International Review of Cell and Molecular Biology

Academic Press is an imprint of Elsevier
525 B Street, Suite 1800, San Diego, CA 92101-4495, USA
225 Wyman Street, Waltham, MA 02451, USA
The Boulevard, Langford Lane, Kidlington, Oxford, OX5 1GB, UK
32 Jamestown Road, London, NW1 7BY, UK
Radarweg 29, PO Box 211, 1000 AE Amsterdam, The Netherlands

First edition 2014

British Library Cataloguing in Publication Data
A catalogue record for this book is available from the British Library

Library of Congress Cataloging-in-Publication Data
A catalog record for this book is available from the Library of Congress

ISBN: 978-0-12-800097-7
ISSN: 1937-6448

PRINTED AND BOUND IN USA
14 15 16 10 9 8 7 6 5 4 3 2 1

CONTRIBUTORS

Josephine C. Adams
School of Biochemistry, University of Bristol, Bristol, United Kingdom

Yasaman Amoozadeh
Keenan Research Center for Biomedical Science, St. Michael's Hospital, and Department of Surgery, University of Toronto, Toronto, Ontario, Canada

Hamid R. Asgari
Tehran University of Medical Sciences, Tehran, Iran

Barry D. Bruce
Department of Biochemistry and Cellular and Molecular Biology, and Department of Microbiology, University of Tennessee, Knoxville, Tennessee, USA

Caspar Bundgaard-Nielsen
Department of Clinical and Experimental Medicine (IKE), Division of Cell Biology, and Integrative Regenerative Medicine Center (IGEN), Linköping University, Linköping, Sweden, and Laboratory for Stem Cell Research, Aalborg University, Aalborg, Denmark

S. John Calise
Department of Oral Biology, University of Florida, Gainesville, Florida, USA

Wendy C. Carcamo
Department of Oral Biology, University of Florida, Gainesville, Florida, USA

Edward K.L. Chan
Department of Oral Biology, University of Florida, Gainesville, Florida, USA

Rebecca Chowdhury
Department of Genetics, Development and Cell Biology, Iowa State University, Ames, Iowa, USA

Artur Cieślar-Pobuda
Department of Clinical and Experimental Medicine (IKE), Division of Cell Biology, and Integrative Regenerative Medicine Center (IGEN), Linköping University, Linköping, Sweden, and Biosystems Group, Institute of Automatic Control, Silesian University of Technology, Gliwice, Poland

Miriam Cohen
Department Cellular and Molecular Medicine, Glycobiology Research and Training Center, University of California, San Diego, California, USA

Ashita M. Dave
Department of Biochemistry and Cellular and Molecular Biology, Knoxville, Tennessee, USA

Ian M.C. Dixon
Department of Physiology, St. Boniface Research Centre, and Manitoba Institute of Child Health, University of Manitoba, Winnipeg, Canada

Caitlin Farris
Department of Genetics, Development and Cell Biology, Iowa State University, Ames, Iowa, USA

Saeid Ghavami
Department of Physiology, St. Boniface Research Centre, and Manitoba Institute of Child Health, University of Manitoba, Winnipeg, Canada

Jillian J. Goetz
Department of Genetics, Development and Cell Biology, Iowa State University, Ames, Iowa, USA

Jerzy Grabarek
Department of Pathology, Pomeranian Medical University, Szczecin, Poland

Huiqing Hu
Department of Microbiology and Molecular Genetics, University of Texas Medical School at Houston, Houston, Texas, USA

Ziyin Li
Department of Microbiology and Molecular Genetics, University of Texas Medical School at Houston, Houston, Texas, USA

Marek J. Łos
Department of Pathology, Pomeranian Medical University, Szczecin, Poland; Department of Clinical and Experimental Medicine (IKE), Division of Cell Biology, and Integrative Regenerative Medicine Center (IGEN), Linköping University, Linköping, Sweden, and BioApplications Enterprises, Winnipeg, Manitoba, Canada

Aleksandar Pantovic
Institute of Microbiology and Immunology, School of Medicine, University of Belgrade, and Clinic of Neurology, Military Medical Academy, Belgrade, Serbia

Mehrdad Rafat
Department of Clinical and Experimental Medicine (IKE), Division of Cell Biology, and Integrative Regenerative Medicine Center (IGEN), and Department of Biomedical Engineering (IMT), Linköping University, Linköping, Sweden

Minoru Satoh
Division of Rheumatology and Clinical Immunology, Department of Medicine, University of Florida, Gainesville, Florida, USA, and Department of Clinical Nursing, School of Health Sciences, University of Occupational and Environmental Health, Kitakyushu, Japan

Richard F. Simmerman
Department of Biochemistry and Cellular and Molecular Biology, Knoxville, Tennessee, USA

Katalin Szaszi
Keenan Research Center for Biomedical Science, St. Michael's Hospital, and Department of Surgery, University of Toronto, Toronto, Ontario, Canada

Jeffrey M. Trimarchi
Department of Genetics, Development and Cell Biology, Iowa State University, Ames, Iowa, USA

Richard P. Tucker
Department of Cell Biology and Human Anatomy, University of California, Davis, California, USA

Ajit Varki
Department of Medicine, and Department Cellular and Molecular Medicine, Glycobiology Research and Training Center, University of California, San Diego, California, USA

Carlos A. von Mühlen
Rheuma Clinic for Rheumatic Diseases, Porto Alegre, Brazil

Agata M. Wasik
Division of Pathology, Department of Laboratory Medicine, Karolinska Institutet, Karolinska University Hospital, Huddinge, Stockholm, Sweden

Qing Zhou
Department of Microbiology and Molecular Genetics, University of Texas Medical School at Houston, Houston, Texas, USA

CHAPTER ONE

Structure and Function of POTRA Domains of Omp85/TPS Superfamily

Richard F. Simmerman[*,1], **Ashita M. Dave**[*,1], **Barry D. Bruce**[*,†,1,2]
[*]Department of Biochemistry and Cellular and Molecular Biology, Knoxville, Tennessee, USA
[†]Department of Microbiology, University of Tennessee, Knoxville, Tennessee, USA
[1]All authors contributed equally to this manuscript
[2]Corresponding author: e-mail address: bbruce@utk.edu

Contents

Abstract

The Omp85/TPS (outer-membrane protein of 85 kDa/two-partner secretion) superfamily is a ubiquitous and major class of β-barrel proteins. This superfamily is restricted to the outer membranes of gram-negative bacteria, mitochondria, and chloroplasts. The common architecture, with an N-terminus consisting of repeats of soluble

International Review of Cell and Molecular Biology, Volume 308
ISSN 1937-6448
http://dx.doi.org/10.1016/B978-0-12-800097-7.00001-4

polypeptide-transport-associated (POTRA) domains and a C-terminal β-barrel pore is highly conserved. The structures of multiple POTRA domains and one full-length TPS protein have been solved, yet discovering roles of individual POTRA domains has been difficult. This review focuses on similarities and differences between POTRA structures, emphasizing POTRA domains in autotrophic organisms including plants and cyanobacteria. Unique roles, specific for certain POTRA domains, are examined in the context of POTRA location with respect to their attachment to the β-barrel pore, and their degree of biological dispensability. Finally, because many POTRA domains may have the ability to interact with thousands of partner proteins, possible modes of these interactions are also explored.

1. INTRODUCTION

The OMs (outer membranes) of gram-negative bacteria, mitochondria, and chloroplasts are unique in their incorporation of β-barrel proteins, while all other biological membranes accommodate α-helical transmembrane proteins exclusively. β-Barrel OMPs (outer-membrane proteins) function as: porins, energy-dependent transporters, protein secretors, protein importers, autotransporters, adhesins, lipases, proteases, and lipid transporters (Wimley, 2003). Correct assembly of these OMPs is dependent upon a conserved family of proteins, Omp85 (outer-membrane protein of 85 kDa) (Voulhoux et al., 2003).

Omp85s share remarkable architectural similarity to a related set of proteins known as TpsB (two-partner secretion B), which are involved in the secretion of TpsA proteins through OMs (Clantin et al., 2007; Kim et al., 2007; Sanchez-Pulido et al., 2003). These two related protein families make up a superfamily of proteins that function as PTBs (polypeptide-transporting β-barrel proteins) (Jacob-Dubuisson et al., 2009). PTBs share a highly conserved domain organization, with an N-terminal region composed of soluble POTRA (polypeptide-transport-associated) domain repeats and a C-terminal transmembrane β-barrel (Sanchez-Pulido et al., 2003). TpsB proteins are defined as class I PTBs and most contain two POTRA domains, while Omp85 proteins are more variable having between one and seven POTRA repeats, and are defined as class II PTBs (Arnold et al., 2010; Kim et al., 2007; Koenig et al., 2010; Sanchez-Pulido et al., 2003).

While it is unclear which class of PTBs evolved first, duplication could have given rise to the two different classes and the different number of POTRA repeats found (Remmert et al., 2010). The fact that PTB members are present in gram-negative bacteria, mitochondria, and chloroplasts

suggests that Omp85 arose early in the evolution of prokaryotes, before the first endosymbiotic event (Habib et al., 2007; Reumann and Keegstra, 1999; Walther et al., 2009). Mitochondrial Sam50 most likely diverged from an Omp85 present in an α-proteobacteria, while the plastid Toc75 is thought to have evolved from a TpsB-like protein present in the cyanobacterial ancestor (Gentle et al., 2004).

While only one complete structure of a TpsB member of the Omp85/TPS superfamily has been experimentally determined (Clantin et al., 2007), the structures of multiple POTRA domains have been solved (Arnold et al., 2010; Gatzeva-Topalova et al., 2008; Kim et al., 2007; Knowles et al., 2008, 2009; Koenig et al., 2010; van den Ent et al., 2008; Zhang et al., 2011). Additionally, the mechanism(s) by which Omp85/TPS and POTRA domains interact allows for specific interactions with multiple partners, thousands of different partners in the case of Toc75 (Iniative, 2000), is fundamental to chloroplast evolution and function and merits further study. Members of the Omp85/TPS superfamily, and even specific POTRA domains, have been proven to be essential for cell growth in both bacteria (Bos et al., 2007; Tashiro et al., 2008) and organelle containing eukaryotes (Hust and Gutensohn, 2006; Patel et al., 2008) yet their exact role in survival is not known.

1.1. Omp85/TPS superfamily in gram-negative bacteria

An OM enveloping a peptidoglycan layer is the defining characteristic of gram-negative bacteria (Costerton et al., 1974). Integrity of the OM depends on the presence of OMPs and a variety of LPS (lipopolysaccharides), which are unique to the outer leaflet of the OM (Gentle et al., 2005; Voulhoux et al., 2003; Wiese and Seydel, 1999). These components are cytosolically synthesized, transported across the inner membrane, through the periplasm, and finally assembled into the OMs (Tamm et al., 2004; Tokuda and Matsuyama, 2004). The protein responsible for OMP insertion was discovered when depletion of Omp85 led to defects in OMP biogenesis (Voulhoux et al., 2003). The family of proteins that functions to insert OMPs into OMs is known as Omp85 proteins, and they make up class II PTBs.

Class I PTBs consists of TpsB proteins that secrete specific TpsA proteins in the TPS (two-partner secretion) systems (Jacob-Dubuisson et al., 2009; Kajava and Steven, 2006). Members of the TpsB family include ShlB of *Serratia marcescens* and FhaC of *Bordetella pertussis* (Surana et al., 2004).

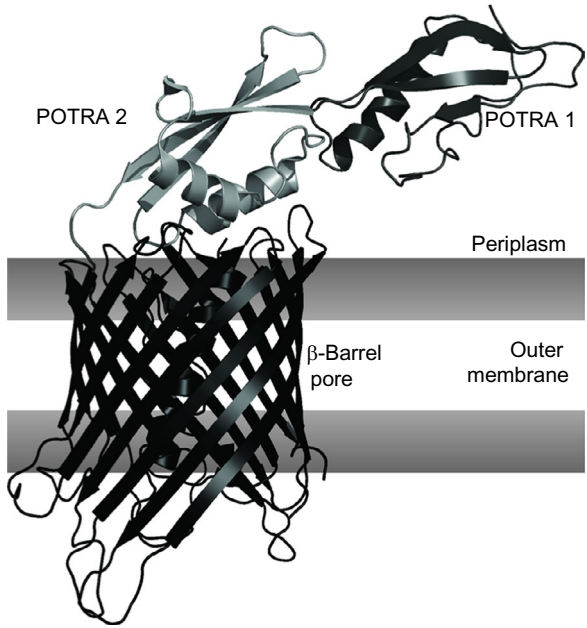

Figure 1.1 Structure of FhaC. FhaC, the TpsB transporter of filamentous hemagglutinin (FHA) from *Bordetella pertussis* has been crystallized and the structure solved at a resolution of 3.15 Å (pdb id: 2QDZ). The pore of the structure is shown in the outer membrane, while the POTRA domains are in the periplasm.

The TpsB protein, FhaC has been crystallized and is represented in Fig. 1.1, and demonstrates the conserved structure present in all members of the Omp85/TPS superfamily (Ertel et al., 2005; Sanchez-Pulido et al., 2003). This protein is the only member of the Omp85/TPS superfamily to be structurally solved in its entirety, only POTRA domains of other members have been structurally solved.

1.2. Omp85/TPS superfamily in organelles

The presence of β-barrel proteins in the OMs of mitochondria and chloroplasts is consistent with their evolutionary origins from α-proteobacteria and cyanobacteria, respectively (Gentle et al., 2005; Patel et al., 2008). Furthermore, mitochondrial Sam50 most likely diverged from an Omp85 present in the α-proteobacteria, while plastid Toc75 is thought to have evolved from a TpsB-like protein present in the cyanobacterial ancestor (Gentle et al., 2004).

1.2.1 Sam50/Tob55, a mitochondrial homolog of bacterial Omp85

Nuclear-encoded and cytosolically synthesized proteins targeted to the mitochondria are translocated through the mitochondrial membranes via the TOM and TIM (translocons at the outer/inner envelope of the mitochondria) (Paschen et al., 2005). β-Barrel proteins destined for the mitochondrial OM follow this path, and are inserted into the OM via the TOB (topogenesis of mitochondrial OM β-barrel proteins), also known as the SAM (sorting and assembly of mitochondria) complex (Paschen et al., 2005). Sam50/Tob55 appears to be the only Omp85 homologue in mitochondria, and was first discovered in *Saccharomyces cerevisiae* (Gentle et al., 2004; Kozjak et al., 2003; Paschen et al., 2005).

1.2.2 Toc75, a plastid homolog of bacterial Omp85

The genome of modern day plastids encodes between 60 and 200 proteins, while the total chloroplast proteome of *Arabidopsis thaliana* is estimated to comprise approximately 2100–4500 proteins (Leister and Kleine, 2008). Therefore, plastids depend on their host nuclei to encode over 95% of the proteins needed to correctly function (Abdullah et al., 2000; Inoue and Potter, 2004). The import of cytosolically translated precursor proteins into the plastid is accomplished by the TOC/TIC (translocon at the outer/inner envelope of the chloroplast) complexes along with soluble chaperones (Schnell et al., 1994), an excellent review of which can be found (Strittmatter et al., 2010). Toc75, the most abundant protein in the OM of the plastid envelope, is a member of the Omp85/TPS superfamily and is believed to form the β-barrel channel in the TOC complex (Gentle et al., 2005). This review will highlight similarities among the Omp85/TPS superfamily and their N-terminal POTRA domains, with an intensive look at phototrophic members of the superfamily. Structural and organizational similarities and differences of POTRA domains will be noted, and possible mechanisms of action will be explored.

2. Omp85/TPS SUPERFAMILY ARCHITECTURE

β-Barrel proteins have been implicated in protein translocation and in the assembly of OMPs in both organelles and bacteria (Moslavac et al., 2005). Bacterial and organellar members of the Omp85/TPS superfamily share a common domain organization (Gentle et al., 2005). The N-terminal regions of the OMP85/TPS superfamily were discovered to share a common three-dimensional structure consisting of repeatable units

made up of two α-helices and three β-strands termed POTRA domains (Sanchez-Pulido et al., 2003). The C-terminus is a highly conserved β-barrel domain comprising 10–16 β-strands (Sanchez-Pulido et al., 2003).

2.1. Highly conserved C-terminal β-barrel domain

The C-terminal β-barrel pore of OMP85/TPSs includes the presence of even numbers of amphipathic, antiparallel β-strands connected by loops of different sizes, forming a cylindrical barrel-like structure across the membrane bilayer. Each strand usually contains 8–11 residues, which is long enough to span biological membranes (Moslavac et al., 2005; Paschen et al., 2005). FhaC, an exporter of filamentous hemagglutinin (FHA) in *B. pertusis* is the only member of the OMP85/TPS superfamily with a solved structure that includes its C-terminus (Clantin et al., 2007), the rest of the structures are of only the N-terminal POTRA domains. It has a 16-stranded β-barrel pore with a width of around 0.8 nm at its restriction point, and has been shown to have both open and closed states (Clantin et al., 2007).

2.2. Soluble N-terminus, containing POTRA domains

Preceding the β-barrel domain is a variable sized domain composed of repeats of POTRA domains. The POTRA domains are always found at the N-termini of OMP85/TPSs and are involved in the assembly of proteins into or translocation across the OMs of mitochondria, chloroplasts, and gram-negative bacteria (Delattre et al., 2011; Gentle et al., 2004, 2005; Knowles et al., 2009; Moslavac et al., 2005; Paschen et al., 2003; Reumann et al., 1999; Sanchez-Pulido et al., 2003; Voulhoux et al., 2003). These domains are also present in the FtsQ/DivIB bacterial division protein family, which is the only known case where POTRA domains are not followed by a transmembrane β-barrel (Sanchez-Pulido et al., 2003).

A typical individual POTRA domain consists of 70–95 amino acids containing three β-strands and two α-helices (Sanchez-Pulido et al., 2003). The repeating POTRA domains are assigned consecutive numbers starting from the N-terminus (Sanchez-Pulido et al., 2003). All members of the Omp85/TPS superfamily have between one and seven repeats of POTRA domains (Arnold et al., 2010; Sanchez-Pulido et al., 2003). The number of POTRA domains varies from one protein and/or organism to another, for example, one POTRA repeat is present in Sam50, FtsQ/DivIB, ShlB, and CGI51; three POTRA repeats are present in YtfM and Toc75; five POTRA repeats are found in D15 of *Haemophilus influenza*, Omp85 of

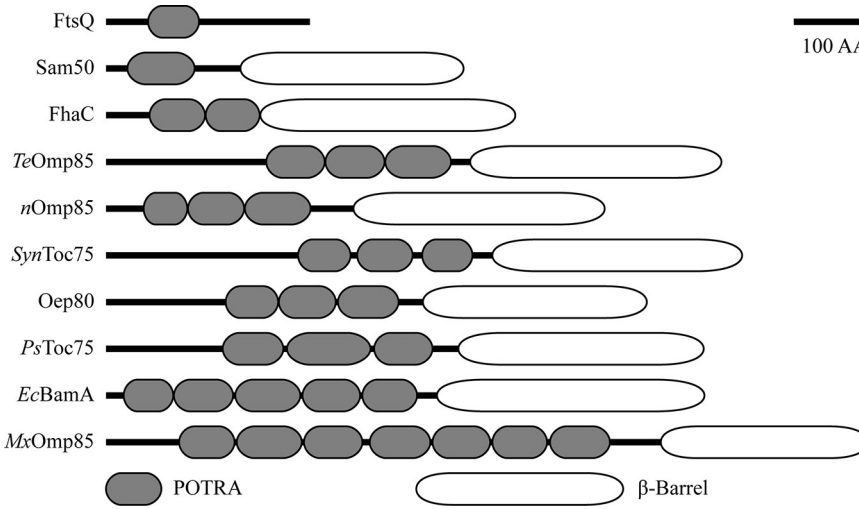

Figure 1.2 Conserved structure of the Omp85/TPS superfamily. POTRA domain-containing proteins are represented in this cartoon. POTRA domains are depicted as gray, while β-barrels are represented as white. FtsQ from *E. coli* is a protein that functions in cell division. Sam50 from *Saccharomyces cervisae* is part of the sorting and assembly machinery that functions in OMP assembly and is found in the mitochondria. FhaC from *B. pertussis* exports FHA. *Te*Omp85, *Mx*Omp85, BamA, and *n*Omp85 from *T.e.*, *M. xanthus*, *E. coli*, and *Nostoc*, respectively, and function in OMP assembly. *Syn*Toc75 from *Synechocystis* sp. PCC 6803 once exported virulence factors. Oep80 from *A. thaliana* functions in the chloroplast in OMP assembly. Toc75 from *Pisum sativum* functions in chloroplast protein import. Proteins and domains are represented to scale.

Neisseria meningitidis, and other bacterial Omp85s; while as many as seven repeats are seen in Mxan5763 of *Myxococcus xanthus* (Arnold et al., 2010; Sanchez-Pulido et al., 2003). This is represented in Fig. 1.2. A recent study of 567 POTRA-domain-containing proteins demonstrated that regardless of total number of POTRA domains present, the most C-terminal POTRA domain was the most conserved followed by the most N-terminal POTRA domain (Arnold et al., 2010). This also suggests that OMP85/TPSs containing multiple POTRA domain repeats may have evolved from a relatively simple ancestor, such as Sam50 containing only one POTRA repeat (Arnold et al., 2010). Notably, it was also demonstrated that POTRA domains from the cyanobacteria *Thermosynechococcus elongatus* (*Te*Omp85) are more closely related to POTRA domains from *A. thaliana* Toc 75 (*At*Toc75) than to proteobacterial Omp85s (Arnold et al., 2010).

These domains appear to be quite antigenic and are often recognized by antibodies raised against the entire protein (e.g., antibodies raised against the POTRA-containing N-terminal portion of the OMP D15, an Omp85

family protein, provide immunity against meningitis caused by *H. influenza*; Loosmore et al., 1997), this high antigenicity has led to the suggestion that they may be a good target to use in vaccines development against: cholera (Ruffolo and Adler, 1996), meningitis (Manning et al., 1998; Yang et al., 1998), gonorrhea (Manning et al., 1998), and syphilis (Cameron et al., 2000; Poolman et al., 2000; Robb et al., 2001).

POTRA domains show very little primary sequence homology, in fact, only glycine and hydrophobic residues forming the core of the domain are conserved between POTRAs (Sanchez-Pulido et al., 2003). However, the secondary sequence was both predicted (Sanchez-Pulido et al., 2003) and shown by crystallization and/or NMR of POTRA domains of BamA (Kim et al., 2007), FhaC (Clantin et al., 2007), FtsQ (van den Ent et al., 2008), *Te*Omp85 (Arnold et al., 2010), and *n*Omp85 (Koenig et al., 2010) to have a conserved structure, which was experimentally determined to have the consensus structure: β–α–α–β–β (Fig. 1.3). A table showing the relationship between primary structure identity and similarity of three-dimensional structure has been constructed for all of the structurally solved POTRA domains (Table 1.1). This table shows that the structural similarities of POTRA domains are not fully explained by sequence, as the most structurally similar POTRA domains are POTRA3 of *Te*Omp85 and *Nostoc*

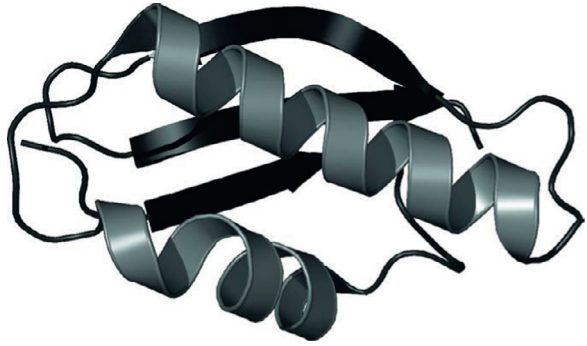

VLRAVQVAGNQVLTQEKVNEIFAPQIGRTLNLRELQAGIEKI
---bbbbb-----hhhhhhhhhhhhh----hhhhhhhhhhhh
NTFYRDNGYILGQVVGTPQVDPDGVVTLQVAE
hhhhhhh-----bbbbbbbb----bbbbbbb-

Figure 1.3 POTRA2 of *Te*Omp85. The primary, secondary, and tertiary structure of POTRA2 of *Te*Omp85 (pdb id: 2X8X) are shown. Under the primary sequence, shown in capital letter, is the secondary structure, represented in b for β-strand, and h for α-helix, the - represents unstructured residues.

Table 1.1 Similarity of POTRA domains

Percent identity																	
	1	2	3	4	5	6	7	8	9	10	11	12	13	14	15		
1		13.9	4.5	5.9	13.2	20.0	11.5	16.4	20.3	12.8	13.6	16.2	10.4	19.2	15.3	1	Bp-FhaC-1
2	6.13		11.8	11.6	6.8	15.3	9.3	12.3	14.7	13.3	15.6	14.9	12.0	7.0	15.9	2	Bp-FhaC-2
3	3.77	4.52		86.8	10.3	7.4	15.9	11.8	10.9	10.1	13.3	13.4	8.7	6.0	6.2	3	Ec-FtsQ-1
4	4.04	4.91	2.06		8.7	10.3	14.3	11.6	12.5	8.6	16.7	14.7	8.6	7.5	6.2	4	Ye-FtsQ-1
5	6.08	4.51	3.06	3.61		16.0	23.5	63.6	26.1	18.8	19.4	11.0	8.0	13.7	16.9	5	No-Omp85-1
6	2.80	5.59	4.37	3.83	2.97		14.3	17.6	54.1	15.6	13.4	21.3	19.2	13.2	13.9	6	No-Omp85-2
7	8.99	3.69	12.05	10.56	1.70	8.46		23.4	16.9	52.4	26.5	12.0	16.9	18.7	31.5	7	No-Omp85-3
8	4.89	2.89	3.07	3.64	1.28	3.69	1.52		21.7	20.8	22.4	9.6	12.0	15.1	16.9	8	Te-Omp85-1
9	3.07	3.46	2.85	3.15	3.32	1.70	11.73	2.69		21.1	19.4	19.7	21.6	14.1	16.4	9	Te-Omp85-2
10	6.77	3.56	7.46	6.21	1.84	3.51	1.11	1.68	6.83		29.4	16.0	10.4	17.3	34.2	10	Te-Omp85-3
11	3.45	2.98	2.17	3.21	1.52	4.00	7.90	1.32	2.42	5.35		12.1	14.9	14.7	26.5	11	Ec-YaeT-1
12	3.74	4.02	2.29	2.52	3.00	3.19	3.72	2.41	2.19	3.53	1.70		14.8	14.5	11.1	12	Ec-YaeT-2
13	3.84	3.91	3.43	3.26	3.97	3.13	4.83	3.98	2.64	4.89	3.53	2.33		15.2	6.8	13	Ec-YaeT-3
14	3.93	4.33	2.66	3.44	2.41	2.52	2.47	2.79	2.49	2.70	2.41	2.04	3.75		10.8	14	Ec-YaeT-4
15	3.57	3.05	2.72	3.39	1.64	3.77	1.34	1.65	3.31	1.53	1.18	2.75	3.12	2.27		15	Ec-YaeT-5
	1	2	3	4	5	6	7	8	9	10	11	12	13	14	15		
RMSD of superimposition (Å)																	

Color scheme								
% Identity	<10	>10	>15	>20	>25	>30	>50	>60
RMSD	>9.0	<9.0	<7.0	<5.0	<3.5	<2.5	<2.0	<1.5

sp. PCC7120 (*n*Omp85), which have a 52.4% identity, but superimpose with an RMSD of 1.11 Å.

POTRA domains were originally identified by searching global hidden Markov models, which identified the POTRA domains by their shared secondary structure (Sanchez-Pulido et al., 2003). The interaction between the adjacent POTRA domains is poorly understood yet is believed to be highly dynamic, based on NMR data of the protein in solution (Knowles et al., 2008). Comparisons of the linkages between tandem POTRA domains in different published crystal structures support this dynamic coupling (Ward et al., 2009). Interestingly, it appears that the POTRA domain closest to the pore tends to have a fixed structure and orientation with respect to the pore (Koenig et al., 2010).

Although the structure and function of the Omp85/TPS superfamily is well conserved, how individual POTRA domains mediate the assembly of OMPs or translocation of polypeptides is still unclear. Solved crystal structures of two POTRA domains of FhaC (Clantin et al., 2007), five POTRA domains of BamA (Kim et al., 2007), three POTRA domains of *n*Omp85 (Koenig et al., 2010), and *Te*Omp85 (Arnold et al., 2010) provide insights into the organization and molecular mechanisms by which these domains may function (Bos et al., 2007).

3. FUNCTION OF Omp85 FAMILY OF PROTEINS

Despite their organizational similarity TpsBs and Omp85s differ fundamentally in their roles: Class I or TpsB members are involved in secretion of other proteins/substrates through the outer bacterial membrane, while Class II or Omp85 members have been shown to function in the biogenesis (Gatzeva-Topalova et al., 2010; Paschen et al., 2005) or insertion of β-barrel proteins into OMs presumably from the periplasmic or equivalent surface (Koenig et al., 2010). Members of the Omp85 family have been shown to be essential for assembly of OM β-barrel proteins into gram-negative OMs (Genevrois et al., 2003; Voulhoux et al., 2003; Wu et al., 2005). Homologues of this family have been found in the genome of all sequenced gram-negative bacteria (Gentle et al., 2004; Voulhoux and Tommassen, 2004), and in the membranes of mitochondria and plastids (Gentle et al., 2005; Voulhoux et al., 2003).

3.1. Role of Omp85 pore

β-Barrels from eukaryotic organelles are thought to facilitate the translocation of precursor proteins through the membranes as well as to aid in assembly of other OMPs (Schleiff and Soll, 2005). However, it should be noted that these organelle-localized members may have an inverted topology relative to their bacterial ancestral members (Reumann et al., 1999). Bacterial proteins destined for the OM are cytosolically translated as precursors with an N-terminal sequence that targets them for secretion via the SecYEG complex (Cross et al., 2009). A model for OMP assembly suggests that nascent OMPs, partially folded via chaperones in the periplasm, are translocated through the SecYEG complex in the cytoplasmic membrane and transferred to an Omp85 protein in the OM (Cross et al., 2009). Because the Omp85 pore is not large enough to accommodate the formation of a new β-barrel (Gentle et al., 2004; Voulhoux et al., 2003), Omp85 may serve as a scaffold that would assist in the insertion of incoming transmembrane spanning β-strands individually or in pairs thereby facilitating the insertion of the OMPs into the membrane at the protein–lipid interface (Gentle et al., 2005). Deletions of POTRA domains (Clantin et al., 2007; Jacob-Dubuisson et al., 2004) support a role of YaeT as a scaffold for other components of the OMP assembly complex.

3.2. Role of POTRA domains

As suggested by their name, POTRA domains play a key role in protein transport (Clantin et al., 2007; Sanchez-Pulido et al., 2003); however, the

mechanism(s) by which they aid the transport of proteins into or across membranes is unclear. A possible mode of interaction for POTRA domains is β-augmentation, a nonsequence-specific interaction between a β-strand of one protein and a β-strand of a second protein (Harrison, 1996), which has been observed in POTRA crystal structures (Gatzeva-Topalova et al., 2008; Kim et al., 2007; Koenig et al., 2010). Unfortunately, there is no information on which of the β-strands would be involved in an *in vivo* interaction since there are no structures of any POTRA domain with a substrate. While the mechanism(s) by which POTRA domains interact is unresolved, what is apparent is that individual POTRA domains of Omp85 proteins interact with OMP precursors (Bennion et al., 2010; Bredemeier et al., 2007; Habib et al., 2007; Kim et al., 2007; Robert et al., 2006; Sklar et al., 2007a; Vuong et al., 2008) and have unique structural characteristics (Gatzeva-Topalova et al., 2008; Koenig et al., 2010; Ward et al., 2009). Furthermore, POTRA domains are necessary for proper functioning of Omp85 proteins (Bos et al., 2007; Bredemeier et al., 2007; Clantin et al., 2007; Ertel et al., 2005; Habib et al., 2007; Kim et al., 2007), with specific POTRA domains vital to the survival of the organism (Bos et al., 2007).

While most of the structurally solved POTRA domains superimpose well, with an average RMSD of 3.7 Å (Table 1.1 and Fig. 1.4), there are differences in their structures that may help in the discovery of the niche that each individual POTRA repeat fills. There is a β-cap on POTRA1 and a

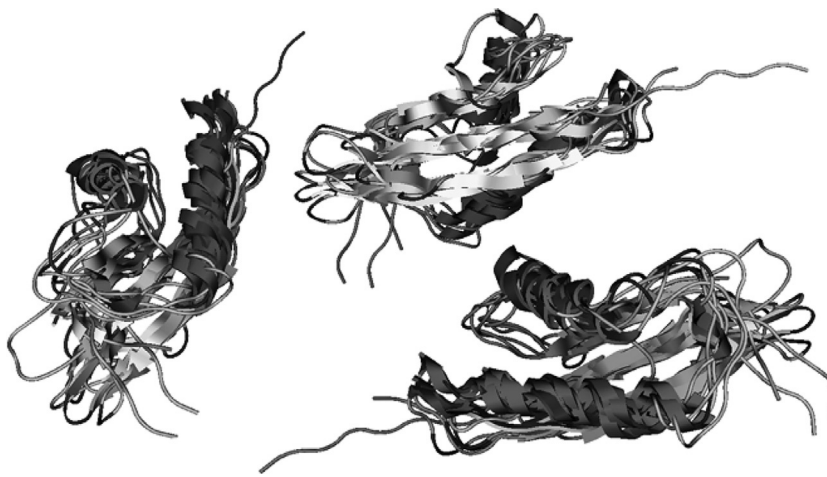

Figure 1.4 Overlay of structurally solved POTRA domains. Solved crystal structures of all solved POTRA domains have been superimposed onto each other. Three different views are present that show the similarity of the tertiary structure of these domains.

β-bulge on POTRA2 of cyanobacterial Omp85s and POTRA3 of BamA (Arnold et al., 2010; Koenig et al., 2010). These may be used as interaction sites for the POTRA domains, and could even function in β-augmentation. POTRA3 of cyanobacterial Omp85s has a loop L1, which may function to help gate the pore (Arnold et al., 2010; Koenig et al., 2010). Phylogenetic analysis shows that POTRAs cluster by their positional number, supporting the hypothesis that their order remains important (Bos et al., 2007). It is interesting that the average RMSD of the most C-terminal POTRA domains of Omp85s is 1.50 Å and the percent identity is 39.4% (Table 1.1). This suggests the most C-terminal POTRA domain is evolutionarily conserved in structure as well as by sequence to a lesser degree. The fact that POTRA5 of Omp85 in *N. meningitidis* is essential for cell viability (Bos et al., 2007) lends support to this hypothesis.

A number of specific interaction partners have been found for specific POTRA domains. The single POTRA domain of Sam50 has been shown to specifically bind β-barrel proteins destined for the mitochondrial OM (Habib et al., 2007). BamA is reported to bind C-terminal peptides of OMPs (Robert et al., 2006). In fact, POTRA5 is necessary for interactions with YfiO, NlpB, and SmpA (all proteins involved in the OM β-barrel protein biogenesis), while POTRA1 is required for an interaction with YfgL (Kim et al., 2007). POTRA1 also interacts with SurA (Sklar et al., 2007b; Vuong et al., 2008), a periplasmic chaperone, using an arginine residue (Bennion et al., 2010). The POTRA domains of *n*Omp85 have an affinity for the C-terminal pore of the protein, and act as a docking site for incoming precursor proteins (Bredemeier et al., 2007). Interestingly, these interactions have been shown to be species-specific (Robert et al., 2006). The identification of interacting partners of POTRA domains of the Omp85 family will help with to uncover roles and mechanism(s) for them.

Deletion studies, which uncovered the necessity of POTRA5 for *N. meningitides*, have been instrumental in the discovery of roles for POTRA domains. In fact, deletion of any POTRA repeat leads to a decrease in either the functionality of the protein machinery they are part of or a loss in cell viability (Bos et al., 2007; Bredemeier et al., 2007; Clantin et al., 2007; Ertel et al., 2005; Habib et al., 2007; Kim et al., 2007). *Escherichia coli* harboring deletions of POTRA1 or POTRA2 of BamA exhibit poor cell growth, while cells with deletions of POTRA3 or POTRA4 do not survive wild-type BamA depletion, and cells without POTRA5 do not survive even when they possess copies of wild-type BamA (Kim et al., 2007). This suggests not only an essential role for POTRA5 but also a dominant negative

interaction *in vivo*. Incorrect β-barrel assembly is correlated with POTRA domain deletions (Bredemeier et al., 2007; Habib et al., 2007). It has been shown that Sam50ΔPOTRA is able to bind, but not release β-barrel precursors, this indicates a role for the POTRA domain in the release of precursor proteins from the SAM complex (Stroud et al., 2011). This was also evidenced by analyzing membrane fractions where *n*Omp85ΔN-term yielded only one stabilized assembly of monomeric Omp85, while membranes containing wild-type *n*OMP85 show formation of a homo-trimeric Omp85 complex (Bredemeier et al., 2007). The deletion studies, structural information, and binding assays help to shed light on the functional roles of POTRA domains of Omp85s.

4. FUNCTIONS OF TWO-PARTNER SECRETION B PROTEINS

TpsBs are involved in polypeptide translocation across membranes (Koenig et al., 2010). FhaC mediates the translocation of FHA, the major adhesin of the whooping cough agent *B. pertussis* to the bacterial surface (Guedin et al., 1998). Clantin et al. (2004) reported the structure of the OM transporter FhaC, a member of the TpsB family of proteins, at a resolution of 3.1 Å. The C-terminal domain of FhaC forms a transmembrane pore comprised of 16 antiparallel β-strands (Clantin et al., 2004), while the N-terminal periplasmic module consists of two globular POTRA domains composed of 75 residues each (Clantin et al., 2007).

4.1. Role of TpsB pore

The β-barrel of FhaC is occluded by a 20-residue long α-helix (H1), residing between the pore and the POTRA domains, and a C-terminal extracellular loop (L6) (Clantin et al., 2007). Although the role of in-plugs are not well understood, it has been observed that one possible function is to stabilize individual β-strands that would be unstable in a lipid bilayer due to their distribution of hydrophobic residues (Naveed et al., 2009). *In silico* analyses of Omp85/TPS superfamily members uncovered conserved motifs within the β-barrel, referred to as motifs 3 and 4, which were seen in FhaC (Fig. 1.5; Clantin et al., 2007; Moslavac et al., 2005). These motifs are defined by two conserved transmembrane β-sheets and may function in the gating of the β-barrel pore (Moslavac et al., 2005). The L6 loop of motif 3, which could insert itself into the pore, is well conserved between FhaC and *Te*Omp85, and has been shown to play an important role in regulation

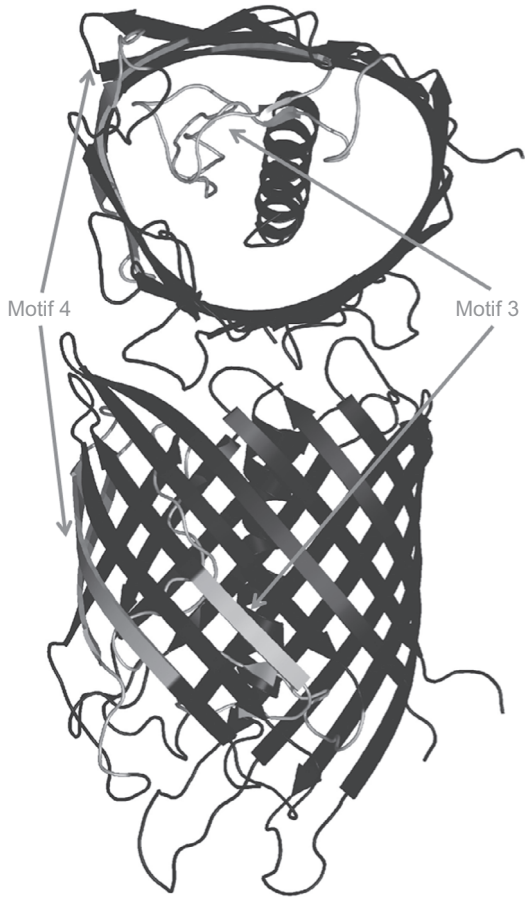

Figure 1.5 Conserved motifs of β-barrel from FhaC. The structure of the only β-barrel pore of the Omp85/TPS superfamily to be solved is shown (pdb id. 2QDZ). The pore here is occluded by an α-helix. Motifs 3 and 4, which are conserved in members of the Omp85/Tps superfamily, are shown in gray.

of polypeptide translocation (Arnold et al., 2010; Clantin et al., 2007). This suggests that L6 may be responsible for regulation of the assembly of OMPs in other *cy*Omp85 (cyanobacterial Omp85) as well.

4.2. Role of POTRA domains of TpsB

TpsA proteins all harbor a conserved, 250-residue long N-terminal TPS domain essential for secretion (Clantin et al., 2004; Hodak et al., 2006) and are involved in adhesion (Borlee et al., 2010), cytolysis, contact-dependent growth inhibition (Aoki et al., 2005), biofilm formation,

proteolysis, and host-cell invasion (Jacob-Dubuisson et al., 2004). The POTRA domains present in the N-terminus of the TpsB proteins interact with the TpsA proteins (Clantin et al., 2007; Hodak et al., 2006).

4.2.1 FhaC

One of the most well-characterized TpsB proteins is FhaC (Clantin et al., 2004, 2007). The structure of FhaC is shown in Fig. 1.1. Using this structure as a template for mutations it was shown that while FhaC still forms a channel with deletion of either POTRA domain, the POTRA domains are very important for the function of FhaC. Deletion of either POTRA domain will abolish secretion of its substrate, FHA, while insertion of residues into the POTRA domains strongly affects secretion (Clantin et al., 2007). POTRA2 is presumed to use β-augmentation during the transport of FHA, and substitutions in this domain have the most severe effect on secretion (Delattre et al., 2011). It has been shown using surface plasmon resonance that POTRA domains (specifically helix 2 of POTRA1) are involved in FHA recognition (Clantin et al., 2007). This interaction was shown to be quite tight with a K_d of ~4.0 μM. The isoelectric points of POTRA1 and FHA are 4.6 and 10.0, respectively, which has led to the suggestion that their interaction may contain a significant electrostatic component (Delattre et al., 2011).

5. PHOTOTROPHIC MEMBERS OF Omp85/TPS

Both oxygenic photosynthetic prokaryotes (i.e., cyanobacteria) and eukaryotes (i.e., plants and algae) contain members of the Omp85/TPS superfamily. These proteins are localized to the OM of the cyanobacteria (Bolter et al., 1998) or the plastid envelope (Bauer et al., 2000; Reumann et al., 1999) in algae or plants, respectively. It has been shown that these proteins are evolutionarily related, having been retained during the process of endosymbiosis (Keegstra et al., 1984). For example, in the model plant *A. thaliana*, the first plant with a sequenced genome (Iniative, 2000), there are three functional Omp85/TPS homologs: sorting assembly machinery of 50 kDa (Sam50) in the mitochondria OM (Gentle et al., 2004; Kozjak et al., 2003; Paschen et al., 2003), outer envelope protein 80 (OEP80), which mediates assembly of proteins into the OM of the chloroplast (Schleiff et al., 2003a), and Toc75-III (Hinnah et al., 1997; Schleiff et al., 2003c; Schnell et al., 1994), which is the central component of the protein translocon of the outer chloroplast envelope.

5.1. Cyanobacterial members of Omp85/TPS superfamily

The first Omp85/TPS member in cyanobacteria was identified in *Synechocystis* sp. PCC 6803 via a limited sequence homology against Toc75 of higher plants (Bolter et al., 1998). Currently there are over 100 (Altschul et al., 1997, 2005) different members of cyanobacterial Omp85/TPS genes that have been identified from a large number of organisms suggesting that this is a universal gene in cyanobacteria. Cyanobacterial *Syn*Toc75 is proposed to export virulence factors across the OM and is essential for the viability of the organism (Bolter et al., 1998; Reumann et al., 1999). *Syn*Toc75 and *Ps*Toc75 share 24% identity (41% similarity) and are similar in size, with *Ps*Toc75 consisting of 809 residues and *Syn*Toc75 containing 861 (Reumann et al., 1999). Furthermore, electrophysiological studies showed that *Syn*Toc75 and Toc75 both form cation-selective channels, which supports roles for the proteins in transport (Bolter et al., 1998; Hinnah et al., 1997). Recent studies show that cyanobacterial Omp85s differ in structure and composition from proteobacterial Omp85s, and are more closely related to chloroplastic Toc75s, with the phototrophic members containing only three POTRA domains instead of five (Arnold et al., 2010).

5.1.1 *Omp85 of* Nostoc *sp. PCC 7120*

Omp85 of *Nostoc* sp. PCC 7120 (*n*Omp85) was identified as a homolog of *Ps*Toc75, the proteins share 19.4% identity and 25.4% similarity (Ertel et al., 2005). The three POTRA domains of *n*Omp85 were recently crystallized with a resolution of 3.8 Å (Koenig et al., 2010). Based on this structure it is clear that the POTRA domains of *n*Omp85 share the common tertiary structure of a three stranded β-sheet packed against two helices as observed in other structures. However, there are several differences including: the N-terminus of POTRA1 is capped by two small β-sheets, random coil is integrated in helix α1 and strand β2 in POTRA2, and POTRA3 has an extended loop (L1) that forms two β-turns between β2 and α2 (Fig. 1.6). POTRA1 and POTRA2 may play roles in substrate recognition and hetero-oligomerization as evidenced by β-augmentation of POTRA1 seen in crystal structures (Arnold et al., 2010; Gatzeva-Topalova et al., 2010) and the two potential protein interaction surfaces present on POTRA2 (Koenig et al., 2010). The structure also revealed the presence of a flexible hinge region containing Pro and/or Gly residues between POTRA1 and POTRA2 corresponding to a flexible region between POTRA2 and POTRA3 of

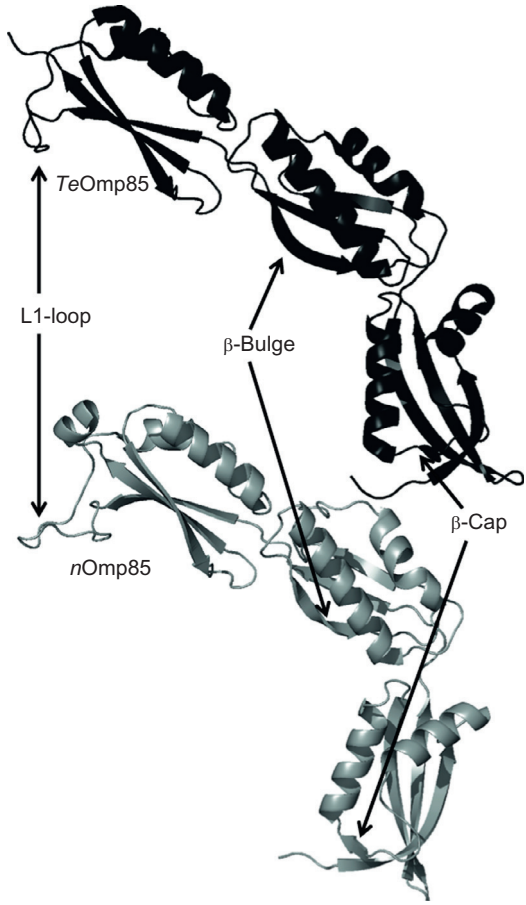

Figure 1.6 POTRA domains from *n*Omp85 and *Te*Omp85. The tertiary structures of the POTRA domains of *n*Omp85 and *Te*Omp85 are shown (pdb ids. 3MC8, 2X8X, respectively). The two POTRA domains can be superimposed with an r.m.s.d. of 0.37 nm, although their primary sequence is only around 50% identical. The features unique to cyanobacterial POTRA domains (L1-loop, β-bulge, and β-cap) are featured.

E. coli BamA, suggesting an equivalent hinge region (Kim et al., 2007; Koenig et al., 2010). Thus, the presence of flexible linker regions might be of importance for substrate-recognizing role of POTRA domains.

5.1.2 Omp85 of T. elongatus

Recently, Arnold et al. (2010) reported the first structure of all three POTRA domains of Omp85 from the cyanobacterium *T. elongatus* (*Te*Omp85) at 1.97 Å resolution. Mature *Te*Omp85 contains an

unstructured proline-rich region located N-terminal to the POTRA domains, followed by three POTRA domains and then a C-terminal pore containing 16 β-strands (Arnold et al., 2010). Residues 67–141 were identified as POTRA1, 142–217 as POTRA2, and 218–301 as POTRA3. POTRA domains of *n*Omp85 and *Te*Omp85 superimpose with an RMSD of 3.7 Å and the similarity between them can be seen in Fig. 1.6.

While POTRA domains are very similar in structure, mutants affecting the POTRA have similar effects on the proteins containing them. The deletion of POTRA domains leads to a destabilization of the pore at higher voltage, which suggests that the POTRA domains play a role in the stabilization of the channel (Arnold et al., 2010). This stabilization of *Te*Omp85 is due to interactions between POTRA3 and β-strands that are part of the pore (Arnold et al., 2010). The electrophysiological measurements of conductance of *Te*Omp85 were the highest reported. They were outside the upper range of other cyOmp85s, *Ps*Toc75, and TpsB proteins; and much higher than those of proteobacterial Omp85s and Sam50s (Arnold et al., 2010). These differences may indicate a similar evolutionary origin between the chloroplastic Omp85 and plant Toc75 homologues.

5.2. Chloroplast members of Omp85/TPS superfamily

Modern chloroplast has a genome (plastome) that codes for a very small amount of genes between 33 (in *Rhizanthella gardneri*) (Delannoy et al., 2011) and 243 (*Cyanidioschyzon merolae*) proteins (Ohta et al., 2003). This limited coding of the plastome is compensated by the large number of proteins that plastids use that are nuclear encoded. For example, *A. thaliana* has a proteome estimated at 3574 (Iniative, 2000). Proteins destined for the chloroplast obtained targeting sequences and the chloroplast had to develop machinery to translocate the cytosolically translated proteins through the outer and inner membranes (Inoue, 2007; Keegstra and Cline, 1999; Keegstra et al., 1984; Ueda et al., 2006). The majority of chloroplast-destined proteins are recognized via cleavable N-terminal targeting sequences termed transit peptides (TPs) discovered over 30 years ago (Chua and Schmidt, 1978; Highfield and Ellis, 1978). There is very little homology in primary sequence or secondary structure in solution among the thousands of known and predicted TPs (Bruce, 2000, 2001; Chotewutmontri et al., 2012).

Different precursor proteins are specifically targeted to six locations in the chloroplast: the OM, intermembrane space, inner membrane, stroma,

thylakoid membrane, or the lumen (Dyall et al., 2004). Regardless of their final destination, most proteins must cross the inner and outer envelope membrane. This translocation is facilitated by the coordinated activity of two protein-translocation complexes known as TOC and TIC (Cline, 2000; Jarvis and Soll, 2001). However, it is the TOC complex that binds precursor first and therefore ensures specificity and directionality of chloroplast protein import (Chen and Li, 2007). Toc34, Toc75, and Toc159 are the components that make up the core TOC complex (Bolter et al., 1998; Schnell et al., 1994; Seedorf et al., 1995). The core TOC complex is sufficient for *in vitro* translocation into lipid vesicles and is estimated to be between 500 kDa and 1 MDa (Chen and Li, 2007; Kikuchi et al., 2006, 2009; Schleiff et al., 2003b,c). Toc75 is a β-barrel translocon at the outer envelope of the chloroplast that was first identified in pea (Perry and Keegstra, 1994; Schnell et al., 1994). In *Arabidopsis* the presence of two paralogs of Toc34, *At*Toc33 and *At*Toc34, along with the four paralogs of Toc159, *At*Toc159, *At*Toc132, *At*Toc120, and *At*Toc90 suggest that distinct classes of TOC complexes could exist (Iniative, 2000; Ivanova et al., 2004; Jackson-Constan and Keegstra, 2001).

5.2.1 Toc75, a plastidic outer-membrane protein of Omp85/TPS superfamily

Toc75 is the only TOC component of cyanobacterial origin (Bolter et al., 1998; Kalanon and McFadden, 2008; Reumann and Keegstra, 1999; Reumann et al., 2005), and is the most abundant protein in the OM of the chloroplast (Nielsen et al., 1997; Seedorf et al., 1995). Toc75 is resistant to thermolysin treatment, salt and high pH extraction and therefore was identified as an integral OMP (Schnell et al., 1994). Toc75 is the only known chloroplast OMP with a cleavable bipartite N-terminal targeting sequence, where the most N-terminal part is a classical TP, cleaved by the SPP, and the C-terminal portion is cleaved in the intermembrane space by an envelope-bound type I signal peptidase (Inoue and Keegstra, 2003). The mature portion of Toc75 possesses two distinct domains typical of OMP85/TPSs: an N-terminal portion consisting of three POTRA domains, and a C-terminal pore made up of 16 β-strands (Sanchez-Pulido et al., 2003).

Toc75 has been shown to oligomerize with itself and other members of the TOC core complex (Nielsen et al., 1997; Reddick et al., 2007; Seedorf et al., 1995), as well as interacting with precursor protein (Hinnah et al., 1997). More specifically, the N-terminus of *Ps*Toc75 was shown to interact

with precursor to the small subunit of RuBisCO (prSSU), but not the mature form of the protein (mSSU) (Ertel et al., 2005). The same study shows that the most N-terminal region is involved in hetero-oligomerization with Toc34 and the C-terminus is involved in the pore formation. This study preceded the structural model of Toc75 containing POTRA domains. Evidence for Toc75 acting as the pore for protein translocation includes: *in vitro* experiments showing that Toc75 interacts with precursor proteins during import, cross-linking data showing an association with envelope-bound import intermediates, and arrest of import into purified chloroplasts by antibodies against Toc75 (Ma et al., 1996; Perry and Keegstra, 1994; Schnell et al., 1994; Tranel et al., 1995). Additionally, patch-clamp analysis provided compelling evidence for the role of Toc75 as a channel-forming protein (Hinnah et al., 1997). Toc75 formed narrow, voltage-gated, cation-selective transmembrane channels with a predicted hydrophilic pore with a constriction zone estimated to be 15.4 Å in diameter (Hinnah et al., 2002). Current through Toc75 was abrogated when a chloroplastic, but not mitochondrial or synthetic, precursor was added, suggesting a specific interaction with the TP (Hinnah et al., 1997). Thus, much evidence supports the role Toc75 and its POTRA domains play in protein import into the chloroplast.

5.2.2 Oep80, a chloroplastic paralog of Toc75

Pisum sativum has two Toc75 paralogs; Toc75, the translocation pore, and Toc75-V, a direct ortholog of an OMP present in the cyanobacterial ancestor (Eckart et al., 2002). Arabidopsis has three Toc75 paralogs that are represented by expressed sequence tags; *At*Toc75-I (shares 60% identity with *At*Toc75-III), *At*Toc75-III (the main pore with 74% identity to *Ps*Toc75), and *At*Toc75-IV (consisting of only 407 amino acids that align with the C-terminus of the other Toc75s) (Jackson-Constan and Keegstra, 2001). *At*Toc75-I is a pseudo-gene with a transposon inserted inside the sequence, and it is not expressed (Baldwin et al., 2005). *At*Toc75-IV does not have a cleavable N-terminal TP, and most likely lacks POTRA domains, as it was not sensitive to protease treatment (Baldwin et al., 2005). The *At*Toc75-III homozygous knockout mutant is embryo lethal (Baldwin et al., 2005).

The fourth *Arabidopsis* homologue of *Ps*Toc75 named *At*OEP80, which shares only 22% identity to *Ps*Toc75 (Eckart et al., 2002; Hinnah et al., 1997), exists as a 70-kD protein (Hsu et al., 2012). A pea ortholog of *At*OEP80, *Ps*Toc75-V, appears to be a 66-kDa protein and is not purified with the TOC complex (Eckart et al., 2002). Inoue et al. demonstrated that

*At*OEP80 is targeted to the OM of the chloroplast by information in its mature sequence and does not utilize the general import pathway for membrane insertion (Inoue and Potter, 2004). *At*OEP80 has been predicted to form a 16 β-stranded porin-like channel with three POTRA domains, and is hypothesized to be involved in the membrane biogenesis (Eckart et al., 2002; Inoue and Potter, 2004; Sveshnikova et al., 2000). T-DNA insertions into the *oep80* gene result in embryo lethality, although at a stage later than the *toc75* knockout. This indicates that while both Toc75 homologs are essential for the viability of plants, they may have distinct functions in chloroplast development (Patel et al., 2008).

Phylogenic analysis of Toc75 from various organisms led to the conclusion that Toc75 and OEP80 represent two independent gene families, both derived from cyanobacteria that had already diverged prior to the endosymbiotic event (Eckart et al., 2002). It is postulated that Toc75 acquired a new role in order to enslave the endosymbiont, while OEP80 retained the function of the ancestral Omp85, which is essential for viability in both bacteria and chloroplasts (Patel et al., 2008). The OEP80 (originally named *At*Toc75-V) is responsible for insertion of OMPs into the chloroplast envelope, and is a member of the Omp85 family that is thought to have diverged from Toc75 before the endosymbiotic event (Inoue and Potter, 2004). The presence of two distinct OMP85/TPS groups makes the chloroplast outer envelope unique among the evolutionary conserved biological membranes of mitochondria and gram-negative bacteria, which appear to have only one homologue each (Inoue and Potter, 2004).

5.3. Unique features of phototrophic Omp85 POTRA domains

The Omp85s of cyanobacteria all possess three POTRA domains, equivalent to the number of POTRA domains present in Toc75 of chloroplasts (Koenig et al., 2010; Sanchez-Pulido et al., 2003). POTRA domains tend to cluster according to their position, and in a cluster analysis of POTRA domains the N- and C-terminal POTRA domains of Toc75, Omp85, and cyanobacterial Omp85 form two distinct groups (Arnold et al., 2010). The similarity of the most N- and C-terminal POTRA domains is also shown in Table 1.1. The C-terminal POTRA domains have the highest homology, suggesting that their function is probably the most conserved and the most important. A knockout of the most C-terminal POTRA domain of Omp85 in *N. meningitidis* is lethal (Bos et al., 2007). This knockout and clustering data suggest that the most C-terminal POTRA domain (especially of

Toc75, Omp85, and cyanobacterial Omp85) may be necessary for organism or plastid survival. The other POTRA domains may have diverged for their specific functions, for example, POTRA3 of *n*Omp85 has a loop between its first β-strand and first α-helix that is conserved in the plastid and cyanobacteria Omp85 members, but is not found within the mitochondria or proteobacteria members (Koenig et al., 2010).

Interestingly, the increased length of POTRA2 in Toc75 of higher plants (e.g., 116 amino acids for POTRA2 of *Ps*Toc75) is not conserved across POTRA2 domains in cyanobacteria and there has yet to be an algal or plant POTRA domain structurally solved. POTRA2 in *n*Omp85 was determined to be 80 residues and POTRA2 in *Te*Omp85 is 70 residues (Arnold et al., 2010; Koenig et al., 2010). The helix α1 and the β-strand β1 of POTRA2 in *n*Omp85 are both interrupted, resulting in a β-bulge that is also present in the third POTRA domain of BamA (Kim et al., 2007; Koenig et al., 2010). Also conserved is a stable orientation for the POTRA2 and POTRA3 domains, and more flexibility between the POTRA2 and POTRA1, which mirrors the flexibility between POTRA2 and POTRA 3 of BamA (Gatzeva-Topalova et al., 2008; Kim et al., 2007; Koenig et al., 2010). POTRA1 of *n*Omp85 has a small two-stranded β-sheet near its N-terminus, which forms a β-cap (Koenig et al., 2010). The first β-strand of the cap is N-terminal to the β1 of POTRA1 and the second β-strand of the cap between α1 and α2 of POTRA1 (Fig. 1.6). The differences unique to POTRA domains that are part of cyanobacterial Omp85s seem conserved and perhaps allow for novel or specialized functioning of these domains.

The hinge region between POTRA2 and POTRA1 could allow POTRA1 the large degree of freedom needed to make adjacent interactions. POTRA1 could change position until it encounters another POTRA1 at which point the ability of POTRA1 to self-dimerize would allow time for the β-barrel pores of the two Toc75s to come into contact with each other. Alternatively, this interaction could compete for an in-plug formation that could occlude the protein-conducting channel. The outer edge of the β-barrels could interact with each other, perhaps via β-augmentation, and this would help to form the 4:4:1 stoichiometry of Toc75:Toc34:Toc159 that is present in the TOC core complex (Agne et al., 2009).

6. POTRA DOMAINS MODE OF ACTION

Although the domain organization of OMP85/TPSs is well conserved, the mechanism by which these domains mediate the assembly of OMPs and polypeptide translocation is not clear. However, crystal

structures (Arnold et al., 2010; Clantin et al., 2004; Kim et al., 2007; Koenig et al., 2010) of several POTRA domains allow for structure-based predictions on how these domains may operate.

6.1. Role and model of action for individual POTRA domains

The unique features of the POTRA domains mentioned above could be biophysical evidence for the unique roles that POTRA domains seem to play in various OMP85/TPSs. The ability of POTRA1 to participate in β-augmentation has been noted in BamA and *n*Omp85 (Gatzeva-Topalova et al., 2008; Kim et al., 2007; Koenig et al., 2010). This β-augmentation has been shown to be able to occur in both parallel and anti-parallel orientations (Heuck et al., 2011; Koenig et al., 2010). TPs have a region toward their C-terminus that has been predicted to form an amphiphilic β-strand (von Heijne et al., 1989), which means that POTRA domains and TPs could interact via β-augmentation.

POTRA1 has been shown to interact with substrates that the Omp85 or TPS translocates through or inserts into biological membranes. For example, POTRA1 of BamA in *E. coli* has been shown to interact with nascent LptD, LamB, and OmpF (all OMPs destined for the OM in *E. coli*), and has been implicated in assembly of BamA into the OM (Bennion et al., 2010; Knowles et al., 2008). POTRA domains belonging to TpsB transporters interact with their TpsA partner (Clantin et al., 2007; Hodak et al., 2006). In particular POTRA1 of FhaC was shown to interact with FHA, although not as well as the entire periplasmic domain of FhaC does (Delattre et al., 2011). This means that POTRA2 of FhaC must interact with the FHA substrate as well. POTRA2 of Toc75 is predicted to be very large and may contain a β-bulge-like POTRA2 of *n*Omp85 or POTRA3 of BamA. If this is the case, POTRA2 of Toc75 will have more residues that could possibly interact with TPs or other members of the TOC machinery.

It has been shown that POTRA domains gate the pore, as constructs without the POTRA-containing N-terminus of *n*Omp85 allow sucrose to diffuse freely into the liposomes they are reconstituted into (Ertel et al., 2005; Koenig et al., 2010). More specifically the most C-terminal POTRA domain, POTRA3, of *n*Omp85 contains a loop deemed L1 loop between the first β-strand and first α-helix. This loop is conserved in chloroplast and cyanobacteria but not mitochondria or proteobacteria, and has been shown to have a gating effect on the pore of *n*Omp85 (Koenig et al., 2010). Another possibility for the observed gating effect on the pore of the translocon is that there are β-strands in the pore that are unstable, and

interaction with other residues could help to stabilize them. In this case residues from the POTRA domains could act as the stabilizing proteins and would be called "in-plug" domains (Naveed et al., 2009).

6.2. Models of POTRA interaction with peptide substrates

While some of the roles for individual POTRA domains have been defined, we will take a look at proteins with structures similar to POTRA domains so that we can analyze possible modes of interaction for the POTRAs.

6.2.1 MHC class I

Class I major histocompatibility complex (MHC) molecules carry short peptides from proteins degraded in the cytoplasm of nucleated vertebrate cells to the cell surface via secretory vesicles (Falk et al., 1991). The tertiary structure of this MHC is strikingly similar to a POTRA domain (Fig. 1.7), although there is a difference in the way that the two different domains behave with respect to interacting with their respective substrates. Class I MHC molecules bind peptides very strongly *in vitro* with fast association rates (Springer et al., 1998) and slow dissociation rates (Buus et al., 1986). In fact, class I MHC molecules are capable of forming complexes with half-lives lasting tens of hours with many different peptide substrates (Khan et al., 2000). This differs from POTRA domains because POTRA domains do not form stable complexes with their substrates. If the binding affinity of POTRA

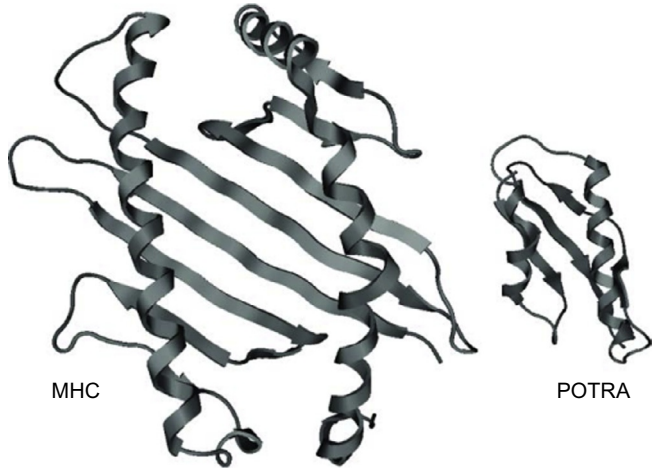

Figure 1.7 Tertiary structure of MHC and POTRA domain. Solved crystal structures of Class I major histocompatibility complex (MHC) from *Homo sapiens* and POTRA2 from *Te*Omp85 (pdb ids. 1DUZ, 2X8X, respectively) are shown.

domains were too high, it would severely hamper the ability of their proteins to export/import substrates or to insert proteins into the OMs. It is possible that the shorter length of α-helices in POTRA domains contributes to a lower affinity for their substrates when compared to MHC molecules. Another way the mode of interaction of POTRA domains and MHC molecules differ is that MHC interactions are specific. Side chains of peptides in the binding groove of MHC molecules reside in specific pockets, showing a sequence dependence on peptide binding (Garrett et al., 1989; Guo et al., 1993; Saper et al., 1991). However, POTRA domains cannot interact specifically with TPs, because there are thousands of different TPs (Bruce, 2000), and only three POTRA domains in Toc75 (Sanchez-Pulido et al., 2003).

6.2.2 Hsp70/DnaK

Another set of molecules that use β-strands to bind their substrates are the molecular chaperones in the 70-kDa heat shock protein (Hsp70) family, present in the cells of all organisms (Zhu et al., 1996). These proteins have constitutive and stress-induced functions (Saito and Uchida, 1978), and are involved in events such as translocation, nascent polypeptide folding, and antiaggregation functions (Rothman, 1989). There are ATP and substrate-binding domains present on Hsp70s (Welch and Feramisco, 1985). The crystallized structure of the substrate-binding domain of DnaK, the Hsp70 that functions in DNA replication in *E. coli* (Saito and Uchida, 1978), has a β-sandwich, composed of eight β-strands inside of five α-helices (Zhu et al., 1996). Peptides interact with the substrate-binding domain by forming hydrogen bonds with the β-sandwich domain of DnaK (Mayer and Bukau, 2005). Hsp70-peptide complexes, like class I MHC interactions, have long half-lives (Schmid et al., 1994). However, DnaK can bind peptides in extended conformations, and the hydrogen bonds formed between DnaK and peptide backbones are generic with few key specificity determining pockets (Zhu et al., 1996).

6.2.3 PDZ domains

PDZ domains are 80–110 residue-containing domains present in the C-terminal portions of signaling proteins of bacteria, yeast, plants, and animals that use β-augmentation to interact with peptides (Boxus et al., 2008; Cho et al., 1992; Ponting, 1997). PDZ domains derived their name from the first three different proteins that they were noticed in: postsynaptic density protein of 95 kDa (PSD95), *Drosophila* disc large tumor suppressor (DlgA),

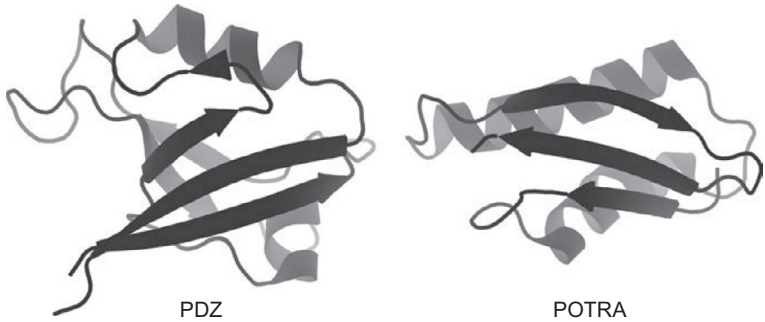

Figure 1.8 Tertiary structure of PDZ and POTRA domain. Solved crystal structures of PDZ domain of PSD-95 from *Rattus norvegicus* and POTRA2 from *Te*Omp85 (pdb ids. 3GSL, 2X8X, respectively).

and zonula occludens-1 protein (Zo-1) (Kennedy, 1995). PDZ domains have six β-sheets and two α-helices. Here, β-augmentation occurs between an exposed β-strand of the PDZ domain and a ligand, including a synthetic peptide used in a crystallization experiment (Lee et al., 2011). Interestingly, the structure of PDZ domains and POTRA domains is highly similar, with both domains ranging in size from 70 to 120 residues (Fig. 1.8), unlike the larger MHC domains. Both β-augmentation interactions in this crystal structure are antiparallel, but parallel interactions can occur (Kim et al., 2007; Koenig et al., 2010). Regions of 100–150 residues present in insulin receptor substrates 1 and 2 also form hydrogen bonds with β-stranded peptides near the exposed edge of a β-sheet (Harrison, 1996).

7. CONCLUDING REMARKS

This review covers the recent progress in the structure and function of the Omp85/TSP superfamily of OMPs. We show that this family is composed of two discreet groups with divergent roles. Moreover, the distinct roles of these two subgroups are ancient and most likely precede the earliest stages of endosymbiosis that gave rise first to mitochondria and then to plastids. Interestingly, both groups are conserved in their general structure and contain a variable number of POTRA domains at their N-terminus followed by a 16-stranded β-barrel structure. Further work is needed to elucidate the role of the individual POTRA domains, however both structural alignments and functional studies suggest that it is the POTRA domain most proximal to the β-barrel that is most conserved and essential. Future work will be needed to elucidate the individual roles of the POTRA domains.

A very interesting area to emerge recently is the apparent duplication and multiple roles that the OMP85 members play in photosynthetic organisms including cyanobacteria and in the OM of the plastid envelope. This is an area that has had considerable advances from genomic analysis but also from recent structural work. Of great interest is the process of how cyanobacterial OMP85 members were redeployed to function in the process of protein import into the plastid. This likely required a topological inversion and meant that the ancestral function essential for cyanobacterial survival was dispensed and the duplicated protein found a new niche and now functions in the biogenesis of the plastid. As new structural data becomes available this will be an exciting area of membrane and organelle biogenesis.

Finally, the role of these Omp85/TPS proteins in the translocation, insertion, and assembly of proteins will be important for a wide range of membrane proteins including other TOC components, OMP assembly machinery, and virulence factor exporters. However, the details of this chaperone role of the POTRA domains in protein folding and assembly will require new structural and genetic approaches in the future.

REFERENCES

Abdullah, F., Salamini, F., Leister, D., 2000. A prediction of the size and evolutionay origin of the proteome of chloroplasts of *Arabidopsis*. Trends Plant Sci. 5, 141–142.

Agne, B., Infanger, S., Wang, F., Hofstetter, V., Rahim, G., Martin, M., Lee, D.W., Hwang, I., Schnell, D., Kessler, F., 2009. A toc159 import receptor mutant, defective in hydrolysis of GTP, supports preprotein import into chloroplasts. J. Biol. Chem. 284, 8670–8679.

Altschul, S.F., Madden, T.L., Schaffer, A.A., Zhang, J., Zhang, Z., Miller, W., Lipman, D.J., 1997. Gapped BLAST and PSI-BLAST: a new generation of protein database search programs. Nucleic Acids Res. 25, 3389–3402.

Altschul, S.F., Wootton, J.C., Gertz, E.M., Agarwala, R., Morgulis, A., Schaffer, A.A., Yu, Y.K., 2005. Protein database searches using compositionally adjusted substitution matrices. FEBS J. 272, 5101–5109.

Aoki, S.K., Pamma, R., Hernday, A.D., Bickham, J.E., Braaten, B.A., Low, D.A., 2005. Contact-dependent inhibition of growth in Escherichia coli. Science 309, 1245–1248.

Arnold, T., Zeth, K., Linke, D., 2010. Omp85 from the thermophilic cyanobacterium Thermosynechococcus elongatus differs from proteobacterial Omp85 in structure and domain composition. J. Biol. Chem. 285, 18003–18015.

Baldwin, A., Wardle, A., Patel, R., Dudley, P., Park, S.K., Twell, D., Inoue, K., Jarvis, P., 2005. A molecular-genetic study of the Arabidopsis Toc75 gene family. Plant Physiol. 138, 715–733.

Bauer, J., Chen, K., Hiltbunner, A., Wehrli, E., Eugster, M., Schnell, D., Kessler, F., 2000. The major protein import receptor of plastids is essential for chloroplast biogenesis. Nature 403, 203–207.

Bennion, D., Charlson, E.S., Coon, E., Misra, R., 2010. Dissection of beta-barrel outer membrane protein assembly pathways through characterizing BamA POTRA 1 mutants of Escherichia coli. Mol. Microbiol. 77, 1153–1171.

Bolter, B., May, T., Soll, J., 1998. A protein import receptor in pea chloroplasts, Toc86, is only a proteolytic fragment of a larger polypeptide. FEBS Lett. 441, 59–62.
Borlee, B.R., Goldman, A.D., Murakami, K., Samudrala, R., Wozniak, D.J., Parsek, M.R., 2010. Pseudomonas aeruginosa uses a cyclic-di-GMP-regulated adhesin to reinforce the biofilm extracellular matrix. Mol. Microbiol. 75, 827–842.
Bos, M.P., Robert, V., Tommassen, J., 2007. Functioning of outer membrane protein assembly factor Omp85 requires a single POTRA domain. EMBO Rep. 8, 1149–1154.
Boxus, M., Twizere, J.C., Legros, S., Dewulf, J.F., Kettmann, R., Willems, L., 2008. The HTLV-1 Tax interactome. Retrovirology 5, 76.
Bredemeier, R., Schlegel, T., Ertel, F., Vojta, A., Borissenko, L., Bohnsack, M.T., Groll, M., von Haeseler, A., Schleiff, E., 2007. Functional and phylogenetic properties of the pore-forming beta-barrel transporters of the Omp85 family. J. Biol. Chem. 282, 1882–1890.
Bruce, B.D., 2000. Chloroplast transit peptides: structure, function and evolution. Trends Cell Biol. 10, 440–447.
Bruce, B.D., 2001. The paradox of plastid transit peptides: conservation of function despite divergence in primary structure. Biochim. Biophys. Acta 1541, 2–21.
Buus, S., Sette, A., Colon, S.M., Jenis, D.M., Grey, H.M., 1986. Isolation and characterization of antigen-Ia complexes involved in T cell recognition. Cell 47, 1071–1077.
Cameron, C.E., Lukehart, S.A., Castro, C., Molini, B., Godornes, C., Van Voorhis, W.C., 2000. Opsonic potential, protective capacity, and sequence conservation of the Treponema pallidum subspecies pallidum Tp92. J. Infect. Dis. 181, 1401–1413.
Chen, K.Y., Li, H.M., 2007. Precursor binding to an 880-kDa Toc complex as an early step during active import of protein into chloroplasts. Plant J. 49, 149–158.
Cho, K.O., Hunt, C.A., Kennedy, M.B., 1992. The rat brain postsynaptic density fraction contains a homolog of the Drosophila discs-large tumor suppressor protein. Neuron 9, 929–942.
Chotewutmontri, P., Reddick, L.E., McWilliams, D.R., Campbell, I.M., Bruce, B.D., 2012. Differential transit peptide recognition during preprotein binding and translocation into flowering plant plastids. Plant Cell 24, 3040–3059.
Chua, N.H., Schmidt, G.W., 1978. Post-translational transport into intact chloroplasts of a precursor the the small subunit of ribulose-1,5-bisphosphate carboxylase. Proc. Natl. Acad. Sci. U.S.A. 75, 6110–6114.
Clantin, B., Hodak, H., Willery, E., Locht, C., Jacob-Dubuisson, F., Villeret, V., 2004. The crystal structure of filamentous hemagglutinin secretion domain and its implications for the two-partner secretion pathway. Proc. Natl. Acad. Sci. U.S.A. 101, 6194–6199.
Clantin, B., Delattre, A.S., Rucktooa, P., Saint, N., Meli, A.C., Locht, C., Jacob-Dubuisson, F., Villeret, V., 2007. Structure of the membrane protein FhaC: a member of the Omp85-TpsB transporter superfamily. Science 317, 957–961.
Cline, K., 2000. Gateway to the chloroplast. Nature 403, 148–149.
Costerton, J.W., Ingram, J.M., Cheng, K.J., 1974. Structure and function of the cell envelope of gram-negative bacteria. Bacteriol. Rev. 38, 87–110.
Cross, B.C., Sinning, I., Luirink, J., High, S., 2009. Delivering proteins for export from the cytosol. Nat. Rev. Mol. Cell Biol. 10, 255–264.
Delannoy, E., Fujii, S., Colas des Francs-Small, C., Brundrett, M., Small, I., 2011. Rampant gene loss in the underground orchid Rhizanthella gardneri highlights evolutionary constraints on plastid genomes. Mol. Biol. Evol. 28, 2077–2086.
Delattre, A.S., Saint, N., Clantin, B., Willery, E., Lippens, G., Locht, C., Villeret, V., Jacob-Dubuisson, F., 2011. Substrate recognition by the POTRA domains of TpsB transporter FhaC. Mol. Microbiol. 81, 99–112.
Dyall, S.D., Brown, M.T., Johnson, P.J., 2004. Ancient invasions: from endosymbionts to organelles. Science 304, 253–257.

Eckart, K., Eichacker, L., Sohrt, K., Schleiff, E., Heins, L., Soll, J., 2002. A Toc75-like protein import channel is abundant in chloroplasts. EMBO Rep. 3, 557–562.
Ertel, F., Mirus, O., Bredemeier, R., Moslavac, S., Becker, T., Schleiff, E., 2005. The evolutionarily related beta-barrel polypeptide transporters from Pisum sativum and Nostoc PCC7120 contain two distinct functional domains. J. Biol. Chem. 280, 28281–28289.
Falk, K., Rotzschke, O., Stevanovic, S., Jung, G., Rammensee, H.G., 1991. Allele-specific motifs revealed by sequencing of self-peptides eluted from MHC molecules. Nature 351, 290–296.
Garrett, T.P., Saper, M.A., Bjorkman, P.J., Strominger, J.L., Wiley, D.C., 1989. Specificity pockets for the side chains of peptide antigens in HLA-Aw68. Nature 342, 692–696.
Gatzeva-Topalova, P.Z., Walton, T.A., Sousa, M.C., 2008. Crystal structure of YaeT: conformational flexibility and substrate recognition. Structure 16, 1873–1881.
Gatzeva-Topalova, P.Z., Warner, L.R., Pardi, A., Sousa, M.C., 2010. Structure and flexibility of the complete periplasmic domain of BamA: the protein insertion machine of the outer membrane. Structure 18, 1492–1501.
Genevrois, S., Steeghs, L., Roholl, P., Letesson, J.J., van der Ley, P., 2003. The Omp85 protein of Neisseria meningitidis is required for lipid export to the outer membrane. EMBO J. 22, 1780–1789.
Gentle, I., Gabriel, K., Beech, P., Waller, R., Lithgow, T., 2004. The Omp85 family of proteins is essential for outer membrane biogenesis in mitochondria and bacteria. J. Cell Biol. 164, 19–24.
Gentle, I.E., Burri, L., Lithgow, T., 2005. Molecular architecture and function of the Omp85 family of proteins. Mol. Microbiol. 58, 1216–1225.
Guedin, S., Willery, E., Locht, C., Jacob-Dubuisson, F., 1998. Evidence that a globular conformation is not compatible with FhaC-mediated secretion of the Bordetella pertussis filamentous haemagglutinin. Mol. Microbiol. 29, 763–774.
Guo, H.C., Madden, D.R., Silver, M.L., Jardetzky, T.S., Gorga, J.C., Strominger, J.L., Wiley, D.C., 1993. Comparison of the P2 specificity pocket in three human histocompatibility antigens: HLA-A*6801, HLA-A*0201, and HLA-B*2705. Proc. Natl. Acad. Sci. U.S.A. 90, 8053–8057.
Habib, S.J., Waizenegger, T., Niewienda, A., Paschen, S.A., Neupert, W., Rapaport, D., 2007. The N-terminal domain of Tob55 has a receptor-like function in the biogenesis of mitochondrial beta-barrel proteins. J. Cell Biol. 176, 77–88.
Harrison, S.C., 1996. Peptide-surface association: the case of PDZ and PTB domains. Cell 86, 341–343.
Heuck, A., Schleiffer, A., Clausen, T., 2011. Augmenting beta-augmentation: structural basis of how BamB binds BamA and may support folding of outer membrane proteins. J. Mol. Biol. 406, 659–666.
Highfield, P.E., Ellis, R.J., 1978. Synthesis and transport of the small subunit of chloroplast ribulose bisphosphate carboxylase. Nature 271, 420–424.
Hinnah, S.C., Hill, K., Wagner, R., Schlicher, T., Soll, J., 1997. Reconstitution of a chloroplast protein import channel. EMBO J. 16, 7351–7360.
Hinnah, S.C., Wagner, R., Sveshnikova, N., Harrer, R., Soll, J., 2002. The chloroplast protein import channel Toc75: pore properties and interaction with transit peptides. Biophys. J. 83, 899–911.
Hodak, H., Clantin, B., Willery, E., Villeret, V., Locht, C., Jacob-Dubuisson, F., 2006. Secretion signal of the filamentous haemagglutinin, a model two-partner secretion substrate. Mol. Microbiol. 61, 368–382.
Hsu, S.C., Nafati, M., Inoue, K., 2012. OEP80, an essential protein paralogous to the chloroplast protein translocation channel Toc75, exists as a 70-kD protein in the Arabidopsis thaliana chloroplast outer envelope. Plant Mol. Biol. 78, 147–158.

Hust, B., Gutensohn, M., 2006. Deletion of core components of the plastid protein import machinery causes differential arrest of embryo development in Arabidopsis thaliana. Plant Biol. (Stuttg.) 8, 18–30.
Iniative, T.A.G., 2000. Analysis of the genome sequence of the flowering plant Arabidopsis thaliana. Nature 408, 796–815.
Inoue, K., 2007. The chloroplast outer envelope membrane: the edge of light and excitement. J. Integr. Plant Biol. 49, 1100–1111.
Inoue, K., Keegstra, K., 2003. A polyglycine stretch is necessary for proper targeting of the protein translocation channel precursor to the outer envelope membrane of chloroplasts. Plant J. 34, 661–669.
Inoue, K., Potter, D., 2004. The chloroplastic protein translocation channel Toc75 and its paralog OEP80 represent two distinct protein families and are targeted to the chloroplastic outer envelope by different mechanisms. Plant J. 39, 354–365.
Ivanova, Y., Smith, M.D., Chen, K., Schnell, D.J., 2004. Members of the Toc159 import receptor family represent distinct pathways for protein targeting to plastids. Mol. Biol. Cell 15, 3379–3392.
Jackson-Constan, D., Keegstra, K., 2001. Arabidopsis genes encoding components of the chloroplastic protein import apparatus. Plant Physiol. 125, 1567–1576.
Jacob-Dubuisson, F., Fernandez, R., Coutte, L., 2004. Protein secretion through autotransporter and two-partner pathways. Biochim. Biophys. Acta 1694, 235–257.
Jacob-Dubuisson, F., Villeret, V., Clantin, B., Delattre, A.S., Saint, N., 2009. First structural insights into the TpsB/Omp85 superfamily. Biol. Chem. 390, 675–684.
Jarvis, P., Soll, J., 2001. Toc, Tic, and chloroplast protein import. Biochim. Biophys. Acta 1541, 64–79.
Kajava, A.V., Steven, A.C., 2006. The turn of the screw: variations of the abundant beta-solenoid motif in passenger domains of Type V secretory proteins. J. Struct. Biol. 155, 306–315.
Kalanon, M., McFadden, G.I., 2008. The chloroplast protein translocation complexes of Chlamydomonas reinhardtii: a bioinformatic comparison of Toc and Tic components in plants, green algae and red algae. Genetics 179, 95–112.
Keegstra, K., Cline, K., 1999. Protein import and routing systems of chloroplasts. Plant Cell 11, 557–570.
Keegstra, K., Werner-Washburne, M., Cline, K., Andrews, J., 1984. The chloroplast envelope: is it homologous with the double membranes of mitochondria and gram-negative bacteria? J. Cell. Biochem. 24, 55–68.
Kennedy, M.B., 1995. Origin of PDZ (DHR, GLGF) domains. Trends Biochem. Sci. 20, 350.
Khan, A.R., Baker, B.M., Ghosh, P., Biddison, W.E., Wiley, D.C., 2000. The structure and stability of an HLA-A*0201/octameric tax peptide complex with an empty conserved peptide-N-terminal binding site. J. Immunol. 164, 6398–6405.
Kikuchi, S., Hirohashi, T., Nakai, M., 2006. Characterization of the preprotein translocon at the outer envelope membrane of chloroplasts by blue native PAGE. Plant Cell Physiol. 47, 363–371.
Kikuchi, S., Oishi, M., Hirabayashi, Y., Lee, D.W., Hwang, I., Nakai, M., 2009. A 1-megadalton translocation complex containing Tic20 and Tic21 mediates chloroplast protein import at the inner envelope membrane. Plant Cell 21, 1781–1797.
Kim, S., Malinverni, J.C., Sliz, P., Silhavy, T.J., Harrison, S.C., Kahne, D., 2007. Structure and function of an essential component of the outer membrane protein assembly machine. Science 317, 961–964.
Knowles, T.J., Jeeves, M., Bobat, S., Dancea, F., McClelland, D., Palmer, T., Overduin, M., Henderson, I.R., 2008. Fold and function of polypeptide transport-associated domains responsible for delivering unfolded proteins to membranes. Mol. Microbiol. 68, 1216–1227.

Knowles, T.J., Scott-Tucker, A., Overduin, M., Henderson, I.R., 2009. Membrane protein architects: the role of the BAM complex in outer membrane protein assembly. Nat. Rev. Microbiol. 7, 206–214.

Koenig, P., Mirus, O., Haarmann, R., Sommer, M.S., Sinning, I., Schleiff, E., Tews, I., 2010. Conserved properties of polypeptide transport-associated (POTRA) domains derived from cyanobacterial Omp85. J. Biol. Chem. 285, 18016–18024.

Kozjak, V., Wiedemann, N., Milenkovic, D., Lohaus, C., Meyer, H.E., Guiard, B., Meisinger, C., Pfanner, N., 2003. An essential role of Sam50 in the protein sorting and assembly machinery of the mitochondrial outer membrane. J. Biol. Chem. 278, 48520–48523.

Lee, J.H., Park, H., Park, S.J., Kim, H.J., Eom, S.H., 2011. The structural flexibility of the shank1 PDZ domain is important for its binding to different ligands. Biochem. Biophys. Res. Commun. 407, 207–212.

Leister, D., Kleine, T., 2008. Towards a comprehensive catalog of chloroplast proteins and their interactions. Cell Res. 18, 1081–1083.

Loosmore, S.M., Yang, Y.P., Coleman, D.C., Shortreed, J.M., England, D.M., Klein, M.H., 1997. Outer membrane protein D15 is conserved among Haemophilus influenzae species and may represent a universal protective antigen against invasive disease. Infect. Immun. 65, 3701–3707.

Ma, Y., Kouranov, A., LaSala, S.E., Schnell, D.J., 1996. Two components of the chloroplast protein import apparatus, IAP86 and IAP75, interact with the transit sequence during the recognition and translocation of precursor proteins at the outer envelope. J. Cell Biol. 134, 315–327.

Manning, D.S., Reschke, D.K., Judd, R.C., 1998. Omp85 proteins of Neisseria gonorrhoeae and Neisseria meningitidis are similar to Haemophilus influenzae D-15-Ag and Pasteurella multocida Oma87. Microb. Pathog. 25, 11–21.

Mayer, M.P., Bukau, B., 2005. Hsp70 chaperones: cellular functions and molecular mechanism. Cell. Mol. Life Sci. 62, 670–684.

Moslavac, S., Mirus, O., Bredemeier, R., Soll, J., von Haeseler, A., Schleiff, E., 2005. Conserved pore-forming regions in polypeptide-transporting proteins. FEBS J. 272, 1367–1378.

Naveed, H., Jackups Jr., R., Liang, J., 2009. Predicting weakly stable regions, oligomerization state, and protein-protein interfaces in transmembrane domains of outer membrane proteins. Proc. Natl. Acad. Sci. U.S.A. 106, 12735–12740.

Nielsen, E., Akita, M., Davila-Aponte, J., Keegstra, K., 1997. Stable association of chloroplastic precursors with protein translocation complexes that contain proteins from both envelope membranes and a stromal Hsp100 molecular chaperone. EMBO J. 16, 935–946.

Ohta, N., Matsuzaki, M., Misumi, O., Miyagishima, S.Y., Nozaki, H., Tanaka, K., Shin, I.T., Kohara, Y., Kuroiwa, T., 2003. Complete sequence and analysis of the plastid genome of the unicellular red alga Cyanidioschyzon merolae. DNA Res. 10, 67–77.

Paschen, S.A., Waizenegger, T., Stan, T., Preuss, M., Cyrklaff, M., Hell, K., Rapaport, D., Neupert, W., 2003. Evolutionary conservation of biogenesis of beta-barrel membrane proteins. Nature 426, 862–866.

Paschen, S.A., Neupert, W., Rapaport, D., 2005. Biogenesis of beta-barrel membrane proteins of mitochondria. Trends Biochem. Sci. 30, 575–582.

Patel, R., Hsu, S.C., Bedard, J., Inoue, K., Jarvis, P., 2008. The Omp85-related chloroplast outer envelope protein OEP80 is essential for viability in Arabidopsis. Plant Physiol. 148, 235–245.

Perry, S.E., Keegstra, K., 1994. Envelope membrane proteins that interact with chloroplastic precursor proteins. Plant Cell 6, 93–105.

Ponting, C.P., 1997. Evidence for PDZ domains in bacteria, yeast, and plants. Protein Sci. 6, 464–468.

Poolman, J.T., Bakaletz, L., Cripps, A., Denoel, P.A., Forsgren, A., Kyd, J., Lobet, Y., 2000. Developing a nontypeable Haemophilus influenzae (NTHi) vaccine. Vaccine 19 (Suppl. 1), S108–S115.
Reddick, L.E., Vaughn, M.D., Wright, S.J., Campbell, I.M., Bruce, B.D., 2007. In vitro comparative kinetic analysis of the chloroplast Toc GTPases. J. Biol. Chem. 282, 11410–11426.
Remmert, M., Biegert, A., Linke, D., Lupas, A.N., Soding, J., 2010. Evolution of outer membrane beta-barrels from an ancestral beta beta hairpin. Mol. Biol. Evol. 27, 1348–1358.
Reumann, S., Keegstra, K., 1999. The endosymbiotic origin of the protein import machinery of chloroplastic envelope membranes. Trends Plant Sci. 4, 302–307.
Reumann, S., Davila-Aponte, J., Keegstra, K., 1999. The evolutionary origin of the protein-translocating channel of chloroplastic envelope membranes: identification of a cyanobacterial homolog. Proc. Natl. Acad. Sci. U.S.A. 96, 784–789.
Reumann, S., Inoue, K., Keegstra, K., 2005. Evolution of the general protein import pathway of plastids (review). Mol. Membr. Biol. 22, 73–86.
Robb, C.W., Orihuela, C.J., Ekkelenkamp, M.B., Niesel, D.W., 2001. Identification and characterization of an in vivo regulated D15/Oma87 homologue in Shigella flexneri using differential display polymerase chain reaction. Gene 262, 169–177.
Robert, V., Volokhina, E.B., Senf, F., Bos, M.P., Van Gelder, P., Tommassen, J., 2006. Assembly factor Omp85 recognizes its outer membrane protein substrates by a species-specific C-terminal motif. PLoS Biol. 4, e377.
Rothman, J.E., 1989. Polypeptide chain binding proteins: catalysts of protein folding and related processes in cells. Cell 59, 591–601.
Ruffolo, C.G., Adler, B., 1996. Cloning, sequencing, expression, and protective capacity of the oma87 gene encoding the Pasteurella multocida 87-kilodalton outer membrane antigen. Infect. Immun. 64, 3161–3167.
Saito, H., Uchida, H., 1978. Organization and expression of the dnaJ and dnaK genes of Escherichia coli K12. Mol. Gen. Genet. 164, 1–8.
Sanchez-Pulido, L., Devos, D., Genevrois, S., Vicente, M., Valencia, A., 2003. POTRA: a conserved domain in the FtsQ family and a class of beta-barrel outer membrane proteins. Trends Biochem. Sci. 28, 523–526.
Saper, M.A., Bjorkman, P.J., Wiley, D.C., 1991. Refined structure of the human histocompatibility antigen HLA-A2 at 2.6 A resolution. J. Mol. Biol. 219, 277–319.
Schleiff, E., Soll, J., 2005. Membrane protein insertion: mixing eukaryotic and prokaryotic concepts. EMBO Rep. 6, 1023–1027.
Schleiff, E., Eichacker, L.A., Eckart, K., Becker, T., Mirus, O., Stahl, T., Soll, J., 2003a. Prediction of the plant beta-barrel proteome: a case study of the chloroplast outer envelope. Protein Sci. 12, 748–759.
Schleiff, E., Jelic, M., Soll, J., 2003b. A GTP-driven motor moves proteins across the outer envelope of chloroplasts. Proc. Natl. Acad. Sci. U.S.A. 100, 4604–4609.
Schleiff, E., Soll, J., Kuchler, M., Kuhlbrandt, W., Harrer, R., 2003c. Characterization of the translocon of the outer envelope of chloroplasts. J. Cell Biol. 160, 541–551.
Schmid, D., Baici, A., Gehring, H., Christen, P., 1994. Kinetics of molecular chaperone action. Science 263, 971–973.
Schnell, D.J., Kessler, F., Blobel, G., 1994. Isolation of components of the chloroplast protein import machinery. Science 266, 1007–1012.
Seedorf, M., Waegemann, K., Soll, J., 1995. A constituent of the chloroplast import complex represents a new type of GTP-binding protein. Plant J. 7, 401–411.
Sklar, J.G., Wu, T., Gronenberg, L.S., Malinverni, J.C., Kahne, D., Silhavy, T.J., 2007a. Lipoprotein SmpA is a component of the YaeT complex that assembles outer membrane proteins in Escherichia coli. Proc. Natl. Acad. Sci. U.S.A. 104, 6400–6405.

Sklar, J.G., Wu, T., Kahne, D., Silhavy, T.J., 2007b. Defining the roles of the periplasmic chaperones SurA, Skp, and DegP in Escherichia coli. Genes Dev. 21, 2473–2484.
Springer, S., Doring, K., Skipper, J.C., Townsend, A.R., Cerundolo, V., 1998. Fast association rates suggest a conformational change in the MHC class I molecule H-2Db upon peptide binding. Biochemistry 37, 3001–3012.
Strittmatter, P., Soll, J., Bolter, B., 2010. The chloroplast protein import machinery: a review. Methods Mol. Biol. 619, 307–321.
Stroud, D.A., Becker, T., Qiu, J., Stojanovski, D., Pfannschmidt, S., Wirth, C., Hunte, C., Guiard, B., Meisinger, C., Pfanner, N., Wiedemann, N., 2011. Biogenesis of mitochondrial beta-barrel proteins: the POTRA domain is involved in precursor release from the SAM complex. Mol. Biol. Cell 22, 2823–2833.
Surana, N.K., Grass, S., Hardy, G.G., Li, H., Thanassi, D.G., Geme 3rd, J.W., 2004. Evidence for conservation of architecture and physical properties of Omp85-like proteins throughout evolution. Proc. Natl. Acad. Sci. U.S.A. 101, 14497–14502.
Sveshnikova, N., Grimm, R., Soll, J., Schleiff, E., 2000. Topology studies of the chloroplast protein import channel Toc75. Biol. Chem. 381, 687–693.
Tamm, L.K., Hong, H., Liang, B., 2004. Folding and assembly of beta-barrel membrane proteins. Biochim. Biophys. Acta 1666, 250–263.
Tashiro, Y., Nomura, N., Nakao, R., Senpuku, H., Kariyama, R., Kumon, H., Kosono, S., Watanabe, H., Nakajima, T., Uchiyama, H., 2008. Opr86 is essential for viability and is a potential candidate for a protective antigen against biofilm formation by Pseudomonas aeruginosa. J. Bacteriol. 190, 3969–3978.
Tokuda, H., Matsuyama, S., 2004. Sorting of lipoproteins to the outer membrane in E. coli. Biochim. Biophys. Acta 1694, IN1–IN9.
Tranel, P.J., Froehlich, J., Goyal, A., Keegstra, K., 1995. A component of the chloroplastic protein import apparatus is targeted to the outer envelope membrane via a novel pathway. EMBO J. 14, 2436–2446.
Ueda, M., Fujimoto, M., Arimura, S., Tsutsumi, N., Kadowaki, K., 2006. Evidence for transit peptide acquisition through duplication and subsequent frameshift mutation of a preexisting protein gene in rice. Mol. Biol. Evol. 23, 2405–2412.
van den Ent, F., Vinkenvleugel, T.M., Ind, A., West, P., Veprintsev, D., Nanninga, N., den Blaauwen, T., Lowe, J., 2008. Structural and mutational analysis of the cell division protein FtsQ. Mol. Microbiol. 68, 110–123.
von Heijne, G., Steppuhn, J., Herrmann, R.G., 1989. Domain structure of mitochondrial and chloroplast targeting peptides. FEBS J. 180, 535–545.
Voulhoux, R., Tommassen, J., 2004. Omp85, an evolutionarily conserved bacterial protein involved in outer-membrane-protein assembly. Res. Microbiol. 155, 129–135.
Voulhoux, R., Bos, M.P., Geurtsen, J., Mols, M., Tommassen, J., 2003. Role of a highly conserved bacterial protein in outer membrane protein assembly. Science 299, 262–265.
Vuong, P., Bennion, D., Mantei, J., Frost, D., Misra, R., 2008. Analysis of YfgL and YaeT interactions through bioinformatics, mutagenesis, and biochemistry. J. Bacteriol. 190, 1507–1517.
Walther, D.M., Rapaport, D., Tommassen, J., 2009. Biogenesis of beta-barrel membrane proteins in bacteria and eukaryotes: evolutionary conservation and divergence. Cell. Mol. Life Sci. 66, 2789–2804.
Ward, R., Zoltner, M., Beer, L., El Mkami, H., Henderson, I.R., Palmer, T., Norman, D.G., 2009. The orientation of a tandem POTRA domain pair, of the beta-barrel assembly protein BamA, determined by PELDOR spectroscopy. Structure 17, 1187–1194.
Welch, W.J., Feramisco, J.R., 1985. Rapid purification of mammalian 70,000-dalton stress proteins: affinity of the proteins for nucleotides. Mol. Cell. Biol. 5, 1229–1237.

Wiese, A., Seydel, U., 1999. Interaction of peptides and proteins with bacterial surface glycolipids: a comparison of glycosphingolipids and lipopolysaccharides. J. Ind. Microbiol. Biotechnol. 23, 414–424.

Wimley, W.C., 2003. The versatile beta-barrel membrane protein. Curr. Opin. Struct. Biol. 13, 404–411.

Wu, T., Malinverni, J., Ruiz, N., Kim, S., Silhavy, T.J., Kahne, D., 2005. Identification of a multicomponent complex required for outer membrane biogenesis in Escherichia coli. Cell 121, 235–245.

Yang, Y., Thomas, W.R., Chong, P., Loosmore, S.M., Klein, M.H., 1998. A 20-kilodalton N-terminal fragment of the D15 protein contains a protective epitope(s) against Haemophilus influenzae type a and type b. Inf. Immun. 66, 3349–3354.

Zhang, H., Gao, Z.Q., Hou, H.F., Xu, J.H., Li, L.F., Su, X.D., Dong, Y.H., 2011. High-resolution structure of a new crystal form of BamA POTRA4-5 from Escherichia coli. Acta Crystallogr. Sect. F: Struct. Biol. Cryst. Commun. 67, 734–738.

Zhu, X., Zhao, X., Burkholder, W.F., Gragerov, A., Ogata, C.M., Gottesman, M.E., Hendrickson, W.A., 1996. Structural analysis of substrate binding by the molecular chaperone DnaK. Science 272, 1606–1614.

CHAPTER TWO

Molecular Cell Biology and Immunobiology of Mammalian Rod/Ring Structures

Wendy C. Carcamo[*,1], S. John Calise[*,1], Carlos A. von Mühlen[†], Minoru Satoh[‡,§], Edward K.L. Chan[*,2]

[*]Department of Oral Biology, University of Florida, Gainesville, Florida, USA
[†]Rheuma Clinic for Rheumatic Diseases, Porto Alegre, Brazil
[‡]Division of Rheumatology and Clinical Immunology, Department of Medicine, University of Florida, Gainesville, Florida, USA
[§]Department of Clinical Nursing, School of Health Sciences, University of Occupational and Environmental Health, Kitakyushu, Japan
[1]These authors contributed equally to this work
[2]Corresponding author: e-mail address: echan@ufl.edu

Contents

International Review of Cell and Molecular Biology, Volume 308
ISSN 1937-6448
http://dx.doi.org/10.1016/B978-0-12-800097-7.00002-6

Abstract

Nucleotide biosynthesis is a highly regulated process necessary for cell growth and replication. Cytoplasmic structures in mammalian cells, provisionally described as rods and rings (RR), were identified by human autoantibodies and recently shown to include two key enzymes of the CTP/GTP biosynthetic pathways, cytidine triphosphate synthetase (CTPS) and inosine monophosphate dehydrogenase (IMPDH). Several studies have described CTPS filaments in mammalian cells, *Drosophila*, yeast, and bacteria. Other studies have identified IMPDH filaments in mammalian cells. Similarities among these studies point to a common evolutionarily conserved cytoplasmic structure composed of a subset of nucleotide biosynthetic enzymes. These structures appear to be a conserved metabolic response to decreased intracellular GTP and/or CTP pools. Antibodies to RR were found to develop in some hepatitis C patients treated with interferon-α and ribavirin. Additionally, the presence of anti-RR antibodies was correlated with poor treatment outcome.

1. INTRODUCTION

We recently reported novel autoantigenic cytoplasmic structures, referred to as rods and rings (RR, Fig. 2.1), detected using autoantibodies in specific patient sera (Carcamo et al., 2011). Many of the patients have hepatitis C virus (HCV) infection and produce anti-RR autoantibodies after treatment with a standard combination therapy of pegylated interferon-α and ribavirin (IFN/R) (Covini et al., 2012). These structures contain cytidine triphosphate synthetase 1 (CTPS1) and inosine monophosphate dehydrogenase 2 (IMPDH2), proteins of 67 and 55 kDa, respectively (Carcamo et al., 2011). Staining by sera from HCV patients and rabbit anti-IMPDH2 antibodies shows perfect colocalization to RR structures. CTPS inhibitors 6-diazo-5-oxo-L-norleucine (DON) and acivicin, as well as the IMPDH2 inhibitors ribavirin and mycophenolic acid (MPA), induce formation of RR in a dose-dependent manner. The induction of RR using these inhibitors has been confirmed in all cancer cell lines and primary cells examined. Our previous report indicated that RR are visualized in undifferentiated mouse embryonic stem cells (ESCs) without the treatment of inhibitors and were disassembled after differentiation with retinoic acid (Fig. 2.1C) (Carcamo et al., 2011). RR can also be found without the use of inhibitors

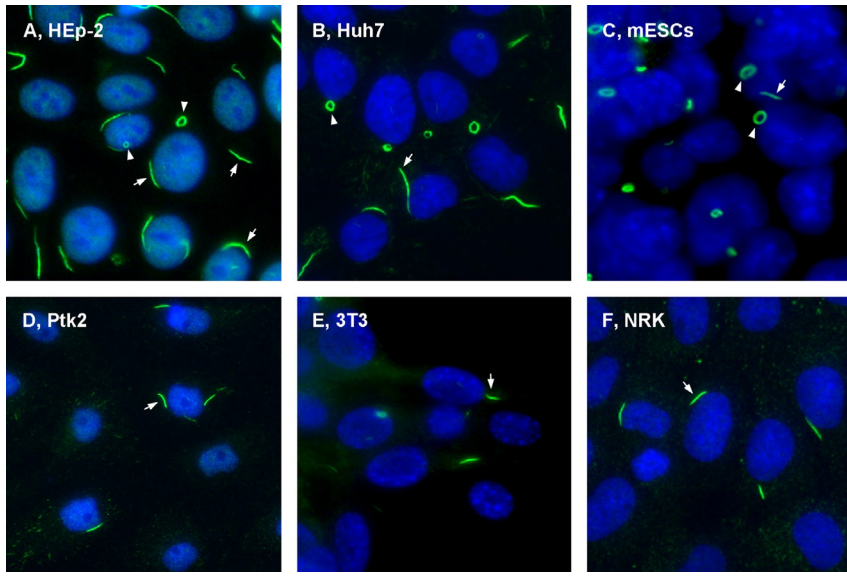

Figure 2.1 Rods and rings (RR) recognized by human autoantibodies. (A) HEp-2 cell substrate from INOVA Diagnostics (San Diego, CA, USA) shows RR recognized by prototype anti-RR serum It2006. (B) Huh7 (human hepatocellular carcinoma) cells exhibit RR induced by 1 mM ribavirin treatment for 24 h. (C) Undifferentiated mouse embryonic stem cells exhibit RR in an unusual ratio of 90% rings to 10% rods. (D–F) RR are present in Ptk2 (male rat kangaroo kidney epithelial cells), 3T3 (mouse fibroblasts), and NRK (normal rat kidney epithelial cells) when incubated in normal growth medium without any treatment. All panels are stained with human prototype anti-RR serum It2006 followed by Alexa 488 goat anti-human IgG (green) and nuclei counterstained with DAPI (blue). Rods (arrows) and rings (arrowheads) are shown throughout each panel.

in Ptk2 (male rat kangaroo kidney epithelial), 3T3 (mouse fibroblast), and NRK (normal rat kidney epithelial) cells (Fig. 2.1D–F), as well as in RAW264.7 (mouse leukemic monocyte/macrophage) cells (unpublished data). RR have also been shown to form in untreated CHO (Chinese hamster ovary) cells transfected with HA-IMPDH (Gunter et al., 2008) and in CHO cells with no extrinsic manipulation at all (Stinton et al., 2013). Therefore, RR expression may be a very interesting biomarker for different types of cells. Various publications from other groups have described novel cytoplasmic filament-like structures that are composed of enzymes involved in either cytidine triphosphate (CTP) or guanosine triphosphate (GTP) nucleotide biosynthesis. Recently, a number of laboratories around the world have concurrently described these structures and assigned them

different names, although it will likely be shown that many of these structures are one in the same. Here, we review all the relevant findings which allow us to speculate that the main function of RR and other macromolecules described is the enhancing of CTP/GTP production when their intracellular levels are lowered; the formation of RR is thus sensitive to lowered cellular levels of GTP/CTP. We refer to these structures as RR for the remainder of this article, as we have referred to them in previous publications.

2. CONSERVED RR STRUCTURES ACROSS SPECIES

Assembly of intracellular protein complexes can serve important functional purposes. Hundreds of metabolic enzymes across diverse organisms form large intracellular bodies inside bacterial microcompartments and eukaryotic microbodies (O'Connell et al., 2012). GW bodies are cytoplasmic structures assembled from miRNA/mRNA–protein complexes that play a role in RNA interference and mRNA degradation (Fritzler and Chan, 2013; Yao et al., 2013). Previous studies have also identified purinosomes and U bodies as functional cytoplasmic structures (An et al., 2008; Liu and Gall, 2007). Various studies show that inhibition of certain enzyme activity by chemical inhibitors or by altering nutrient levels can induce formation of other filaments. Acetyl-CoA, involved in fatty acid synthesis, has been shown to assemble into filaments in mammalian cells and yeast in response to citrate (Kleinschmidt et al., 1969; Schneiter et al., 1996). Acetyl-CoA filaments, as well as glutamine synthetase filaments in yeast, show that enzyme activity and nutrient starvation play a role in filament polymerization (Beaty and Lane, 1983; Narayanaswamy et al., 2009; Vagelos et al., 1962). Nutrient deprivation plays a similar role to the nucleotide biosynthetic enzyme inhibitors described above in reducing nucleotide levels and, therefore, depleting nucleotide levels may be a direct cause of the formation of RR. Since CTPS1 and IMPDH2 are key RR components, it is speculated that formation of RR helps increase cellular production of GTP and CTP.

2.1. Nematin in mammalian cells

The earliest report on RR-like structures is the work by Willingham et al. (1987), who described a novel cytoplasmic filament named nematin that is practically identical to rods shown in Fig. 2.1 (Willingham et al., 1987). The structures were observed by immunofluorescence staining using a monoclonal

antibody referred to as antinematin. The monoclonal antibody was derived from a BALB/c mouse that was immunized with SR-BALB 3T3 cells and thus can be classified as an autoantibody, as it was later shown positive for staining of mouse 3T3 cells. Most cells exhibited only one of these structures, but occasionally more than one were present. Some structures took on a distinct doughnut shape, which appears to be indistinguishable from the rings shown in Fig. 2.1. Through colocalization studies, the filaments were identified to be independent of tubulin or vimentin. The presence of these filaments was examined in nine different mammalian cell lines and they determined that rat and mouse cells expressed the nematin structure at a higher frequency, while chick embryo cells contained virtually no such structures. This observation is consistent with our recent observations that a rat (NRK), rat kangaroo (Ptk2), and two mouse (3T3, RAW264.7) cell lines express RR while incubated in typical growth medium alone; this effect has not been seen in any human cell lines examined to date. Fixation methods affected the stability of the structures, with formaldehyde acting as the best fixative. With the use of light and electron microscopy and microinjection, they identified this filament as a novel cytoplasmic structure without a lipid bilayer membrane. They concluded that the antigen recognized by the monoclonal antibody was a protein and that it may be a differentiation marker. Although the antigen was not identified, immunoprecipitation analysis revealed that the antigen was a 58-kDa protein, very close in size to IMPDH. Additionally, cells were found to have a higher frequency of nematin right after thawing and DMSO treatment did not induce filament formation; we also found this to be true for RR. This study was not continued to determine the identity of the antigen, but these similarities suggest that this may be the first publication to identify the novel cytoplasmic structure that we have described as RR.

2.2. IMPDH filaments induced by MPA in mammalian cells

The second report of a filament composed of a nucleotide biosynthetic enzyme was from Ji et al. (2006), who discovered that IMPDH inhibitors induced formation of rods composed of IMPDH and that the structure was reversible with the addition of guanosine or GTPγS. Cells treated with MPA induced the clustering of IMPDH in as little as 30 min, with full linear/rod and annular/ring structures observed after 24 h. MPA treatment also caused a mobility shift of the IMPDH band in SDS-PAGE detectable in Western blotting. The band shift was preventable with the use of guanosine, which also caused the disassembly of the IMPDH aggregates.

The aggregation of IMPDH was associated with the loss of enzymatic activity, as expected from the putative inhibitory action of MPA. They determined that GTP levels are important for the prevention and reversal of IMPDH aggregates; direct binding of GTP to IMPDH reverses the conformational changes in the protein caused by MPA. The structures identified by Ji et al. are the same as RR, although their data suggest that IMPDH is capable of polymerizing in the absence of other proteins. RR formation was also detected in HeLa cells treated with MPA using a rabbit anti-IMPDH antibody and our patient autoantibody (unpublished).

Another report by Gunter et al. (2008) described these putatively identical structures in rat retinal cells, and confirmed the findings related to MPA by Ji et al. (2006). Their work focused on characterizing the differences between the two isoforms of IMPDH, especially related to intracellular localization during various phases of development of the rat retina, since mutations in the IMPDH1 gene have been shown to contribute to several related retinal diseases (Bowne et al., 2002, 2006; Kennan et al., 2002). Their major finding that propelled further investigation was that an isoform switch occurs during development around P10 (postnatal day 10). In the early development of retinae, IMPDH type 1 is undetectable while type 2 is present, but after P10, the type 1 variants α and γ become the dominant forms. This led them to examine the subcellular distribution of both isoforms and their variants, hoping that localization may provide clues to the function of the IMPDH isoforms. Intriguingly, they observed that in developing rat retinae, type 1 tended to aggregate into these "intracellular macrostructures," as they refer to these RR-like structures in their report, at a higher rate than type 2; this is contrary to our laboratory's typical thinking, as we have only shown that type 2 is present in RR and have yet to document the inclusion of type 1 in the polymerization process. Curiously, they did not see the same spontaneous formation in adult retinae, despite the dominance of IMPDH type 1α and 1γ later in development. This contradiction could be explained by high intracellular GTP levels within the photoreceptors; the group did find that cells supplemented with guanosine prior to expression of IMPDH1 could not form the structures. They utilized CHO cells to compare the expression of transiently and stably transfected HA-tagged IMPDH type 1 and type 2 compared to endogenous isoforms of IMPDH in nontransfected cells. It is important to note that these macrostructures formed in CHO cells that were untreated beyond the transfection, the first indication of RR formation without the use of IMPDH inhibitors outside of the work done by Willingham et al. (1987).

Additionally, the study of Gunter et al. (2008) built upon the work done by Ji et al. (2006) related to macrostructure formation due to decreased intracellular GTP levels. While Ji et al. hypothesized that the conformational changes brought about by binding of inhibitors to IMPDH caused aggregation, Gunter et al. (2008) rejected that hypothesis and decided that the intracellular GTP levels must be a major factor and set out to prove it. First, they confirmed the other group's findings by reproducing the reversal of structure formation using guanosine supplementation. They also noted that a low percentage of untreated cells contained these macrostructures and suggested that a spectrum of IMPDH distribution from cell to cell may play an important role. Decoyinine, which blocks *de novo* synthesis of guanine nucleotides by inhibiting GMP synthetase (GMPS), the enzyme directly downstream of IMPDH, did not affect enzymatic activity of IMPDH but encouraged formation of RR. To further support their hypothesis, they also utilized reverse-phase HPLC and measured that intracellular GTP levels were reduced by over 80% following treatment with MPA; guanosine supplementation reversed this effect and increased GTP levels to above that of control cells. These findings led them to believe that the RR-like macrostructures may be a result of substrate channeling, so they examined the subcellular distribution of transiently expressed HA-tagged GMPS and endogenous aminoimidazole carboxamide ribonucleotide formyltransferase (ATIC), an enzyme upstream of IMPDH, in CHO cells treated with MPA. They observed only diffuse cytoplasmic staining with no localization of these enzymes to any RR-like macrostructures, ruling out their substrate channeling hypothesis.

In 2012, a report from the same group documented their most recent findings regarding IMPDH polymerization and the Bateman domains of both isoforms (Thomas et al., 2012). The Bateman domain is a conserved region found in a wide variety of proteins across different species, important in allosteric regulation (Bateman, 1997; Kemp, 2004). Mutations in the Bateman domain have been implicated in several diseases (Ignoul and Eggermont, 2005), but its role in IMPDH has not been fully characterized to date. Its importance in the regulation of nucleotide homeostasis *in vivo* was established in 2008 by Pimkin and Markham using *Escherichia coli* with a Bateman domain deletion in the IMPDH gene; the bacteria were unable to utilize exogenously supplied purine bases to maintain normal ATP and GTP levels (Pimkin and Markham, 2008). Scott et al. (2004) observed ATP binding to the Bateman domain of purified human IMPDH2 that increased catalytic activity by fourfold, although other laboratories have

been unable to reproduce these data. Thomas et al. (2012) hypothesized that the Bateman domain, which varies between the two IMPDH isoforms, may explain their differential inclinations to polymerize. Several IMPDH1/2 chimera constructs were used to demonstrate that the N-terminal 244 amino acids, which include the Bateman domain, determine the isoform's tendency to form macrostructures. This is based on isoform-specific nucleotide-binding capabilities that induce conformational changes, which alter communication between the Bateman domain and the catalytic domain, suggesting that both domains are important to polymerization and subcellular localization. Additional examination of retinitis pigmentosa-causing mutations R224P and D226N by the same group yielded the observation that the R224P mutation inhibited ATP binding and decreased the tendency of the mutant protein to polymerize, while the D226N mutation appeared similar to the wild type with, perhaps, a slight reduction in ATP binding. Their results hint that future studies of these mutations may provide us with more clues into the formation and function of these structures.

2.3. *Drosophila* cytoophidia—CTPS filaments

There are several recent studies reporting RR-like structures in different systems. Liu (2010) identified an RR-like intracellular structure containing CTPS in *Drosophila* cells. The structures, referred to as cytoophidia (cell serpents), were identified in all major *Drosophila* cell types within the ovary and other tissues, such as brain, gut, trachea, testis, accessory gland, salivary gland, and lymph gland. The structure was recognized by an antibody against Cup protein that was believed to have cross-reactivity. Using two GFP-protein trap fly stocks from the Carnegie Protein Trap Library, CTPS was identified as a component of cytoophidia (Liu, 2010). Cytoophidia were also determined to be associated with the microtubular network but not associated with centrioles. Two types of structures were identified as macro- and microcytoophidia based on their length.

In a follow-up study, the same laboratory reported similar structures in human HeLa P4 cells using an anti-CTPS antibody (Chen et al., 2011). Cytoophidium formation was increased by treatment with CTPS inhibitor DON. Knocking down CTPS caused the cytoophidia to disappear, although it is unknown if the disappearance is due to the requirement of CTPS or the decrease in protein. Azaserine, another CTPS inhibitor, showed effects similar to those of DON. Identification of cytoophidia in

HeLa and clustering of CTPS suggests that these structures are identical to RR. Cytoophidia and RR have clear similarities and both structures have been determined to be unassociated with centrioles. Although the expression frequency of cytoophidia varies, both structures can be induced with DON and both structures were detected with antibodies to CTPS.

The most recent report from Liu's laboratory builds on the knowledge of cytoophidia by focusing on the roles of the three isoforms of CTPS present in *Drosophila melanogaster* (Azzam and Liu, 2013). Their results indicate that only isoform C localizes to the cytoophidium, while isoform A localizes to the nucleus and isoform B appears diffuse in the cytoplasm. Although isoform A does not seem to be incorporated into the cytoophidium, its expression is still important for the formation of the structure; a mutation disturbing isoform A expression in the nucleus prevents cytoophidium formation in the cytoplasm just as mutations to isoform C arrest cytoophidium assembly. Additionally, when isoform C was overexpressed in ovarian cells, the length and thickness of the structures increased significantly; in embryonic cells, where cytoophidia are less commonly observed, overexpression stimulated assembly of cytoophidia. Azzam and Liu also examined the protein domains that differed between the three isoforms and how they affected cytoophidium development. They identified a unique N-terminal domain in isoform C required for cytoophidium assembly, suggesting that isoform C is the fully functional form of CTP synthetase; a truncated isoform C lacking this 56-aa segment could not assemble the structures. It is likely that their results regarding this N-terminal segment could be replicated in human cells, as this region is highly conserved among species. They also showed that overexpression of the synthetase domain prevents cytoophidium formation.

2.4. Rod-like filaments in *Saccharomyces cerevisiae*

Another recent study from Noree et al. (2010) identified nine proteins that formed rod-like filaments in *S. cerevisiae*. The filaments were identified using GFP-tagged proteins; they also verified that the tag did not play a role in the formation of the filaments because the same filaments were observed when the GFP tag was changed to an HA epitope tag. Additionally, the tagged version of each protein did not affect growth or viability of cells. The nine proteins are Glt1p (glutamate synthase), Psa1p (GDP–mannose pyrophosphorylase), Ura7p/Ura8p (CTP synthase), Gcd2p (eIF2B-δ), Gcd6p (eIF2B-ε), GCD7p (eIF2B-β), Gcn3p (eIF2B-α), and Sui2p (eIF2B-α). Some of the nine proteins colocalized to form four distinct

filaments. They observed that the Ura7p filaments were increased when cells were grown to saturation and concluded that this was due to a decrease in available carbon sources. In addition, treating cells with sodium azide to alter energy status caused an increase in Ura7p and Psa1p filaments. CTPS filaments were identified in all three cell types in the *Drosophila* egg chamber. They concluded that the different complexes form in response to environmental conditions either to promote or inhibit particular enzymatic processes, and not as a stress response. Additionally, CTPS filament assembly is caused by the regulation of enzyme activity by the binding of specific ligands such as CTP.

2.5. CTPS filaments in *Caulobacter crescentus*

The recent report from Ingerson-Mahar et al. (2010) identifies a possible function of CTPS filaments in the fresh water bacterium *C. crescentus*. They demonstrated that CTPS formed filaments along the inner curve of the bacterium using electron cryotomography. This bacterial CTPS enzyme has a bifunctional role; as a filament, it regulates the curvature of *C. crescentus* and performs its catalytic function. They treated cells with the irreversible CTPS inhibitor DON and showed the disruption of the CTPS filament. They determined via electron cryotomography that CTPS colocalizes with the filament and is required for its formation. In addition, an *E. coli* CTPS homolog was able to form filaments both *in vivo* and *in vitro*. They concluded that CTPS is a negative regulator of cell curvature by mediating CreS. However, the mechanism of how CTPS controls cellular curvature remains unclear.

2.6. Loukoumasomes in rat sympathetic neurons

Ramer et al. (2010) described an intracellular organelle present in a subset of rat sympathetic ganglion neurons. These doughnut-like bodies, named "loukoumasomes" from the Greek words for doughnut (*loukoumas*) and body (*soma*), are quite similar in size to RR at ~6 μm in diameter, but only appear once per neuron. Like RR, loukoumasomes have also been observed in rod or "figure 8" forms, although the ring-like shape is the most prevalent phenotype reported. Loukoumasomes can be recognized throughout the cytoplasm and initial axon segment of these specific neuronal cells and associate with nematosomes as well as centrosomes and their primary cilia, although the structures themselves are not centrosomes. To date, γ-tubulin, myosin IIb, and cenexin have been confirmed as components of the

loukoumasome, while βIII tubulin is presented as an additional potential component, as different antibodies have provided the group with varying results.

Ramer's group hypothesizes that loukoumasomes are potentially active structures that maneuver between the perinuclear compartment and the axon; this idea is supported by their observation that an antibody to non-muscle heavy chain myosin recognized the loukoumasome structure. They hypothesize that this organelle is dynamic and may supply centrosomes with γ-tubulin to conserve cell shape. Cenexin, a protein associated with centrioles and ciliary development, also localizes to loukoumasomes, which may implicate this organelle plays a role in maintaining primary cilia. Despite the fact that RR and loukoumasomes have not been found to contain common proteins, it is intriguing that these structures, which appear phenotypically identical to RR, are potentially mobile within the cell because the mobility of RR has yet to be shown. At the least, there must be a mechanism for aggregation of proteins into the RR structure, and there may yet be a link between RR and loukoumasomes.

In summary, RR-like filaments have been identified in a wide range of species as described above. RR-like filaments have been identified in human, mouse, rat, rat kangaroo, Chinese hamster, *Drosophila*, yeast, and bacteria. Filament sizes range from <1 to 50 μm, with bacteria expressing the smallest structures and *Drosophila* expressing the largest ones (summarized in Table 2.1). The structures have also been identified in some cancer cell lines, primary cells, and stem cells as discussed above.

3. KNOWN COMPONENTS OF RR

3.1. Cytidine triphosphate synthetase

The observation that two known components in RR are CTPS1 and IMPDH2 implicates the association of these structures with CTP and GTP biosynthesis. CTP and GTP are essential building blocks of DNA and RNA and are involved in a multitude of pathways in both prokaryotes and eukaryotes. They serve as energy carriers, participate in cellular signaling, and act as important cofactors in enzymatic reactions. Nucleotide biosynthesis can occur via *de novo* pathways or the salvage pathway and is tightly regulated by the cell. CTPS is a glutamine amidotransferase enzyme that catalyzes the conversion of uridine triphosphate (UTP) to CTP and is a key enzyme in nucleic acid and phospholipid biosynthesis (Fig. 2.2). Two human isoforms, CTPS1 and CTPS2, are 74% identical at the amino acid

Table 2.1 Comparison of various reported RR-like cytoplasmic filament structures

Group	Rods/rings; components	Sizes	Induction method	Detection	Species/cell types	Similarities versus Carcamo et al. (2011)	Differences versus Carcamo et al. (2011) (Carcamo et al., 2011)	Other Comments
Carcamo et al. (2011)	Both detected; CTPS1, IMPDH2	3–10 μm rod length; 2–5 μm ring diameter	CTPS1 and IMPDH2 inhibitors: DON, acivicin, ribavirin, MPA	IMDPH2 and CTPS1 antibodies and human autoantibodies	Human: HeLa, HEp-2, K562, HCT116; mouse 3T3, primary cardiomyocytes, fibroblasts, ESCs	–	–	–
Willingham et al. (1987)	Both detected; nematin, 58 kDa	0.5–3 μm rod length	Not induced	Mouse IgG3 mAb	Human KB; bovine MDBK; rat NRK; mouse 3T3	Not enriched in vimentin or tubulin; Prevalent in newly thawed cells; Fixation methods affect structure	–	mAb Stains mouse skin and CNS; Not abundant in human cell lines
Ji et al. (2006)	Both detected; IMPDH	0.1 to >1 μm in diameter	IMPDH inhibitor MPA	IMPDH antibody	Human: MCF7, CEM, K66/B5	Untreated cells show IMPDH dispersed in cytoplasm;	–	Mobility shift of IMPDH after MPA treatment in Western blot

						Aggregates in 30 min after MPA treatment; mature rods by 24 h; No association with other organelles		Guanosine, guanine, GMP, GDP, GTP disassemble rods; MPA causes aggregation of IMPDH on glass slides
Gunter et al. (2008)	Both detected; IMPDH	2–10 μm in length	IMPDH inhibitor MPA	IMPDH antibody, HA-IMPDH1/2	Rat retina; CHO	Same as Ji et al. above	RR in untreated CHO; IMPDH1 detected	RR found in developing rat retinae and CHO with no induction by inhibitor
Liu (2010)	Both detected as cytoophidia; CTPS	<1–50 μm rod length, depends on stages	Not induced	Three CTPS antibodies, GFP-CTPS	Drosophila follicle cells, nurse cells, oocytes	Cytoophidia are not associated with centrioles	CTPS functional in cytoophidium; Associated with the microtubular network but does not overlap	–
Chen et al. (2011)	Both detected; CTPS	2-10 μm rod length	CTPS inhibitor DON	CTPS antibody	Human HeLa P4	DON increases the	Only 40% RR can be induced	DON induced apoptosis and

Continued

Table 2.1 Comparison of various reported RR-like cytoplasmic filament structures—cont'd

Group	Rods/rings; components	Sizes	Induction method	Detection	Species/cell types	Similarities versus Carcamo et al. (2011)	Differences versus Carcamo et al. (2011) (Carcamo et al., 2011)	Other Comments
						formation of cytoophidia	at 4 μg/mL of DON	induced filament formation in *Drosophila* ovaries
Noree et al. (2010)	Only rods; CTPS Ura7p	0.5-3 μm length	Nutrient deprivation or CTPS inhibition	GFP-protein in yeast	*S. cerevisiae*, *D. melanogaster*	Filament formation is due to regulation of enzymatic activity	The tag on the protein does not affect the formation of the filament	Kinase inhibitor staurosporine increased filament formation
Ingerson-Mahar et al. (2010)	Only rods; CTPS	390–790 nm length	Not induced or CTPS overexpression	mCherry–CTPS	*C. crescentus*, *E. coli*	–	DON disrupts rods; Overexpression increase length of rods	CTPS interacts with CreS
Ramer et al. (2010)	Both detected; γ-tubulin, myosin IIb, cenexin	~6 μm diameter	Not induced	Antibodies to γ-tubulin, myosin IIb, cenexin; SDL.3D10 Ab	Rat sympathetic ganglion neurons	Phenotypical appearance	Specific to cell type; no common components	Potentially a mechanism for intracellular transport

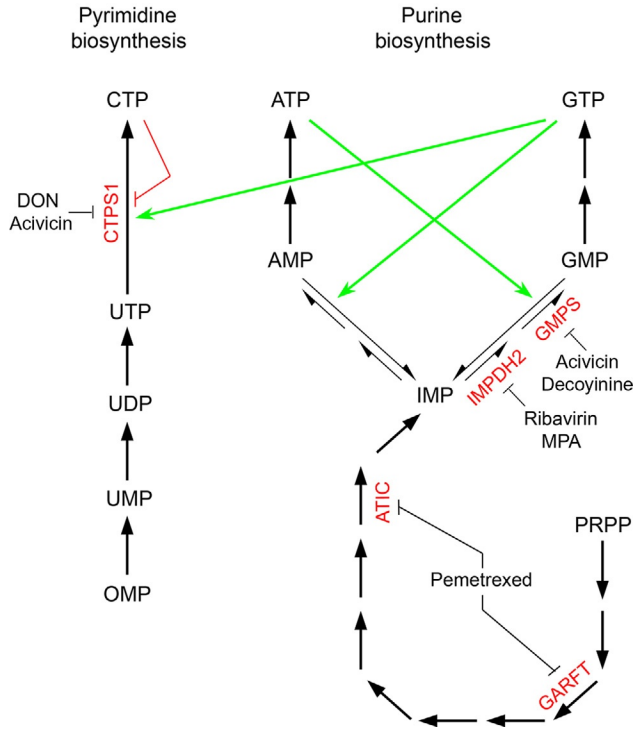

Figure 2.2 A schematic of RR components CTPS1 and IMPDH2 within the purine and pyrimidine biosynthesis pathways. The sites of inhibition for DON, acivicin, ribavirin, MPA, decoyinine, and pemetrexed that induce RR formation are shown in red. IMPDH2 is an enzyme involved in the GTP biosynthesis pathway that catalyzes the conversion of IMP into XMP, which is then converted by GMPS into GMP, a precursor to the production of GTP. CTPS1 is an enzyme involved in the CTP biosynthesis pathway and catalyzes the conversion of UTP to CTP. Arrows signify steps in the pathway. Green arrows signify activation of pyrimidine and purine biosynthesis pathways by ATP and GTP. Red angled line signifies inhibition of the pyrimidine biosynthesis pathway by end product CTP. The pathway schematic is adapted from Hofer et al. (2001).

level (Kursula et al., 2006). There are two CTPS isozymes in *S. cerevisiae*, URA7 and URA8, which correspond to the mammalian CTPS1 and CTPS2, respectively. The enzyme consists of the N-terminal synthetase domain and the C-terminal glutaminase domain. The latter catalyzes the deamination of glutamine. CTPS is an established target for antiviral, antineoplastic, and antiparasitic therapy (Dereuddre-Bosquet et al., 2004; Hofer et al., 2001; Verschuur et al., 2000).

3.2. Inosine monophosphate dehydrogenase

IMPDH is also tightly regulated and catalyzes the conversion of IMP into xanthosine 5′-monophosphate, which is the rate-limiting step in the *de novo* synthesis of guanine nucleotides (Fig. 2.2) (Jackson et al., 1975; Weber et al., 1996). IMPDH exists as two 55 kDa isoforms, IMPDH1 and IMPDH2, with 84% amino acid sequence identity and forms independent tetramers when active (Colby et al., 1999). IMPDH is an important regulator of cell proliferation and is a known target in the treatment of neoplastic and viral diseases. MPA, an IMPDH inhibitor, has been used as an immunosuppressive agent for organ transplants and autoimmune diseases (Allison and Eugui, 1993; Franklin and Cook, 1969; Sintchak et al., 1996). Another IMPDH inhibitor, ribavirin, is currently being used in the treatment of HCV (Hong and Cameron, 2002; Zhou et al., 2003).

3.3. Other candidate components

Immunoprecipitation of K562 cell extract using anti-RR-positive HCV patient sera shows that some anti-RR antibody-positive sera named 604, 605, and 611 pull down a common 55 kDa doublet (Fig. 2.3A, red dots), which corresponds to IMPDH1/2. Although CTPS1 and IMPDH2 are known RR components, other sera with anti-RR antibodies by immunofluorescence do not immunoprecipitate IMPDH or CTPS protein (Fig. 2.3A, 603, 606, 608, 609, 610, and 612). Immunofluorescence analysis shows serum 609 (anti-RR-positive, 55 kDa doublet-negative) and serum 611 (anti-RR-positive, 55 kDa doublet-positive) both recognize the same structure costained with rabbit anti-IMPDH2 (Fig. 2.3B–J). To date, three studies have identified IMPDH and five have identified CTPS as components of the RR-like filaments, as summarized in Table 2.1. Liu speculates that these structures may be composed of additional components, as seen in the yeast Ura7p and Ura8p filaments (Liu, 2011). Willingham et al. (1987) identified that nematin filaments were not enriched in vimentin or tubulin. Our study also concluded that RR are neither enriched in vimentin, tubulin, or actin, nor associated with any known cytoplasmic structures (Carcamo et al., 2011). In addition, we investigated the colocalization of RR with centrioles and determined that RR are not primary cilia because the structures are not attached to the centrioles.

Recently, a study by Probst et al. confirmed IMPDH2 as the primary antigen for human anti-RR autoantibodies using their newly developed recombinant cell-based indirect immunofluorescence assay. This study showed that

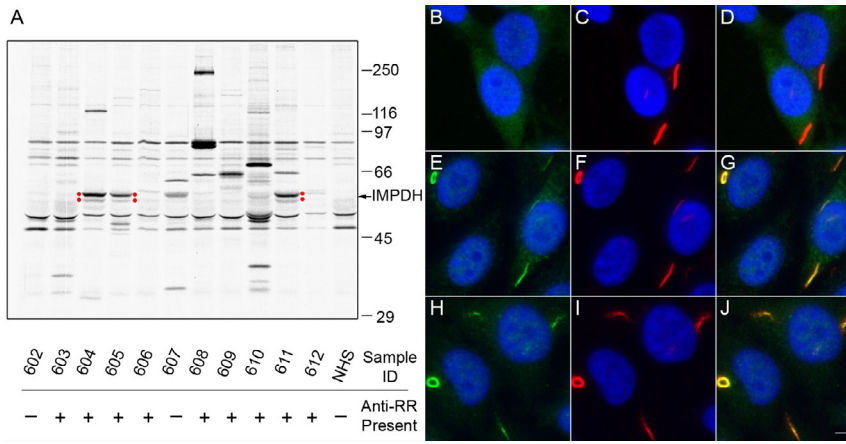

Figure 2.3 Patient autoantibodies recognize multiple components of RR. (A) Immunoprecipitation of K562 cell lysates using hepatitis C patient sera 602–612 and correlation with the presence of anti-RR antibodies by immunofluorescence. Sera 604, 605, and 611 show a common 55-kDa doublet (red dots) corresponding to IMPDH and are also positive for anti-RR antibodies. In contrast, sera 603, 606, 608, 609, 610, and 612 have anti-RR antibodies but do not immunoprecipitate the 55-kDa doublet. To confirm RR detected from patients were all the same structure, double staining of HEp-2 cells was performed with rabbit anti-IMPDH2 (C, F, I) and serum 607 (anti-RR negative, B), serum 609 (anti-RR positive but did not immunoprecipitate the 55 kDa doublet, E), or serum 611 (anti-RR positive and immunoprecipitated the 55 kDa doublet, H). Since RR are recognized by both serum 611 and 609, serum 609 most likely recognizes other unidentified RR component(s). Nuclei are counterstained with DAPI. Panels D, G, and J are merged images. Scale bar: 10 μm.

anti-RR-positive patient sera reacted with recombinant IMPDH2 but did not react at all with recombinant CTPS, causing the group to name CTPS an "unlikely target" of anti-RR antibodies (Probst et al., 2013). To date, only one anti-CTPS antibody has been able to recognize RR structures in INOVA HEp-2 slides (Table 2.2). It is likely that the native conformation of CTPS and the manner in which CTPS is incorporated into the structure limits available epitopes such that many antibodies are unable to recognize RR in immunofluorescence. While we know from the report by Probst et al. that anti-RR antibodies from patient sera likely do not recognize CTPS, it is also possible that CTPS is not present in RR structures under certain conditions, since its presence has only been confirmed by this single antibody under unknown cellular conditions in a commercial slide, and has not been confirmed under any other conditions. Further studies are required to confirm the presence of CTPS in RR structures induced with various methods.

Table 2.2 Antibodies tested for RR staining by indirect immunofluorescence

Protein	Antibody species	Producer	Catalog no.	RR detection
IMPDH2[a]	Rabbit	Abcam	Ab75790	No
IMPDH2	Rabbit	Proteintech	12948-1-AP	Yes
IMPDH2	Rabbit	Aviva	ARP54365_P050	Yes
IMPDH2	Rabbit	Aviva	ARP54366_P050	Yes
CTPS1	Rabbit	Abcam	Ab65045	No
CTPS1	Rabbit	Jim Wilhelm's lab[b]		Yes
CTPS1	Mouse	Sigma	WH0001503M1	No
CTPS1	Rabbit	Santa Cruz	Sc-101925	Lot specific[c]
CTPS2	Rabbit	Aviva	ARP62443_P050	No
CTPS2	Rabbit	Proteintech	12852-1-AP	No
TYMS	Mouse	Maria Zajac-Kaye's lab	TS-106	No
DHFR	Rabbit	Spring Bioscience	E18220	No
UMPS	Mouse	Abgent	AT4467a	No
PCYT1A	Mouse	Abgent	AT3244a	No
ATIC	Rabbit	Aviva	ARP46095_T100	No
ATIC	Rabbit	Aviva	ARP46094_T100	No
HPRT	Rabbit	Aviva	ARP48471_P050	No
GMPS	Rabbit	Aviva	ARP48619_P050	No

[a]ATIC, aminoimidazole carboxamide ribonucleotide formyltransferase; CTPS, cytidine triphosphate synthetase; DHFR, dihydrofolate reductase; GMPS, guanine monophosphate synthetase; HPRT, hypoxanthine-guanine phosphoribosyl transferase; IMPDH, inosine monophosphate dehydrogenase; PCYT1A, phosphocholine cytidylyl transferase A; TYMS, thymidylate synthetase; UMPS, Uridine monophosphate synthetase.
[b]Carcamo et al. (2011).
[c]CTPS1 antibody from Santa Cruz was tested three times due to inconsistent reports; Liu reported that this antibody detected RR (Liu, 2010). However, we determined that detection of RR with this antibody was lot-specific. Only one lot was able to detect RR while another lot could only detect RR at 1:50 with very weak staining.

3.3.1 Nucleotide biosynthetic enzymes

As stated above, RR are composed of IMPDH2 and CTPS1 and may include other enzymes involved in purine and pyrimidine biosynthesis pathways. Due to the large size of the RR structure, we speculate that RR may be composed of other additional components. For example, in GW bodies,

which are known to range from 0.1 to 0.3 μm in diameter, more than 10 proteins have been identified (Eystathioy et al., 2002; Jakymiw et al., 2007). With rods being ~3–10 μm in length and rings ~2–5 μm in diameter, it is very reasonable to postulate that RR are composed of additional enzymes involved in nucleotide biosynthesis. There is experimental support for this consideration because we have observed RR formation in cells treated with 10 μM pemetrexed for 24 h. Pemetrexed is a chemotherapeutic drug that inhibits thymidine synthetase, dihydrofolate reductase, glycinamide ribonucleotide formyltransferase (GARFT), and ATIC. The fact that pemetrexed induced RR formation in HeLa cells suggests that some of these enzymes may be components of RR, although Gunter et al. (2008) were unable to identify GMPS as a component of RR after directly inhibiting the enzyme with decoyinine. Thymidine synthetase is an interesting candidate RR protein because it is the critical enzyme for the production of thymidine triphosphate (TTP). Additional thymidine synthetase inhibitors 5-fluorouracil and gemcitibane were also tested but they did not induce RR formation. We were also unable to detect RR using a mouse antibody to thymidine synthetase (generously provided by Dr. Maria Zajac-Kaye); however, these data cannot completely rule out that thymidine synthetase may be localized to RR. Similarly, rabbit anti-dihydrofolate reductase antibody (E18220; Spring Bioscience, Pleasanton, CA, USA) was unable to detect RR formed after treatment with pemetrexed. Thus, it remains necessary to examine whether RR may be composed of GARFT or ATIC, enzymes involved in the purine biosynthesis pathway (Fig. 2.2).

3.3.2 RR candidate proteins from microarray screening

A recent report by Stinton et al. (2013) utilized a protein/peptide microarray to identify an assortment of additional candidate RR autoantibody target antigens. In the protein microarray, anti-RR-positive human sera were screened for reactivity with a wide array of antigens and compared to screening of normal and unrelated autoantibody controls. This technique, that had not been previously used in RR study, indicated several new potential targets for anti-RR antibodies: Myc-associated zinc finger protein (MAZI), voltage-dependent anion channel 1 (VDAC1), ankyrin repeat and sterile alpha motif domain containing 6 (ANKS6), actin-related protein 1 homolog A (ARP1), as well as three uncharacterized peptides with unknown functions (Stinton et al., 2013). Intriguingly, these candidate antigens are functionally similar and are involved in purine metabolism, protein folding, and polymerization, indicating a promising link to RR. The signal strength and

consistency of the four distinct clones associated with MAZI, also known as purine binding factor 1 (Pur-1), combined with the role of MAZI as a purine binding transcription factor make it the most intriguing candidate RR protein from this assay. VDAC1, which interacts with proteins that control apoptosis, localizes to the outer mitochondrial membrane, where it also interacts with the rest of the cell to maintain metabolic reactions. The reactivity of anti-RR sera with ANKS6, related to protein folding, and ARP1, the major subunit of dynactin, represents possible explanations for how proteins aggregate and conform into RR structures. Reactivity of anti-RR sera with these proteins is a novel and attractive finding, but the positive signals for these proteins on a microarray cannot elucidate their association with or localization to the RR structure. The validation of these candidate proteins as RR components will require additional studies related to the actual structure as well as human anti-RR antibodies.

3.3.3 Methods in RR component identification

RR that are induced by CTPS/IMPDH inhibitors are readily dissociated after cell lysis with detergents such as 0.3% Nonidet P40 or 0.5% Triton-X; therefore, attempts to purify RR for the identification of additional components using mass spectrometry have not been feasible to date. If mass spectrometry can identify any of these enzymes discussed above as potential components, they can possibly be confirmed as RR components by using inhibitors to those enzymes to detect whether RR are formed. However, many antibodies of known RR components do not recognize RR, as shown in Table 2.2. This inability of certain antibodies to recognize RR structures may depend on the conformational changes of the individual component upon assimilation into the RR structure. Techniques such as mass spectrometry may be necessary to fully characterize the RR structure; interference with epitope–paratope interactions on the three-dimensional structure of RR may prevent us from using immunofluorescence colocalization studies to identify new components. It is also likely that the composition of RR varies based on current intracellular conditions and availability of essential enzymes.

4. BIOLOGICAL FUNCTION OF RR

4.1. Nucleotide biosynthesis associated with RR

In human cell cultures maintained to date, RR are not found in more than a very low percent of cells. Curiously, nonhuman cell lines, such as rat NRK

cells, rat kangaroo Ptk2 cells, and mouse cell lines 3T3 and RAW264.7, have an increased tendency for RR formation without any treatment at all, which remains to be explained. While RR formation can appear in anywhere from 10% to 80% of untreated nonhuman cells, a percentage seemingly dependent on a number of variables associated with cell culture, inhibitors of CTPS and IMPDH are known to induce RR formation in 90–100% of cells from all species tested, detectable by both patient autoantibodies and rabbit anti-IMPDH2 antibodies (Carcamo et al., 2011). Comparing IMPDH inhibitors ribavirin and MPA to CTPS inhibitors DON and acivicin at a relatively high concentration (2 mM), IMPDH inhibitors are consistently faster at inducing RR in only 15–30 min versus CTPS inhibitors which require 2–3 h to induce comparable levels of RR (Carcamo et al., 2011). Most studies report that the inhibition of these enzymes causes RR-like filament formation, with the only exception in *C. crescentus* when CTPS inhibitor DON disassembles CTPS filaments as described earlier (Ingerson-Mahar et al., 2010). Noree et al. (2010) specifically identified Ura7p (CTPS) filaments as being affected by levels of nutrients. Some key differences between reports are summarized in Table 2.1.

4.2. Rod versus ring configurations

As described in Section 1, the cytoplasmic structures provisionally named rods and rings were identified using HCV patient sera. The rods and rings are distinct structures visualized via indirect immunofluorescence. It is unknown whether rods and rings have different functions, but it is reasonable to hypothesize that there is interconversion between the two forms. This speculation is derived in part from the appearance of intermediate structures (Fig. 2.4B–G) that are observed via immunofluorescence. Although RR can be induced in various cell lines, there are differences in size and the percentage of cells forming rods versus rings. HeLa cells were determined to have rods measuring 5–10 μm while THP-1 cells formed shorter rods measuring 2–3 μm. Additional time-point immunofluorescence data and live cell imaging of the formation of RR induced by MPA and decoyinine suggest that the structures start off small and increase in size until reaching full/mature size of 5–10 μm (Carcamo et al., 2013; Thomas et al., 2012).

4.3. Induced versus native RR

RR can be induced in cancer cells and primary cells using IMPDH/CTPS inhibitors in as short as 15 min with IMPDH inhibitors and 3 h with CTPS

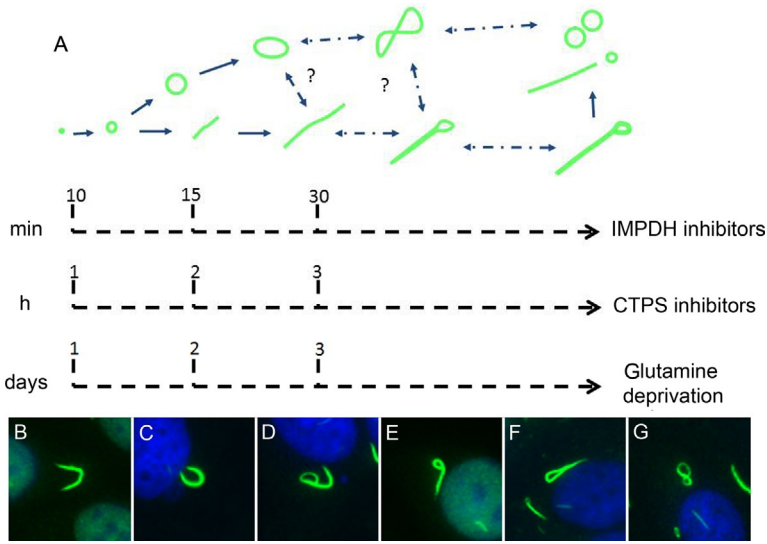

Figure 2.4 RR induction timeline showing hypothetical interconversion between rods and rings. (A) This panel summarizes the overall timeline of IMPDH and CTPS inhibitors or glutamine deprivation inducing the formation of RR in different cell lines. Some RR structures may be interchangeable, as indicated by double-sided arrows. Question marks indicate the uncertainty as to whether or not these structures interconvert between the rod and ring forms. The timelines indicate induction time for RR using IMPDH inhibitors (ribavirin or MPA), CTPS inhibitors (DON or acivicin), and glutamine deprivation. (B–G) Various forms of intermediate RR structures, uncommonly observed compared to the typical rod and ring structures, are depicted here. These structures are likely going through a folding/unfolding process. They include a bent rod (B), an open ring (C), a spiral-shaped structure possibly composed of a rod and ring linked together (D), a rod curling or uncurling at its end (E), a "sewing pin" or "stem-loop" structure (F), and a "figure 8" structure that may be two rings linked together or one ring folding in 3D space (G). Structures in panels (F) and (G) were previously described by Carcamo et al. (2011).

inhibitors (Carcamo et al., 2011). Figure 2.4A summarizes the putative formation of RR using IMPDH/CTPS inhibitors and the induction time required for the formation of mature RR. Additionally, RR can be induced in cancer cells via glutamine deprivation for 48 h (Carcamo et al., 2013). However, RR are observed in almost 100% of cultured undifferentiated mouse ESCs without the addition of inhibitors or treatment to induce glutamine deprivation. This phenomenon was previously explained by our hypothesis that since mouse ESCs are highly proliferative, their increased intracellular GTP/CTP requirements caused a decrease in the available GTP/CTP pools, which caused RR formation (Carcamo et al., 2011). However, our recent finding that NRK, Ptk2, 3T3, and RAW264.7 cells

exhibit RR formation with no extrinsic manipulation, coupled with similar findings regarding CHO cells by other laboratories (Gunter et al., 2008; Stinton et al., 2013), contradicts our previous hypothesis. While NRK and RAW264.7 cells proliferate very rapidly in our hands, we have not seen a markedly increased proliferation rate in 3T3 or Ptk2 cells compared to human cell lines HeLa or HEp-2. For this reason, RR formation in mouse ESCs may not be solely related to proliferation rate and increased GTP/CTP requirements; there may simply be innate differences in nucleotide metabolism and sensitivity to GTP/CTP levels between rats, mice, marsupials, hamsters, and humans that causes the formation of these structures. RR structures induced with CTPS/IMPDH inhibitors or by glutamine deprivation as well as RR in mESCs and NRK, Ptk2, 3T3, and RAW264.7 cells can be readily detected with patient anti-RR sera or anti-IMPDH2 antibodies, as well as certain anti-CTPS1 antibodies, suggesting that induced RR and native RR are structurally similar. However, it is unclear whether they have the same molecular composition, due to observed differences in the ratio of rods to rings in cells that are induced versus native RR in mESCs. RR, as independent structures, may have different functions, as 90% of RR in ESCs are rings, while cells that are treated with CTPS/IMPDH inhibitors or deprived of glutamine have ~90% rods (Table 2.3). NRK, Ptk2, 3T3, and RAW264.7 cells naturally exhibit the typical ratio of ~90% rods to ~10% rings, indicating that there may be stem cell-specific attributes unrelated to species that cause a unique ratio of these structures. Proliferation is decreased after induction of RR with CTPS/IMPDH inhibitors; this is observed as a clear decrease in the number of mitotic cells after treatment with inhibitors compared to untreated controls. Since ESCs are highly proliferating cells that possess a unique ratio of 9:1 rings to rods, it is possible that the ring is playing a specific role in ESCs that is either nonexistent or utilized to a lesser extent in the other cell lines examined to date. This role may be

Table 2.3 Methods of RR induction and quantification of rods versus rings

Induction method	Cell types	Rods versus rings percentage
IMPDH/CTPS inhibitors	Cancer and primary cells	90% rods
Glutamine deprivation	HeLa	90% rods
Uninduced	NRK, Ptk2, 3T3, RAW264.7	90% rods
Uninduced	Mouse ESCs	90% rings

related to rapid ESC proliferation, which is supported by the fact that IMPDH2 and CTPS1 are known to be required for cell proliferation (Kursula et al., 2006; Sintchak et al., 1996).

4.4. Cytoplasmic versus nuclear rods

In addition to the cytoplasmic RR structures discussed so far, recent data show RR detected within the nucleus. Nuclear RR are observed after treatment with CTPS or IMPDH inhibitors or glutamine deprivation. Although they are located within the nucleus, they may be similar to cytoplasmic RR. Multiple z-stack images of a nucleus containing a short rod clearly demonstrated the structure within the nucleus (Fig. 2.5); additional cells were observed with rings within the nucleus. These rod and ring structures were present within the nucleus and were co-stained by both patient autoantibodies and rabbit anti-IMPDH2 antibody (data not shown). Nuclear rods were determined to range in size from 1.6 to 4.5 μm, while cytoplasmic rods ranged from 2.5 to 16.8 μm when counted from the same cell preparations. Nuclear rods were substantially shorter than cytoplasmic rods; the mean size of cytoplasmic rods was 8.4 μm and the mean size of nuclear rods was 3.2 μm. This was determined by quantitating nuclear and cytoplasmic RR from 66 cells. Although nuclear rods and cytoplasmic rods are highly similar structures, it is unknown whether they have the same function due to the difference in their subcellular locations. Studies suggest that IMPDH binds single-stranded RNA and DNA and modulates localization or degradation of a set of mRNAs (Hedstrom, 2009; McLean et al., 2004).

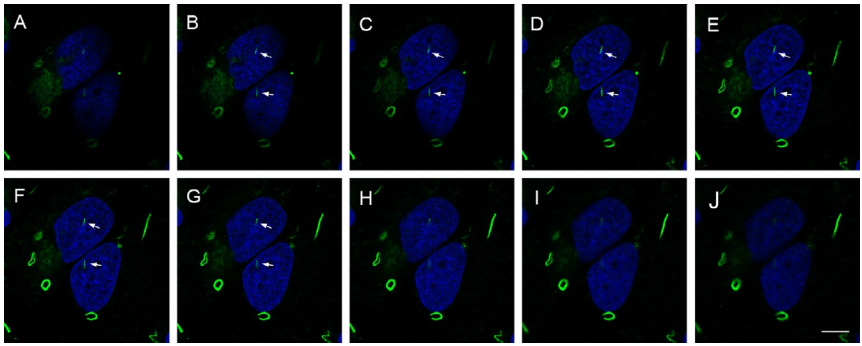

Figure 2.5 Rods and rings in the nucleus. HeLa cells treated with DON form RR detected by human It2006 (green). (A–J) A confocal z-stack cutting shows shorter rods (arrows) within the nucleus (0.39 μm thickness per section). Nuclei are counterstained with DAPI. Scale bar: 5 μm.

4.5. Technical difficulties in rod/ring detection

The study of RR formation and function has been limited by several obstacles. First, detection of RR antibodies in patient serum depends on the commercial antinuclear antibody slides used. Most antinuclear antibody slides do not show RR staining; HEp-2 slides from INOVA Diagnostics, Inc. (San Diego, CA, USA) consistently present RR staining with our prototype anti-RR serum but similar slides from Immuno Concepts (Sacramento, CA, USA) are negative. After determining that RR can be induced with glutamine deprivation, we speculate that RR detected in INOVA slides may be due to techniques used to increase proliferation, which may cause limitations in availability of nutrients in the medium. Additionally, not all antibodies can detect the apparently conformational epitope(s) expressed on the RR structures as compared to monomeric proteins in the cytoplasm. Table 2.2 includes all the antibodies we have tested for their ability to recognize RR on INOVA or homemade slides to date. While all the antibodies can detect monomeric or SDS-denatured proteins by Western blot, only three out of four anti-IMPDH2 antibodies were able to detect RR structures by immunofluorescence. Liu (2010) detected RR-like structures in *Drosophila* using an anti-CTPS1 antibody. However, the same anti-CTPS1 antibody did not detect RR when tested in our laboratory. This was due to variation between lots; not all lots were able to detect RR. Therefore, the inability of an antibody to detect RR does not rule out that target antigen from being a component of the RR structure. It is also noteworthy to indicate that various fixation methods have not affected our ability to properly detect RR structures. Fixation methods including acetone at −20 °C for 5 min, 3:1 acetone:methanol at −20 °C for 10 min, and 3% paraformaldehyde in PBS at room temperature for 10 min followed by 0.1% Triton-X in PBS have all preserved the structure and allowed for proper binding of the antibodies used (Carcamo et al., 2011).

5. IMMUNOBIOLOGY OF RR—AUTOIMMUNE RESPONSE

5.1. Autoantibodies in rheumatic diseases as cellular and molecular probes

Autoantibodies directed against intracellular antigens are a characteristic feature of human autoimmune diseases, such as systemic lupus erythematosus, scleroderma (Fritzler, 1993), and Sjögren's syndrome (Chan and Andrade, 1992), certain malignancies (Covini et al., 1997; Soo Hoo et al., 2002; Zhang et al., 2001), and paraneoplastic syndromes (Satoh et al., 2009;

Tan, 1989; Tan et al., 1988). Studies in systemic rheumatic diseases have provided strong evidence that autoantibodies are produced by antigen-driven responses (Radic and Weigert, 1994; Tan et al., 1988; Tillman et al., 1992) and that autoantibodies can be reporters from the immune system revealing the identity of antigens involved in the autoimmune disease pathogenesis (Tan, 1989). Some of these autoantibodies serve as disease-specific markers and are directed against intracellular macromolecular complexes or particles such as nucleosomes, small nuclear ribonucleoproteins, centromere antigens, and Ro cytoplasmic RNPs (Hardin, 1986; Tan, 1989; Tan et al., 1988). There has been significant progress in identifying many intracellular autoantigens over the last two decades (Satoh et al., 2007, 2009).

The study of human autoantibodies and their use as probes of cell structure and function has had an important impact on the disciplines of molecular and cell biology (Chan and Fritzler, 2013; Tan, 1991). First, the majority of autoantibodies studied have been shown to bind to highly conserved determinants on ubiquitous cellular proteins (Tan, 1989; Tan et al., 1988). Second, many of the autoantibodies associated with systemic rheumatic diseases are often directed to functional macromolecules rather than to structural components. These include DNA, histones, and HMG of the nucleosome and heterochromatin protein HP1 (Furuta et al., 1997), the snRNP complex, various centromere and kinetochore components (CENPs), components of the nucleolus, and other subcellular structures such as Cajal bodies (a.k.a. coiled bodies) (Andrade et al., 1991) and GW bodies (a.k.a. mammalian processing bodies or P bodies) (Fritzler and Chan, 2013; Jakymiw et al., 2006; Yao et al., 2013). Third, in systems amenable to testing, autoantibodies have been shown capable of inhibiting the enzymatic or cellular functions served by the autoantigens. Examples include the inhibition of aminoacylation of transfer RNAs by anti-tRNA synthetase antibodies, the relaxation of supercoiled DNA by anti-topoisomerase I antibodies, inhibition of precursor mRNA splicing by anti-Sm/RNP antibodies, and the inhibition of RNA transcription by anti-RNA polymerases. Taken together, these observations suggest that the conserved epitopes recognized by human autoantibodies are often the functional or active sites of these intracellular proteins (Tan, 1989; Tan et al., 1988). For immunologists, one of the interesting objectives is the identification of macromolecules and organelles, such as the nucleolus (Alderuccio et al., 1991; Chan et al., 1991; Ochs et al., 1996), Golgi complex (Chan and Fritzler, 1998; Eystathioy et al., 2000; Stinton et al., 2004), Cajal bodies (Andrade et al., 1991; Chan et al., 1994), and GW/P

bodies (Chan and Fritzler, 2013; Fritzler and Chan, 2013; Satoh et al., 2013), as targets of autoimmune responses and how this may explain pathogenesis of autoimmune diseases. For cell biologists, attempts to unravel cellular events can be enhanced by the availability of specific autoantibody probes.

5.2. Anti-RR and chronic HCV infection and therapy

HCV is a small positive-sense single-stranded RNA virus that causes acute and chronic hepatitis in humans (Boyer et al., 2002; Hoofnagle, 2002). HCV is one of the major causative agents of liver disease worldwide, with more than 180 million people infected (Alter and Seeff, 2000; Boyer et al., 2002). It is estimated that 3–4 million people are newly infected each year (Boyer et al., 2002). In the United States, HCV-related chronic liver disease is a leading cause of liver transplantation and causes thousands of deaths annually (Charlton, 2001). Although therapeutic options are improving, viral clearance fails in about 80% of infected patients, resulting in a chronic viral disease (Seeff, 1997). In 4–20% of patients with chronic hepatitis, liver cirrhosis develops within 20 years, with 1–5% of these patients developing hepatocellular carcinoma. Persistent HCV infections are facilitated by the ability of the virus to incorporate adaptive mutations in the host and exist as a genetically distinct quasispecies. The persistent infection may also result from the ability of the virus to disrupt host defense by blocking phosphorylation and the function of interferon regulatory factor-3, an antiviral signaling molecule (Foy et al., 2003). Unlike hepatitis A and B viruses, there is no vaccine to prevent HCV infection; therefore, current treatment is a combination therapy of pegylated interferon-alpha (IFN-α) and ribavirin, which results in sustained clearance of serum HCV-RNA. However, this treatment is only efficacious in approximately 50% of patients (Fried et al., 2002; Hadziyannis et al., 2004; Manns et al., 2001) and, as described in further detail below, autoantibodies to RR are most commonly associated with HCV patients who have undergone IFN/ribavirin therapy. Several host factors such as age, stage of liver fibrosis, body mass index, liver steatosis, insulin resistance, ethnicity, IL28B single nucleotide polymorphisms, and viral genotype can potentially influence the treatment outcome (Kau et al., 2008; Smith et al., 2011). For instance, patients with HCV genotypes 2 or 3 respond more favorably to treatment than patients with genotypes 1 or 4 (Simmonds et al., 2005). Therefore, new antiviral compounds that are more effective and more easily tolerated need to be developed. One of the biggest challenges in developing and implementing new therapies for HCV infection is finding the appropriate models to examine the translational capability.

5.2.1 Molecular structure and interactions with HCV

A major breakthrough in HCV research occurred when the complete sequence of the viral genome was identified and cloned by Choo et al. (1989). HCV is the only member of the *Hepacivirus* genus that belongs to the *Flaviviridae* family (Dustin and Rice, 2007; Lauer and Walker, 2001). Structural analysis of the virus revealed that the genetic material is surrounded by a protective nucleocapsid composed mainly of the protein core (C) and further protected by a lipid envelope (Rosenberg, 2001). The lipid envelope contains two major glycoproteins, envelope protein 1 (E1) and E2, that are embedded in the envelope (Op De Beeck and Dubuisson, 2003). The genome consists of a single open reading frame that is ~9600 nucleotides long, which is made into a single polyprotein (3010 or 3033 amino acids) product (Kato, 2000; Ohba et al., 1996). The HCV genome is flanked by two nontranslated regions, which are essential in the replication and synthesis of viral proteins. Viral and cellular proteases mediate the processing of the polyprotein into structural (core, E1, E2, and p7) and nonstructural proteins (NS2, NS3, NS4A, NS4B, NS5A, and NS5B) (Bartenschlager and Lohmann, 2000; Lohmann et al., 1996; Penin et al., 2004). The HCV life cycle is entirely cytoplasmic and replication occurs mainly in hepatocytes, but the virus may also replicate in peripheral blood mononuclear cells. The virus enters the host cells through a complex interaction between virions and cell surface molecules CD81, LDL receptor, scavenger receptor class B type 1, Claudin-1, and Occludin (Bartosch and Cosset, 2006; Cocquerel et al., 2006; Evans et al., 2007; Kohaar et al., 2010). Additionally, Niemann-Pick C1-like 1 cholesterol absorption receptor was identified as a new HCV entry factor (Ray, 2012; Sainz et al., 2012). Once inside the cell, the virus takes over the intracellular machinery to replicate (Lindenbach and Rice, 2005). Due to its high mutation rate caused by the RNA-dependent RNA polymerase, which lacks 3′–5′ exonuclease activity (Pavio and Lai, 2003), HCV is considered a quasispecies composed of six genotypes with several subtypes (Simmonds et al., 2005). The six genotypes have differences in geographic distribution, disease progression, and response to therapy. Genotypes 1, 2, and 3 are distributed worldwide, with genotypes 1a and 1b accounting for 60% of global infections. In the United States, genotypes 1a and 2b are more commonly encountered. What remains unknown is whether any of the HCV proteins are associated with RR or form viral-self protein macromolecular complexes during various stages of pathogenesis, which may explain the apparent specificity of anti-RR with HCV patients.

5.2.2 HCV and autoantibodies

Autoimmune manifestations of HCV include both organ- and nonorgan-specific autoantibodies, seropositivity, and cryoglobulins to immunological diseases such as glomerulonephritis, vasculitis, and mixed cryoglobulinemia (Cresta et al., 1999; Ferri and Zignego, 2000; Hadziyannis, 1997). In chronic HCV infection, smooth muscle antibodies, which react with cytoskeleton antigens of smooth muscle cells, are found in 10–66% of cases. The prevalence of antinuclear antibodies ranges from 6% to 22% and they are usually presented at a low titer (1:40–1:80) (Bortolotti et al., 1996; Kammer et al., 1999; Lenzi et al., 1999; Luo et al., 1998). Anti-liver–kidney–microsomal antibodies, antibodies against epitopes on cytochrome P450, are found in the cytoplasm of hepatocytes and proximal renal tubes. Anti-liver–kidney–microsomal antibodies are detected in up to 10% of chronic HCV patients (Drygiannakis et al., 2001). Other antibodies such as anti-asialoglycoprotein receptor, antiliver membrane antigen, antiliver cytosol antigen, antihepatocyte plasma membrane, antithyroglobulin, antithyroid peroxidase, antithyroid microsome, antiphospholipid, antineutrophil cytoplasmic, and many other autoantibodies have also been described in patients with HCV infection (Dammacco et al., 2000; McMurray and Elbourne, 1997; Obermayer-Straub and Manns, 2001). Although the roles of these antibodies are unclear, each antibody is directed against a certain intracellular antigen probably released during cell death and presented to the immune system. Most studies have not observed significant differences in clinical and biochemical parameters between chronic HCV patients with or without positive serum autoantibodies (Luo et al., 1998; Valentini et al., 1999).

5.3. Autoimmune response to rod/ring structures in HCV infection

There are few reports to date that have examined the potential role of anti-RR antibodies in the overall immune response of hepatitis C patients. However, these few reports agree upon the notion that anti-RR antibodies seem to have an almost exclusive presence in hepatitis C patients that have undergone IFN/R therapy. That is, anti-RR antibodies are not seen in healthy individuals or hepatitis C patients that have yet to be treated; this finding was recently re-affirmed by Stinton et al. (2013), who did not observe anti-RR antibodies in any of the 301 untreated HCV patients that they screened. One of the first studies on anti-RR *in vivo* actually examined the presence of anti-IMPDH2 antibodies by ELISA in various patient groups (Seelig et al., 2011). They reported that anti-IMPDH2 antibodies

are more prevalent in HCV-RNA carriers (35.2%, $n=108$) and anti-actin-positive patients suspected of autoimmune hepatitis (31%, $n=42$) than in HBV-DNA-positive patients (6.2%, $n=113$), hospitalized HCV-RNA-negative patients (5%, $n=100$), patients with antinuclear antibodies (13.7%, $n=51$), suspected primary biliary cirrhosis patients with type M2 antimitochondrial antibodies (3.2%, $n=31$), and healthy individuals (2%, $n=100$) (Seelig et al., 2011). It should be emphasized that the ELISA did not exactly measure anti-RR antibodies, but anti-IMPDH2 antibodies instead, and so this information is useful but does not tell a complete story. The authors suggest that the higher prevalence of anti-IMPDH2 in HCV-RNA carriers is potentially related to the polymerization of RR caused by ribavirin that is seen *in vitro*, but a direct link between the two cannot be made from these data. The next major finding on anti-RR *in vivo* was that these antibodies are more prevalent in patients that do not respond to therapy or relapse after therapy than in patients who clear the virus (33% vs. 11%, $p=0.037$) (Covini et al., 2012). In a follow-up study by Carcamo et al., two separate cohorts of HCV patients were examined. In a patient cohort from the United States, anti-RR titers were significantly higher in nonresponders/relapsers (median = 1:3200) than in responders (1:100, $p=0.0016$), while titers in Italian patients were shown to be elevated in relapsers versus nonresponders ($p=0.0040$) and responders ($p=0.015$) (Carcamo et al., 2013). A third report from Brazil by Keppeke et al. confirmed the previous reports of exclusivity of this antibody to HCV and also found that 38% of HCV patients ($n=108$) treated with IFN/R were positive for anti-RR, while patients on an interferon-α-only regimen ($n=23$) or ribavirin-only regimen ($n=3$) did not present these antibodies. This group also found that anti-RR-positive HCV patients retained their positivity for at least 6–12 months after the discontinuation of IFN/R therapy (Keppeke et al., 2012). Thus far, studies have shown that anti-RR autoantibodies do not appear to be associated with certain ethnicities, as these autoantibodies have been found in Italians as well as various ethnicities of Americans and Brazilians.

5.4. Clinical implications of anti-rods/rings autoantibodies

Examination of the clinical implications of anti-RR autoantibodies has proven to be complicated thus far, as there are some reported cases that contradict the generally accepted idea that these antibodies are unique to HCV patients who have undergone IFN/R therapy. In a preliminary study by

Carcamo et al. (2009), about 30% of 23 sera positive for anti-RR were negative for HCV. However, since that study, published data have not proved any non-HCV patients to be positive for anti-RR; although ~0.8% of 4754 patients examined during the National Health and Nutrition Examination Survey (NHANES) showed positive for anti-RR, the detailed medical histories of these patients were not examined for history of hepatitis C (Satoh et al., 2012). Therefore, the only recent exception to this trend is the appearance of anti-RR antibodies in one HCV-negative patient suffering from systemic lupus erythematosus (Calise et al., 2014). Despite this information, there is still strong evidence of a role for anti-RR autoantibodies in HCV, as anti-RR antibodies were detected at a higher rate in nonresponding/relapsing patients than in patients who responded to therapy (33% vs. 11%, $p = 0.037$) (Covini et al., 2012), as was mentioned in the previous section. Additionally, extreme differences in anti-RR titers between confirmed HCV patients (1:50 to >1:819,200) (Calise et al., 2014; Carcamo et al., 2014) and potentially healthy patients from the NHANES study (1:80 to 1:1280) remain unexplained (Satoh et al., 2012). Although these initial reports on anti-RR autoantibodies have advanced our overall knowledge of the RR structure and its potential to play numerous roles in humans, not enough evidence has been gathered to assign any diagnostic or prognostic value to anti-RR antibodies or the structure itself.

5.4.1 Ribavirin as a therapeutic agent

Ribavirin is believed to be the cause of RR formation in HCV patients who have undergone months of therapeutic exposure, leading to the production of anti-RR autoantibodies. Due to ribavirin induction of RR in tissue culture cells (Carcamo et al., 2011; Gunter et al., 2008), it is unknown whether ribavirin alone or the coexposure to interferon in HCV treatment is required for the production of anti-RR in selected patients. Ribavirin is only approved for the treatment of HCV, but it is currently in trial for the treatment of other viral infections. Although there are a few cases of patients with anti-RR antibodies that do not have HCV, the presence of anti-RR antibodies in HCV patients is highly correlated with the effects of ribavirin treatment, which leads to RR formation and stimulation of the host immune system.

5.4.2 MPA as a therapeutic agent

MPA (commonly marketed as the prodrug mycophenolate mofetil, or MMF) is currently used for the treatment of systemic lupus erythematosus and to prevent organ rejection after transplantation. Although MPA has

been shown to induce RR formation *in vitro*, lupus patients treated with MPA do not develop anti-RR antibodies, with just one exception to date; a single lupus patient, negative for HCV, HBV, and other infectious diseases, consistently tested positive for anti-RR autoantibodies at titers up to 1:1600 over a period of 4 years (Calise et al., 2014). Interestingly, lupus patients are also often continuously exposed to type I interferon, the cytokine that plays a major role in the disease pathogenesis (Baechler et al., 2003; Bennett et al., 2003). Thus, continuous exposure of interferon does not help induce anti-RR antibodies in lupus patients undergoing MPA treatment. This suggests that this specific inhibitor of IMPDH alone or together with endogenous interferon is not sufficient to induce anti-RR autoantibody formation.

6. CONCLUDING REMARKS AND FUTURE PERSPECTIVES

Recent studies show that mammalian cells cluster critical enzymes into RR as a metabolic response to decreased intracellular GTP and/or CTP pools, although the mechanism of formation and function(s) of RR are not completely understood. RR contain two nucleotide biosynthetic enzymes, CTPS and IMPDH, but we speculate that these structures may be composed of other enzymes of the same pathways. This hypothesis is based in part on the relatively large physical dimensions of the structure and on the fact that there are anti-RR autoantibodies from many HCV patients that do not appear to recognize CTPS or IMPDH. Assembly of both CTPS and IMPDH may be due to the close interaction between both enzymes during nucleotide biosynthesis. Many studies suggest the possibility of a conserved RR structure composed of nucleotide biosynthetic enzymes that is sensitive to lowered levels of GTP/CTP.

Our identification of abundant RR in mouse undifferentiated ESCs, as well as Ptk2, NRK, 3T3, and RAW264.7 cells, is intriguing as these structures are found without apparent extrinsic manipulation. Chen et al. have described the effects of DON on the filaments and *Drosophila* oogenesis, suggesting a biological function in development, which may contribute to the reasoning behind the presence of RR in ESCs (Chen et al., 2011). Our group has also identified that a percentage of HCV patients treated with IFN/R produce autoantibodies against RR. Covini et al. (2012) examined the prevalence of anti-RR antibodies in other diseases and concluded that anti-RR antibodies are highly specific to HCV patients after treatment, but not before treatment. Anti-RR antibodies were determined to be more prevalent in patients that do not respond to therapy. Since HCV patients

are treated with ribavirin and it has been shown that ribavirin can induce RR formation *in vitro* (Carcamo et al., 2011; Gunter et al., 2008), ribavirin treatment in HCV patients may cause RR formation, which leads to the induction of autoantibodies against these structures when they are released to the host immune system during cell turnover. Studies thus far imply that RR structures have novel clinical and biological significance.

RR were identified using human autoantibodies produced by HCV patients treated with IFN/R. HCV patients that do not respond to therapy or relapse tend to have higher anti-RR antibody titers. RR were determined to be composed of nucleotide biosynthesis enzymes CTPS1 and IMPDH2. RR formed from the inhibition of CTPS1 or IMPDH2 or in response to glutamine deprivation are consistently correlated with a decrease in intracellular levels of CTP/GTP. Therefore, RR may represent polymerization of nucleotide biosynthetic enzymes in response to a decrease in intracellular CTP or GTP levels in order to return CTP/GTP levels to an optimal level for cellular function. While current evidence strongly supports our working hypothesis, further experiments are required to ascertain the details of this highly complex metabolic process.

ACKNOWLEDGMENTS

Many undergraduates and other fellows have participated in the development of this research and their contributions are acknowledged: Erwin Lam, Natasha Deming, Pabina Dhawan, Yasmany Dominguez, Steven J. Ross, Brad Pauley, Stephanie Tamayo, Claire Krueger, Gerson Keppeke, Joyce Yin, and Hyun-Min Jung. We also thank many collaborators who have spent their valuable time and effort providing invaluable discussion and/or reagents: Luis E. C. Andrade, Nicola Bizzaro, Angela Ceribelli, Giovanni Covini, Marvin J. Fritzler, Hideko Kasahara, Chen Liu, Daniel L. Purich, Naohiro Terada, and Maria Zajac-Kaye.

REFERENCES

Alderuccio, F., Chan, E.K.L., Tan, E.M., 1991. Molecular characterization of an autoantigen of PM-Scl in the polymyositis/scleroderma overlap syndrome: a unique and complete human cDNA encoding an apparent 75-kD acidic protein of the nucleolar complex. J. Exp. Med. 173, 941–952.

Allison, A.C., Eugui, E.M., 1993. Immunosuppressive and other effects of mycophenolic acid and an ester prodrug, mycophenolate mofetil. Immunol. Rev. 136, 5–28.

Alter, H.J., Seeff, L.B., 2000. Recovery, persistence, and sequelae in hepatitis C virus infection: a perspective on long-term outcome. Semin. Liver Dis. 20, 17–35.

An, S., Kumar, R., Sheets, E.D., Benkovic, S.J., 2008. Reversible compartmentalization of de novo purine biosynthetic complexes in living cells. Science 320, 103–106.

Andrade, L.E.C., Chan, E.K.L., Raska, I., Peebles, C.L., Roos, G., Tan, E.M., 1991. Human autoantibody to a novel protein of the nuclear coiled body: immunological characterization and cDNA cloning of p80-coilin. J. Exp. Med. 173, 1407–1419.

Azzam, G., Liu, J.L., 2013. Only one isoform of Drosophila melanogaster CTP synthase forms the cytoophidium. PLoS Genet. 9, e1003256.
Baechler, E.C., Batliwalla, F.M., Karypis, G., Gaffney, P.M., Ortmann, W.A., Espe, K.J., et al., 2003. Interferon-inducible gene expression signature in peripheral blood cells of patients with severe lupus. Proc. Natl. Acad. Sci. U.S.A. 100, 2610–2615.
Bartenschlager, R., Lohmann, V., 2000. Replication of hepatitis C virus. J. Gen. Virol. 81, 1631–1648.
Bartosch, B., Cosset, F.L., 2006. Cell entry of hepatitis C virus. Virology 348, 1–12.
Bateman, A., 1997. The structure of a domain common to archaebacteria and the homocystinuria disease protein. Trends Biochem. Sci. 22, 12–13.
Beaty, N.B., Lane, M.D., 1983. Kinetics of activation of acetyl-CoA carboxylase by citrate. Relationship to the rate of polymerization of the enzyme. J. Biol. Chem. 258, 13043–13050.
Bennett, L., Palucka, A.K., Arce, E., Cantrell, V., Borvak, J., Banchereau, J., et al., 2003. Interferon and granulopoiesis signatures in systemic lupus erythematosus blood. J. Exp. Med. 197, 711–723.
Bortolotti, F., Vajro, P., Balli, F., Giacchino, R., Crivellaro, C., Barbera, C., et al., 1996. Non-organ specific autoantibodies in children with chronic hepatitis C. J. Hepatol. 25, 614–620.
Bowne, S.J., Sullivan, L.S., Blanton, S.H., Cepko, C.L., Blackshaw, S., Birch, D.G., et al., 2002. Mutations in the inosine monophosphate dehydrogenase 1 gene (IMPDH1) cause the RP10 form of autosomal dominant retinitis pigmentosa. Hum. Mol. Genet. 11, 559–568.
Bowne, S.J., Sullivan, L.S., Mortimer, S.E., Hedstrom, L., Zhu, J., Spellicy, C.J., et al., 2006. Spectrum and frequency of mutations in IMPDH1 associated with autosomal dominant retinitis pigmentosa and leber congenital amaurosis. Invest. Ophthalmol. Vis. Sci. 47, 34–42.
Boyer, J.L., Chang, E.B., Collyar, D.E., DeLeve, L.D., Feinberg, J., Judge, T.A., et al., 2002. National Institutes of Health Consensus Development Conference Statement: management of hepatitis C 2002 (June 10-12, 2002). Gastroenterology 123, 2082–2099.
Calise, S.J., Carcamo, W.C., Ceribelli, A., Dominguez, Y., Satoh, M., Chan, E.K.L., 2014. Antibodies to rods and rings. In: Shoenfeld, Y., Gershwin, M.E., Meroni, P.L. (Eds.), Autoantibodies. Elsevier Science, San Diego, CA.
Carcamo, W.C., Yao, B., Satoh, M., Reeves, W.H., Liu, C., Covini, G., et al., 2009. Cytoplasmic rings/rods as autoimmune targets of emerging human autoantibodies associated with HCV virus infection and interferon therapy. In: Conrad, K., Chan, E.K.L., Fritzler, M.J., Humbel, R.L., von Landenberg, P., Shoenfeld, Y. (Eds.), From Pathogenesis to Therapy of Autoimmune Diseases. Pabst Science Publishers, Lengerich, Germany, pp. 127–134.
Carcamo, W.C., Satoh, M., Kasahara, H., Terada, N., Hamazaki, T., Chan, J.Y., et al., 2011. Induction of cytoplasmic rods and rings structures by inhibition of the CTP and GTP synthetic pathway in mammalian cells. PLoS One 6, e29690.
Carcamo, W.C., Calise, S.J., Krueger, C.E., Purich, D.L., Chan, E.K.L., 2014. Glutamine deprivation initiates reversible assembly of cytoplasmic rods and rings. Cell. Mol. Life Sci., in revision.
Carcamo, W.C., Ceribelli, A., Calise, S.J., Krueger, C., Liu, C., Daves, M., et al., 2013. Differential reactivity to IMPDH2 by anti-rods/rings autoantibodies and unresponsiveness to pegylated interferon-alpha/ribavirin therapy in US and Italian HCV patients. J. Clin. Immunol. 33, 420–426.
Chan, E.K.L., Andrade, L.E.C., 1992. Antinuclear antibodies in Sjogren's syndrome. Rheum. Dis. Clin. North Am. 18, 551–570.

Chan, E.K.L., Fritzler, M.J., 1998. Autoantibodies to Golgi Apparatus antigens. In: Conrad, K., Humbel, R.L., Meurer, M., Shoenfeld, Y., Tan, E.M. (Eds.), Pathogenic and Diagnostic Relevance of Autoantibodies. Proceedings of the 4th Dresden Symposium on Autoantibodies. Pabst Science Publishers, Scottsdale, AZ, pp. 85–100.

Chan, E.K.L., Fritzler, M.J., 2013. Introduction: the GW body story as an example of autoantibodies with significant impacts to molecular cell biology. Adv. Exp. Med. Biol. 768, 1–4.

Chan, E.K.L., Imai, H., Hamel, J.C., Tan, E.M., 1991. Human autoantibody to RNA polymerase I transcription factor hUBF. Molecular identity of nucleolus organizer region autoantigen NOR-90 and ribosomal RNA transcription upstream binding factor. J. Exp. Med. 174, 1239–1244.

Chan, E.K.L., Takano, S., Andrade, L.E., Hamel, J.C., Matera, A.G., 1994. Structure, expression and chromosomal localization of human p80-coilin gene. Nucleic Acids Res. 22, 4462–4469.

Charlton, M., 2001. Hepatitis C infection in liver transplantation. Am. J. Transplant. 1, 197–203.

Chen, K., Zhang, J., Tastan, O.Y., Deussen, Z.A., Siswick, M.Y., Liu, J.L., 2011. Glutamine analogs promote cytoophidium assembly in human and Drosophila cells. J. Genet. Genomics 38, 391–402.

Choo, Q.L., Kuo, G., Weiner, A.J., Overby, L.R., Bradley, D.W., Houghton, M., 1989. Isolation of a cDNA clone derived from a blood-borne non-A, non-B viral hepatitis genome. Science 244, 359–362.

Cocquerel, L., Voisset, C., Dubuisson, J., 2006. Hepatitis C virus entry: potential receptors and their biological functions. J. Gen. Virol. 87, 1075–1084.

Colby, T.D., Vanderveen, K., Strickler, M.D., Markham, G.D., Goldstein, B.M., 1999. Crystal structure of human type II inosine monophosphate dehydrogenase: implications for ligand binding and drug design. Proc. Natl. Acad. Sci. U.S.A. 96, 3531–3536.

Covini, G., Chan, E.K.L., Nishioka, M., Morshed, S.A., Reed, S.I., Tan, E.M., 1997. Immune response to cyclin B1 in hepatocellular carcinoma. Hepatology 25, 75–80.

Covini, G., Carcamo, W.C., Bredi, E., von Muhlen, C.A., Colombo, M., Chan, E.K.L., 2012. Cytoplasmic rods and rings autoantibodies developed during pegylated interferon and ribavirin therapy in patients with chronic hepatitis C. Antivir. Ther. 17, 805–811.

Cresta, P., Musset, L., Cacoub, P., Frangeul, L., Vitour, D., Poynard, T., et al., 1999. Response to interferon alpha treatment and disappearance of cryoglobulinaemia in patients infected by hepatitis C virus. Gut 45, 122–128.

Dammacco, F., Sansonno, D., Piccoli, C., Racanelli, V., D'Amore, F.P., Lauletta, G., 2000. The lymphoid system in hepatitis C virus infection: autoimmunity, mixed cryoglobulinemia, and Overt B-cell malignancy. Semin. Liver Dis. 20, 143–157.

Dereuddre-Bosquet, N., Roy, B., Routledge, K., Clayette, P., Foucault, G., Lepoivre, M., 2004. Inhibitors of CTP biosynthesis potentiate the anti-human immunodeficiency virus type 1 activity of 3TC in activated peripheral blood mononuclear cells. Antiviral Res. 61, 67–70.

Drygiannakis, D., Lionis, C., Drygiannakis, I., Pappas, G., Kouroumalis, E., 2001. Low prevalence of liver-kidney microsomal autoantibodies of type 1 (LKM1) in hepatitis C seropositive subjects on Crete, Greece. BMC Gastroenterol. 1, 4.

Dustin, L.B., Rice, C.M., 2007. Flying under the radar: the immunobiology of hepatitis C. Annu. Rev. Immunol. 25, 71–99.

Evans, M.J., von Hahn, T., Tscherne, D.M., Syder, A.J., Panis, M., Wolk, B., et al., 2007. Claudin-1 is a hepatitis C virus co-receptor required for a late step in entry. Nature 446, 801–805.

Eystathioy, T., Jakymiw, A., Fujita, D.J., Fritzler, M.J., Chan, E.K.L., 2000. Human autoantibodies to a novel Golgi protein golgin-67: high similarity with golgin-95/gm 130 autoantigen. J. Autoimmun. 14, 179–187.
Eystathioy, T., Chan, E.K.L., Tenenbaum, S.A., Keene, J.D., Griffith, K., Fritzler, M.J., 2002. A phosphorylated cytoplasmic autoantigen, GW182, associates with a unique population of human mRNAs within novel cytoplasmic speckles. Mol. Biol. Cell 13, 1338–1351.
Ferri, C., Zignego, A.L., 2000. Relation between infection and autoimmunity in mixed cryoglobulinemia. Curr. Opin. Rheumatol. 12, 53–60.
Foy, E., Li, K., Wang, C., Sumpter Jr., R., Ikeda, M., Lemon, S.M., et al., 2003. Regulation of interferon regulatory factor-3 by the hepatitis C virus serine protease. Science 300, 1145–1148.
Franklin, T.J., Cook, J.M., 1969. The inhibition of nucleic acid synthesis by mycophenolic acid. Biochem. J. 113, 515–524.
Fried, M.W., Shiffman, M.L., Reddy, K.R., Smith, C., Marinos, G., Goncales Jr., F.L., et al., 2002. Peginterferon alfa-2a plus ribavirin for chronic hepatitis C virus infection. N. Engl. J. Med. 347, 975–982.
Fritzler, M.J., 1993. Autoantibodies in scleroderma. J. Dermatol. 20, 257–268.
Fritzler, M.J., Chan, E.K.L., 2013. The discovery of GW bodies. Adv. Exp. Med. Biol. 768, 5–21.
Furuta, K., Chan, E.K.L., Kiyosawa, K., Reimer, G., Luderschmidt, C., Tan, E.M., 1997. Heterochromatin protein HP1Hsbeta (p25beta) and its localization with centromeres in mitosis. Chromosoma 106, 11–19.
Gunter, J.H., Thomas, E.C., Lengefeld, N., Kruger, S.J., Worton, L., Gardiner, E.M., et al., 2008. Characterisation of inosine monophosphate dehydrogenase expression during retinal development: differences between variants and isoforms. Int. J. Biochem. Cell Biol. 40, 1716–1728.
Hadziyannis, S.J., 1997. The spectrum of extrahepatic manifestations in hepatitis C virus infection. J. Viral Hepat. 4, 9–28.
Hadziyannis, S.J., Sette Jr., H., Morgan, T.R., Balan, V., Diago, M., Marcellin, P., et al., 2004. Peginterferon-alpha2a and ribavirin combination therapy in chronic hepatitis C: a randomized study of treatment duration and ribavirin dose. Ann. Intern. Med. 140, 346–355.
Hardin, J.A., 1986. The lupus autoantigens and the pathogenesis of systemic lupus erythematosus. Arthritis Rheum. 29, 457–460.
Hedstrom, L., 2009. IMP dehydrogenase: structure, mechanism, and inhibition. Chem. Rev. 109, 2903–2928.
Hofer, A., Steverding, D., Chabes, A., Brun, R., Thelander, L., 2001. Trypanosoma brucei CTP synthetase: a target for the treatment of African sleeping sickness. Proc. Natl. Acad. Sci. U.S.A. 98, 6412–6416.
Hong, Z., Cameron, C.E., 2002. Pleiotropic mechanisms of ribavirin antiviral activities. Prog. Drug Res. 59, 41–69.
Hoofnagle, J.H., 2002. Course and outcome of hepatitis C. Hepatology 36, S21–S29.
Ignoul, S., Eggermont, J., 2005. CBS domains: structure, function, and pathology in human proteins. Am. J. Physiol. Cell Physiol. 289, C1369–C1378.
Ingerson-Mahar, M., Briegel, A., Werner, J.N., Jensen, G.J., Gitai, Z., 2010. The metabolic enzyme CTP synthase forms cytoskeletal filaments. Nat. Cell Biol. 12, 739–746.
Jackson, R.C., Weber, G., Morris, H.P., 1975. IMP dehydrogenase, an enzyme linked with proliferation and malignancy. Nature 256, 331–333.
Jakymiw, A., Ikeda, K., Fritzler, M.J., Reeves, W.H., Satoh, M., Chan, E.K.L., 2006. Autoimmune targeting of key components of RNA interference. Arthritis Res. Ther. 8, R87.

Jakymiw, A., Pauley, K.M., Li, S., Ikeda, K., Lian, S., Eystathioy, T., et al., 2007. The role of GW/P-bodies in RNA processing and silencing. J. Cell Sci. 120, 1317–1323.
Ji, Y., Gu, J., Makhov, A.M., Griffith, J.D., Mitchell, B.S., 2006. Regulation of the interaction of inosine monophosphate dehydrogenase with mycophenolic acid by GTP. J. Biol. Chem. 281, 206–212.
Kammer, A.R., van der Burg, S.H., Grabscheid, B., Hunziker, I.P., Kwappenberg, K.M., Reichen, J., et al., 1999. Molecular mimicry of human cytochrome P450 by hepatitis C virus at the level of cytotoxic T cell recognition. J. Exp. Med. 190, 169–176.
Kato, N., 2000. Genome of human hepatitis C virus (HCV): gene organization, sequence diversity, and variation. Microb. Comp. Genomics 5, 129–151.
Kau, A., Vermehren, J., Sarrazin, C., 2008. Treatment predictors of a sustained virologic response in hepatitis B and C. J. Hepatol. 49, 634–651.
Kemp, B.E., 2004. Bateman domains and adenosine derivatives form a binding contract. J. Clin. Invest. 113, 182–184.
Kennan, A., Aherne, A., Palfi, A., Humphries, M., McKee, A., Stitt, A., et al., 2002. Identification of an IMPDH1 mutation in autosomal dominant retinitis pigmentosa (RP10) revealed following comparative microarray analysis of transcripts derived from retinas of wild-type and Rho(-/-) mice. Hum. Mol. Genet. 11, 547–557.
Keppeke, G.D., Nunes, E., Ferraz, M.L., Silva, E.A., Granato, C., Chan, E.K.L., et al., 2012. Longitudinal Study of a Human Drug-Induced Model of Autoantibody to Cytoplasmic Rods/Rings following HCV Therapy with Ribavirin and Interferon-alpha. PLoS One 7, e45392.
Kleinschmidt, A.K., Moss, J., Lane, D.M., 1969. Acetyl coenzyme A carboxylase: filamentous nature of the animal enzymes. Science 166, 1276–1278.
Kohaar, I., Ploss, A., Korol, E., Mu, K., Schoggins, J.W., O'Brien, T.R., et al., 2010. Splicing diversity of the human OCLN gene and its biological significance for hepatitis C virus entry. J. Virol. 84, 6987–6994.
Kursula, P., Flodin, S., Ehn, M., Hammarstrom, M., Schuler, H., Nordlund, P., et al., 2006. Structure of the synthetase domain of human CTP synthetase, a target for anticancer therapy. Acta Crystallogr. Sect. F Struct. Biol. Cryst. Commun. 62, 613–617.
Lauer, G.M., Walker, B.D., 2001. Hepatitis C virus infection. N. Engl. J. Med. 345, 41–52.
Lenzi, M., Bellentani, S., Saccoccio, G., Muratori, P., Masutti, F., Muratori, L., et al., 1999. Prevalence of non-organ-specific autoantibodies and chronic liver disease in the general population: a nested case-control study of the Dionysos cohort. Gut 45, 435–441.
Lindenbach, B.D., Rice, C.M., 2005. Unravelling hepatitis C virus replication from genome to function. Nature 436, 933–938.
Liu, J.L., 2010. Intracellular compartmentation of CTP synthase in Drosophila. J. Genet. Genomics 37, 281–296.
Liu, J.L., 2011. The enigmatic cytoophidium: compartmentation of CTP synthase via filament formation. Bioessays 33, 159–164.
Liu, J.L., Gall, J.G., 2007. U bodies are cytoplasmic structures that contain uridine-rich small nuclear ribonucleoproteins and associate with P bodies. Proc. Natl. Acad. Sci. U.S.A. 104, 11655–11659.
Lohmann, V., Koch, J.O., Bartenschlager, R., 1996. Processing pathways of the hepatitis C virus proteins. J. Hepatol. 24, 11–19.
Luo, J.C., Hwang, S.J., Li, C.P., Lu, R.H., Chan, C.Y., Wu, J.C., et al., 1998. Clinical significance of serum auto-antibodies in Chinese patients with chronic hepatitis C: negative role of serum viral titre and genotype. J. Gastroenterol. Hepatol. 13, 475–479.
Manns, M.P., McHutchison, J.G., Gordon, S.C., Rustgi, V.K., Shiffman, M., Reindollar, R., et al., 2001. Peginterferon alfa-2b plus ribavirin compared with interferon alfa-2b plus ribavirin for initial treatment of chronic hepatitis C: a randomised trial. Lancet 358, 958–965.

McLean, J.E., Hamaguchi, N., Belenky, P., Mortimer, S.E., Stanton, M., Hedstrom, L., 2004. Inosine 5'-monophosphate dehydrogenase binds nucleic acids in vitro and in vivo. Biochem. J. 379, 243–251.
McMurray, R.W., Elbourne, K., 1997. Hepatitis C virus infection and autoimmunity. Semin. Arthritis Rheum. 26, 689–701.
Narayanaswamy, R., Levy, M., Tsechansky, M., Stovall, G.M., O'Connell, J.D., Mirrielees, J., et al., 2009. Widespread reorganization of metabolic enzymes into reversible assemblies upon nutrient starvation. Proc. Natl. Acad. Sci. U.S.A. 106, 10147–10152.
Noree, C., Sato, B.K., Broyer, R.M., Wilhelm, J.E., 2010. Identification of novel filament-forming proteins in Saccharomyces cerevisiae and Drosophila melanogaster. J. Cell Biol. 190, 541–551.
Obermayer-Straub, P., Manns, M.P., 2001. Hepatitis C and D, retroviruses and autoimmune manifestations. J. Autoimmun. 16, 275–285.
Ochs, R.L., Stein Jr., T.W., Chan, E.K.L., Ruutu, M., Tan, E.M., 1996. cDNA cloning and characterization of a novel nucleolar protein. Mol. Biol. Cell 7, 1015–1024.
O'Connell, J.D., Zhao, A., Ellington, A.D., Marcotte, E.M., 2012. Dynamic reorganization of metabolic enzymes into intracellular bodies. Annu. Rev. Cell Dev. Biol. 28, 89–111.
Ohba, K., Mizokami, M., Lau, J.Y., Orito, E., Ikeo, K., Gojobori, T., 1996. Evolutionary relationship of hepatitis C, pesti-, flavi-, plantviruses, and newly discovered GB hepatitis agents. FEBS Lett. 378, 232–234.
Op De Beeck, A., Dubuisson, J., 2003. Topology of hepatitis C virus envelope glycoproteins. Rev. Med. Virol. 13, 233–241.
Pavio, N., Lai, M.M., 2003. The hepatitis C virus persistence: how to evade the immune system? J. Biosci. 28, 287–304.
Penin, F., Dubuisson, J., Rey, F.A., Moradpour, D., Pawlotsky, J.M., 2004. Structural biology of hepatitis C virus. Hepatology 39, 5–19.
Pimkin, M., Markham, G.D., 2008. The CBS subdomain of inosine 5'-monophosphate dehydrogenase regulates purine nucleotide turnover. Mol. Microbiol. 68, 342–359.
Probst, C., Radzimski, C., Blocker, I.M., Teegen, B., Bogdanos, D.P., Stocker, W., et al., 2013. Development of a recombinant cell-based indirect immunofluorescence assay (RC-IFA) for the determination of autoantibodies against "rings and rods"-associated inosine-5'-monophosphate dehydrogenase 2 in viral hepatitis C. Clin. Chim. Acta 418, 91–96.
Radic, M.Z., Weigert, M., 1994. Genetic and structural evidence for antigen selection of anti-DNA antibodies. Annu. Rev. Immunol. 12, 487–520.
Ramer, M.S., Cruz Cabrera, M.A., Alan, N., Scott, A.L., Inskip, J.A., 2010. A new organellar complex in rat sympathetic neurons. PLoS One 5, e10872.
Ray, K., 2012. Hepatitis: NPC1L1 identified as a novel HCV entry factor. Nat. Rev. Gastroenterol. Hepatol. 9, 124.
Rosenberg, S., 2001. Recent advances in the molecular biology of hepatitis C virus. J. Mol. Biol. 313, 451–464.
Sainz Jr., B., Barretto, N., Martin, D.N., Hiraga, N., Imamura, M., Hussain, S., et al., 2012. Identification of the Niemann-Pick C1-like 1 cholesterol absorption receptor as a new hepatitis C virus entry factor. Nat. Med. 18, 281–285.
Satoh, M., Chan, E.K.L., Sobel, E.S., Kimpel, D.L., Yamasaki, Y., Narain, S., et al., 2007. Clinical implication of autoantibodies in patients with systemic rheumatic diseases. Expert Rev. Clin. Immunol. 3, 721–738.
Satoh, M., Vazquez-Del Mercado, M., Chan, E.K.L., 2009. Clinical interpretation of antinuclear antibody tests in systemic rheumatic diseases. Mod. Rheumatol. 19, 219–228.
Satoh, M., Chan, E.K.L., Ho, L.A., Rose, K.M., Parks, C.G., Cohn, R.D., et al., 2012. Prevalence and sociodemographic correlates of antinuclear antibodies in the United States. Arthritis Rheum. 64, 2319–2327.

Satoh, M., Chan, J.Y., Ceribelli, A., Del-Mercado, M.V., Chan, E.K.L., 2013. Autoantibodies to argonaute 2 (Su antigen). Adv. Exp. Med. Biol. 768, 45–59.
Schneiter, R., Hitomi, M., Ivessa, A.S., Fasch, E.V., Kohlwein, S.D., Tartakoff, A.M., 1996. A yeast acetyl coenzyme A carboxylase mutant links very-long-chain fatty acid synthesis to the structure and function of the nuclear membrane-pore complex. Mol. Cell. Biol. 16, 7161–7172.
Scott, J.W., Hawley, S.A., Green, K.A., Anis, M., Stewart, G., Scullion, G.A., et al., 2004. CBS domains form energy-sensing modules whose binding of adenosine ligands is disrupted by disease mutations. J. Clin. Invest. 113, 274–284.
Seeff, L.B., 1997. Natural history of hepatitis C. Hepatology 26, 21S–28S.
Seelig, H.P., Appelhans, H., Bauer, O., Bluthner, M., Hartung, K., Schranz, P., et al., 2011. Autoantibodies against inosine-5'-monophosphate dehydrogenase 2–characteristics and prevalence in patients with HCV-infection. Clin. Lab. 57, 753–765.
Simmonds, P., Bukh, J., Combet, C., Deleage, G., Enomoto, N., Feinstone, S., et al., 2005. Consensus proposals for a unified system of nomenclature of hepatitis C virus genotypes. Hepatology 42, 962–973.
Sintchak, M.D., Fleming, M.A., Futer, O., Raybuck, S.A., Chambers, S.P., Caron, P.R., et al., 1996. Structure and mechanism of inosine monophosphate dehydrogenase in complex with the immunosuppressant mycophenolic acid. Cell 85, 921–930.
Smith, K.R., Suppiah, V., O'Connor, K., Berg, T., Weltman, M., Abate, M.L., et al., 2011. Identification of improved IL28B SNPs and haplotypes for prediction of drug response in treatment of hepatitis C using massively parallel sequencing in a cross-sectional European cohort. Genome Med. 3, 57.
Soo Hoo, L., Zhang, J.Y., Chan, E.K.L., 2002. Cloning and characterization of a novel 90 kDa 'companion' auto-antigen of p62 overexpressed in cancer. Oncogene 21, 5006–5015.
Stinton, L.M., Eystathioy, T., Selak, S., Chan, E.K.L., Fritzler, M.J., 2004. Autoantibodies to protein transport and messenger RNA processing pathways: endosomes, lysosomes, Golgi complex, proteasomes, assemblyosomes, exosomes, and GW bodies. Clin. Immunol. 110, 30–44.
Stinton, L.M., Myers, R.P., Coffin, C.S., Fritzler, M.J., 2013. Clinical associations and potential novel antigenic targets of autoantibodies directed against rods and rings in chronic hepatitis C infection. BMC Gastroenterol. 13, 50.
Tan, E.M., 1989. Antinuclear antibodies: diagnostic markers for autoimmune diseases and probes for cell biology. Adv. Immunol. 44, 93–151.
Tan, E.M., 1991. Autoantibodies in pathology and cell biology. Cell 67, 841–842.
Tan, E.M., Chan, E.K.L., Sullivan, K.F., Rubin, R.L., 1988. Antinuclear antibodies (ANAs): diagnostically specific immune markers and clues toward the understanding of systemic autoimmunity. Clin. Immunol. Immunopathol. 47, 121–141.
Thomas, E.C., Gunter, J.H., Webster, J.A., Schieber, N.L., Oorschot, V., Parton, R.G., et al., 2012. Different characteristics and nucleotide binding properties of inosine monophosphate dehydrogenase (IMPDH) isoforms. PLoS One 7, e51096.
Tillman, D.M., Jou, N.T., Hill, R.J., Marion, T.N., 1992. Both IgM and IgG anti-DNA antibodies are the products of clonally selective B cell stimulation in (NZB x NZW) F1 mice. J. Exp. Med. 176, 761–779.
Vagelos, P.R., Alberts, A.W., Martin, D.B., 1962. Activation of acetyl-CoA carboxylase and associated alteration of sedimentation characteristics of the enzyme. Biochem. Biophys. Res. Commun. 8, 4–8.
Valentini, G., Mantelli, A., Persico, M., Tuccillo, C., Del Vecchio Blanco, G., Morisco, F., et al., 1999. Serological and clinical markers of autoimmune disease in HCV-infected subjects with different disease conditions. Clin. Exp. Rheumatol. 17, 75–79.
Verschuur, A.C., Van Gennip, A.H., Leen, R., Meinsma, R., Voute, P.A., van Kuilenburg, A.B., 2000. In vitro inhibition of cytidine triphosphate synthetase activity by

cyclopentenyl cytosine in paediatric acute lymphocytic leukaemia. Br. J. Haematol. 110, 161–169.
Weber, G., Prajda, N., Abonyi, M., Look, K.Y., Tricot, G., 1996. Tiazofurin: molecular and clinical action. Anticancer Res 16, 3313–3322.
Willingham, M.C., Richert, N.D., Rutherford, A.V., 1987. A novel fibrillar structure in cultured cells detected by a monoclonal antibody. Exp. Cell Res. 171, 284–295.
Yao, B., Li, S., Chan, E.K.L., 2013. Function of GW182 and GW Bodies in siRNA and miRNA Pathways. Adv. Exp. Med. Biol. 768, 71–96.
Zhang, J.Y., Zhu, W., Imai, H., Kiyosawa, K., Chan, E.K.L., Tan, E.M., 2001. De-novo humoral immune responses to cancer-associated autoantigens during transition from chronic liver disease to hepatocellular carcinoma. Clin. Exp. Immunol. 125, 3–9.
Zhou, S., Liu, R., Baroudy, B.M., Malcolm, B.A., Reyes, G.R., 2003. The effect of ribavirin and IMPDH inhibitors on hepatitis C virus subgenomic replicon RNA. Virology 310, 333–342.

CHAPTER THREE

Modulation of Glycan Recognition by Clustered Saccharide Patches

Miriam Cohen[†,1], **Ajit Varki**[*,†,1]
[*]Department of Medicine, University of California, San Diego, California, USA
[†]Department Cellular and Molecular Medicine, Glycobiology Research and Training Center, University of California, San Diego, California, USA
[1]Corresponding authors: e-mail address: micohen@ucsd.edu; a1varki@ucsd.edu

Contents

International Review of Cell and Molecular Biology, Volume 308
ISSN 1937-6448
http://dx.doi.org/10.1016/B978-0-12-800097-7.00003-8

Abstract

All cells in nature are covered with a dense and complex array of glycan chains. Specific recognition and binding of glycans is a critical aspect of cellular interactions, both within and between species. Glycan–protein interactions tend to be of low affinity but high specificity, typically utilizing multivalency to generate the affinity required for biologically relevant binding. This review focuses on a higher level of glycan organization, the formation of clustered saccharide patches (CSPs), which can constitute unique ligands for highly specific interactions. Due to technical challenges, this aspect of glycan recognition remains poorly understood. We present a wealth of evidence for CSPs-mediated interactions, and discuss recent advances in experimental tools that are beginning to provide new insights into the composition and organization of CSPs. The examples presented here are likely the tip of the iceberg, and much further work is needed to elucidate fully this higher level of glycan organization.

1. INTRODUCTION: GLYCOME COMPLEXITY IN NATURE

Glycans are the most diverse of the four fundamental cellular macromolecules (Marth, 2008). Glycan diversity exceeds that of DNA and RNA (with their four nucleoside constituents) and proteins (with their 20 amino acids) because the latter molecules are strictly linear. Glycans combine dozens of possible monosaccharide units into branched structures whose diversity results from linear or branched α or β linkages between monosaccharides. Thus the glycome is comprised of many unique glycans (Marth, 2008; Varki and Sharon, 2009) that can be either free (e.g., hyaluronan), or attached to proteins (glycoproteins and proteoglycans) or lipids (glycolipids). The biosynthesis of glycans and their modifications are not template-driven; rather they are the product of multiple sometimes competing, enzymatic activities. This creates vast glycan diversity. In addition, a range of glycan variations can be found on each glycosylation site, a pattern referred to as glycosylation microheterogeneity (Kornfeld and Kornfeld, 1985).

Glycans cover the surfaces of all cells in nature, forming a dense and complex layer known as the glycocalyx. Glycans are also abundant on secreted proteins and in the extracellular matrix (ECM). Every known cell is covered in glycans suggesting that the glycome is as essential to life as a genome, transcriptome, proteome, lipidome, or a metabolome (Varki, 2011). The diversity of glycan modifications generates a unique glycan "topography" for each protein, cell, and tissue. Like a forest canopy, glycome complexity

is recognizable at various levels: the identity and modification of outer or terminal monosaccharide core structure (*leaves* and *flowers*), the linkage to the underlying sugar (*stems*), the identity, and arrangement of the underlying glycans (*branches*), the structural attributes of the underlying glycans (*tree trunks*), and finally, the spatial organization of the oligosaccharides in relation to components of the intact cell surface (the *forest* itself) (Cohen and Varki, 2010). Because glycans comprise the outer face of cells, cellular interactions within and between species typically involve glycan binding and recognition. Indeed, many examples of biological recognition by glycans have been documented, typically involving glycan-binding proteins (GBPs). These interactions include antibody recognition, pathogen binding, cell adhesion, cell–cell interactions, and signaling (Ohtsubo and Marth, 2006; Sharon, 2006; Varki and Varki, 2007).

2. GLYCAN RECOGNITION BY GBPs

Glycan interactions with GBPs are often very specific, and each type of structure in the glycan forest can mediate specific interactions with certain GBPs (reviewed in Cohen and Varki, 2010). Although highly specific, these interactions often tend to be of weak affinity (K_d values in micromolar to millimolar range) (Collins and Paulson, 2004; Cummings and Esko, 2009; Varki, 1994). Glycans often achieve biologically significant binding via multivalent avidity, with their interaction involving more than one pair of partners in close physical proximity. This review focuses on GBP interactions at the highest level of glycan complexity (the *forest*), which are not well represented by current analytical techniques, even by modern glycan microarrays. At this level of glycan complexity "clustered saccharide patches" (CSPs) can be formed by multiple glycans interacting with each other, with or without involvement of proteins or lipids. The spatial organization of glycans within such patches can influence the specificity of their interaction with GBPs.

The two major groups of GBPs are lectins and sulfated glycosaminoglycan-binding proteins (Varki et al., 2009a). This review will focus on lectins, but many of the principles discussed may apply to other types of GBPs. Lectin-binding specificity is often defined by the structure of the terminal glycan, the linkage to the underlying glycans, the structure of the underlying glycans, and the type of linkage (N- or O-) to the underlying protein/lipid (Cummings and Esko, 2009; Varki, 1994; Varki et al., 2009a; Weis and Drickamer, 1996). Lectin–glycan interactions are typically

stabilized in two ways: by hydrogen bonding between amino acids in the carbohydrate-recognition domain (CRD) and the glycan hydroxyl groups, and by van der Waals packing of the hydrophobic glycan face against the aromatic amino acid side chain (Weis and Drickamer, 1996). Because these interactions tend to be weak, multivalency is often required to generate biologically relevant binding (Dam and Brewer, 2008). There are three different ways to achieve this: simple multivalency, spatial clustering of the GBPs, or clustering of the glycans into a saccharide patch.

The typical CRD of a GBP accommodates 1–4 monosaccharides (Weis and Drickamer, 1996), in some cases simple multivalency of either the GBP or the glycans is sufficient to promote binding (Fig. 3.1A). For example, the influenza hemagglutinin has a very low affinity, but high specificity for its sialylated glycan ligands. The multivalency of the hemagglutinin trimer and the large number and density of hemagglutinin molecules on the virus envelope together promote high avidity binding. In similar fashion, a

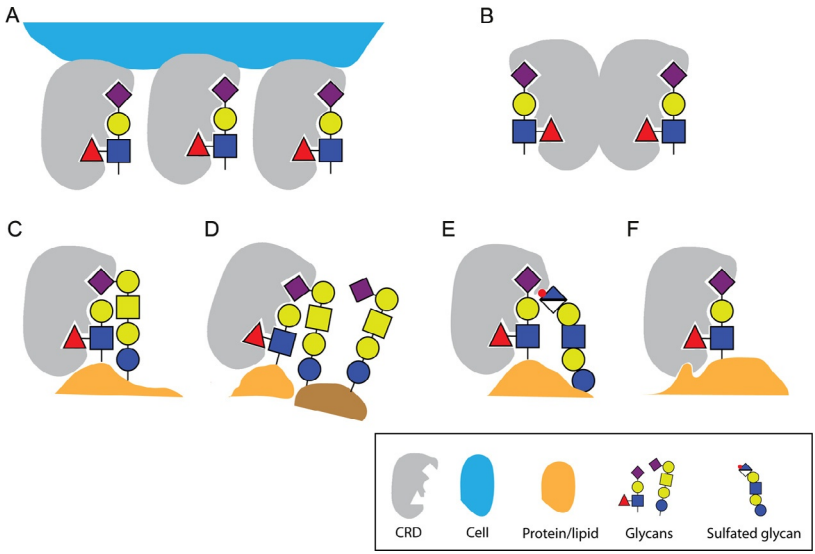

Figure 3.1 *Models of multivalent glycan binding to a carbohydrate recognition domain (CRD).* (A) Simple multivalent binding of multiple proteins to multiple glycans. (B) Multimerization of glycan-binding proteins (GBPs) can significantly enhance the affinity for glycan binding. (C–F) Binding to a clustered saccharide patch (CSP) enhances both affinity and specificity of GBP–glycan interactions. CSP may be formed by multiple glycans located on a single (C), or several (D) proteins or lipids, or by a glycan-sulfate cluster (E), or a patch comprised of glycan and adjacent peptide sequence (F).

precomplexing of recombinant soluble influenza hemagglutinins with antibodies is required for specific binding to glycans on microarrays (Stevens et al., 2006). In many cases, the high-density presentation of glycans on a microarray is sufficient to allow binding of GBP (Rillahan and Paulson, 2011). Another possible way to enhance carbohydrate–protein interactions is multivalent aggregation of the GBPs (Fig. 3.1B). For example, a pentamer of cholera toxin B subunit binds to ganglioside GM1 at a K_d value of ~40 nM (Kuziemko et al., 1996; Merritt et al., 1994). Experimental reports on avidity suggest that such multivalent interaction increase the binding affinity by a minimum of an order of magnitude compared to typical protein–carbohydrate interactions (Kuziemko et al., 1996). A third potential way to enhance both affinity and specificity of GBP–glycan interactions is by binding to a "CSP," in which several closely spaced saccharides interact to generate a specific recognition epitope (see Fig. 3.1C–F for variations in this theme) (Varki, 1994). This review focuses on this third aspect of GBP biology, which is currently poorly understood.

3. CONCEPT OF CSPs

The clustering of glycans into CSPs can be caused by multiple glycans located on a single underlying protein or lipid (Fig. 3.1C). Clusters can also involve glycans attached to two or more proteins or lipids (Fig. 3.1D). Binding patches can include glycans only, glycan-sulfates (Fig. 3.1E), or glycans and their adjacent peptide sequences (Fig. 3.1F). Within CSPs glycans are presumably presented in a distinct spatial organization that can fit the CRD pocket like a key into a lock. Since the CRD pocket can accommodate only a small number of glycans, an optimal presentation of glycans in relation to the amino acids could greatly stabilize their interactions. Saccharide clusters are stabilized by *cis* carbohydrate–carbohydrate interactions such as hydrogen bridges, hydrophobic surfaces, and ionic interactions (typically Ca^{2+} or Mg^{2+}) (Spillmann and Burger, 1996). A carbohydrate–carbohydrate interaction between glycosphingolipids also stabilizes glycosynapse microdomains (see Section 9; Hakomori, 2003). In our own work, we found that clusters of sialylated oligosaccharides and A/B blood group antigens on human erythrocytes are dispersed when a single monosaccharide is cleaved off the A/B antigen, suggesting that their spatial structure is maintained by the glycan (see Section 6; Cohen et al., 2009). The multiple lines of evidence for GBP recognition of CSPs are discussed in Sections 4–11 of this review.

Glycans are ideal molecules for mediating initial interactions since GBP–glycan interactions are highly specific but relatively weak, and thus readily reversible. Furthermore, glycan organization in CSPs can generate a unique topology even for proteins/cells with very similar glycan content (Cohen et al., 2009). Due to the complex nature of CSPs, it is extremely difficult to experimentally recreate them *in vitro* and on glycan microarrays, although several attempts have been made (see Section 11). However, there is an abundance of direct and indirect evidence for CSP-mediated binding, in particular for sialylated CSPs, which we focus on here.

Sialic acids are a family of monosaccharides typically found at the outer terminal end of glycans. They are specifically recognized by certain lectins such as Siglecs (Sialic acid-binding Ig-like lectins), and by antibodies and pathogens (Crocker et al., 2007; Varki and Angata, 2006; Varki and Varki, 2007). As with other glycans, specificity for sialic acid binding can be determined at all levels of the sialylated forest canopy (the Sialome), from modifications of the terminal monosaccharide (the *leaves* and *flowers*) to the spatial organization of the glycans (the *forest*) (Brinkman-Van der Linden and Varki, 2000; Cohen and Varki, 2010; Varki, 2008). Binding and recognition of sialic acids is known to be involved in interactions between protein–protein, protein–cell, cell–cell, cell–matrix, and is also involved in pathogen recognition.

In this review, we present examples of a spectrum of possible CSPs: on heavily glycosylated proteins (Fig. 3.2A), including CSPs formed on the cell membrane by glycosphingolipids (Fig. 3.2B) or glycoproteins (Fig. 3.2C); and CSPs on pathogens (Fig. 3.2D). All of these CSPs mediate specific interactions with certain GBPs or antibodies. We also discuss the existence of CSPs in glycosynapses, a type of glycan microdomain that mediates cell–cell and cell–ECM adhesion and signaling (Fig. 3.2E). While this review is biased toward sialylated CSPs, nonsialylated clustered patches (e.g., mannosylated clusters on HIV, Section 8.2) also exist and may be very common. Thus these examples are likely the tip of the iceberg. We expect the field to develop quickly. Recent advances in experimental tools, such as glycan arrays and lipid arrays are already providing new insight into the composition and organization of saccharides that are recognized by GBPs.

4. EVIDENCE FOR CSPs ON HEAVILY GLYCOSYLATED PROTEINS

On heavily glycosylated proteins like mucins, the polypeptide core can be completely hidden under a dense array of glycan chains. As a result, binding by other proteins is often mediated solely by the glycans, and their

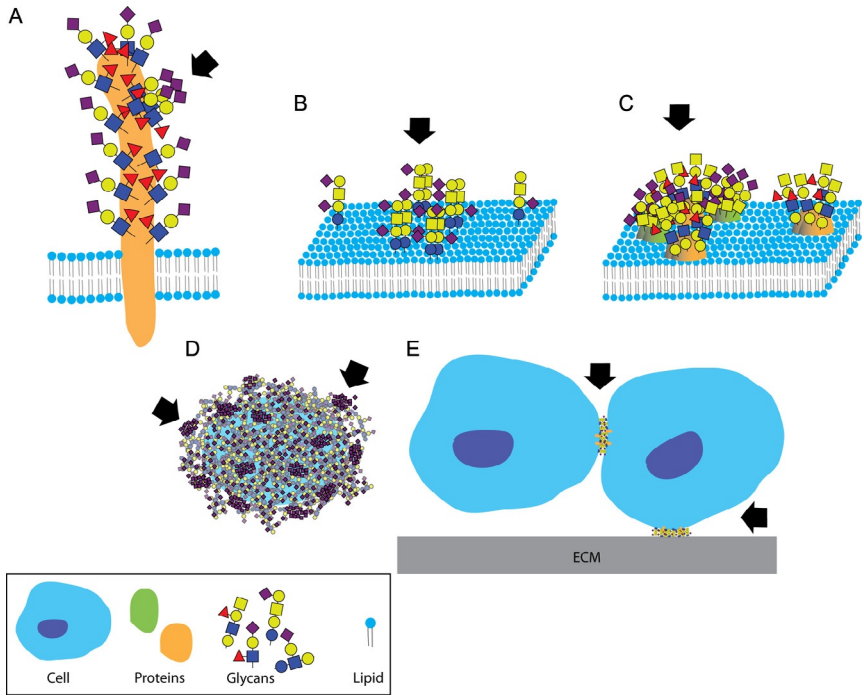

Figure 3.2 *Clustered Saccharide Patches exist at spatial scales spanning several orders of magnitude*. CSPs may form on heavily glycosylated proteins (A), on cell membranes because of interactions between two or more glycosphingolipids (B) or glycoproteins (C). CSPs can also form on pathogen polysaccharides (D). Glycosynapses are clustered glycan microdomains, which mediate cell–cell and cell–extracellular matrix adhesion and signaling (E). Arrows indicate likely CSPs.

structure and spatial arrangement can be important for recognition. These glycans are also interacting with one another in ways that restrict their motion, or cause them to cluster. Thus the complex spatial presentation of glycans in CSPs can generate novel ligands that are specifically recognized by an antibody or a receptor. We present here four examples of pathogen proteins, antibodies, and lectins that bind their targets only when glycans are clustered at high density on glycoconjugates.

4.1. Malarial merozoite recognition of clustered sialoglycans on glycophorins

Plasmodium falciparum is a major cause of human malaria. *P. falciparum* merozoites circulating in the blood invade erythrocytes via specific pathways that are either sialic acid-dependent (SAD) or -independent (SAID). The

SAD pathways are mediated by interaction between proteins from the *P. falciparum* Duffy binding-like family (e.g., pfEBA-175 and pfEBA-140), and glycophorins on erythrocytes (Oh and Chishti, 2005). Glycophorins (A, B, and C) are the major sialoglycoproteins on human erythrocytes. The extracellular domain of glycophorin A (GpA) is glycosylated with 16 O-linked glycans (primarily Neu5Acα2-3Gal(Neu5Acα2-6)GalNAcα1-*O*-Ser/Thr, with minor variations) and one sialylated N-linked glycan (Thomas and Winzler, 1969; Tomita et al., 1978). Glycophorin B (GpB) is highly homologous to GpA, but is shorter and has only 11 O-linked glycans on its extracellular domain (Anstee, 1990; Sim et al., 1994; Tomita et al., 1978). Although both GpA and GpB are modified with similar O-linked oligosaccharides, glycan distribution along the extracellular domain is unique for each protein (Anstee, 1990). Glycophorin C (GpC) is broadly similar to GpA, and contains about 13 O-linked glycans and one N-linked glycan (Anstee, 1990).

Binding of pfEBA-175 to erythrocytes is SAD, and can be inhibited by sialidase pretreatment. pfEBA-175 selectively binds to a clustered patch of six O-linked glycans on the N-terminal peptide region of a GpA dimer. However, this interaction cannot be competed by free sialic acids or by fetuin, despite the fact that the latter contains three non-adjacent O-linked glycans, which are identical to the tetrasaccharide on GpA (Orlandi et al., 1992). Furthermore, despite its high homology to GpA, soluble GpB cannot inhibit pfEBA-175 binding to erythrocytes or to GpA (Sim et al., 1994). In contrast, soluble GpA can effectively inhibit pfEBA-175 binding to erythrocytes, and inhibition with Neu5Acα2-3lactose requires a 100-fold higher concentration (Orlandi et al., 1992). pfEBA-175 binds to N-deglycosylated GpA, indicating that the sialylated N-linked glycan on GpA is not required for binding (Orlandi et al., 1992).

Taken together it is clear that the sialylated O-linked tetrasaccharide structure by itself is not the ligand for pfEBA-175, and other element(s) on GpA are required for binding. Two possible scenarios can be proposed. One is that pfEBA-175 binds to a cluster comprised of O-linked sialoglycans but also recognizes the underlying GpA peptide. The other is that GpA N-terminal peptide conformation presents the glycans in a novel clustered patch that is specifically recognized by pfEBA-175 (Sim et al., 1994). From the crystal structure of pfEBA-175 RII region (which is the erythrocyte-binding domain), it appears that the pfEBA-175 dimer binds to a clustered patch of six oligosaccharides presented on GpA (Tolia et al., 2005). Six potential glycan-binding sites were identified on the RII dimer: four are

located in the two channels of the dimer, and two are exposed to the top of the surface. Mutation analysis confirmed that all six sites are important for pfEBA-175 binding to GpA and to erythrocytes. Interestingly, several well-ordered sulfate molecules were observed in the channels and on one face of the dimer (Tolia et al., 2005). The GpA tetrasaccharide can be modeled into all six binding sites simultaneously, suggesting that pfEBA-175 ligand is a clustered patch of six *O*-glycans on the N-terminal of a GpA dimer (Tolia et al., 2005). The fact that the N-terminal peptide region of GpA and GpB is rapidly evolving among primates suggests that it is under selection pressure by the malarial pathogen (Baum et al., 2002). Consistent with this conclusion, natural human polymorphisms of this peptide sequence generate the MN blood groups (Anstee, 1990; Sadler et al., 1979). There is also evidence for rapid evolution of this peptide in five populations that have been exposed to malaria, suggesting that MN blood group polymorphism may indeed affect malarial parasite invasion (Ko et al., 2011).

There is similar evidence that another *Plasmodium* protein pfEBA-140 (BAEBL) binds to a sialylated clustered patch that includes the sialylated N-linked glycan on glycophorin C (GpC) combined with an additional unknown element. pfEBA-140 is a polymorphic Duffy binding-like receptor, each variant being identified by four amino acids in the RII region. It was determined that the BAEBL-VSTK variant recognizes GpC on erythrocytes since it does not bind to Gerbich-negative erythrocytes, which express a truncated form of GpC (Anstee, 1990; Mayer et al., 2002). The RII domain of BAEBL-VSTK has two arginine residues (Arg, R114, and R52) that are critical for binding to GpC (Jiang et al., 2009). Positively charged Arg residues are a conserved motif for sialic acid binding by Siglecs and sialidases (Varki and Angata, 2006). Erythrocyte treatment with sialidases reduces the binding of BAEBL-VSTK by 90% (Kobayashi et al., 2010), confirming sialic acid-mediated binding. Similar to pfEBA-175, fetuin does not inhibit BAEBL–VSTK interactions with erythrocytes (Kobayashi et al., 2010), despite carrying sialylated *N*-glycans with structures similar to those of GpC. In contrast to pfEBA-175, *N*-deglycosylated GpC cannot inhibit BAEBL-VSTK binding to erythrocytes, but soluble N-glycosylated GpC can. Thus the N-linked glycan is an essential component of the BAEBL-VSTK ligand on GpC. However, the isolated N-linked glycans that were cleaved from GpC cannot inhibit BAEBL-VSTK binding to erythrocytes themselves (Mayer et al., 2006). In addition, soluble GpA, which also contains a single similar N-linked glycan does not inhibit

BAEBL-VSTK binding to erythrocytes (Mayer et al., 2006) (although BAEBL-VSTK can bind to GpA on SDS-Page, Maier et al., 2003). It appears that both N-linked glycans and sialylation of GpC are required for BAEBL-VSTK binding (Malpede et al., 2013). However, the single N-linked glycan on GpC by itself is not the ligand for BAEBL-VSTK. Taken together the data suggest that similar to the pfEBA-175-GpA interaction, a cluster of N-linked glycan with other element(s) on GpC form the ligand for BAEBL-VSTK binding. The involvement of O-linked glycans in the binding was not tested, and a cluster of N-linked and O-linked glycans remains a possibility for BAEBL-VSTK binding. Alternatively, there is evidence for heparan sulfate involvement in the SAD invasion pathway of BAEBL-VSTK and GpC. Heparitinase (heparin sulfate-specific lyase) treatment inhibits merozoite invasion by a maximum of 35%, compared to almost 60% inhibition by sialidase treatment. Combined treatment with both enzymes inhibits invasion to similar extent as sialidase treatment alone, suggesting that sialic acid and heparan sulfate mediate invasion through the same pathway (Kobayashi et al., 2010). Furthermore, heparitinase treatment reduces pfEBA-140 (VSTK) binding to erythrocytes by 30–40%, and incubation with heparin (highly sulfated heparan sulfate) completely abolished binding (Kobayashi et al., 2010).

In summary, there is strong evidence that pfEBA-175 binds to a clustered patch of six *O*-glycans on the N-terminal peptide of a GpA dimer (Tolia et al., 2005). And while pfEBA-140 (BAEBL-VSTK) binding requires N-linked glycosylation on GpC, the isolated N-linked glycans are not sufficient for binding. In addition, there is evidence that heparan sulfate may be involved in the SAD pathway of BAEBL-VSTK-mediated invasion. Although erythrocytes express only small amounts of heparan sulfate (Drzeniek et al., 1999), it is possible that heparan sulfate stabilizes a sialylated cluster that is recognized by BAEBL-VSTK (Kobayashi et al., 2010; Vogt et al., 2004).

4.2. Antibody recognition of sialylated Lewis antigens on mucins

Clusters of Sialyl-Lewis^a (Siaα2-3Galβ1-3(Fucα1-4)GlcNAcβ-, SLe^a) on plasma proteins are differentially recognized by three monoclonal antibodies that were raised against SLe^a. The Lewis antigens are formed by addition of fucose to *N*-acetylglucosamine on glycolipid or glycoprotein in either α1–3 or α1–4 linkage (Stanley and Cummings, 2009). Le^a and Le^b are known as blood group antigens, as they are secreted into the plasma as glycolipids and

then incorporated into erythrocytes in individuals that are secretors. In contrast, the Le^x and Le^y antigens are expressed only on a few cell types and are not found associated with erythrocytes (Lloyd, 2000). All of the Lewis group epitopes are expressed in high densities by many carcinomas (Lloyd, 2000; Yuriev et al., 2005). Elevated levels of SLe^a bearing glycoconjugates are found in the peripheral blood of pancreatic cancer patients, and patients with acute and chronic pancreatitis, obstructive jaundice, and liver cirrhosis (Bhat et al., 2012). SLe^a is the canonical epitope for cancer/carbohydrate antigen 19-9 (CA 19-9), and is used as a biomarker for cancer diagnostics (Bhat et al., 2012; Molina et al., 2012).

Several other monoclonal antibodies are available for diagnostics: 9L426 was raised against purified SLe^a, 1B.844 antibody was raised against CA19-9 mucin antigen, and 121SLE which is comprised of mAb 19-9 and mucins that were isolated from ovarian cyst of a Lewis (a + b-) patient and further purified by immunediffusion (Gustafsson, 1990; Partyka et al., 2012). Not surprisingly, 9L426 antibody is very specific for SLe^a epitope, however both 1B.844 and 121SLE bind to additional glycan structures on glycan microarrays. For example, they both bind well to a SLe^a epitope that contains *N*-glycolylneuraminic acid (Neu5Gc), and to the SLe^c structure (SLe^a missing a fucose) (Partyka et al., 2012). Multiplexed comparison of antibodies binding to pancreatic cancer patient plasma samples revealed differential recognition of SLe^a epitopes on plasma proteins by these antibodies. The three antibodies were immobilized on microarrays, and plasma proteins from patients were incubated with these arrays. The captured proteins were then probed by each of the three antibodies, resulting in all possible antibody-pair combinations. The various capture–detection pair combinations generally showed the same pattern of recognition across the plasma samples, indicating that all three antibodies essentially recognize the same epitope (SLe^a). However, plasma proteins captured by one antibody were not always recognized by the other antibodies (Partyka et al., 2012). For example, plasma proteins from three of eleven patients were uniquely detected by 121SLE antibody but not by 9L426 and 1B.844 antibodies. In contrast, plasma proteins from two of eleven patients were recognized by 9L426 and 1B.844 antibodies but not by 121SLE (Partyka et al., 2012). This indicates that each antibody recognize a slightly different SLe^a containing epitope on the proteins. Thus the SLe^a epitopes likely form various clustered patches on the tumor-derived mucin-like proteins in plasma, which are specifically recognized by each of the antibodies. Again, we have a case where a defined glycan is necessary but not sufficient for recognition by different GBPs.

4.3. Antibody recognition of mucin-related tumor antigens Tn, TF, and STn

Incomplete mucin glycosylation in carcinomas leads to the exposure and reorganization of cryptic glycans that can be in clustered patches that are specifically recognized by certain antibodies. Examples of such cryptic glycans include the Tn (GalNAc-α1-*O*-Ser/Thr) and T (Galβ1-3GalNAc-α1-*O*-Ser/Thr) antigens, both of which have been reported in carcinomas (Springer, 1984, 1997; Varki et al., 2009b), and Sialyl-Tn (Siaα2-6GalNAc-α1-*O*-Ser/Thr, STn), which is found in some adenocarcinomas (Zhang et al., 1995).

Mucins are a family of large glycoproteins that contain variable number of tandem repeats rich in proline, threonine and serine, and are extensively O-glycosylated at the Ser/Thr residues (Itzkowitz et al., 1989; Kufe, 2009). Altered expression and incomplete glycosylation of mucins in carcinomas results in the expression of glycan epitopes that are normally cryptic. For example, mutation in the T-synthase enzyme (Cosmc) results in expression of Tn antigen, and can lead to the formation of STn (Ju et al., 2008). Reduced sialic acid O-acetylation can also expose the underlying STn structure (Itzkowitz et al., 1989; Varki et al., 2009b). Analysis of the binding pattern of two monoclonal antibodies that were raised against STn, TKH2, and B72.3 suggests that non-O-acetylated STn glycans are organized in clustered patches on colon carcinomas but not on normal tissues.

TKH2 antibody was generated following immunization with ovine submaxillary mucins (OSM) (Kjeldsen et al., 1988), which are exclusively glycosylated with STn. B72.3 antibody was generated following immunization with human breast carcinoma cells (Thor et al., 1986). Both antibodies do not bind to normal colon tissue, but interact with colon cancer tissues (Itzkowitz et al., 1989; Ogata et al., 1998). TKH2 does not bind to O-acetylated sialic acids, but de-O-acetylation of normal and cancer tissues with sodium hydroxide results in an increase in TKH2 staining (Ogata et al., 1995, 1998). This supports the hypothesis that sialic acid moieties are masked by O-acetylation in normal tissues, and de-O-acetylated in cancer tissues. In contrast, B72.3 staining was not affected by sodium hydroxide treatment (Ogata et al., 1998), however, unlike TKH2, this antibody was raised against carcinoma cells. Importantly, B72.3 strongly binds neoglycoproteins bearing STn-trimers, but poorly interacts with monomeric-STn neoglycoproteins (Ogata et al., 1998). Taken together, these findings demonstrate that in colon carcinoma tissues at least three non-O-acetylated STn epitopes form

a clustered patch that is specifically recognized by B72.3 antibody. In contrast, in normal colonic tissue STn is found in O-acetylated nonclustered potentially monomeric form (Ogata et al., 1998).

Since carcinomas express aberrant glycosylation, attempts have been made to generate anti-cancer vaccines by injecting patients with immunogenic proteins bearing the aberrant glycans. Cancer patients produce low levels of IgM antibodies against STn and Tn epitopes. These anti-STn antibodies can bind to OSM, suggesting recognition of clustered STn epitope (Adluri et al., 1995). In order to elicit production of IgG antibodies, patients were vaccinated with neoglycoproteins comprised of keyhole limpet hemocyanin (KLH) conjugated to STn (STn–KLH), or to Tn (KLH–Tn). While the vaccination enhanced the production of corresponding natural IgM antibodies, IgG antibodies from these patients reacted only with STn and Tn epitopes on synthetic conjugates (Adluri et al., 1995). The fact that IgG antibodies failed to interact with STn and Tn epitopes from natural sources such as OSM and asialoglycophorin indicates that the neoglycoproteins do not mimic the natural cancer epitope. In contrast, IgG antibodies from patients that were vaccinated with OSM reacted with both synthetic and naturally occurring STn epitopes (Adluri et al., 1995). In a separate approach, IgG monoclonal antibodies (MLS 128 and MLS 132) that were raised against human colorectal cancer cell line LS 180 were shown to specifically recognize a cluster of Tn or a cluster of STn, respectively. Immunoaffinity columns containing MLS 128 (Numata et al., 1990) or MLS 132 (Tanaka et al., 1999) antibodies were loaded with tryptic digest of OSM or asialo-OSM. All the peptides that were captured by MLS 128 contained a cluster of three or four consecutive residues of Tn antigen on a Ser-Thr-Thr glycopeptides (Nakada et al., 1991, 1993). Conversely, all the peptides captured by MLS 132 reacted with a cluster of four STn antigens on OSM peptides (Tanaka et al., 1999). Taken together it is clear that on cancer cells STn and Tn epitopes are organized in immunogenic clusters that are specifically and differentially recognized by different antibodies. As with some of the prior examples, a defined glycan is *necessary but not sufficient* for recognition by different GBPs.

4.4. Lectin binding to CA125 antigen

CA125 antigen is the most prominent marker for serous ovarian cancer; it is the extracellular domain of MUC16 mucin and is heavily O-glycosylated (Bouanene and Miled, 2010; Yin et al., 2002). It has an unusual expression of sialylated branched core 1 antennae in the core 2 glycans. Despite having a

comparable content of Sias in α2-3-linkage and α2-6-linkage, the binding pattern of recombinant soluble Siglec-Fc chimeras was found to be unique for each of three CA125 isolates. This suggests recognition by the Siglecs of sialylated CSPs that are unique for each isolate.

CA125 was isolated from three different sources: ovarian carcinoma patients (pfCA125), ovarian carcinoma cell line (clCA125), and noncancer source (pCA125). The isolates were extensively analyzed by lectin-affinity columns (Jankovic and Milutinovic, 2008), and by binding of recombinant human Siglecs to immobilized CA125 (Mitic et al., 2012). Overall the three CA125 isolates appeared to have similar sialylation patterns, as both *Maackia amurensis* lectin (MAA, recognizes Siaα2-3Galβ1-R/3-*O*-sulfate-Galβ1-R) and *Sambucus nigra* agglutinin (SNA, binds to Siaα2-6Gal/GalNAc) recognized all isolates at a similar extent (Mitic et al., 2012). Thus the proportion of Sias in α2-3- and α2-6-linkage is comparable between all three isolates. In contrast, six Fc-chimeric Siglec proteins (Siglec-2, 3, 6, 7, 9, and 10) differentially bound to the CA125 isolates. The isolate from ovarian carcinoma patients, pfCA125, was exclusively recognized by Siglec-2, 3, 6, and 7; the ovarian carcinoma cell line isolate, clCA125, was exclusively recognized by Siglec-9 and 10; and the pCA125 isolate from a noncancer source was recognized by Siglec-2, 3, 6, 9, and 10 (Mitic et al., 2012). Note that all these Siglecs can bind to various glycan structures containing Sias in α2-3- and α2-6-linkage. Specifically, Siglec-2 binds non-9-*O*-acetylated Siaα2-6Gal/GalNAc (Brinkman-Van der Linden et al., 2002; Sjoberg et al., 1994; Varki and Angata, 2006), Siglec-3 binds mostly Siaα2-6Gal and Siaα2-3Gal (Brinkman-Van der Linden and Varki, 2000), Siglec-7 preferably binds to branched α2-6-linked Sias, such as Galβ1-3(Siaα2-6)HexNAc (Angata and Varki, 2000; Yamaji et al., 2002), Siglec-6 binds Siaα2-6GalNAc (STn) (Brinkman-Van der Linden and Varki, 2000; Patel et al., 1999), Siglec-9 and Siglec-10 preferably bind to Siaα2-3Galβ1-4GlcNAc, although they bind to Siaα2-6Gal as well (Varki and Angata, 2006). All these are structures that are recognized by MAA and SNA, which bind to the three CA125 isolates in a comparable manner (Mitic et al., 2012). Thus the differential binding by Siglec-chimeras implies a higher order organization of the sialylated glycans on CA125, likely in sialylated CSPs.

5. CLUSTERED PATCHES OF SIALYLATED GANGLIOSIDES ON CELL SURFACES

Gangliosides are sialylated glycosphingolipids, composed of a ceramide lipid tail attached to an oligosaccharide chain that contains between

one to five sialic acid residues. Gangliosides typically form clusters on the plasma membrane, and are important components of the nervous system. Saccharides from two or more neighboring gangliosides can form a clustered patch that is uniquely recognized by antibodies. The formation of such CSPs can elicit novel antibodies. Alternatively, it can mask antibody recognition of a single ganglioside. Here we present examples of antibodies that specifically recognize aberrant CSPs, and show that clustered patch formation on melanoma cells can mask antibody recognition.

5.1. Autoantibody recognition of ganglioside complexes in immune neuropathies

Autoantibodies from patients can specifically recognize heterogeneous ganglioside clusters and yet do not react with the constituent gangliosides individually. Autoantibody–ganglioside interactions are a critical pathogenic factor in a subset of autoimmune neuropathies, including multifocal motor neuropathy (MMN), Guillain–Barré (GBS) and Miller-Fisher (MFS) syndromes (Willison and Yuki, 2002; Yuki and Hartung, 2012). Anti-ganglioside antibodies trigger inappropriate activation of the complement cascade, which may induce nerve injury in GBS and MFS patients (Kaida and Kusunoki, 2010; Willison et al., 2008). Serum IgG autoantibodies against GM1, GD1a, GT1a, and/or GQ1b gangliosides are associated with nerve injury in GBS and MFS patients (Greenshields et al., 2009; Willison and Yuki, 2002). IgM autoantibodies against GM1 and GM2 have been reported in the serum of MMN patients (Nobile-Orazio et al., 2010; Willison and Yuki, 2002). Because these antibodies are characteristic of the acute phase of the disease, they are useful diagnostic markers. However, acute phase sera from 8% to 17% of GBS patients does not react with purified gangliosides such as GM1, GM2, GM3, GD1a, GD1b, GD3, GalNAc-GD1a, GT1b, and GQ1b. Instead the serum IgG strongly reacted with ganglioside mixtures (Kaida et al., 2004, 2007; Kusunoki and Kaida, 2011).

Gangliosides are localized in glycosynapse microdomains (see Section 9 below), with the oligosaccharide side chain protruding from the plasma membrane. The sialylated oligosaccharide chains may form a saccharide cluster that can itself be specifically recognized by antibodies. Indeed, sera from certain neuropathy patients that do not react with an individual ganglioside do react with a complex of two different gangliosides (Kaida et al., 2004; Kanzaki et al., 2008; Mauri et al., 2012; Nobile-Orazio et al., 2010; Willison and Yuki, 2002). Conversely, antibody recognition of a single ganglioside may be masked in the ganglioside complex by the neighboring glycans (Ogawa et al., 2009). For example, a GA1/GQ1b ganglioside mixture

can be recognized by monoclonal anti-GQ1b antibody but not by monoclonal anti-GA1 antibody (Ogawa et al., 2009). Similarly, anti-GM1 IgM reactivity with GM1 is abolished or substantially reduced in GM1/GD1a ganglioside mixture (Nobile-Orazio et al., 2010).

The epitope recognized by serum antibodies was identified by extensive analysis of antibody binding to a mixture of two gangliosides. Two gangliosides were mixed and separated on thin layer chromatography (TLC) in a solvent that allowed overlapping in the same lane. Serum IgG from GBS patients reacted strongly with the overlapping portion, but did not react with the individual gangliosides (Kaida et al., 2007; Kusunoki and Kaida, 2011). Similarly, serum IgG bound strongly to wells coated with mixtures of GD1a/GD1b, GM1/GD1a, GD1b/GT1b, GM1/GT1b, or GM1/GD1b but not with the individual gangliosides in enzyme-linked immunosorbent assay (ELISA) (Kaida et al., 2004, 2007). Most of the anti-GD1a/GD1b- or anti-GM1/GD1a-positive sera also reacted with GM1/GD1b and GM1/GT1b ganglioside mixtures. This suggests that serum antibodies recognize a clustered epitope formed by a combination of Galβ1-3GalNAc (on GD1b or GM1) and Neu5Acα2-3Galβ1-3GalNAc (on the GT1b or GD1a) (Willison et al., 2008).

Serum antibodies from MFS patients can be divided into three groups: GQ1b- or GT1a-specific, GQ1b/GM1-reactive, and GQ1b/GD1a-reactive. GQ1b/GM1-reactive antibodies bind to ganglioside complexes containing a combination of Galβ1-3GalNAc and Neu5Acα2-8 Neu5Acα2-3Galβ1-3GalNAc in the terminal residue of ganglio-*N*-tetraose, including GQ1b/GD1b, GT1a/GD1b and GT1a/GM1 complexes. GQ1b/GD1a-reactive antibodies bind to complexes containing Neu5Acα2-3Galβ1-3GalNAc and Neu5Acα2-8Neu5Acα2-3Galβ1-3GalNAc, including GT1a/GD1a, GQ1b/GT1b and GT1a/GT1b (Kaida et al., 2006; Kusunoki and Kaida, 2011; Ogawa et al., 2009; Willison et al., 2008). In addition to the terminal sialic acid residues, the binding of certain antibodies may require one or two sialic acids on the internal galactose as well. For example, GQ1b/GA1 and GT1a/GA1 have the same terminal structure as the GQ1b/GM1 complex, but are missing one sialic acid on an internal galactose. GQ1b/GM1-reactive sera do not react with these complexes (Ogawa et al., 2009). IgM antibodies from sera of chronic neuropathy patients (MMN, chronic inflammatory demyelinating polyradiculoneuropathy and IgM paraproteinemic neuropathy) recognized GT1b/GM1, GT1b/GM2, and GM2/GD1b complexes (Nobile-Orazio et al., 2010). Additional evidence was obtained by glycan microarray studies

(see Section 11.1). Taken together from these examples, it is clear that gangliosides form specific sialylated CSPs that are detected by autoantibodies from neuropathy patients.

5.2. Antibody recognition of ganglioside complexes on melanoma cells

Heterogeneous ganglioside cluster formation on melanoma cells inhibits recognition of GM2, GM3, and GD3 by certain antibodies. Gangliosides are overexpressed in tumor cells and thus are putative targets for cancer vaccines (Heimburg-Molinaro et al., 2011). GM3 and GD3 are the predominant gangliosides expressed in melanoma tissues and cell lines (Lloyd et al., 1992; Tsuchida et al., 1989). Despite the uniformly high GM3 content, monoclonal antibodies against GM3 selectively interact with certain melanoma cell lines but not others (Lloyd et al., 1992; Wakabayashi et al., 1984). For example, the three anti-GM3 monoclonal antibodies, M2590 (IgM), CMR6 (IgM), and DH2 (IgG3), reacted only with one out of six melanoma cell lines tested (B78, mouse melanoma). Unlike the other five cell lines, B78 expresses only GM3. The other five cell lines express GM2, GD3 or other gangliosides in addition to GM3 (Lloyd et al., 1992). Similarly, anti-GD3 and anti-GM2 monoclonal antibodies (IgG3) reacted poorly with certain cell lines despite the high content of GD3 and GM2 in these cells. This phenomenon was observed on cells in suspension as well as in monolayers. To rule out that the lack of reactivity is due to crypticity effect (steric interference caused by neighboring glycoproteins), the cells were pretreated with trypsin-EDTA buffer or with pronase. Neither of the protease treatments significantly increased reactivity with anti-GM3 or anti-GD3 antibodies (Lloyd et al., 1992). Thus antibodies specific for GM3, GM2, and GD3 failed to recognize their ganglioside epitope when certain other gangliosides were present on the plasma membrane. This suggests the formation of a new epitope comprised of two or more gangliosides in a heterogeneous cluster. Gangliosides in the cluster are no longer exposed to antibody recognition, thus the single ganglioside is masked by formation of a CSP epitope.

Heterogenous GM1/GM3 clusters were also observed in normal mouse fibroblasts by immune-electron microscopy (Fujita et al., 2007). Antibodies against GM3 (monoclonal) and GM1 (polyclonal) detected clusters of $<$100 nm in diameter. GM3 and GM1 clusters were mostly segregated from each other, however, in 13.3% of the cases GM1 and GM3 co-clustered (Fujita et al., 2007). It is therefore likely that a CSP comprised of gangliosides is formed in these cells.

6. CLUSTERED PATCHES OF SIALYLATED GLYCOPROTEINS ON CELL SURFACES

The neutral ABH(O) blood group antigens stabilize sialylated clusters on human erythrocytes, unique for each blood type, that are differentially recognized by sialic acid-binding proteins. Erythrocytes from all three blood groups display a comparable amount of sialic acids (Bulai et al., 2003), most of which is found on glycophorins (see Section 4.1; Anstee, 1990). However, we found that three sialic acid binding proteins that are all specific for sialic acid in α2–6 linkage (and do not bind to ABH antigens) differentially interact with erythrocytes from each blood type (Cohen et al., 2009). While human Siglec-2 (CD22) binds to erythrocytes with blood group preference A > O > B, the pandemic human influenza hemagglutinin (A/South Carolina/1/18) binds equally to erythrocytes from all blood groups, and the plant lectin *Sambucus nigra* agglutinin (SNA) binding preference is A > B > O (Cohen and Varki, 2010; Cohen et al., 2009). Although a minor fraction of the glycan modifications on glycophorins contain the ABH antigens, it cannot explain the striking difference in Siglec-2 and SNA binding to erythrocytes from blood type B and O. Both lectins have comparable binding patterns in ELISA assay and on microarrays with strong preference to Siaα2-6Gal/GalNAc (Brinkman-Van der Linden et al., 2002; Padler-Karavani et al., 2012; Sjoberg et al., 1994; Varki and Angata, 2006). Although SNA binds to 9-*O*-acetylated sialic acids (Padler-Karavani et al., 2012) and Siglec-2 preferably binds to non-9-*O*-acetylated sialic acids (Brinkman-Van der Linden et al., 2002). But 9-*O*-acetylated Neu5Ac comprise less than 1.5% of the total sialic acids on erythrocytes and is comparable between the three blood groups (Bulai et al., 2003). Thus 9-O-acetylation cannot explain the differential binding of SNA and Siglec-2.

The majority of the ABH(O) blood group antigens on erythrocytes are found on the anion transport protein (band 3) and the glucose transport protein (band 4.5), which unlike glycophorins, are not much sialylated (Anstee, 1990). The blood type H antigen structure (Fucα1-2Galβ-R) is the precursor for both blood type A (GalNAcα1-3[Fucα1-2]Galβ-R) and blood type B (Galα1-3[Fucα1-2]Galβ-R) antigens (Greenwell, 1997; Hosoi, 2008). Note that these ABH(O) blood group antigens are neutral oligosaccharides that differ only in respect to a single terminal saccharide. Interestingly, blood type A and B antigens stabilize sialylated CSPs on the plasma membrane, but blood type H antigen does not. From electron microscopy analysis blood

type A antigens are organized in the periphery of sialylated clusters, and blood type B antigens are found in the center of sialylated clusters. In membranes of blood type O erythrocytes, very small sialylated clusters are formed and the blood type H antigens are not associated with them. Selective enzymatic cleavage of the terminal GalNAc and Gal from blood type A and B antigens, respectively, disperse the clusters and convert Siglec-2 and SNA binding in the expected direction (Cohen and Varki, 2010; Cohen et al., 2009). There is some evidence for co-localization of band 3 and GpA, which are the two most abundant proteins on the human erythrocyte membranes (Che and Cherry, 1995; Telen and Chasis, 1990; Young et al., 2000). However the interaction is not stable enough to be detected by standard methods such as co-immunoprecipitation, and fluorescence resonance energy transfer (Cohen et al., 2009; Jarolim et al., 1994; Telen and Chasis, 1990; Young et al., 2000), suggesting that band 3 and GpA do not form a stable protein complex. Taken together it is clear that sialylated clustered patches are formed on the plasma membrane of human erythrocytes, and are likely stabilized by carbohydrate–carbohydrate interactions with blood type A and B terminal saccharides. Lectin binding to sialylated ligands can be enhanced or reduced by the cluster formation resulting differential binding to cells presenting sialic acids with similar structure, linkage, and underlying sugars.

7. ENZYME RECOGNITION OF CLUSTERED GLYCANS: *O*-SIALOGLYCOPROTEIN ENDOPEPTIDASE

Proteolytic cleavage requires enzyme recognition of the target protein, and most endopeptidases recognize specific amino acid sequence motifs adjacent to the cleavage site (Turk et al., 2012). In contrast, *O*-sialoglycoprotein endopeptidase (OSGPase) binds to a clustered sialylated glycan patch on many different O-linked-glycan containing mucins and cleaves the adjacent peptide. This enzyme was first identified in the bacterium *Pasteurella haemolytica* (Abdullah et al., 1991; Lee et al., 1994; Mellors and Lo, 1995), but has homologs in all kingdoms of life (Nichols et al., 2006; Seki et al., 2002). The amino acid sequence of the *Pasteurella* enzyme substrate must contain at least 30% serine/threonine residues, thus presenting a mucin-like array of O-linked glycans (Mellors and Lo, 1995; Mellors and Sutherland, 1994). Terminal sialic acids on the O-linked oligosaccharides are also required for enzyme recognition, although sialic acids by themselves are not sufficient ligands for the enzyme (Abdullah et al., 1992; Sutherland et al., 1992).

OSGPase binds and cleaves only proteins with dense arrays of sialylated O-linked glycans, such as GpA (Mellors and Lo, 1995). As mentioned earlier, GpA contains 15 O-linked glycans and 1 N-linked glycan. Eleven of the O-linked glycans are found on serine/threonine residues that are clustered between amino acids 2–26 on the N-terminal domain, and the other four are located between amino acids 37–50 (Tomita et al., 1978). The major cleavage site of OSGPAse is the peptide bond at Arg-31-Asp-32 (Abdullah et al., 1992), which is adjacent to the O-glycosylation sites. Another example is CD43 (leukosialin, sialophorin): the extracellular domain of human CD43 is comprised of 234 amino acid, and 70–85 O-linked sialoglycans, an average of one O-linked sialoglycan per every three amino acids (Cyster et al., 1991). In keeping with this, OSGPase cleaves this protein to very small fragments (Sutherland et al., 1992). In contrast to the homogenous O-glycosylation of CD43, the 330–550 amino acid extracellular domain of CD45 (leukocyte common Ag) can be divided to three subdomains: an O-linked glycosylation region, and two separate cysteine-rich regions (Thomas, 1989; Tomita et al., 1978). The O-linked region spans about 177 amino acids at the very tip of the N-terminal domain, and is comprised of 34% serine/threonine residues, which are O-glycosylated. The two cysteine-rich domains are heavily N-linked glycosylated (Thomas, 1989). OSGPase digests only the O-linked glycosylation region of CD45, leaving the N-linked glycosylated region intact (Sutherland et al., 1992). Other examples of densely O-sialoglycosylated proteins that are cleaved by the enzyme are: bovine submaxillary mucins (Norgard et al., 1993a), hyaluronan receptor CD44 (Sutherland et al., 1992), CD34 (Sutherland et al., 1992), and epitectin (Hu et al., 1994).

OSGPase does not digest proteins that present sialylated O-linked glycans that are not densely packed, for example, bovine fetuin (Akai et al., 2003; Nwosu et al., 2011), or human IgA1 (Mattu et al., 1998), both of which contain only a small cluster of 3–4 O-linked sialylated glycans (Sutherland et al., 1992). The enzyme also does not digest N-linked sialoglycoproteins, over 30 of which have been tested to date (Mellors and Sutherland, 1994; Sutherland et al., 1992). When presented with an intact cell, the enzyme specifically cleaves only mucin-like sialoglycoproteins (Hu et al., 1994). Taken together it is clear that this enzyme requires a patch of sialylated O-linked glycans for binding to the target protein, and it cleaves that peptide bond adjacent to the O-glycosylated cluster. On the other hand, there is no specific sialoglycan sequence required for recognition. Thus OSGPase is apparently recognizing

some form of clustered sialylated patch that is common to all mucin-type glycoproteins, despite the different *O*-glycan structures.

8. CSPs ON PATHOGENS

8.1. Glycan clusters on bacterial capsular polysaccharides

There is evidence for antibody or Siglec recognition of saccharide clusters on bacteria capsules. Certain IgG-type monoclonal antibodies exclusively bind to intact type III group B Streptococcus (GBS III) but do not bind purified capsular polysaccharide (CPS) or comparable glycans on a microarray. Both gram-positive and gram-negative bacteria express extracellular polysaccharides that can form capsules and biofilms, both of which are major virulence factors (Bazaka et al., 2011). GBS is the major cause for pneumonia, septicemia, and meningitis in newborns (Maisey et al., 2008; Pincus et al., 1998, 2012), and has a capsular polysaccharide (CPS) that forms the outermost layer of the bacteria. The CPS helps bacteria to evade the host immune system by masking antigenic determinants, mimicking host glycans or by interfering with complement-mediated killing (Cieslewicz et al., 2005; Nizet and Esko, 2009). The GBS CPS is typically comprised of repeating monosaccharide units that are joined by glycosidic linkages to serotype-specific configuration (Bazaka et al., 2011; Cieslewicz et al., 2005). The CPS of GBS is comprised of 3–4 monosaccharide units: glucose (Glc), galactose (Gal), and *N*-acetylneuraminic acid (Neu5Ac) that may be O-acetylated, and in some serotypes *N*-acetylglucosamine (GlcNAc) is also present. These monosaccharides are polymerized in nine different configurations, unique for each serotype (Cieslewicz et al., 2005; Lewis et al., 2004). For example, the capsular polysaccharide of GBS III (CPSIII) is comprised of the repeating subunit Glcβ1-6 (Neu5Acα2-3Galβ1-4)GlcNAcβ1-3Gal (Wessels et al., 1987).

Three IgG-type monoclonal antibodies derived by immunization with intact CPSIII conjugated to tetanus toxoid: S3.1A6 (IgG1), S3.2A6 (IgG1), and S3.1B1 (IgG2a) (Zou et al., 1999), can bind and opsonize live GBS *in vitro* (Pincus et al., 2012). Immunization with tetanus toxoid conjugates typically yields antibodies that primarily recognize conformational structures (Kasper et al., 1996; Marques et al., 1994). None of the three antibodies bind to sialoglycans on the glycoarrays, including oligosaccharide structures that were recognized by other GBS type-III-specific antibodies (Pincus et al., 2012). S3.1B1 antibody binds equally well to sialidase-treated or untreated type III GBS in ELISA assay, suggesting that the sialic acid Neu5Ac is not part of the epitope recognized by this antibody (Pincus

et al., 2012). However, S3.1B1 antibody does not bind to *S. pneumoniae* type 14, which has the same core structure as desialylated CPSIII (Zou et al., 1999). This could be due to incomplete digestion by sialidase, or it may indicate that S3.1B1 ligand is stabilized by additional structure on CPSIII (Pincus et al., 2012). Despite the fact that the antibodies were derived by immunization with CPSIII, S3.1A6, and S3.2A6 preferably bind intact type III GBS over purified CPSIII in ELISA assay. These two antibodies do not bind desialylated GBS, indicating that Neu5Ac is a critical component of their ligand. Similarly, monoclonal antibody SS8 (IgG2a) that was derived by immunization with heat-killed type III GBS bound to intact type III GBS bacteria but not to CPSIII (Egan et al., 1983), suggesting that spatial organization of the glycans comprising SS8 ligand on intact bacteria is critical for the antibody recognition. Although the glycan components remain the same in purified CPSIII, the spatial organization is not preserved and the ligand is apparently scrambled, preventing antibody recognition (Pincus et al., 2012).

In addition to the cluster-specific IgG-type antibodies mentioned here, IgM-type antibodies preferably bound intact type III GBS over CPSIII. These antibodies were elicited by immunization with head-killed GBS (Egan et al., 1983; Pincus et al., 1998). However, unlike the IgG antibodies, the IgM antibodies bound to relevant structures on glycan microarray, with the exception of one antibody (SB3). In contrast to the other antibodies that were tested, SB3 binds to both intact GBS and desialylated GBS suggesting that it may recognize a completely different component of the capsid (Pincus et al., 2012). Taken together, it appears that the capsid of type III GBS is organized in immunogenic saccharide clusters that are stabilized by the sialic acid Neu5Ac.

In like manner a variety of different recombinant soluble human Siglecs bind differentially to various GBS serotypes, despite the fact that they all contain the same Neu5Acα2-3Galβ1-4GlcNAc sequence (Carlin et al., 2007, 2009). These are further examples wherein a single glycan sequence is necessary but not sufficient for recognition by various antibodies and GBPs. The best explanation for these findings is that unique CSPs are being recognized.

8.2. Antibody recognition of *N*-glycans clusters on HIV gp120

While the focus of this review has been sialylated CSPs, a recent prominent example involving mannose-containing glycans deserves special attention. Highly ordered mannose clusters on HIV gp120 monomers are comprised

of an intrinsic patch of unprocessed $Man_{5-9}GlcNAc_2$ glycans, flanked by a rim of complex glycans, surrounded by trimer-associated Manα1-2Man patch. This clustered mannose patch is recognized by the 2G12 neutralizing antibody. Additional CSPs on gp120, comprised of several N-linked oligomannose clustered with a short peptide sequence are recognized by other broadly neutralizing antibodies, PGT 125–128, PGT 130, and PG9. The HIV envelope protein Env is comprised of two noncovalently bound glycoproteins: the transmembrane subunit gp41 and the external subunit gp120. The gp120 subunit has an average of 25 N-linked glycosylation sites, and the position of these sites is highly conserved between HIV isolates and clades (Li et al., 2009; Scanlan et al., 2007a; Zhang et al., 2004). The glycosylation of gp120 results in a tightly packed cluster of oligomannose, which is evidently not found on mammalian cell surfaces (Balzarini, 2006). The formation of this unique cluster starts with the addition of $Glc_3Man_9GlcNAc_2$ precursor to the N-linked glycosylation sites in the ER. Glucose residues are then cleaved by α-glucosidases I and II to produce $Man_9GlcNAc_2$ or D2-, D3-$Man_8GlcNAc_2$, depending on the cell type (Bonomelli et al., 2011; Doores et al., 2010; Sanders et al., 2002). Further processing of the oligomannose chains to produce complex glycans is limited by the high density of mannose residues and by steric consequences of gp120 trimerization. As a result only a limited area on the gp120 trimer is accessible for glycan processing. Indeed, mass spectrometry analysis confirms that less than 2% of the total glycans on gp120 are complex glycans (Scanlan et al., 2007a; Zhu et al., 2000). Taken together, it was suggested that each gp120 monomer has an intrinsic patch of unprocessed $Man_{5-9}GlcNAc_2$ glycans, flanked by a rim of complex glycans, surrounded by trimer-associated Manα1-2Man patch (Li et al., 2009; Scanlan et al., 2007a; Zhu et al., 2000). This uniquely conserved HIV-specific glycosylation pattern was found in HIV isolates from clades A, B, and C and in simian immunodeficiency virus (SIV) (Scanlan et al., 2007a).

Given that the clustered oligomannose patch appears to be conserved for HIV viruses and does not exist on mammalian cells, it is potentially a good target for vaccine design. It was shown that the broadly neutralizing 2G12 human anti-HIV antibodies bind to the intrinsic mannose patch at the center of this complex mannose cluster (Calarese et al., 2003; Li et al., 2009; Scanlan et al., 2002). The high mannose patch can be mimicked on cultured cells by inhibition of $Man_9GlcNAc_2$ trimming with kifunensine, a mannose analog that competitively inhibits type 1 ER and Golgi α-mannosidases. The 2G12 antibody bound to the abundant oligomannose-type glycans on

kifunensine-inhibited human 293T cells, and to human CEACAM1 protein that was expressed in these cells. Like gp120, this protein has a 120 kDa highly mannosylated extracellular domain, when it was expressed in 293T cells in the presence of kifunensine (Scanlan et al., 2007b). Although 2G12 recognizes terminal Manα1-2Man residues on high mannose glycans (Sanders et al., 2002; Scanlan et al., 2002, 2007b), the spatial organization of mannose in the cluster is important for the binding and neutralization of HIV isolates with 2G12 (Astronomo et al., 2010; Scanlan et al., 2007b). Antibodies that were generated against high mannose clusters were ineffective against primary HIV isolates. For example, *Saccharomyces cerevisiae* yeast with a deletion in the α1-3 mannosyltransferase gene ΔMnn1, or a deletion of three genes (ΔOch1 ΔMnn1 ΔMnn4) in the N-linked glycosylation pathway, expresses high density of $Man_9GlcNAc_2$ or $Man_8GlcNAc_2$ oligosaccharides, respectively. Although 2G12 antibody can bind these yeasts, immunization with these mutants results in antibodies that bind gp120 but fail to neutralize primary HIV isolates (Agrawal-Gamse et al., 2011; Dunlop et al., 2010; Luallen et al., 2008). Similarly, a mannose binding molecule, cyanovirin-N, binds to gp120 and can neutralize laboratory-adapted strains, but only very weakly neutralize primary HIV isolates (Scanlan et al., 2007a). Many attempts were made to mimic the mannose cluster on gp120 protein by chemically synthesizing compounds containing multiple Man_{9}-$GlcNAc_2$ chains attached to a rigid scaffold at various densities (Astronomo et al., 2010; Joyce et al., 2008; Krauss et al., 2007). All these compounds were recognized by 2G12 antibody, and induced robust carbohydrate-specific antibody responses in immunized animals, but failed to elicit broadly neutralizing antibodies against HIV.

In addition to 2G12, other broadly neutralizing antibodies for HIV were shown to interact with the densely packed oligomannose Man_8 and Man_9 on the gp120 protein. The PGT monoclonal antibodies 125–128 and 130 bound specifically to $Man_8GlcNAc_2$ and $Man_9GlcNAc_2$ on glycan array (Pejchal et al., 2011; Walker et al., 2011). Unlike 2G12, binding of these antibodies to pg120 can be competed out with Man_9 but not with monomeric mannose or Man_4, suggesting that they bind to a different epitope (Walker et al., 2011). Despite forming 11–16 hydrogen bonds with a number of terminal mannose on gp120, only two of the $Man_{8-9}GlcNAc_2$ oligosaccharides (position 332 and/or 301) are critical for binding of PGT 127–128 antibodies (Pejchal et al., 2011; Walker et al., 2011). In addition, a short peptide at the C-terminal V3 stem is required for binding (Pejchal et al., 2011). This suggests that PGT 127–128 antibodies bind to

a specific CSP comprised of several mannose residues and a peptide, which is stabilized by one or two N-linked oligomannose. Another broadly neutralizing antibody, PG9, binds to a cluster comprised of $Man_5GlcNAc_2$, $Man_4GlcNAc_2$, and a β-sheet strand (McLellan et al., 2011).

Taken together these findings suggest that the spatial organization of mannose residues in the intrinsic patch is stabilized by the flanking glycans. Thus, in order to generate high potency HIV-broadly neutralizing antibodies the entire mannose CSP must be taken into account.

9. GLYCOSYNAPSES: CELL INTERACTIONS AND SIGNALING VIA CSPs

Glycosynapses are a type of cell surface microdomain that are stabilized by carbohydrate–carbohydrate interactions, and mediate adhesion and signaling between two cells or between cells and the ECM (Hakomori, 2002; Hakomori and Handa, 2002; Todeschini and Hakomori, 2008). Glycosynapse microdomains are classified by their content and function to three types: Type I are comprised of GSLs clustered with signaling proteins; Type II are comprised of O-linked mucin-type glycoproteins clustered with Src family kinases; and Type III are comprised of GSLs, N-glycosylated adhesion receptor, tetraspanins, and signaling proteins (Hakomori, 2004; Todeschini and Hakomori, 2008). All of the glycosynapses are stabilized by *cis* carbohydrate–carbohydrate interactions between GSLs, and are distinctively different from lipid rafts and caveolae microdomains (Hakomori, 2003).

In Type I glycosynapses, the glycosylated N-terminal domain of a GSL cluster stabilizes a saccharide cluster on the plasma membrane and GSL lipid tails interact with signaling proteins. These glycosynapses mediate cell–cell adhesion and signaling either through carbohydrate–protein interactions or carbohydrate–carbohydrate interactions between two cells (Todeschini and Hakomori, 2008). The carbohydrate–protein-mediated adhesions typically involve a "lock and key" type interaction between gangliosides and GBPs, for example, galectin-1 interaction with GM1 microdomain (Hakomori, 2004; Siebert et al., 2005). In contrast, carbohydrate–carbohydrate-mediated cell–cell adhesion is described as a zipper or a gear wheel in which a perfect fit between interacting carbohydrates is required for adhesion (Spillmann and Burger, 1996). Carbohydrate–carbohydrate interactions are stabilized primarily by van der Waal's forces, although dipole–dipole and hydrogen bonds may also form between the molecules. In most cases,

carbohydrate–carbohydrate interactions require the presence of bivalent cations (Ca^{2+} or Mg^{2+}) (Spillmann and Burger, 1996; Todeschini and Hakomori, 2008). Examples of carbohydrate–carbohydrate-mediated adhesion by type I glycosynapses include: Le^x-to-Le^x (Galβ1-4(Fucα1-3) GlcNAc) interactions between two cells to induce auto-aggregation of mouse tetratocarcinoma F9 cells (Eggens et al., 1989; Hakomori, 2004); GM3 (Neu5Acα2-3Galβ1-4Glcβ1-Cer) on B16 mouse melanoma cells interaction with Gg3 (GalNAcβ1-4Galβ1-4Glcβ1-Cer) on L5178 mouse lymphoma cells (Kojima and Hakomori, 1989), or with lactosylceramide (Galβ1-4Glcβ1-Cer) on endothelial cells (Kojima and Hakomori, 1991); Le^y (Fucα1-2Galβ1-4(Fucα1-3)GlcNAc) in mouse uterus epithelium with blood group H antigen (Fucα1-2Gal) (Zhu et al., 1995); and human embryonal carcinoma cells aggregation by interaction of globoside Gb4 (GalNAβ3Galα4Galβ4Glcβ1Cer) *cis* with Gb4, GalGb4 or *trans* with nLc_4 (Le^x precursor, Galβ1-4GlcNAc) on a neighboring cell (Song et al., 1998).

Type II glycosynapses are comprised of O-linked mucin-type glycoproteins clustered with Src family kinases, and are not very well studied. The best example is the MUC1-containing microdomains that were isolated from low-density membrane fraction of T cells (Hakomori, 2004). These microdomains include three mucin-type glycoproteins (MUC1, PSGL-1, and CD45), and three Src family kinases (Yes, Fyn, and lck56) (Agrawal et al., 1998a,b). MUC1 proteins cluster at the leading edge of activated T cells, an area that is also associated with gangliosides (Correa et al., 2003). MUC1 interactions with receptor proteins may induce signaling to mediate T-cell activation and migration (Hakomori, 2004). PSGL-1 mediates selectin binding (see Section 10.2) and CD45 is involved in regulating T-cell activation via the TCR (Altin and Sloan, 1997). Taken together the data indicate that type II glycosynapses are involved in carbohydrate-mediated cell adhesion and signaling (Hakomori, 2004).

Type III glycosynapses mediate cell–ECM adhesion, and are comprised of GSLs, an N-glycosylated adhesion receptor (e.g., integrin), tetraspanin, and signaling proteins (Todeschini and Hakomori, 2008). Integrins are a family of α/β hetrodimeric proteins that mediate cell–cell and cell–ECM adhesion (Scales and Parsons, 2011). Integrins that bind to ECM components (laminin, collagen, and fibrinogen) often associate with tetraspanins, which are palmitoylated and N-glycosylated transmembrane proteins (Bassani and Cingolani, 2012). *Cis* interactions among integrins, tetraspanin, and gangliosides depend on the N-glycosylation level on all the glycosynapse

components (Ono et al., 2000, 2001; Todeschini and Hakomori, 2008). Transmembrane signaling proteins are also stabilized by interactions between the N-linked glycans, cytoplasmic signaling proteins are stabilized by interactions with the GSLs lipid tail. Examples of type III glycosynapses include GM3/tetraspanin CD9 inhibition of cell motility and proliferation through modulation of integrin and FGF receptor function (Hakomori, 2004; Todeschini and Hakomori, 2008); and GM2/GM3/tetraspanin CD82 complex inhibit activation of hepatocyte growth factor by the tyrosine kinase receptor Met, and cross-talk with integrin α3β1 (Todeschini and Hakomori, 2008).

In conclusion, glycosynapse microdomains are comprised of GSLs, glycoproteins, and signaling proteins that are stabilized by *cis* carbohydrate–carbohydrate interactions. Such CSP-containing glycosynapses are involved in carbohydrate-dependent cell–cell and cell–ECM adhesion, and induce cell activation, motility, and growth.

10. RECOGNITION OF COMBINED SACCHARIDE–PEPTIDE PATCHES

In addition to specific glycan epitopes, several amino acids of the core protein can be required for receptor recognition, in some cases, forming an oligosaccharide–peptide patch. Sometimes the amino acids are sulfated and may be substituted for sulfated oligosaccharides. Here, we present two examples of oligosaccharide–peptide patch recognition.

10.1. *O*-sialoglycopeptide recognition by paired immunoglobulin-like receptors

The ligand for paired immunoglobulin-like receptors type 2 (PILRs) is comprised of a cluster of sialylated core 1-type O-linked glycan chain and a protein determinant (Sun et al., 2012; Wang et al., 2008a). PILRs belong to one of the paired receptor family, which consists of a pair of inhibiting (PILRα) and activating (PILRβ) receptors, are predominantly expressed in immune cells (Mousseau et al., 2000). One of the best studied ligands for PILRs is mouse CD99 (mCD99), an O-glycosylated protein that is expressed on all leukocyte lineages, and highly expressed on activated T cells (Schenkel et al., 2002; Shiratori et al., 2004; Tabata et al., 2008). O-glycosylation of threonine residues 45 and 50 on mCD99 is required for recognition by both PILRα and PILRβ. However, PILRα binding to mCD99 is not affected by a single alanine mutation of either threonine

45 (T45A) or threonine 50 (T50A). In contrast, mutation of T45A inhibits the binding of PILRβ to mCD99 (Tabata et al., 2008; Wang et al., 2008a). It was further shown that the O-glycosylation is likely comprised of a sialylated core 1-type structure. Both core 2 branching and desialylation inhibit PILRs binding to mCD99 (Sun et al., 2012; Wang et al., 2008a). Although sialylated core 1 structures are likely found on additional surface proteins on the cells, PILRs do not bind to parental cells that were not transfected with mCD99. Furthermore, PILRs do not bind sialylated oligomeric glycans on ELISA-like binding assay (Sun et al., 2012). Thus sialylated core 1 structure by itself is not the ligand for PILR binding (Wang et al., 2008a).

In addition to the sialylated core 1 structure, the PILR ligand is comprised of an adjacent protein determinant. Both mouse and human PILRα bind mCD99 but not human CD99 (hCD99), although both present similar glycosylation structures ($Neu5Ac_{1\text{-}2}Hex_1HexNAc_1$) (Sun et al., 2012). As mentioned above, mCD99 has two adjacent O-glycosylation sites (Thr-45 and Thr-50) each independently sufficient to promote PILRα binding (Tabata et al., 2008; Wang et al., 2008a). In contrast, hCD99 has only one occupied O-glycosylation site on Thr-41, which corresponds to Thr-45 site on mCD99. Insertion of the mCD99 amino acids region between Pro-46 and Thr-50 (^{46}PKAPT^{50}) to hCD99 was sufficient for PILRα binding (Sun et al., 2012). Since only one O-glycosylation site is sufficient to promote PILRα binding, the PILRα ligand is comprised of one sialylated core 1-type O-glycosylation and an adjacent protein motif (Sun et al., 2012). Additional PILRs ligands that have similar binding motifs are PILR-associating neural protein (Kogure et al., 2011), neuronal differentiation and proliferation factor-1, collectin-12 (Sun et al., 2012), and herpes simplex virus-1 glycoprotein B (Wang et al., 2009).

10.2. P- and L-selectin recognition of clustered *O*-sialoglycan-sulfated epitopes

P- and L-selectin bind to a clustered patch comprised of sialic acid, fucose, and sulfate residues at a specific spatial orientation on their protein ligands. Selectins are transmembrane glycoproteins that mediate cell–cell interactions, P-selectin is expressed on activated vascular epithelium and platelets, L-selectin is constitutively expressed on leukocytes, and E-selectin is expressed on sites of inflammation (Konstantopoulos and Thomas, 2009; Varki, 1994, 1997). Selectins weakly interact with sialylated, fucosylated lactosaminoglycans such as Sialyl-Lewis^x (Siaα2-3Galβ1-4(Fucα1-3) GlcNAcβ-, SLe^x), or its isomer Sialyl-Lewis^a (Siaα2-3Galβ1-3(Fucα1-4)

GlcNAcβ-, SLe^a). In addition, P- and L-selectins can also bind certain sulfated molecules like heparin (Norgard et al., 1993b; Varki, 1994). In contrast, E-selectin binding is sulfation-independent, and requires sialylated fucosylated N-linked glycans (Kanamori et al., 2002; Lenter et al., 1994; Levinovitz et al., 1993; Zöllner and Vestweber, 1996). Careful analysis of selectin binding requirements to their natural protein ligands reveals that the composition, charge, and spatial organization of monosaccharides and sulfate epitopes are important for binding. The cluster may be formed by oligosaccharide and sulfated peptide (e.g., P-selectin glycoprotein ligand-1 (PSGL-1)), more than one oligosaccharide chain (e.g., CD24) or form on a single oligosaccharide chain (e.g., 6-sulfo-SLe^x on GlyCAM-1). Here, we discuss the former two clusters.

PSGL-1 is a dimeric mucin type glycoprotein that was originally identified as P-selectin ligand (Moore et al., 1992) but can interact with L- and E-selectins as well (McEver and Cummings, 1997; Moore, 1998). The extracellular domain of human PSGL-1 is densely O-glycosylated with *O*-glycans that are neutral, mono- or disialylated forms of the core 2 tetrasaccharide Galβ1-4GlcNAcβ1-6(Galβ1-3)GalNAcα1-OH. Core 2 modifications include SLe^x and α1,3Fuc structures (Moore, 1998; Wilkins et al., 1996). In addition to the extensive glycosylation, PSGL-1 contains up to three sulfated tyrosine residues (Tyr-46, Tyr-48, and Tyr-51) (Pouyani and Seed, 1995; Wilkins et al., 1995). Both O-linked glycosylation and sulfation are required for P- and L-selectin binding (McEver, 2002; Norgard et al., 1993b). The exact epitope for P- and L-selectin binding on PSGL-1 was identified by analysis of glycosulfopeptides corresponding to the N-terminal amino acid residues 45–61 of human PSGL-1. The synthesized glycosulfopeptides contained between 1 and 3 sulfated tyrosines, and were O-glycosylated at Thr-57 with different core 2 structures with SLe^x determinant (Leppanen et al., 2003; Leppänen et al., 2002). Both P- and L-selectin required core 2 SLe^x determinant, and a minimum of two adjacent sulfated Tyr in close proximity to the glycosylation site for binding. L-selectin binding requires the sulfated Tyr to be immediately adjacent to the glycosylation site (Tyr-48 and Tyr-51) in contrast to P-selectin that is not as selective (Leppanen et al., 2003). This distinction is interesting because L-selectin can bind to O-linked core 2 6-sulfo SLe^x structures (e.g., on GlyCAM-1 and CD34), in contrast to P-selectin which requires the sulfated Tyr for binding (Hemmerich and Rosen, 2000; Hernandez Mir et al., 2009; Kanamori et al., 2002). However, optimal binding of both P- and L-selectin was obtained only when all three

Tyr residues were sulfated. Elongation or desialylation of the glycosylated chain inhibits P- and L-selectin binding determinant (Leppanen et al., 2003; Leppänen et al., 2002), indicating that the spatial distance between SLe^x and sulfated tyrosines is important for an optimal fit in the binding pocket. This suggests the core 2 O-linked SLe^x and 2–3 sulfated tyrosines form a cluster on PSGL-1 that is recognized by P- and L-selectins.

Another example is human CD24 (heat-stable antigen), a small mucin-type GPI-anchored protein that has O-sialoglycosyl modifications on nearly half of its amino acids (Pirruccello and LeBien, 1986). Unlike PSGL-1, CD24 does not contain a sulfated Tyr residue (Aigner et al., 1997). However, certain CD24 glycoforms contain a sulfated glucuronylneolactose carbohydrate modification (HNK-1) sulfate-3GlcAβ1-3Galβ1-4GlcNAcβ1-3Galβ1-4Glc (Aigner et al., 1997; Chou et al., 1986; Sammar et al., 1994). P- and L-selectin bind to sulfated glycosphingolipids containing the HNK-1 epitope *in vitro* (Needham and Schnaar, 1993). O-linked glycosylation, sialylation and the HNK-1 modification are all required for P-selectin binding to CD24 (Aigner et al., 1997). In contrast, treatment with endoglycosidase F to remove N-linked glycans does not affect P-selectin binding to human CD24 (Aigner et al., 1997). Only certain glycoforms of CD24 contain SLe^x modifications (Aigner et al., 1997, 1998), but these modifications are required to mediate CD24-dependent rolling and adhesion by selectins (Aigner et al., 1998). Taken together, the data indicate that P- and L-selectin bind to a cluster of SLe^x and sulfated glucuronylneolactose on CD24.

11. EXPERIMENTAL RECREATION OF CSPs

Given how little is really understood about CSPs, recreating the composition and spatial organization of glycans in a natural CSP in an *in vitro* setting is very difficult. However useful information can be obtained by spotting glycan mixtures, neoglycoproteins, and glycans on dendrimeric scaffold onto glycan microarrays, a relatively new approach to the study of glycans (Feizi et al., 2003). In the context of CSPs, a drawback of the microarray approach is the static state of the printed glycans. The cell membrane is a fluidic lipid bilayer environment, in which lateral movement can be a significant factor in mediating multivalent interactions. In order to mimic the membrane environment more closely, fluidic microarrays have been designed. Here, we briefly present evidence for CSPs recognition in glycan microarrays and fluidic microarrays.

11.1. GBP binding to mixed glycan clusters on glycan microarrays

Microarrays are a great tool for high-throughput analysis of GBP interactions with various glycan epitopes. A large number of glycan libraries comprised of synthetic glycans, glycans isolated from natural sources or a mixture of both are currently available to researchers (Lonardi et al., 2010; Padler-Karavani et al., 2012; Rillahan and Paulson, 2011). Glycans are immobilized on these arrays by various covalent and noncovalent methods. Covalent immobilization is most commonly achieved by functionalization of the glycans with thiol or amine groups, for example, and applying to an appropriate reactive surface. This approach yields a high-density glycan surface with known orientation (Rillahan and Paulson, 2011). Noncovalent methods include glycan adsorption to nitrocellulose, oxidized polystyrene, electrostatic or hydrophobic surfaces, which yields glycans in random orientation. In addition the glycans can be biotinylated and immobilized on streptavidin-conjugated surface, or tagged with DNA and immobilized to complementary DNA (Rillahan and Paulson, 2011). Binding of GBPs to glycan arrays is influenced by the length and flexibility of the linker, the underlying glycan structures and the glycan densities. This was demonstrated by cross-comparison of lectin binding to otherwise identical terminal sialylated glycan structures between two glycan array platforms (Padler-Karavani et al., 2012). Furthermore, due to the multivalent nature of GBPs interactions with glycan epitope, the spacing (density) and orientation of glycans on the array are important factors for binding (Taylor and Drickamer, 2009; Zhang et al., 2010a).

One approach for controlling the spacing between glycan epitopes is to conjugate glycan epitopes to a carrier protein, for example, albumin, generating a multivalent glycoconjugate termed neoglycoprotein (Roy, 1996; Stowell and Lee, 1980). The neoglycoproteins are then mixed with non-glycosylated spacer proteins (e.g., BSA) at a known ratio, and the mixture is immobilized on an array (Zhang et al., 2010b). The distance between neighboring neoglycoproteins is determined by the ratio between spacer proteins and neoglycoproteins, and can be estimated from the spacer protein dimensions. For example, in a tightly packed monolayer of 1:7 neoglycoprotein to BSA mixture, on average, there should be one neoglycoprotein in the middle of each group of eight molecules. BSA dimensions are approximately $35\ \text{Å} \times 35\ \text{Å} \times 70\ \text{Å}$, with the assumption that BSA molecules adhere to the surface with the 70 Å side parallel to

the surface, the distance between two neighboring neoglycoproteins should be about 140 Å (Zhang et al., 2010a). This approach provides a distinction between two modes of multivalent binding of GBP to glycan cluster. The nonglycosylated spacer proteins will not affect multivalent binding of GBP to several glycan epitopes that are presented on a single neoglycoprotein. Conversely, the spacer protein will inhibit multivalent binding of GBP to several glycan epitopes that are presented on two (or more) different neoglycoproteins, forming a homogenous CSP (Zhang et al., 2010a). Interestingly in this array the average spacing between the centers of two neighboring neoglycoproteins (140 Å) is too large for efficient energy transfer between donor and acceptor. Critical distance for Förster resonance energy transfer (FRET) is ~90 Å (Adams et al., 1991; Ishikawa-Ankerhold et al., 2012). Thus a CSP formation does not necessarily require the core proteins to form a stable complex or to physically interact.

Binding of the plant lectin concanavalin A (Con A) to mannose and glucose was examined using this approach. ConA bound at a similar apparent K_d value to a uniform layer of Glc-α-BSA, Man-α-BSA, or Man6-BSA. ConA binding to Man6-BSA was not affected by adding BSA spacer at 1:7 Man6-BSA/BSA ratio, suggesting that ConA binds to several mannose epitopes on a single neoglycoprotein. In contrast, adding the BSA spacer at 1:7 ratio abolished ConA binding to Glc-α-BSA and to Man-α-BSA. Thus ConA forms multivalent interactions with glycans on two or more neoglycoprotein (Zhang et al., 2010a), indicating specific recognition of homogenous clustered patch of mannose or glucose. Another example for homogenous CSP binding is the binding of *Vicia villosa* lectin B4 (VVL-B4) to GalNAc. VVL-B4 binding to neoglycoproteins presenting GalNAc with various underlying structures is inhibited by adding the BSA spacer proteins (Zhang et al., 2010a). This method can be used to tease out binding of commercially available antibodies and patient serum to CSPs. For example, the binding properties of five IgM and IgG1 type monoclonal antibodies for blood group A (GalNAcα1-3(Fucα1-2)Galβ-) and A1 (GalNAcα1-3(Fucα1-2)Galβ1-3GlcNAcβ1-3Galβ1-4Glc) were tested. All five antibodies tightly bound to blood group A and A1 epitopes on the array with low apparent K_d value (Zhang et al., 2010b). However, adding BSA spacer at 1:7 ratio abolished the binding of one of the tested antibodies (IgM) to blood group A1 epitope but not to the blood group A epitope. Two of the antibodies (IgM and IgG1) exhibit additional strong binding to

GalNAcα1-3Galβ-epitope on the array, which was abolished by adding BSA spacer (Zhang et al., 2010b).

Composition and spatial organization of naturally occurring CSPs on cells could be very complex and difficult to mimic on the above kind of microarray. Instead, spotting mixtures of two different glycans on an array provides a simplified version of heterogeneous saccharide patches. Theoretically, a mixture of 1:1 should generate a surface in which the two glycans are evenly distributed (Liang et al., 2011). Antibody or GBP binding to a mixed surface can be then compared with the binding to a uniform layer of its specific ligand. A change in the binding K_d is an indication to the effect of neighboring glycans on antibody–ligand interactions. The binding can be reduced due to steric hindrance by the neighboring glycans, can remain unaffected, or can be enhanced by the formation of a novel epitope comprised of two or more neighboring glycans (Liang et al., 2011). For example, the binding of an antibody against the glycosphingolipid SSEA3 (Stage-Specific Embryonic Antigen 3, Gb5) was tested on an array with 1:1 mixtures of SSEA3 with six other glycosphingolipids of the globo-series glycolipids (SSEA4, Globo H, Gb4, Gb3, Gb2, and Bb2) (Kannagi et al., 1983; Liang et al., 2011). With exception of the SSEA3/SSEA4 mixture, antibody binding to SSEA3 was reduced in the mixed surface presumably due to steric hindrance by neighboring glycans. Not surprisingly, the steric hindrance was directly proportional to the length of the neighboring glycan. Interestingly, however, higher antibody binding to SSEA3/SSEA4 mixture was observed compared with binding to SSEA3 alone (Liang et al., 2011). Although the antibody did cross-react with SSEA4 directly, the binding intensity to SSEA3/SSEA4 mixture was higher than the intensity of the average binding to SSEA3 and to SSEA4. This suggests that a cluster of SSEA3 and SSEA4 generates the preferred ligand for the antibody.

In another approach, two types of oligomannose (Man4 and Man9) were conjugated to a second-generation dendrimetric scaffold at different ratios. The oligomannose dendrimers were spotted on a microarray, creating clusters of oligomannose with 9:0, 0:9, 6:3, 3:6, and 5:4 Man4:Man9 ratio (Liang et al., 2011; Wang et al., 2008b). The HIV neutralizing antibody, 2G12 preferably bound to the 5:4 dendrimer with half of the binding K_d compared with the other dendrimers (13.47 nM compared with 30.34–47.4 nM). In theory, at 5:4 ratio every Man9 is flanked with Man4 thus potentially presenting a new clustered epitope comprised of both oligomers (Liang et al., 2011).

11.2. Combinatorial glycoarrays and fluidic glycan microarrays

Combinatorial glycoarrays and lipid microarrays are another approach to study binding to glycosphingolipid mixtures. In examples of this approach, a mixture of glycolipids/lipids is printed onto a polyvinylidene difluoride membranes affixed to glass slides. The lipid tail binds noncovalently to the hydrophobic surface and the oligosaccharide head group is free to interact with GBPs and antibodies (Kanter et al., 2006; Rinaldi et al., 2012). The combinatorial glycoarray is used to compare the interactions with a single ganglioside compared to interactions with its heterodimeric ganglioside mixtures (Rinaldi et al., 2012). Lipid microarrays typically include lipid extracts from a variety of tissues, biological fluids, and cells (Kanter et al., 2006).

Combinatorial glycoarrays were used to identify antibodies against ganglioside complexes in sera from neuropathy patients (see Section 5.1). In addition, combinatorial glycoarrays were used to study the binding of certain bacterial toxins and lectins to gangliosides and ganglioside complexes. For example, the gangliosides GD1b and GT1b are known to be part of the binding complex of Tetanus neurotoxin fragment (TeNT HC) on neuronal cells, and were shown to colocalize in immunofluorescence studies (Deinhardt et al., 2006). In agreement with these findings, TeNT HC binds very strongly both to GD1b and to GT1b on the combinatorial glycoarray and the binding is not affected by ganglioside complex formation. In contrast, TeNT HC strongly binds to GQ1b on the glycoarray, but does not bind to GQ1b/GM2 mixture (Rinaldi et al., 2009). Interestingly, although TeNT HC does not bind to the single gangliosides GD3, GM1, GD1a, or GT1a, it reacts strongly with heterodimers of these gangliosides with GD3, suggesting the formation of a neo binding epitope for TeNT HC in the GD3-containing ganglioside complexes (Rinaldi et al., 2009, 2010). Other evidence to the formation of GD3-containing complexes comes from the binding pattern of human Siglec-7-Fc to the combinatorial glycoarrays. Human Siglec-7 is a CD33-related Siglec that preferably binds to Neu5Acα2-8Neu5Ac containing structures, such as GD3 (Crocker et al., 2007). Siglec-7-Fc strongly binds to GD3 on the glycoarray, but does not bind to the GD3 when it is mixed with GM1, GD1a, or GT1a, suggesting that the GD3 epitope is masked in the cluster probably by the formation of a neo epitope (Rinaldi et al., 2009, 2010).

As discussed above, in most glycan microarrays the glycan epitopes are immobilized to the surface of the array either covalently or noncovalently. However, the cell membrane is a fluidic lipid bilayer environment, in which lateral movement is a significant factor in mediating multivalent interactions

(Yamazaki et al., 2005; Zhu et al., 2009). Several approaches have been taken to generate lipid microarrays (Brian and McConnell, 1984; Castellana and Cremer, 2007; Groves and Boxer, 2002; Tanaka and Sackmann, 2005). Lipid bilayer platform technology is the most robust and quantitative method (Deng et al., 2008). In this approach cholesterol is dispersed and immobilized by covalent linking to a brush layer of poly(ethyleneglycol) (PEG). Small unilamellar vesicles (SUV) are then deposited onto the PEG-cholesteryl surface to form a lipid bilayer. The cholesterol molecules stabilize the lower leaflet of the bilayer while maintaining the fluidity of the outer layer (Deng et al., 2008). Different glycoproteins and glycolipids can be incorporated into the SUV at varying concentrations in order to form a fluidic glycan microarray (Bricarello et al., 2010; Deng et al., 2008; Zhu et al., 2009).

Fluidic glycan microarrays were used to study the interaction of pathogens with their known glycan receptors. For example, type 1 adhesin FimH, located at the tip of *Escherichia coli* pili, bind to mannose on host cells (Harris et al., 2001; Krogfelt et al., 1990; Schembri and Klemm, 1998). *E. coli* binding to a density gradient fluidic array of mannose-linked lipids at densities ranging from 0 to 0.3 nm^{-2} was quantified (Zhu et al., 2009). At a critical mannose concentration of 0.1 nm^{-2}, the number of bound bacteria was increased by an order of magnitude. At this concentration the inter-mannose distance is ~4 nm, which is 2 orders of magnitude shorter than the distance between two pili. Thus the binding of FimH to the array switched from monovalent binding to a trivalent binding (Zhu et al., 2009), suggesting that clustered mannose is a preferred ligand for FimH.

12. CONCLUSIONS AND PERSPECTIVES

The idea that glycans can cluster into discreet patches, and that these CSPs can influence glycan recognition and function was proposed two decades ago as a possible explanation for the extraordinary specificity of selectins for certain ligands, despite their recognition of commonly occurring glycans (Varki, 1994). In this review we present an abundance of indirect evidence to support the existence of CSPs on proteins, cells and pathogens, and evidence that glycan clustering influences their recognition by GBPs. It is likely that glycan microdomains are mostly stabilized by carbohydrate–carbohydrate interactions, which are too weak to withstand the standard biochemical methods used to study protein–protein interactions (e.g., immunoprecipitation). Furthermore, the spatial organization of

glycans in CSPs is critical for GBP recognition. Attempts to isolate them for study *in vitro* inevitably disperse the clusters (e.g., CSPs on GBS III capsid, Section 8.1). Imaging of the relative positions of glycans in CSPs is also very difficult, since imaging typically requires binding of antibodies and GBPs to a target epitope. The density and distribution of glycans in CSPs may mask recognition of individual glycans, and thus prevent their visualization within the CSP (e.g., ganglioside complexes, Section 5). Alternate approaches that directly label the glycans (using click chemistry Baskin et al., 2007 or periodate oxidation and aniline-catalyzed oxime ligation Ramya et al., 2013) also alters the glycans and potentially changes the organization of the CSP and its interaction with GBPs. Recreating natural CSPs *in vitro* and on glycan or lipid arrays is a major challenge, though technology is improving (see Section 11). Screens of antibody and GBP binding to arrays containing glycan mixtures will eventually provide a reference database of naturally occurring glycan epitopes and the molecules that bind them in their native conformation. Progress toward this goal will require advances in glycan microarray technology and perhaps even new ideas about how to generate an array of CSPs with realistic clustering properties.

Obtaining direct physical evidence of CSP formation will require technologies that do not rely on protein/antibody detection, or chemical modification of the glycans. Such methods may include crystallography, nuclear magnetic resonance (NMR) spectroscopy, or advanced microscopy methods. X-ray crystallography is not well suited to study structure of heavily glycosylated proteins such as mucins, because the heterogeneity and flexibility of glycan bonds prevents crystallization (Gerken, 1993). However, 2D crystallography methods can now visualize two-dimensional crystals of membrane proteins in a lipid environment (Kang et al., 2013; Raunser and Walz, 2009) and on living cells (Gualtieri et al., 2011). Glycans in CSPs are stabilized by *cis* interactions, so their movement should be constrained relative to glycans that are not associated with CSPs. Thus it may be possible to adapt 2D crystallography for the structural analysis of CSPs on membranes. NMR spectroscopy is another experimental tool to study glycan structure at atomic resolution. This method is typically used to analyze purified glycans or a simple mixture of glycans in solution using ^{1}H and ^{13}C isotopes (Shriver et al., 2012). Although the structure of the glycosaminoglycan heparan sulfate has been studied using NMR, the heterogeneity of glycans on mucin-like proteins may be too overwhelming for this method. Thus study of CSPs on proteins using liquid state NMR is very challenging. Recent developments in solid-state NMR enable analysis of proteins in the

cell membrane. To compensate for the high signal-to-noise ratio and increase sensitivity, proteins are labeled with fluorine (^{19}F), which is scarce in natural membranes (Koch et al., 2012). However, while the resolution is not yet sufficient to study CSPs, glycan labeling with heavy isotopes in combination with a high power energy source (e.g., synchrotron) will perhaps allow the study of CSPs on membranes.

Direct visualization of CSPs on the plasma membrane may become possible with improved high-resolution microscopy methods for imaging unlabeled hydrated samples. Advances in atomic force microscopy (AFM) and near field scanning optical microscopy allow imaging of single molecules on the plasma membrane with nanometer spatial resolution (Betzig and Trautman, 1992; Hinterdorfer et al., 2012; van Zanten et al., 2010). Using these methods enabled imaging of the spatial organization of peptidoglycan in living bacteria, nanodomains in yeast membranes, and the spatial organization of molecules in lipid rafts (reviewed in Hinterdorfer et al., 2012). In addition, the thickness and spatial distribution of glycocalyx in the plasma membrane of cultured cells was visualized using a combination of AFM and light microscopy (Bai and Wang, 2012). However, the resolution is currently not sufficient for CSP imaging and further developments are needed to enable analysis of glycan distribution within the CSP.

Considering the huge diversity of glycans, their biochemical properties, and their important role in cellular recognition and binding it is very likely that glycans are often organized into meaningful clusters of the kind discussed here. While current technology does not allow for direct imaging of CSPs, their existence and biological importance can be inferred from the wealth of evidence for CSP-specific recognition presented in this review.

ACKNOWLEDGMENTS

We thank Lingquan Deng and Stevan Springer for their critical comments on the manuscript.

REFERENCES

Abdullah, K.M., Lo, R.Y., Mellors, A., 1991. Cloning, nucleotide sequence, and expression of the Pasteurella haemolytica A1 glycoprotease gene. J. Bacteriol. 173, 5597–5603.

Abdullah, K.M., Udoh, E.A., Shewen, P.E., Mellors, A., 1992. A neutral glycoprotease of Pasteurella haemolytica A1 specifically cleaves O-sialoglycoproteins. Infect. Immun. 60, 56–62.

Adams, S.R., Harootunian, A.T., Buechler, Y.J., Taylor, S.S., Tsien, R.Y., 1991. Fluorescence ratio imaging of cyclic AMP in single cells. Nature 349, 694–697.

Adluri, S., Helling, F., Ogata, S., Zhang, S., Itzkowitz, S.H., Lloyd, K.O., Livingston, P.O., 1995. Immunogenicity of synthetic TF-KLH (keyhole limpet hemocyanin) and

sTn-KLH conjugates in colorectal carcinoma patients. Cancer Immunol. Immunother. 41, 185–192.
Agrawal, B., Krantz, M.J., Parker, J., Longenecker, B.M., 1998a. Expression of MUC1 mucin on activated human T cells: implications for a role of MUC1 in normal immune regulation. Cancer Res. 58, 4079–4081.
Agrawal, B., Krantz, M.J., Reddish, M.A., Longenecker, B.M., 1998b. Cancer-associated MUC1 mucin inhibits human T-cell proliferation, which is reversible by IL-2. Nat. Med. 4, 43–49.
Agrawal-Gamse, C., Luallen, R.J., Liu, B., Fu, H., Lee, F.H., Geng, Y., Doms, R.W., 2011. Yeast-elicited cross-reactive antibodies to HIV Env glycans efficiently neutralize virions expressing exclusively high-mannose N-linked glycans. J. Virol. 85, 470–480.
Aigner, S., Sthoeger, Z.M., Fogel, M., Weber, E., Zarn, J., Ruppert, M., Zeller, Y., Vestweber, D., Stahel, R., Sammar, M., Altevogt, P., 1997. CD24, a mucin-type glycoprotein, is a ligand for P-selectin on human tumor cells. Blood 89, 3385–3395.
Aigner, S., Ramos, C.L., Hafezi-Moghadam, A., Lawrence, M.B., Friederichs, J., Altevogt, P., Ley, K., 1998. CD24 mediates rolling of breast carcinoma cells on P-selectin. FASEB J. 12, 1241–1251.
Akai, R., Kinoshita, M., Kakehi, K., Lee, Y.C., 2003. A method for detecting O-glycanase in biological samples using a combination of MALDI-TOF mass spectrometry and time-resolved fluorimetry. Analyst 128, 440–446.
Altin, J.G., Sloan, E.K., 1997. The role of CD45 and CD45-associated molecules in T cell activation. Immunol. Cell Biol. 75, 430–445.
Angata, T., Varki, A., 2000. Siglec-7: a sialic acid-binding lectin of the immunoglobulin superfamily. Glycobiology 10, 431–438.
Anstee, D.J., 1990. Blood group-active surface molecules of the human red blood cell. Vox Sang. 58, 1–20.
Astronomo, R.D., Kaltgrad, E., Udit, A.K., Wang, S.K., Doores, K.J., Huang, C.Y., Pantophlet, R., Paulson, J.C., Wong, C.H., Finn, M.G., Burton, D.R., 2010. Defining criteria for oligomannose immunogens for HIV using icosahedral virus capsid scaffolds. Chem. Biol. 17, 357–370.
Bai, K., Wang, W., 2012. Spatio-temporal development of the endothelial glycocalyx layer and its mechanical property in vitro. J. R. Soc. Interface. 9, 2290–2298.
Balzarini, J., 2006. Inhibition of HIV entry by carbohydrate-binding proteins. Antiviral Res. 71, 237–247.
Baskin, J.M., Prescher, J.A., Laughlin, S.T., Agard, N.J., Chang, P.V., Miller, I.A., Lo, A., Codelli, J.A., Bertozzi, C.R., 2007. Copper-free click chemistry for dynamic in vivo imaging. Proc. Natl. Acad. Sci. U. S. A. 104, 16793–16797.
Bassani, S., Cingolani, L.A., 2012. Tetraspanins: interactions and interplay with integrins. Int. J. Biochem. Cell Biol. 44, 703–708.
Baum, J., Ward, R.H., Conway, D.J., 2002. Natural selection on the erythrocyte surface. Mol. Biol. Evol. 19, 223–229.
Bazaka, K., Crawford, R.J., Nazarenko, E.L., Ivanova, E.P., 2011. Bacterial extracellular polysaccharides. Adv. Exp. Med. Biol. 715, 213–226.
Betzig, E., Trautman, J.K., 1992. Near-field optics: microscopy, spectroscopy, and surface modification beyond the diffraction limit. Science 257, 189–195.
Bhat, K., Wang, F., Ma, Q., Li, Q., Mallik, S., Hsieh, T.C., Wu, E., 2012. Advances in biomarker research for pancreatic cancer. Curr. Pharm. Des. 18, 2439–2451.
Bonomelli, C., Doores, K.J., Dunlop, D.C., Thaney, V., Dwek, R.A., Burton, D.R., Crispin, M., Scanlan, C.N., 2011. The glycan shield of HIV is predominantly oligomannose independently of production system or viral clade. PLoS One 6, e23521.
Bouanene, H., Miled, A., 2010. Conflicting views on the molecular structure of the cancer antigen CA125/MUC16. Dis. Markers 28, 385–394.

Brian, A.A., McConnell, H.M., 1984. Allogeneic stimulation of cytotoxic T cells by supported planar membranes. Proc. Natl. Acad. Sci. U. S. A. 81, 6159–6163.
Bricarello, D.A., Mills, E.J., Petrlova, J., Voss, J.C., Parikh, A.N., 2010. Ganglioside embedded in reconstituted lipoprotein binds cholera toxin with elevated affinity. J. Lipid Res. 51, 2731–2738.
Brinkman-Van der Linden, E.C.M., Varki, A., 2000. New aspects of siglec binding specificities, including the significance of fucosylation and of the sialyl-Tn epitope. J. Biol. Chem. 275, 8625–8632.
Brinkman-Van der Linden, E.C.M., Sonnenburg, J.L., Varki, A., 2002. Effects of sialic acid substitutions on recognition by Sambucus nigra agglutinin and Maackia amurensis hemagglutinin. Anal. Biochem. 303, 98–104.
Bulai, T., Bratosin, D., Pons, A., Montreuil, J., Zanetta, J.P., 2003. Diversity of the human erythrocyte membrane sialic acids in relation with blood groups. FEBS Lett. 534, 185–189.
Calarese, D.A., Scanlan, C.N., Zwick, M.B., Deechongkit, S., Mimura, Y., Kunert, R., Zhu, P., Wormald, M.R., Stanfield, R.L., Roux, K.H., Kelly, J.W., Rudd, P.M., Dwek, R.A., Katinger, H., Burton, D.R., Wilson, I.A., 2003. Antibody domain exchange is an immunological solution to carbohydrate cluster recognition. Science 300, 2065–2071.
Carlin, A.F., Lewis, A.L., Varki, A., Nizet, V., 2007. Group B streptococcal capsular sialic acids interact with siglecs (immunoglobulin-like lectins) on human leukocytes. J. Bacteriol. 89, 1231–1237.
Carlin, A.F., Chang, Y.C., Areschoug, T., Lindahl, G., Hurtado-Ziola, N., King, C.C., Varki, A., Nizet, V., 2009. Group B Streptococcus suppression of phagocyte functions by protein-mediated engagement of human Siglec-5. J. Exp. Med. 206, 1691–1699.
Castellana, E.T., Cremer, P.S., 2007. Imaging large arrays of supported lipid bilayers with a macroscope. Biointerphases 2, 57–63.
Che, A., Cherry, R.J., 1995. Loss of rotational mobility of band 3 proteins in human erythrocyte membranes induced by antibodies to glycophorin A. Biophys. J. 68, 1881–1887.
Chou, D.K., Ilyas, A.A., Evans, J.E., Costello, C., Quarles, R.H., Jungalwala, F.B., 1986. Structure of sulfated glucuronyl glycolipids in the nervous system reacting with HNK-1 antibody and some IgM paraproteins in neuropathy. J. Biol. Chem. 261, 11717–11725.
Cieslewicz, M.J., Chaffin, D., Glusman, G., Kasper, D., Madan, A., Rodrigues, S., Fahey, J., Wessels, M.R., Rubens, C.E., 2005. Structural and genetic diversity of group B streptococcus capsular polysaccharides. Infect. Immun. 73, 3096–3103.
Cohen, M., Varki, A., 2010. The sialome-far more than the sum of its parts. OMICS 14, 455–464.
Cohen, M., Hurtado-Ziola, N., Varki, A., 2009. ABO blood group glycans modulate sialic acid recognition on erythrocytes. Blood 114, 3668–3676.
Collins, B.E., Paulson, J.C., 2004. Cell surface biology mediated by low affinity multivalent protein-glycan interactions. Curr. Opin. Chem. Biol. 8, 617–625.
Correa, I., Plunkett, T., Vlad, A., Mungul, A., Candelora-Kettel, J., Burchell, J.M., Taylor-Papadimitriou, J., Finn, O.J., 2003. Form and pattern of MUC1 expression on T cells activated in vivo or in vitro suggests a function in T-cell migration. Immunology 108, 32–41.
Crocker, P.R., Paulson, J.C., Varki, A., 2007. Siglecs and their roles in the immune system. Nat. Rev. Immunol. 7, 255–266.
Cummings, R.D., Esko, J.D., 2009. Principles of glycan recognition. In: Varki, A., Cummings, R.D., Esko, J.D., Freeze, H.H., Stanley, P., Bertozzi, C.R., Hart, G.W., Etzler, M.E. (Eds.), Essentials of Glycobiology. Cold Spring Harbor Laboratory Press, Cold Spring Harbor, NY, pp. 387–402.

Cyster, J.G., Shotton, D.M., Williams, A.F., 1991. The dimensions of the T lymphocyte glycoprotein leukosialin and identification of linear protein epitopes that can be modified by glycosylation. EMBO J. 10, 893–902.
Dam, T.K., Brewer, C.F., 2008. Effects of clustered epitopes in multivalent ligand-receptor interactions. Biochemistry 47, 8470–8476.
Deinhardt, K., Berninghausen, O., Willison, H.J., Hopkins, C.R., Schiavo, G., 2006. Tetanus toxin is internalized by a sequential clathrin-dependent mechanism initiated within lipid microdomains and independent of epsin1. J. Cell Biol. 174, 459–471.
Deng, Y., Wang, Y., Holtz, B., Li, J., Traaseth, N., Veglia, G., Stottrup, B.J., Elde, R., Pei, D., Guo, A., Zhu, X.Y., 2008. Fluidic and air-stable supported lipid bilayer and cell-mimicking microarrays. J. Am. Chem. Soc. 130, 6267–6271.
Doores, K.J., Bonomelli, C., Harvey, D.J., Vasiljevic, S., Dwek, R.A., Burton, D.R., Crispin, M., Scanlan, C.N., 2010. Envelope glycans of immunodeficiency virions are almost entirely oligomannose antigens. Proc. Natl. Acad. Sci. U. S. A. 107, 13800–13805.
Drzeniek, Z., Stocker, G., Siebertz, B., Just, U., Schroeder, T., Ostertag, W., Haubeck, H.D., 1999. Heparan sulfate proteoglycan expression is induced during early erythroid differentiation of multipotent hematopoietic stem cells. Blood 93, 2884–2897.
Dunlop, D.C., Bonomelli, C., Mansab, F., Vasiljevic, S., Doores, K.J., Wormald, M.R., Palma, A.S., Feizi, T., Harvey, D.J., Dwek, R.A., Crispin, M., Scanlan, C.N., 2010. Polysaccharide mimicry of the epitope of the broadly neutralizing anti-HIV antibody, 2G12, induces enhanced antibody responses to self oligomannose glycans. Glycobiology 20, 812–823.
Egan, M.L., Pritchard, D.G., Dillon, H.C.J., Gray, B.M., 1983. Protection of mice from experimental infection with type III group B Streptococcus using monoclonal antibodies. J. Exp. Med. 158, 1006–1011.
Eggens, I., Fenderson, B., Toyokuni, T., Dean, B., Stroud, M., Hakomori, S.-I., 1989. Specific interaction between Lex and Lex determinants. A possible basis for cell recognition in preimplantation embryos and in embryonal carcinoma cells. J. Biol. Chem. 264, 9476–9484.
Feizi, T., Fazio, F., Chai, W., Wong, C.H., 2003. Carbohydrate microarrays—a new set of technologies at the frontiers of glycomics. Curr. Opin. Struct. Biol. 13, 637–645.
Fujita, A., Cheng, J., Hirakawa, M., Furukawa, K., Kusunoki, S., Fujimoto, T., 2007. Gangliosides GM1 and GM3 in the living cell membrane form clusters susceptible to cholesterol depletion and chilling. Mol. Biol. Cell 18, 2112–2122.
Gerken, T.A., 1993. Biophysical approaches to salivary mucin structure, conformation and dynamics. Crit. Rev. Oral Biol. Med. 4, 261–270.
Greenshields, K.N., Halstead, S.K., Zitman, F.M., Rinaldi, S., Brennan, K.M., O'Leary, C., Chamberlain, L.H., Easton, A., Roxburgh, J., Pediani, J., Furukawa, K., Furukawa, K., Goodyear, C.S., Plomp, J.J., Willison, H.J., 2009. The neuropathic potential of anti-GM1 autoantibodies is regulated by the local glycolipid environment in mice. J. Clin. Invest. 119, 595–610.
Greenwell, P., 1997. Blood group antigens: molecules seeking a function? Glycoconj. J. 14, 159–173.
Groves, J.T., Boxer, S.G., 2002. Micropattern formation in supported lipid membranes. Acc. Chem. Res. 35, 149–157.
Gualtieri, E.J., Guo, F., Kissick, D.J., Jose, J., Kuhn, R.J., Jiang, W., Simpson, G.J., 2011. Detection of membrane protein two-dimensional crystals in living cells. Biophys. J. 100, 207–214.
Gustafsson, B., 1990. Isotype determination of monoclonal antibodies by immunodiffusion. Methods Mol. Biol. 5, 623–625.

Hakomori, S., 2002. The glycosynapse. Proc. Natl. Acad. Sci. U. S. A. 99, 225–232.
Hakomori, S., 2003. Structure, organization, and function of glycosphingolipids in membrane. Curr. Opin. Hematol. 10, 16–24.
Hakomori, S., 2004. Glycosynapses: microdomains controlling carbohydrate-dependent cell adhesion and signaling. An. Acad. Bras. Cienc. 76, 553–572.
Hakomori, S., Handa, K., 2002. Glycosphingolipid-dependent cross-talk between glycosynapses interfacing tumor cells with their host cells: essential basis to define tumor malignancy. FEBS Lett. 531, 88–92.
Harris, S.L., Spears, P.A., Havell, E.A., Hamrick, T.S., Horton, J.R., Orndorff, P.E., 2001. Characterization of Escherichia coli type 1 pilus mutants with altered binding specificities. J. Bacteriol. 183, 4099–4102.
Heimburg-Molinaro, J., Lum, M., Vijay, G., Jain, M., Almogren, A., Rittenhouse-Olson, K., 2011. Cancer vaccines and carbohydrate epitopes. Vaccine 29, 8802–8826.
Hemmerich, S., Rosen, S.D., 2000. Carbohydrate sulfotransferases in lymphocyte homing. Glycobiology 10, 849–856.
Hernandez Mir, G., Helin, J., Skarp, K.P., Cummings, R.D., Makitie, A., Renkonen, R., Leppanen, A., 2009. Glycoforms of human endothelial CD34 that bind L-selectin carry sulfated sialyl Lewis x capped O- and N-glycans. Blood 114, 733–741.
Hinterdorfer, P., Garcia-Parajo, M.F., Dufrene, Y.F., 2012. Single-molecule imaging of cell surfaces using near-field nanoscopy. Acc. Chem. Res. 45, 327–336.
Hosoi, E., 2008. Biological and clinical aspects of ABO blood group system. J. Med. Invest. 55, 174–182.
Hu, R.-H., Mellors, A., Bhavanandan, V.P., 1994. Cleavage of epitectin, a mucin-type sialoglycoprotein, from the surface of human laryngeal carcinoma cells by a glycoprotease from Pasteurella haemolytica. Arch. Biochem. Biophys. 310, 300–309.
Ishikawa-Ankerhold, H.C., Ankerhold, R., Drummen, G.P., 2012. Advanced fluorescence microscopy techniques—FRAP, FLIP, FLAP, FRET and FLIM. Molecules 17, 4047–4132.
Itzkowitz, S.H., Yuan, M., Montgomery, C.K., Kjeldsen, T., Takahashi, H.K., Bigbee, W.L., Kim, Y.S., 1989. Expression of Tn, sialosyl-Tn, and T antigens in human colon cancer. Cancer Res. 49, 197–204.
Jankovic, M.M., Milutinovic, B.S., 2008. Glycoforms of CA125 antigen as a possible cancer marker. Cancer Biomark 4, 35–42.
Jarolim, P., Rubin, H.L., Liu, S.C., Cho, M.R., Brabec, V., Derick, L.H., Yi, S.J., Saad, S.T., Alper, S., Brugnara, C., et al., 1994. Duplication of 10 nucleotides in the erythroid band 3 (AE1) gene in a kindred with hereditary spherocytosis and band 3 protein deficiency (band 3PRAGUE). J. Clin. Invest. 93, 121–130.
Jiang, L., Duriseti, S., Sun, P., Miller, L.H., 2009. Molecular basis of binding of the Plasmodium falciparum receptor BAEBL to erythrocyte receptor glycophorin C. Mol. Biochem. Parasitol. 168, 49–54.
Joyce, J.G., Krauss, I.J., Song, H.C., Opalka, D.W., Grimm, K.M., Nahas, D.D., Esser, M.T., Hrin, R., Feng, M., Dudkin, V.Y., Chastain, M., Shiver, J.W., Danishefsky, S.J., 2008. An oligosaccharide-based HIV-1 2G12 mimotope vaccine induces carbohydrate-specific antibodies that fail to neutralize HIV-1 virions. Proc. Natl. Acad. Sci. U. S. A. 105, 15684–15689.
Ju, T., Lanneau, G.S., Gautam, T., Wang, Y., Xia, B., Stowell, S.R., Willard, M.T., Wang, W., Xia, J.Y., Zuna, R.E., Laszik, Z., Benbrook, D.M., Hanigan, M.H., Cummings, R.D., 2008. Human tumor antigens Tn and sialyl Tn arise from mutations in Cosmc. Cancer Res. 68, 1636–1646.
Kaida, K., Kusunoki, S., 2010. Antibodies to gangliosides and ganglioside complexes in Guillain-Barre syndrome and Fisher syndrome: mini-review. J. Neuroimmunol. 223, 5–12.

Kaida, K., Morita, D., Kanzaki, M., Kamakura, K., Motoyoshi, K., Hirakawa, M., Kusunoki, S., 2004. Ganglioside complexes as new target antigens in Guillain-Barre syndrome. Ann. Neurol. 56, 567–571.

Kaida, K., Kanzaki, M., Morita, D., Kamakura, K., Motoyoshi, K., Hirakawa, M., Kusunoki, S., 2006. Anti-ganglioside complex antibodies in Miller Fisher syndrome. J. Neurol. Neurosurg. Psychiatry 77, 1043–1046.

Kaida, K., Morita, D., Kanzaki, M., Kamakura, K., Motoyoshi, K., Hirakawa, M., Kusunoki, S., 2007. Anti-ganglioside complex antibodies associated with severe disability in GBS. J. Neuroimmunol. 182, 212–218.

Kanamori, A., Kojima, N., Uchimura, K., Muramatsu, T., Tamatani, T., Berndt, M.C., Kansas, G.S., Kannagi, R., 2002. Distinct sulfation requirements of selectins disclosed using cells that support rolling mediated by all three selectins under shear flow - L-selectin prefers carbohydrate 6-sulfation to tyrosine sulfation, whereas P-selectin does not. J. Biol. Chem. 277, 32578–32586.

Kang, H.J., Lee, C., Drew, D., 2013. Breaking the barriers in membrane protein crystallography. Int. J. Biochem. Cell Biol. 45, 636–644.

Kannagi, R., Cochran, N.A., Ishigami, F., Hakomori, S., Andrews, P.W., Knowles, B.B., Solter, D., 1983. Stage-specific embryonic antigens (SSEA-3 and −4) are epitopes of a unique globo-series ganglioside isolated from human teratocarcinoma cells. EMBO J. 2, 2355–2361.

Kanter, J.L., Narayana, S., Ho, P.P., Catz, I., Warren, K.G., Sobel, R.A., Steinman, L., Robinson, W.H., 2006. Lipid microarrays identify key mediators of autoimmune brain inflammation. Nat. Med. 12, 138–143.

Kanzaki, M., Kaida, K., Ueda, M., Morita, D., Hirakawa, M., Motoyoshi, K., Kamakura, K., Kusunoki, S., 2008. Ganglioside complexes containing GQ1b as targets in Miller Fisher and Guillain-Barre syndromes. J. Neurol. Neurosurg. Psychiatry 79, 1148–1152.

Kasper, D.L., Paoletti, L.C., Wessels, M.R., Guttormsen, H.K., Carey, V.J., Jennings, H.J., Baker, C.J., 1996. Immune response to type III group B streptococcal polysaccharide-tetanus toxoid conjugate vaccine. J. Clin. Invest. 98, 2308–2314.

Kjeldsen, T., Clausen, H., Hirohashi, S., Ogawa, T., Iijima, H., Hakomori, S., 1988. Preparation and characterization of monoclonal antibodies directed to the tumor-associated O-linked sialosyl-2——6 alpha-N-acetylgalactosaminyl (sialosyl-Tn) epitope. Cancer Res. 48, 2214–2220.

Ko, W.Y., Kaercher, K.A., Giombini, E., Marcatili, P., Froment, A., Ibrahim, M., Lema, G., Nyambo, T.B., Omar, S.A., Wambebe, C., Ranciaro, A., Hirbo, J.B., Tishkoff, S.A., 2011. Effects of natural selection and gene conversion on the evolution of human glycophorins coding for MNS blood polymorphisms in malaria-endemic African populations. Am. J. Hum. Genet. 88, 741–754.

Kobayashi, K., Kato, K., Sugi, T., Takemae, H., Pandey, K., Gong, H., Tohya, Y., Akashi, H., 2010. Plasmodium falciparum BAEBL binds to heparan sulfate proteoglycans on the human erythrocyte surface. J. Biol. Chem. 285, 1716–1725.

Koch, K., Afonin, S., Ieronimo, M., Berditsch, M., Ulrich, A.S., 2012. Solid-state (19)F-NMR of peptides in native membranes. Top. Curr. Chem. 306, 89–118.

Kogure, A., Shiratori, I., Wang, J., Lanier, L.L., Arase, H., 2011. PANP is a novel O-glycosylated PILRalpha ligand expressed in neural tissues. Biochem. Biophys. Res. Commun. 405, 428–433.

Kojima, N., Hakomori, S., 1989. Specific interaction between gangliotriaosylceramide (Gg3) and sialosyllactosylceramide (GM3) as a basis for specific cellular recognition between lymphoma and melanoma cells. J. Biol. Chem. 264, 20159–20162.

Kojima, N., Hakomori, S., 1991. Cell adhesion, spreading, and motility of GM3-expressing cells based on glycolipid-glycolipid interaction. J. Biol. Chem. 266, 17552–17558.

Konstantopoulos, K., Thomas, S.N., 2009. Cancer cells in transit: the vascular interactions of tumor cells. Annu. Rev. Biomed. Eng. 11, 177–202.
Kornfeld, R., Kornfeld, S., 1985. Assembly of asparagine-linked oligosaccharides. Annu. Rev. Biochem. 54, 631–664.
Krauss, I.J., Joyce, J.G., Finnefrock, A.C., Song, H.C., Dudkin, V.Y., Geng, X., Warren, J.D., Chastain, M., Shiver, J.W., Danishefsky, S.J., 2007. Fully synthetic carbohydrate HIV antigens designed on the logic of the 2G12 antibody. J. Am. Chem. Soc. 129, 11042–11044.
Krogfelt, K.A., Bergmans, H., Klemm, P., 1990. Direct evidence that the FimH protein is the mannose-specific adhesin of Escherichia coli type 1 fimbriae. Infect. Immun. 58, 1995–1998.
Kufe, D.W., 2009. Mucins in cancer: function, prognosis and therapy. Nat. Rev. Cancer 9, 874–885.
Kusunoki, S., Kaida, K., 2011. Antibodies against ganglioside complexes in Guillain-Barre syndrome and related disorders. J. Neurochem. 116, 828–832.
Kuziemko, G.M., Stroh, M., Stevens, R.C., 1996. Cholera toxin binding affinity and specificity for gangliosides determined bysurface plasmon resonance. Biochemistry 35, 6375–6384.
Lee, C.W., Lo, R.Y.C., Shewen, P.E., Mellors, A., 1994. The detection of the sialoglycoprotease gene and assay for sialoglycoprotease activity among isolates of Pasteurella haemolytica A1 strains, serotypes A13, A14, T15 and A16. FEMS Microbiol. Lett. 121, 199–206.
Lenter, M., Levinovitz, A., Isenmann, S., Vestweber, D., 1994. Monospecific and common glycoprotein ligands for E- and P-selectin on myeloid cells. J. Cell Biol. 125, 471–481.
Leppänen, A., Penttilä, L., Renkonen, O., McEver, R.P., Cummings, R.D., 2002. Glycosulfopeptides with O-glycans containing sialylated and polyfucosylate d polylactosamine bind with low affinity to P-selectin. J. Biol. Chem. 277, 39749–39759.
Leppanen, A., Yago, T., Otto, V.I., McEver, R.P., Cummings, R.D., 2003. Model Glycosulfopeptides from P-selectin Glycoprotein Ligand-1 Require Tyrosine Sulfation and a Core 2-branched O-Glycan to Bind to L-selectin. J. Biol. Chem. 278, 26391–26400.
Levinovitz, A., Mühlhoff, J., Isenmann, S., Vestweber, D., 1993. Identification of a glycoprotein ligand for E-selectin on mouse myeloid cells. J. Cell Biol. 121, 449–459.
Lewis, A.L., Nizet, V., Varki, A., 2004. Discovery and characterization of sialic acid O-acetylation in group B Streptococcus. Proc. Natl. Acad. Sci. U. S. A. 101, 11123–11128.
Li, H., Xu, C.F., Blais, S., Wan, Q., Zhang, H.T., Landry, S.J., Hioe, C.E., 2009. Proximal glycans outside of the epitopes regulate the presentation of HIV-1 envelope gp120 helper epitopes. J. Immunol. 182, 6369–6378.
Liang, C.H., Wang, S.K., Lin, C.W., Wang, C.C., Wong, C.H., Wu, C.Y., 2011. Effects of neighboring glycans on antibody-carbohydrate interaction. Angew. Chem. Int. Ed. Engl. 50, 1608–1612.
Lloyd, K.O., 2000. The chemistry and immunochemistry of blood group A, B, H, and Lewis antigens: past, present and future. Glycoconj. J. 17, 531–541.
Lloyd, K.O., Gordon, C.M., Thampoe, I.J., DiBenedetto, C., 1992. Cell surface accessibility of individual gangliosides in malignant melanoma cells to antibodies is influenced by the total ganglioside composition of the cells. Cancer Res. 52, 4948–4953.
Lonardi, E., Balog, C.I., Deelder, A.M., Wuhrer, M., 2010. Natural glycan microarrays. Exp. Rev. Proteomics 7, 761–774.
Luallen, R.J., Lin, J., Fu, H., Cai, K.K., Agrawal, C., Mboudjeka, I., Lee, F.H., Montefiori, D., Smith, D.F., Doms, R.W., Geng, Y., 2008. An engineered Saccharomyces cerevisiae strain binds the broadly neutralizing human immunodeficiency virus

type 1 antibody 2G12 and elicits mannose-specific gp120-binding antibodies. J. Virol. 82, 6447–6457.
Maier, A.G., Duraisingh, M.T., Reeder, J.C., Patel, S.S., Kazura, J.W., Zimmerman, P.A., Cowman, A.F., 2003. Plasmodium falciparum erythrocyte invasion through glycophorin C and selection for Gerbich negativity in human populations. Nat. Med. 9, 87–92.
Maisey, H.C., Doran, K.S., Nizet, V., 2008. Recent advances in understanding the molecular basis of group B Streptococcus virulence. Expert Rev. Mol. Med. 10, e27.
Malpede, B.M., Lin, D.H., Tolia, N.H., 2013. Molecular basis for sialic acid-dependent receptor recognition by Plasmodium falciparum erythrocyte binding antigen 140/BAEBL. J. Biol. Chem. 288, 12406–12415.
Marques, M.B., Kasper, D.L., Shroff, A., Michon, F., Jennings, H.J., Wessels, M.R., 1994. Functional activity of antibodies to the group B polysaccharide of group B streptococci elicited by a polysaccharide-protein conjugate vaccine. Infect. Immun. 62, 1593–1599.
Marth, J.D., 2008. A unified vision of the building blocks of life. Nat. Cell Biol. 10, 1015–1016.
Mattu, T.S., Pleass, R.J., Willis, A.C., Kilian, M., Wormald, M.R., Lellouch, A.C., Rudd, P.M., Woof, J.M., Dwek, R.A., 1998. The glycosylation and structure of human serum IgA1, Fab, and Fc regions and the role of N-glycosylation on Fc alpha receptor interactions. J. Biol. Chem. 273, 2260–2272.
Mauri, L., Casellato, R., Ciampa, M.G., Uekusa, Y., Kato, K., Kaida, K., Motoyama, M., Kusunoki, S., Sonnino, S., 2012. Anti-GM1/GD1a complex antibodies in GBS sera specifically recognize the hybrid dimer GM1-GD1a. Glycobiology 22, 352–360.
Mayer, D.C., Mu, J.B., Feng, X., Su, X.Z., Miller, L.H., 2002. Polymorphism in a Plasmodium falciparum erythrocyte-binding ligand changes its receptor specificity. J. Exp. Med. 196, 1523–1528.
Mayer, D.C., Jiang, L., Achur, R.N., Kakizaki, I., Gowda, D.C., Miller, L.H., 2006. The glycophorin C N-linked glycan is a critical component of the ligand for the Plasmodium falciparum erythrocyte receptor BAEBL. Proc. Natl. Acad. Sci. U. S. A. 103, 2358–2362.
McEver, R.P., 2002. Selectins: lectins that initiate cell adhesion under flow. Curr. Opin. Cell Biol. 14, 581–586.
McEver, R.P., Cummings, R.D., 1997. Role of PSGL-1 binding to selectins in leukocyte recruitment. J. Clin. Invest. 100, 485–492.
McLellan, J.S., Pancera, M., Carrico, C., Gorman, J., Julien, J.P., Khayat, R., Louder, R., Pejchal, R., Sastry, M., Dai, K., O'Dell, S., Patel, N., Shahzad-ul-Hussan, S., Yang, Y., Zhang, B., Zhou, T., Zhu, J., Boyington, J.C., Chuang, G.Y., Diwanji, D., Georgiev, I., Kwon, Y.D., Lee, D., Louder, M.K., Moquin, S., Schmidt, S.D., Yang, Z.Y., Bonsignori, M., Crump, J.A., Kapiga, S.H., Sam, N.E., Haynes, B.F., Burton, D.R., Koff, W.C., Walker, L.M., Phogat, S., Wyatt, R., Orwenyo, J., Wang, L.X., Arthos, J., Bewley, C.A., Mascola, J.R., Nabel, G.J., Schief, W.R., Ward, A.B., Wilson, I.A., Kwong, P.D., 2011. Structure of HIV-1 gp120 V1/V2 domain with broadly neutralizing antibody PG9. Nature 480, 336–343.
Mellors, A., Lo, R.Y.C., 1995. O-sialoglycoprotease from Pasteurella haemolytica. Methods Enzymol. 248, 728–740.
Mellors, A., Sutherland, D.R., 1994. Tools to cleave glycoproteins. Trends Biotechnol. 12, 15–18.
Merritt, E.A., Sarfaty, S., van, den Akker, F., L'Hoir, C., Martial, J.A., Hol, W.G.J., 1994. Crystal structure of cholera toxin B-pentamer bound to receptor GM1 pentasaccharide. Protein Sci. 3, 166–175.
Mitic, N., Milutinovic, B., Jankovic, M., 2012. Assessment of sialic acid diversity in cancer- and non-cancer related CA125 antigen using sialic acid-binding Ig-like lectins (Siglecs). Dis. Markers 32, 187–194.

Molina, V., Visa, L., Conill, C., Navarro, S., Escudero, J.M., Auge, J.M., Filella, X., Lopez-Boado, M.A., Ferrer, J., Fernandez-Cruz, L., Molina, R., 2012. CA 19-9 in pancreatic cancer: retrospective evaluation of patients with suspicion of pancreatic cancer. Tumour Biol. 33, 799–807.

Moore, K.L., 1998. Structure and function of P-selectin Glycoprotein ligand-1. Leuk. Lymphoma 29, 1–15.

Moore, K.L., Stults, N.L., Diaz, S., Smith, D.F., Cummings, R.D., Varki, A., McEver, R.P., 1992. Identification of a specific glycoprotein ligand for P-selectin (CD62) on myeloid cells. J. Cell Biol. 118, 445–456.

Mousseau, D.D., Banville, D., L'Abbe, D., Bouchard, P., Shen, S.H., 2000. PILRalpha, a novel immunoreceptor tyrosine-based inhibitory motif-bearing protein, recruits SHP-1 upon tyrosine phosphorylation and is paired with the truncated counterpart PILRbeta. J. Biol. Chem. 275, 4467–4474.

Nakada, H., Numata, Y., Inoue, M., Tanaka, N., Kitagawa, H., Funakoshi, I., Fukui, S., Yamashina, I., 1991. Elucidation of an essential structure recognized by an anti-GalNAc_-Ser(Thr) monoclonal antibody (MLS 128). J. Biol. Chem. 266, 12402–12405.

Nakada, H., Inoue, M., Numata, Y., Tanaka, N., Funakoshi, I., Fukui, S., Mellors, A., Yamashina, I., 1993. Epitopic structure of Tn glycophorin A for an anti-Tn antibody (MLS 128). Proc. Natl. Acad. Sci. U. S. A. 90, 2495–2499.

Needham, L.K., Schnaar, R.L., 1993. The HNK-1 reactive sulfoglucuronyl glycolipids are ligands for L-selectin and P-selectin but not E-selectin. Proc. Natl. Acad. Sci. U. S. A. 90, 1359–1363.

Nichols, C.E., Johnson, C., Lockyer, M., Charles, I.G., Lamb, H.K., Hawkins, A.R., Stammers, D.K., 2006. Structural characterization of Salmonella typhimurium YeaZ, an M22 O-sialoglycoprotein endopeptidase homolog. Proteins 64, 111–123.

Nizet, V., Esko, J.D., 2009. Bacterial and viral infections. In: Varki, A., Cummings, R.D., Esko, J.D., Freeze, H.H., Stanley, P., Bertozzi, C.R., Hart, G.W., Etzler, M.E. (Eds.), Essentials of Glycobiology. Cold Spring Harbor Laboratory Press, Cold Spring Harbor, NY, pp. 537–552.

Nobile-Orazio, E., Giannotta, C., Briani, C., 2010. Anti-ganglioside complex IgM antibodies in multifocal motor neuropathy and chronic immune-mediated neuropathies. J. Neuroimmunol. 219, 119–122.

Norgard, K.E., Han, H., Powell, L., Kriegler, M., Varki, A., Varki, N.M., 1993a. Enhanced interaction of L-selectin with the high endothelial venule ligand via selectively oxidized sialic acids. Proc. Natl. Acad. Sci. U. S. A. 90, 1068–1072.

Norgard, K.E., Moore, K.L., Diaz, S., Stults, N.L., Ushiyama, S., McEver, R.P., Cummings, R.D., Varki, A., 1993b. Characterization of a specific ligand for P-selectin on myeloid cells. A minor glycoprotein with sialylated O-linked oligosaccharides. J. Biol. Chem. 268, 12764–12774.

Numata, Y., Nakada, H., Fukui, S., Kitagawa, H., Ozaki, K., Inoue, M., Kawasaki, T., Funakoshi, I., Yamashina, I., 1990. A monoclonal antibody directed to Tn antigen. Biochem. Biophys. Res. Commun. 170, 981–985.

Nwosu, C.C., Seipert, R.R., Strum, J.S., Hua, S.S., An, H.J., Zivkovic, A.M., German, B.J., Lebrilla, C.B., 2011. Simultaneous and extensive site-specific N- and O-glycosylation analysis in protein mixtures. J. Proteome Res. 10, 2612–2624.

Ogata, S., Ho, I., Chen, A., Dubois, D., Maklansky, J., Singhal, A., Hakomori, S., Itzkowitz, S.H., 1995. Tumor-associated sialylated antigens are constitutively expressed in normal human colonic mucosa. Cancer Res. 55, 1869–1874.

Ogata, S., Koganty, R., Reddish, M., Longenecker, B.M., Chen, A., Perez, C., Itzkowitz, S.H., 1998. Different modes of sialyl-Tn expression during malignant transformation of human colonic mucosa. Glycoconj. J. 15, 29–35.

Ogawa, G., Kaida, K., Kusunoki, S., Ueda, M., Kimura, F., Kamakura, K., 2009. Antibodies to ganglioside complexes consisting of asialo-GM1 and GQ1b or GT1a in Fisher and Guillain-Barre syndromes. J. Neuroimmunol. 214, 125–127.
Oh, S.S., Chishti, A.H., 2005. Host receptors in malaria merozoite invasion. Curr. Top. Microbiol. Immunol. 295, 203–232.
Ohtsubo, K., Marth, J.D., 2006. Glycosylation in cellular mechanisms of health and disease. Cell 126, 855–867.
Ono, M., Handa, K., Withers, D.A., Hakomori, S.I., 2000. Glycosylation effect on membrane domain (GEM) involved in cell adhesion and motility: a preliminary note on functional _3, _5-CD82 glycosylation complex in ldlD 14 cells. Biochem. Biophys. Res. Commun. 279, 744–750.
Ono, M., Handa, K., Sonnino, S., Withers, D.A., Nagai, H., Hakomori, S., 2001. GM3 ganglioside inhibits CD9-facilitated haptotactic cell motility: coexpression of GM3 and CD9 is essential in the downregulation of tumor cell motility and malignancy. Biochemistry 40, 6414–6421.
Orlandi, P.A., Klotz, F.W., Haynes, J.D., 1992. A malaria invasion receptor, the 175-kilodalton erythrocyte binding antigen of Plasmodium falciparum recognizes the terminal Neu5Ac(alpha 2–3)Gal-sequences of glycophorin A. J. Cell Biol. 116, 901–909.
Padler-Karavani, V., Song, X., Yu, H., Hurtado-Ziola, N., Huang, S., Muthana, S., Chokhawala, H.A., Cheng, J., Verhagen, A., Langereis, M.A., Kleene, R., Schachner, M., de Groot, R.J., Lasanajak, Y., Matsuda, H., Schwab, R., Chen, X., Smith, D.F., Cummings, R.D., Varki, A., 2012. Cross-comparison of protein recognition of sialic acid diversity on two novel sialoglycan microarrays. J. Biol. Chem. 287, 22593–22608.
Partyka, K., Maupin, K.A., Brand, R.E., Haab, B.B., 2012. Diverse monoclonal antibodies against the CA 19-9 antigen show variation in binding specificity with consequences for clinical interpretation. Proteomics 12, 2212–2220.
Patel, N., Brinkman-Van der Linden, E.C.M., Altmann, S.W., Gish, K., Balasubramanian, S., Timans, J.C., Peterson, D., Bell, M.P., Bazan, J.F., Varki, A., Kastelein, R.A., 1999. OB-BP1/Siglec-6 - A leptin- and sialic acid-binding protein of the immunoglobulin superfamily. J. Biol. Chem. 274, 22729–22738.
Pejchal, R., Doores, K.J., Walker, L.M., Khayat, R., Huang, P.S., Wang, S.K., Stanfield, R.L., Julien, J.P., Ramos, A., Crispin, M., Depetris, R., Katpally, U., Marozsan, A., Cupo, A., Maloveste, S., Liu, Y., McBride, R., Ito, Y., Sanders, R.W., Ogohara, C., Paulson, J.C., Feizi, T., Scanlan, C.N., Wong, C.H., Moore, J.P., Olson, W.C., Ward, A.B., Poignard, P., Schief, W.R., Burton, D.R., Wilson, I.A., 2011. A potent and broad neutralizing antibody recognizes and penetrates the HIV glycan shield. Science 334, 1097–1103.
Pincus, S.H., Smith, M.J., Jennings, H.J., Burritt, J.B., Glee, P.M., 1998. Peptides that mimic the group B streptococcal type III capsular polysaccharide antigen. J. Immunol. 160, 293–298.
Pincus, S.H., Moran, E., Maresh, G., Jennings, H.J., Pritchard, D.G., Egan, M.L., Blixt, O., 2012. Fine specificity and cross-reactions of monoclonal antibodies to group B streptococcal capsular polysaccharide type III. Vaccine 30, 4849–4858.
Pirruccello, S.J., LeBien, T.W., 1986. The human B cell-associated antigen CD24 is a single chain sialoglycoprotein. J. Immunol. 136, 3779–3784.
Pouyani, T., Seed, B., 1995. PSGL-1 recognition of P-selectin is controlled by a tyrosine sulfation consensus at the PSGL-1 amino terminus. Cell 83, 333–343.
Ramya, T.N., Weerapana, E., Cravatt, B.F., Paulson, J.C., 2013. Glycoproteomics enabled by tagging sialic acid- or galactose-terminated glycans. Glycobiology 23, 211–221.
Raunser, S., Walz, T., 2009. Electron crystallography as a technique to study the structure on membrane proteins in a lipidic environment. Annu. Rev. Biophys. 38, 89–105.

Rillahan, C.D., Paulson, J.C., 2011. Glycan microarrays for decoding the glycome. Annu. Rev. Biochem. 80, 797–823.
Rinaldi, S., Brennan, K.M., Goodyear, C.S., O'Leary, C., Schiavo, G., Crocker, P.R., Willison, H.J., 2009. Analysis of lectin binding to glycolipid complexes using combinatorial glycoarrays. Glycobiology 19, 789–796.
Rinaldi, S., Brennan, K.M., Willison, H.J., 2010. Heteromeric glycolipid complexes as modulators of autoantibody and lectin binding. Prog. Lipid Res. 49, 87–95.
Rinaldi, S., Brennan, K.M., Willison, H.J., 2012. Combinatorial glycoarray. Methods Mol. Biol. 808, 413–423.
Roy, R., 1996. Syntheses and some applications of chemically defined multivalent glycoconjugates. Curr. Opin. Struct. Biol. 6, 692–702.
Sadler, J.E., Paulson, J.C., Hill, R.L., 1979. The role of sialic acid in the expression of human MN blood group antigens. J. Biol. Chem. 254, 2112–2119.
Sammar, M., Aigner, S., Hubbe, M., Schirrmacher, V., Schachner, M., Vestweber, D., Altevogt, P., 1994. Heat-stable antigen (CD24) as ligand for mouse P-selectin. Int. Immunol. 6, 1027–1036.
Sanders, R.W., Venturi, M., Schiffner, L., Kalyanaraman, R., Katinger, H., Lloyd, K.O., Kwong, P.D., Moore, J.P., 2002. The mannose-dependent epitope for neutralizing antibody 2G12 on human immunodeficiency virus type 1 glycoprotein gp120. J. Virol. 76, 7293–7305.
Scales, T.M., Parsons, M., 2011. Spatial and temporal regulation of integrin signalling during cell migration. Curr. Opin. Cell Biol. 23, 562–568.
Scanlan, C.N., Pantophlet, R., Wormald, M.R., Ollmann Saphire, E., Stanfield, R., Wilson, I.A., Katinger, H., Dwek, R.A., Rudd, P.M., Burton, D.R., 2002. The broadly neutralizing anti-human immunodeficiency virus type 1 antibody 2G12 recognizes a cluster of alpha1 → 2 mannose residues on the outer face of gp120. J. Virol. 76, 7306–7321.
Scanlan, C.N., Offer, J., Zitzmann, N., Dwek, R.A., 2007a. Exploiting the defensive sugars of HIV-1 for drug and vaccine design. Nature 446, 1038–1045.
Scanlan, C.N., Ritchie, G.E., Baruah, K., Crispin, M., Harvey, D.J., Singer, B.B., Lucka, L., Wormald, M.R., Wentworth, P.J., Zitzmann, N., Rudd, P.M., Burton, D.R., Dwek, R.A., 2007b. Inhibition of mammalian glycan biosynthesis produces non-self antigens for a broadly neutralising, HIV-1 specific antibody. J. Mol. Biol. 372, 16–22.
Schembri, M.A., Klemm, P., 1998. Heterobinary adhesins based on the Escherichia coli FimH fimbrial protein. Appl. Environ. Microbiol. 64, 1628–1633.
Schenkel, A.R., Mamdouh, Z., Chen, X., Liebman, R.M., Muller, W.A., 2002. CD99 plays a major role in the migration of monocytes through endothelial junctions. Nat. Immunol. 3, 143–150.
Seki, Y., Ikeda, S., Kiyohara, H., Ayabe, H., Seki, T., Matsui, H., 2002. Sequencing analysis of a putative human O-sialoglycoprotein endopeptidase gene (OSGEP) and analysis of a bidirectional promoter between the OSGEP and APEX genes. Gene 285, 101–108.
Sharon, N., 2006. Carbohydrates as future anti-adhesion drugs for infectious diseases. Biochim. Biophys. Acta 1760, 527–537.
Shiratori, I., Ogasawara, K., Saito, T., Lanier, L.L., Arase, H., 2004. Activation of natural killer cells and dendritic cells upon recognition of a novel CD99-like ligand by paired immunoglobulin-like type 2 receptor. J. Exp. Med. 199, 525–533.
Shriver, Z., Capila, I., Venkataraman, G., Sasisekharan, R., 2012. Heparin and heparan sulfate: analyzing structure and microheterogeneity. Handb. Exp. Pharmacol. 207, 159–176.
Siebert, H.C., Born, K., Andre, S., Frank, M., Kaltner, H., von der Lieth, C.W., Heck, A.J., Jimenez-Barbero, J., Kopitz, J., Gabius, H.J., 2005. Carbohydrate chain of ganglioside

GM1 as a ligand: identification of the binding strategies of three 15 mer peptides and their divergence from the binding modes of growth-regulatory galectin-1 and cholera toxin. Chemistry 12, 388–402.
Sim, B.K., Chitnis, C.E., Wasniowska, K., Hadley, T.J., Miller, L.H., 1994. Receptor and ligand domains for invasion of erythrocytes by Plasmodium falciparum. Science 264, 1941–1944.
Sjoberg, E.R., Powell, L.D., Klein, A., Varki, A., 1994. Natural ligands of the B cell adhesion molecule CD22beta can be masked by 9-O-acetylation of sialic acids. J. Cell Biol. 126, 549–562.
Song, Y., Withers, D.A., Hakomori, S., 1998. Globoside-dependent adhesion of human embryonal carcinoma cells, based on carbohydrate-carbohydrate interaction, initiates signal transduction and induces enhanced activity of transcription factors AP1 and CREB. J. Biol. Chem. 273, 2517–2525.
Spillmann, D., Burger, M.M., 1996. Carbohydrate-carbohydrate interactions in adhesion. J. Cell. Biochem. 61, 562–568.
Springer, G.F., 1984. T and Tn, general carcinoma autoantigens. Science 224, 1198–1206.
Springer, G.F., 1997. Immunoreactive T and Tn epitopes in cancer diagnosis, prognosis, and immunotherapy. J. Mol. Med. (Berl.) 75, 594–602.
Stanley, P., Cummings, R.D., 2009. Structures common to different glycans. In: Varki, A., Cummings, R.D., Esko, J.D., Freeze, H.H., Stanley, P., Bertozzi, C.R., Hart, G.W., Etzler, M.E. (Eds.), Essentials of Glycobiology. Cold Spring Harbor Laboratory Press, Cold Spring Harbor, NY, pp. 175–198.
Stevens, J., Blixt, O., Glaser, L., Taubenberger, J.K., Palese, P., Paulson, J.C., Wilson, I.A., 2006. Glycan microarray analysis of the hemagglutinins from modern and pandemic influenza viruses reveals different receptor specificities. J. Mol. Biol. 355, 1143–1155.
Stowell, C.P., Lee, V.C., 1980. Neoglycoproteins: the preparation and application of synthetic glycoproteins. Adv. Carbohydr. Chem. Biochem. 37, 225–281.
Sun, Y., Senger, K., Baginski, T.K., Mazloom, A., Chinn, Y., Pantua, H., Hamidzadeh, K., Ramani, S.R., Luis, E., Tom, I., Sebrell, A., Quinones, G., Ma, Y., Mukhyala, K., Sai, T., Ding, J., Haley, B., Shadnia, H., Kapadia, S.B., Gonzalez, L.C., Hass, P.E., Zarrin, A.A., 2012. Evolutionarily conserved paired immunoglobulin-like receptor alpha (PILRalpha) domain mediates its interaction with diverse sialylated ligands. J. Biol. Chem. 287, 15837–15850.
Sutherland, D.R., Abdullah, K.M., Cyopick, P., Mellors, A., 1992. Cleavage of the cell-surface O-sialoglycoproteins CD34, CD43, CD44, and CD45 by a novel glycoprotease from Pasteurella haemolytica. J. Immunol. 148, 1458–1464.
Tabata, S., Kuroki, K., Wang, J., Kajikawa, M., Shiratori, I., Kohda, D., Arase, H., Maenaka, K., 2008. Biophysical characterization of O-glycosylated CD99 recognition by paired Ig-like type 2 receptors. J. Biol. Chem. 283, 8893–8901.
Tanaka, M., Sackmann, E., 2005. Polymer-supported membranes as models of the cell surface. Nature 437, 656–663.
Tanaka, N., Nakada, H., Inoue, M., Yamashina, I., 1999. Binding characteristics of an anti-Siaalpha2-6GalNAc_-Ser/Thr (sialyl Tn) monoclonal antibody (MLS 132). Eur. J. Biochem. 263, 27–32.
Taylor, M.E., Drickamer, K., 2009. Structural insights into what glycan arrays tell us about how glycan-binding proteins interact with their ligands. Glycobiology 19, 1155–1162.
Telen, M.J., Chasis, J.A., 1990. Relationship of the human erythrocyte Wrb antigen to an interaction between glycophorin A and band 3. Blood 76, 842–848.
Thomas, M.L., 1989. The leukocyte common antigen family. Annu. Rev. Immunol. 7, 339–369.
Thomas, D.B., Winzler, R.J., 1969. Structural studies on human erythrocyte glycoproteins. Alkali-labile oligosaccharides. J. Biol. Chem. 244, 5943–5946.

Thor, A., Ohuchi, N., Szpak, C.A., Johnston, W.W., Schlom, J., 1986. Distribution of oncofetal antigen tumor-associated glycoprotein-72 defined by monoclonal antibody B72.3. Cancer Res. 46, 3118–3124.
Todeschini, A., Hakomori, S.I., 2008. Functional role of glycosphingolipids and gangliosides in control of cell adhesion, motility, and growth, through glycosynaptic microdomains. Biochim. Biophys. Acta 1780, 421–433.
Tolia, N.H., Enemark, E.J., Sim, B.K., Joshua-Tor, L., 2005. Structural basis for the EBA-175 erythrocyte invasion pathway of the malaria parasite Plasmodium falciparum. Cell 122, 183–193.
Tomita, M., Furthmayr, H., Marchesi, V.T., 1978. Primary structure of human erythrocyte glycophorin A. Isolation and characterization of peptides and complete amino acid sequence. Biochemistry 17, 4756–4770.
Tsuchida, T., Saxton, R.E., Morton, D.L., Irie, R.F., 1989. Gangliosides of human melanoma. Cancer 63, 1166–1174.
Turk, B., Turk du, S.A., Turk, V., 2012. Protease signalling: the cutting edge. EMBO J. 31, 1630–1643.
van Zanten, T.S., Gomez, J., Manzo, C., Cambi, A., Buceta, J., Reigada, R., Garcia-Parajo, M.F., 2010. Direct mapping of nanoscale compositional connectivity on intact cell membranes. Proc. Natl. Acad. Sci. U. S. A. 107, 15437–15442.
Varki, A., 1994. Selectin ligands. Proc. Natl. Acad. Sci. U. S. A. 91, 7390–7397.
Varki, A., 1997. Sialic acids as ligands in recognition phenomena. FASEB J. 11, 248–255.
Varki, A., 2008. Sialic acids in human health and disease. Trends Mol. Med. 14, 351–360.
Varki, A., 2011. Evolutionary forces shaping the Golgi glycosylation machinery: why cell surface glycans are universal to living cells. Cold Spring Harb. Perspect Biol. 3 (6), pii: a005462. http://dx.doi.org/10.1101/cshperspect.a005462.
Varki, A., Angata, T., 2006. Siglecs—the major subfamily of I-type lectins. Glycobiology 16, 1R–27R.
Varki, A., Sharon, N., 2009. Historical background and overview. In: Varki, A., Cummings, R.D., Esko, J.D., Freeze, H.H., Stanley, P., Bertozzi, C.R., Hart, G.W., Etzler, M.E. (Eds.), Essentials of Glycobiology. Cold Spring Harbor Laboratory Press, Cold Spring Harbor, NY, pp. 1–22.
Varki, N.M., Varki, A., 2007. Diversity in cell surface sialic acid presentations: implications for biology and disease. Lab Invest. 87, 851–857.
Varki, A., Etzler, M.E., Cummings, R.D., Esko, J.D., 2009a. Discovery and classification of glycan-binding proteins. In: Varki, A., Cummings, R.D., Esko, J.D., Freeze, H.H., Stanley, P., Bertozzi, C.R., Hart, G.W., Etzler, M.E., Varki, A., Cummings, R.D., Esko, J.D., Freeze, H.H., Stanley, P., Bertozzi, C.R., Hart, G.W., Etzler, M.E. (Eds.), Essentials of Glycobiology. Cold Spring Harbor Laboratory Press, Cold Spring Harbor, NY, pp. 375–386.
Varki, A., Kannagi, R., Toole, B.P., 2009b. Glycosylation changes in cancer. In: Varki, A., Cummings, R.D., Esko, J.D., Freeze, H.H., Stanley, P., Bertozzi, C.R., Hart, G.W., Etzler, M.E. (Eds.), Essentials of Glycobiology. Cold Spring Harbor Laboratory Press, Cold Spring Harbor, NY, pp. 617–632.
Vogt, A.M., Winter, G., Wahlgren, M., Spillmann, D., 2004. Heparan sulphate identified on human erythrocytes: a Plasmodium falciparum receptor. Biochem. J. 381, 593–597.
Wakabayashi, S., Saito, T., Shinohara, N., Okamoto, S., Tomioka, H., Taniguchi, M., 1984. Syngeneic monoclonal antibodies against melanoma antigens with species specificity and interspecies cross-reactivity. J. Invest. Dermatol. 83, 128–133.
Walker, L.M., Huber, M., Doores, K.J., Falkowska, E., Pejchal, R., Julien, J.P., Wang, S.K., Ramos, A., Chan-Hui, P.Y., Moyle, M., Mitcham, J.L., Hammond, P.W., Olsen, O.A., Phung, P., Fling, S., Wong, C.H., Phogat, S., Wrin, T., Simek, M.D., Koff, W.C.,

Wilson, I.A., Burton, D.R., Poignard, P., 2011. Broad neutralization coverage of HIV by multiple highly potent antibodies. Nature 477, 466–470.
Wang, J., Shiratori, I., Satoh, T., Lanier, L.L., Arase, H., 2008a. An essential role of sialylated O-linked sugar chains in the recognition of mouse CD99 by paired Ig-like type 2 receptor (PILR). J. Immunol. 180, 1686–1693.
Wang, S.K., Liang, P.H., Astronomo, R.D., Hsu, T.L., Hsieh, S.L., Burton, D.R., Wong, C.H., 2008b. Targeting the carbohydrates on HIV-1: interaction of oligomannose dendrons with human monoclonal antibody 2G12 and DC-SIGN. Proc. Natl. Acad. Sci. U. S. A. 105, 3690–3695.
Wang, J., Fan, Q., Satoh, T., Arii, J., Lanier, L.L., Spear, P.G., Kawaguchi, Y., Arase, H., 2009. Binding of herpes simplex virus glycoprotein B (gB) to paired immunoglobulin-like type 2 receptor alpha depends on specific sialylated O-linked glycans on gB. J. Virol. 83, 13042–13045.
Weis, W.I., Drickamer, K., 1996. Structural basis of lectin-carbohydrate recognition. Annu. Rev. Biochem. 65, 441–473.
Wessels, M.R., Pozsgay, V., Kasper, D.L., Jennings, H.J., 1987. Structure and immunochemistry of an oligosaccharide repeating unit of the capsular polysaccharide of type III group B Streptococcus. A revised structure for the type III group B streptococcal polysaccharide antigen. J. Biol. Chem. 262, 8262–8267.
Wilkins, P.P., Moore, K.L., McEver, R.P., Cummings, R.D., 1995. Tyrosine sulfation of P-selectin glycoprotein ligand-1 is required for high affinity binding to P-selectin. J. Biol. Chem. 270, 22677–22680.
Wilkins, P.P., McEver, R.P., Cummings, R.D., 1996. Structures of the O-glycans on P-selectin glycoprotein ligand-1 from HL-60 cells. J. Biol. Chem. 271, 18732–18742.
Willison, H.J., Yuki, N., 2002. Peripheral neuropathies and anti-glycolipid antibodies. Brain 125, 2591–2625.
Willison, H.J., Halstead, S.K., Beveridge, E., Zitman, F.M., Greenshields, K.N., Morgan, B.P., Plomp, J.J., 2008. The role of complement and complement regulators in mediating motor nerve terminal injury in murine models of Guillain-Barre syndrome. J. Neuroimmunol. 201–202, 172–182.
Yamaji, T., Teranishi, T., Alphey, M.S., Crocker, P.R., Hashimoto, Y., 2002. A small region of the natural killer cell receptor, Siglec-7, is responsible for its preferred binding to alpha 2,8-disialyl and branched alpha 2,6-sialyl residues. A comparison with Siglec-9. J. Biol. Chem. 277, 6324–6332.
Yamazaki, V., Sirenko, O., Schafer, R.J., Nguyen, L., Gutsmann, T., Brade, L., Groves, J.T., 2005. Cell membrane array fabrication and assay technology. BMC Biotechnol. 5, 18.
Yin, B.W.T., Dnistrian, A., Lloyd, K.O., 2002. Ovarian cancer antigen CA125 is encoded by the MUC16 mucin gene. Int. J. Cancer 98, 737–740.
Young, M.T., Beckmann, R., Toye, A.M., Tanner, M.J., 2000. Red-cell glycophorin A-band 3 interactions associated with the movement of band 3 to the cell surface. Biochem. J. 350 (Pt 1), 53–60.
Yuki, N., Hartung, H.P., 2012. Guillain-Barre syndrome. N. Engl. J. Med. 366, 2294–2304.
Yuriev, E., Farrugia, W., Scott, A.M., Ramsland, P.A., 2005. Three-dimensional structures of carbohydrate determinants of Lewis system antigens: implications for effective antibody targeting of cancer. Immunol. Cell Biol. 83, 709–717.
Zhang, S., Walberg, L.A., Ogata, S., Itzkowitz, S.H., Koganty, R.R., Reddish, M., Gandhi, S.S., Longenecker, B.M., Lloyd, K.O., Livingston, P.O., 1995. Immune sera and monoclonal antibodies define two configurations for the sialyl Tn tumor antigen. Cancer Res. 55, 3364–3368.
Zhang, M., Gaschen, B., Blay, W., Foley, B., Haigwood, N., Kuiken, C., Korber, B., 2004. Tracking global patterns of N-linked glycosylation site variation in highly variable viral

glycoproteins: HIV, SIV, and HCV envelopes and influenza hemagglutinin. Glycobiology 14, 1229–1246.
Zhang, Y., Li, Q., Rodriguez, L.G., Gildersleeve, J.C., 2010a. An array-based method to identify multivalent inhibitors. J. Am. Chem. Soc. 132, 9653–9662.
Zhang, Y., Campbell, C., Li, Q., Gildersleeve, J.C., 2010b. Multidimensional glycan arrays for enhanced antibody profiling. Mol. Biosyst. 6, 1583–1591.
Zhu, Z.M., Kojima, N., Stroud, M.R., Hakomori, S.-I., Fenderson, B.A., 1995. Monoclonal antibody directed to Ley oligosaccharide inhibits implantation in the mouse. Biol. Reprod. 52, 903–912.
Zhu, X., Borchers, C., Bienstock, R.J., Tomer, K.B., 2000. Mass spectrometric characterization of the glycosylation pattern of HIV-gp120 expressed in CHO cells. Biochemistry 39, 11194–11204.
Zhu, X.Y., Holtz, B., Wang, Y., Wang, L.X., Orndorff, P.E., Guo, A., 2009. Quantitative glycomics from fluidic glycan microarrays. J. Am. Chem. Soc. 131, 13646–13650.
Zöllner, O., Vestweber, D., 1996. The E-selectin ligand-1 is selectively activated in Chinese hamster ovary cells by the _(1,3)-fucosyltransferases IV and VII. J. Biol. Chem. 271, 33002–33008.
Zou, W., Mackenzie, R., Therien, L., Hirama, T., Yang, Q., Gidney, M.A., Jennings, H.J., 1999. Conformational epitope of the type III group B Streptococcus capsular polysaccharide. J. Immunol. 163, 820–825.

CHAPTER FOUR

New Insights into the Molecular Mechanisms of Mitosis and Cytokinesis in Trypanosomes

Qing Zhou, Huiqing Hu, Ziyin Li[1]
Department of Microbiology and Molecular Genetics, University of Texas Medical School at Houston, Houston, Texas, USA
[1]Corresponding author: e-mail address: ziyin.Li@uth.tmc.edu

Contents

Abstract

Trypanosoma brucei, a unicellular eukaryote and the causative agent of human sleeping sickness, possesses multiple single-copy organelles that all need to be duplicated and segregated during cell division. Trypanosomes undergo a closed mitosis in which the mitotic spindle is anchored on the nuclear envelope and connects the kinetochores made of novel protein components. Cytokinesis in trypanosomes is initiated from the anterior tip of the new flagellum attachment zone, and proceeds along the

International Review of Cell and Molecular Biology, Volume 308
ISSN 1937-6448
http://dx.doi.org/10.1016/B978-0-12-800097-7.00004-X

longitudinal axis without the involvement of the actomyosin contractile ring, the well-recognized cytokinesis machinery conserved from yeast to humans. Trypanosome appears to employ both evolutionarily conserved and trypanosome-specific proteins to regulate its cell cycle, and has evolved certain cell cycle regulatory pathways that are either distinct between its life cycle stages or different from its human host. Understanding the mechanisms of mitosis and cytokinesis in trypanosomes not only would shed novel light on the evolution of cell cycle control, but also could provide new drug targets for chemotherapy.

1. INTRODUCTION

Trypanosoma brucei spp. (comprising *Trypanosoma brucei brucei* and the human infective forms *T. b. rhodesiense* and *T. b. gambiense*) are early branching, flagellated protozoan parasites causing sleeping sickness in human and nagana in cattle in 36 countries of sub-Saharan Africa, where they impose devastating impacts on human health and agriculture. The current WHO estimate indicates that about 30,000 people are infected per year and over 70 million people are at risk of infection (http://www.who.int/mediacentre/factsheets/fs259/en/). This disease places a heavy financial burden on the people living in Africa. It can be cured with medication if diagnosed early; however, it is fatal if left untreated. Unfortunately, the currently available drugs all have severe side effects; therefore, development of new drugs is urgently needed for combating this dreadful pathogen.

Trypanosomes are transmitted between mammalian hosts by the tsetse fly, *Glossina* spp. Within the insect host, the parasite is initially established in the midgut of the fly after a healthy fly takes a bloodmeal from an infected mammalian host, and subsequently it migrates to the salivary glands of the fly, where it prepares for transmission to the new mammalian host. Within the mammalian host, the parasite lives freely and proliferates by binary fission in the bloodstream since it is capable of escaping the host immune responses through antigenic variation (McCulloch, 2004). Antigenic variation involves the sequential expression of antigenically distinct variable surface glycoproteins (VSGs) that are linked to the membrane of the cell by a glycosylphosphatidylinositol (GPI) anchor. Upon uptake by the tsetse fly, bloodstream trypanosomes lose their VSG coat but instead express a different surface coat composed of procyclins, which are also GPI anchored on the plasma membrane (Roditi and Liniger, 2002). Due to the expression of the procyclin surface proteins, the parasite that lives in the insect host is

generally referred to as the procyclic form, which proliferates by binary fission in the midgut of the insect, similar to the bloodstream form of the parasite.

Most studies on trypanosome cell cycle control have been carried out in the procyclic and bloodstream forms of the parasite because these two forms can be easily cultured *in vitro* and many genetic tools are available for gene manipulation. For example, gene knockouts, gene replacements, and *in situ* epitope tagging can be readily generated through homologous recombination. Tetracycline-inducible ectopic overexpression and RNA interference (RNAi) have been routinely practiced in almost all the laboratories that use trypanosomes as the model system. Moreover, forward genetic approaches through the use of genomic RNAi library (Morris et al., 2002) and the mariner-based transposon mutagenesis (Leal et al., 2004) offer great prospects for screening numerous mutants. Finally, with the development of efficient tandem affinity purification (Schimanski et al., 2005), high-throughput genome-wide RNAi analysis (Alsford et al., 2011), and proteome-wide quantitative mass spectrometry (Urbaniak et al., 2012), trypanosome has become an excellent model organism for carrying out basic science research, including the understanding of the molecular mechanisms of mitosis and cytokinesis, which would potentially reveal novel regulatory pathways that could be good drug targets for chemotherapy.

2. CELL STRUCTURE OF *T. brucei*

It has been well established that the shape of a trypanosome cell is maintained by a subpellicular array of microtubules, which are cross-linked to the plasma membrane and to each other, forming a cage-like structure with all the single-copy organelles positioned at distinct locations within the cell (Fig. 4.1A). The single flagellum, which possesses an axoneme consisting of the canonical 9 + 2 array of microtubules and a large lattice-like structure termed paraflagellar rod (PFR), exits from the flagellar pocket at the posterior portion of the cell, attaches to the cell body along most of its length via a specialized cytoskeletal structure termed flagellum attachment zone (FAZ), and extends to the anterior tip of the cell (Fig. 4.1). The subpellicular microtubules all have an intrinsic polarity, with their plus (+) ends located at the posterior end of the cell, which is the opposite orientation to that of the flagellar axoneme microtubules, which have their plus (+) ends located at the anterior tip of the cell. During cell division, the subpellicular microtubules do not break down, and newly synthesized microtubules are

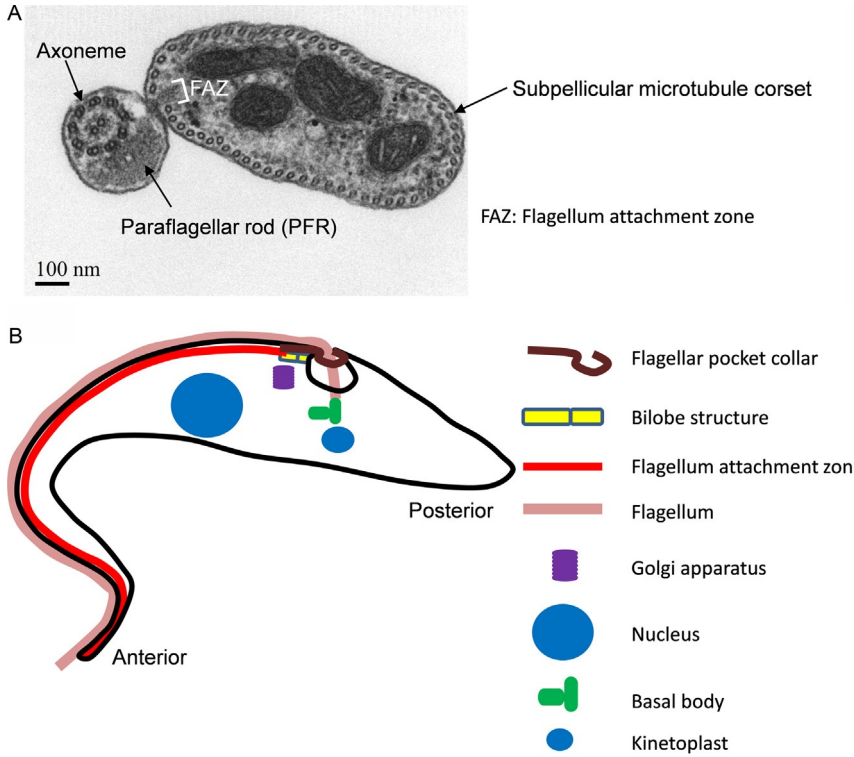

Figure 4.1 The cell structure of *Trypanosoma brucei*. (A) Cross-section of a trypanosome cell visualized under the transmission EM. The flagellar axoneme, paraflagellar rod (PFR), flagellum attachment zone (FAZ) filament, and the subpellicular microtubule corset are indicated. (B) Schematic illustration of a trypanosome cell showing the relative locations of its single-copied organelles.

integrated into the old microtubule array. Therefore, the microtubule corset appears to be inherited by the two daughter cells in a semiconservative manner (Sherwin and Gull, 1989).

The FAZ is composed of a single protein filament and a specialized set of four microtubules that associate with the smooth endoplasmic reticulum (Kohl et al., 1999). The complete protein composition of the FAZ filament is still not known, but a number of proteins have been localized to the FAZ filament, and RNAi of some of these FAZ proteins impairs the assembly of the new FAZ filament and causes defective cytokinesis (Morriswood et al., 2013; Vaughan et al., 2008; Zhou et al., 2011). The flagellar basal body, which functions as the microtubule organizing center (MTOC)

in trypanosomes and nucleates the flagellar axoneme microtubules, is located at the posterior portion of the cell, where it is physically connected, through a so-called tripartite attachment complex (TAC) across the mitochondrial membrane (Ogbadoyi et al., 2003), with the kinetoplast, the cell's unusual mitochondrial DNA complex that is composed of several dozen maxicircles and several thousand minicircles topologically interlocked and condensed into a disk-shaped structure. Unlike fungi and animals, a trypanosome cell possesses a single mitochondrion, which extends throughout the cell body and whose fission is tightly coupled with cell abscission. Trypanosome also contains a single Golgi apparatus, which undergoes *de novo* synthesis and is segregated during the cell cycle (He et al., 2004). The Golgi apparatus associates tightly with an ER exit site (ERES), which also undergoes duplication and segregation during the cell cycle. Between the old Golgi apparatus and the newly assembled Golgi apparatus, there is a bilobed cytoskeletal structure marked by TbCentrin2, one of the five centrin proteins in trypanosomes (He et al., 2005), with one of its lobe associating with the old Golgi and the other lobe with the new, growing Golgi apparatus. The precise function of the bilobe structure is still not clear, but it appears to be essential for Golgi duplication. The relative locations of the single-copy organelles and cytoskeletal structures are depicted in Fig. 4.1B.

3. CELL CYCLE OF *T. brucei*

3.1. Duplication and segregation of organelles and cytoskeletal structures

3.1.1 Basal body

To ensure successful cell division, all the single-copy organelles must be precisely replicated, maintained at specific locations, and faithfully segregated to the daughter cells. During trypanosome cell cycle, basal body is the first organelle to be duplicated, which constitutes the first cytoskeletal event of the cell cycle. Although the basal body structure has been well described, the existence of a second premature basal body (probasal body) is often overlooked, and due to the lack of a good basal body marker, the probasal body is frequently not identified experimentally. The most commonly used basal body marker, YL 1/2, is a monoclonal antibody raised against the tyrosinated α-tubulin in the basal body, which only labels the mature basal body (Fig. 4.2). Despite its limitation to stain only the mature basal body, YL 1/2 can be readily used to monitor the duplication and segregation of the basal bodies during the cell cycle. At the G1 phase, there is a

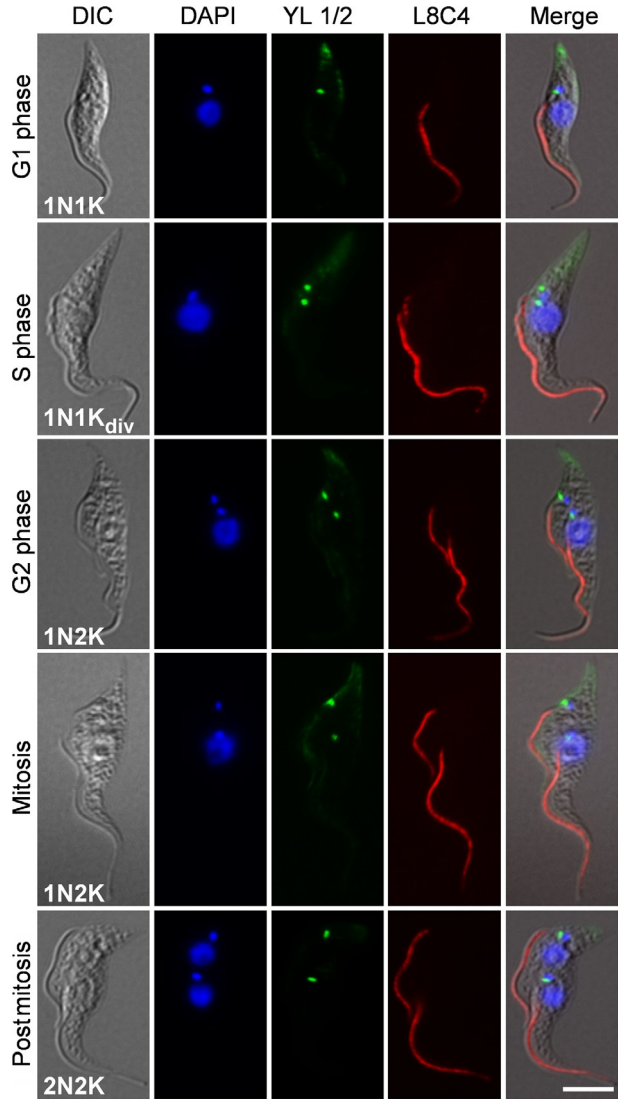

Figure 4.2 Duplication and segregation of basal body and flagellum during the cell cycle in trypanosomes. Procyclic trypanosomes were immunostained with YL 1/2 antibody and L8C4 antibody to label the basal body and flagellum, respectively, and then counterstained with DAPI to stain the nuclear and kinetoplast DNA. Bar: 5 μm.

single mature basal body per cell, which sits near the base of the old flagellum and associates with the single kinetoplast. At the S phase, the basal body duplicates, and the duplicated basal bodies are slightly separated but remain associated with the duplicated but not separated kinetoplasts. During G2 and

the subsequent cell cycle phases, the duplicated basal bodies are well separated, leading to the segregation of the duplicated kinetoplasts (Fig. 4.2). Through electron microscopy and electron tomography techniques, Lacomble et al. (2010) described in detail the duplication and rotation of the probasal body and mature basal body. At the start of the cell cycle, the probasal body is positioned anterior to the mature basal body of the old flagellum. During the transition from G1 to S phase, the probasal body becomes mature and elongates to form the transition zone and then the axoneme of the new flagellum. In the meantime, two new probasal bodies are formed in the vicinity of the two mature basal bodies. The new basal body then undergoes an anticlockwise rotation around the old basal body and repositions from the anterior to the posterior side of the old flagellum. The rotation and the subsequent migration of the new basal body toward the posterior portion of the cell result in the division of the flagellar pockets and appear to be required for cell morphogenesis (Lacomble et al., 2010).

As the only visible MTOC in trypanosomes, basal body is structurally similar to the centrosome in animals. Three key components of the centrosome, SAS-4/CPAP, SAS-6, and BLD10/CEP135, constitute the evolutionarily conserved and ancestral module (Carvalho-Santos et al., 2010). Trypanosomes appear to express the well-conserved SAS-4/CPAP and SAS-6 homologs and a divergent BLD10/CEP135 homolog (Carvalho-Santos et al., 2010), but whether these homologs are *bona fide* basal body proteins and whether they play any roles in basal body biogenesis remain to be determined. Other than these putative basal body components, a number of proteins have been localized to the basal body and are involved in basal body duplication and/or segregation. γ-Tubulin, a key component of the γ-tubulin complex located at the spindle pole body (SPB) of the budding yeast, was the first protein to be localized to the basal body in trypanosomes (Scott et al., 1997). The major function of γ-tubulin, however, is to nucleate the flagellum axoneme microtubules and is not involved in regulating basal body duplication or segregation (McKean et al., 2003). TBBC, which stands for *T. brucei* Basal Body Component, is a large protein consisting almost entirely of the coiled coil structure and is mainly localized to the mature basal body (Dilbeck et al., 1999). RNAi of TBBC compromises the connection of the new flagellum to the old flagellum (Absalon et al., 2007), although its potential role in basal body duplication/segregation remains to be explored. The mammalian ortholog of TBBC is not known, but anti-TBBC antibody detects a protein in HeLa cell extract and immunostaining of HeLa cells are confined to the centrosomes, suggesting the presence of a close homolog of TBBC in the mammalian centrosomes.

A NIMA (Never-In-Mitosis gene A)-like kinase, TbNRKC, is localized to both the premature and mature basal bodies, and RNAi-mediated silencing of TbNRKC in procyclic trypanosomes results in overproduction of basal bodies that fail to segregate, suggesting a role of TbNRKC in basal body segregation (Pradel et al., 2006). In mammals, the Polo-like kinase 4 or SAK (Snk/Plk-akin kinase) regulates centrosome duplication (Habedanck et al., 2005). Trypanosomes express a single PLK homolog, TbPLK, which is initially enriched at the basal body and, surprisingly, is required for basal body segregation but not duplication, likely by regulating the rotation of the duplicated basal bodies (Ikeda and de Graffenried, 2012; Lozano-Nunez et al., 2013). Centrin, an EF hand-containing calcium-binding protein, constitutes another conserved component of the centrosome in animals. Trypanosomes express five centrin-like proteins, an unusually large number of such proteins in a unicellular organism (He et al., 2005). At least three of the five centrin homologs, TbCentrin1, TbCentrin2, and TbCentrin4, are found at the mature basal body, and RNAi-mediated knockdown of TbCentrin1 clearly inhibits basal body duplication (He et al., 2005). However, a role for TbCentrin2 and TbCentrin4 in basal body duplication and/or segregation remains to be clarified due to the controversial observations made by different research groups (He et al., 2005; Selvapandiyan et al., 2007, 2012; Shi et al., 2008). The precise mechanism underlying basal body segregation is still not well understood, but it was suggested that posterior migration of the newly formed basal body is controlled by the elongation of the new flagellum and the new FAZ filament (Absalon et al., 2007).

3.1.2 Kinetoplast

Due to its tight association with the basal body (Fig. 4.2), kinetoplast segregation likely is controlled by the movement of the basal body toward the posterior portion (Robinson and Gull, 1991). Kinetoplast replication occurs prior to nuclear DNA replication and is well coordinated with the latter. It apparently occurs concurrently with the repositioning of the newly formed basal body (Gluenz et al., 2011). Regulation of kinetoplast replication is under tight control in a manner that is reminiscent of the nuclear DNA replication licensing system (Klingbeil and Shapiro, 2009; Li et al., 2008b; Liu et al., 2009). A mitochondrial HslVU protease, a eubacterial counterpart of the eukaryotic 26S proteasome, plays an essential role in preventing kinetoplast rereplication, thus maintaining the copy number of both the minicircle and maxicircle DNA in the kinetoplast (Li et al., 2008b). TbHslVU regulates a key mitochondrial helicase, TbPIF2, which maintains

the copy number of the maxicircle DNA (Liu et al., 2009), but the TbHslVU substrate(s) involved in controlling minicircle DNA replication remains to be identified. Once kinetoplast replication is completed, the kinetoplast undergoes symmetrical division by an unknown mechanism, resulting in the production of two equal-sized kinetoplasts in cells that are generally at the G2 phase of the cell cycle (Fig. 4.2). Segregation of the duplicated kinetoplasts is mediated by the separation of the duplicated basal bodies (Robinson and Gull, 1991), due to their tight physical association mediated by the TAC (Ogbadoyi et al., 2003). Three proteins have been identified as components of the TAC, p166 (Zhao et al., 2008), AEP-1 (Ochsenreiter et al., 2008), and p197 (Gheiratmand et al., 2013), and depletion of these proteins by RNAi all causes defects in kinetoplast segregation, suggesting the essential requirement of the TAC for kinetoplast segregation.

3.1.3 Flagellum and FAZ

The new flagellum is assembled when the new basal body is matured (Fig. 4.2, S phase). The short, newly formed flagellum is located in the existing flagellar pocket, and the tip of the new flagellum is attached to the old flagellum through the flagellum connector, an unusual motile transmembrane junction (Briggs et al., 2004). When the new flagellum outgrows the flagellar pocket, the PFR forms, and the flagellum is physically attached to cell body through FAZ. Following cell cycle progression, the new flagellum elongates and the FAZ also elongates (Fig. 4.2). However, the assembly of the flagellar axoneme and the assembly of the FAZ filament do not appear to be interdependent. In trypanosome cells deficient in intraflagellar transport, the flagellar axoneme is not assembled, but a short flagellar membrane still forms, which extends out of the flagellar pocket and is attached to the cell body via a short FAZ (Absalon et al., 2008; Davidge et al., 2006; Kohl et al., 2003). Conversely, trypanosome mutants that fail to assemble the FAZ filament can still assemble a full-length flagellum with normal axoneme and PFR (Vaughan et al., 2008; Zhou et al., 2011). Despite the essential role of FAZ in flagellum attachment, precisely how the FAZ filament is assembled remains poorly understood. To date, at least nine proteins have been found to localize to the FAZ filament, and RNAi knockdown of some FAZ proteins each results in defects in new FAZ assembly (Lacomble et al., 2012; LaCount et al., 2002; Morriswood et al., 2013; Oberholzer et al., 2011; Vaughan et al., 2008; Woods et al., 2013; Zhou et al., 2011), suggesting

the complexity of the FAZ filament and the requirement of multiple proteins for FAZ filament assembly.

3.1.4 Bilobe structure

The bilobe is a cytoskeletal structure originally identified as an unknown structure labeled by the 20H5 antibody raised against the *Chlamydomonas reinhardtii* Centrin and by anti-trypanosome TbCentrin2 antibody (He et al., 2005). Like other single-copy organelles in trypanosomes, the bilobe structure also undergoes duplication and segregation during the cell cycle (Fig. 4.3). At the G1 phase, 20H5 marks a single bilobe structure (Fig. 4.3, arrow) in addition to the basal body (Fig. 4.3, arrowhead). At the S phase, the bilobe structure is replicated, but the duplicated bilobe structures are not separated. At later cell cycle stages during which the basal bodies are separated and the nuclei are segregated, the bilobe structures are also segregated (Fig. 4.3). More than 10 proteins have been shown to localize to the bilobe structure (He et al., 2005; Morriswood et al., 2009, 2013; Shi et al., 2008; Zhou et al., 2010), and by immuno-EM the ultrastructure of the bilobe structure was revealed, which appears like a hairpin structure connecting the flagellar pocket collar and the FAZ filament (Esson et al., 2012). The exact function of the bilobe structure is still not clear, but it appears to be required for Golgi duplication (He et al., 2005). The old Golgi associates with the posterior lobe of the bilobe structure and the new Golgi is associated with the anterior lobe of the bilobe structure (He et al., 2004, 2005). In TbCentrin2 RNAi cells, duplication of the bilobe structure is impaired, resulting in defective duplication of the Golgi apparatus (He et al., 2005).

3.1.5 Golgi apparatus

Golgi duplication in trypanosomes likely is through *de novo* biogenesis, in which new Golgi is assembled next to the new ERES (He et al., 2004). During the G1 phase of the cell cycle, the trypanosome cell possesses a single Golgi apparatus, labeled by anti-GRASP (Golgi reassembly and stacking protein) antibody, which closely associates with the ERES, marked by EYFP (enhanced yellow fluorescent protein)-tagged Sec31 (Fig. 4.4). At the S phase, a small new Golgi appears, and both the new and old Golgi still associate with the duplicated ERESs, and during later stages of the cell cycle, such as G2 phase, mitotic, and postmitotic phases, the duplicated Golgi are further separated and the associated ERESs also undergo separation (Fig. 4.4). The mechanisms underlying Golgi duplication and segregation

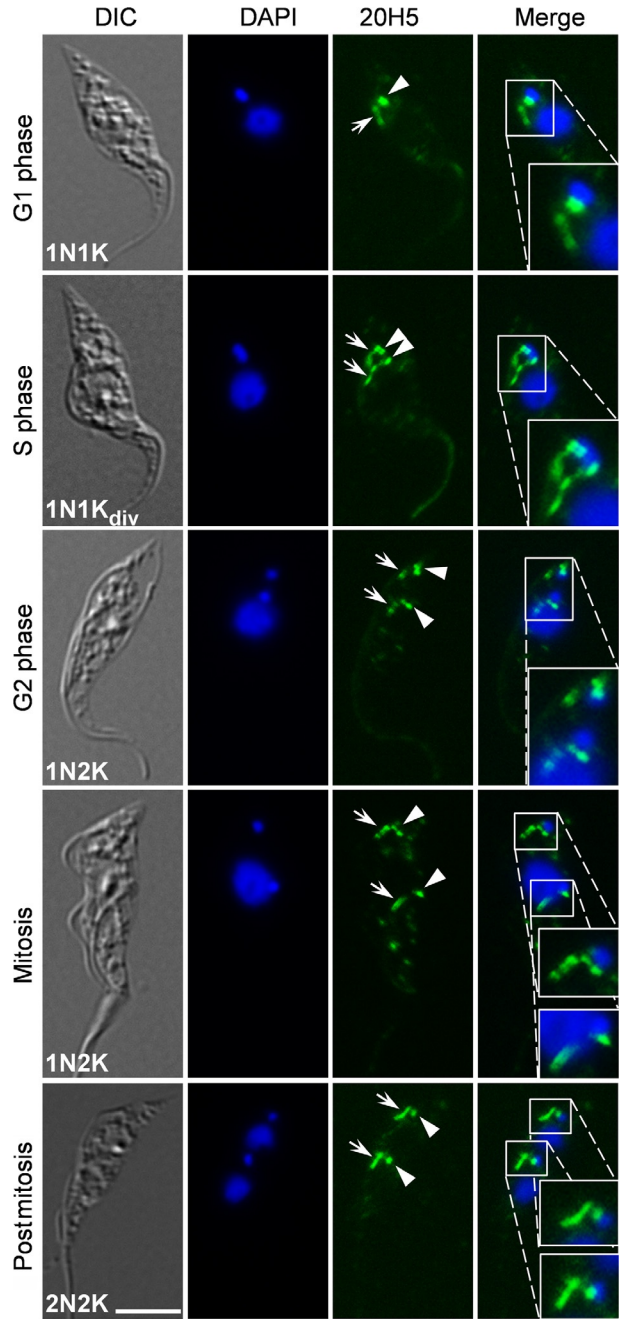

Figure 4.3 Duplication and segregation of bilobe, a novel cytoskeletal structure during the cell cycle. Procyclic trypanosome cells were fixed in methanol, immunostained with the 20H5 antibody, which stains the basal body (arrowheads) and the bilobe structure (arrows), and counterstained with DAPI for nuclear and kinetoplast DNA. Bar: 5 μm.

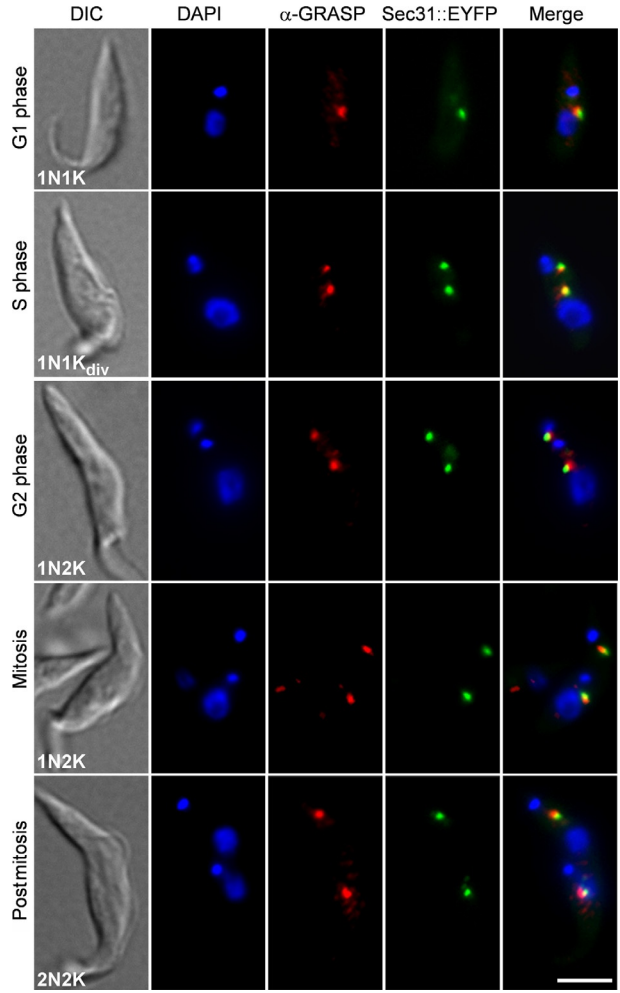

Figure 4.4 Duplication and segregation of Golgi and the ER exit site during the cell cycle. Procyclic trypanosome cells expressing EYFP-tagged Sec31, a marker of the ER exit site, were immunostained with anti-GRASP antibody, a marker of the Golgi, and counterstained with DAPI for nuclear and kinetoplast DNA. Bar: 5 μm.

are still poorly defined, but presumably the segregation of Golgi could be dependent on the elongation of the flagellum and the FAZ filament and the posterior migration of the new basal body. Such a mechanism appears to be involved in the segregation of bilobe structure, ERES, and kinetoplast as well, but this has not been experimentally confirmed.

3.1.6 Mitochondrion

Trypanosomes contain a single mitochondrion that extends throughout the cell body. Unlike the mitochondria in yeasts and animals which undergo frequent fission and fusion throughout the cell cycle, trypanosome mitochondrion only undergoes a single fission event during cytokinesis. Mitochondrial fission and fusion in yeast involves three factors, Fis1p, Dnm1p, and Mdv1p (Shaw and Nunnari, 2002). The trypanosome genome encodes homologs of Fis1p and Dnm1p (Chanez et al., 2006; Morgan et al., 2004), but no homolog of Mdv1p was found, likely due to the divergence of the sequence. Ablation of the dynamin homolog by RNAi in the procyclic form of *T. brucei* blocks mitochondrial fission and results in precise cytokinesis arrest (Chanez et al., 2006; Morgan et al., 2004), suggesting the conserved role of dynamin in regulating mitochondrial fission in trypanosomes. The result also highlights the requirement of mitochondrial division for cell division. It also suggests that mitochondrion division in trypanosomes is well coordinated with cell division, but the underlying mechanism remains to be explored.

3.2. Repertoire of cyclins and cyclin-dependent kinases

Cyclins and cyclin-dependent kinases (CDKs) are the fundamental regulators of the eukaryotic cell cycle. Through periodic synthesis and degradation of the cyclin partner, the CDK is sequentially activated and inactivated (Johnson and Walker, 1999). In the budding yeast *Saccharomyces cerevisiae*, nine cyclins are identified, with three of them, Cln1–Cln3, regulating the G1/S transition and the rest of them, Clb1–Clb6, driving the cell cycle through S phase to mitosis. Strikingly, all the nine cyclins bind to the same CDK, Cdc28, and due to the cell cycle stage-specific expression of cyclins, Cdc28 is activated at different cell cycle stages (Kuntzel et al., 1996). In striking contrast, in the fission yeast *Schizosaccharomyces pombe* only a single cyclin, Cdc13, and a single CDK, Cdc2, are required for controlling cell cycle progression across the G1/S and G2/M transitions, respectively (Humphrey and Pearce, 2005). The cyclin and CDK system in animals is more complex than that in the budding and fission yeasts. To date, at least 8 cyclin families, consisting of a total of 15 cyclins, and at least 9 CDKs are directly involved in cell cycle control in animals (Harper and Brooks, 2005). These cyclins and CDKs form distinct complexes and are involved in different cell cycle stages. Control of the G1/S transition is regulated by Cdk4, Cdk6, and the D-type cyclins. Regulation of S-phase progression requires Cdk2 and the

E-type cyclin, and regulation of the G2/M transition requires Cdk1, Cdk2, and their A-type and B-type cyclin partners (Harper and Brooks, 2005; Malumbres and Barbacid, 2005).

In trypanosomes, at least 10 cyclins (CYC2–CYC11) and 11 *C*dc2-*r*elated *k*inases (CRK1–CRK4 and CRK6–CRK12) were identified (Hammarton, 2007). This large number of cyclins and CDKs found in the trypanosome genome appears to suggest a rather complex cyclin–CDK system than one would expect for a unicellular eukaryote. The function of some of these cyclins and CRKs has been characterized and demonstrated to be involved in cell cycle control. The CYC2–CRK1 pair and the CYC6–CRK3 pair are likely the primary cyclin–CRK complexes for promoting the G1/S and G2/M transitions, respectively (Hammarton et al., 2003, 2004; Li and Wang, 2003; Tu and Wang, 2004). CYC2 is homologous to the PHO80 cyclins in yeast and CYC6 is a homolog of the B-type cyclin found in plants (Li and Wang, 2003). However, CYC4 and CYC8, which are related to CYC2 and CYC6, respectively, are also involved in the G1/S transition and the G2/M transition, respectively, but their role(s) in cell cycle control appears to be rather limited since RNAi of CYC4 and CYC8 only generates minor cell cycle defects (Li and Wang, 2003). Strikingly, CYC2 also interacts with CRK3 and likely is also involved in the G2/M transition (Gourguechon et al., 2007; Van Hellemond et al., 2000). CYC2 also interacts with CRK2, which is also required for the G1/S transition (Gourguechon et al., 2007; Tu and Wang, 2005). Recently, CRK1 was found to interact with at least four PHO80-like cyclins, CYC2, CYC4, CYC5, and CYC7, and RNAi of each of the four cyclins resulted in defects in G1/S transition (Liu et al., 2013). CRK9, an extraordinarily large CDK homolog with a large sequence insertion in its catalytic domain, appears to regulate mRNA trans-splicing by phosphorylating an RNA polymerase II subunit, RPB1 (Badjatia et al., 2013a). This discovery questions whether CRK9 is involved in cell cycle control. Biochemical purification of CRK9-associated proteins led to the identification of a novel cyclin, CYC12, and RNAi-mediated silencing of CYC12 also disrupted mRNA trans-splicing (Badjatia et al., 2013b). These results suggest that CRK9 does not play any role in cell cycle regulation but rather is involved in mRNA splicing. Altogether, these findings suggest that at least two CRKs (CRK1 and CRK2) and four cyclins (CYC2, CYC4, CYC5, and CYC7) are important for promoting the cell cycle transition from G1 to S phase, whereas CRK3 and three cyclins (CYC2, CYC6, and CYC8) are involved in the G2/M transition. No cyclin and CRK have

been found to play a role in the S phase. Additionally, homologs of the CDK inhibitors are also not identified, presumably due to their divergent sequence that has escaped the homology-based search against the trypanosome proteome. Nevertheless, the presence of an unexpected large number of cyclins and CDKs in an early branching unicellular eukaryote suggests the complexity of the cell cycle control system, which may reflect the complex life cycle of trypanosomes during which the parasite has to deal with different living environments, such as in the mammalian host and the tsetse fly host, for successful cell proliferation.

3.3. Life cycle stage-specific differences in cell cycle regulation

The life cycle of trypanosomes involves the transmission between mammalian hosts and the insect vector, tsetse fly. During the cyclic transmission, trypanosome cells undergo differentiation, which is characterized by morphological restructuring, surface coat switching, and biochemical adaptation (McKean, 2003). The most distinct morphological difference between the different life cycle forms of trypanosomes is the relative position of the kinetoplast. In the procyclic form, the kinetoplast is posterior and when it replicates and segregates, one kinetoplast remains posterior, but the other kinetoplast is positioned between the two segregating nuclei, resulting in the KNKN configuration (from posterior to anterior) of cells before cytokinesis initiation. In the bloodstream form, however, the kinetoplast replicates and segregates in the posterior portion of the cell, and both daughter kinetoplasts remain in the posterior region throughout the cell cycle, thus resulting in the KKNN configuration of cells before cytokinesis. In addition to the morphological difference between the life cycle forms, life cycle-specific differences in many other cellular processes, including chromatin structure (Schlimme et al., 1993), glucose transport (Munoz-Antonia et al., 1991), maintenance of plasma membrane potential (Van der Heyden and Docampo, 2002), cell motility (Broadhead et al., 2006), and cell cycle regulation (Hammarton et al., 2003; Li and Wang, 2006; Tu and Wang, 2004) have also been discovered. Nevertheless, the molecular mechanisms underlying these distinctions between the two life cycle forms remain poorly understood.

The fundamental architecture of the organelles, the cytoskeletal structures, and the overall cell shape between the life cycle forms appears to be of no significant difference. However, there apparently are fundamental differences in the cell cycle checkpoint systems between the two life cycle

stages. When mitosis is impaired by chemical intervention, such as Rhizoxin-induced malformation of the mitotic spindle (Ploubidou et al., 1999; Robinson et al., 1995), or by genetic interference, such as RNAi-mediated knockdown of mitotic cyclin or CRK which causes mitotic defects (Hammarton et al., 2003; Li and Wang, 2003; Tu and Wang, 2004), the procyclic form of trypanosomes is still capable of completing its cytokinesis, leading to the production of anucleate cells. This suggests that either the procyclic trypanosomes lack the mitosis to cytokinesis checkpoint or the mitotically defective procyclic trypanosomes are able to bypass the mitosis–cytokinesis checkpoint. In the bloodstream form, however, cells with defective mitosis, which is caused by similar knockdown of the mitotic cyclin and CRK (Hammarton et al., 2003; Tu and Wang, 2004), are apparently unable to initiate cytokinesis, suggesting that the mitosis–cytokinesis checkpoint is operational in the bloodstream trypanosomes or that the bloodstream cells with mitotic defects are not capable of bypassing the checkpoint. In striking contrast to the procyclic trypanosomes, these mitotically defective and cytokinesis-arrested bloodstream trypanosomes are able to enter the next round of cell cycle repeatedly, albeit still mitotically defective, resulting in the production of giant cells with polyploid DNA that are not able to be segregated (Hammarton et al., 2003; Li and Wang, 2006; Tu and Wang, 2004). These interesting observations argue that bloodstream trypanosomes appear to lack the checkpoint system that controls the entry to the next G1 phase of the cell cycle in the absence of cytokinesis. Overall, it is clear that the two life cycle forms of trypanosomes employ distinct cell cycle checkpoint control systems.

4. REGULATION OF MITOSIS

4.1. Closed mitosis in *T. brucei*

Eukaryotic cells must faithfully segregate their genetic material to the daughter cells during mitosis. It has long been established that lower and higher eukaryotes achieve this in strikingly distinct ways. Higher eukaryotes undergo an open mitosis, with the nuclear envelope completely disassembled at the G2/M transition and then reassembled upon the completion of mitosis. In contrast, many lower eukaryotes undergo a closed mitosis in which the nuclear envelope remains intact throughout mitosis and mitosis occurs within the nucleus. In the closed mitosis, proteins and molecules involved in mitosis are transported in and out of the nucleus through the nuclear pore complexes that are embedded in the nuclear envelope and serve

as molecular sieves. Like many other lower eukaryotes, trypanosome also undergoes a closed mitosis. Throughout mitosis the nuclear envelope does not break down, which was easily detected by immunofluorescence microscopy with an antibody against a nuclear envelope protein and by electron microscopy (Ogbadoyi et al., 2000). Through biochemical purification followed by mass spectrometry, the trypanosome nuclear pole complex was characterized, which shares a similar architecture to that of fungi and animals (DeGrasse et al., 2009).

4.2. Spindle structure and assembly

It has been well recognized that trypanosome cells do not possess centrioles, but instead have the flagellar basal body as the cell's MTOC, which is involved in nucleating the flagellar axoneme microtubules and has little role in spindle assembly. Since mitosis is closed, the mitotic spindle is formed within the nucleus, with the two poles of the spindle located at the opposite ends of the nucleus, which are potentially the spindle poles in trypanosomes (Ogbadoyi et al., 2000). However, it is not clear whether trypanosomes possess a spindle pole structure similar to the SPB found in fungi. A search for the homologs of yeast SPB proteins in the trypanosome genome only identified the components of the γ-tubulin complex, which is known to localize to the flagellar basal body, the cell's only visible MTOC. Intriguingly, two proteins, the Tousled-like kinase TbTLK1 and a nuclear pore complex component, TbNup92, are found to localize to the spindle poles during mitosis in trypanosomes (DeGrasse et al., 2009; Li et al., 2007). RNAi of TbTLK1 results in defects in spindle formation in trypanosomes, suggesting that TbTLK1 is likely involved in spindle assembly. The potential role of TbNup92 in spindle assembly remains to be explored.

Using a monoclonal antibody against β-tubulin, KMX-1, the mitotic spindle can be readily detected during early to late mitotic phases in trypanosomes. Here, we report the morphological and conformational changes of the spindle during mitotic progression, which represents the first detailed illustration of the various shapes of the mitotic spindle in trypanosomes (Fig. 4.5). The spindle structure becomes clearly visible at metaphase, during which the spindle is short in length and appears like a diamond in shape, with the kinetochores of the chromosomes all aligned in the equator of the spindle (Fig. 4.5A). The spindle then gradually elongates, presumably through the sliding of the overlapping interpolar spindle microtubules which in general is mediated by kinesin motor proteins and/or through the separation of

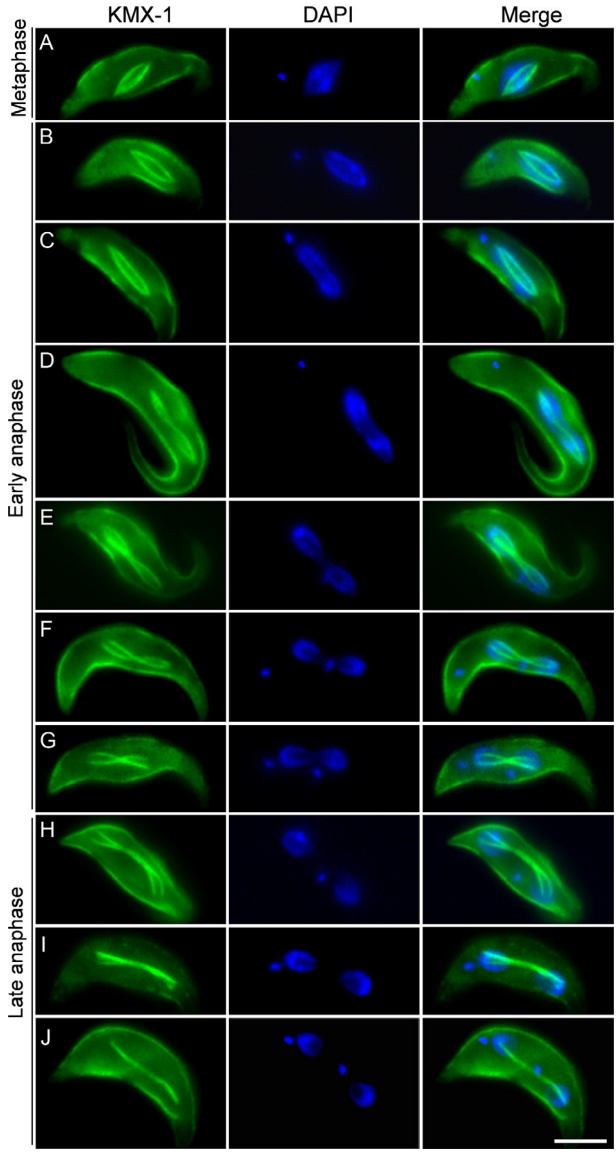

Figure 4.5 Morphology of the mitotic spindle during various stages of mitosis in the procyclic trypanosomes. Cells were immunostained with KMX-1, which stains the β-tubulin in the spindle in trypanosomes, and counterstained with DAPI for nuclear and kinetoplast DNA. Bar: 5 μm.

the spindle poles. This elongation of spindle microtubules correlates with the gradual segregation of chromosomes, which is often referred to as the anaphase of the cell cycle (Fig. 4.5B–G). The spindle structure in trypanosomes appears to contain less microtubule fibers than that in fungi and animals, and as a result the metaphase spindle and anaphase spindle appear to comprise only two lines of microtubules (more spindle microtubules may exist, but they are not visible), with both ends of the two lines merged together to form the SPBs that associate with or are an integral part of the nuclear envelope (Fig. 4.5A–C) (Ogbadoyi et al., 2000). Strikingly, during early anaphase when the spindle is elongated, the two visible microtubule lines start to twist by an unknown mechanism, thus making the shape of the spindle resemble the Arabic number 8, with the SPB likely remaining intact (Fig. 4.5D, E). This "8"-shaped spindle then apparently undergoes some conformational change by transforming from a closed conformation to an open bifurcated conformation assuming an "X" shape (Fig. 4.5F, G), which likely involves the disassembly of the SPB complex, although this is still not clear and needs to be further investigated. At later stages of anaphase, the spindle is further elongated, resulting in farther segregation of the duplicated nuclei. The spindle microtubules at late anaphase appear to bundle vigorously, leading to the transformation of the "X"-shaped spindle to a single microtubule bundle that connects the two far segregated nuclei (Fig. 4.5H–J). Prior to cytokinesis, the spindle bundle disappears.

Little is known about how the bipolar mitotic spindle is assembled in trypanosomes. It is generally accepted that spindle microtubules in animals are nucleated either by centrosomes or through chromatin-mediated pathways and that spindle microtubules in fungi are nucleated by SPBs embedded in the nuclear envelope. Unlike the organisms containing centrosomes or SPBs, spindle assembly in acentrosomal cells rely exclusively on chromatin-mediated pathways in which microtubules are nucleated and stabilized near the kinetochores (Dumont and Desai, 2012). Once the bipolar spindle is assembled, its maintenance is dependent on the cooperative action of microtubule motors, such as the Kinesin-5 family, which are plus end-directed motors, the Kinesin-14 family, which are minus end-directed motors, and the Kinesin-13 family, which are microtubule depolymerases (Gatlin and Bloom, 2010). Both the Kinesin-5 and Kinesin-13 kinesins subject to phosphorylation by Aurora A kinase and Aurora B kinase, respectively, and this phosphorylation is required for assembly of a bipolar spindle. Moreover, Aurora B kinase also plays an additional role in chromosome biorientation by correcting

microtubule–kinetochore misattachments, which also helps establish the bipolar spindle (Carmena et al., 2009). Finally, the spindle assembly checkpoint (SAC) monitors microtubule–kinetochore attachment errors, and when an attachment error is detected by the SAC, anaphase onset is delayed through inhibiting the activity of the anaphase promoting complex/cyclosome (APC/C) (Peters, 2006).

The lack of centrosomes or SPBs in trypanosome cells argues that establishment of a bipolar spindle is most likely dependent on chromatin-mediated pathways. To support such a notion, the proteins that are known to be required for centrosome-directed spindle assembly, such as Aurora A kinase and Kinesin-5, appear to be missing in trypanosomes. In contrast, the proteins that are implicated in chromatin-based pathways, such as Aurora B kinase and Kinesin-13, are present in trypanosomes and are involved in regulating spindle formation and the dynamics of spindle microtubules (Chan et al., 2010; Li and Wang, 2006; Tu et al., 2006; Wickstead et al., 2010). Intriguingly, despite the lack of a Kinesin-5 homolog in trypanosomes, two highly divergent orphan kinesins, TbKIN-A and TbKIN-B, cooperate with the Aurora B kinase homolog, TbAUK1, to regulate spindle assembly (Li et al., 2008a,c). Both TbKIN-A and TbKIN-B associate with nuclear DNA and the central spindle and interact with TbAUK1, but how the two kinesins promote spindle assembly is still not known. Unlike any other eukaryotes, trypanosomes express a greatly expanded repertoire of the Kinesin-13 family, and one of this family, TbKif13-1, is involved in regulating the dynamics of spindle microtubules (Chan et al., 2010; Wickstead et al., 2010). Nevertheless, it remains unclear whether TbKif13-1 plays any role in maintaining kinetochore–microtubule interactions as its mammalian counterpart. Further in-depth investigation is necessary to explore the mechanistic roles of the mitotic kinesins in controlling spindle assembly and spindle microtubule dynamics.

Homologs for most of the APC/C components have been identified in trypanosomes, which apparently form a functional ubiquitin E3 ligase that is required for metaphase–anaphase transition and is also involved in controlling the stability of the mitotic cyclin, CYC6 (Bessat et al., 2013; Kumar and Wang, 2005). The latter function of the APC/C in trypanosomes may suggest another role of the complex in promoting mitotic exit. However, homologs for most of the SAC complex except Mad2 are missing in the trypanosome genome (Berriman et al., 2005). Surprisingly, TbMad2 is localized to the basal body (Akiyoshi and Gull, 2013a), arguing against its involvement in monitoring kinetochore–microtubule interaction errors

during bipolar spindle assembly. Therefore, the lack of a SAC complex and the safeguard control mechanism in trypanosomes cannot be ruled out, which may highlight the unusual mechanism underlying spindle assembly and kinetochore–microtubule interactions in trypanosomes.

4.3. Kinetochore and its unusual protein composition

The kinetochore is a complex structure that establishes the attachment of spindle microtubules to chromosomes and is thus essential for faithful chromosome segregation. Under the transmission electron microscope, the kinetochore in vertebrate animals appears as a trilaminar stack of plates situated on opposite sides of the centromere of mitotic chromosomes (Brinkley and Stubblefield, 1966). The outer plate contains microtubule-interacting proteins (such as CENP-E, etc.) and the SAC proteins, whereas the inner plate is immediately adjacent to the centromere and is organized on a chromatin structure containing nucleosomes with a specialized histone named CENP-A, which substitutes histone H3 in the centromere region, auxiliary proteins, and centromere DNA (Chan et al., 2005). Electron microscopic studies show that the mitotic chromosomes of trypanosomes also possess an electron-dense structure typical of the canonical kinetochore found in other eukaryotic organisms (Ogbadoyi et al., 2000). However, the observed number of kinetochore appears not to exceed 8 (Solari, 1995), but there are more than 100 chromosomes. This suggests either a non-conventional function of the kinetochore or the existence of alternative chromosome segregation mechanism(s) (Ogbadoyi et al., 2000). It is also very likely that those chromosomes without detectable kinetochores may contain smaller kinetochores whose ultrastructure is not readily visible by electron microscopy.

Despite the presence of canonical kinetochore structure in trypanosomes, the protein components of the kinetochore were largely unknown (Berriman et al., 2005). Only a few kinetochore protein homologs were found based on sequence homology (Berriman et al., 2005), which include the inner kinetochore protein MCAK (Kinesin-13 family kinesins) and the outer kinetochore protein TOG/MOR1. Surprisingly, the TOG/MOR1 homolog was found to be localized to the cytosol without enrichment in the nucleus in procyclic trypanosomes (our unpublished data), suggesting that it is either not a kinetochore component in trypanosomes or not a *bona fide* homolog of TOG/MOR1. Recently, 19 candidate kinetochore proteins were identified in trypanosomes by using localization-based screening

and proteomics approach, and RNAi-mediated knockdown of these kinetochore proteins resulted in severe chromosome mis-segregation (Akiyoshi and Gull, 2013b). All of the 19 kinetochore proteins bear no detectable sequence homology to the kinetochore proteins in other eukaryotes, suggesting that trypanosomes employ a chromosome segregation mechanism involving novel kinetochore components (Akiyoshi and Gull, 2013b).

4.4. Novel chromosomal passenger complex and its role in mitosis

Chromosomal passengers are proteins that move from the centromere to the midzone of the spindle during mitosis. The first passenger protein identified is an inner centromere protein called INCENP (Cooke et al., 1987), which was later found to interact with an essential mitotic kinase, the Aurora B kinase (Adams et al., 2000; Kaitna et al., 2000). It is now well known that the chromosomal passenger complex (CPC) is composed of the enzymatic subunit Aurora B and three regulatory components, INCENP, Survivin, and Borealin (Ruchaud et al., 2007). The three regulatory CPC proteins form a localization module, forming a three-helix bundle among the INCENP amino terminus, Survivin and Borealin (Jeyaprakash et al., 2007). This bundle is required for CPC localization to the centromere of chromosomes, which is mediated by the baculovirus IAP repeat domain of Survivin and the C-terminus of Borealin (Jeyaprakash et al., 2007). This bundle is also required for CPC localization to the spindle midzone and the anaphase midbody that is involved in cytokinesis initiation, but the precise mechanism remains a mystery. The CPC is present in all the eukaryotes examined so far, and all the four components are evolutionarily conserved from fungi to humans (Carmena et al., 2012).

Trypanosomes, however, express a unique CPC that only consists of three components (Li et al., 2008a). This novel CPC is composed of the well-conserved Aurora B kinase homolog, TbAUK1 (Li and Wang, 2006; Tu et al., 2006), and two hypothetical protein, TbCPC1 and TbCPC2. TbCPC1 appears to contain a so-called IN-box motif that is originally found in INCENP and is involved in binding to Aurora B kinase. However, TbCPC1 is relatively small, with an observed molecular mass of around 30 kDa, whereas the INCENP homologs found in many other organisms from yeast to human have a molecular mass of over 100 kDa. Nevertheless, the presence of the IN box suggests that TbCPC1 is a structural and likely also functional homolog of INCENP. TbCPC2 is extremely divergent and exhibits no significant sequence homology to

the well-conserved CPC proteins found in fungi and animals (Li et al., 2008a,c). TbCPC2 could act as a functional homolog of Borealin or Survivin, but this still needs to be investigated.

Despite the structure distinction, the trypanosome CPC still exhibits a dynamic subcellular localization pattern typical of the canonical CPC found in animals. It is concentrated in the nucleus at G2 phase, and then migrates from the chromosome centromeres to the central portion of the mitotic spindle during metaphase to anaphase transition. Subsequently, it moves from the central spindle to the anterior tip of the new FAZ during the transition from mitosis to cytokinesis. Since trypanosome cells undergo a closed mitosis without breaking down the nuclear envelope during mitosis, this suggests that the CPC has to be exported out of the nucleus across the nuclear membrane. The detailed mechanism behind the nuclear export of the CPC is not clear. Finally, the complex travels along the cleavage furrow which ingresses longitudinally from the anterior tip of the new FAZ toward the posterior end of the cell (Li et al., 2008a, 2009) (also see Fig. 4.6 and below for detailed description). Since the three noncatalytic CPC proteins in animals are known to function as a single structural unit to target Aurora B kinase to various subcellular locations during mitosis (Jeyaprakash et al., 2007), it is not clear whether the two noncatalytic CPC proteins in trypanosomes play similar roles like the animal CPC components. Additionally, INCENP has an additional function by acting as a substrate activator of Aurora B kinase (Bishop and Schumacher, 2002). Since TbCPC1 is a structural homolog of INCENP, it will be necessary to determine whether TbCPC1 also has a role in activating TbAUK1. Further investigation of the function of the two CPC proteins would help understand the regulation of TbAUK1 and the mechanistic roles of TbAUK1 in mitosis and cytokinesis.

5. MECHANISMS OF CYTOKINESIS

5.1. Coordination of mitosis with cytokinesis

Eukaryotes employ a number of cell cycle checkpoint systems to ensure the fidelity of cell division. For example, DNA damage checkpoint monitors the DNA damages generated during the cell cycle, and when DNA damages are detected, cell cycle progression is slowed down, allowing the cell to repair the DNA damage before continuation of the cell cycle. The abscission checkpoint control system, which is triggered by the Aurora B kinase through phosphorylating a subunit of the endosomal sorting complex

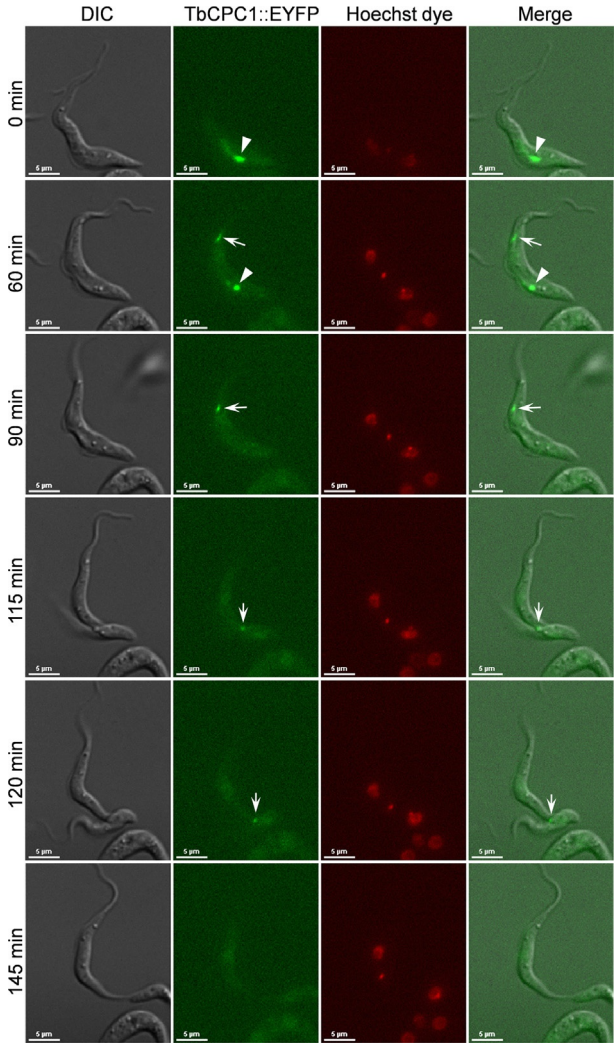

Figure 4.6 Cytokinesis initiation, progression, and completion in procyclic trypanosomes and the dynamic localization of the CPC during cytokinesis. A procyclic cell expressing EYFP-tagged TbCPC1 was visualized under the fluorescence microscope and the time-course live image was taken at various times to monitor the progress of cytokinesis and the localization of TbCPC1. Live cells were stained with Hoechst dye to label the nuclear and kinetoplast DNA. Arrowheads point to the TbCPC1 fluorescence signal at the central spindle, whereas the arrows indicate the TbCPC1 fluorescence signal at the anterior tip of the new FAZ and the cleavage furrow. Bars: 5 μm.

required for transport-III (Carlton et al., 2012), delays abscission until the chromatin bridge stuck in the cell division plane is resolved (Carmena et al., 2012). In all the eukaryotes studied to date, inhibition of mitotic progression unanimously blocks cytokinesis, resulting in the production of polyploid cells. Intriguingly, transition from mitosis to cytokinesis in the procyclic form of trypanosomes appears to be poorly coordinated. This interesting phenotype was originally observed when procyclic trypanosome cells were treated with Rhizoxin, a microtubule poison that disrupts the assembly of spindle microtubules and hence inhibits mitosis, anucleate cells, termed zoids, were produced (Ploubidou et al., 1999; Robinson et al., 1995), suggesting that cytokinesis can occur in the absence of mitosis in procyclic trypanosomes. Such observations were further confirmed by genetic interference with mitosis through RNAi-mediated silencing of mitotic genes, such as the mitotic cyclin, CYC6, and its partner, CRK3 (Hammarton et al., 2003; Li and Wang, 2003; Tu and Wang, 2004). These studies suggest that procyclic trypanosomes likely lack a checkpoint system for controlling mitosis–cytokinesis transition. Since basal body duplication and segregation appears to constitute the first cytoskeletal event in trypanosome cell cycle and inhibition of basal body duplication or segregation completely arrests cytokinesis (Das et al., 1994), it suggests that posterior migration of the basal body, which is believed to be controlled by the elongation of the new flagellum and the FAZ filament (Absalon et al., 2007), likely functions as the primary driving force for cytokinesis in procyclic trypanosomes, although the roles of the CPC, TbPLK, and other unidentified cytokinesis regulators should not be undermined.

5.2. Unusual mode of cytokinesis

Cytokinesis is the final step of the cell cycle during which two daughter cells physically separate after the duplication and segregation of chromosomes and organelles. Cytokinesis begins when the site of the future cleavage furrow is defined, and in fungi and animals it can be generally divided into the following steps: selection of the cell division plane, assembly of the contractile ring, constriction and disassembly of the contractile ring, and separation of daughter cells by membrane fusion (Pollard and Wu, 2010). Positioning the cleavage plane is critical for symmetrical cytokinesis, and at the site of cell division plane a contractile ring, which is composed of the myosin motor protein, actin filaments, and many other proteins, is assembled and attached to the plasma membrane (Barr and Gruneberg, 2007). The mechanism of

cytokinesis through the actomyosin contractile ring structure likely appeared in the common ancestor of amoebas, fungi, and animals, which share most of the genes used for cytokinesis (Pollard and Wu, 2010). Plants use a different cytokinesis mechanism, the membrane fusion machinery, in which the plant cells fuse membrane vesicles to build new membrane between the daughter cells (Otegui et al., 2005). The mechanism of cytokinesis in the organisms that branched earlier than algae and plants, such as the protozoan parasites trypanosomes and Giardia, also appears to be different from that in fungi and animals because these parasites apparently lack myosin II. Further investigation of the mechanism of cytokinesis in early branching protozoa would help understand the evolution of the cytokinesis regulatory machinery.

Cytokinesis in trypanosomes appears to be different from that in fungi and animals, not only because there is no evidence to support the existence of the actomyosin contractile ring-based cytokinesis machinery (Garcia-Salcedo et al., 2004) but also because cytokinesis cleavage furrow ingression occurs along the longitudinal axis from the anterior tip of the new FAZ toward the posterior tip of the cell between the two flagella (Li et al., 2008a,c, 2009; Vaughan and Gull, 2003, 2008). The precise selection site of the cytokinesis cleavage plane in trypanosomes is still not defined, but several lines of evidence strongly suggest that the anterior tip of the new FAZ is implicated (Robinson et al., 1995). As further support to this hypothesis, trypanosome mutants defective in intraflagellar transport, which generate a short new flagellum and a short new FAZ, undergo asymmetrical cell division to produce a small daughter cell with a short flagellum and a short FAZ (Kohl et al., 2003). The trypanosome mutant defective in new FAZ assembly due to the depletion of a FAZ filament protein CC2D also undergoes unequal cell division, but this produces a small daughter cell with a short FAZ and a full-length flagellum (Zhou et al., 2011). The latter study further reinforces the notion that it is the new FAZ, but not the flagellum, that defines the cytokinesis cleavage plane in trypanosomes.

5.3. Regulation of cytokinesis by CPC

Initiation of cytokinesis in animals is known to be initiated by two evolutionarily conserved protein kinases, Aurora B kinase and Polo-like kinase (PLK), both of which are enriched at the central spindle and the anaphase midbody. The central spindle is critical for positioning and establishment of the actomyosin contractile ring. The two kinases act cooperatively to

regulate, through phosphorylation, a common downstream factor, the so-called centralspindlin complex that is composed of a Kinesin-6 family member, MKLP1, and a Rho GTPase activating protein, MgcRacGAP, in mammals (Mishima et al., 2002). The centralspindlin complex then binds to Ect2, a Rho GEF (guanine nucleotide exchange factor), and recruits the latter to the midbody (Somers and Saint, 2003). Ect2 is required to activate RhoA, a small GTPase, leading to the concentration of the latter in the equatorial region of the cell membrane (Piekny et al., 2005). Activation of RhoA further promotes actin polymerization and myosin II activation, leading to the formation of the actomyosin contractile ring (Carmena, 2008; Glotzer, 2005). Interestingly, the fission yeast Aurora B kinase homolog Ark1 is not essential for cytokinesis (Petersen and Hagan, 2003), suggesting that regulation of actomyosin ring assembly in fission yeast likely involves a mechanism distinct from that in budding yeast and animals. Like in animals, the PLK in fungi is essential for cytokinesis by functioning as an upstream component of the SIN (septum initiation network) or MEN (mitotic exit network) comprising a number of proteins, such as MOB1, DBF2, and Cdc14, all of which are conserved between budding and fission yeasts (Gruneberg and Nigg, 2003). Some of these SIN/MEN pathway components also have their mammalian homologs, which are also essential for cytokinesis in mammals. However, how they are regulated by PLK in mammals remains poorly understood (D'Amours and Amon, 2004).

Although trypanosomes display a different mode of cytokinesis and lack the actomyosin-based cytokinesis apparatus, the Aurora B kinase homolog, TbAUK1, and the PLK homolog, TbPLK, are both implicated in cytokinesis (Hammarton et al., 2007; Kumar and Wang, 2006; Li and Wang, 2006; Tu et al., 2006). TbAUK1 functions as a crucial chromosomal passenger protein and plays multiple roles in mitosis (Li and Wang, 2006; Li et al., 2008a,c, 2009; Tu et al., 2006). It is also required for cytokinesis initiation, furrow ingression, and abscission (Li and Wang, 2006; Li et al., 2008a,c, 2009; Tu et al., 2006); however, the precise mechanisms of TbAUK1 in cytokinesis are still a mystery, mainly because none of its downstream factors in the cytokinesis pathway has been identified. Like the CPC in animals, the trypanosome CPC is also enriched on the central spindle during late mitosis (Fig. 4.6, 0 min), but it is not clear whether the central spindle in trypanosomes defines the cytokinesis cleavage plane as it does in animals. However, unlike the animal CPC that stays on the central spindle region upon the completion of mitosis, the trypanosome CPC starts to relocate to the anterior tip of the new FAZ (Fig. 4.6, 60 min), which is known to constitute the

initiation site of cytokinesis in trypanosomes. However, it remains to be determined whether the CPC proteins at the anterior tip of the new FAZ are newly synthesized proteins or are the old CPC proteins translocalized from the central spindle. When the CPC is only confined to the anterior tip of the new FAZ (Fig. 4.6, 90 min), cytokinesis is initiated, and when the cleavage furrow ingresses toward the posterior end of the cell, the CPC travels along the furrow (Fig. 4.6, 115 and 120 min). At the final stage of cytokinesis during which the two daughter cells are connected at the posterior ends, the CPC disappears, likely because they are degraded (our unpublished data). This dynamic pattern of CPC localization during mitosis–cytokinesis transition and during cytokinesis progression, together with the genetic evidence (Li and Wang, 2006; Tu et al., 2006), strongly suggests a role for the CPC in cytokinesis initiation, progression, and completion.

5.4. Regulation of cytokinesis by other proteins

A highly divergent Rho-like small GTPase, TbRHP, and its RhoGAP, TbOCRL, were identified in trypanosomes (Abbasi et al., 2011). RNAi-mediated silencing of both proteins each leads to defective cytokinesis, and the phenotype resembles that of the TbAUK1 RNAi mutant (Abbasi et al., 2011), implying that TbRHP and TbOCRL might function in TbAUK1-mediated pathway. Unlike in humans where active RhoA is concentrated at the cytokinesis initiation site (Piekny et al., 2005), however, TbRHP is diffusely localized throughout the cytosol (Abbasi et al., 2011). Nevertheless, the identification of a RhoA-like small GTPase and its activation partner as crucial cytokinesis regulators suggests that a RhoA-mediated cytokinesis pathway is indeed operating in trypanosomes. However, it is not clear whether they function downstream of TbAUK1 and whether TbAUK1 can activate TbRHP. Intriguingly, TbRHP appears to regulate cytokinesis through its interaction with TRACK (Abbasi et al., 2011), which is the trypanosome homolog of the receptor for activated C kinase 1 (RACK1) and is involved in regulating cytokinesis onset and progression (Rothberg et al., 2006). Given the absence of the actomyosin contractile ring in trypanosomes, the mechanistic role of TbRHP in cytokinesis remains to be explored.

Like in animals, the trypanosome genome also encodes a few SIN/MEN pathway proteins, such as the homologs of MOB1 and DBF2 kinase, both of which are essential for cytokinesis in trypanosomes (Hammarton et al., 2005; Ma et al., 2010). Strikingly, both the MOB1 homolog and the DBF2

homolog in trypanosomes appear to play distinct roles in different life cycle forms. MOB1 appears to regulate cytokinesis completion in the bloodstream form and the positioning of cleavage furrow in the procyclic form (Hammarton et al., 2005). DBF2 homolog is essential for cytokinesis initiation in the bloodstream form, but is not required for cytokinesis in the procyclic form (Ma et al., 2010 and our unpublished observation). Surprisingly, unlike in yeast where MOB1 and DBF2 interact with each other, the two homologs do not interact *in vivo* in trypanosomes (Ma et al., 2010), which argues whether they act in the same pathway as their yeast counterparts. Nevertheless, these observations suggest that the cytokinesis regulatory pathways found in fungi and animals are likely also operating in trypanosomes.

It has been well accepted that regulation of cytokinesis involves more than 100 proteins in the cleavage furrow in fungi and animals (Pollard and Wu, 2010; Skop et al., 2004), and a conserved core of about 20 cytokinesis proteins are found in most animal cells (Glotzer, 2005). However, additional cytokinesis proteins are not conserved among animal cells. The number of proteins known to be involved in cytokinesis in trypanosomes is rather limited, with less than a dozen of proteins identified as putative cytokinesis regulators, including a type III phosphatidylinositol 4-kinase (Rodgers et al., 2007), KMP-11 (Li and Wang, 2008), a protein arginine methyltransferase (Fisk et al., 2010), a small GTPase (ARL2) (Price et al., 2010), Katanin and Spastin (Benz et al., 2012), an F-box protein (CFB2) (Benz and Clayton, 2007), a microtubule-associated protein (AIR9) (May et al., 2012), adenylyl cyclases (Salmon et al., 2012), and a kinetoplastid-specific kinesin, TbKIN-C, and its partner kinesin, TbKIN-D (Hu et al., 2012a,b). However, the precise mechanistic roles of these proteins in cytokinesis are not well established, and none of these proteins was found concentrated at the cytokinesis cleavage furrow or at the anterior tip of the new FAZ, thus ruling out their direct participation in cytokinesis.

5.5. Unusual roles of PLK in organelle duplication and cytokinesis

The PLKs are evolutionarily conserved serine/threonine protein kinases and are localized to various mitotic structures, such as centrosomes, nucleus, central spindle, and anaphase midbody, where they play multiple essential roles in mitotic entry, bipolar spindle assembly, chromosome segregation, mitotic exit, and cytokinesis (Archambault and Glover, 2009; Barr et al., 2004). All the PLKs possess a canonical catalytic domain in the N-terminus and a C-terminal Polo-box domain consisting of one or two

Polo-box motifs, which plays a regulatory role in controlling PLK localization and substrate binding (Barr et al., 2004).

The PLK homolog in *T. brucei*, TbPLK, exhibits a characteristic PLK structure, with a catalytic kinase domain in its N-terminus and two Polo-box motifs in its C-terminus (Graham et al., 1998). TbPLK exhibits a dynamic localization pattern during the cell cycle. It is initially expressed during the S phase and is found in the basal body (de Graffenried et al., 2008; Umeyama and Wang, 2008). When the cell cycle proceeds, TbPLK is enriched in the bilobe structure that is undergoing duplication. After the bilobe is replicated and the duplicated bilobe structures start to segregate, TbPLK is found at the growing tip of new FAZ filament during late S phase, G2 phase, and early mitotic phases, such as metaphase and early anaphase (de Graffenried et al., 2008). However, at late anaphase and telophase during which the CPC is detected at the anterior tip of the new FAZ, TbPLK disappears from the anterior tip of the new FAZ (Li et al., 2010). Strikingly, unlike the PLK homologs found in any other organisms, TbPLK is not localized to the nucleus throughout the cell cycle (de Graffenried et al., 2008; Kumar and Wang, 2006) despite the presence of a nuclear localization signal located between the kinase domain and the Polo-box motif (Sun and Wang, 2011; Yu et al., 2012). Importantly, consistent with its absence in the nucleus, TbPLK apparently does not play an essential role in mitosis since RNAi of TbPLK in both the procyclic and bloodstream forms does not cause any detectable mitotic defects (Hammarton et al., 2007; Kumar and Wang, 2006).

The function of TbPLK appears to correlate with its subcellular localization. Depletion of TbPLK by RNAi causes defective segregation of the duplicated basal bodies (Hammarton et al., 2007; Ikeda and de Graffenried, 2012), presumably by inhibiting the rotation of the new basal body (Lozano-Nunez et al., 2013). RNAi of TbPLK also causes defective bilobe duplication, leading to defects in assembling the duplicated Golgi apparatus (de Graffenried et al., 2008). Moreover, TbPLK deficiency also compromises the assembly of the new FAZ filament, resulting in detachment of the new flagellum (Ikeda and de Graffenried, 2012; Lozano-Nunez et al., 2013). Since TbPLK is required for basal body segregation and inhibition of basal body segregation inhibits cell division, it is still not clear whether TbPLK is directly involved in cytokinesis initiation. TbPLK appears to exert its effect primarily during the S phase because it is highly expressed at S phase during which basal body duplicates and rotation of the new basal body occurs (Lozano-Nunez et al., 2013; Umeyama and Wang, 2008). However, since

TbPLK remains associated with the FAZ filament until early anaphase and cytokinesis initiation is known to initiate at anaphase in other eukaryotes, it is likely that TbPLK also plays a direct role in cytokinesis. In this regard, TbPLK presumably regulates certain cytokinesis regulatory proteins at the anterior tip of the FAZ filament. Such proteins are, unfortunately, still not identified, which hinders our understanding of the mechanistic roles of TbPLK in regulating cytokinesis.

5.6. Roles of flagellum and FAZ in furrow positioning and cytokinesis initiation

Defining the cytokinesis cleavage plane is fundamental to cells for symmetrical cell division to generate two identical daughter cells. In animals, the division plane is defined by the position of the central spindle, which is critical for the establishment of the actomyosin contractile ring. In trypanosomes, however, the cleavage plane is placed between the two flagella along the longitudinal axis, which appears to be in parallel with the mitotic spindle, and is initiated from the anterior tip of the new FAZ filament (Robinson et al., 1995; Vaughan and Gull, 2003). Growing evidence suggests that the new FAZ may provide structural information for positioning the cleavage plane (Robinson et al., 1995). Trypanosome mutants with a short new FAZ filament and an old full-length FAZ are capable of undergoing an asymmetrical cell division, producing a small-sized daughter cell with the short new FAZ and a normal-sized daughter cell containing the old full-length FAZ (Zhou et al., 2011). On the other hand, since positioning and elongation of the FAZ filament is defined by the flagellum (Kohl et al., 1999), the growth of the new flagellum thus also plays a critical role in positioning the cleavage plane. This hypothesis is supported by the observation that trypanosome mutants with defective flagellum assembly can undergo an asymmetrical cytokinesis by producing a small-sized daughter cell with a short flagellum and a normal-sized daughter cell with a full-length flagellum (Kohl et al., 2003). The proposed role of the anterior tip of the FAZ as the initiation site of cytokinesis is further confirmed by the discovery that the CPC, a crucial regulator of cytokinesis, is localized to the anterior tip of the new FAZ before cytokinesis initiation (Li et al., 2008a,c, 2009).

6. CONCLUSIONS AND PERSPECTIVES

During the past decade, significant advances in the understanding of the molecular mechanism of mitosis and cytokinesis in trypanosomes have

been made, and it is now well accepted that most cell cycle regulatory pathways conserved from fungi to humans are also present in trypanosomes. However, trypanosomes have evolved some unusual cell cycle checkpoint systems and employ many trypanosome-specific cell cycle regulators to compensate for the absence of the regulators that are conserved in other eukaryotes. It is also well accepted that significant differences in cell cycle control exist between different life cycle stages.

Many questions with regard to the cell cycle control in trypanosomes remain unanswered. For example, what are the components of the cytokinesis cleavage furrow? What are the cell cycle checkpoints and how do they control cell cycle progression? How does the CPC travel across the nuclear envelope and how does CPC promote cytokinesis? What is the abscission machinery and how does the machinery cleave the membrane and the microtubule cytoskeleton? Future work should apply a combination of biochemical, genetic, and proteomics approaches for further exploration of trypanosome-specific cell cycle regulatory pathways and for identification of novel cell cycle regulators. There is no doubt that such endeavors will significantly advance our fundamental understanding of the mechanisms of mitosis and cytokinesis in trypanosomes and would also provide novel drug targets for chemotherapeutic intervention.

ACKNOWLEDGMENTS

We apologize to our colleagues whose work could not be cited due to space constraints. We thank members of the Li laboratory for critical reading of the manuscript. We also thank Dr. Keith Gull of the University of Oxford for providing the L8C4 antibody and Dr. Graham Warren of Max F. Perutz Laboratories in Austria for anti-GRASP antibody. Work in the Li laboratory is supported by the NIH Grants R01AI101437 and R21AI093897.

REFERENCES

Abbasi, K., DuBois, K.N., Leung, K.F., Dacks, J.B., Field, M.C., 2011. A novel Rho-like protein TbRHP is involved in spindle formation and mitosis in trypanosomes. PLoS One 6, e26890.

Absalon, S., Kohl, L., Branche, C., Blisnick, T., Toutirais, G., Rusconi, F., Cosson, J., Bonhivers, M., Robinson, D., Bastin, P., 2007. Basal body positioning is controlled by flagellum formation in *Trypanosoma brucei*. PLoS One 2, e437.

Absalon, S., Blisnick, T., Kohl, L., Toutirais, G., Dore, G., Julkowska, D., Tavenet, A., Bastin, P., 2008. Intraflagellar transport and functional analysis of genes required for flagellum formation in trypanosomes. Mol. Biol. Cell 19, 929–944.

Adams, R.R., Wheatley, S.P., Gouldsworthy, A.M., Kandels-Lewis, S.E., Carmena, M., Smythe, C., Gerloff, D.L., Earnshaw, W.C., 2000. INCENP binds the Aurora-related kinase AIRK2 and is required to target it to chromosomes, the central spindle and cleavage furrow. Curr. Biol. 10, 1075–1078.

Akiyoshi, B., Gull, K., 2013a. Evolutionary cell biology of chromosome segregation: insights from trypanosomes. Open Biol. 3, 130023.
Akiyoshi, B., Gull, K., 2013b. Identification of kinetochore proteins in *Trypanosoma brucei*. In: The 5th Kinetoplastid Molecular Cell Biology Meeting. Woods Hole, MA, April 21–25, 2013, p. 39.
Alsford, S., Turner, D.J., Obado, S.O., Sanchez-Flores, A., Glover, L., Berriman, M., Hertz-Fowler, C., Horn, D., 2011. High-throughput phenotyping using parallel sequencing of RNA interference targets in the African trypanosome. Genome Res. 21, 915–924.
Archambault, V., Glover, D.M., 2009. Polo-like kinases: conservation and divergence in their functions and regulation. Nat. Rev. Mol. Cell Biol. 10 (4), 265–275.
Badjatia, N., Ambrosio, D.L., Lee, J.H., Gunzl, A., 2013a. Trypanosome cdc2-related kinase 9 controls spliced leader RNA cap4 methylation and phosphorylation of RNA polymerase II subunit RPB1. Mol. Cell. Biol. 33, 1965–1975.
Badjatia, N., Ambrosio, D.L., Nguyen, B., Gunzl, A., 2013b. Characterization of cdc2-related kinase 9 (CRK9), a key enzyme in trypanosome gene expression. In: 5th Kinetoplastid Molecular Cell Biology Meeting. Woods Hole, MA, April 21–25, 2013.
Barr, F.A., Gruneberg, U., 2007. Cytokinesis: placing and making the final cut. Cell 131, 847–860.
Barr, F.A., Sillje, H.H., Nigg, E.A., 2004. Polo-like kinases and the orchestration of cell division. Nat. Rev. Mol. Cell Biol. 5 (6), 429–440.
Benz, C., Clayton, C.E., 2007. The F-box protein CFB2 is required for cytokinesis of bloodstream-form *Trypanosoma brucei*. Mol. Biochem. Parasitol. 156, 217–224.
Benz, C., Clucas, C., Mottram, J.C., Hammarton, T.C., 2012. Cytokinesis in bloodstream stage *Trypanosoma brucei* requires a family of katanins and spastin. PLoS One 7, e30367.
Berriman, M., Ghedin, E., Hertz-Fowler, C., Blandin, G., Renauld, H., Bartholomeu, D.C., Lennard, N.J., Caler, E., Hamlin, N.E., Haas, B., Bohme, U., Hannick, L., Aslett, M.A., Shallom, J., Marcello, L., Hou, L., Wickstead, B., Alsmark, U.C., Arrowsmith, C., Atkin, R.J., Barron, A.J., Bringaud, F., Brooks, K., Carrington, M., Cherevach, I., Chillingworth, T.J., Churcher, C., Clark, L.N., Corton, C.H., Cronin, A., Davies, R.M., Doggett, J., Djikeng, A., Feldblyum, T., Field, M.C., Fraser, A., Goodhead, I., Hance, Z., Harper, D., Harris, B.R., Hauser, H., Hostetler, J., Ivens, A., Jagels, K., Johnson, D., Johnson, J., Jones, K., Kerhornou, A.X., Koo, H., Larke, N., Landfear, S., Larkin, C., Leech, V., Line, A., Lord, A., Macleod, A., Mooney, P.J., Moule, S., Martin, D.M., Morgan, G.W., Mungall, K., Norbertczak, H., Ormond, D., Pai, G., Peacock, C.S., Peterson, J., Quail, M.A., Rabbinowitsch, E., Rajandream, M.A., Reitter, C., Salzberg, S.L., Sanders, M., Schobel, S., Sharp, S., Simmonds, M., Simpson, A.J., Tallon, L., Turner, C.M., Tait, A., Tivey, A.R., Van Aken, S., Walker, D., Wanless, D., Wang, S., White, B., White, O., Whitehead, S., Woodward, J., Wortman, J., Adams, M.D., Embley, T.M., Gull, K., Ullu, E., Barry, J.D., Fairlamb, A.H., Opperdoes, F., Barrell, B.G., Donelson, J.E., Hall, N., Fraser, C.M., Melville, S.E., El-Sayed, N.M., 2005. The genome of the African trypanosome *Trypanosoma brucei*. Science 309, 416–422.
Bessat, M., Knudsen, G., Burlingame, A.L., Wang, C.C., 2013. A minimal anaphase promoting complex/cyclosome (APC/C) in *Trypanosoma brucei*. PLoS One 8, e59258.
Brinkley, B.R., Stubblefield, E., 1966. The fine structure of the kinetochore of mammalian cell in vitro. Chromosoma 19 (1), 28–43.
Bishop, J.D., Schumacher, J.M., 2002. Phosphorylation of the carboxyl terminus of inner centromere protein (INCENP) by the Aurora B Kinase stimulates Aurora B kinase activity. J. Biol. Chem. 277, 27577–27580.
Briggs, L.J., McKean, P.G., Baines, A., Moreira-Leite, F., Davidge, J., Vaughan, S., Gull, K., 2004. The flagella connector of *Trypanosoma brucei*: an unusual mobile transmembrane junction. J. Cell Sci. 117, 1641–1651.

Broadhead, R., Dawe, H.R., Farr, H., Griffiths, S., Hart, S.R., Portman, N., Shaw, M.K., Ginger, M.L., Gaskell, S.J., McKean, P.G., Gull, K., 2006. Flagellar motility is required for the viability of the bloodstream trypanosome. Nature 440, 224–227.

Carlton, J.G., Caballe, A., Agromayor, M., Kloc, M., Martin-Serrano, J., 2012. ESCRT-III governs the Aurora B-mediated abscission checkpoint through CHMP4C. Science 336, 220–225.

Carmena, M., 2008. Cytokinesis: the final stop for the chromosomal passengers. Biochem. Soc. Trans. 36, 367–370.

Carmena, M., Ruchaud, S., Earnshaw, W.C., 2009. Making the Auroras glow: regulation of Aurora A and B kinase function by interacting proteins. Curr. Opin. Cell Biol. 21, 796–805.

Carmena, M., Wheelock, M., Funabiki, H., Earnshaw, W.C., 2012. The chromosomal passenger complex (CPC): from easy rider to the godfather of mitosis. Nat. Rev. Mol. Cell Biol. 13, 789–803.

Carvalho-Santos, Z., Machado, P., Branco, P., Tavares-Cadete, F., Rodrigues-Martins, A., Pereira-Leal, J.B., Bettencourt-Dias, M., 2010. Stepwise evolution of the centriole-assembly pathway. J. Cell Sci. 123, 1414–1426.

Chan, G.K., Liu, S.T., Yen, T.J., 2005. Kinetochore structure and function. Trends Cell Biol. 15, 589–598.

Chan, K.Y., Matthews, K.R., Ersfeld, K., 2010. Functional characterisation and drug target validation of a mitotic kinesin-13 in *Trypanosoma brucei*. PLoS Pathog. 6, e1001050.

Chanez, A.L., Hehl, A.B., Engstler, M., Schneider, A., 2006. Ablation of the single dynamin of *T. brucei* blocks mitochondrial fission and endocytosis and leads to a precise cytokinesis arrest. J. Cell Sci. 119, 2968–2974.

Cooke, C.A., Heck, M.M., Earnshaw, W.C., 1987. The inner centromere protein (INCENP) antigens: movement from inner centromere to midbody during mitosis. J. Cell Biol. 105, 2053–2067.

D'Amours, D., Amon, A., 2004. At the interface between signaling and executing anaphase—Cdc14 and the FEAR network. Genes Dev. 18, 2581–2595.

Das, A., Gale Jr., M., Carter, V., Parsons, M., 1994. The protein phosphatase inhibitor okadaic acid induces defects in cytokinesis and organellar genome segregation in *Trypanosoma brucei*. J. Cell Sci. 107 (Pt. 12), 3477–3483.

Davidge, J.A., Chambers, E., Dickinson, H.A., Towers, K., Ginger, M.L., McKean, P.G., Gull, K., 2006. Trypanosome IFT mutants provide insight into the motor location for mobility of the flagella connector and flagellar membrane formation. J. Cell Sci. 119, 3935–3943.

de Graffenried, C.L., Ho, H.H., Warren, G., 2008. Polo-like kinase is required for Golgi and bilobe biogenesis in *Trypanosoma brucei*. J. Cell Biol. 181, 431–438.

DeGrasse, J.A., DuBois, K.N., Devos, D., Siegel, T.N., Sali, A., Field, M.C., Rout, M.P., Chait, B.T., 2009. Evidence for a shared nuclear pore complex architecture that is conserved from the last common eukaryotic ancestor. Mol. Cell. Proteomics 8, 2119–2130.

Dilbeck, V., Berberof, M., Van Cauwenberge, A., Alexandre, H., Pays, E., 1999. Characterization of a coiled coil protein present in the basal body of *Trypanosoma brucei*. J. Cell Sci. 112 (Pt. 24), 4687–4694.

Dumont, J., Desai, A., 2012. Acentrosomal spindle assembly and chromosome segregation during oocyte meiosis. Trends Cell Biol. 22, 241–249.

Esson, H.J., Morriswood, B., Yavuz, S., Vidilaseris, K., Dong, G., Warren, G., 2012. Morphology of the trypanosome bilobe, a novel cytoskeletal structure. Eukaryot. Cell. 11, 761–772.

Fisk, J.C., Zurita-Lopez, C., Sayegh, J., Tomasello, D.L., Clarke, S.G., Read, L.K., 2010. TbPRMT6 is a type I protein arginine methyltransferase that contributes to cytokinesis in *Trypanosoma brucei*. Eukaryot. Cell. 9, 866–877.

Garcia-Salcedo, J.A., Perez-Morga, D., Gijon, P., Dilbeck, V., Pays, E., Nolan, D.P., 2004. A differential role for actin during the life cycle of *Trypanosoma brucei*. EMBO J. 23, 780–789.

Gatlin, J.C., Bloom, K., 2010. Microtubule motors in eukaryotic spindle assembly and maintenance. Semin. Cell Dev. Biol. 21, 248–254.

Gheiratmand, L., Brasseur, A., Zhou, Q., He, C.Y., 2013. Biochemical characterization of the bi-lobe reveals a continuous structural network linking the bi-lobe to other single-copied organelles in *Trypanosoma brucei*. J. Biol. Chem. 288, 3489–3499.

Glotzer, M., 2005. The molecular requirements for cytokinesis. Science 307, 1735–1739.

Gluenz, E., Povelones, M.L., Englund, P.T., Gull, K., 2011. The kinetoplast duplication cycle in Trypanosoma brucei is orchestrated by cytoskeleton-mediated cell morphogenesis. Mol. Cell. Biol. 31, 1012–1021.

Gourguechon, S., Savich, J.M., Wang, C.C., 2007. The multiple roles of cyclin E1 in controlling cell cycle progression and cellular morphology of *Trypanosoma brucei*. J. Mol. Biol. 368, 939–950.

Graham, T.M., Tait, A., Hide, G., 1998. Characterisation of a polo-like protein kinase gene homologue from an evolutionary divergent eukaryote, *Trypanosoma brucei*. Gene 207, 71–77.

Gruneberg, U., Nigg, E.A., 2003. Regulation of cell division: stop the SIN! Trends Cell Biol. 13, 159–162.

Habedanck, R., Stierhof, Y.D., Wilkinson, C.J., Nigg, E.A., 2005. The Polo kinase Plk4 functions in centriole duplication. Nat. Cell Biol. 7, 1140–1146.

Hammarton, T.C., 2007. Cell cycle regulation in *Trypanosoma brucei*. Mol. Biochem. Parasitol. 153, 1–8.

Hammarton, T.C., Clark, J., Douglas, F., Boshart, M., Mottram, J.C., 2003. Stage-specific differences in cell cycle control in *Trypanosoma brucei* revealed by RNA interference of a mitotic cyclin. J. Biol. Chem. 278, 22877–22886.

Hammarton, T.C., Engstler, M., Mottram, J.C., 2004. The *Trypanosoma brucei* cyclin, CYC2, is required for cell cycle progression through G1 phase and for maintenance of procyclic form cell morphology. J. Biol. Chem. 279, 24757–24764.

Hammarton, T.C., Lillico, S.G., Welburn, S.C., Mottram, J.C., 2005. *Trypanosoma brucei* MOB1 is required for accurate and efficient cytokinesis but not for exit from mitosis. Mol. Microbiol. 56, 104–116.

Hammarton, T.C., Kramer, S., Tetley, L., Boshart, M., Mottram, J.C., 2007. *Trypanosoma brucei* Polo-like kinase is essential for basal body duplication, kDNA segregation and cytokinesis. Mol. Microbiol. 65, 1229–1248.

Harper, J.V., Brooks, G., 2005. The mammalian cell cycle: an overview. Methods Mol. Biol. 296, 113–153.

He, C.Y., Ho, H.H., Malsam, J., Chalouni, C., West, C.M., Ullu, E., Toomre, D., Warren, G., 2004. Golgi duplication in *Trypanosoma brucei*. J. Cell Biol. 165, 313–321.

He, C.Y., Pypaert, M., Warren, G., 2005. Golgi duplication in Trypanosoma brucei requires Centrin2. Science 310, 1196–1198.

Hu, H., Hu, L., Yu, Z., Chasse, A.E., Chu, F., Li, Z., 2012a. An orphan kinesin in trypanosomes cooperates with a kinetoplastid-specific kinesin to maintain cell morphology through regulating subpellicular microtubules. J. Cell Sci. 125, 4126–4136.

Hu, L., Hu, H., Li, Z., 2012b. A kinetoplastid-specific kinesin is required for cytokinesis and for maintenance of cell morphology in *Trypanosoma brucei*. Mol. Microbiol. 83, 565–578.

Humphrey, T., Pearce, A., 2005. Cell cycle molecules and mechanisms of the budding and fission yeasts. Methods Mol. Biol. 296, 3–29.

Ikeda, K.N., de Graffenried, C.L., 2012. Polo-like kinase is necessary for flagellum inheritance in *Trypanosoma brucei*. J. Cell Sci. 125, 3173–3184.

Jeyaprakash, A.A., Klein, U.R., Lindner, D., Ebert, J., Nigg, E.A., Conti, E., 2007. Structure of a Survivin-Borealin-INCENP core complex reveals how chromosomal passengers travel together. Cell 131, 271–285.
Johnson, D.G., Walker, C.L., 1999. Cyclins and cell cycle checkpoints. Annu. Rev. Pharmacol. Toxicol. 39, 295–312.
Kaitna, S., Mendoza, M., Jantsch-Plunger, V., Glotzer, M., 2000. Incenp and an aurora-like kinase form a complex essential for chromosome segregation and efficient completion of cytokinesis. Curr. Biol. 10, 1172–1181.
Klingbeil, M.M., Shapiro, T.A., 2009. Unraveling the secrets of regulating mitochondrial DNA replication. Mol. Cell 35, 398–400.
Kohl, L., Sherwin, T., Gull, K., 1999. Assembly of the paraflagellar rod and the flagellum attachment zone complex during the *Trypanosoma brucei* cell cycle. J. Eukaryot. Microbiol. 46, 105–109.
Kohl, L., Robinson, D., Bastin, P., 2003. Novel roles for the flagellum in cell morphogenesis and cytokinesis of trypanosomes. EMBO J. 22, 5336–5346.
Kumar, P., Wang, C.C., 2005. Depletion of anaphase-promoting complex or cyclosome (APC/C) subunit homolog APC1 or CDC27 of *Trypanosoma brucei* arrests the procyclic form in metaphase but the bloodstream form in anaphase. J. Biol. Chem. 280, 31783–31791.
Kumar, P., Wang, C.C., 2006. Dissociation of cytokinesis initiation from mitotic control in a eukaryote. Eukaryot. Cell. 5, 92–102.
Kuntzel, H., Schulz, A., Ehbrecht, I.M., 1996. Cell cycle control and initiation of DNA replication in Saccharomyces cerevisiae. Biol. Chem. 377, 481–487.
Lacomble, S., Vaughan, S., Gadelha, C., Morphew, M.K., Shaw, M.K., McIntosh, J.R., Gull, K., 2010. Basal body movements orchestrate membrane organelle division and cell morphogenesis in *Trypanosoma brucei*. J. Cell Sci. 123, 2884–2891.
Lacomble, S., Vaughan, S., Deghelt, M., Moreira-Leite, F.F., Gull, K., 2012. A *Trypanosoma brucei* protein required for maintenance of the flagellum attachment zone and flagellar pocket ER domains. Protist 163, 602–615.
LaCount, D.J., Barrett, B., Donelson, J.E., 2002. *Trypanosoma brucei* FLA1 is required for flagellum attachment and cytokinesis. J. Biol. Chem. 277, 17580–17588.
Leal, S., Acosta-Serrano, A., Morris, J., Cross, G.A., 2004. Transposon mutagenesis of Trypanosoma brucei identifies glycosylation mutants resistant to concanavalin A. J. Biol. Chem. 279, 28979–28988.
Li, Z., Wang, C.C., 2003. A PHO80-like cyclin and a B-type cyclin control the cell cycle of the procyclic form of *Trypanosoma brucei*. J. Biol. Chem. 278, 20652–20658.
Li, Z., Wang, C.C., 2006. Changing roles of aurora-B kinase in two life cycle stages of *Trypanosoma brucei*. Eukaryot. Cell. 5, 1026–1035.
Li, Z., Wang, C.C., 2008. KMP-11, a basal body and flagellar protein, is required for cell division in *Trypanosoma brucei*. Eukaryot. Cell. 7, 1941–1950.
Li, Z., Gourguechon, S., Wang, C.C., 2007. Tousled-like kinase in a microbial eukaryote regulates spindle assembly and S-phase progression by interacting with Aurora kinase and chromatin assembly factors. J. Cell Sci. 120, 3883–3894.
Li, Z., Lee, J.H., Chu, F., Burlingame, A.L., Gunzl, A., Wang, C.C., 2008a. Identification of a novel chromosomal passenger complex and its unique localization during cytokinesis in *Trypanosoma brucei*. PLoS One 3, e2354.
Li, Z., Lindsay, M.E., Motyka, S.A., Englund, P.T., Wang, C.C., 2008b. Identification of a bacterial-like HslVU protease in the mitochondria of Trypanosoma brucei and its role in mitochondrial DNA replication. PLoS Pathog. 4, e1000048.
Li, Z., Umeyama, T., Wang, C.C., 2008c. The chromosomal passenger complex and a mitotic kinesin interact with the Tousled-like kinase in trypanosomes to regulate mitosis and cytokinesis. PLoS One 3, e3814.

Li, Z., Umeyama, T., Wang, C.C., 2009. The Aurora Kinase in *Trypanosoma brucei* plays distinctive roles in metaphase-anaphase transition and cytokinetic initiation. PLoS Pathog. 5, e1000575.

Li, Z., Umeyama, T., Li, Z., Wang, C.C., 2010. Polo-like kinase guides cytokinesis in *Trypanosoma brucei* through an indirect means. Eukaryot. Cell. 9, 705–716.

Liu, B., Wang, J., Yaffe, N., Lindsay, M.E., Zhao, Z., Zick, A., Shlomai, J., Englund, P.T., 2009. Trypanosomes have six mitochondrial DNA helicases with one controlling kinetoplast maxicircle replication. Mol. Cell 35, 490–501.

Liu, Y., Hu, H., Li, Z., 2013. The cooperative roles of PHO80-like cyclins in regulating the G1/S transition and posterior cytoskeletal morphogenesis in *Trypanosoma brucei*. Mol. Microbiol. 90, 130–146.

Lozano-Nunez, A., Ikeda, K.N., Sauer, T., de Graffenried, C.L., 2013. An analogue-sensitive approach identifies basal body rotation and flagellum attachment zone elongation as key functions of PLK in *Trypanosoma brucei*. Mol. Biol. Cell 24, 1321–1333.

Ma, J., Benz, C., Grimaldi, R., Stockdale, C., Wyatt, P., Frearson, J., Hammarton, T.C., 2010. Nuclear DBF-2-related kinases are essential regulators of cytokinesis in bloodstream stage *Trypanosoma brucei*. J. Biol. Chem. 285, 15356–15368.

Malumbres, M., Barbacid, M., 2005. Mammalian cyclin-dependent kinases. Trends Biochem. Sci. 30, 630–641.

May, S.F., Peacock, L., Almeida Costa, C.I., Gibson, W.C., Tetley, L., Robinson, D.R., Hammarton, T.C., 2012. The *Trypanosoma brucei* AIR9-like protein is cytoskeleton-associated and is required for nucleus positioning and accurate cleavage furrow placement. Mol. Microbiol. 84, 77–92.

McCulloch, R., 2004. Antigenic variation in African trypanosomes: monitoring progress. Trends Parasitol. 20, 117–121.

McKean, P.G., 2003. Coordination of cell cycle and cytokinesis in *Trypanosoma brucei*. Curr. Opin. Microbiol. 6, 600–607.

McKean, P.G., Baines, A., Vaughan, S., Gull, K., 2003. Gamma-tubulin functions in the nucleation of a discrete subset of microtubules in the eukaryotic flagellum. Curr. Biol. 13, 598–602.

Mishima, M., Kaitna, S., Glotzer, M., 2002. Central spindle assembly and cytokinesis require a kinesin-like protein/RhoGAP complex with microtubule bundling activity. Dev. Cell 2, 41–54.

Morgan, G.W., Goulding, D., Field, M.C., 2004. The single dynamin-like protein of *Trypanosoma brucei* regulates mitochondrial division and is not required for endocytosis. J. Biol. Chem. 279, 10692–10701.

Morris, J.C., Wang, Z., Drew, M.E., Englund, P.T., 2002. Glycolysis modulates trypanosome glycoprotein expression as revealed by an RNAi library. EMBO J. 21, 4429–4438.

Morriswood, B., He, C.Y., Sealey-Cardona, M., Yelinek, J., Pypaert, M., Warren, G., 2009. The bilobe structure of *Trypanosoma brucei* contains a MORN-repeat protein. Mol. Biochem. Parasitol. 167, 95–103.

Morriswood, B., Havlicek, K., Demmel, L., Yavuz, S., Sealey-Cardona, M., Vidilaseris, K., Anrather, D., Kostan, J., Djinovic-Carugo, K., Roux, K.J., Warren, G., 2013. Novel bilobe components in *Trypanosoma brucei* identified using proximity-dependent biotinylation. Eukaryot. Cell. 12, 356–367.

Munoz-Antonia, T., Richards, F.F., Ullu, E., 1991. Differences in glucose transport between blood stream and procyclic forms of Trypanosoma brucei rhodesiense. Mol. Biochem. Parasitol. 47, 73–81.

Oberholzer, M., Langousis, G., Nguyen, H.T., Saada, E.A., Shimogawa, M.M., Jonsson, Z.O., Nguyen, S.M., Wohlschlegel, J.A., Hill, K.L., 2011. Independent analysis of the flagellum surface and matrix proteomes provides insight into flagellum signaling in mammalian-infectious *Trypanosoma brucei*. Mol. Cell. Proteomics 10, M111.010538.

Ochsenreiter, T., Anderson, S., Wood, Z.A., Hajduk, S.L., 2008. Alternative RNA editing produces a novel protein involved in mitochondrial DNA maintenance in trypanosomes. Mol. Cell. Biol. 28, 5595–5604.
Ogbadoyi, E., Ersfeld, K., Robinson, D., Sherwin, T., Gull, K., 2000. Architecture of the *Trypanosoma brucei* nucleus during interphase and mitosis. Chromosoma 108, 501–513.
Ogbadoyi, E.O., Robinson, D.R., Gull, K., 2003. A high-order trans-membrane structural linkage is responsible for mitochondrial genome positioning and segregation by flagellar basal bodies in trypanosomes. Mol. Biol. Cell 14, 1769–1779.
Otegui, M.S., Verbrugghe, K.J., Skop, A.R., 2005. Midbodies and phragmoplasts: analogous structures involved in cytokinesis. Trends Cell Biol. 15, 404–413.
Peters, J.M., 2006. The anaphase promoting complex/cyclosome: a machine designed to destroy. Nat. Rev. Mol. Cell Biol. 7, 644–656.
Petersen, J., Hagan, I.M., 2003. *S. pombe* aurora kinase/survivin is required for chromosome condensation and the spindle checkpoint attachment response. Curr. Biol. 13, 590–597.
Piekny, A., Werner, M., Glotzer, M., 2005. Cytokinesis: welcome to the Rho zone. Trends Cell Biol. 15, 651–658.
Ploubidou, A., Robinson, D.R., Docherty, R.C., Ogbadoyi, E.O., Gull, K., 1999. Evidence for novel cell cycle checkpoints in trypanosomes: kinetoplast segregation and cytokinesis in the absence of mitosis. J. Cell Sci. 112 (Pt. 24), 4641–4650.
Pollard, T.D., Wu, J.Q., 2010. Understanding cytokinesis: lessons from fission yeast. Nat. Rev. Mol. Cell Biol. 11, 149–155.
Pradel, L.C., Bonhivers, M., Landrein, N., Robinson, D.R., 2006. NIMA-related kinase TbNRKC is involved in basal body separation in *Trypanosoma brucei*. J. Cell Sci. 119, 1852–1863.
Price, H.P., Peltan, A., Stark, M., Smith, D.F., 2010. The small GTPase ARL2 is required for cytokinesis in *Trypanosoma brucei*. Mol. Biochem. Parasitol. 173, 123–131.
Robinson, D.R., Gull, K., 1991. Basal body movements as a mechanism for mitochondrial genome segregation in the trypanosome cell cycle. Nature 352, 731–733.
Robinson, D.R., Sherwin, T., Ploubidou, A., Byard, E.H., Gull, K., 1995. Microtubule polarity and dynamics in the control of organelle positioning, segregation, and cytokinesis in the trypanosome cell cycle. J. Cell Biol. 128, 1163–1172.
Rodgers, M.J., Albanesi, J.P., Phillips, M.A., 2007. Phosphatidylinositol 4-kinase III-beta is required for Golgi maintenance and cytokinesis in *Trypanosoma brucei*. Eukaryot. Cell. 6, 1108–1118.
Roditi, I., Liniger, M., 2002. Dressed for success: the surface coats of insect-borne protozoan parasites. Trends Microbiol. 10, 128–134.
Rothberg, K.G., Burdette, D.L., Pfannstiel, J., Jetton, N., Singh, R., Ruben, L., 2006. The RACK1 homologue from *Trypanosoma brucei* is required for the onset and progression of cytokinesis. J. Biol. Chem. 281, 9781–9790.
Ruchaud, S., Carmena, M., Earnshaw, W.C., 2007. Chromosomal passengers: conducting cell division. Nat. Rev. Mol. Cell Biol. 8, 798–812.
Salmon, D., Bachmaier, S., Krumbholz, C., Kador, M., Gossmann, J.A., Uzureau, P., Pays, E., Boshart, M., 2012. Cytokinesis of Trypanosoma brucei bloodstream forms depends on expression of adenylyl cyclases of the ESAG4 or ESAG4-like subfamily. Mol. Microbiol. 84, 225–242.
Schimanski, B., Nguyen, T.N., Gunzl, A., 2005. Highly efficient tandem affinity purification of trypanosome protein complexes based on a novel epitope combination. Eukaryot. Cell. 4, 1942–1950.
Schlimme, W., Burri, M., Bender, K., Betschart, B., Hecker, H., 1993. *Trypanosoma brucei brucei*: differences in the nuclear chromatin of bloodstream forms and procyclic culture forms. Parasitology 107 (Pt. 3), 237–247.

Scott, V., Sherwin, T., Gull, K., 1997. Gamma-tubulin in trypanosomes: molecular characterisation and localisation to multiple and diverse microtubule organising centres. J. Cell Sci. 110 (Pt. 2), 157–168.

Selvapandiyan, A., Kumar, P., Morris, J.C., Salisbury, J.L., Wang, C.C., Nakhasi, H.L., 2007. Centrin1 is required for organelle segregation and cytokinesis in *Trypanosoma brucei*. Mol. Biol. Cell 18, 3290–3301.

Selvapandiyan, A., Kumar, P., Salisbury, J.L., Wang, C.C., Nakhasi, H.L., 2012. Role of centrins 2 and 3 in organelle segregation and cytokinesis in Trypanosoma brucei. PLoS One 7, e45288.

Shaw, J.M., Nunnari, J., 2002. Mitochondrial dynamics and division in budding yeast. Trends Cell Biol. 12, 178–184.

Sherwin, T., Gull, K., 1989. Visualization of detyrosination along single microtubules reveals novel mechanisms of assembly during cytoskeletal duplication in trypanosomes. Cell 57, 211–221.

Shi, J., Franklin, J.B., Yelinek, J.T., Ebersberger, I., Warren, G., He, C.Y., 2008. Centrin4 coordinates cell and nuclear division in T. brucei. J. Cell Sci. 121, 3062–3070.

Skop, A.R., Liu, H., Yates 3rd, J., Meyer, B.J., Heald, R., 2004. Dissection of the mammalian midbody proteome reveals conserved cytokinesis mechanisms. Science 305, 61–66.

Solari, A.J., 1995. Mitosis and genome partition in trypanosomes. Biocell 19, 65–84.

Somers, W.G., Saint, R., 2003. A RhoGEF and Rho family GTPase-activating protein complex links the contractile ring to cortical microtubules at the onset of cytokinesis. Dev. Cell 4, 29–39.

Sun, L., Wang, C.C., 2011. The structural basis of localizing polo-like kinase to the flagellum attachment zone in *Trypanosoma brucei*. PLoS One 6, e27303.

Tu, X., Wang, C.C., 2004. The involvement of two cdc2-related kinases (CRKs) in *Trypanosoma brucei* cell cycle regulation and the distinctive stage-specific phenotypes caused by CRK3 depletion. J. Biol. Chem. 279, 20519–20528.

Tu, X., Wang, C.C., 2005. Coupling of posterior cytoskeletal morphogenesis to the G1/S transition in the Trypanosoma brucei cell cycle. Mol. Biol. Cell 16, 97–105.

Tu, X., Kumar, P., Li, Z., Wang, C.C., 2006. An aurora kinase homologue is involved in regulating both mitosis and cytokinesis in *Trypanosoma brucei*. J. Biol. Chem. 281, 9677–9687.

Umeyama, T., Wang, C.C., 2008. Polo-like kinase is expressed in S/G2/M phase and associated with the flagellum attachment zone in both procyclic and bloodstream forms of *Trypanosoma brucei*. Eukaryot. Cell. 7, 1582–1590.

Urbaniak, M.D., Guther, M.L., Ferguson, M.A., 2012. Comparative SILAC proteomic analysis of Trypanosoma brucei bloodstream and procyclic lifecycle stages. PLoS One 7, e36619.

Van der Heyden, N., Docampo, R., 2002. Significant differences between procyclic and bloodstream forms of Trypanosoma brucei in the maintenance of their plasma membrane potential. J. Eukaryot. Microbiol. 49, 407–413.

Van Hellemond, J.J., Neuville, P., Schwarz, R.T., Matthews, K.R., Mottram, J.C., 2000. Isolation of *Trypanosoma brucei* CYC2 and CYC3 cyclin genes by rescue of a yeast G(1) cyclin mutant. Functional characterization of CYC2. J. Biol. Chem. 275, 8315–8323.

Vaughan, S., Gull, K., 2003. The trypanosome flagellum. J. Cell Sci. 116, 757–759.

Vaughan, S., Gull, K., 2008. The structural mechanics of cell division in *Trypanosoma brucei*. Biochem. Soc. Trans. 36, 421–424.

Vaughan, S., Kohl, L., Ngai, I., Wheeler, R.J., Gull, K., 2008. A repetitive protein essential for the flagellum attachment zone filament structure and function in *Trypanosoma brucei*. Protist 159, 127–136.

Wickstead, B., Carrington, J.T., Gluenz, E., Gull, K., 2010. The expanded Kinesin-13 repertoire of trypanosomes contains only one mitotic Kinesin indicating multiple extranuclear roles. PLoS One 5, e15020.

Woods, K., Nic a'Bhaird, N., Dooley, C., Perez-Morga, D., Nolan, D.P., 2013. Identification and characterization of a stage specific membrane protein involved in flagellar attachment in *Trypanosoma brucei*. PLoS One 8, e52846.

Yu, Z., Liu, Y., Li, Z., 2012. Structure-function relationship of the Polo-like kinase in *Trypanosoma brucei*. J. Cell Sci. 125, 1519–1530.

Zhao, Z., Lindsay, M.E., Roy Chowdhury, A., Robinson, D.R., Englund, P.T., 2008. p166, a link between the trypanosome mitochondrial DNA and flagellum, mediates genome segregation. EMBO J. 27, 143–154.

Zhou, Q., Gheiratmand, L., Chen, Y., Lim, T.K., Zhang, J., Li, S., Xia, N., Liu, B., Lin, Q., He, C.Y., 2010. A comparative proteomic analysis reveals a new bi-lobe protein required for bi-lobe duplication and cell division in *Trypanosoma brucei*. PLoS One 5, e9660.

Zhou, Q., Liu, B., Sun, Y., He, C.Y., 2011. A coiled-coil- and C2-domain-containing protein is required for FAZ assembly and cell morphology in *Trypanosoma brucei*. J. Cell Sci. 124, 3848–3858.

CHAPTER FIVE

Reprogramming and Carcinogenesis—Parallels and Distinctions

Agata M. Wasik[*], Jerzy Grabarek[†], Aleksandar Pantovic[‡], Artur Cieślar-Pobuda[§,¶], Hamid R. Asgari[||], Caspar Bundgaard-Nielsen[§,#], Mehrdad Rafat[§,††], Ian M.C. Dixon[**], Saeid Ghavami[,1], Marek J. Łos[†,§,‡‡,1,2]**

[*]Division of Pathology, Department of Laboratory Medicine, Karolinska Institutet, Karolinska University Hospital, Huddinge, Stockholm, Sweden
[†]Department of Pathology, Pomeranian Medical University, Szczecin, Poland
[‡]Institute of Microbiology and Immunology, School of Medicine, University of Belgrade, and Clinic of Neurology, Military Medical Academy, Belgrade, Serbia
[§]Department of Clinical and Experimental Medicine (IKE), Division of Cell Biology, and Integrative Regenerative Medicine Center (IGEN), Linköping University, Linköping, Sweden
[¶]Biosystems Group, Institute of Automatic Control, Silesian University of Technology, Gliwice, Poland
[||]Tehran University of Medical Sciences, Tehran, Iran
[#]Laboratory for Stem Cell Research, Aalborg University, Aalborg, Denmark
[**]Department of Physiology, St. Boniface Research Centre, and Manitoba Institute of Child Health, University of Manitoba, Winnipeg, Canada
[††]Department of Biomedical Engineering (IMT), Linköping University, Linköping, Sweden
[‡‡]BioApplications Enterprises, Winnipeg, Manitoba, Canada
[1]Both authors share senior authorship
[2]Corresponding author: e-mail address: marek.los@liu.se

Contents

International Review of Cell and Molecular Biology, Volume 308
ISSN 1937-6448
http://dx.doi.org/10.1016/B978-0-12-800097-7.00005-1

Abstract

Rapid progress made in various areas of regenerative medicine in recent years occurred both at the cellular level, with the Nobel prize-winning discovery of reprogramming (generation of induced pluripotent stem (iPS) cells) and also at the biomaterial level. The use of four transcription factors, Oct3/4, Sox2, c-Myc, and Klf4 (called commonly "Yamanaka factors") for the conversion of differentiated cells, back to the pluripotent/embryonic stage, has opened virtually endless and ethically acceptable source of stem cells for medical use. Various types of stem cells are becoming increasingly popular as starting components for the development of replacement tissues, or artificial organs. Interestingly, many of the transcription factors, key to the maintenance of stemness phenotype in various cells, are also overexpressed in cancer (stem) cells, and some of them may find the use as prognostic factors. In this review, we describe various methods of iPS creation, followed by overview of factors known to interfere with the efficiency of reprogramming. Next, we discuss similarities between cancer stem cells and various stem cell types. Final paragraphs are dedicated to interaction of biomaterials with tissues, various adverse reactions generated as a result of such interactions, and measures available, that allow for mitigation of such negative effects.

ABBREVIATIONS

CSC cancer stem cells
ECM extracellular matrix
ES cell embryonic stem cell
GFP green fluorescent protein
GSK3 glycogen synthase kinase-3
iPS induced pluripotent stem
MSFs myocardial scar fibroblasts
RB retinoblastoma protein
RGD arginine–glycine–aspartic acid
Shc Src homology 2 domain containing

1. INTRODUCTION

Reprogramming, or reversing adult (partially) differentiated cell into a cell with properties very closely resembling those of embryonic stem (ES) cells, called "induced pluripotent stem" (iPS) cells, by the expression of a set of transcription factors, was first achieved in 2006 (Takahashi and Yamanaka, 2006). Initially, the induction of pluripotent stem cells was carried out by introduction of four factors, Oct3/4, Sox2, c-Myc, and Klf4 (called commonly "Yamanaka factors") to murine (embryonic) fibroblasts,

under ES cell culture conditions. Nowadays, protocols exist, where only two or three factors are used, with c-Myc appearing to enhance the process only rather than being indispensible. For example, Li and colleagues reprogrammed cells without introducing Sox2 transcription factor, showing that only Oct4, Klf4 and glycogen synthase kinase-3 (GSK3) inhibitor CHIR 99021 are sufficient for murine embryonic fibroblasts reprogramming. They indicate that GSK3 inhibitor can replace the reprogramming-related effects of Sox2 transcription factor (Banito et al., 2009; Li et al., 2009b).

While initial reprogramming procedures were performed in murine embryonic or adult fibroblasts, it is becoming increasingly evident that (i) "younger" cells are reprogrammed with higher efficiency, (ii) cells that by their nature already express some of the reprogramming factors become reprogrammed with higher frequency and by using only some of the Yamanaka factors (Kim et al., 2009b), and (iii) cells that express lower amounts of p53 are also reprogrammed with higher efficiency. The later observation indicates that preprogramming itself induces enormous cellular stress, and thus it is a powerful inducer of p53-activated cell death, or senescence triggered by p53, $p16^{INK4a}$, and $p21^{CIP1}$ (Banito et al., 2009; Menendez et al., 2010). Thus, modern reprogramming protocols typically include apoptosis and/or senescence inhibitors in the reprogramming medium.

2. OVERVIEW OF REPROGRAMMING METHODS

Before transcription factor-based reprogramming protocol had been published by Yamanaka group, such process could only be achieved either by transfer of nuclei of mature, differentiated cells into oocytes from which pronuclei were removed, or by fusion with ES cells (Moawad et al., 2011). Somatic cell nuclear transfer has sometimes been used in humans, but it is controversial because of ethical issues related to human egg destruction (Wilmut et al., 1997).

One of the most efficient methods to generate iPS cells is lentiviral transduction of Yamanaka factors (Nakagawa et al., 2008). In this approach, retroviruses integrate into host's genome and allow for sustained expression of reprogramming factors at a sufficient level. Interestingly, newly generated iPS cells are able to methylate and switch off the expression of lentivirally introduced Yamanaka factors, while relying instead on the expression of the same intrinsic transcription factors (Hotta and Ellis,

2008). Lentiviruses have been used for the delivery of Yamanaka factors in a monocistronic form (one factor per virus), or as a multifactor cassette (polycistronic, offered, i.e., by Millipore) in a single lentiviral particle (Sommer et al., 2009). Lentiviral delivery of Yamanaka factors, like other retroviral methods, carry significant risk of insertion mutagenesis related to their genomic integration (Hockemeyer et al., 2008; Sommer et al., 2009); therefore, while they are a valuable research tools, they cannot be safely used in the clinic.

Contrary to report by Hotta and Ellis (2008), viral transgenes may not always be inactivated completely, and during the longer culture period they may reactivate. It has been shown that chimeric mice produced from viral iPS cells frequently developed tumors, because of reactivation of c-Myc expressing virus, used as one of the original Yamanaka factors (Nakagawa et al., 2008). Some Yamanaka factors are also frequently upregulated by certain tumors and their expression level generally correlates with increased metastatic potential and thus with bad prognosis (see below) (Huang et al., 2011; Lengerke et al., 2011).

Adenoviral vectors are another option for the delivery of reprogramming factors. They do not integrate into host's genome, and some adenoviral vectors deliver genes with high efficiency to certain cell types like hepatocytes. In general however, lower efficiency and shorter expression kinetics, that would require repeated transductions to maintaining an adequate level of transgene expression makes adenoviral vectors less suitable for the task (Esteban et al., 2010; Sommer et al., 2009).

Reprogramming has been successfully achieved by Fusaki et al. (2009) using Sendai virus-based delivery of Yamanaka factors (nonintegrating RNA virus). As the used Sendai virus-based vector was replication-deficient, its copies became diluted during cell divisions, and eventually virus-free iPS cells were available. Remaining Sendai virus-harboring cells could be removed using antibody recognizing hemagglutinin-neuraminidase surface marker (expressed only on Sendai virus-infected cells). Thus, this reprogramming technique works without changes to genome.

Precisely due to the above highlighted safety issues, labs around the world aim at developing efficient nonviral reprogramming methods. In this way, one could obtain iPS cells without introducing changes into their genome (beside epigenetic changes). Such methods include (i) minicircle vectors, (ii) PiggyBac transposon system, (iii) already mentioned episomal vectors, and (iv) the delivery of Yamanaka factors as proteins. The common

denominator of such methods is much lower reprogramming efficiency as compared to lentiviral vectors-based reprogramming.

Minicircle vectors-based reprogramming was for the first time described in 2010 (Jia et al., 2010). Minicircle vectors are circular, nonviral DNA elements that are generated by PhiC31 integrase-based intramolecular recombination from parental plasmids that contain sequences of interest (i.e., Oct3/4, Sox2, Nanog, Lin28, green fluorescent protein (GFP)). Expression of minicircle-coded genes lasts weeks, and occurs in both dividing and nondividing cells. Minicircle vectors get introduced (transfected) into cells with higher efficiency, and typically yield higher expression levels of desired proteins, as they are less likely to be inactivated by cellular mechanisms targeting foreign nucleic acids. The plasmid used by Jia et al. (2010) contains a single cassette of four reprogramming factors and GFP as a marker sequence, all separated by self-cleavage peptide 2A sequences.

PiggyBac transposon reprogramming was first proposed by Kaji et al. (2009). In this method, transgene sequence can be removed from integration site without changing host's DNA. The PiggyBac transposon carries a cassette that contains all four reprogramming factors, linked with 2A self-cleavage peptides. For removal purposes, the cassette containing reprogramming factors is flanked by *lox*P sites (Kaji et al., 2009). To remove the exogenous reprogramming factors, iPS cells were transiently transfected with Cre. This system minimizes genome modification in iPS cells and enables complete elimination of nucleic acid sequences encoding exogenous reprogramming factors.

High-efficiency, synthetic mRNA-based reprogramming was recently described (Warren et al., 2010). To achieve that, authors used large quantities of synthetic mRNAs coding for Yamanaka factors, modified to overcome innate antiviral responses. Since mRNA is translated to protein in the cytoplasm they do not have to enter the nucleus, thus further minimizing chance of unwanted modifications of hosts DNA. This method appears to work fast and efficiently (reprogramming in just 2-week period, much shorter than lentiviral vector-based reprogramming, and 4% efficiency—several orders of magnitude higher than lentiviral vector-based reprogramming) (Warren et al., 2010). The major drawback is the need to produce large quantities of high-quality, very long stretches of synthetic mRNA (rather technically challenging and expensive). Furthermore, the cellular RISC (RNA-induced silencing complex) system attempts to degrade such synthetic mRNAs (mechanism of RNA destruction like in RNA-interference technology) (van den Berg et al., 2008). To overcome that

problem, researchers tested synthetic mRNAs chemically modified so that they were not readily recognized as a foreign RNA. As an alternative to chemical synthesis, *in vitro* transcription systems exist, which allow for the synthesis of desired mRNAs.

Protein-based reprogramming carries the advantage that it does not cause any genetic changes. As already mentioned, current methods of protein-based reprogramming are several order of magnitudes less efficient that lentiviral delivery of Yamanaka factors (Kim et al., 2009; Esteban et al., 2010). Typically, synthesized in bacteria Yamanaka factors are modified so that they express basic amino acids or other transport peptides enabling to cross the cell membrane (Hauff et al., 2005). Table 5.1 summarizes current reprogramming methods highlighting their most important advantages and disadvantages.

Beside reprogramming, and subsequent differentiation into desired cell type, several authors have recently reported the possibility of trans-differentiation, or conversion of one cell type to another one, while bypassing the iPS-state. Here are some examples. Recently, conversion of pancreatic cells to hepatocytes by the treatment with dexamethasone was reported (Eberhard and Jockusch, 2010). Another group converted B cells into hematopoietic multipotent progenitors and then reprogrammed them into T cells and macrophages (Cobaleda, 2010). Vierbuchen et al. (2010) describe direct conversion of fibroblasts into neurons by the expression of neural-lineage-specific transcription factors Ascl1, Brn2/Pou3f2, and Myt1l. Direct conversion of myocardial scar fibroblasts (MSFs) to cardiomyocytes by infection of human MSFs with a lentivirus vector encoding the potent cardiogenic transcription factor myocardin was achieved (van Tuyn et al., 2007). Those are just a few examples of the strong scientific interest into direct conversion of one cell type into another.

3. REPROGRAMMING, ANTIPROLIFERATIVE RESPONSE, APOPTOSIS, AND SENESCENCE

An activation of the antiproliferative response during reprogramming has been shown by several authors (Banito et al., 2009). The role of tumor suppressors in reprogramming is inherent at different levels and highlights how stressful the reprogramming is for the cell (Marion et al., 2009). p53 converts various upstream cellular-stress signals into downstream responses including cell cycle arrest, senescence, DNA repair, and apoptosis (Vincent and Los, 2011). Several groups analyzed whether the expression of the

Table 5.1 Advantages/disadvantages of different reprogramming techniques/vectors

Vector	Advantages	Disadvantages
Lentivirus	Sustained expression of reprogramming factors (Hotta and Ellis, 2008) Can be used to transduce both proliferating and nondividing cells (Patel and Yang, 2010)	Insertion mutagenesis which may lead to cancer (Yu et al., 2009)
Adenovirus	Transient expression causes removal of viral vector following reprogramming (Okita et al., 2008) No genomic integration thus preventing insertional mutagenesis (Okita et al., 2008)	Low reprogramming efficiency (Okita et al., 2008) Requires repeated transduction in order to successfully reprogram fibroblasts (Okita et al., 2008)
Sendai virus	Efficient introduction of genomic material into host cells (Fusaki et al., 2009) Can affect several types of cells (Fusaki et al., 2009) No genomic integration thus preventing insertional mutagenesis (Fusaki et al., 2009)	Transfected cells tend to contain viral remains following transduction that requires additional techniques for removal (Okita and Yamanaka, 2011)
Plasmids	Long-term transient gene expression allows reprogramming with only a single transfection (Yu et al., 2009) Episomal gene expression prevents insertional mutagenesis (Yu et al., 2009) Plasmids are lost following repeated culturing (Yu et al., 2009) Can be used in a wide variety of cells (Yu et al., 2009)	Low transfection efficiency (Fusaki et al., 2009) Successful reprogramming requires several plasmids (Jia et al., 2010)
Minicircle	Higher transfection efficiency than plasmids (Jia et al., 2010) Unlike standard plasmids, minicircles does not contain bacterial DNA (Jia et al., 2010) Can reprogram somatic cells using only one vector (Jia et al., 2010)	Low transfection efficiency compared to viral techniques (Jia et al., 2010; Okita et al., 2008).

Continued

Table 5.1 Advantages/disadvantages of different reprogramming techniques/vectors—cont'd

Vector	Advantages	Disadvantages
	Longer expression that plasmids (Jia et al., 2010) Minicircle vectors are lost following repeated culturing (Jia et al., 2010) Can be used in a wide variety of cells (Jia et al., 2010)	
PiggyBac transposon	Sustained expression allow for a higher reprogramming efficiency (Woltjen et al., 2009) Reprogramming vectors can theoretically be removed to produce vector-free iPS cells (Woltjen et al., 2009)	Cells might contain remains of vector following reprogramming (Jia et al., 2010) Low reprogramming efficiency compared to viral techniques (Jia et al., 2010; Okita et al., 2008)
mRNA	No introduction of ectopic DNA (Plews et al., 2010) The small size of mRNA molecules results in a high introduction into the cells with a low cytotoxicity (Plews et al., 2010) Better control of the reprogramming (Plews et al., 2010) Good reprogramming efficiency (Okita and Yamanaka, 2011)	mRNA is degraded within 2 or 3 days. As such, repeated transfection is required for successful reprogramming (Plews et al., 2010)
Proteins	No introduction of ectopic nucleic acids (Kim et al., 2009a)	Proteins produced by bacteria might be misfolded or lack essential modifications (Plews et al., 2010) Proteins provided as cell lysate contain several poorly defined substances beside the reprogramming factors (Plews et al., 2010) Low reprogramming efficiency (Kim et al., 2009a)

reprogramming factors is sufficient to trigger directly an antiproliferative response and showed that the expression of the four Yamanaka factors, or combinations of Oct4, Sox2, and Klf4, in human or murine fibroblasts induces p53 and $p21^{CIP1}$ (Banito and Gil, 2010; Hong et al., 2009; Kawamura et al., 2009). Moreover, the same studies also suggest that a combination of Oct4 and Sox2 or even the individual factors is also sufficient to trigger the activation of p53 and/or $p21^{CIP1}$ (Banito et al., 2009; Kawamura et al., 2009). The main determinants of p53 activation during reprogramming have not been clearly established (Fig. 5.1). The expression of the four Yamanaka factors in human fibroblasts results in oxidative stress and subsequent DNA damage, which leads to the activation of p53 (Egler et al., 2005; Vafa et al., 2002). In addition to p53, transcriptional profiling revealed that reprogramming also activates other genes involved in DNA replication and cell cycle progression such as: POLI, RCF4, MCM5, CCND1, CCND, and the cyclin-dependent kinase inhibitors $p21^{CIP1}$ and $p16^{INK4a}$ (Banito et al., 2009; Mikkelsen et al., 2008; Sridharan et al., 2009).

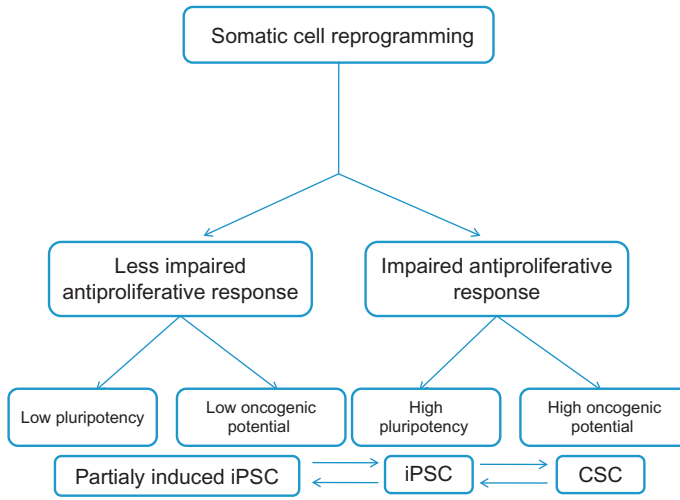

Figure 5.1 The relationship between antiproliferative response, pluripotency, and oncogenesis. Antiproliferative response is activated during reprogramming. At the same time expression of reprogramming factors impairs antiproliferative response by causing mutations on the main tumor suppressor genes. This impairment makes reprogramming more susceptible but increase the possibility for oncogenic transformation. Cell commitment depends on this complex interplay.

3.1. Apoptosis and senescence as outcomes of aborted reprogramming

Murine and human fibroblasts expressing reprogramming factors suffer a cell-cycle arrest that presents multiple characteristics of senescence, such as upregulation of $p16^{INK4a}$ (Banito et al., 2009). Upregulation of both BAX and its antagonist molecule BCL2 in response to the expression of Oct4, Sox2, and Klf4 enhance reprogramming (Kawamura et al., 2009). Other reports suggest that the expression of the reprogramming factors synergizes with the induction of DNA damage to trigger apoptosis. In such a scenario, the expression of BCL2 restores the ability of these cells to be reprogrammed (Marion et al., 2009). Therefore reprogramming is limited by both antiproliferative responses as happens during tumor suppression, in which both senescence and apoptosis are implicated.

3.2. Tumor suppressor loss, differentiation, and oncogenic transformation

Antiproliferative response is activated during the reprogramming process. However, this response is an obstacle in the development of pluripotent cell. Suppression of antiproliferative response increases the efficiency of reprogramming to a more dedifferentiated state but at the same time increases the oncogenic potential of cells. Genomic alterations that occur during reprogramming can cause inefficient antiproliferative response, enhance reprogramming, and increase susceptibility for oncogenic transformation. Commitment of the cell depends on these complex relations (Fig. 5.1).

Several groups have shown that knocking down p53 in human or murine cells significantly increase the efficiency of reprogramming (Banito and Gil, 2010; Hong et al., 2009; Kawamura et al., 2009; Marion et al., 2009). The expression of MDM2 or a dominant-negative mutant of p53 also results in enhanced reprogramming, whereas the activation of p53 through different strategies reduced the reprogramming efficiency (Kawamura et al., 2009; Marion et al., 2009), emphasizing the importance of controlling p53 activity to modulate reprogramming. Similarly, low levels or absence of $p16^{INK4a}$ or $p21^{CIP1}$ expression leads to more efficient and faster reprogramming in mouse and human cells (Banito et al., 2009; Li et al., 2009).

Genomic instability that occurs during and after reprogramming (i.e., prolonged passaging of iPS cells) may contribute to the increase of transformation potential of iPS cells (Gore et al., 2011). Mutations in the p53 and $p16^{INK4a}$/retinoblastoma protein (RB) pathways are found in the majority

of tumors, thus any changes that would destabilize those pathways in iPS cells are particularly dangerous, as they would increase the probability of the emergence of iPS-derived tumors.

Defects in the p53 or the $p16^{INK4a}$/RB pathways have an impact on tumorigenesis as they appear to be especially common in tumors showing plasticity and loss of differentiation characteristics, thus increasing the pool of cancer stem cells (CSC) (Banito et al., 2009). p53 loss was associated with poorly differentiated thyroid cancers (Fagin et al., 1993), breast cancer (de Cremoux et al., 1999; Kochhar et al., 2005; Miller et al., 2005; Mizuno et al., 2010), lung cancer (Junttila et al., 2010), and hematopoietic system malignancies (Chylicki et al., 2000; Feinstein et al., 1992). Collateral mutations of p53 and PTEN are the most common tumor suppressor aberrations in glioblastomas, which are poorly differentiated, developmentally plastic brain tumors derived from the neuronal stem/progenitor cells (Zheng et al., 2008). Deletion of the three RB family proteins triggers the reprogramming of MEFs to generate CSC-like cells (Liu et al., 2009).

4. REPROGRAMMING AND AUTOPHAGY

4.1. Autophagy

Autophagy is a catabolic process that is initiated in cells which is facing stress or starvation conditions (Abounit et al., 2012) and, beside apoptosis and necrosis, if hyperactivated, it may constitute a separate cell death mechanism, removing damaged cells (Ghavami et al., 2010; Yoshimori, 2004). There are three major forms of autophagy: (1) macroautophagy, (2) microautophagy, and (3) chaperone-mediated autophagy. During macroautophagy, parts of the cytoplasm and whole damaged organelles are sequestered into double-membrane autophagosomes (Ghavami et al., 2012a; Rotter and Rothermel, 2012). Macroautophagy could be also involved in sequestration of damaged and misfolded proteins (Gustafsson and Gottlieb, 2009). Following autophagosomes formation, they will fuse with lysosomes to generate single-membrane autophagolysosomes, where degradation of their contents occurs (Yoshimori, 2004). Microautophagy refers to direct engulfment of the organelle by lysosomes without formation of autophagosomes (Rotter and Rothermel, 2012). The third form of autophagy, referred to as chaperone-mediated autophagy, is initiated when proteins (mainly cytosolic) carrying a KFERQ amino acid motif are directed by a complex of chaperone proteins to combine with lysosomes, via the latter's LAMP 2A receptors, for engulfment and degradation (Rotter and Rothermel, 2012).

The molecular mechanisms that regulate autophagy are not yet fully characterized, however, genetic studies in yeast have identified a set of autophagy-related genes (*ATG*) such as *ATG*5, *ATG*12, *ATG*16, *ATG*8, and *ATG*7, which are the major regulators for molecular signaling pathways in autophagy (Ghavami et al., 2012b; Nakatogawa et al., 2009).

Four major steps could be distinguished during the course of autophagy: initiation, elongation, closure, and maturation. Initiation is considered as an autophagosomal membrane isolation step that is driven by an upstream signal (i.e., an ATG14–Beclin 1–hVPS34 complex). The establishment of this complex is required for the formation of phagophores (Abounit et al., 2012; Kang et al., 2011). hVPS34 (phosphatylinositol 3-kinase), one of the key players in the initiation step, is a member of the class III PI3 kinases. hVPS34 is inhibited by protein (Beclin-1) or chemical [3-methyladenine (3-MA)] factors, which results in disruption of the initiation complex (Wu et al., 2010).

Elongation involves the formation of a double-membrane structure comprised of an ATG512-16 complex and LC3. LC3 is a mammalian homologue of yeast ATG8 (Ghavami et al., 2011). LC3 is converted to LC3-I via proteolytic cleavage of its C-terminus by ATG4. Then, two E3- and E2-like enzymes, ATG7 and ATG3, respectively, drive the covalent conjugation of phosphatidylethanolamine to LC3-I, thus forming LC3-II. Similarly, ATG5 becomes covalently bound to ATG12 in the presence of another E2-like enzyme, ATG10. Finally, ATG7 coordinates the formation of the ATG5-12-16 complex (Hanada et al., 2007).

Closure consists of final adjustments to LC3-II and ATG5-12-16 in forming the double-membrane autophagosome. LC3-II in the autophagosome membrane interacts with p62, which is a cargo for ubiquitinated misfolded proteins and organelles. LC3-II is extensively used to measure autophagy flux, the rate of formation of autophagosomes, and is considered the golden standard for autophagometer scale (Rubinsztein et al., 2009). Maturation is the final step in the autophagic process, and mainly describes the translocation and fusion of autophagosomes with lysosomes to form autolysosomes (Ravikumar et al., 2010). It is here in the autolysosomes that sequestered, damaged proteins and organelles are finally degraded, and their components recycled or disposed of (Abounit et al., 2012).

4.2. Autophagy and stem cells

High basal level of autophagy has been reported in human mesenchymal stem cells, whereas after differentiation autophagy is largely downregulated and even undetectable in some cases (Oliver et al., 2012). Hypoxic

conditions facilitate MSCs self-renewal (Lee et al., 2013), whereas autophagy inhibition has been shown to facilitate hypoxia-induced apoptosis in MSCs (Zhang et al., 2012b). Similarly, high basal autophagy level has been shown in hematopoietic stem cells (HSCs), dermal and epidermal stem cells (Salemi et al., 2012) with a trend to decrease to a basal level activity after differentiation (Salemi et al., 2012). Different groups have demonstrated that *ATG7* knock down in murine HSCs resulted in decelerated HSCs self-renewal and negatively affected myeloproliferation (Liu et al., 2010; Mortensen et al., 2011). In contrast, upregulation of autophagy genes has also been shown during neuronal differentiation in mouse embryonic olfactory bulb (Vazquez et al., 2012). Vazquez et al. (2012) also demonstrated that chemical inhibition of autophagy pathway will block the nervous system development in this animal.

Autophagy also plays a central role in controlling somatic reprogramming. Chen et al. (2011) have shown that autophagy is a positive regulator of pluripotency and that rapamycin facilitates mouse embryonic fibroblast reprogramming to pluripotent stem cells. In this context, autophagy may negatively regulate cellular apoptosis and senescence and therefore positively affecting the reprogramming progress (Menendez et al., 2011). On the other hand, in some experimental systems, mitochondrial-targeted autophagy (mitophagy) (Jangamreddy and Los, 2012) facilitates reprogramming via decreasing reactive oxygen species production (Fimia et al., 2007; Vazquez et al., 2012).

4.3. Possible role of autophagy in iPS cell generation

As we have previously indicated, autophagy is a quality control mechanism, which guarantees normal cell function at different stages of cellular life (Jia et al., 2011a). Transcription factors Oct3/4, Sox2, c-Myc, and Klf4 are employed to reprogram differentiated cells toward an embryonic-like state (Marchetto et al., 2010), called iPS. Interestingly, iPS cells not only express stem cell markers, but also stem cell characteristics including anaerobic metabolism, low reactive oxygen species generation and decrease in mitochondrial mass and number (Armstrong et al., 2010; Prigione et al., 2010; Suhr et al., 2010). It has been suggested that the decrease in mitochondrial numbers contributes to lower generation of superoxide ions in iPS cells as compared to their progenitors (Vessoni et al., 2012).

Autophagy plays an important role during differentiation of hematopoietic progenitor cells to erythrocytes and adipocytes by selective mitochondrial

autophagy (Lafontan, 2008; Singh and Cuervo, 2011). Thus it could be hypothesized that autophagy might also participate in reprogramming of differentiated cells to pluripotent form during iPS generation. The observed lower mitochondria numbers in iPS cells may be achieved by selectively targeting mitochondria (mitophagy). Additionally, autophagy may actively facilitate generation of cells with pluripotent stem cell properties via lysosomal degradation of proteins typical for more differentiated cellular stage. Lastly, autophagy may also play a role during phenotype-conversion process by improving protein synthesis via amino acids recycling. Therefore, autophagy could be considered as a potential mechanism, participating not only during cell differentiation, but also throughout reprogramming, or even transdifferentiation processes.

5. REPROGRAMMING FACTORS AND CARCINOGENESIS

Cancer cells and stem cells share certain characteristics, like the ability of self-renewal (Reya et al., 2001), and already discussed above expression of certain stemness factors, including Yamanaka factors. Many pathways that are altered in cancer cells regulate functions of embryonic and adult stem cells. Reprogramming factors (Yamanaka factors) are at the same time proto-oncogenes and may directly affect the proliferation. On the other hand, Yamanaka factors expression is associated with a high level of genomic instability and also indirectly affects proliferation. In Table 5.2, we list the key genes important for the induction of iPS cells, and their function in oncogenic transformation, tumor progression, dissemination or (poor) prognosis.

Besides being part of the Yamanaka reprogramming cocktail, c-Myc and Klf4 are well-known proto-oncogenes, they also play a role in stem-cell self-renewal. Both above facts emphasize the parallels between the induction of pluripotency and carcinogenesis. The Klf4 encodes a transcription factor that is associated with both tumor suppression and oncogenesis. As transcriptional repressor of p53, Klf4 acts as a context-dependent proto-oncogene (Rowland et al., 2005). Klf4 and c-Myc lead to DNA replication stress and genomic instability. Comparative genomic hybridization analysis of iPS cells has revealed occasional presence of genomic deletions and amplifications, a signature suggestive for oncogene-induced DNA replication stress. The genomic aberrations were to a significant degree dependent on c-Myc expression and their presence could explain why p53 inactivation facilitates reprogramming (Marion et al., 2009). The expression of some

Table 5.2 Examples of the cancer types in which transcription factors important for cell reprogramming are expressed

Reprogramming factors	Cancer type and observed association	References
Sox2	Nasopharyngeal cancer *Clinical prognosis*	Wang et al. (2012)
	Melanoma *Cell invasion*	Girouard et al. (2012)
	Colon cancer *Cell invasion and metastases*	Neumann et al. (2011)
	Osteosarcomas *Survival and self-renewal*	Basu-Roy et al. (2012)
	Gastric cancer	Matsuoka et al. (2012)
	Lung cancer *Transformation*	Chen et al. (2012)
	Prostate cancer	Jia et al. (2011b)
	Breast cancer	Stolzenburg et al. (2012)
Oct4	Gastric cancer *Negative prognostic factor*	Matsuoka et al. (2012)
	Oral squamous cell carcinoma	Chiou et al. (2008) and Tsai et al. (2011)
Klf4	Breast cancer *Good prognosis*	Nagata et al. (2012)
	Leukemias *Different Klf4 mRNA levels mirror differentiation state, not a prognostic factor*	Guo and Tang (2012)
	Squamous cell carcinoma *Poor prognosis*	Chen et al. (2008)
	Breast cancer	Rowland et al. (2005)
Nanog	Hepatocellular carcinoma	Shan et al. (2012)
	Breast cancer *Poor prognosis*	Nagata et al. (2012)
	Oral squamous cell carcinoma (OSCC) (Nanog/Oct-4/CD133 coexpression) *Poor prognosis*	Chiou et al. (2008)

Continued

Table 5.2 Examples of the cancer types in which transcription factors important for cell reprogramming are expressed—cont'd

Reprogramming factors	Cancer type and observed association	References
Lin28	Breast cancer *Poor prognosis*	Feng et al. (2012)
	Transformation	Viswanathan et al. (2009)
	Lung cancer *Transformation*	Viswanathan et al. (2009)
	Colon cancer *Transformation*	Viswanathan et al. (2009)
	Cervical cancer *Transformation*	Viswanathan et al. (2009)
	Germ cell tumors *Transformation* Extragonadal germ cells tumors *Transformation(diagnostic marker)*	West et al. (2009) and Cao et al. (2011)
	Ovarian cancer (coexpressed with Oct4) *cell growth and survival*	Peng et al. (2010)

oncogenes such as c-Myc in epithelial tumors is sufficient to reactivate an ES cell-like transcriptional signature.

Other reprogramming factors, such as Sox2 and Lin28, have been documented as oncogenes in small cell lung and esophageal squamous-cell carcinomas and germ-cell tumors (Bass et al., 2009; West et al., 2009). Aggressive, poorly differentiated tumors also express high levels of the ES cell-associated factors (Ben-Porath et al., 2008). Lengerke and colleagues have shown that Sox2 is expressed in a variety of early stage postmenopausal breast cancers and associated metastatic lymph nodes. They conclude that Sox2 plays an early role in breast carcinogenesis and high expression may promote metastases (Lengerke et al., 2011). Others have demonstrated that Sox2 alone or Sox2/Oct4A expression in hepatocellular cancer could serve as a prognostic marker, predicting the outcome of the treatment of hepatocellular cancer patients even at an early stage of the diseases. Thus, Sox2 and Oct4A are predictors of poor prognosis for patients undergoing resection of hepatocellular cancer (Huang et al., 2011).

6. STEMNESS FACTORS AS TRANSCRIPTION FACTORS—EFFECTS IN TRANSFORMATION AND REPROGRAMMING

Functionally, Yamanaka factors are transcription factors that regulate the expression of a number of genes, including some of the reprogramming factors. Below we discuss the regulatory functions of selected Yamanaka factors.

c-Myc proto-oncogene is a transcription factor that regulates a number of genes involved mainly in proliferation and DNA replication. It is overexpressed in many tumor types, thus not surprisingly, it is also at least partially responsible for tumor formation in tissues derived from iPS cells (Okita et al., 2007). Nakagawa et al. (2008) and Wernig et al. (2008) showed independently that the iPS cells generation from mouse embryonic fibroblast using only three Yamanaka's factors, omitting c-Myc, is possible; however, the lack of retroviral c-Myc does not exclude endogenous c-Myc recruitment in the iPS cells generation process. Interestingly, in the study by Nakagawa et al. 6 of 37 chimeras derived from iPS cells generated using four Yamanaka's factors died of tumor within 100 days, while all 26 chimeras derived from three factors cocktail (without c-Myc), survived during the 100 days. Also, the iPS cells generation from human adult fibroblast is possible when retroviral c-Myc is absent, although with the lower reprogramming efficiency (Nakagawa et al., 2008). Further attempts to resolve the importance of c-Myc in iPS cells generation clarified that different properties of c-Myc are responsible for carcinogenic transformation and different for the iPS cells generation. Hence, oncogenic c-Myc could be replaced by genetically engineered c-Myc or other Myc family member L-Myc, which fulfills both criteria (Nakagawa et al., 2010).

Sox2 is a transcription factor belonging to the SOXB1 group of Sry-related HMG box. Sox2 heteredimerizes with another transcription factor Oct4 and together they are important for activating genes important for stem cells maintenance (Lefebvre et al., 2007). Sox2 and Oct4 have been found at high levels in many types of tumors, for example, neuroblastoma (Yang et al., 2012), gliomas (Guo et al., 2012), liver cancer (Huang et al., 2011) and are of importance for the outcome of cancer therapy (Hu et al., 2012; Stolzenburg et al., 2012). However, Cantz et al. (2008) showed that HeLa and MCF-7 cancer cell lines are Oct4-negative and in accordance, the Oct4 promoter is hypermethylated in those cells. Suo et al. (2005)

demonstrated that Oct4 pseudogenes, which are not important for iPS cell generation, in addition to, or instead of Oct4 gene are variably expressed in different cancer types and therefore the role of Oct4 gene in cancrogenesis is debatable.

Klf-4, depending on its target genes, may have multiple, sometimes opposing, roles in regulating cell proliferation, apoptosis and differentiation (Evans and Liu, 2008). Its dual role extends to the cancer cells where Klf-4 can act as both tumor suppressor and an oncogene depending on the cancer type. The first function has been found, for example, in gastric cancer (Zhang et al., 2012a) or B-cell malignancies (Kharas et al., 2007). The fluctuating Klf-4 levels can also mirror the differentiation state of malignant cells (Guo and Tang, 2012). One of the functions of Klf-4 is suppression of the Wnt/β-catenin signaling. Hence, disturbed Wnt/β-catenin is associated with the tumorigenesis. Klf4-β-catenin interaction is crucial for regulating telomere length (Hoffmeyer et al., 2012). Klf4 also interacts with p53–p21 pathway (Zhang et al., 2000) by downregulating p53 promoter, as described for breast cancer cells (Rowland et al., 2005). The p53 protein is a well-known tumor suppressor and its mutations are frequently associated with the tumor progression. Hong et al. (2009) showed that the suppression of p53 and p21 results in increased efficiency of iPS cell generation in mice and in human.

Lin28 and Nanog, although not included in the original Yamanaka's "cocktail", are currently used in some protocols for the cell reprogramming. Lin28 and its human homologue Lin28B regulate let-7 miRNA by blocking let-7 precursor from processing (Viswanathan et al., 2008). Both the repression of let-7 (Kumar et al., 2008; Nadiminty et al., 2012) and the expression of Lin28 have been associated with tumorigenicity (Viswanathan et al., 2009). Among other functions, Nanog drives the expression of Oct4. Several studies showed the expression of Nanog in the context of cancer cells (Jeter et al., 2009; Zbinden et al., 2010). However, there are 11 human Nanog pseudogenes (Booth and Holland, 2004), whose function might differ from Nanog gene and those might be of importance for tumorigenicity. For example, Nanog pseudogene 8 has been associated with tumorigenecity and cell proliferation (Uchino et al., 2012; Zhang et al., 2006).

7. DIFFERENCES AND SIMILARITIES BETWEEN iPS CELLS AND CSC

iPS cells exhibit similar behavior not only to stem cells but they also may have some similarities to CSC, particularly with respect to expression of

certain stemness factors, and proliferative properties. CSC, so far reported in several human solid and hematological tumors, are able to initiate tumor formation and metastasis (Galli et al., 2004; Ribatti, 2012). They are associated with chemo- and radiotherapy resistance and poor patient prognosis (Saigusa et al., 2009). Some of them express specific cell surface markers like CD133 (Beier et al., 2008; Tirino et al., 2008; Zhou et al., 2007). Moreover, CSC express increased levels of anti-apoptotic proteins in comparison to mature cell types from the same tissue which could explain CSC's resistance to cytotoxic drugs (Bitarte et al., 2011; Ribatti, 2012). Like iPS cells, CSC may have gene expression profile different from respective, normal progenitor cells (Reya et al., 2001), possess high proliferation rate and thus positivity for Ki-67 (Tirino et al., 2008).

CSC and iPS cells exhibit several similarities that we summarize in Table 5.3, furthermore iPS cells form teratomas when injected into tissues (Hanley et al., 2010; Miura et al., 2009). Moreover, differentiated tissues that originate from iPS cells have an increased propensity to form tumors.

Table 5.3 Differences and similarities between iPS and cancer stem cells

Feature	iPS cells	Cancer stem cells
Tumor formation	Increased propensity to form teratomas (Hanley et al., 2010; Miura et al., 2009)	Form tumors by definition (Galli et al., 2004; Ribatti, 2012)
p53	p53 loss increases pluripotency (Hanna et al., 2009; Hong et al., 2009; Kawamura et al., 2009)	p53 loss increases tumor initiation frequency (Godar et al., 2008; Zhang et al., 2008)
Senescence	Premature senescence (Feng et al., 2010)	Reduced senescence (Karimi-Busheri et al., 2010; Sabisz and Skladanowski, 2009)
Cell cycle	Short G1 phase, abbreviated cell cycle (Ghule et al., 2011), arrest in G2 phase after DNA damage (Momcilovic et al., 2010)	Long G2 phase, high proportion of cells in the G2 (Chappell and Dalton, 2010; Harper et al., 2010; Tirino et al., 2008)
Treatment resistance	Hypersensitivity to DNA-damaging agents, induction of apoptosis (Momcilovic et al., 2010)	Resistance to DNA-damaging agents, efficient DNA repair (Bao et al., 2006)
Gene expression	Small differences between iPS cells and ES cells gene expression (Yu et al., 2009)	Gene expression different in CSC and tumor cells (Reya et al., 2001)

Formation of tumors seems to depend on the origin of cells. iPS cells derived from different adult tissues may vary in their capacities to differentiate into certain tissues, and may vary substantially in their teratoma-forming propensity (Miura et al., 2009; Yamanaka, 2009). The increased tendency of iPS cell-derived tissues to form tumors may be directly connected to the use of c-Myc in some protocols for generation of iPS cells. Retroviral introduction of c-Myc may result in tumor formation in even ~50% of chimeric mice generated from iPS cells (Okita et al., 2007). Although reprogramming methods exist that do not use c-Myc (Nakagawa et al., 2008; Wernig et al., 2008), they are less efficient, the reprogramming is protracted, and pluripotency is weakened (Yamanaka, 2009). Furthermore, the other three reprogramming factors may also cause tumors (Yamanaka, 2009), and they are often overexpressed in subset of cancer cells (Huang et al., 2011; Lengerke et al., 2011).

Senescence induction during reprogramming is another crucial aspect contributing to lowered efficiency of iPS production and culture, as well as playing pivotal role in CSC biology. Factors and processes involved in reprogramming evoke cellular senescence and therefore impair successful reprogramming to pluripotent stem cells (Banito et al., 2009). It has been shown that human iPS-derived early blood progenitor cells appear to undergo premature senescence (Feng et al., 2010). It was also suggested that in order to control the efficiency of iPS generation, senescence may be activated by tumor suppressors like p53 and p16(INK4a) (Banito and Gil, 2010).

CSC seem to behave in a distinct way. CSC found among MCF-7 breast cancer cells showed significantly reduced propensity to undergo senescence, which could be a result of increased telomerase activity and a low level of p21 protein. These cells also had a reduced level of reactive oxygen species, and more active DNA single-strand break repair pathway (Karimi-Busheri et al., 2010). Sabisz and Skladanowski (2009) observed in turn that A549 cells treated with DNA-damaging antitumor drugs revealed premature senescence; however, a small fraction of them (CSC) escaped from senescence and lead to regrowth of tumor cell population.

One of the most intriguing issues concerning iPS cells involves the fact that p53 may prevent pluripotency. It turns out that when p53 is damaged, or deleted from cell genome—cells more easily become iPS cells (Hong et al., 2009; Kawamura et al., 2009), and the generation of iPS cells may increase even up to 20% in cells without p53 (Hong et al., 2009). p53 loss mainly contributes to reprogramming by accelerating cell cycle progression (Hanna et al., 2009). To enhance the reprogramming of cells one may target

p53 pathway in a safer way, by carrying-out the process under hypoxic conditions (Bae et al., 2012; Yoshida et al., 2009) or in the presence of ascorbic acid (Esteban et al., 2010). Alternatively, inhibition of p53 is achieved by the increase of expression of SV40 large T antigen or Rem2 GTPase (Stadtfeld and Hochedlinger, 2010). However, both manipulations carry an increased risk of oncogenic transformation.

Undoubtedly loss of p53 plays also an important role in CSC biology. Several scientific groups reported that CSC derived from p53-null mice have a high tumor-initiating frequency (Zhang et al., 2008) and link the loss of p53 function to increased expression of CD44, which promotes expansion of tumor-initiating cells (Godar et al., 2008). These chapters suggest that loss of p53 permits expansion of presumptive CSC especially in mouse mammary tumors and in human breast cell lines. Suppression of CSC phenotype is an additional activity by which p53 can inhibit tumors.

CSC, as already mentioned, are often resistant to DNA damage inducers, and show greater DNA repair capacity than their non-stem-like counterparts (Bao et al., 2006). For example, CSC contribute to radioresistance of glioma cells through preferential activation of the DNA damage checkpoint response and an increase in DNA repair capacity. Tumor cells expressing CD133 (a marker for brain (cancer) stem cells) survived ionizing radiation and their fraction was enriched in gliomas following ionizing irradiation (Bao et al., 2006). However, human iPS cells exhibit hypersensitivity to DNA-damaging agents following gamma-irradiation, which results in rapid induction of apoptosis (Momcilovic et al., 2010). Expression of pluripotency factors in iPS cells did not appear to be diminished after irradiation (Momcilovic et al., 2010). Moreover, high degree of similarity in DNA damage responses between iPS cells and ES cells was found. After irradiation, similar to ES cells, iPS cells activated checkpoint signaling, evidenced by phosphorylation of ATM, NBS1, CHEK2, TP53, and localization of ATM to the double-strand breaks (Momcilovic et al., 2010).

Both CSC and iPS cells have altered cell cycle as compared to normal and stem cells. Experiments carried out by Ghule and coworkers revealed that human iPS cells have a short G1 phase and an abbreviated cell cycle (16–18 h). Furthermore, histone locus bodies are formed and reorganized shortly after mitosis within 1.5–2 h (Ghule et al., 2011). Other results suggest in turn that the expression of reprogramming factors increase the percentage of cells arrested in G1 without significant induction of apoptosis (Banito et al., 2009). It was also reported that exposure of iPS cells to

DNA-damaging agents results in arrest of cell cycle progression in the G2 phase and the population display high percentage of cells in S phase (Momcilovic et al., 2010).

CSC subpopulations of epithelial, breast, and prostate carcinoma are characterized by high proportion of cells in the G2 phase, which may suggest that they spend a consistently longer time in G2 (Harper et al., 2010). Longer G2 phase was also observed by Chappell and Dalton (2010) suggesting longer time for DNA repair in CSC.

Growing body of evidence collected mainly in the last three decades shows important role of epigenetic changes in carcinogenesis and cancer progression (Hellebrekers et al., 2007; Rius and Lyko, 2012). Low-resolution scanning of genomes of ES, iPS, and cancer cells revealed largely overlapping but not identical pattern of DNA methylation (Doi et al., 2009).

8. INTERACTION OF BIOMATERIALS WITH CELLS

Some earlier biomaterials tested in animals have caused higher incidence of oncogenic transformation within the surrounding tissues (Denishefsky et al., 1967). One possible mechanism responsible for such events is Ras pathway activation via the interaction of integrins (types β_1, $\alpha_V\beta_3$, or $\alpha_6\beta_4$) with their ligands and subsequent activation of Shc (Src homology 2 domain containing). Activated Shc in turn triggers the Ras/MAPK signaling cascade that then alters gene expression (Wary et al., 1996), sometimes leading to oncogenic transformation (see below). Therefore, we felt that a dedicated chapter covering interactions of biomaterials with cells is needed.

Due to pathologies or traumatic injuries, organs or tissues can lose their function. Thus, there is a large need for engineered replacements, including joints, heart valves, corneas, and intraocular lenses made from a number of different biomaterials (Binyamin et al., 2006; Hench, 1980). A biomaterial can be defined as any substance, synthetic or natural in origin, that is used to replace or restore function to a body tissue or organ, maybe continuously or intermittently in contact with body fluids, cells, and tissues, and can be divided into ceramics, polymers, metals, and composites (Binyamin et al., 2006). Initially, research focused on producing biomaterials that did not elicit a biological response from the host, that is, a bioinert material. By the 1980s a shift developed, where new biomaterials were designed to interact with the surrounding cells and tissues (Hench and Wilson, 1984). This include biomaterials that mimic the extracellular matrix (ECM) or release

soluble factors that influence activity of the surrounding cells (Hench and Thompson, 2010; Place et al., 2009).

Orthopedic replacements should be capable of supporting functional loading and for this reason, metal biomaterials are often used due to their excellent mechanical strength (Zreiqat et al., 2005). Titanium alloys (e.g. Ti-6Al-4V) are commonly used as bioinert metalic biomaterials (Zhao et al., 2012). In order to sustain functional loading, the implant should be anchored to the bone, through the actions of osteogenic cells. It was found that osteoblasts were able to adhere to titanium through production of ECM proteins that was absorbed onto the surface of titanium (Matsuura et al., 2000). The quantities of ECM proteins produced were, however, insufficient while some proteins were not produced at all, leading to inadequate bone anchorage. To improve the integration of implant into the bone, it has been attempted to alter the surface of metal biomaterials to combine the excellent mechanical features of metal biomaterials with a bioactive surface. Examples of bioactive surfaces include hydroxy-apatite, that is the main mineral component of normal bone, and Bioglass (Hench and Thompson, 2010; Zreiqat et al., 2005). Bioglass is a type of bioactive glass consisting of Na_2O, CaO, P_2O_5 and SiO_2. When Bioglass is implanted into bone tissue, an ion exchange between the Bioglass surface and the surrounding fluids initiates. This ion exchange leads to absorbance of Ca, PO_4, and CO_3 that later crystallize to form hydroxyl carbonate apatite. Surrounding osteoblasts will then integrate the newly formed Bioglass surface with the surrounding bone. Bioglass has been bound to the surface of titanium implants, where the Bioglass allows strong integration of the titanium-Bioglass implant (Hench and Thompson, 2010). The effects of different orthopedic or dental biomaterials on osteoblast function are presented in Table 5.4. In summary, both hydroxy apatite coating and Bioglass positively affect the bone integration of implants (Hench and Thompson, 2010; Zreiqat et al., 2005).

Bioactive surfaces have been investigated as a tool in tissue engineering, with much of the research being focused on mimicking the ECM. Biomaterials based on components of the ECM may direct differentiation of pluripotent stem cells toward different lineages (Table 5.5; Dickinson et al., 2011). Besides serving as structural support, the ECM provides biochemical and mechanical signals to the cells, mainly mediated by integrins, which helps control cell fate (Eshghi and Schaffer, 2008). Integrins are transmembrane proteins that serve to link the intracellular compartment with the ECM. Binding the ECM components vitronectin and fibronectin with

Table 5.4 Genes upregulated in osteoblasts in response to the surface of different biomaterials and their effects

Biomaterial	Protein/gene	Effect	References
Titanium alloy	Vinculin	Formation of focal adhesions leading to stronger cell adhesion to biomaterial	Räisänen et al. (2000)
	NDRG1	Marker of stress response	Zhao et al. (2012)
	TGFβI	Stimulates cell migration while inhibiting cell adhesion	
	Ferritin	Intracellular storage of iron. Upregulates pro-inflammatory mediators	
Hydroxy-apatite coating	β_1 integrin	Activates Shc in response to integrin-ECM binding	Zreiqat et al. (2005)
	Shc	Stimulates RAS/MAPK signaling	
Gold	Vinculin	Formation of focal adhesions leading to stronger cell adhesion	Räisänen et al. (2000)
	$\alpha_6\beta_4$ integrin	Activates Shc in response to integrin-ECM binding	
Bioglass	RCL	Initiates cell cycle	Xynos et al. (2000)
	Cyclin D	Causes progression from G1 phase to S phase of the mitosis	
	Cyclin K		
	CDKN1A		
	Insulin like growth factor II	Osteoblast homeostasis	
	VEGF	Enhances osteogenic differentiation of osteoblasts	
	β_1 Integrin	Activates Shc in response to ECM components	
	MAPK	Components of the MAPK signaling pathways, thus indicating activity of the MAPK signaling cascade	
	MAP2K		
	MAPK3		
	CD44	Marker of osteocytic differentiation	

Table 5.5 Differentiation of pluripotent stem cells in response to biomaterials coated with different ECM components

ECM component	Differentiation of pluripotent stem cells	References
Collagen I	Cardiomyogenic lineage	Sato et al. (2006)
Collagen IV	Hematopoietic cells Smooth muscle cells	Schenke-Layland et al. (2008)
Laminin	Neural cells Pancreatic islet cells	Dickinson et al. (2011)
Fibronectin	Mesodermal and ectodermal lineages	Dickinson et al. (2011)

integrins of the types β_1, $\alpha_V\beta_3$ or $\alpha_6\beta_4$ activates the cytosolic protein Shc resulting in activation of the Ras/MAPK signaling cascade that in turn alters gene expression (Wary et al., 1996). Integrins bind to small peptides in the ECM adhesive components, termed RGD (arginine–glycine–aspartic acid) (Ruoslahti and Pierschbacher, 1987). Using phosphonic acid groups as linker molecules, titanium may be covalently covered with RGD peptides. These peptides bind to $\alpha_V\beta_3$ integrins and engage the subsequent Ras/MAP signaling cascade, inducing adhesion of osteoblasts to the implant. These events also subsequently induce the proliferation of fibroblasts and osteogenic differentiation resulting in a strong incorporation of the implant into the surrounding bone (Auernheimer et al., 2005).

Despite the obvious advantages of using biomaterials, negative reactions have been noted. While traditional biomaterials strived to reach bioinertness, most of them do produce some biological foreign body response. Zhao et al. (2012) found that osteoblasts reacted to supposedly bioinert biomaterials like titanium alloys by an increased production of inflammatory proteins (Table 5.5). This manifested as formation of a fibrous cap that separated the implant from the surrounding tissues. Since the biomaterial and the fibrous cap do not adhere to each other, this severely weakens the ability of the implant to withstand mechanical loading (Hench, 1980).

During the 1950s and 1960s studies indicated that mice and rats that were implanted with solid materials including plastic, metals, and glass had a high risk of developing sarcoma (Denishefsky et al., 1967). The originator cells of the sarcoma were eventually isolated and identified as pericytes, which are pluripotent stem cells serving as progenitors of small blood vessels.

Development of a fibrous capsule surrounding the implant required neovascularization that is why the pericytes proliferated. Hyperplasia of the pericytes increases the risk of developing genetic errors, which could result in formation of precarcinogenous cells and eventually malignancies. Despite the findings in rodents, no human cases of foreign body-related cancers were known at that time (Brand, 1994). Newer studies focused on metals like cobalt, iron, nickel, and chromium that are released to the body by metal biomaterials like hip replacements, and can be found in liver, lymph nodes, and spleen (Case et al., 1994). Chromium ions pass the cell membranes through membrane anion transporters. In the cell, chromium is reduced and can form covalent interactions with the DNA, thereby causing double-strand DNA breaks (Singh et al., 1998). Thus chronic chromium exposure has been linked with an increased risk of malignancies (Parry et al., 2010; Tsaousi et al., 2010).

9. CLOSING REMARKS

The rapidly developing field of regenerative medicine will certainly revolutionize clinical handling of numerous diseases in not so distant future. In medicine and biomaterials science, there has been a paradigm shift from replacement to regeneration of tissues and organs, and consequently a shift from synthetic to natural-based biomaterials to enhance the interactions between the body and biomaterials. Therefore, it is critical to gain sufficient understanding about the nature and consequences of interactions between biomaterials introduced to the body and the induced biological responses. As outlined above, the focus of dedicated research has been mostly on an inflammatory reaction and possible carcinogenic effects of biomaterials. There is an urgent need to look into those interactions at a mechanistic level. For example, (i) how cell death and cell survival processes are affected by those interactions (Jain et al., 2013; Jangamreddy and Los, 2012; Maddika et al., 2007), (ii) if and how certain genetic markers may influence carcinogenic process in the vicinity of implanted biomaterials (Denishefsky et al., 1967; Wiechec, 2011; Wiechec et al., 2013), and (iii) what are the long-term effects of coexistence of biomaterial and cells. It is crucial to fully characterize iPS cells and explore complex relations between pluripotency reprogramming and carcinogenes before their use for therapeutic applications in humans. New generation of anticancer drugs that preferentially target CSC (Jangamreddy et al., 2013) may help decreasing the risk of transplant-induced malignancies.

ACKNOWLEDGMENTS

S. G. was supported by Parker B Francis fellowship in Respiratory Disease. A. C. P. acknowledges a fellowship from Integrative Regenerative Medicine Center (IGEN). M. J. L. kindly acknowledge the core/startup support from Linkoping University, from Integrative Regenerative Medicine Center (IGEN), from Cancerfonden (CAN 2013/391), and from VR-NanoVision (K2012-99X-22325-01-5).

REFERENCES

Abounit, K., Scarabelli, T.M., McCauley, R.B., 2012. Autophagy in mammalian cells. World J. Biol. Chem. 3, 1–6.

Armstrong, L., Tilgner, K., Saretzki, G., Atkinson, S.P., Stojkovic, M., Moreno, R., Przyborski, S., Lako, M., 2010. Human induced pluripotent stem cell lines show stress defense mechanisms and mitochondrial regulation similar to those of human embryonic stem cells. Stem Cells 28, 661–673.

Auernheimer, J., Zukowski, D., Dahmen, C., Kantlehehner, M., Enderle, A., Goodman, S.L., Kessler, H., 2005. Titanium implant materials with improved biocompatibility through coating with phosphonate-anchored cyclic RGD peptides. ChemBioChem 6, 2034–2040.

Bae, D., Mondragon-Teran, P., Hernandez, D., Ruban, L., Mason, C., Bhattacharya, S.S., Veraitch, F.S., 2012. Hypoxia enhances the generation of retinal progenitor cells from human induced pluripotent and embryonic stem cells. Stem Cells Dev. 21, 1344–1355.

Banito, A., Gil, J., 2010. Induced pluripotent stem cells and senescence: learning the biology to improve the technology. EMBO Rep. 11, 353–359.

Banito, A., Rashid, S.T., Acosta, J.C., Li, S., Pereira, C.F., Geti, I., Pinho, S., Silva, J.C., Azuara, V., Walsh, M., Vallier, L., Gil, J., 2009. Senescence impairs successful reprogramming to pluripotent stem cells. Genes Dev. 23, 2134–2139.

Bao, S., Wu, Q., McLendon, R.E., Hao, Y., Shi, Q., Hjelmeland, A.B., Dewhirst, M.W., Bigner, D.D., Rich, J.N., 2006. Glioma stem cells promote radioresistance by preferential activation of the DNA damage response. Nature 444, 756–760.

Bass, A.J., Watanabe, H., Mermel, C.H., Yu, S., Perner, S., Verhaak, R.G., Kim, S.Y., Wardwell, L., Tamayo, P., Gat-Viks, I., Ramos, A.H., Woo, M.S., Weir, B.A., Getz, G., Beroukhim, R., O'Kelly, M., Dutt, A., Rozenblatt-Rosen, O., Dziunycz, P., Komisarof, J., Chirieac, L.R., Lafargue, C.J., Scheble, V., Wilbertz, T., Ma, C., Rao, S., Nakagawa, H., Stairs, D.B., Lin, L., Giordano, T.J., Wagner, P., Minna, J.D., Gazdar, A.F., Zhu, C.Q., Brose, M.S., Cecconello, I., Jr, U.R., Marie, S.K., Dahl, O., Shivdasani, R.A., Tsao, M.S., Rubin, M.A., Wong, K.K., Regev, A., Hahn, W.C., Beer, D.G., Rustgi, A.K., Meyerson, M., 2009. SOX2 is an amplified lineage-survival oncogene in lung and esophageal squamous cell carcinomas. Nat. Genet. 41, 1238–1242.

Basu-Roy, U., Seo, E., Ramanathapuram, L., Rapp, T.B., Perry, J.A., Orkin, S.H., Mansukhani, A., Basilico, C., 2012. Sox2 maintains self renewal of tumor-initiating cells in osteosarcomas. Oncogene 31, 2270–2282.

Beier, D., Wischhusen, J., Dietmaier, W., Hau, P., Proescholdt, M., Brawanski, A., Bogdahn, U., Beier, C.P., 2008. CD133 expression and cancer stem cells predict prognosis in high-grade oligodendroglial tumors. Brain Pathol. 18, 370–377.

Ben-Porath, I., Thomson, M.W., Carey, V.J., Ge, R., Bell, G.W., Regev, A., Weinberg, R.A., 2008. An embryonic stem cell-like gene expression signature in poorly differentiated aggressive human tumors. Nat. Genet. 40, 499–507.

Binyamin, G., Shafi, B., Mery, C., 2006. Biomaterials: a primer for surgeons. Semin. Paediatr. Surg. 15, 276–283.

Bitarte, N., Bandres, E., Boni, V., Zarate, R., Rodriguez, J., Gonzalez-Huarriz, M., Lopez, I., Javier Sola, J., Alonso, M.M., Fortes, P., Garcia-Foncillas, J., 2011. MicroRNA-451 is involved in the self-renewal, tumorigenicity, and chemoresistance of colorectal cancer stem cells. Stem Cells 29, 1661–1671.

Booth, H.A., Holland, P.W., 2004. Eleven daughters of NANOG. Genomics 84, 229–238.

Brand, K.G., 1994. Do implanted medical devices cause cancer? J. Biomater. Appl. 8, 325–343.

Cantz, T., Key, G., Bleidissel, M., Gentile, L., Han, D.W., Brenne, A., Scholer, H.R., 2008. Absence of OCT4 expression in somatic tumor cell lines. Stem Cells 26, 692–697.

Cao, D., Liu, A., Wang, F., Allan, R.W., Mei, K., Peng, Y., Du, J., Guo, S., Abel, T.W., Lane, Z., Ma, J., Rodriguez, M., Akhi, S., Dehiya, N., Li, J., 2011. RNA-binding protein LIN28 is a marker for primary extragonadal germ cell tumors: an immunohistochemical study of 131 cases. Mod. Pathol. 24, 288–296.

Case, C.P., Langkamer, V.G., James, C., Palmer, M.R., Kemp, A.J., Heap, P.F., Solomon, L., 1994. Widespread Dissemination of Metal Debris from Implants. J. Bone Joint Surg. 76-B, 701–712.

Chappell, J., Dalton, S., 2010. Altered cell cycle regulation helps stem-like carcinoma cells resist apoptosis. BMC Biol. 8, 63.

Chen, Y.J., Wu, C.Y., Chang, C.C., Ma, C.J., Li, M.C., Chen, C.M., 2008. Nuclear Kruppel-like factor 4 expression is associated with human skin squamous cell carcinoma progression and metastasis. Cancer Biol. Ther. 7, 777–782.

Chen, T., Shen, L., Yu, J., Wan, H., Guo, A., Chen, J., Long, Y., Zhao, J., Pei, G., 2011. Rapamycin and other longevity-promoting compounds enhance the generation of mouse induced pluripotent stem cells. Aging Cell 10, 908–911.

Chen, S., Xu, Y., Chen, Y., Li, X., Mou, W., Wang, L., Liu, Y., Reisfeld, R.A., Xiang, R., Lv, D., Li, N., 2012. SOX2 gene regulates the transcriptional network of oncogenes and affects tumorigenesis of human lung cancer cells. PLoS One 7, e36326.

Chiou, S.H., Yu, C.C., Huang, C.Y., Lin, S.C., Liu, C.J., Tsai, T.H., Chou, S.H., Chien, C.S., Ku, H.H., Lo, J.F., 2008. Positive correlations of Oct-4 and Nanog in oral cancer stem-like cells and high-grade oral squamous cell carcinoma. Clin. Cancer Res. 14, 4085–4095.

Chylicki, K., Ehinger, M., Svedberg, H., Gullberg, U., 2000. Characterization of the molecular mechanisms for p53-mediated differentiation. Cell Growth Differ. 11, 561–571.

Cobaleda, C., 2010. Reprogramming of B cells. Methods Mol. Biol. 636, 233–250.

de Cremoux, P., Salomon, A.V., Liva, S., Dendale, R., Bouchind'homme, B., Martin, E., Sastre-Garau, X., Magdelenat, H., Fourquet, A., Soussi, T., 1999. p53 mutation as a genetic trait of typical medullary breast carcinoma. J. Natl. Cancer Inst. 91, 641–643.

Denishefsky, I., Oppenheimer, E.T., Heritier-Watkins, O., Bella, A., Willhite, M., 1967. Biochemical changes in the connective tissue pocket surrounding subcutaeously imbedded films. Cancer Res. 27, 833–837.

Dickinson, L.E., Kusuma, S., Gerecht, S., 2011. Reconstructing the differentiation niche of embryonic stem cells using biomaterials. Macromol. Rapid Commun. 11, 36–49.

Doi, A., Park, I.H., Wen, B., Murakami, P., Aryee, M.J., Irizarry, R., Herb, B., Ladd-Acosta, C., Rho, J., Loewer, S., Miller, J., Schlaeger, T., Daley, G.Q., Feinberg, A.P., 2009. Differential methylation of tissue- and cancer-specific CpG island shores distinguishes human induced pluripotent stem cells, embryonic stem cells and fibroblasts. Nat. Genet. 41, 1350–1353.

Eberhard, D., Jockusch, H., 2010. Clonal and territorial development of the pancreas as revealed by eGFP-labelled mouse chimeras. Cell Tissue Res. 342, 31–38.

Egler, R.A., Fernandes, E., Rothermund, K., Sereika, S., de Souza-Pinto, N., Jaruga, P., Dizdaroglu, M., Prochownik, E.V., 2005. Regulation of reactive oxygen species, DNA damage, and c-Myc function by peroxiredoxin 1. Oncogene 24, 8038–8050.

Eshghi, S., Schaffer, D.V., 2008. Engineering microenviroments to control stem cell fate and function. StemBook, 1–12.

Esteban, M.A., Wang, T., Qin, B., Yang, J., Qin, D., Cai, J., Li, W., Weng, Z., Chen, J., Ni, S., Chen, K., Li, Y., Liu, X., Xu, J., Zhang, S., Li, F., He, W., Labuda, K., Song, Y., Peterbauer, A., Wolbank, S., Redl, H., Zhong, M., Cai, D., Zeng, L., Pei, D., 2010. Vitamin C enhances the generation of mouse and human induced pluripotent stem cells. Cell Stem Cell 6, 71–79.

Evans, P.M., Liu, C., 2008. Roles of Krupel-like factor 4 in normal homeostasis, cancer and stem cells. Acta Biochim. Biophys. Sin. (Shanghai) 40, 554–564.

Fagin, J.A., Matsuo, K., Karmakar, A., Chen, D.L., Tang, S.H., Koeffler, H.P., 1993. High prevalence of mutations of the p53 gene in poorly differentiated human thyroid carcinomas. J. Clin. Invest. 91, 179–184.

Feinstein, E., Gale, R.P., Reed, J., Canaani, E., 1992. Expression of the normal p53 gene induces differentiation of K562 cells. Oncogene 7, 1853–1857.

Feng, Q., Lu, S.J., Klimanskaya, I., Gomes, I., Kim, D., Chung, Y., Honig, G.R., Kim, K.S., Lanza, R., 2010. Hemangioblastic derivatives from human induced pluripotent stem cells exhibit limited expansion and early senescence. Stem Cells 28, 704–712.

Feng, C., Neumeister, V., Ma, W., Xu, J., Lu, L., Bordeaux, J., Maihle, N.J., Rimm, D.L., Huang, Y., 2012. Lin28 regulates HER2 and promotes malignancy through multiple mechanisms. Cell Cycle (Georgetown, Tex.) 11, 2486–2494.

Fimia, G.M., Stoykova, A., Romagnoli, A., Giunta, L., Di Bartolomeo, S., Nardacci, R., Corazzari, M., Fuoco, C., Ucar, A., Schwartz, P., Gruss, P., Piacentini, M., Chowdhury, K., Cecconi, F., 2007. Ambra1 regulates autophagy and development of the nervous system. Nature 447, 1121–1125.

Fusaki, N., Ban, H., Nishiyama, A., Saeki, K., Hasegawa, M., 2009. Efficient induction of transgene-free human pluripotent stem cells using a vector based on Sendai virus, an RNA virus that does not integrate into the host genome. Proc. Jpn. Acad., Ser. B, Phys. Biol. Sci. 85, 348–362.

Galli, R., Binda, E., Orfanelli, U., Cipelletti, B., Gritti, A., De Vitis, S., Fiocco, R., Foroni, C., Dimeco, F., Vescovi, A., 2004. Isolation and characterization of tumorigenic, stem-like neural precursors from human glioblastoma. Cancer Res. 64, 7011–7021.

Ghavami, S., Eshragi, M., Ande, S.R., Chazin, W.J., Klonisch, T., Halayko, A.J., McNeill, K.D., Hashemi, M., Kerkhoff, C., Los, M., 2010. S100A8/A9 induces autophagy and apoptosis via ROS-mediated cross-talk between mitochondria and lysosomes that involves BNIP3. Cell Res. 20, 314–331.

Ghavami, S., Mutawe, M.M., Sharma, P., Yeganeh, B., McNeill, K.D., Klonisch, T., Unruh, H., Kashani, H.H., Schaafsma, D., Los, M., Halayko, A.J., 2011. Mevalonate cascade regulation of airway mesenchymal cell autophagy and apoptosis: a dual role for p53. PLoS One 6, e16523.

Ghavami, S., Cunnington, R.H., Yeganeh, B., Davies, J.J., Rattan, S.G., Bathe, K., Kavosh, M., Los, M.J., Freed, D.H., Klonisch, T., Pierce, G.N., Halayko, A.J., Dixon, I.M., 2012a. Autophagy regulates trans fatty acid-mediated apoptosis in primary cardiac myofibroblasts. Biochim. Biophys. Acta 1823, 2274–2286.

Ghavami, S., Mutawe, M.M., Schaafsma, D., Yeganeh, B., Unruh, H., Klonisch, T., Halayko, A.J., 2012b. Geranylgeranyl transferase 1 modulates autophagy and apoptosis in human airway smooth muscle. Am. J. Physiol. Lung Cell. Mol. Physiol. 302, L420–L428.

Ghule, P.N., Medina, R., Lengner, C.J., Mandeville, M., Qiao, M., Dominski, Z., Lian, J.B., Stein, J.L., van Wijnen, A.J., Stein, G.S., 2011. Reprogramming the pluripotent cell cycle: restoration of an abbreviated G1 phase in human induced pluripotent stem (iPS) cells. J. Cell. Physiol. 226, 1149–1156.

Girouard, S.D., Laga, A.C., Mihm, M.C., Scolyer, R.A., Thompson, J.F., Zhan, Q., Widlund, H.R., Lee, C.W., Murphy, G.F., 2012. SOX2 contributes to melanoma cell invasion. Lab. Invest. 92, 362–370.

Godar, S., Ince, T.A., Bell, G.W., Feldser, D., Donaher, J.L., Bergh, J., Liu, A., Miu, K., Watnick, R.S., Reinhardt, F., McAllister, S.S., Jacks, T., Weinberg, R.A., 2008. Growth-inhibitory and tumor-suppressive functions of p53 depend on its repression of CD44 expression. Cell 134, 62–73.

Gore, A., Li, Z., Fung, H.L., Young, J.E., Agarwal, S., Antosiewicz-Bourget, J., Canto, I., Giorgetti, A., Israel, M.A., Kiskinis, E., Lee, J.H., Loh, Y.H., Manos, P.D., Montserrat, N., Panopoulos, A.D., Ruiz, S., Wilbert, M.L., Yu, J., Kirkness, E.F., Izpisua Belmonte, J.C., Rossi, D.J., Thomson, J.A., Eggan, K., Daley, G.Q., Goldstein, L.S., Zhang, K., 2011. Somatic coding mutations in human induced pluripotent stem cells. Nature 471, 63–67.

Guo, X., Tang, Y., 2012. KLF4 translation level is associated with differentiation stage of different pediatric leukemias in both cell lines and primary samples. Clin. Exp. Med. 13, 99–107.

Guo, Y., Liu, S., Wang, P., Zhao, S., Wang, F., Bing, L., Zhang, Y., Ling, E.A., Gao, J., Hao, A., 2013. Expression profile of embryonic stem cell-associated genes Oct4, Sox2 and Nanog in human gliomas. Histopathology 59, 763–775.

Gustafsson, A.B., Gottlieb, R.A., 2009. Autophagy in ischemic heart disease. Circ. Res. 104, 150–158.

Hanada, T., Noda, N.N., Satomi, Y., Ichimura, Y., Fujioka, Y., Takao, T., Inagaki, F., Ohsumi, Y., 2007. The Atg12-Atg5 conjugate has a novel E3-like activity for protein lipidation in autophagy. J. Biol. Chem. 282, 37298–37302.

Hanley, J., Rastegarlari, G., Nathwani, A.C., 2010. An introduction to induced pluripotent stem cells. Br. J. Haematol. 151, 16–24.

Hanna, J., Saha, K., Pando, B., van Zon, J., Lengner, C.J., Creyghton, M.P., van Oudenaarden, A., Jaenisch, R., 2009. Direct cell reprogramming is a stochastic process amenable to acceleration. Nature 462, 595–601.

Harper, L.J., Costea, D.E., Gammon, L., Fazil, B., Biddle, A., Mackenzie, I.C., 2010. Normal and malignant epithelial cells with stem-like properties have an extended G2 cell cycle phase that is associated with apoptotic resistance. BMC Cancer 10, 166.

Hauff, K., Zamzow, C., Law, W.J., De Melo, J., Kennedy, K., Los, M., 2005. Peptide-based approaches to treat asthma, arthritis, other autoimmune diseases and pathologies of the central nervous system. Arch. Immunol. Ther. Exp. 53, 308–320.

Hellebrekers, D.M., Griffioen, A.W., van Engeland, M., 2007. Dual targeting of epigenetic therapy in cancer. Biochim. Biophys. Acta 1775, 76–91.

Hench, L., 1980. Biomaterials. Science 208, 826–831.

Hench, L., Thompson, I., 2010. Twenty-first century challenges for biomaterials. J. R. Soc. Interface. 7, 379–391.

Hench, L., Wilson, J., 1984. Surface-Active Biomaterials. Science 226, 630–636.

Hockemeyer, D., Soldner, F., Cook, E.G., Gao, Q., Mitalipova, M., Jaenisch, R., 2008. A drug-inducible system for direct reprogramming of human somatic cells to pluripotency. Cell Stem Cell 3, 346–353.

Hoffmeyer, K., Raggioli, A., Rudloff, S., Anton, R., Hierholzer, A., Del Valle, I., Hein, K., Vogt, R., Kemler, R., 2012. Wnt/beta-catenin signaling regulates telomerase in stem cells and cancer cells. Science 336, 1549–1554.

Hong, H., Takahashi, K., Ichisaka, T., Aoi, T., Kanagawa, O., Nakagawa, M., Okita, K., Yamanaka, S., 2009. Suppression of induced pluripotent stem cell generation by the p53-p21 pathway. Nature 460, 1132–1135.

Hotta, A., Ellis, J., 2008. Retroviral vector silencing during iPS cell induction: an epigenetic beacon that signals distinct pluripotent states. J. Cell. Biochem. 105, 940–948.

Hu, X., Ghisolfi, L., Keates, A.C., Zhang, J., Xiang, S., Lee, D.K., Li, C.J., 2012. Induction of cancer cell stemness by chemotherapy. Cell Cycle (Georgetown, Tex.) 11, 2691–2698.

Huang, P., Qiu, J., Li, B., Hong, J., Lu, C., Wang, L., Wang, J., Hu, Y., Jia, W., Yuan, Y., 2011. Role of Sox2 and Oct4 in predicting survival of hepatocellular carcinoma patients after hepatectomy. Clin. Biochem. 44, 582–589.

Jain, M.V., Paczulla, A.M., Klonisch, T., Dimgba, F.N., Rao, S.B., Roberg, K., Schweizer, F., Lengerke, C., Davoodpour, P., Palicharla, V.R., Maddika, S., Los, M., 2013. Interconnections between apoptotic, autophagic and necrotic pathways: implications for cancer therapy development. J. Cell. Mol. Med. 17, 12–29.

Jangamreddy, J.R., Los, M.J., 2012. Mitoptosis, a novel mitochondrial death mechanism leading predominantly to activation of autophagy. Hepat. Mon. 12, e6159.

Jangamreddy, J.R., Ghavami, S., Grabarek, J., Kratz, G., Wiechec, E., Fredriksson, B.A., Rao, R.K., Cieślar-Pobuda, A., Panigrahi, S., Los, M.J., 2013. Salinomycin induces activation of autophagy, mitophagy and affects mitochondrial polarity: differences between primary-, and cancer cells. Biochim. Biophys. Acta 1833, 2057–2069. http://dx.doi.org/10.1016/j.bbamcr.2013.04.011.

Jeter, C.R., Badeaux, M., Choy, G., Chandra, D., Patrawala, L., Liu, C., Calhoun-Davis, T., Zaehres, H., Daley, G.Q., Tang, D.G., 2009. Functional evidence that the self-renewal gene NANOG regulates human tumor development. Stem Cells 27, 993–1005.

Jia, F., Wilson, K.D., Sun, N., Gupta, D.M., Huang, M., Li, Z., Panetta, N.J., Chen, Z.Y., Robbins, R.C., Kay, M.A., Longaker, M.T., Wu, J.C., 2010. A nonviral minicircle vector for deriving human iPS cells. Nat. Methods 7, 197–199.

Jia, W., Pua, H.H., Li, Q.J., He, Y.W., 2011a. Autophagy regulates endoplasmic reticulum homeostasis and calcium mobilization in T lymphocytes. J. Immunol. 186, 1564–1574.

Jia, X., Li, X., Xu, Y., Zhang, S., Mou, W., Liu, Y., Lv, D., Liu, C.H., Tan, X., Xiang, R., Li, N., 2011b. SOX2 promotes tumorigenesis and increases the anti-apoptotic property of human prostate cancer cell. J. Mol. Cell Biol. 3, 230–238.

Junttila, M.R., Karnezis, A.N., Garcia, D., Madriles, F., Kortlever, R.M., Rostker, F., Brown Swigart, L., Pham, D.M., Seo, Y., Evan, G.I., Martins, C.P., 2010. Selective activation of p53-mediated tumour suppression in high-grade tumours. Nature 468, 567–571.

Kaji, K., Norrby, K., Paca, A., Mileikovsky, M., Mohseni, P., Woltjen, K., 2009. Virus-free induction of pluripotency and subsequent excision of reprogramming factors. Nature 458, 771–775.

Kang, R., Zeh, H.J., Lotze, M.T., Tang, D., 2011. The Beclin 1 network regulates autophagy and apoptosis. Cell Death Differ. 18, 571–580.

Karimi-Busheri, F., Rasouli-Nia, A., Mackey, J.R., Weinfeld, M., 2010. Senescence evasion by MCF-7 human breast tumor-initiating cells. Breast Cancer Res. 12, R31.

Kawamura, T., Suzuki, J., Wang, Y.V., Menendez, S., Morera, L.B., Raya, A., Wahl, G.M., Izpisua Belmonte, J.C., 2009. Linking the p53 tumour suppressor pathway to somatic cell reprogramming. Nature 460, 1140–1144.

Kharas, M.G., Yusuf, I., Scarfone, V.M., Yang, V.W., Segre, J.A., Huettner, C.S., Fruman, D.A., 2007. KLF4 suppresses transformation of pre-B cells by ABL oncogenes. Blood 109, 747–755.

Kim, D., Kim, C.H., Moon, J.I., Chung, Y.G., Chang, M.Y., Han, B.S., Ko, S., Yang, E., Cha, K.Y., Lanza, R., Kim, K.S., 2009a. Generation of human induced pluripotent stem cells by direct delivery of reprogramming proteins. Cell Stem Cell 4, 472–476.

Kim, J.B., Greber, B., Arauzo-Bravo, M.J., Meyer, J., Park, K.I., Zaehres, H., Scholer, H.R., 2009b. Direct reprogramming of human neural stem cells by OCT4. Nature 461, 649–653.

Kochhar, R., Howard, E.M., Umbreit, J.N., Lau, S.K., 2005. Metaplastic breast carcinoma with squamous differentiation: molecular and clinical analysis of six cases. Breast J. 11, 367–369.

Kumar, M.S., Erkeland, S.J., Pester, R.E., Chen, C.Y., Ebert, M.S., Sharp, P.A., Jacks, T., 2008. Suppression of non-small cell lung tumor development by the let-7 microRNA family. Proc. Natl. Acad. Sci. U.S.A. 105, 3903–3908.

Lafontan, M., 2008. Advances in adipose tissue metabolism. Int. J. Obes. (Lond) 32 (Suppl. 7), S39–S51.

Lee, Y., Jung, J., Cho, K.J., Lee, S.K., Park, J.W., Oh, I.H., Kim, G.J., 2013. Increased SCF/c-kit by hypoxia promotes autophagy of human placental chorionic plate-derived mesenchymal stem cells via regulating the phosphorylation of mTOR. J. Cell. Biochem. 114, 79–88.

Lefebvre, V., Dumitriu, B., Penzo-Mendez, A., Han, Y., Pallavi, B., 2007. Control of cell fate and differentiation by Sry-related high-mobility-group box (Sox) transcription factors. Int. J. Biochem. Cell Biol. 39, 2195–2214.

Lengerke, C., Fehm, T., Kurth, R., Neubauer, H., Scheble, V., Muller, F., Schneider, F., Petersen, K., Wallwiener, D., Kanz, L., Fend, F., Perner, S., Bareiss, P.M., Staebler, A., 2011. Expression of the embryonic stem cell marker SOX2 in early-stage breast carcinoma. BMC Cancer 11, 42.

Li, H., Collado, M., Villasante, A., Strati, K., Ortega, S., Canamero, M., Blasco, M.A., Serrano, M., 2009. The Ink4/Arf locus is a barrier for iPS cell reprogramming. Nature 460, 1136–1139.

Li, W., Zhou, H., Abujarour, R., Zhu, S., Young Joo, J., Lin, T., Hao, E., Schöler, H.R., Hayek, A., Ding, S., 2009b. Generation of human-induced pluripotent stem cells in the absence of exogenous Sox2. Stem Cells 27, 2992–3000. http://dx.doi.org/10.1002/stem.240.

Liu, Y., Clem, B., Zuba-Surma, E.K., El-Naggar, S., Telang, S., Jenson, A.B., Wang, Y., Shao, H., Ratajczak, M.Z., Chesney, J., Dean, D.C., 2009. Mouse fibroblasts lacking RB1 function form spheres and undergo reprogramming to a cancer stem cell phenotype. Cell Stem Cell 4, 336–347.

Liu, F., Lee, J.Y., Wei, H., Tanabe, O., Engel, J.D., Morrison, S.J., Guan, J.L., 2010. FIP200 is required for the cell-autonomous maintenance of fetal hematopoietic stem cells. Blood 116, 4806–4814.

Maddika, S., Ande, S.R., Panigrahi, S., Paranjothy, T., Weglarczyk, K., Zuse, A., Eshraghi, M., Manda, K.D., Wiechec, E., Los, M., 2007. Cell survival, cell death and cell cycle pathways are interconnected: implications for cancer therapy. Drug Resist. Updat. 10, 13–29.

Marchetto, M.C., Carromeu, C., Acab, A., Yu, D., Yeo, G.W., Mu, Y., Chen, G., Gage, F.H., Muotri, A.R., 2010. A model for neural development and treatment of Rett syndrome using human induced pluripotent stem cells. Cell 143, 527–539.

Marion, R.M., Strati, K., Li, H., Murga, M., Blanco, R., Ortega, S., Fernandez-Capetillo, O., Serrano, M., Blasco, M.A., 2009. A p53-mediated DNA damage response limits reprogramming to ensure iPS cell genomic integrity. Nature 460, 1149–1153.

Matsuoka, J., Yashiro, M., Sakurai, K., Kubo, N., Tanaka, H., Muguruma, K., Sawada, T., Ohira, M., Hirakawa, K., 2012. Role of the stemness factors sox2, oct3/4, and nanog in gastric carcinoma. J. Surg. Res. 174, 130–135.

Matsuura, T., Hosokawa, R., Okamoto, K., Kimoto, T., Akagawa, Y., 2000. Diverse mechanisms of osteoblast spreading on hydroxyappatit and titanium. Biomaterials 21, 1121–1127.

Menendez, S., Camus, S., Izpisua Belmonte, J.C., Menendez, S., Camus, S., Izpisua Belmonte, J.C., 2010. p53: guardian of reprogramming. Cell cycle (Georgetown, Tex.) 9, 3887–3891.

Menendez, J.A., Vellon, L., Oliveras-Ferraros, C., Cufi, S., Vazquez-Martin, A., 2011. mTOR-regulated senescence and autophagy during reprogramming of somatic cells to pluripotency: a roadmap from energy metabolism to stem cell renewal and aging. Cell cycle (Georgetown, Tex.) 10, 3658–3677.

Mikkelsen, T.S., Hanna, J., Zhang, X., Ku, M., Wernig, M., Schorderet, P., Bernstein, B.E., Jaenisch, R., Lander, E.S., Meissner, A., 2008. Dissecting direct reprogramming through integrative genomic analysis. Nature 454, 49–55.

Miller, L.D., Smeds, J., George, J., Vega, V.B., Vergara, L., Ploner, A., Pawitan, Y., Hall, P., Klaar, S., Liu, E.T., Bergh, J., 2005. An expression signature for p53 status in human breast cancer predicts mutation status, transcriptional effects, and patient survival. Proc. Natl. Acad. Sci. U.S.A. 102, 13550–13555.

Miura, K., Okada, Y., Aoi, T., Okada, A., Takahashi, K., Okita, K., Nakagawa, M., Koyanagi, M., Tanabe, K., Ohnuki, M., Ogawa, D., Ikeda, E., Okano, H., Yamanaka, S., 2009. Variation in the safety of induced pluripotent stem cell lines. Nat. Biotechnol. 27, 743–745.

Mizuno, H., Spike, B.T., Wahl, G.M., Levine, A.J., 2010. Inactivation of p53 in breast cancers correlates with stem cell transcriptional signatures. Proc. Natl. Acad. Sci. U.S.A. 107, 22745–22750.

Moawad, A.R., Choi, I., Zhu, J., Campbell, K.H., 2011. Ovine oocytes vitrified at germinal vesicle stage as cytoplast recipients for somatic cell nuclear transfer (SCNT). Cell Reprogram. 13, 289–296.

Momcilovic, O., Knobloch, L., Fornsaglio, J., Varum, S., Easley, C., Schatten, G., 2010. DNA damage responses in human induced pluripotent stem cells and embryonic stem cells. PLoS One 5, e13410.

Mortensen, M., Soilleux, E.J., Djordjevic, G., Tripp, R., Lutteropp, M., Sadighi-Akha, E., Stranks, A.J., Glanville, J., Knight, S., Jacobsen, S.E., Kranc, K.R., Simon, A.K., 2011. The autophagy protein Atg7 is essential for hematopoietic stem cell maintenance. J. Exp. Med. 208, 455–467.

Nadiminty, N., Tummala, R., Lou, W., Zhu, Y., Shi, X.B., Zou, J.X., Chen, H., Zhang, J., Chen, X., Luo, J., deVere White, R.W., Kung, H.J., Evans, C.P., Gao, A.C., 2012. MicroRNA let-7c is downregulated in prostate cancer and suppresses prostate cancer growth. PLoS One 7, e32832.

Nagata, T., Shimada, Y., Sekine, S., Hori, R., Matsui, K., Okumura, T., Sawada, S., Fukuoka, J., Tsukada, K., 2012. Prognostic significance of NANOG and KLF4 for breast cancer. Breast Cancer. [Epub ahead of print].

Nakagawa, M., Koyanagi, M., Tanabe, K., Takahashi, K., Ichisaka, T., Aoi, T., Okita, K., Mochiduki, Y., Takizawa, N., Yamanaka, S., 2008. Generation of induced pluripotent stem cells without Myc from mouse and human fibroblasts. Nat. Biotechnol. 26, 101–106.

Nakagawa, M., Takizawa, N., Narita, M., Ichisaka, T., Yamanaka, S., 2010. Promotion of direct reprogramming by transformation-deficient Myc. Proc. Natl. Acad. Sci. U.S.A. 107, 14152–14157.

Nakatogawa, H., Suzuki, K., Kamada, Y., Ohsumi, Y., 2009. Dynamics and diversity in autophagy mechanisms: lessons from yeast. Nat. Rev. Mol. Cell Biol. 10, 458–467.

Neumann, J., Bahr, F., Horst, D., Kriegl, L., Engel, J., Luque, R.M., Gerhard, M., Kirchner, T., Jung, A., 2011. SOX2 expression correlates with lymph-node metastases and distant spread in right-sided colon cancer. BMC Cancer 11, 518.

Okita, K., Yamanaka, S., 2011. Induced pluripotent stem cells: opportunities and challenges. Philos. Trans. R. Soc. Lond., B, Biol. Sci. 366, 2198–2207.

Okita, K., Ichisaka, T., Yamanaka, S., 2007. Generation of germline-competent induced pluripotent stem cells. Nature 448, 313–317.

Okita, K., Nakagawa, M., Hyenjong, H., Ichisaka, T., Yamanaka, S., 2008. Generation of mouse induced pluripotent stem cells without viral vectors. Science 322, 949–953.

Oliver, L., Hue, E., Priault, M., Vallette, F.M., 2012. Basal autophagy decreased during the differentiation of human adult mesenchymal stem cells. Stem Cells Dev. 21, 2779–2788.

Parry, M.C., Bhabra, G., Sood, A., Machado, F., Cartwright, L., Saunders, M., Ingham, E., Newson, R., Blom, A.W., Case, C.P., 2010. Thresholds for indirect DNA damage across cellular barriers for orthopaedic biomaterials. Biomaterials 31, 4477–4483.

Patel, M., Yang, S., 2010. Advances in reprogramming somatic cells to induced pluripotent stem cells. Stem Cell Rev. 6, 367–380.
Peng, S., Maihle, N.J., Huang, Y., 2010. Pluripotency factors Lin28 and Oct4 identify a subpopulation of stem cell-like cells in ovarian cancer. Oncogene 29, 2153–2159.
Place, E.S., Evans, N.D., Stevens, M.M., 2009. Complexity in Biomaterials for tissue engineering. Nat. Mater. 8, 457–470.
Plews, J.R., Li, J., Jones, M., Moore, H.D., Mason, C., Andrews, P.W., Na, J., 2010. Activation of pluripotency genes in human fibroblast cells by a novel mRNA based approach. PLoS One 5, e14397.
Prigione, A., Fauler, B., Lurz, R., Lehrach, H., Adjaye, J., 2010. The senescence-related mitochondrial/oxidative stress pathway is repressed in human induced pluripotent stem cells. Stem Cells 28, 721–733.
Räisänen, L., Könönen, M., Juhanoja, J., Varpavaara, P., Hautaniemi, J., Kivilahti, J., Hormia, M., 2000. Expression of cell adhesion complexes in epithelial cells seeded on biomaterial surfaces. J. Biomed. Mater. Res. 49, 79–87.
Ravikumar, B., Sarkar, S., Davies, J.E., Futter, M., Garcia-Arencibia, M., Green-Thompson, Z.W., Jimenez-Sanchez, M., Korolchuk, V.I., Lichtenberg, M., Luo, S., Massey, D.C., Menzies, F.M., Moreau, K., Narayanan, U., Renna, M., Siddiqi, F.H., Underwood, B.R., Winslow, A.R., Rubinsztein, D.C., 2010. Regulation of mammalian autophagy in physiology and pathophysiology. Physiol. Rev. 90, 1383–1435.
Reya, T., Morrison, S.J., Clarke, M.F., Weissman, I.L., 2001. Stem cells, cancer, and cancer stem cells. Nature 414, 105–111.
Ribatti, D., 2012. Cancer stem cells and tumor angiogenesis. Cancer Lett. 321, 13–17.
Rius, M., Lyko, F., 2012. Epigenetic cancer therapy: rationales, targets and drugs. Oncogene 31, 4257–4265.
Rotter, D., Rothermel, B.A., 2012. Targets, trafficking, and timing of cardiac autophagy. Pharmacol. Res. 66, 494–504.
Rowland, B.D., Bernards, R., Peeper, D.S., 2005. The KLF4 tumour suppressor is a transcriptional repressor of p53 that acts as a context-dependent oncogene. Nat. Cell Biol. 7, 1074–1082.
Rubinsztein, D.C., Cuervo, A.M., Ravikumar, B., Sarkar, S., Korolchuk, V., Kaushik, S., Klionsky, D.J., 2009. In search of an "autophagomometer" Autophagy 5, 585–589.
Ruoslahti, E., Pierschbacher, M.D., 1987. New perspectives in cell adhesion: RGD and integrins. Science 238, 491–497.
Sabisz, M., Skladanowski, A., 2009. Cancer stem cells and escape from drug-induced premature senescence in human lung tumor cells: implications for drug resistance and in vitro drug screening models. Cell cycle (Georgetown, Tex.) 8, 3208–3217.
Saigusa, S., Tanaka, K., Toiyama, Y., Yokoe, T., Okugawa, Y., Ioue, Y., Miki, C., Kusunoki, M., 2009. Correlation of CD133, OCT4, and SOX2 in rectal cancer and their association with distant recurrence after chemoradiotherapy. Ann. Surg. Oncol. 16, 3488–3498.
Salemi, S., Yousefi, S., Constantinescu, M.A., Fey, M.F., Simon, H.U., 2012. Autophagy is required for self-renewal and differentiation of adult human stem cells. Cell Res. 22, 432–435.
Sato, H., Takahashi, M., Ise, H., Yamada, A., Hirose, S.-i., Tagawa, Y.-i., Morimoto, H., Izawa, A., Ikeda, U., 2006. Collagen synthesis is require for ascorbic acid-enhanced differentiation of mouse embryonic stem cells into cardiomyocytes. Biochem. Biophys. Res. Commun. 342, 107–112.
Schenke-Layland, K., Rhodes, K.E., Angelis, E., Butylkova, Y., Heydarkhan-Hagvall, S., Gekas, C., Zhang, R., Goldhaber, J.I., Mikkola, H.K., Plath, K., Robb, M.W., 2008. Reprgrammed mouse fibroblasts differentiate into cells of the cardiovascular and hematopoietic lineages. Stem Cells 26, 1537–1546.
Shan, J., Shen, J., Liu, L., Xia, F., Xu, C., Duan, G., Xu, Y., Ma, Q., Yang, Z., Zhang, Q., Ma, L., Liu, J., Xu, S., Yan, X., Bie, P., Cui, Y., Bian, X.W., Qian, C., 2012. Nanog

regulates self-renewal of cancer stem cell through IGF pathway in human hepatocellular carcinoma. Hepatology 56, 1004–1014.
Singh, R., Cuervo, A.M., 2011. Autophagy in the cellular energetic balance. Cell Metab. 13, 495–504.
Singh, J., Carlisle, D.L., Pritchard, D.E., Patierno, S.R., 1998. Chromium-induced genotoxicity and apoptosis: relationship to chromium carcinogenesis (review). Oncol. Rep. 5, 1307–1325.
Sommer, C.A., Stadtfeld, M., Murphy, G.J., Hochedlinger, K., Kotton, D.N., Mostoslavsky, G., 2009. Induced pluripotent stem cell generation using a single lentiviral stem cell cassette. Stem Cells 27, 543–549.
Sridharan, R., Tchieu, J., Mason, M.J., Yachechko, R., Kuoy, E., Horvath, S., Zhou, Q., Plath, K., 2009. Role of the murine reprogramming factors in the induction of pluripotency. Cell 136, 364–377.
Stadtfeld, M., Hochedlinger, K., 2010. Induced pluripotency: history, mechanisms, and applications. Genes Dev. 24, 2239–2263.
Stolzenburg, S., Rots, M.G., Beltran, A.S., Rivenbark, A.G., Yuan, X., Qian, H., Strahl, B.D., Blancafort, P., 2012. Targeted silencing of the oncogenic transcription factor SOX2 in breast cancer. Nucleic Acids Res. 40, 6725–6740.
Suhr, S.T., Chang, E.A., Tjong, J., Alcasid, N., Perkins, G.A., Goissis, M.D., Ellisman, M.H., Perez, G.I., Cibelli, J.B., 2010. Mitochondrial rejuvenation after induced pluripotency. PLoS One 5, e14095.
Suo, G., Han, J., Wang, X., Zhang, J., Zhao, Y., Dai, J., 2005. Oct4 pseudogenes are transcribed in cancers. Biochem. Biophys. Res. Commun. 337, 1047–1051.
Takahashi, K., Yamanaka, S., 2006. Induction of pluripotent stem cells from mouse embryonic and adult fibroblast cultures by defined factors. Cell 126, 663–676.
Tirino, V., Desiderio, V., d'Aquino, R., De Francesco, F., Pirozzi, G., Graziano, A., Galderisi, U., Cavaliere, C., De Rosa, A., Papaccio, G., Giordano, A., 2008. Detection and characterization of CD133+ cancer stem cells in human solid tumours. PLoS One 3, e3469.
Tsai, L.L., Yu, C.C., Chang, Y.C., Yu, C.H., Chou, M.Y., 2011. Markedly increased Oct4 and Nanog expression correlates with cisplatin resistance in oral squamous cell carcinoma. J. Oral Pathol. Med. 40, 621–628.
Tsaousi, A., Jones, E., Case, C.P., 2010. The in vitro genotoxicity of orthopaedic ceramic (Al2O3) and metal (CoCr alloy) particles. Mutat. Res. 697, 1–9.
Uchino, K., Hirano, G., Hirahashi, M., Isobe, T., Shirakawa, T., Kusaba, H., Baba, E., Tsuneyoshi, M., Akashi, K., 2012. Human Nanog pseudogene8 promotes the proliferation of gastrointestinal cancer cells. Exp. Cell Res. 318, 1799–1807.
Vafa, O., Wade, M., Kern, S., Beeche, M., Pandita, T.K., Hampton, G.M., Wahl, G.M., 2002. c-Myc can induce DNA damage, increase reactive oxygen species, and mitigate p53 function: a mechanism for oncogene-induced genetic instability. Mol. Cell 9, 1031–1044.
van den Berg, A., Mols, J., Han, J., 2008. RISC-target interaction: cleavage and translational suppression. Biochim. Biophys. Acta 1779, 668–677.
van Tuyn, J., Pijnappels, D.A., de Vries, A.A., de Vries, I., van der Velde-van Dijke, I., Knaan-Shanzer, S., van der Laarse, A., Schalij, M.J., Atsma, D.E., 2007. Fibroblasts from human postmyocardial infarction scars acquire properties of cardiomyocytes after transduction with a recombinant myocardin gene. FASEB J. 21, 3369–3379.
Vazquez, P., Arroba, A.I., Cecconi, F., de la Rosa, E.J., Boya, P., de Pablo, F., 2012. Atg5 and Ambra1 differentially modulate neurogenesis in neural stem cells. Autophagy 8, 187–199.
Vessoni, A.T., Muotri, A.R., Okamoto, O.K., 2012. Autophagy in stem cell maintenance and differentiation. Stem Cells Dev. 21, 513–520.

Vierbuchen, T., Ostermeier, A., Pang, Z.P., Kokubu, Y., Sudhof, T.C., Wernig, M., 2010. Direct conversion of fibroblasts to functional neurons by defined factors. Nature 463, 1035–1041.
Vincent, F.C., Los, M.J., 2011. New potential instrument to fight hepatocellular cancer by restoring p53. Hepat. Mon. 11, 331–332.
Viswanathan, S.R., Daley, G.Q., Gregory, R.I., 2008. Selective blockade of microRNA processing by Lin28. Science 320, 97–100.
Viswanathan, S.R., Powers, J.T., Einhorn, W., Hoshida, Y., Ng, T.L., Toffanin, S., O'Sullivan, M., Lu, J., Phillips, L.A., Lockhart, V.L., Shah, S.P., Tanwar, P.S., Mermel, C.H., Beroukhim, R., Azam, M., Teixeira, J., Meyerson, M., Hughes, T.P., Llovet, J.M., Radich, J., Mullighan, C.G., Golub, T.R., Sorensen, P.H., Daley, G.Q., 2009. Lin28 promotes transformation and is associated with advanced human malignancies. Nat. Genet. 41, 843–848.
Wang, X., Liang, Y., Chen, Q., Xu, H.M., Ge, N., Luo, R.Z., Shao, J.Y., He, Z., Zeng, Y.X., Kang, T., Yun, J.P., Xie, F., 2012. Prognostic significance of SOX2 expression in nasopharyngeal carcinoma. Cancer Invest. 30, 79–85.
Warren, L., Manos, P.D., Ahfeldt, T., Loh, Y.H., Li, H., Lau, F., Ebina, W., Mandal, P.K., Smith, Z.D., Meissner, A., Daley, G.Q., Brack, A.S., Collins, J.J., Cowan, C., Schlaeger, T.M., Rossi, D.J., 2010. Highly efficient reprogramming to pluripotency and directed differentiation of human cells with synthetic modified mRNA. Cell Stem Cell 7, 618–630.
Wary, K.K., Mainiero, F., Isakoff, S.J., Marcantonio, E.E., Giancotti, F.G., 1996. The adaptor protein Shc couples a class of integrins to the control of cell cycle progression. Cell 87, 733–743.
Wernig, M., Meissner, A., Cassady, J.P., Jaenisch, R., 2008. c-Myc is dispensable for direct reprogramming of mouse fibroblasts. Cell Stem Cell 2, 10–12.
West, J.A., Viswanathan, S.R., Yabuuchi, A., Cunniff, K., Takeuchi, A., Park, I.H., Sero, J.E., Zhu, H., Perez-Atayde, A., Frazier, A.L., Surani, M.A., Daley, G.Q., 2009. A role for Lin28 in primordial germ-cell development and germ-cell malignancy. Nature 460, 909–913.
Wiechec, E., 2011. Implications of genomic instability in the diagnosis and treatment of breast cancer. Expert Rev. Mol. Diagn. 11, 445–453.
Wiechec, E., Overgaard, J., Kjeldsen, E., Hansen, L.L., 2013. Chromosome 1q25.3 copy number alterations in primary breast cancers detected by multiplex ligation-dependent probe amplification and allelic imbalance assays and its comparison with fluorescent in situ hybridization assays. Cell. Oncol. (Dordr.) 36, 113–120.
Wilmut, I., Schnieke, A.E., McWhir, J., Kind, A.J., Campbell, K.H., 1997. Viable offspring derived from fetal and adult mammalian cells. Nature 385, 810–813.
Woltjen, K., Michael, I.P., Mohseni, P., Desai, R., Mileikovsky, M., Hamalainen, R., Cowling, R., Wang, W., Liu, P., Gertsenstein, M., Kaji, K., Sung, H.K., Nagy, A., 2009. piggyBac transposition reprograms fibroblasts to induced pluripotent stem cells. Nature 458, 766–770.
Wu, Y.T., Tan, H.L., Shui, G., Bauvy, C., Huang, Q., Wenk, M.R., Ong, C.N., Codogno, P., Shen, H.M., 2010. Dual role of 3-methyladenine in modulation of autophagy via different temporal patterns of inhibition on class I and III phosphoinositide 3-kinase. J. Biol. Chem. 285, 10850–10861.
Xynos, I.D., Edgar, A.J., Buttery, L.D.K., Hench, L., Polak, J.M., 2000. Gene-expression profiling of human osteoblasts following treatment with the ionic products of Bioglass 45S5 dissolution. J. Biomed. Mater. Res. 55, 151–157.
Yamanaka, S., 2009. A fresh look at iPS cells. Cell 137, 13–17.
Yang, S., Zheng, J., Ma, Y., Zhu, H., Xu, T., Dong, K., Xiao, X., 2012. Oct4 and Sox2 are overexpressed in human neuroblastoma and inhibited by chemotherapy. Oncol. Rep. 28, 186–192.

Yoshida, Y., Takahashi, K., Okita, K., Ichisaka, T., Yamanaka, S., 2009. Hypoxia enhances the generation of induced pluripotent stem cells. Cell Stem Cell 5, 237–241.
Yoshimori, T., 2004. Autophagy as a bulk protein degradation system: it plays various roles. Tanpakushitsu kakusan koso 49, 1029–1032.
Yu, J., Hu, K., Smuga-Otto, K., Tian, S., Stewart, R., Slukvin, I.I., Thomson, J.A., 2009. Human induced pluripotent stem cells free of vector and transgene sequences. Science 324, 797–801.
Zbinden, M., Duquet, A., Lorente-Trigos, A., Ngwabyt, S.N., Borges, I., Ruiz i Altaba, A., 2010. NANOG regulates glioma stem cells and is essential in vivo acting in a cross-functional network with GLI1 and p53. EMBO J. 29, 2659–2674.
Zhang, W., Geiman, D.E., Shields, J.M., Dang, D.T., Mahatan, C.S., Kaestner, K.H., Biggs, J.R., Kraft, A.S., Yang, V.W., 2000. The gut-enriched Kruppel-like factor (Kruppel-like factor 4) mediates the transactivating effect of p53 on the p21WAF1/Cip1 promoter. J. Biol. Chem. 275, 18391–18398.
Zhang, J., Wang, X., Li, M., Han, J., Chen, B., Wang, B., Dai, J., 2006. NANOGP8 is a retrogene expressed in cancers. FEBS J. 273, 1723–1730.
Zhang, M., Behbod, F., Atkinson, R.L., Landis, M.D., Kittrell, F., Edwards, D., Medina, D., Tsimelzon, A., Hilsenbeck, S., Green, J.E., Michalowska, A.M., Rosen, J.M., 2008. Identification of tumor-initiating cells in a p53-null mouse model of breast cancer. Cancer Res. 68, 4674–4682.
Zhang, N., Zhang, J., Shuai, L., Zha, L., He, M., Huang, Z., Wang, Z., 2012a. Kruppel-like factor 4 negatively regulates beta-catenin expression and inhibits the proliferation, invasion and metastasis of gastric cancer. Int. J. Oncol. 40, 2038–2048.
Zhang, Q., Yang, Y.J., Wang, H., Dong, Q.T., Wang, T.J., Qian, H.Y., Xu, H., 2012b. Autophagy activation: a novel mechanism of atorvastatin to protect mesenchymal stem cells from hypoxia and serum deprivation via AMP-activated protein kinase/mammalian target of rapamycin pathway. Stem Cells Dev. 21, 1321–1332.
Zhao, M., An, M., Wang, Q., Liu, X., Lai, W., Zhao, X., Wei, S., Ji, J., 2012. Quantitative proteomic analysis of human osteoblast-like MG-63 cells in response to bioinert implant material titanium and polyetheretherketone. J. Proteome 75, 3560–3573.
Zheng, H., Ying, H., Yan, H., Kimmelman, A.C., Hiller, D.J., Chen, A.J., Perry, S.R., Tonon, G., Chu, G.C., Ding, Z., Stommel, J.M., Dunn, K.L., Wiedemeyer, R., You, M.J., Brennan, C., Wang, Y.A., Ligon, K.L., Wong, W.H., Chin, L., DePinho, R.A., 2008. p53 and Pten control neural and glioma stem/progenitor cell renewal and differentiation. Nature 455, 1129–1133.
Zhou, L., Wei, X., Cheng, L., Tian, J., Jiang, J.J., 2007. CD133, one of the markers of cancer stem cells in Hep-2 cell line. Laryngoscope 117, 455–460.
Zreiqat, H., Valenzuela, S.M., Nissan, B.B., Roecst, R., Knabe, C., Radlanski, R.J., Renz, H., Evans, P.J., 2005. The effect of surface chemistry modification of titanium alloy on signalling pathways in human osteoblasts. Biomaterials 26, 7579–7586.

CHAPTER SIX

New Insights into Functions, Regulation, and Pathological Roles of Tight Junctions in Kidney Tubular Epithelium

Katalin Szaszi[*,†,1], **Yasaman Amoozadeh**[*,†]
[*]Keenan Research Center for Biomedical Science, St. Michael's Hospital, Toronto, Ontario, Canada
[†]Department of Surgery, University of Toronto, Toronto, Ontario, Canada
[1]Corresponding author: e-mail address: szaszik@smh.ca

Contents

Abstract

Epithelial tight junctions (TJs) seal off the intercellular space to generate a paracellular barrier as well as a selective transport pathway. They also maintain apicobasal polarization of cells. In addition, TJs serve as signaling platforms that orchestrate many epithelial

International Review of Cell and Molecular Biology, Volume 308
ISSN 1937-6448
http://dx.doi.org/10.1016/B978-0-12-800097-7.00006-3

functions. The past years have brought about a remarkable increase in our understanding of the structure and function of TJs. The overall aim of this review is to provide an update on this new knowledge, with special emphasis on TJs in the kidney tubular epithelium. TJs are key determinants of tubular transport processes, contributing to ion and fluid homeostasis. They are also central organizers of the structure of the tubular epithelium and many aspects of tubular cell functions, beyond transport processes. Many pathological states in the kidney, including inflammation, acute kidney injury, and chronic progressive diseases affect the tubular TJs, with important consequences with regards to the pathogenesis and pathophysiology of various nephropathies. In fact, altered TJ structure and function are increasingly recognized as a key step in the generation of renal diseases. In this review, we provide an overview of the protein composition, function and regulation of TJs in the kidney tubules, as well as their involvement and role in diseases.

1. INTRODUCTION

The tubular epithelium is well adapted for efficient transport of large volumes of water, ions, and substances. This function adjusts the composition of the primary filtrate generated by the glomeruli, and is vital for ion and fluid homeostasis. Two fundamental characteristics allow the epithelium to perform these tasks. First, the layer generates a permeability barrier that blocks passive movement of substances both through the cells and the intercellular space, which is sealed off by junctional complexes. Second, epithelial cells contain highly regulated specialized transport pathways. Key to the directional transport processes is the high degree of apicobasal polarity of the cells, that have distinct apical (facing the lumen), lateral (facing the neighboring cell), and basal (facing the renal tissue) sides. Whereas the apical and lateral membranes are divided by the intercellular junctions, components of the basal and lateral membranes can freely mix, and the whole area is referred to as the basolateral membrane. The apical and basolateral membranes have unique lipid and protein compositions and functions, including differential expression of transport proteins (Fig. 6.1A). The overall permeability of an epithelial layer is determined by the combined function of all transcellular and paracellular transport proteins. Transcellular transport is achieved by the coordinated action of transport proteins localized at the apical and basolateral sides. Importantly, the differential expression of transporters at these two sides is the basis for vectorial transport (Fig. 6.1A) (Nelson, 2003). In contrast, the paracellular pathway allows only selective passive transport of ions, water, and small solutes. The electrochemical

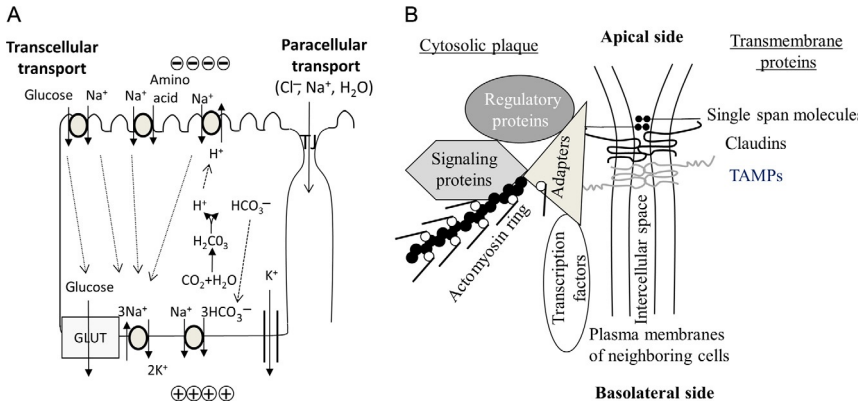

Figure 6.1 (A) Simplified scheme of directional NaCl transport in the proximal tubules. This example illustrates how the differential localization of transport proteins can mediate vectorial transcellular transport. Transcellular transport generates a transepithelial electrical and chemical driving force for paracellular transport. Please note that for the sake of clarity not all transporter types expressed in the cells are shown. (B) Overview of types of proteins at the TJs. The transcellular proteins bind to adapters that connect them to the actomyosin ring. Adapters also bind various regulatory proteins involved in the regulation of TJs, and also localize signaling intermediates and TJ-regulated transcription factors.

gradient that drives paracellular transport is generated by the transcellular transport processes (Tsukita and Furuse, 2000). The tubular epithelium is an excellent example of this general principle. The barrier and permeability properties of the layer show large variations in distinct segments which correlates with the overall transport functions of the specific segment. The intercellular junctions and specifically the tight junctions (TJs) fundamentally determine epithelial characteristics through their effects on cell polarity and paracellular transport (Hartsock and Nelson, 2008). In the past years, our understanding of the TJs has significantly increased. This review provides an overview of the exciting new knowledge of the structure, protein components, functions and regulation of TJs, with special focus on the tubular epithelium.

The four types of intercellular junctions that connect epithelial cells are the TJs, adheres junctions (AJs), desmosomes, and gap junctions (Anderson and Van Itallie, 2009; Delva et al., 2009; Rudini and Dejana, 2008; Sohl and Willecke, 2004). These multiprotein complexes can be distinguished based on their composition and functions, although there is some degree of

overlap. TJs, AJs, and desmosomes show similar principle organization: all three contain unique transmembrane and associated cytosolic proteins that are linked to the cytoskeleton. The TJs and AJs interact with actomyosin structures, while the desmosomes are anchored to the intermediate filaments. The focus of this review is the TJ, the apical–most junctional complex. These structures are responsible for the permeability barrier and paracellular pathway and also contribute to apicobasal polarity. We discuss these "classic" gate and fence functions in Section 2.2.

The major function of the AJs and the desmosomes is to generate cell–cell adhesion and resistance against mechanical forces (Delva et al., 2009; Rudini and Dejana, 2008). Both structures contain integral membrane proteins belonging to the cadherin family: epithelial AJs express classical cadherins (predominantly E-cadherin), while desmosomes have desmosomal cadherins. These complexes form Ca^{2+}-dependent bridges between neighboring cells that organize and maintain the epithelial monolayer. The gap junctions differ from the other three complexes. The connexins that make up these junctions form hydrophilic ion channels that directly connect the cytoplasm of neighboring cells. Such a connection allows rapid communication between cells to organize coordinated fast responses of the whole monolayer.

Importantly, the AJs, TJs, and desmosomes also act as signaling hubs that relay information from the environment to modify and organize vital cellular functions. Although this role was first recognized in the case of the AJs, the TJs are now emerging as regulators of epithelial growth, differentiation and motility. These "nonclassical functions" will be the topic of Section 3. The junctional complexes also affect each other. For example, the formation and maintenance of the AJs and TJs are interconnected, and so are some of their signaling functions. Thus, although we focus on the TJs, it is important to note the existence of functional overlaps, especially when functions cannot be clearly separated.

A number of well-established and commercially available tubular cell lines have been used to obtain insights into the general properties of TJs. Various lines that originate from different parts of the tubules are also invaluable tools for exploring the cell biology and physiology of specific segments of the tubules (Bens and Vandewalle, 2008; Prozialeck et al., 2006). However, care should be taken, as most cell lines show somewhat mixed phenotypes. The most widely used tubular lines include several proximal tubule-like cells such as the Lilly Laboratories cell porcine kidney 1 ($LLC\text{-}PK_1$), the opossum kidney (OK) and the human kidney-2 cells, the

distal tubule-like Madin–Darby canine kidney (MDCK) and the inner medullary collective duct cells. Under the right culture conditions, these cell lines can form well-polarized layers with mature TJs. The MDCK cells are particularly favored models of polarized epithelial cells, and a large portion of our knowledge on polarized traffic and junctions was obtained using this cell line. It is important to note that many cell lines were established decades ago and by now several subtypes have developed, with differences in their permeability properties and expression of junctional proteins (e.g., Dukes et al., 2011). These differences are not always recognized, but might explain some inconsistencies between studies. Nevertheless, experiments using overexpression or knockdown of the TJ protein of interest in cell lines followed by functional assessments played a key role in developing our current models of the TJs.

2. STRUCTURE AND FUNCTION OF TJs

2.1. Morphology of TJs

TJs (zonula occludens (ZO)) are present in all epithelial and endothelial cells. They are located apically from the other three junctions and form a belt-like structure that circumscribes the cell. Various early studies provided detailed description of the intriguing morphology of the TJs decades before their molecular components were identified. Transmission electron microscopy revealed that the membranes of two neighboring cells form direct contact points at the TJs, which were referred to as "kissing points" (Farquhar and Palade, 1963). In these areas, the membranes of the adjacent cells seem to fuse to seal off the intercellular space. More detailed pictures obtained using freeze fracture electron microscopy showed the TJs as anastomozing continuous fibrils found on the cytoplasmic leaflet with corresponding grooves on the exoplasmic leaflet (Staehelin, 1973, 1974). These fibrils are referred to as the TJ strands. They form a net-like meshwork composed of particles within the membrane that encircles the cell. Interestingly, these early studies also revealed large variations in the morphology and complexity of the TJ strands found in different epithelial cells. Most notably, in some cells the TJs show up not as fibrils, but as discontinuous particles (Claude and Goodenough, 1973). Based on systematic comparisons between the TJ morphology and the properties of transepithelial transport in different epithelial layers, Claude proposed a logarithmic correlation between the TJ strand number and the electrical resistance (Claude, 1978). Indeed, in many epithelial cells, more complex strands were associated with increased

resistance and lower permeability. However, many examples were also uncovered where resistance did not correlate well with the number of TJ strands. We now know that permeability best correlates with the properties of the proteins in the strands. The molecular basis of the described structure and the identity of the strand-forming proteins however remained unknown for several more years. The first TJ proteins identified during the 1980s were not transmembrane but cytoplasmic proteins (Tsukita and Furuse, 1998). The real breakthrough in our understanding of the TJs came with the discovery of the integral membrane components of the TJs. The first such protein, occludin, was identified by the group of Shoichiro Tsukita 20 years ago (Furuse et al., 1993). This was followed by the discovery of the first two claudins, claudin-1 and -2, by the same group (Furuse et al., 1998a). These seminal discoveries indeed revolutionized the field of TJ research and started us on a path toward real understanding of the TJs. Since then, the number of identified TJ proteins has increased significantly (Furuse, 2010; Schneeberger and Lynch, 2004). In the next sections, we first provide a brief overview of TJ functions followed by a description of the major TJ-associated proteins.

2.2. Classic functions of TJs: gate and fence

TJs generate a permeability barrier and maintain the polarization of the epithelia. These two functions are referred to as "gate and fence."

2.2.1 Gate function

The TJs have a dual role in permeability: they seal off the intercellular space to generate a permeability barrier between the two sides of the epithelial layer, but at the same time also create a selective pathway that allows passage of some ions and solutes (Shen et al., 2011). Segments of the tubular epithelium show large variations in their permeability due to two major factors. First, plasma membrane transporters catalyzing transcellular transport differ in the various segments, resulting in differences in transcellular transport and the generated electrochemical driving forces. Second, there are also large variations in the TJ gate properties in different tubular segments.

In various epithelial layers, the paracellular pathway exhibits unique characteristics that are specific for the given epithelium. Thus, differences can be observed in overall permeability, ion selectivity, and size cutoff for nonionic solutes. These properties together are referred to as permselectivity. For an exciting historical look-back on how our understanding of permselectivity evolved, the readers are directed to an excellent review by

Anderson and Van Itallie (2009). To gain more insights into the properties of the TJ pathway, its permeability toward molecular tracers with progressively increasing size was explored. This "size profiling" revealed the existence of two distinct pathways. One is a high capacity pathway with a steep size cut-off for solutes larger than ~4 Å, which was labeled the pore pathway. In contrast, the second pathway, termed the "leak pathway" allows transport of larger solutes (Knipp et al., 1997; Van Itallie et al., 2008; Watson et al., 2001). The surprising finding that transport through the leak pathway can be altered independent from changes in ion permeability substantiates the notion that these two pathways are indeed distinct (Watson et al., 2001).

The *pore pathway* is generated by the claudin family of transmembrane proteins. It mediates paracellular ion transport and exhibits ionic charge selectivity. Transepithelial resistance (TER) is often used to characterize its properties. To assess TER, cells are grown on a permeable support (filter) or in an Ussing chamber. TER is measured across the whole epithelial monolayer using electrodes. It has to be kept in mind however, that although it is a good indicator of the properties of the pore pathway, TER is actually influenced by the resistance of both the paracellular and transcellular pathways. As a further complication, the measurement is also affected by the resistance of the space between the basal membrane and the cell support (Lo et al., 1999). Thus, although a useful and easy-to-measure parameter, TER does not entirely reflect the properties of the paracellular pathway. Two new techniques, two-path impedance spectroscopy (Gunzel et al., 2012; Krug et al., 2009b) and electric cell–substrate impedance sensing (Lo et al., 1999; Tiruppathi et al., 1992) can overcome these problems by offering means to separate paracellular resistance from other influencing factors.

The *leak pathway* that mediates the flux of larger solutes does not show charge selectivity, but has a size cutoff (Shen et al., 2011). The exact molecular nature and properties of this pathway remain unknown. The transport of larger solutes is thought to occur through temporary breaks in the dynamic TJ strands, or at the sites where three cells meet (tricellular tight junctions (tTJs)) (Shen et al., 2011). However, how selectivity of this pathway is achieved is not clear: why don't small charged molecules and ions pass through it indiscriminately? The permeability of the leak pathway is usually assessed by measuring the transepithelial flux of tracer molecules, such as fluorescently tagged dextran of various sizes or radioactive inulin. Due to the size cutoff of this pathway, larger molecules do not readily permeate through it; and this property is used to distinguish between paracellular

and transcellular transport of the tracers. Importantly, many studies on TJ functions do not distinguish between the two types of permeability pathways. More systematic approaches will be needed to enhance our understanding of the molecular nature of the leak pathway and of the relationship between the two types of paracellular pathways.

2.2.2 Fence function

The TJ complex also generates a barrier within the plasma membrane to establish and maintain apicobasal polarity, that is, the different compositions of the two membrane compartments. The TJs prevent free diffusion and mixing of lipid and protein components between the two compartments, referred to as the fence function. Establishment and maintenance of apicobasal polarity requires the interaction between the junctions and specialized polarity proteins complexes (Schluter and Margolis, 2012). This will be discussed in Section 2.3.6.

2.3. Tight junction proteins

TJ-associated proteins fall into two categories: transmembrane and associated cytoplasmic proteins (Chiba et al., 2008; Furuse, 2010; Fig. 6.1B). The transmembrane proteins can be further subdivided into three major types: claudins, tight junction-associated Marvel proteins (TAMP), and single span proteins. TJ-associated cytosolic proteins are collectively referred to as the cytoplasmic plaque, and they include a large array of adapters, signaling proteins, transcription factors, and cytoskeletal components (Fig. 6.1B).

2.3.1 Claudin family

2.3.1.1 Structure and homology

Claudins are small molecular weight (21–28 kDa) integral membrane proteins with four transmembrane domains (tetraspan proteins) (Fig. 6.2A). They belong to the PMP22/EMP/MP20/claudin superfamily (PFAM family 00822) (Van Itallie and Anderson, 2006). They incorporate into the TJ strands that typically contain multiple claudin isoforms. Claudins are essential components of the TJs, and they determine permselectivity (Angelow et al., 2008; Tsukita and Furuse, 2000; Van Itallie and Anderson, 2004). With recent additions, the human claudin family has now expanded from the original 24 members to 27 (Lal-Nag and Morin, 2009; Mineta et al., 2011). All claudins show some degree of homology to each other, but some are more homologous. Based on a phylogenetic tree, the family has been subdivided into two major groups. The classic claudin group includes

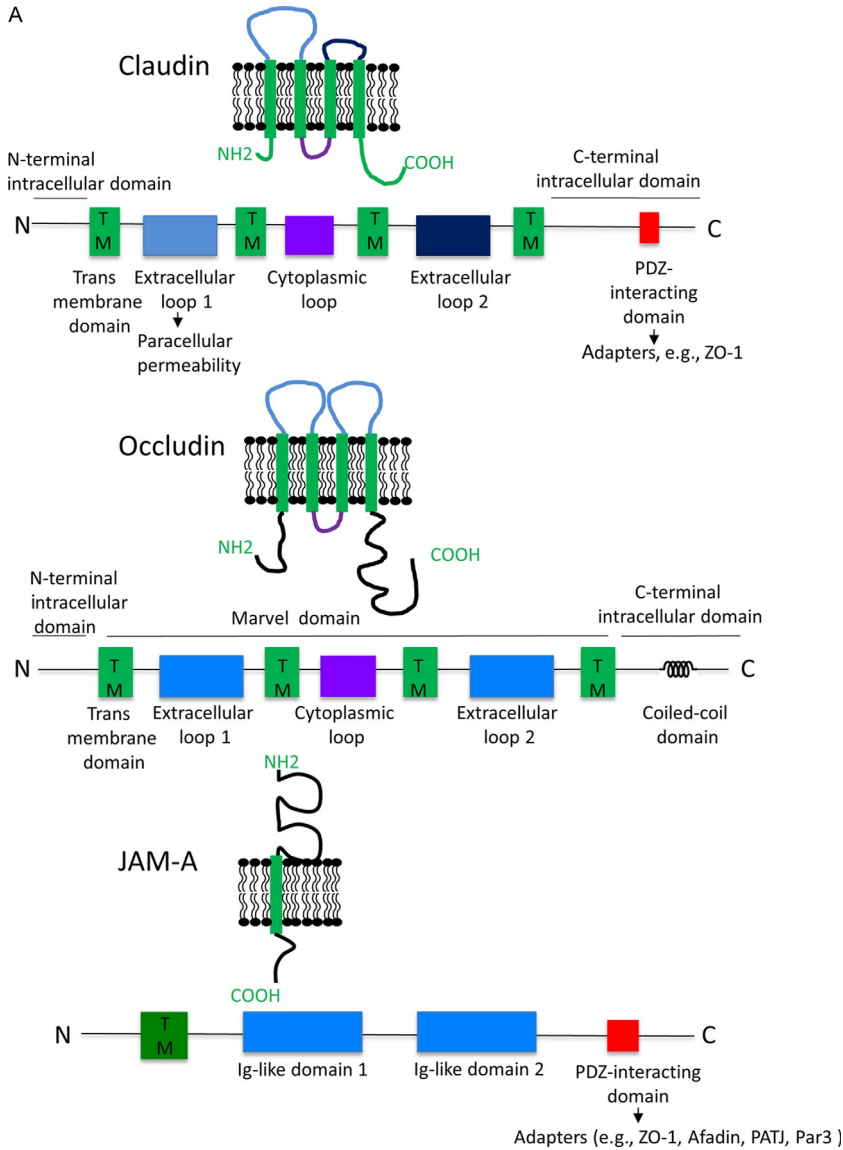

Figure 6.2—Cont'd

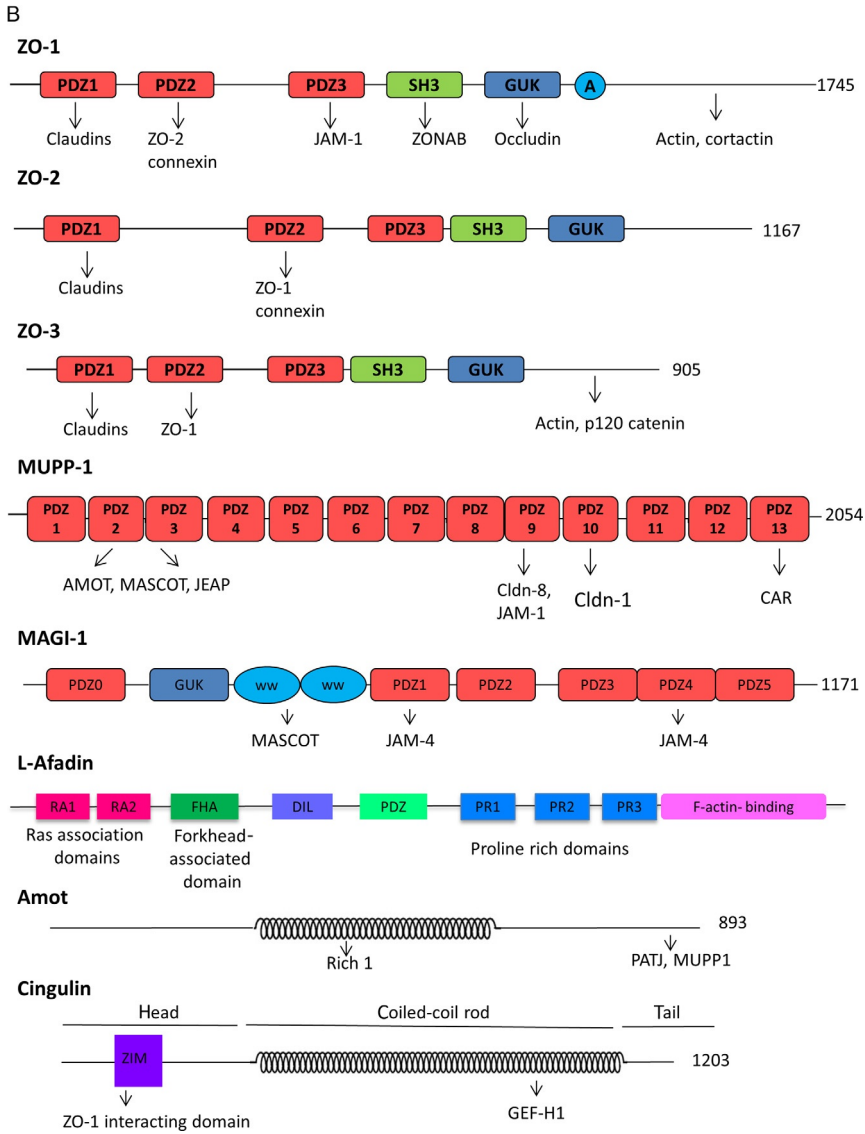

Figure 6.2 Structure of some of the transmembrane TJ proteins (A) and multidomain adapters in the cytosolic plaque (B).

claudin 1–10, 14, 15, 17, 19, and the nonclassic group contains claudin 11–13, 16, 18, 20–24, although the exact place of some of the claudins is still debated (Krause et al., 2008; Lal-Nag and Morin, 2009). Claudins form complex homo- and heterotypic interactions with one another as well as other TJ membrane proteins. The extracellular loops of claudins in adjacent cells form *trans* interactions, which are key for the generation of the paracellular barrier and permeability pathway. The two extracellular loops differ in length, and the larger first loop contains a conserved GLWxxC(8–10 aa)C motif. Elegant mutational and domain swapping experiments demonstrated that the charged amino acids within this loop are critical for determining the ion selectivity and permeability of the paracellular pathway (e.g., Colegio et al., 2002; Van Itallie and Anderson, 2006). Both the N- and C-terminal portions of claudins are cytoplasmic. The C-terminal domain of various claudins is highly variable both in lengths (21–63 amino acids) and sequence. It connects claudins to intracellular proteins through a post-synaptic density 95, Disc large (Dlg), ZO-1 (PDZ)-binding motif that mediates interaction with adapters. In contrast, the N-terminus is short, and its function is yet to be established. In addition to the *trans* interactions, claudins within the same cell also bind each other through *cis* interactions, which is mediated by the transmembrane domains. Such interactions regulate insertion into the TJ strand and possibly also modulate functions. Interestingly, the amino acid sequences of the first and fourth transmembrane regions are highly conserved; while the sequences of the second and third are more diverse. Such differences might underlie specific affinities of claudins for other claudins and TJ proteins.

2.3.1.2 Function

Claudins play central role in the gate functions. The dual nature of the TJ gate (barrier and permeability) is evident in claudin functions. They not only create a barrier preventing free diffusion of solutes but also generate the paracellular pore pathway with unique cation- or anion-selectivity (Colegio et al., 2002; Van Itallie and Anderson, 2004). The first indication that claudins are TJ strand-forming proteins came from pioneering studies by the Tsukita group. Overexpression of claudin-1 in fibroblasts lacking endogenous claudins proved to be sufficient to induce the formation of TJ strand-like networks at the plasma membrane (Furuse et al., 1998b). In the following years, a large array of silencing and overexpression experiments performed in various epithelial cell lines combined with physiological measurements to detect changes in resistance and ion permeability

revealed that specific claudins have unique properties (Anderson and Van Itallie, 2009; Van Itallie et al., 2003). These studies resulted in a functional classification of claudins into four groups (Schulzke et al., 2012). Claudins that reduce permeability are referred to as *sealing* (or barrier forming) claudins (1, 3, 5, 11, 14, 19), while those that specifically enhance permeability are the *channel forming*, also known as pore-forming claudins. This latter group can be further subdivided into *cation-selective* (2, 10b, 15) and *anion-selective* (10a, 17) claudins. The other two groups contain claudins with *inconsistent* (4, 7, 8, and 16) or *unknown* (6, 9, 12, 13, 18, 20–27) functions. Of course, these groups are bound to change in the future as our knowledge about incompletely characterized claudins will improve.

Importantly, epithelial tissues express multiple claudins, and their TJ strands are a mosaic of different claudins. The complex, tissue-specific expression pattern poses a significant challenge to uncovering the *in vivo* functions of individual claudins, since epithelial permselectivity is determined not only by the presence or absence of individual claudins, but by the overall claudin expression profile. In fact, changes in the expression of a specific claudin might have different effects depending on the cell lines studied, which might explain inconsistencies in the literature. Thus, the function of a single claudin has to be assessed in the context of the expression profile of all claudins in the tissue investigated. In this respect, studies using knockout mouse models and the analysis of diseases caused by natural claudin mutations provided valuable information (Furuse, 2009). Typically, knockout or mutation of a specific claudin results in complex phenotypes, involving increased epithelial leakiness due the lack of sealing function and/or transport changes due to the absence of specific ion permeability pathways. But in addition, there is accumulating evidence demonstrating that claudins might affect expression of other claudins. Thus, the absence of one claudin can alter the expression of other claudins, further complicating the phenotype. Exciting new observations also suggest that in addition to their "classic" functions, some claudins can regulate cell survival and motility. This opens up an exciting new area of claudin research (Balda and Matter, 2009; Matter et al., 2005; see Section 3). The complex phenotypes of knockout mice reflect these functions of claudins too.

2.3.2 Expression and function of claudins in different tubule segments

Paracellular ion transport through the pathway formed by claudins is a passive process driven by the transepithelial electrochemical gradient. The paracellular permeability and ionic conductance of the TJs vary along

the nephron, with a decrease in overall leakiness from the proximal tubules toward the collecting ducts. In addition, there are also large differences in the driving forces in different segments, due to differential transcellular transport processes along the nephron that alter the composition of the filtrate. Claudin expression was characterized in the tubules by several researchers using Northern analysis and immunohistochemistry. Overall, claudins 1–4, 7,8, 10–12, 16, 17, and 19 were found in different tubule segments (Kirk et al., 2010; Kiuchi-Saishin et al., 2002; Krug et al., 2012; Lee et al., 2006b; Reyes et al., 2002). In addition, claudins 5 and 15 are also present in the kidney, but seem to be expressed only in endothelial cells. However, reports on claudin expression do not always agree, which might be partially due to cross-reaction of antibodies between claudin isoforms. Further, some species-specific differences in claudin localization were also reported (e.g., Gonzalez-Mariscal et al., 2006). Nevertheless, claudin expression profiles in different segments can be well correlated with segmental variations in the paracellular pathway (Fig. 6.3). As a rule, the proximal, more leaky segments express channel-forming claudins (e.g., claudin 2 and 10), while the distal parts with reduced paracellular permeability and solute transport typically express sealing claudins (e.g., claudins 1, 3, 11, and 14). There are excellent reviews on claudins in various tubule segment (Balkovetz, 2009; Hou et al., 2012; Li et al., 2011; Muto et al., 2012).

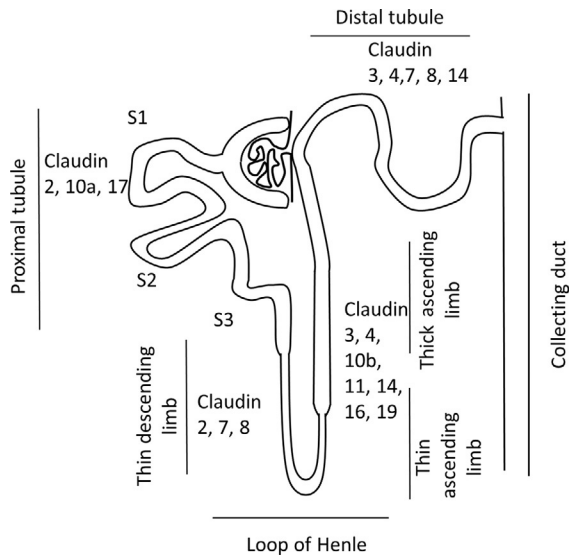

Figure 6.3 Tubular segments and the corresponding claudin expression pattern.

The proximal tubules mediate the largest volume of transport. Based on morphological and functional properties, it can be further divided into three distinct parts. Segment 1 (S1), which is the early and middle convoluted portion of the proximal tubule, exhibits the largest rate of solute transport. Epithelial cells in this segment have well-developed brush borders that enlarge the apical surface area. They are also very rich in mitochondria supplying energy for the transport processes. Segment 2 (S2) includes the end of the convoluted and beginning of the straight part, while Segment 3 (S3) is the distal portion of the straight part. Fluid transport rates gradually decrease toward the S2 and S3 segments and the transporting phenotype as well as the brush border of the epithelium in these segments becomes less pronounced. The proximal tubules reabsorb two-thirds of the NaCl content of the primary filtrate (Aronson and Giebisch, 1997; Rector, 1983). Na^+ and Cl^- reabsorption takes place through both transcellular and paracellular routes. Apical transporters involved in transcellular Na^+ absorption include Na^+/H^+ exchanger isoform 3, and Na^+-coupled cotransporters (Na^+-glucose and Na^+-amino acid transporters), while the basolateral side contains the HCO_3^-/Na^+ cotransporter and Na^+/K^+ ATPase. The initial portions of the proximal tubule preferentially reabsorb HCO_3^- over Cl^-, and the generated electrochemical force drives passive Cl^- reabsorption in more distal parts of the proximal tubule. Cl^- reabsorption in turn generates a positive potential in the lumen that helps passive Na^+ reabsorption (Liu and Cogan, 1986). The proximal tubules express two channel-forming claudins, the cation-selective claudin-2 and anion-selective claudin-10a (Enck et al., 2001; Gunzel et al., 2009; Kiuchi-Saishin et al., 2002; Reyes et al., 2002). Claudin-2 is the best characterized channel-forming claudin in the kidney (Amasheh et al., 2002; Furuse et al., 2001; Hou et al., 2006; Yu, 2009). Its overexpression in various cell lines decreases TER, an effect that is attributed to increased cation-selective TJ permeability (Amasheh et al., 2002; Furuse et al., 2001). Short interfering RNA-mediated claudin-2 silencing experiments in MDCK cells further supported that claudin-2 increases cation-selective permeability. When claudin-2 was silenced, decreased permeability toward Na^+ was registered and the preference of the paracellular pathway toward Na^+ over Cl^- disappeared (Hou et al., 2006). Structure–function analysis revealed that the cation selectivity is due to a negatively charged site within the pore formed by claudin-2 that mediates electrostatic interactions with permeating cations (Yu et al., 2009). In contrast, the claudin-2 channel was found to be relatively impermeable to uncharged solutes (Amasheh et al., 2002; Furuse et al., 2001). Surprisingly however, it was recently shown to

mediate water transport (Rosenthal et al., 2010). A knockout mouse model verified the key role of claudin-2 in proximal tubule Na^+ reabsorption: the S2 segment of these mice showed significantly reduced transepithelial reabsorption of Na^+, Cl^-, and water, and the loss of Na^+ selectivity of the paracellular pathway (Muto et al., 2010). Claudin-10a is a major anion-selective claudin expressed in the proximal tubule. Claudin-10 exists in six splice variants, and of these claudin-10a increases permeability toward small anions, but reduces permeability toward large organic anions (Gunzel et al., 2009). Interestingly, the claudin-10b splice variant, expressed in the Henle's loop has entirely different properties. Although both variants form low-resistance pores when expressed in tubular cell lines, claudin-10b was found to be more selective for cations than claudin-10a (Van Itallie et al., 2006). Claudin-10a is probably not the only paracellular anion channel in the proximal nephron, as recently the anion-selective claudin 17 was also shown to be expressed there (Krug et al., 2012). Taken together, claudin-2 likely mediates paracellular Na^+ transport, while claudin-10a and 17 are responsible for paracellular Cl^- reabsorption in the proximal tubules. The relative permeability of Na^+ and Cl^- (P_{Na}/P_{Cl}) varies between different segments of the proximal tubules (Berry and Rector, 1978; Schafer et al., 1974). Although it is suggestive that segmental expression of claudin-2 and 10a might account for such permeability differences, this notion remains to be tested.

The Henle's loop consists of the thin descending, thin ascending, and thick ascending limbs (TAL). The specific distribution and function of claudins in these segments is a prerequisite for the countercurrent mechanism, which depends on the water impermeability of the ascending limb associated with selective absorption of NaCl. The *thin descending limb* still shows some similarities with the proximal tubules, as it contains claudin-2. In addition, claudin-7 and -8 are also expressed here, but the exact function of these is under debate (Enck et al., 2001; Li et al., 2004). Overexpression studies suggest that claudin-8 might have an indirect effect on permeability, through the regulation of claudin-2. Notably, claudin-8 overexpression resulted in enhanced barrier functions, which was at least in part attributed to reducing claudin-2 synthesis, resulting in a decrease in claudin-2 expression. Claudin-8 was also shown to displace claudin-2 from the junctions (Angelow et al., 2007b).

More distal portions of the Henle's loop express several cation channel-forming claudins, including 10b, 16, and 19, as well as sealing claudins (3, 11, and 14), and claudin-4, the function of which remains undecided (Elkouby-Naor et al., 2008; Gonzalez-Mariscal et al., 2006; Ohta et al., 2006).

Claudin-3 and -4 attracted special interest, because their extracellular loops bind the endotoxin of the bacterium *Clostridium perfringens*, which results in their removal from the TJs. This elevates permeability, suggesting that these are sealing claudins (Fujita et al., 2000; Sonoda et al., 1999). This is further supported by findings that overexpression of these claudins in tubular cells enhances the barrier (Borovac et al., 2012; Milatz et al., 2010; Van Itallie et al., 2001). In fact, claudin-3 probably forms a seal against all ions (Milatz et al., 2010). However, the exact function of claudin-4 remains undecided, as contradicting findings have been reported. Claudin-4 silencing in the porcine tubular cell line LLC-PK_1 was found to reduce Cl^- permeability (Hou et al., 2006). These findings do not substantiate the role of claudin-4 as a sealing claudin. In contrast, claudin-4 overexpression in MDCK cells resulted in decreased cation permeability (Van Itallie et al., 2001), and in proximal tubule-like OK cells overexpression of claudin-4 reduced both Na^+ and Cl^- permeability, leading to significantly reduced TER (Borovac et al., 2012). This effect however was associated with an increase in claudin-1, -6, and -9 mRNA levels, suggesting a possible indirect effect. A similar complex effect could explain results from yet another study that contradict the sealing function of claudin-4. In the collective duct claudin-4 formed an anion-selective paracellular pathway (Hou et al., 2010), and interestingly, this required interaction with claudin-8. These studies therefore highlighted some of the difficulties in studying the properties of individual claudins. The complex interactions between claudins might explain the contradicting results obtained in different cell lines. Taken together, claudin-4, similar to claudin-8 might exert its effect through the regulation of other claudins. This possibility however will need further experimental verification.

The TAL reabsorbs about one-third of the filtered Na^+, and much of the remaining bicarbonate. This segment also plays a major role in both K^+ homeostasis and Ca^{2+} and Mg^{2+} reabsorption (Hou and Goodenough, 2010). Apical K^+ channels that mediate K^+ secretion contribute to the development of a lumen-positive transepithelial voltage that in turn drives the passive paracellular reabsorption of both Na^+ and divalent cations. Two claudins, claudin-16 and -19, were found to play a key role in this process (Angelow et al., 2007a; Gunzel and Yu, 2009; Hou and Goodenough, 2010; Ohta et al., 2006). Mutations in these claudins cause the hereditary disorder familial hypomagnesemia with hypercalciuria and nephrocalcinosis (FHHNC). This syndrome is associated with Ca^{2+} and Mg^{2+} wasting, and will be discussed in more detail in Section 5.1. The TAL also expresses

claudin-11 and -14. Based on overexpression studies, both of these reduce cation permeability (Ben-Yosef et al., 2003; Van Itallie et al., 2003). Claudin-11 and -14 knockout mice show slightly enhanced urine Ca^{2+} and Mg^{2+} levels (Elkouby-Naor et al., 2008). As discussed in Section 5.1, recent studies suggest that claudin-14 acts as a regulator of claudin-16 and -19, that in turn play key role in Ca^{2+} transport (Gong et al., 2012). In line with this notion, variants of claudin-14 are associated with elevated risk of kidney stones (Thorleifsson et al., 2009).

The distal nephron consists of the distal convoluted tubule, the connecting tubule, and the collecting duct. Together these are referred to as the aldosterone-sensitive distal nephron. These segments play a vital role in the control of extracellular volume and blood pressure. In these segments, up to 10% of the remaining NaCl is reabsorbed (Hou, 2012). An apical Na^+ channel coupled with the basolateral Na^+/K^+ ATPase is responsible for the transepithelial Na^+ absorption, which generates a negative luminal transepithelial potential. This in turn can drive Cl^- absorption through the paracellular pathway. Transcellular Na^+ absorption and K^+ secretion in these segments are under the control of aldosterone. Several claudins are expressed in these parts, including claudin-3, -4, -7, -8, and -14 (Hou, 2012).

Multiple studies suggest that claudin-8 might be a key regulator of paracellular permeability in the collecting duct, partly through the regulation of other claudins. In collecting duct cell lines coimmunoprecipitation and colocalization experiments demonstrated that claudin-4 and -8 interact with each other (Hou et al., 2010). As mentioned earlier, claudin-4 was implicated in Cl^- transport, since its silencing in LLC-PK_1 cells resulted in decreased Cl^- permeability (Hou et al., 2006). The assembly of claudin-4 into TJ strands required its interaction with claudin-8, and the absence of claudin-8 reduced the recruitment of claudin-4. Thus, claudin-8 might play a key role in the collecting duct Cl^- permeability through the regulation of claudin-4. In addition, claudin-8 was also shown to increase barrier properties through decreasing proton, ammonium and bicarbonate permeability, and is therefore likely to play an important role in acid–base homeostasis (Angelow et al., 2006). Importantly, claudin-8 in the mouse nephron was found to be expressed along the aldosterone-sensitive distal nephron (Li et al., 2004). Although there are currently no data available about the role of claudin-8 in aldosterone-sensitive reabsorption, in colon cells claudin-8 expression was found to be increased by aldosterone. This effect was necessary to form a paracellular seal that prevents Na^+ back-leak (Amasheh et al., 2009).

Claudin-7 is also expressed in high levels in the distal convoluted tubules and collecting ducts (Alexandre et al., 2005; Li et al., 2004; Reyes et al., 2002). Although the exact function of this claudin is still not clarified, when overexpressed in the porcine tubular cell line LLC-PK_1 it increased TER, decreased and increased paracellular Cl^- and Na^+ conductance, respectively (Alexandre et al., 2005). Silencing claudin-7 in collecting duct cells reduced TER without affecting ion selectivity of the paracellular pathway (Hou et al., 2010). Consistent with a potential role of claudin-7 as a nonselective ion barrier, claudin-7 knockout mice die within 12 days after birth from severe salt wasting and chronic dehydration. Urinary Na^+, Cl^-, and K^+ excretion in these mice is significantly elevated (Tatum et al., 2010). Loss of a nonselective paracellular barrier in the collecting duct is consistent with this phenotype: reduced sealing between the cells causes back leak of ions and disrupts Na^+ and Cl^- reabsorption. This also leads to fluid loss that in turn elevates aldosterone levels, causing increased K^+ excretion.

Taken together, the segmental expression of claudins appears to explain segmental differences in the paracellular permeability that plays a major role in the overall tubular transport.

2.3.3 Tight junction-associated Marvel proteins family

This newly defined family (also referred to as the Marvel family proteins) consists of occludin, tricellulin, and MarvelD3 (Mariano et al., 2011). These tetraspan proteins contain a conserved Marvel (MAL and related proteins for vesicle traffic and membrane link) domain formed by their predicted transmembrane helices. This structural motif was originally discovered in proteins involved in membrane apposition and fusion events. All three proteins incorporate into TJ strands. Despite the high degree of similarities in these proteins, when compared based on a number of criteria they all exhibit unique properties and functions too (Raleigh et al., 2010).

Occludin was the first TJ membrane protein identified by the Tsukita group (Furuse et al., 1993). It is present in all TJs and is often used as a marker of the TJs (Cummins, 2012). Several occludin variants have been identified, that are produced by differential splicing and alternative promoter usage. We do not know what the functional differences between these occludin variants are, although some were found to exhibit distinct subcellular distribution (Mankertz et al., 2002). The 522-amino acid, 65-kDa variant is referred to as occludin (Gu et al., 2008; Mankertz et al., 2002; Muresan et al., 2000). This protein has two extracellular loops, four transmembrane domains and intracellular C- and N-terminal portions, as well as the above-mentioned

Marvel domain (Fig. 6.2A). The C-terminal region interacts with the adapter proteins ZO-1, -2, and -3, and regulates intracellular trafficking and dimerization (Cummins, 2012; Feldman et al., 2005). The extracellular loops also play a role in localization. Occludin was shown to cooligomerize with claudins, that probably controls its localization to the TJs (Cording et al., 2012; Furuse et al., 1998b).

Despite its status as the first identified TJ membrane protein, the exact function of occludin remains unresolved. Overexpression and down-regulation studies failed to provide a clear picture. Some findings suggest that it has roles in TJ formation and regulation. Expression of occludin in fibroblasts that lack TJs induced the formation of TJ-like strands (Furuse et al., 1996). In MDCK cells occludin overexpression elevated TER, but surprisingly it also increased the paracellular flux of small molecular weight tracers (Balda et al., 1996; McCarthy et al., 1996). Expression of occludin mutants lacking the N-terminal portion or the extracellular domains led to defective barrier functions and decreased TER. But even more surprisingly, this was also associated with enhanced paracellular flux of small tracers (Bamforth et al., 1999). These studies raise the possibility that occludin might contribute to the leak pathway. In contrast, knockdown of occludin in MDCK cells caused no major alterations in the TJ structure or fence function but caused an increase in mono- and divalent cation permeability (Yu et al., 2005). It is important to note however, that in these experiments occludin knockdown also decreased the expression of claudin-1 and -7 and increased claudin-3 and -4. Similarly, expression of mutant occludin proteins in MDCK cells also leads to the accumulation of claudin-4 (Balda et al., 2000). Thus, the observed effects on barrier functions might be due to changes in claudins rather than the direct effect of occludin at the TJs. Nonetheless, how occludin regulates claudin expression remains to be established.

An occludin knockout mouse model provided further clues suggesting that occludin does not directly regulate gate functions but has other roles. The mice are viable and show no obvious TJ morphological phenotype (Saitou et al., 2000; Schulzke et al., 2005). Instead, they have postnatal growth retardation and histological abnormalities that include chronic inflammation and hyperplasia of the gastric epithelium. Overall these findings point to the possible role of occludin as a signal organizing molecule. Indeed, several studies suggest that occludin is important for cell–cell adhesion and TJ signaling functions (see Section 3). Knockdown of occludin in MDCK cells leads to defects in the extrusion of apoptotic cells, and alterations in the actin cytoskeleton and Rho GTPase regulation (Yu et al., 2005). Occludin was

also implicated in the formation of cell–cell adhesion. Its overexpression in fibroblasts promotes weak cell–cell adhesion (Van Itallie and Anderson, 1997). Further, an exciting new study showed that occludin localizes to the centrosomes in dividing MDCK cells, suggesting possible additional roles in growth regulation (Runkle et al., 2011). Occludin might have a role in inflammation too, as it was suggested to modulate the transmigration of neutrophil leukocytes through epithelial layers (Huber et al., 2000). Specifically, mutations in the N-terminal portion of occludin upregulated, while mutations in the extracellular domains inhibited neutrophil transmigration. Finally, the presence of occludin was also shown to modulate the sensitivity of epithelial cells for cytokine-induced TJ alterations (Van Itallie et al., 2010). Taken together, these and other studies suggest that rather than being a direct contributor to barrier functions and paracellular permeability, occludin might have a role in TJ assembly, maintenance and remodeling, as well as in signaling.

Tricellulin (MarvelD2) is the only protein known to be concentrated at the tTJs where three cells make contact. At these sites, TJ strands expand along the lateral membrane of all three cells to form vertical strands and a central tube (Ikenouchi et al., 2005). The exact protein structure of this tube remains to be established, but tricellulin likely contributes to its generation. Four isoforms of the human tricellulin gene have been identified with the longest gene, TRIC-a (558-amino acid long, 65-kDa protein) referred to as tricellulin (Mariano et al., 2011; Riazuddin et al., 2006). Occludin and tricellulin show high degree of homology in their C-terminal cytoplasmic domains through which both proteins bind to ZO-1 (Riazuddin et al., 2006). However, ZO-1 binding is dispensable for the incorporation of tricellulin into claudin-based TJ strands. Although tricellulin is highly concentrated in the tTJs, under some conditions it can be found at the bicellular TJs (bTJs) (Ikenouchi et al., 2005). How is tricellulin targeted to the tTJs? During TJ development, tricellulin localizes to the edges of elongating bTJs (Ikenouchi et al., 2008). Interestingly, when occludin is silenced, tricellulin becomes localized mostly at the bTJs, implying that the presence of occludin might exclude tricellulin from bTJs and/or enhance its delivery to the tTJs (Ikenouchi et al., 2008). Moreover, tricellulin and occludin were reported to form heteromeric complexes (Westphal et al., 2010), although this remains controversial (Raleigh et al., 2010). According to a model based on multiple studies, tricellulin and occludin are transported together to the edges of elongating bicellular junctions but upon establishment of the tTJs, they dissociate. A newly identified tTJ-associated membrane protein,

the lypolysis-stimulated lipoprotein receptor (a receptor for triacyl-glycerol-rich lipoproteins) was shown to bind tricellulin (Furuse et al., 2012; Masuda et al., 2011). This protein might act as a landmark that recruits tricellulin to tTJs to form the vertical TJ strands.

The exact function of tricellulin remains to be established. Interestingly, tricellulin mutations cause a recessive form of nonsyndromatic deafness, with no obvious other epithelial phenotype (Riazuddin et al., 2006). When overexpressed in cell lines, tricellulin increases TJ strand cross-linking, suggesting that it might organize strands (Ikenouchi et al., 2008). On the other hand, tricellulin silencing results in disorganized tTJs with compromised barrier, decreased TER and elevated flux of small tracer molecules (Ikenouchi et al., 2005). At least in some cells, tricellulin might also have a sealing function at the bTJs. This conclusion is supported by experiments using different levels of tricellulin expression. If the expression levels are low, tricellulin localizes exclusively at the tTJs, but with higher expression it is also incorporated into the bTJs. Tricellulin at the tTJs was shown to form a barrier only against macromolecules, while at the bTJs it appeared to act as a barrier against all solutes (Krug et al., 2009a). Taken together, tricellulin likely has an important role in TJ sealing and regulating the passage of macromolecules.

MarvelD3 is the third member of the TAMP family. Similar to its relatives, it also has alternatively spliced isoforms that show broad tissue distribution. MarvelD3 colocalizes with occludin at the TJs. However, similar to occludin, its silencing by RNA interference does not affect the formation of functional TJs, but causes an elevation in TER. Like occludin, it might exert its effects on TER through interactions with other TAMP proteins and/or claudins (Cording et al., 2012). MarvelD3 is able to partially compensate for occludin or tricellulin loss, but it cannot fully restore all lost functions, substantiating the existence of distinct roles for the three proteins (Raleigh et al., 2010).

2.3.4 Single-span transmembrane proteins of TJs

Single-span proteins at the TJs can be divided into two categories: immunoglobulin superfamily members, and others. None of these proteins are incorporated into the TJ strands, and they likely contribute to TJ regulation and signaling. Overall, the role of these proteins in the kidney remains not well established. The immunoglobulin family proteins at the TJs include the coxsackie and adenovirus receptor (CAR) (Coyne and Bergelson, 2005) and the three junction-associated molecules (JAM-A, -B, and -C, also

referred to as JAM-1, -2, or -3) (Bazzoni, 2003; Mandell and Parkos, 2005). JAMs are glycoproteins that contain two immunoglobulin folds in their extracellular domains. In addition to endothelial and epithelial cells, circulating leukocytes and platelets also express JAMs suggesting a role in immune functions (Bazzoni, 2003). JAM-A appears to stabilize the TJ barrier and its knockdown in cell lines induces leakiness (Bazzoni et al., 2000; Liu et al., 2000). However, this might be an indirect effect, as JAM-A silencing was also shown to elevate the expression of the pore-forming claudins 10 and 15. JAM-A also regulates the small GTPase Rap1, which has a key role in junction formation (Mandell et al., 2005).

Single span TJ transmembrane proteins that do not have immunoglobulin domains include Crumbs homologue 3 (Crb3), a polarity complex protein (see Section 2.3.6) and blood vessel epicardial substance (Bves) (Balda and Matter, 2008). This latter protein may contribute to the establishment and/or maintenance of epithelial integrity and polarity and to signaling, including the regulation of the small GTPase RhoA (Russ et al., 2011).

2.3.5 Cytosolic plaque proteins

The integral membrane proteins of the TJs interact with a large array of cytoplasmic proteins that collectively form the cytoplasmic plaque (Fig. 6.1B). These interactions regulate junction assembly/disassembly and gate functions, but also control gene transcription, proliferation, migration, cell polarity, and cytoskeleton organization (Guillemot et al., 2008b). The plaque contains various adapter (scaffolding), cytoskeletal and signaling proteins, that couple the membrane proteins to the cytoskeleton and small GTPases, that have a central role in TJ regulation (Ivanov, 2008; Kapus and Szaszi, 2006; Rodgers and Fanning, 2011).

The modular structure of adapter proteins enables them to act as scaffolds assembling large protein networks (Fig. 6.2B). One of the most important protein–protein binding domain present in many junctional adapters is the PDZ domain. This is a sequence of 80–90 amino acids that has a central role in junction assembly and regulation. It binds the COOH-terminal T/SXV residues of various target proteins, including many of the transmembrane junction proteins (Lee and Zheng, 2010). Small variations in the context surrounding the PDZ domains ensure binding specificity. Adapter proteins containing PDZ domains form the structural backbone of the TJs. They anchor integral membrane proteins to other members of the cytosolic plaque and to the cytoskeleton. This creates a complex network of protein–protein interactions that controls TJ assembly and function. Here, we will give a

brief overview of the major TJ plaque proteins. For more details, the reader is directed to excellent recent reviews (Bauer et al., 2010; Citi et al., 2012; Fanning and Anderson, 2009; Furuse, 2010; Gonzalez-Mariscal et al., 2008, 2012; Guillemot et al., 2008b).

2.3.5.1 PDZ domain containing TJ-associated adapters

ZO-1, -2, and -3 are the best-characterized PDZ domain containing adapters in the cytoplasmic plaque (Fanning and Anderson, 2009). In fact, ZO-1 was the first identified TJ-associated protein (Stevenson et al., 1986). Its homologues ZO-2 and -3 were found through the analysis of proteins that coprecipitate with ZO-1 (Gumbiner et al., 1991; Haskins et al., 1998). The ZO proteins belong to the membrane-associated guanyl kinase (MAGUK) family (Fig. 6.2B). They contain several protein–protein interaction domains, including PDZ, SH3, guanylate kinase homology, and F-actin-binding domains. Experiments using RNA interference revealed that ZO-1 and -2 are indispensable for the formation of TJs (Adachi et al., 2006; Umeda et al., 2006). ZO proteins also bind AJ and desmosome proteins, and have critical roles in the maintenance of those structures too. Targeted disruption of either ZO-1 or -2 in mice prevents the formation of cell junctions and results in embryonic lethality (Katsuno et al., 2008; Xu et al., 2008). How do ZO proteins regulate junction assembly? We do not have a complete answer to this question, but the ability of ZO proteins to organize and cross-link junctional proteins into higher order arrays and to link them to the underlying cortical cytoskeleton is likely a key factor (Fanning and Anderson, 2009).

Other PDZ domain containing scaffolding proteins, such as MAGI (membrane-associated guanylyl kinase inverted) 1–3 and MUPP-1 (multi-PDZ domain protein) are also important regulators of junction assembly, and contribute to TJ-mediated regulation of signaling and cell growth. Polarity complexes, that are involved in the establishment and maintenance of apicobasal polarity also contain PDZ domain proteins (Assemat et al., 2008; Dow and Humbert, 2007; see Section 2.3.6). Angiomotin (Amot), and its relatives angiomotin-like-protein-1 (also known as Junction Enriched and Associated Protein, JEAP) and angiomotin-like-protein-2 (also called MAGI-associated coiled-coil tight junction protein, MASCOT) constitute a newly characterized group of related adapters with emerging important functions in junction assembly and signaling (Guillemot et al., 2008b). Amot was first characterized in endothelial cells, but multiple recent studies associate it with important functions in epithelia as well. It localizes

cdc42 activation to the forming junctions, thereby promoting junction assembly. Amot also interacts with the Hippo pathway transcription coactivator Yes-associated protein (YAP), thereby regulating cell growth and contact inhibition (see Section 3.3; Zhao et al., 2011).

AF6/afadin is a PDZ domain containing adapter found both at the TJs and AJs (Mandai et al., 1997). It was shown to interact with ZO-1 during junction formation and its knockdown in MDCK cells impaired the formation of both AJs and TJs (Ooshio et al., 2010). This effect might be at least in part due to the role of afadin in local Rap1 signaling during epithelial morphogenesis (Severson et al., 2009). Afadin is targeted by the Ras signaling pathway, suggesting a potential role in oncogenic transformation (Guillemot et al., 2008b). It interacts with immunoglobulin family proteins (nectins at the AJs and JAMs at the TJs) and the Eph tyrosine kinase receptor family (Guillemot et al., 2008b; Ogita et al., 2010; Ooshio et al., 2010).

2.3.5.2 Non-PDZ domain containing TJ-associated proteins

These are mostly involved in signaling, and include kinases, phosphatases, transcription factors and small GTPases and their regulators. Some adapters also lack PDZ domains. Two such related proteins are cingulin and paracingulin (also called JACOP, that stands for junction-associated coiled-coil protein; Citi et al., 2012). These proteins have significant sequence homology and consist of a globular head, a coiled-coil rod domain and a globular tail (Fig. 6.2B). They have a role in connecting TJ membrane proteins with the cytoskeleton (Citi et al., 2012; Cordenonsi et al., 1999; Ohnishi et al., 2004). Cingulin is recruited to the junctions through binding to ZO-1 (Umeda et al., 2004). Since it also binds myosin, it may convey contractility-mediated regulatory signals to the TJs (Cordenonsi et al., 1999). Knockdown and knockout studies revealed that cingulin does not contribute directly to TJ strand formation, but regulates gene expression, maybe through its effect on Rho family GTPases (Citi et al., 2012). Paracingulin is present both in AJs and TJs, but is also recruited to stress fibers (Ohnishi et al., 2004). Similar to cingulin, it has a role in localized regulation of the small GTPases Rac and RhoA (Guillemot et al., 2008a; see Section 3.2).

2.3.6 Polarity protein complexes

Apicobasal polarization refers to the asymmetrical distribution of proteins and lipids at the two distinct membrane compartments. Polarity is a fundamental feature of epithelial cells, and is the basis for specialized epithelial

functions, including directional transport. Accordingly, the generation and maintenance of apicobasal polarization is central for normal kidney development and functions. In recent years, the characterization of the polarity complexes brought a significant increase in our understanding of how apicobasal polarity is established and maintained. This process involves the interplay between three multiprotein complexes and the intercellular junction proteins (Fig. 6.4; Assemat et al., 2008; Pieczynski and Margolis, 2011; Schluter and Margolis, 2012). The three-core polarity complexes are the apically localized Crumbs and Partitioning defective (Par), and the lateral Scribble complex. These complexes are evolutionarily conserved and were first characterized in *Drosophila* and *Caenorhabditis elegans*, but were later found to play vital roles in mammalian epithelia. Through their multilateral interactions and mutual antagonisms, that is still not fully explored, these protein complexes segregate the apical and basolateral membrane. They also target and retain junctional proteins at the border between them to promote junction formation. Establishment of the TJs is a central event in the generation of polarity, because the TJs physically separate the two domains and prevent intermixing of lipids and proteins. The Crumbs complex consists of the integral membrane protein Crumbs (Crb), and two adapters, protein associated with lin seven 1 (Pals1) and Pals-associated tight junction protein (PATJ) (Fig. 6.4). The Par complex includes two adapters,

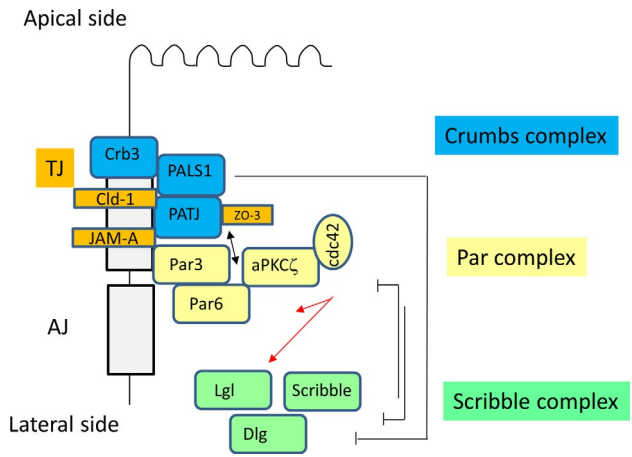

Figure 6.4 Core polarity complex proteins. The figure shows only some of the known interactions between these proteins. The red arrow indicates phosphorylation.

Par3 and 6 and the atypical protein kinase C (aPKC) (Assemat et al., 2008; Dow and Humbert, 2007). The Crumbs complex has an important role in targeting and connecting the Par complex to the TJs. Crb is a single-span integral membrane protein associated with the TJs. Of the three Crb isoforms, Crb3 is the predominant kidney protein (Makarova et al., 2003). Pals1 and PATJ are MAGUK proteins with multiple protein–protein interaction motifs, including PDZ domains. Pals1 is targeted to the TJs by binding PATJ, a protein with multiple PDZ domains, that can also bind directly to ZO-3, claudin-1, and JAM-A (Adachi et al., 2009; Roh et al., 2002). PatJ also binds Crb. These interactions provide a direct link between the TJs and the polarity complexes. The Par complex proteins Par3 and 6 are also multidomain scaffold proteins. Par3 was shown to bind to JAM-A (Ebnet et al., 2001). Importantly, this complex interacts with cdc42, the activation of which is required for the establishment of apicobasal polarity. Phosphorylation is an important modulator of protein–protein interactions in the polarity network. The Par proteins localize aPKC, a serine/threonine kinase to the apical side, which in turn phosphorylates and regulates them. The basal polarity complex consists of scribble (Scrib), Dlg, and lethal giant larvae (Lgl) (Roberts et al., 2012). The exact role of the Scrib complex in apicobasal polarity remains to be established (Pieczynski and Margolis, 2011). The Scribble complex is associated with the lateral membrane, but also has various interactions with the apical polarity complex proteins. For example, Lgl interacts with the Par polarity complex. Importantly, a multitude of studies now show that this complex has a key role in signaling, and interacts with numerous signaling pathways. All members of the Scrib complex have been shown to act as tumor suppressors. Scrib is a large, cytoplasmic scaffold protein that binds Lgl through its N-terminal, which is necessary for its targeting to the lateral membrane. Mammals contain multiple Lgl proteins (Lgl1–4) with similar and/or redundant functions. In the renal epithelium Lgl1 is highly expressed. The third member of the complex is Dlg, an adapter protein that is the funding member of the MAGUK family proteins with PDZ domains. Similar to Lgl, in mammalian cells four Dlg genes have been identified (Roberts et al., 2012). Dlg is also localized in the lateral membrane, however how exactly it interacts with the other two components remains to be determined.

Taken together, the combined function of the polarity complexes is central for epithelial morphogenesis and TJ maintenance. Future studies will no doubt refine our understanding of how these proteins fulfill their vital functions.

3. "NONCLASSIC" FUNCTIONS OF TJs

3.1. Tight junctions as signaling platforms

It is now well established that similar to the AJs, the TJs also act as signal integrating and initiating platforms that orchestrate many epithelial functions. In fact the TJ signaling network is bidirectional: TJ-associated signaling molecules affect cell functions (outside-in signaling), but the TJs themselves are also targeted by multiple signaling pathways (inside-out signaling). One of the best known example of such bidirectional signaling is the control of small GTPases and the cytoskeleton, which are regulated by and are major regulators of the TJs (see Sections 3.2 and 4.3). For the sake of clarity we will discuss these two arms of TJ-associated signaling separately, but the intertwined nature of these complex pathways should always be kept in mind.

Initial evidence suggesting that the TJs have signaling roles came from downregulation and overexpression experiments, which demonstrated that altered expression levels of various TJ-associated molecules affect multiple cell functions. In fact, in cancer cells many TJ proteins show altered expression (Escudero-Esparza et al., 2011), and the development of cancer is frequently associated with the failure of epithelial cells to form TJs and to establish apicobasal polarity. Alterations in the composition of TJs, or TJ disruption affect proliferation and migration, and promote epithelial–mesenchymal transition (EMT; Martin and Jiang, 2009). While the underlying mechanisms are still poorly understood, TJs clearly affect the cytoskeleton, small molecular weight GTPases, gene transcription, proliferation, cell migration, and EMT. Many signaling molecules are specifically localized to the TJs, providing the structural basis for bidirectional signaling networks. TJ-associated kinases and phosphatases include the Src family kinase c-Yes, the serine phosphatase PP2A, the lipid phosphatase PTEN, and WNK4, a kinase that regulates ion transport in the kidney, and contributes to the development of hypertension (Gamba, 2005). Small GTPases at the TJs include membrane traffic regulator Rab proteins, the cytoskeleton regulator Rho family small GTPases, and the Ras family member Rap1 (Guillemot et al., 2008b). Regulators of these proteins are also present. Some receptors are also colocalized with junctions, and interactions with junction proteins could affect activation and trafficking of these. Another mode whereby TJs regulate receptors is by segregating them from coreceptors or ligands. Such mechanisms control the ErbB family that is a potent

regulator of cell growth (Carraway and Carraway, 2007). Surprisingly, several transcription factors are also found at the TJs. Indeed, controlling nucleocytoplasmic shuttling is a potent mode of transcription factor regulation. Accordingly, their retention at the TJ cytosolic plaque inhibits, while release from these interactions triggers nuclear accumulation. This mechanism can translate environmental information through the state of the junctions to gene transcription. In addition to transcription factors, TJ adapter proteins were also found to shuttle between the nucleus and the periphery. The following sections will discuss some of the important signaling and regulatory roles of the TJs.

3.2. Regulation of small GTPases by junctional proteins

Four small GTPase proteins were implicated in the establishment of cell polarity, and the generation of junctions: three members of the Rho family (RhoA, Rac, and cdc42) and the Ras family protein Rap1 (Pannekoek et al., 2009; Samarin and Nusrat, 2009). In a typical bidirectional signaling network, these proteins not only regulate junctions, but are also regulated by them. Small GTPase proteins cycle between inactive (GDP-bound) and active (GTP-bound) states, a mechanism that allows for signaling inputs to rapidly turn them on and off (Fig. 6.5). The activation/inactivation cycle is controlled by three regulator families (Cherfils and Zeghouf, 2013). GDP dissociation inhibitors (GDIs) bind to the GDP-coupled small GTPases, preventing their activation and localizing them to the cytosol. GDI has to dissociate prior to activation of the small GTPase by guanine nucleotide exchange factors (GEFs) that stimulate the exchange of GDP to GTP. In contrast, GTPase-activating proteins (GAPs) enhance the intrinsic GTPase activity of the proteins to promote cleavage of GTP, thereby leading to their inactivation (Moon and Zheng, 2003; Rossman et al., 2005). Active RhoA, Rac, and cdc42 stimulate various effectors to control actin polymerization, myosin phosphorylation, and cytoskeletal organization. They regulate a large array of cellular functions, including junction formation, gene transcription, proliferation and migration (Hall, 2005; Jaffe and Hall, 2005). Our knowledge about junction-dependent control of small GTPases was largely enhanced by the introduction of fluorescent probes and imaging techniques that revealed the spatiotemporal activation/inactivation patterns of specific GTPases (Pertz, 2011; Yoshizaki et al., 2003). Live imaging showed coordinated and localized activation of Rac, RhoA, cdc42, and Rap1 at the junctions at different stages of cell–cell contact formation, controlled by GEFs and GAPs that are recruited to the junctions by adapters.

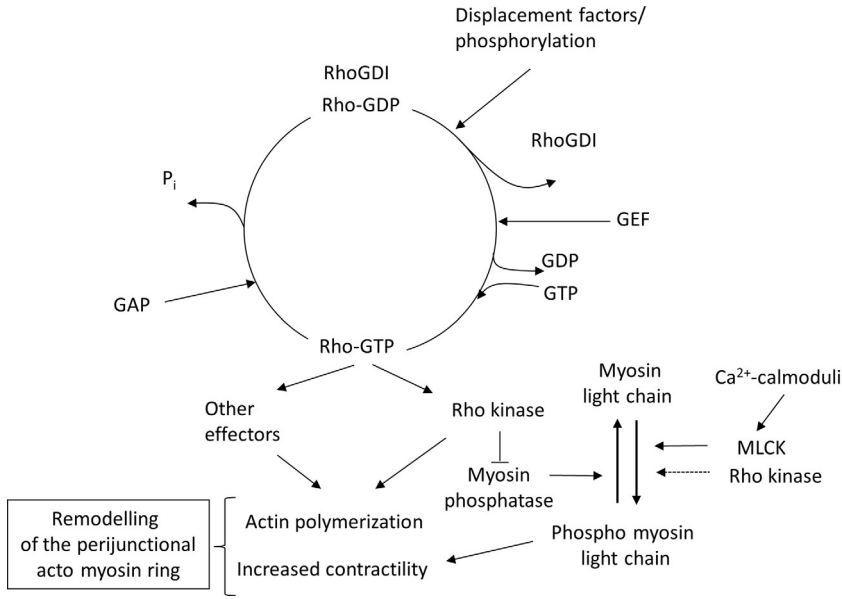

Figure 6.5 Activation/inactivation cycle of RhoA, and its role in myosin light chain phosphorylation and remodeling of the actomyosin ring. GEF, guanine nucleotide exchange factors; GDI, GDP dissociation inhibitor; GAP, GTPase activator protein.

The complex interplay between the junctions and small GTPases is best characterized during the process of new cell–cell contact formation. AJ molecules play a central role in the initiation of new contacts. Nectins, a group of immunoglobulin-like molecules, cooperate with cadherins to promote the assembly of AJs (Ogita et al., 2010; Sato et al., 2006). TJs form apically from the nascent AJs, although the exact molecular events controlling this are largely unknown. Nevertheless, nectin-based signaling and small GTPase-mediated actin reorganization seem to play a central role in TJ formation. Formation of nectin-based contacts induces c-Src-dependent activation of Rap1. In epithelial cells two GEFs, C3G and PDZ–GEF, have been implicated in Rap1 activation at the new junctions (Pannekoek et al., 2009). C3G directly binds to E-cadherin, while PDZ–GEFs bind the MAGI proteins. Activated Rap1 in turn binds the adapter afadin that appears to play a key role in AJ formation (Sato et al., 2006). Active Rap1 controls E-cadherin vesicular sorting and recruitment to the surface and promotes actin cytoskeleton remodeling that induces junction maturation (Pannekoek et al., 2009). Importantly, Rap1 can also signal to activate Rho family small GTPases, although the exact underlying mechanisms remain poorly characterized

(Sato et al., 2006). Activation of cdc42 and Rac by nectin- and cadherin-based cell–cell contacts requires c-Src and Rap1 (Sato et al., 2006). Cdc42 activation is regulated by the GEF Tuba and the GAP Rich1. Active cdc42 in turn controls the formation of the Par polarity complex and the establishment of apicobasal polarity (Kim, 2000; Yamanaka et al., 2001). Tuba is recruited to the junctions by ZO proteins, and Rich1 binds to Amot (Otani et al., 2006; Wells et al., 2006). The Par polarity complex is both a target and regulator of Rac and cdc42. Par6 binds both of these small GTPases, and Par3 and the junctional adapter paracingulin directly bind and recruit the Rac GEF Tiam-1 (Chen and Macara, 2005; Guillemot et al., 2008a). Tiam-1 activation is also stimulated by phosphatidyl-inositol-3 kinase. Once these interactions induce localized activation of Rac and cdc42, a feedback loop is established to promote the formation and maturation of cadherin-based adhesions and the perijunctional actomyosin ring. Rap1 also has a role in recruiting myosin IIb to the junctions (Smutny et al., 2010). During the early stages of junction establishment active Rac1 accumulates at the tips of lamellipodia-like structures in the junctional area (Ehrlich et al., 2002). The relocalization of Rac to the edges of the newly formed junctions is associated with actin polymerization and junction stabilization (Braga et al., 1997). In contrast, the role of RhoA during junction formation is less clear. Active RhoA specifically accumulates at the edges of newly formed cell–cell contacts, and RhoA-dependent myosin phosphorylation is necessary for the lateral expansion of the junctions (Yamada and Nelson, 2007). ARHGEF11, a member of the regulator of G proteins–RhoGEF family was shown to associate with ZO-1, and it might regulate RhoA-dependent myosin light chain (MLC) phosphorylation at the early cell–cell contacts (Itoh et al., 2012). Another GEF that may contribute to spatially restricted RhoA activation during junction assembly is p114RhoGEF, which is recruited by cingulin (Terry et al., 2011). Interestingly, cingulin and paracingulin can also sequester the RhoA and Rac activator GEF-H1 at the junctions (Aijaz et al., 2005). This however likely does not have a role in junction formation. Instead, binding of GEF-H1 to the junctional adapters occurs as cell layers reach confluence and inhibits its activity, leading to downregulation of RhoA signaling and cell proliferation (Aijaz et al., 2005; Guillemot et al., 2008a).

Taken together, interactions between the polarity complex and junctional scaffolds provide a mechanism for spatially and temporally controlled activation/inactivation of small GTPases. This drives cell polarization and junction assembly and organizes the perijunctional cytoskeleton to stabilize

the junctions (Citi et al., 2012). Whether these junction-bound regulators contribute to junction maintenance in established epithelial layers remains to be explored. It is conceivable that at least some of them can shuttle between the junctions and other cellular locations to promote small GTPase activation induced by different signals. GEF-H1, for example, is activated by Ca^{2+}-removal-induced junction disruption and mediates Rho activation (Ly et al., 2013; Samarin et al., 2007). Binding of GEFs and GAPs to junctional adapters could therefore be important not only for localized small GTPase activation, but could also represent a more general regulatory mechanism, similar to the control of transcription factors.

3.3. Regulation of proliferation and gene expression by TJs

Contact inhibition of proliferation, that is, the phenomenon that cells stop proliferating upon contact formation has been described several decades ago (Fisher and Yeh, 1967), but the underlying mechanisms are only now emerging. Importantly, loss of contact inhibition is a hallmark of cancer. The first indications that the integral membrane proteins in the TJs can affect proliferation came from observations made using knockout mice. Absence of occludin, JAM-A, or claudin-15 is associated with enhanced cell proliferation (Laukoetter et al., 2007; Schulzke et al., 2005; Tamura et al., 2008). In intestinal cells, downregulation of JAM-A stimulates the kinase Akt, which promotes phosphorylation, nuclear translocation and increased transcriptional activity of β-catenin, thereby promoting proliferation (Nava et al., 2011). There is accumulating evidence that various claudins also regulate proliferation, but the underlying mechanisms are not known. Claudin-15 knockout mice showed enhanced proliferation of intestinal cryptic cells, resulting in the development of megaintestine (Tamura et al., 2008). A large number of studies also found dysregulation of claudin expression in various cancers (e.g., Escudero-Esparza et al., 2011; Lee et al., 2010; Shang et al., 2012; Takehara et al., 2009; Turksen and Troy, 2011; Zavala-Zendejas et al., 2010). Altered claudin expression in many cases correlates with invasiveness of the cancer. Silencing or overexpression of specific claudins provided further experimental evidence for a role of claudins in migration and proliferation (Ikari et al., 2011a,b). This role was hypothesized to be at least in part due to their general effects on epithelial microenvironment and homeostasis (Tsukita et al., 2008). Occludin also affects cell proliferation. Interestingly, in MDCK cells occludin was shown to localize to the centrosomes during interphase, and to regulate mitotic entry and centrosome

separation in a phosphorylation-dependent manner (Runkle et al., 2011). Occludin and its splice variants were also found to affect apoptosis and the extrusion of apoptotic cells (Gu et al., 2008; Yu et al., 2005).

Tissue culture models verify that cells in an intact epithelial monolayer do not proliferate. Subconfluent cultures have reduced expression of many transmembrane TJ proteins, and some plaque proteins are present in the nucleus. Importantly, upon the establishment of junctions, TJ proteins not only show increased expression, but they also sequester many signal regulators and transcription factors at the periphery, thereby suppressing gene transcription and proliferation (Farkas et al., 2012; Rathinam et al., 2011).

An increasing number of proteins are known to shuttle between the junctions and the nucleus. These proteins have been collectively called nuclear and adherent junction complex components (NACos) (Balda and Matter, 2009; McCrea et al., 2009). They can bind either to the AJs (e.g., β-catenin) or the TJs, or in some cases both. The first identified TJ-associated NACos protein was symplekin (Keon et al., 1996). This protein regulates proliferation and differentiation probably through its effects on mRNA polyadenylation (Balda and Matter, 2009). It can bind ZO-1 and was also suggested to regulate junction functions. This finding suggests that NACos proteins might have not only dual localization, but also dual functions. Several proteins that were initially characterized as TJ cytosolic plaque proteins later proved to also shuttle between the junctions and the nucleus. Most notably, in proliferating epithelial cells ZO-1 and -2 are localized at the nucleus. ZO proteins likely affect gene expression indirectly through the regulation of transcription factors including AP1 and ZO-1 nucleic acid binding protein (ZONAB/DbpA) (Balda and Matter, 2009; Bauer et al., 2010). Levels of the Y-box transcription factor ZONAB in the nucleus are high in proliferating cells when ZO-1 expression is low. In contrast, in confluent cells ZO-1 sequesters ZONAB at the junctions (Lima et al., 2010). ZONAB controls proliferation through multiple mechanisms, both as a transcription factor, and as a scaffold that binds other regulators. Its active (nuclear) form promotes cell cycle progression by upregulating Cyclin D1. This effect involves interaction between ZONAB and symplekin (Kavanagh et al., 2006). ZONAB also forms a complex with cell division kinase (CDK) 4, and regulates its nuclear localization (Lima et al., 2010; Sourisseau et al., 2006). ZONAB can also bind to the guanine nucleotide exchange factor GEF-H1 that stimulates Cyclin D1 through this transcription factor (Nie et al., 2009). Finally, stress-induced activation of ZONAB can also induce posttranscriptional upregulation of the prosurvival molecule p21

(Nie et al., 2012). Cyclin D1, along with the associated CDK4, is an important regulator of cell cycle progression, and all three ZO proteins were shown to regulate its localization, stability, and expression (Capaldo et al., 2011; Gonzalez-Mariscal et al., 2009, 2012; Huerta et al., 2007; Sourisseau et al., 2006; Tapia et al., 2009).

Another important pathway with inputs from the junctions is the Hippo pathway (Genevet and Tapon, 2011; Harvey and Hariharan, 2012). This is an evolutionally conserved signaling pathway that controls proliferation, differentiation, stem cell activity and cell death, and has a central role in determining epithelial tissue size. In fact, in the last few years the Hippo pathway has emerged as a major mediator of contact inhibition. Many inputs that control this pathway are associated with the cell junctions and polarity complexes. Through these the activity of the pathway reflects cell density and intactness of the junctions. The core of the Hippo pathway is a phosphorylation cascade that regulates the nuclear localization of two transcription factors, Taz and Yap, whose targets include progrowth and antiapoptotic genes. At low cell density, Taz and Yap are nuclear and drive proliferation (Harvey and Hariharan, 2012). In contrast, in layers with high density these factors are phosphorylated and localize to the cytoplasm, which is associated with decreased proliferation. Yap can also localize to the junctions through its binding to Crb3, Pals1, and Amot. Overall, although key details of the interactions between the junctions and the Hippo pathway remain to be established, regulation of Taz and Yap is a central mechanism in growth control by the junctions.

4. REGULATION OF TJs

Adaptation of epithelial transport processes to changing needs is central to homeostasis. Accordingly, reabsorption and secretion processes in the kidney tubules are acutely affected both by alterations in the composition of the filtrate and by various hormones. The paracellular ion transport is crucial for maintaining continuous transepithelial transport since it prevents the buildup of a transepithelial electrochemical gradient that would stop transcellular transport. Further, in contrast to the cellular transporters, the paracellular pathway does not saturate over a large concentration range. The TJs must maintain the barrier at all times, while also allowing alterations in paracellular transport to take place. Since the solute flux is passive, any change in the electrochemical gradient is reflected in the magnitude of the transport. However, coordination of transcellular and paracellular transport can

enhance the efficiency of epithelial transport. Indeed, various mechanisms have developed, through which the presence of certain substrates can alter paracellular transport. A powerful example is the effect of Na^+-coupled apical transporters on the paracellular pathway, which will be discussed below. Furthermore, it is becoming increasingly clear that the properties of the paracellular pathway are controlled by many inputs both under physiological and pathological conditions. For example, a number of hormones, growth factors and inflammatory mediators are known to affect paracellular permeability, causing both acute and chronic changes.

The TJs are dynamic structures that undergo continuous assembly and disassembly, controlled by a multitude of signaling pathways. Physiological junction regulation and pathological junction disruption most likely involve similar pathways and mechanisms, and the outcome is likely determined by the magnitude and timing of the signal. What are the molecular mechanisms that control the TJs? We do not have a complete answer to this question. In principle, modifications can be achieved by two ways: either by changing the properties of TJ components *in situ* or by altering the composition of the junctions through retrieval of specific constituents or insertion of new proteins. It is possible that both of these mechanisms are involved, although there is more evidence supporting the second one. Junction assembly is controlled by complex protein–protein interactions, which are in turn affected by posttranslational modifications, including phosphorylation of TJ proteins (Dorfel and Huber, 2012; Gonzalez-Mariscal et al., 2008). The cytoskeleton has long been known as a key regulator of the TJs, and it was recently shown to control endocytosis of TJ proteins (Shen, 2012). Finally, synthesis and degradation of the different components are also under tight control, which likely underlies longer-term remodeling. Indeed, changes in the expression of TJ proteins may be critical to meet physiological needs but may also occur under pathological conditions.

4.1. Protein–protein interactions and posttranslational modifications of TJ proteins

Multilateral *cis* interactions between TJ membrane proteins, mediated by their transmembrane helices, promote their insertion into the TJ strand. Insertion of occludin for example requires a claudin backbone (Cording et al., 2012; Furuse et al., 1998b). Claudins also regulate each other: claudin-4 and -8 were shown to interact in the Golgi and to be cotransported to the TJs (Hou et al., 2010). The binding between the TJ membrane proteins and the adapters that connect them to the cytoskeleton

is also a prerequisite for junction formation and maintenance. These crucial dynamic protein–protein interactions are affected by various posttranslational modifications. Many TJ transmembrane proteins are phosphorylated on multiple sites, and this regulates their insertion into the TJ strands and their interactions with other proteins. For example, the C-terminal cytoplasmic tail of occludin is heavily phosphorylated and this controls its localization (Sakakibara et al., 1997). The growing list of kinases targeting occludin includes various protein kinase C (PKC) isoforms, protein kinase A (PKA), extracellular signal-regulated kinase (ERK), casein kinase (CK) 1 and 2, and Rho kinase (ROK) (Cummins, 2012; Dorfel and Huber, 2012). In addition, several phosphatases also regulate occludin phosphorylation, including the serine phosphatase PP1, the threonine phosphatase PP2A and the tyrosine phosphatase density-enhanced phosphatase-1 (Nunbhakdi-Craig et al., 2002; Sallee and Burridge, 2009; Seth et al., 2007). Some of the phosphorylation events stabilize occludin at the TJs, whereas others destabilize it. For example, PKCη and PKCζ phosphorylate several C-terminal threonine sites, thereby promoting occludin localization to the TJs (Jain et al., 2011; Suzuki et al., 2009). In contrast, c-*Src*-mediated tyrosine phosphorylation weakens binding between occludin and ZO-1 and causes release of occludin from the TJs (Elias et al., 2009). There is ample evidence that phosphorylation alters interactions between occludin and other TJ proteins. For example, the phosphorylation state of S408 controls binding between occludin, ZO-1 and claudin-1 and -2 (Raleigh et al., 2011). Moreover inhibition of CK2-mediated occludin phosphorylation on S408 reduces paracellular cation flux, suggesting an important functional role for these interactions.

Many claudins are also phosphoproteins, and several of the kinases targeting occludin also mediate claudin phosphorylation. Claudins are phosphorylated by PKC, PKA, ERK, c-Src, ROK, as well as WNK kinase and the ephrin receptor kinases (Gamba, 2005; Gonzalez-Mariscal et al., 2008). Similar to occludin, several claudins require phosphorylation for insertion into the TJs (Schulzke et al., 2012). For example, claudin-2 was shown to be heavily phosphorylated on its C-terminus, and its phosphorylation on serine 208 is necessary for membrane retention (Van Itallie et al., 2012b).

Phosphorylation also regulates some of the TJ cytoplasmic plaque proteins. The functional significance of phosphorylation of the ZO proteins is not well known, but it might determine localization, for example, to the nucleus (Gonzalez-Mariscal et al., 2012). Taken together, these data strongly imply that junction regulation involves phosphorylation-dependent changes in the dynamic protein–protein interactions within the TJs.

Other known posttranslational modifications include palmitoylation that is necessary for insertion of several claudins into the TJs (Van Itallie et al., 2005). Claudin-2 is SUMOylated, which might regulate its expression (Van Itallie et al., 2012a). Finally, the role of ubiquitination in regulating occludin and claudin expression, endocytosis and localization is also starting to emerge (Murakami et al., 2009).

4.2. Membrane trafficking

While studying the membrane dynamics of a GFP-tagged claudin-3 molecule in mouse Eph4 epithelial cells, the Tsukita group described a remarkable dynamic behavior (Matsuda et al., 2004). Claudin-3 forms homotypic *trans* interactions. In confluent layers, individual cells constantly remodel their TJs to move within the cellular sheets, without losing structural continuity. During this remodeling, the membranes from the two opposing cells containing GFP-claudin-3 were coendocytosed into one of the cells. Moreover, this process was even more pronounced during repair of an injured layer. Surprisingly, other TJ proteins, such as occludin, JAM, and ZO-1, were not endocytosed together with claudin-3. The authors labeled this process as a "peculiar internalization of the claudin" and concluded that fine regulation of the endocytotic process is important for TJ integrity and remodeling (Matsuda et al., 2004). We now know that many TJ proteins undergo continuous endocytosis and recycling to the plasma membrane. This ongoing cycling is likely the basis of rapid junction remodeling both under physiological and pathological conditions. Proteins that control vesicular trafficking, including Rab family small GTPases can be found at the TJs (Guillemot et al., 2008b; Nishimura and Sasaki, 2009). Trafficking of TJ proteins is controlled by the actin cytoskeleton, myosin phosphorylation, and the microtubules (Rodgers and Fanning, 2011).

Endocytosis of junction proteins is best characterized in intestinal cells, and much less data are available in kidney cells. However, the mechanisms described are likely similar in all epithelial cells. All classical endocytotic pathways have been implicated in junction protein endocytosis under different conditions. Uncoupling of the junctions, for example, by Ca^{2+} removal induces wholesale, clathrin-dependent and ROK-mediated endocytosis of both AJ and TJ proteins (Ivanov et al., 2005). Under these conditions, the proteins were found to accumulate in large actin-coated intracellular vacuoles that originate from the apical plasma membrane. AJ and TJ proteins however do not always internalize simultaneously. Large-scale caveolar

endocytosis of TJ but not AJ molecules was induced by the *Escherichia coli* cytotoxic necrotizing factor-1 (CNF-1), which activates Rho, Rac, and cdc42 (Hopkins et al., 2003). Interestingly, CNF-1 also delocalized the TJ-associated pool of phosphorylated MLC. Under these conditions, occludin was present in early and recycling endosomes, but not in late endosomes, suggesting that it is recycled to the surface and does not get degraded. Yet another internalization mechanism was described in cells stimulated by the proinflammatory cytokine interferon-γ (IFN-γ), where TJ proteins but not AJ proteins were macropinocytosed (Bruewer et al., 2005). Proinflammatory cytokines including IFN-γ and tumor necrosis factor-alpha (TNF-α) were also shown to induce myosin-dependent caveolar endocytosis of occludin (Shen, 2012). Moreover, this was demonstrated not only in cell lines, but also in a series of elegant studies that used live imaging in animals (Marchiando et al., 2010). Taken together, continuous internalization is likely to contribute to the normal turnover of TJ and AJ proteins. During this process, the proteins might get recycled or degraded in the late endosomes. In resting state the continuous endocytosis and exocytosis are in balance, and the process does not affect TJ function. However, various stimuli, including inflammatory cytokines can induce selective endocytosis of the TJ proteins, thereby altering gate functions. Finally, more disruptive stimuli can enhance the internalization of both AJ and TJ proteins, thereby impairing not only the barrier, but also the fence function, cell–cell adhesion and polarity (Capaldo and Nusrat, 2009; Chalmers and Whitley, 2012; Ivanov, 2008; Shen, 2012).

Although there are still large gaps in our knowledge of how trafficking of TJ proteins is modulated, several regulatory factors have been identified. As discussed in section 4.1, phosphorylation can alter protein–protein interactions that affect localization. Rab family small GTPases also play crucial roles. These proteins are master regulators of vesicular trafficking, and can direct proteins specifically to distinct subcellular sites along actin and microtubule filament tracks (Nishimura and Sasaki, 2009). Targeted transport of proteins is a prerequisite for establishing junctions and apicobasal polarity. Rab proteins regulate the assembly and disassembly of epithelial apical junctions (Nishimura and Sasaki, 2009). Rab8, Rab13 and its binding partners junctional Rab13-binding protein (JRAB)/molecule interacting with CasL-like 2 (MICAL-L2) mediate the endocytosis and recycling of occludin and claudin-1. Thus, these proteins play a central role in the formation of functional TJs (Terai et al., 2006; Yamamura et al., 2008).

4.3. Cytoskeletal regulation of TJs

The cytoskeleton and specifically actomyosin-based contractility is well recognized as a mediator of physiological and pathological TJ regulation. Structural studies have demonstrated a close association between the TJs and the perijunctional actomyosin ring that is found at the border of the apical and lateral membrane (Rodgers and Fanning, 2011; Turner, 2000). Actin-binding scaffold proteins, such as ZO1–3 and the myosin-binding adapter cingulin connect the integral TJ proteins with the actomyosin ring (Rodgers and Fanning, 2011). Disruption of F-actin by drugs that inhibit actin polymerization, for example, cytochalasin B reduces TER (Meza et al., 1980) and decreases TJ strand numbers (Madara et al., 1986). Nevertheless, when actin is disrupted, the paracellular permeability pathway retains its size selectivity, suggesting that the effect is not due to a nonspecific loss of the barrier. Myosin-dependent contractility also regulates gate functions. Cell contractility is determined by the phosphorylation state of nonmuscle MLC (Fig. 6.5; Somlyo and Somlyo, 2003). Enhanced MLC phosphorylation elevates contractility. MLC phosphorylation in turn is regulated by two major pathways. The classical pathway involves Ca^{2+}-calmodulin-dependent activation of the myosin light chain kinase (MLCK) that phosphorylates MLC on threonine 18 and serine 19. The second pathway involves the small GTPase RhoA and its downstream effector ROK. ROK inhibits MLC phosphatase, thereby enhancing MLC phosphorylation. In addition, in some cells ROK was also found to directly phosphorylate MLC (Somlyo and Somlyo, 2003). Interestingly, experimental evidence suggests that the contribution of these two pathways to MLC phosphorylation is not the same in epithelial cells of different origin. MLCK is an important regulator of intestinal epithelial contractility (Cunningham and Turner, 2012), but in the kidney tubular cell lines LLC-PK_1 and MDCK MLC phosphorylation is predominantly mediated by the Rho–ROK pathway (Di Ciano-Oliveira et al., 2005; Szaszi et al., 2005). Irrespective of the upstream mechanisms however, the central role of myosin-mediated contractility in the regulation of epithelial permeability is supported by a large array of experimental data (Kapus and Szaszi, 2006; Turner, 2000). Increased MLC phosphorylation elevates paracellular permeability. Many stimuli, including pathogens and inflammatory cytokines increase paracellular permeability by altering myosin phosphorylation (Ivanov, 2008). In LLC-PK_1 cells expression of a dominant negative, non-phosphorylatable myosin prevented permeability rise induced by plasma

membrane potential changes and TNF-α (Kakiashvili et al., 2009; Waheed et al., 2010). The regulation of junctions however seems to require finely tuned MLC activity. Resting MLC phosphorylation is necessary for maintaining barrier and both a decrease and an increase in the level of phospho-MLC or RhoA activity can elevate permeability. In MDCK cells elimination of basal myosin activity by 2,3-butanedione monoxime, an inhibitor of myosin II ATPase induced marked increase in paracellular permeability (Castillo et al., 2002). On the other hand, sustained activation of RhoA and ROK, that leads to increased MLC phosphorylation, can enhance barrier functions in tubular cells (Martin-Martin et al., 2012).

Rac, cdc42, and RhoA, that are central regulators of actin polymerization and myosin phosphorylation, also play a key role not only in junction assembly, but also maintenance. Various signaling pathways converge on these proteins to induce alteration in junction functions. However, similar to contractility, both enhanced and reduced RhoA activity can lead to junction disruption (Hopkins et al., 2003; Jou et al., 1998; Miyake et al., 2006; Nusrat et al., 1995; Utech et al., 2005). Whether these effects are due to alterations in the actin cytoskeleton or myosin-mediated contractility, or both, remains to be established. Many of the junction-associated regulators of Rho proteins also affect junction maintenance. Depletion of two junction-associated Rho GEFs, GEF-H1, and p114RhoGEF caused an increase in paracellular permeability (Benais-Pont et al., 2003; Terry et al., 2011). p114RhoGEF forms a junction regulating signaling complex with cingulin, myosin IIA and ROK (Terry et al., 2011).

What is the molecular mechanism whereby phosphomyosin regulates the TJs? In principle, myosin may act as a force generating motor protein, and/or as an adapter and integrator of various permeability-altering inputs. Since alterations in myosin phosphorylation also affect the actin cytoskeleton, and vice versa, the effects of the above-described manipulations might be indirect.

Overall, whether acting directly, or through the actin cytoskeleton, myosin might control protein–protein interactions at the junctions, and/or endocytosis of transmembrane proteins. Indeed, there is evidence for both. The activity of MLCK that regulates myosin-dependent contractility was shown to affect the interaction between actin and junctional adapters. In addition, evidence is accumulating that contractility controls dynamic assembly/disassembly of the junctions, probably by affecting membrane trafficking of the junctional components. Stimulus-induced endocytosis of junction proteins was shown to be myosin-dependent (Hopkins et al.,

2003; Ivanov et al., 2004; Samarin et al., 2007; Schwarz et al., 2007; Shen, 2012; Shen et al., 2006). ROK also controls localization of TJ proteins, probably through the regulation of their endocytosis (Samarin et al., 2007; Walsh et al., 2001).

In transporting epithelia such as the intestinal cells and the kidney tubules, the cytoskeleton coordinates transcellular and paracellular flux. This mechanism ensures efficient transepithelial transport by preventing the buildup of inhibitory electrical and osmotic gradients, and allowing a paracellular pathway for enhanced transport of substances. This mechanism was first described in intestinal cells, where the activation of the apical Na^+-coupled glucose uptake was found to increase paracellular flux of water and solutes (Turner, 2000). This effect was mediated by enhanced contractility (Kapus and Szaszi, 2006; Turner, 2000). Such coupling also exists in kidney tubular cells: apical Na^+-coupled transporters enhance myosin phosphorylation and paracellular permeability in LLC-PK_1 cells (Waheed et al., 2010). While the central role of phosphomyosin was shown in both intestinal and tubular cells, the upstream mechanisms whereby apical transport elevates phosphomyosin differ in these two cell types. In intestinal cells p38 MAP kinase-induced, Na^+/H^+-exchanger-mediated alkalinization plays a central role, and leads to MLCK-dependent myosin phosphorylation. In tubular cells, myosin phosphorylation is induced through plasma membrane depolarization triggered by the electrogenic Na^+-cotransporters. Depolarization activates the Rho exchange factor GEF-H1 through an ERK-dependent mechanism and induces MLC phosphorylation through RhoA and ROK. Elevated contractility in turn mediates enhanced paracellular transport of small molecules (Szaszi et al., 2005; Waheed et al., 2010).

Taken together, the following general mode of myosin-dependent permeability increase has emerged. A multitude of pathways that affect TJs do so by altering the organization of the perijunctional actomyosin belt. Myosin phosphorylation is controlled through MLCK, and/or Rho/ROK, while the actin changes are mediated by Rho, Rac, and cdc42 activity. Remodeling of the perijunctional actomyosin alters trafficking of TJ proteins, increasing endocytosis and/or decreasing exocytosis. The end result is elevation in paracellular permeability (decrease in TER).

5. KIDNEY DISEASE AND TJs

Increased knowledge about the role of various TJ proteins in tubular transport allows us to gain new insight into their potential contribution to

diseases. Changes in TJ protein expression or function alter kidney ion and fluid handling, with important consequences for ion and fluid homeostasis. Indeed, mutations or genetic variants of claudins have already been associated with specific diseases. The tubular epithelium is also increasingly recognized as an active contributor to both acute kidney injury and chronic kidney disease (CKD). Since many pathological states, including inflammation and oxygen deprivation directly affect junctions, disruption of paracellular transport and signaling through the TJs is emerging as a key step in tubular pathology. Section 5.1 will provide an overview of the role of the TJs in kidney pathology.

5.1. Mutations affecting TJ functions in kidney

5.1.1 Claudin mutations and variants

In the past years, several disease-causing mutations in claudin genes have been characterized. We are now aware of two types of disease causing "claudinopathies": Familiar hypomagnesemia with hypercalciuria and nephrocalcinosis (FHHNC), and hypercalciuria associated with kidney stone disease. FHHNC is an autosomal recessive renal tubular disorder that is associated with disturbed Mg^{2+} and Ca^{2+} homeostasis. The disease usually presents with kidney stones, recurring urinary tract infections, polyuria, and polydipsia. It often also associates with convulsions and carpopedal spasm, a typical muscle spasm of the hands and feet due to tetany. It also causes early onset CKD (Benigno et al., 2000). The cause of this disease is a loss-of-function mutation in the CLDN16 (previously known as paracellin-1) or the CLDN19 gene that encode claudin-16 and -19, respectively. A number of different mutations of these two genes have been associated with the disease. Interestingly, in the subset of patients with mutations of CLDN19 the disease also involves visual impairment (Konrad et al., 2006). CLDN 16 and 19 knockout mice phenocopy the disease (Himmerkus et al., 2008; Hou et al., 2007, 2009; Shan et al., 2009). Initially claudin-16 and/or -19 were thought to form divalent cation-selective pores in the TAL, where the majority of Mg^{2+} reabsorption takes place. However, evidence from *in vitro* studies did not support this hypothesis (Hou et al., 2005, 2008). Instead, it seems likely that claudin-16 and 19 interact to form monovalent cation-selective channels, which are necessary for the generation of an electrochemical gradient that drives Mg^{2+} and Ca^{2+} reabsorption in the TAL.

Hypercalciuria is a major risk factor for Ca^{2+}-containing kidney stones. Recently, genome-wide association studies showed that common, synonymous variants in the CLDN14 gene confer risk of kidney stones and low

bone mineral density (Thorleifsson et al., 2009; Vezzoli et al., 2011). Claudin14 is expressed in the TAL (Ben-Yosef et al., 2003; Elkouby-Naor et al., 2008; Gong et al., 2012). When exposed to high Ca^{2+} dietary conditions, claudin-14 knockout animals develop hypermagnesaemia, hypomagnesiuria, and hypocalciuria. These findings substantiate a key role for claudin-14 in Ca^{2+} and Mg^{2+} homeostasis. Recently, claudin-14 was found to block the paracellular cation channel generated by claudin-16 and -19, suggesting that it regulates Ca^{2+} absorption through its effects on these claudins (Gong et al., 2012). In order to match Ca^{2+} excretion to changes in serum Ca^{2+} the kidneys alter Ca^{2+} reabsorption. This mechanism helps to maintain serum Ca^{2+} concentration within the normal range. Ca^{2+}-sensing receptors (CaSR) play an important role in regulating renal calcium reabsorption and calcium homeostasis. Under normal dietary conditions, the expression of claudin-14 in the TAL is suppressed by microRNAs. In a mouse model elevated serum Ca^{2+} was shown to induce a marked increase in claudin-14 mRNA in the kidneys. This effect required the CaSR, and resulted in elevated urinary Ca^{2+} excretion (Dimke et al., 2013). Taken together, an exciting mechanism is emerging that can fine-tune Ca^{2+} reabsorption/excretion. Activation of the CaSR in the TAL by elevated levels of Ca^{2+} in the serum and tubular filtrate stimulates claudin-14 expression. This is mediated at least in part through microRNAs. Claudin-14 in turn blocks the formation of cation channels generated by claudin-16 and -19, thereby reducing the electrochemical gradient for paracellular reabsorption of Ca^{2+}. This increases Ca^{2+} excretion, which can normalize serum Ca^{2+} levels. Disturbances in this fine control can increase urine Ca^{2+} levels that promotes kidney stone formation.

5.1.2 Pseudohypoaldosteronism type II

Mutations in the WNK4 gene cause pseudohypoaldosteronism type II (also known as Gordon syndrome), an autosomal-dominant disorder associated with hyperkalemia, hyperchloremic metabolic acidosis and hypertension. Two WNK kinases, WNK1 and WNK4 are predominantly expressed in the distal convoluted tubule and collecting duct. They regulate the activity of apical and paracellular ion transport pathways. Interestingly, claudins 1–4 are among the many identified targets of WNKs. Expression of WNK4 containing the disease-causing mutation in a tubular cell line resulted in enhanced claudin phosphorylation, indicating a possible gain-of-function effect, that likely contributes to altered transport processes (Yamauchi et al., 2004).

5.2. TJ and polarity changes caused by inflammation and ischemia–reperfusion

There is overwhelming evidence that inflammation is a major contributor to loss of function in acute kidney injury and CKD. Inflammation of the tubules and the surrounding interstitium is referred to as tubulointerstitial inflammation (TI) (or tubulointerstitial nephritis). This state involves focal tubular necrosis, interstitial edema, and infiltration of leukocytes into the interstitial space. As discussed later, inflammation also has a major effect on epithelial junctions. Acute and chronic TI evolves through an interplay between the epithelium and inflammatory cells, and is a self-augmenting pathological process, that can culminate in fibrosis (Fig. 6.6). Several inflammatory mediators play key roles in the generation and maintenance of TI. Importantly, the tubular cells are now recognized as both initiators and

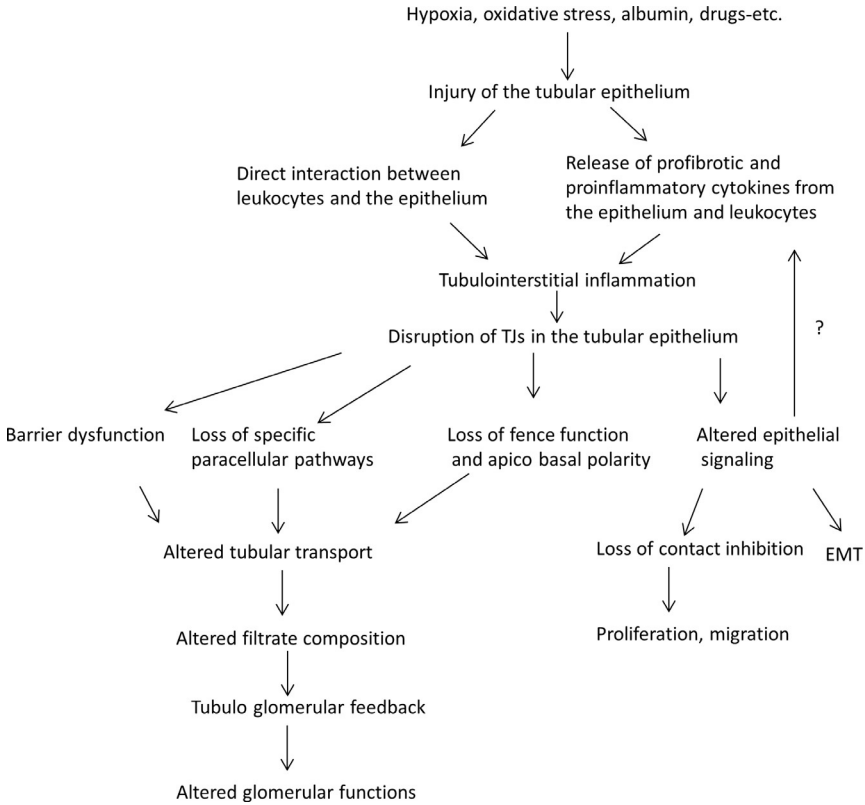

Figure 6.6 Mechanisms involved in the generation of TI and interstitial fibrosis, and epithelial–mesenchymal cross talk.

targets of inflammation. Many injury-causing factors can trigger inflammatory responses in the epithelium. One of the most common initiators of acute TI is ischemia–reperfusion injury, that often leads to acute renal failure, a condition that has high mortality to this day (Kinsey et al., 2008; Lu et al., 2012; Thurman, 2007). The renal tubules are very susceptible to hypoxic injury because of the high energy demands of their transport processes. Ischemia and experimental ATP depletion have been shown to disrupt the actin cytoskeleton and the junctional complexes in tubular cells, leading to loss of polarity (Gopalakrishnan et al., 1998; Kellerman and Bogusky, 1992; Molitoris, 2004; Tsukamoto and Nigam, 1999). Hypoxia and reactive oxidants are also potent triggers for the production of inflammatory cytokines by the tubular cells (Lee et al., 2011; Thurman, 2007). The tubular epithelium also expresses Toll-like receptors (TLR), a pattern recognition receptor family that regulates innate immune responses (Lu et al., 2012). These receptors are stimulated by danger-associated molecular pattern molecules (DAMPs) released by damaged tissues. Thus, TLRs can mediate the response to tissue injury, including hypoxic damage (Rosin and Okusa, 2011). Hypoxic injury also induces the expression of kidney injury protein-1 (KIM-1). This immunoglobulin family protein enhances phagocytosis of damaged cells by the epithelium (Ichimura et al., 2008), which further augments the inflammatory response. Yet another common and important factor that can trigger epithelial inflammation is albumin, which can be significant in nephropathies when glomerular damage causes proteinuria (Rodriguez-Iturbe and Garcia Garcia, 2010; Vallon, 2011). Irrespective of the trigger, inflammatory responses in the epithelium stimulate the production and release of chemokines and proinflammatory cytokines (Fig. 6.6). These act as chemoattractants for leukocytes. The infiltrating, activated leukocytes are also a rich source of various inflammatory mediators, and initiate a positive feedback that augments inflammation. In addition to affecting the epithelium through the released cytokines, leukocytes also directly interact with the tubular layer. Excessive leukocyte transmigration though the epithelial layer can lead to enhanced junction disruption due to several mechanisms. The interaction between leukocytes and the epithelium induces signaling pathways (e.g., leading to enhanced myosin phosphorylation) that can trigger disassembly of junctions (Schnoor and Parkos, 2008). Leukocytes can also release proteases that cleave junction components to promote transepithelial leukocyte migration.

In acute TI, the epithelial damage causes tubular dysfunction, and can culminate in renal failure. The tubular epithelium however has a high

regenerative capacity, and tubular functions may be restored. Inflammatory cytokines likely enhance regeneration too. As mentioned earlier, transmembrane TJ proteins might contribute to such regenerative processes through the regulation of proliferation and migration. Sustained, unresolved inflammation on the other hand contributes to the development of progressive interstitial fibrosis. Indeed, TI is increasingly recognized as an important early phase leading to the development of CKD. Regardless of its initial cause, CKD is characterized by tubulointerstitial fibrosis, during which the normal tissue is replaced by large amounts of extracellular matrix, reducing the number of functional nephrons. Importantly, the impairment of kidney function correlates well with the magnitude of the tubular damage. Overall, the process is progressive toward kidney failure and end-stage kidney disease.

Despite the importance of inflammation in kidney injury, the effect of cytokines on the TJs in the tubules is much less explored than in the intestinal epithelium, where inflammation has been recognized as a key pathogenic factor for a longer time. It is likely that the responses of tubular cells to inflammatory cytokines are in many aspects similar to those observed in the intestinal epithelium. In intestinal cells cytokines cause marked elevation in permeability, which is probably due to enhanced endocytosis of TJ proteins (Schulzke et al., 2009). Expression of various TJ proteins is also altered. However, due to the large variations in the composition and permeability properties of the TJs along the nephron, it is very likely that unique differences exist in the responses of various tubular segments. Also, although basic regulatory mechanisms, for example, the role of actin and myosin might be the same, specific differences clearly exist in some of the signaling mechanisms. For example, as mentioned earlier, in tubular cells ROK plays a larger role than MLCK. The specific responses of various tubular segments however remain to be established.

Studies using LLC-PK_1 and MDCK cell lines have shown that inflammatory cytokines including IFN-γ and TNF-α, as well as their combination cause complex responses. These cytokines were shown to induce an initial drop in TER, and enhanced paracellular permeability toward larger solutes, followed by an increase in TER (Kakiashvili et al., 2009; Lechner et al., 1999; Leone et al., 2007; Mullin et al., 1992; Patrick et al., 2006; Van Itallie et al., 2010). Interestingly, occludin plays a key role in modifying the sensitivity of the cells to the cytokines, probably due to its effects on caveolin-1 (Van Itallie et al., 2010). There is also evidence that inflammatory cytokines also affect the junctions in tubular cells through myosin. TNF-α-induced elevated

permeability of small molecular tracers in tubular cells was mediated by phosphomyosin that was induced through GEF-H1-dependent Rho/ROK activation (Kakiashvili et al., 2009). Interestingly, the TNF-α-induced activation of GEF-H1 was found to be mediated by the epidermal growth factor receptor (EGFR; Kakiashvili et al., 2009, 2011; Waheed et al., 2013). Indeed, transactivation of the EGFR is emerging as an important mechanism in kidney pathology. In addition to TNF-α, the fibrogenic peptide hormone angiotensin II, that plays a key role in CKD, was also found to activate the EGFR in tubular cells (Lautrette et al., 2005). Epidermal growth factor (EGF) family ligands on the other hand were shown to modulate TJ functions and composition. For example, in MDCK cells EGF alters claudin expression and elevates TER (Flores-Benitez et al., 2007; Ikari et al., 2011c; Singh et al., 2007).

Taken together, disruption of the junctions and particularly the TJs is emerging as a central step associated with tubular injury. Importantly, more work will be needed to entirely understand the underlying mechanisms.

5.3. Consequences of altered junction function in kidney epithelium

Disruption of the TJs could have multiple consequences, both beneficial and harmful. As a beneficial effect, cytokine-induced junction disruption might promote wound healing and regeneration of the epithelial layer (Waheed et al., 2013). However, the reduced paracellular barrier and/or lack of specific paracellular pathways could impair the effectiveness of the tubular transport processes, leading to back leak of the filtrate or reduced absorption of specific ions and solutes. The altered ion composition of the tubular filtrate in turn affects glomerular functions through the tubuloglomerular feedback mechanism (Fig. 6.6) (Lee et al., 2006a; Singh and Okusa, 2011). The disruption of the TJs also leads to the loss of the fence function and affects apicobasal polarity. Indeed, ischemia was shown to induce redistribution of apical proteins, including microvillar actin and villin to the basolateral membrane (Brown et al., 1997). Mislocalization of the basolateral Na^+–K^+ ATPase further impairs vectorial transport. Interestingly, correct targeting of the Na^+–K^+ ATPase was also shown to be necessary for TJ organization, and therefore mistargetting of this transporter might further augment junction disruption (Rajasekaran and Rajasekaran, 2003). Finally, the disruption of intercellular junctions can also affect junctional signaling. Since a number of signaling components and transcription factors are inhibited through sequestration at the junctions, their release can cause activation. Some of these effects might contribute to regeneration, for

example, through enhanced proliferation and migration. However, they might also further augment inflammatory responses, and can contribute to tumor formation. Importantly, as discussed in section 5.4, junction disruption has also emerged as an important input for epithelial plasticity and EMT.

5.4. Epithelial plasticity and EMT

Plasticity is a genetically determined property of epithelial cells, whereby they can lose their epithelial phenotype and acquire mesenchymal properties, such as increased motility. The best known role of this process is during rapid and effective monolayer repair after injury. Upon adequate stimuli epithelial cells can undergo EMT, or its more advanced form, epithelial–myofibroblast transition(Carew et al., 2012; Masszi and Kapus, 2011b). During EMT cells lose their epithelial characteristics, including junctions and apicobasal polarity, and acquire mesenchymal properties. They become matrix-producing, motile and contractile, apoptosis-resistant fibroblasts or myofibroblasts. EMT has been classified into three types based on the biological processes it is associated with. Accordingly, type 1 is developmental EMT, type 2 takes place during wound healing and may contribute to organ fibrosis, while type 3 is cancer EMT (Kalluri and Weinberg, 2009). EMT was suggested to play an important role in kidney fibrosis (Carew et al., 2012). The accumulation of myofibroblasts shows strong correlation with the severity and progression of fibrotic diseases. Myofibroblasts are thought to originate from multiple sources, including the tubular epithelium, although recent studies have questioned this paradigm (Quaggin and Kapus, 2011). EMT is induced by inflammatory cytokines and growth factors released by the injured epithelium and inflammatory cells. The most important such factor is transforming growth factor β1 (TGFβ1). EMT requires the activation/inactivation of a multitude of transcription factors and microRNAs that mediate the dramatic phenotypic change. The cytoskeleton and intercellular junctions undergo major remodeling, leading to loss of the perijunctional actomyosin ring. Stress fibers and peripheral F-actin branches become more pronounced. These structures also become positive for α-smooth muscle actin (SMA), an actin isoform typically absent from epithelial cells. The intermediate filaments undergo a cytokeratin-to-vimentin switch. The junctions are also dismantled, and expression of many junctional proteins decreases. E-cadherin transcription can be suppressed by repressor transcription factors including Snail, Zeb, E47, and KLF8, and

possibly Twist, as well as indirectly acting factors such as Goosecoid, E2.2, and FoxC2 (Burns and Thomas, 2010). Claudins and occludin are also suppressed in kidney tubular cell models of EMT (Carrozzino et al., 2005; Martinez-Estrada et al., 2006; Medici et al., 2006). Some of the listed transcription factors regulate the expression of claudins (Carrozzino et al., 2005; Ikenouchi et al., 2003; Martinez-Estrada et al., 2006; Medici et al., 2006; Ohkubo and Ozawa, 2004; Vincent et al., 2009). Junctional proteins might also be cleaved by various proteases, such as matrix metalloproteases (Bojarski et al., 2004; Lochter et al., 1997).

Importantly, the junctions seem to be not only targets, but also regulators of EMT. The presence of intact junctions is protective against TGFβ1-induced EMT (Masszi et al., 2004). Disruption of the junctions induces activation of the Rho/ROK and Rac/Pak pathways, which stimulates myocardin-related transcription factor (MRTF) that controls the expression of many cytoskeletal proteins including SMA (Fan et al., 2007; Masszi and Kapus, 2011a; Masszi et al., 2010; Sebe et al., 2008). Recent findings suggest that altered expression of TJ membrane proteins might also affect EMT. Overexpression of claudin-1 in liver cells induced the expression of the transcription factors Slug and Zeb1, thereby leading to EMT-like changes, including reduced E-cadherin and β-catenin and elevated N-cadherin and Vimentin expression (Suh et al., 2012). Although similar effects have not yet been demonstrated in tubular cells, the expression of some TJ proteins in the kidney is altered by conditions that promote fibrosis. For example, the immunosuppressant drugs cyclosporine A and sirolimus were shown to elevate claudin-1 and reduce claudin-2 expression in tubular cell lines (Martin-Martin et al., 2010, 2011, 2012). These drugs are used in combination to reduce transplant rejection, but were also found to promote tubular EMT and kidney fibrosis (McMorrow et al., 2005; Slattery et al., 2005). Expression of claudin-1 was also increased in an endotoxin-induced mouse acute kidney injury model, and in MDCK cells exposed to EGF. Conversely, claudin-1 is reduced by H_2O_2 treatment (Eadon et al., 2012; Gonzalez et al., 2009; Singh and Harris, 2004). Claudin-2 levels on the other hand are decreased by EGF, H_2O_2, and metabolic acidosis (Balkovetz et al., 2009; Gonzalez et al., 2009; Singh and Harris, 2004). Taken together, these findings point to the possibility that altered claudin levels might promote EMT and fibrosis.

Accumulating new data suggest that the epithelial–mesenchymal cross talk plays an even more important physiological and pathological role in the kidney than previously recognized. Most notably, mediators released from the injured epithelium have important effects on mesenchymal cells.

For example, profibrotic factors such as TGFβ1 were found to be released by the injured epithelium which can affect local pericytes to induce pericyte–myofibroblast transition (Wu et al., 2013). Disruption of the epithelial TJs could be an important trigger for such cross talk. Finally, it is also becoming increasingly clear that epithelial plasticity involves a full range of morphogenic changes. In fact, epithelial layers repair injured parts via the process of sheet migration, wherein cells migrate into a denuded area as a unit, and cells facing the intact areas maintain cell–cell contacts (Rorth, 2009; Szaszi et al., 2012). Moreover, cells adjacent to the injury site might undergo partial EMT. The regulation and the signaling events associated with such a partial loss of junctions remain largely unknown.

Future studies will be needed to explore the underlying mechanisms and the exact functional consequences of altered expression of various TJ proteins in the tubules.

6. CONCLUDING REMARKS

The past years have brought about a tremendous increase in our understanding of the structure, function, regulation, and physiological role of the TJs in the kidney tubules. The exciting new findings also raised many unanswered further questions. Future work will have to further address the correlation of the transport-specificity and capacity with expression and alterations in various claudins in different tubular segments. Another important question is whether cellular transport processes affect the paracellular transport other than influencing driving forces? TJs proteins also clearly affect each others expression, but the underlying mechanisms are unknown. We are now starting to recognize the role of "claudinopathies" in genetically inherited diseases. Having uncovered the central role of claudins in tubular transport, it will be exciting to see if claudin mutations are also associated with susceptibility to imbalances or dysregulation of ion and fluid homeostasis, including hypertension. Finally, it is increasingly likely that claudins and other TJ proteins can act as modulators/effectors of injury repair, epithelial plasticity and kidney fibrosis. Indeed, while much research has focused on the role of glomerular epithelial cells, that is, podocytes as the quintessential players in the pathogenesis of CKDs, the contribution of the tubules has so far been understudied and possibly underestimated. With the emerging role of TJ proteins in kidney disease pathogenesis, this aspect warrants reevaluation. Such a tubular and TJ-centered approach will likely uncover exciting new knowledge about the role of genetic and acquired "tubulopathies" in kidney diseases.

ACKNOWLEDGMENTS

This work was funded by the Kidney Foundation of Canada and the Natural Sciences and Engineering Research Council of Canada (NSERC). K. S. is a recipient of an Ontario Early Researcher Award. The authors would like to thank Dr. Andras Kapus for his helpful comments on the manuscript.

REFERENCES

Adachi, M., Inoko, A., Hata, M., Furuse, K., Umeda, K., Itoh, M., Tsukita, S., 2006. Normal establishment of epithelial tight junctions in mice and cultured cells lacking expression of ZO-3, a tight-junction MAGUK protein. Mol. Cell. Biol. 26, 9003–9015.

Adachi, M., Hamazaki, Y., Kobayashi, Y., Itoh, M., Tsukita, S., Furuse, M., 2009. Similar and distinct properties of MUPP1 and Patj, two homologous PDZ domain-containing tight-junction proteins. Mol. Cell. Biol. 29, 2372–2389.

Aijaz, S., D'Atri, F., Citi, S., Balda, M.S., Matter, K., 2005. Binding of GEF-H1 to the tight junction-associated adaptor cingulin results in inhibition of Rho signaling and G1/S phase transition. Dev. Cell 8, 777–786.

Alexandre, M.D., Lu, Q., Chen, Y.H., 2005. Overexpression of claudin-7 decreases the paracellular Cl- conductance and increases the paracellular Na+ conductance in LLC-PK1 cells. J. Cell Sci. 118, 2683–2693.

Amasheh, S., Meiri, N., Gitter, A.H., Schoneberg, T., Mankertz, J., Schulzke, J.D., Fromm, M., 2002. Claudin-2 expression induces cation-selective channels in tight junctions of epithelial cells. J. Cell Sci. 115, 4969–4976.

Amasheh, S., Milatz, S., Krug, S.M., Bergs, M., Amasheh, M., Schulzke, J.D., Fromm, M., 2009. Na+ absorption defends from paracellular back-leakage by claudin-8 upregulation. Biochem. Biophys. Res. Commun. 378, 45–50.

Anderson, J.M., Van Itallie, C.M., 2009. Physiology and function of the tight junction. Cold Spring Harb. Perspect. Biol. 1, a002584.

Angelow, S., Kim, K.J., Yu, A.S., 2006. Claudin-8 modulates paracellular permeability to acidic and basic ions in MDCK II cells. J. Physiol. 571, 15–26.

Angelow, S., El-Husseini, R., Kanzawa, S.A., Yu, A.S., 2007a. Renal localization and function of the tight junction protein, claudin-19. Am. J. Physiol. Renal Physiol. 293, F166–F177.

Angelow, S., Schneeberger, E.E., Yu, A.S., 2007b. Claudin-8 expression in renal epithelial cells augments the paracellular barrier by replacing endogenous claudin-2. J. Membr. Biol. 215, 147–159.

Angelow, S., Ahlstrom, R., Yu, A.S., 2008. Biology of claudins. Am. J. Physiol. Renal Physiol. 295, F867–F876.

Aronson, P.S., Giebisch, G., 1997. Mechanisms of chloride transport in the proximal tubule. Am. J. Physiol. 273, F179–F192.

Assemat, E., Bazellieres, E., Pallesi-Pocachard, E., Le Bivic, A., Massey-Harroche, D., 2008. Polarity complex proteins. Biochim. Biophys. Acta 1778, 614–630.

Balda, M.S., Matter, K., 2008. Tight junctions at a glance. J. Cell Sci. 121, 3677–3682.

Balda, M.S., Matter, K., 2009. Tight junctions and the regulation of gene expression. Biochim. Biophys. Acta 1788, 761–767.

Balda, M.S., Whitney, J.A., Flores, C., Gonzalez, S., Cereijido, M., Matter, K., 1996. Functional dissociation of paracellular permeability and transepithelial electrical resistance and disruption of the apical-basolateral intramembrane diffusion barrier by expression of a mutant tight junction membrane protein. J. Cell Biol. 134, 1031–1049.

Balda, M.S., Flores-Maldonado, C., Cereijido, M., Matter, K., 2000. Multiple domains of occludin are involved in the regulation of paracellular permeability. J. Cell. Biochem. 78, 85–96.

Balkovetz, D.F., 2009. Tight junction claudins and the kidney in sickness and in health. Biochim. Biophys. Acta 1788, 858–863.
Balkovetz, D.F., Chumley, P., Amlal, H., 2009. Downregulation of claudin-2 expression in renal epithelial cells by metabolic acidosis. Am. J. Physiol. Renal Physiol. 297, F604–F611.
Bamforth, S.D., Kniesel, U., Wolburg, H., Engelhardt, B., Risau, W., 1999. A dominant mutant of occludin disrupts tight junction structure and function. J. Cell Sci. 112 (Pt. 12), 1879–1888.
Bauer, H., Zweimueller-Mayer, J., Steinbacher, P., Lametschwandtner, A., Bauer, H.C., 2010. The dual role of zonula occludens (ZO) proteins. J. Biomed. Biotechnol. 2010, 402593.
Bazzoni, G., 2003. The JAM family of junctional adhesion molecules. Curr. Opin. Cell Biol. 15, 525–530.
Bazzoni, G., Martinez-Estrada, O.M., Orsenigo, F., Cordenonsi, M., Citi, S., Dejana, E., 2000. Interaction of junctional adhesion molecule with the tight junction components ZO-1, cingulin, and occludin. J. Biol. Chem. 275, 20520–20526.
Benais-Pont, G., Punn, A., Flores-Maldonado, C., Eckert, J., Raposo, G., Fleming, T.P., Cereijido, M., Balda, M.S., Matter, K., 2003. Identification of a tight junction-associated guanine nucleotide exchange factor that activates Rho and regulates paracellular permeability. J. Cell Biol. 160, 729–740.
Benigno, V., Canonica, C.S., Bettinelli, A., von Vigier, R.O., Truttmann, A.C., Bianchetti, M.G., 2000. Hypomagnesaemia-hypercalciuria-nephrocalcinosis: a report of nine cases and a review. Nephrol. Dial. Transplant. 15, 605–610.
Bens, M., Vandewalle, A., 2008. Cell models for studying renal physiology. Pflugers Arch. 457, 1–15.
Ben-Yosef, T., Belyantseva, I.A., Saunders, T.L., Hughes, E.D., Kawamoto, K., Van Itallie, C.M., Beyer, L.A., Halsey, K., Gardner, D.J., Wilcox, E.R., Rasmussen, J., Anderson, J.M., Dolan, D.F., Forge, A., Raphael, Y., Camper, S.A., Friedman, T.B., 2003. Claudin 14 knockout mice, a model for autosomal recessive deafness DFNB29, are deaf due to cochlear hair cell degeneration. Hum. Mol. Genet. 12, 2049–2061.
Berry, C.A., Rector Jr., F.C., 1978. Relative sodium-to-chloride permeability in the proximal convoluted tubule. Am. J. Physiol. 235, F592–F604.
Bojarski, C., Weiske, J., Schoneberg, T., Schroder, W., Mankertz, J., Schulzke, J.D., Florian, P., Fromm, M., Tauber, R., Huber, O., 2004. The specific fates of tight junction proteins in apoptotic epithelial cells. J. Cell Sci. 117, 2097–2107.
Borovac, J., Barker, R.S., Rievaj, J., Rasmussen, A., Pan, W., Wevrick, R., Alexander, R.T., 2012. Claudin-4 forms a paracellular barrier, revealing the interdependence of claudin expression in the loose epithelial cell culture model opossum kidney cells. Am. J. Physiol. Cell Physiol. 303, C1278–C1291.
Braga, V.M., Machesky, L.M., Hall, A., Hotchin, N.A., 1997. The small GTPases Rho and Rac are required for the establishment of cadherin-dependent cell-cell contacts. J. Cell Biol. 137, 1421–1431.
Brown, D., Lee, R., Bonventre, J.V., 1997. Redistribution of villin to proximal tubule basolateral membranes after ischemia and reperfusion. Am. J. Physiol. 273, F1003–F1012.
Bruewer, M., Utech, M., Ivanov, A.I., Hopkins, A.M., Parkos, C.A., Nusrat, A., 2005. Interferon-gamma induces internalization of epithelial tight junction proteins via a macropinocytosis-like process. FASEB J. 19, 923–933.
Burns, W.C., Thomas, M.C., 2010. The molecular mediators of type 2 epithelial to mesenchymal transition (EMT) and their role in renal pathophysiology. Expert Rev. Mol. Med. 12, e17.
Capaldo, C.T., Nusrat, A., 2009. Cytokine regulation of tight junctions. Biochim. Biophys. Acta 1788, 864–871.

Capaldo, C.T., Koch, S., Kwon, M., Laur, O., Parkos, C.A., Nusrat, A., 2011. Tight function zonula occludens-3 regulates cyclin D1-dependent cell proliferation. Mol. Biol. Cell 22, 1677–1685.
Carew, R.M., Wang, B., Kantharidis, P., 2012. The role of EMT in renal fibrosis. Cell Tissue Res. 347, 103–116.
Carraway, C.A., Carraway, K.L., 2007. Sequestration and segregation of receptor kinases in epithelial cells: implications for ErbB2 oncogenesis. Sci. STKE 2007, re3.
Carrozzino, F., Soulie, P., Huber, D., Mensi, N., Orci, L., Cano, A., Feraille, E., Montesano, R., 2005. Inducible expression of Snail selectively increases paracellular ion permeability and differentially modulates tight junction proteins. Am. J. Physiol. Cell Physiol. 289, C1002–C1014.
Castillo, A.M., Reyes, J.L., Sanchez, E., Mondragon, R., Meza, I., 2002. 2,3-butanedione monoxime (BDM), a potent inhibitor of actin-myosin interaction, induces ion and fluid transport in MDCK monolayers. J. Muscle Res. Cell Motil. 23, 223–234.
Chalmers, A.D., Whitley, P., 2012. Continuous endocytic recycling of tight junction proteins: how and why? Essays Biochem. 53, 41–54.
Chen, X., Macara, I.G., 2005. Par-3 controls tight junction assembly through the Rac exchange factor Tiam1. Nat. Cell Biol. 7, 262–269.
Cherfils, J., Zeghouf, M., 2013. Regulation of small GTPases by GEFs, GAPs, and GDIs. Physiol. Rev. 93, 269–309.
Chiba, H., Osanai, M., Murata, M., Kojima, T., Sawada, N., 2008. Transmembrane proteins of tight junctions. Biochim. Biophys. Acta 1778, 588–600.
Citi, S., Pulimeno, P., Paschoud, S., 2012. Cingulin, paracingulin, and PLEKHA7: signaling and cytoskeletal adaptors at the apical junctional complex. Ann. N. Y. Acad. Sci. 1257, 125–132.
Claude, P., 1978. Morphological factors influencing transepithelial permeability: a model for the resistance of the zonula occludens. J. Membr. Biol. 39, 219–232.
Claude, P., Goodenough, D.A., 1973. Fracture faces of zonulae occludentes from "tight" and "leaky" epithelia. J. Cell Biol. 58, 390–400.
Colegio, O.R., Van Itallie, C.M., McCrea, H.J., Rahner, C., Anderson, J.M., 2002. Claudins create charge-selective channels in the paracellular pathway between epithelial cells. Am. J. Physiol. Cell Physiol. 283, C142–C147.
Cordenonsi, M., D'Atri, F., Hammar, E., Parry, D.A., Kendrick-Jones, J., Shore, D., Citi, S., 1999. Cingulin contains globular and coiled-coil domains and interacts with ZO-1, ZO-2, ZO-3, and myosin. J. Cell Biol. 147, 1569–1582.
Cording, J., Berg, J., Kading, N., Bellmann, C., Tscheik, C., Westphal, J.K., Milatz, S., Gunzel, D., Wolburg, H., Piontek, J., Huber, O., Blasig, I.E., 2012. In tight junctions claudins regulate the interactions between occludin, tricellulin and marvelD3, which, inversely, modulate claudin oligomerization. J. Cell Sci. 126, 554–564.
Coyne, C.B., Bergelson, J.M., 2005. CAR: a virus receptor within the tight junction. Adv. Drug Deliv. Rev. 57, 869–882.
Cummins, P.M., 2012. Occludin: one protein, many forms. Mol. Cell. Biol. 32, 242–250.
Cunningham, K.E., Turner, J.R., 2012. Myosin light chain kinase: pulling the strings of epithelial tight junction function. Ann. N. Y. Acad. Sci. 1258, 34–42.
Delva, E., Tucker, D.K., Kowalczyk, A.P., 2009. The desmosome. Cold Spring Harb. Perspect. Biol. 1, a002543.
Di Ciano-Oliveira, C., Lodyga, M., Fan, L., Szaszi, K., Hosoya, H., Rotstein, O.D., Kapus, A., 2005. Is myosin light-chain phosphorylation a regulatory signal for the osmotic activation of the Na+-K+-2Cl- cotransporter? Am. J. Physiol. Cell Physiol. 289, C68–C81.
Dimke, H., Desai, P., Borovac, J., Lau, A., Pan, W., Alexander, R.T., 2013. Activation of the Ca2+-sensing receptor increases renal claudin-14 expression and urinary Ca2+ excretion. Am. J. Physiol. Renal Physiol. 304, F761–F769.

Dorfel, M.J., Huber, O., 2012. A phosphorylation hotspot within the occludin C-terminal domain. Ann. N. Y. Acad. Sci. 1257, 38–44.
Dow, L.E., Humbert, P.O., 2007. Polarity regulators and the control of epithelial architecture, cell migration, and tumorigenesis. Int. Rev. Cytol. 262, 253–302.
Dukes, J.D., Whitley, P., Chalmers, A.D., 2011. The MDCK variety pack: choosing the right strain. BMC Cell Biol. 12, 43.
Eadon, M.T., Hack, B.K., Xu, C., Ko, B., Toback, F.G., Cunningham, P.N., 2012. Endotoxemia alters tight junction gene and protein expression in the kidney. Am. J. Physiol. Renal Physiol. 303, F821–F830.
Ebnet, K., Suzuki, A., Horikoshi, Y., Hirose, T., Meyer Zu Brickwedde, M.K., Ohno, S., Vestweber, D., 2001. The cell polarity protein ASIP/PAR-3 directly associates with junctional adhesion molecule (JAM). EMBO J. 20, 3738–3748.
Ehrlich, J.S., Hansen, M.D., Nelson, W.J., 2002. Spatio-temporal regulation of Rac1 localization and lamellipodia dynamics during epithelial cell-cell adhesion. Dev. Cell 3, 259–270.
Elias, B.C., Suzuki, T., Seth, A., Giorgianni, F., Kale, G., Shen, L., Turner, J.R., Naren, A., Desiderio, D.M., Rao, R., 2009. Phosphorylation of Tyr-398 and Tyr-402 in occludin prevents its interaction with ZO-1 and destabilizes its assembly at the tight junctions. J. Biol. Chem. 284, 1559–1569.
Elkouby-Naor, L., Abassi, Z., Lagziel, A., Gow, A., Ben-Yosef, T., 2008. Double gene deletion reveals lack of cooperation between claudin 11 and claudin 14 tight junction proteins. Cell Tissue Res. 333, 427–438.
Enck, A.H., Berger, U.V., Yu, A.S., 2001. Claudin-2 is selectively expressed in proximal nephron in mouse kidney. Am. J. Physiol. Renal Physiol. 281, F966–F974.
Escudero-Esparza, A., Jiang, W.G., Martin, T.A., 2011. The Claudin family and its role in cancer and metastasis. Front. Biosci. 16, 1069–1083.
Fan, L., Sebe, A., Peterfi, Z., Masszi, A., Thirone, A.C., Rotstein, O.D., Nakano, H., McCulloch, C.A., Szaszi, K., Mucsi, I., Kapus, A., 2007. Cell contact-dependent regulation of epithelial-myofibroblast transition via the rho-rho kinase-phospho-myosin pathway. Mol. Biol. Cell 18, 1083–1097.
Fanning, A.S., Anderson, J.M., 2009. Zonula occludens-1 and -2 are cytosolic scaffolds that regulate the assembly of cellular junctions. Ann. N. Y. Acad. Sci. 1165, 113–120.
Farkas, A.E., Capaldo, C.T., Nusrat, A., 2012. Regulation of epithelial proliferation by tight junction proteins. Ann. N. Y. Acad. Sci. 1258, 115–124.
Farquhar, M.G., Palade, G.E., 1963. Junctional complexes in various epithelia. J. Cell Biol. 17, 375–412.
Feldman, G.J., Mullin, J.M., Ryan, M.P., 2005. Occludin: structure, function and regulation. Adv. Drug Deliv. Rev. 57, 883–917.
Fisher, H.W., Yeh, J., 1967. Contact inhibition in colony formation. Science 155, 581–582.
Flores-Benitez, D., Ruiz-Cabrera, A., Flores-Maldonado, C., Shoshani, L., Cereijido, M., Contreras, R.G., 2007. Control of tight junctional sealing: role of epidermal growth factor. Am. J. Physiol. Renal Physiol. 292, F828–F836.
Fujita, K., Katahira, J., Horiguchi, Y., Sonoda, N., Furuse, M., Tsukita, S., 2000. Clostridium perfringens enterotoxin binds to the second extracellular loop of claudin-3, a tight junction integral membrane protein. FEBS Lett. 476, 258–261.
Furuse, M., 2009. Knockout animals and natural mutations as experimental and diagnostic tool for studying tight junction functions in vivo. Biochim. Biophys. Acta 1788, 813–819.
Furuse, M., 2010. Molecular basis of the core structure of tight junctions. Cold Spring Harb. Perspect. Biol. 2, a002907.
Furuse, M., Hirase, T., Itoh, M., Nagafuchi, A., Yonemura, S., Tsukita, S., 1993. Occludin: a novel integral membrane protein localizing at tight junctions. J. Cell Biol. 123, 1777–1788.

Furuse, M., Fujimoto, K., Sato, N., Hirase, T., Tsukita, S., 1996. Overexpression of occludin, a tight junction-associated integral membrane protein, induces the formation of intracellular multilamellar bodies bearing tight junction-like structures. J. Cell Sci. 109 (Pt. 2), 429–435.

Furuse, M., Fujita, K., Hiiragi, T., Fujimoto, K., Tsukita, S., 1998a. Claudin-1 and -2: novel integral membrane proteins localizing at tight junctions with no sequence similarity to occludin. J. Cell Biol. 141, 1539–1550.

Furuse, M., Sasaki, H., Fujimoto, K., Tsukita, S., 1998b. A single gene product, claudin-1 or -2, reconstitutes tight junction strands and recruits occludin in fibroblasts. J. Cell Biol. 143, 391–401.

Furuse, M., Furuse, K., Sasaki, H., Tsukita, S., 2001. Conversion of zonulae occludentes from tight to leaky strand type by introducing claudin-2 into Madin-Darby canine kidney I cells. J. Cell Biol. 153, 263–272.

Furuse, M., Oda, Y., Higashi, T., Iwamoto, N., Masuda, S., 2012. Lipolysis-stimulated lipoprotein receptor: a novel membrane protein of tricellular tight junctions. Ann. N. Y. Acad. Sci. 1257, 54–58.

Gamba, G., 2005. Role of WNK kinases in regulating tubular salt and potassium transport and in the development of hypertension. Am. J. Physiol. Renal Physiol. 288, F245–F252.

Genevet, A., Tapon, N., 2011. The Hippo pathway and apico-basal cell polarity. Biochem. J. 436, 213–224.

Gong, Y., Renigunta, V., Himmerkus, N., Zhang, J., Renigunta, A., Bleich, M., Hou, J., 2012. Claudin-14 regulates renal Ca(+)(+) transport in response to CaSR signalling via a novel microRNA pathway. EMBO J. 31, 1999–2012.

Gonzalez, J.E., DiGeronimo, R.J., Arthur, D.E., King, J.M., 2009. Remodeling of the tight junction during recovery from exposure to hydrogen peroxide in kidney epithelial cells. Free Radic. Biol. Med. 47, 1561–1569.

Gonzalez-Mariscal, L., Namorado Mdel, C., Martin, D., Sierra, G., Reyes, J.L., 2006. The tight junction proteins claudin-7 and -8 display a different subcellular localization at Henle's loops and collecting ducts of rabbit kidney. Nephrol. Dial. Transplant. 21, 2391–2398.

Gonzalez-Mariscal, L., Tapia, R., Chamorro, D., 2008. Crosstalk of tight junction components with signaling pathways. Biochim. Biophys. Acta 1778, 729–756.

Gonzalez-Mariscal, L., Tapia, R., Huerta, M., Lopez-Bayghen, E., 2009. The tight junction protein ZO-2 blocks cell cycle progression and inhibits cyclin D1 expression. Ann. N. Y. Acad. Sci. 1165, 121–125.

Gonzalez-Mariscal, L., Bautista, P., Lechuga, S., Quiros, M., 2012. ZO-2, a tight junction scaffold protein involved in the regulation of cell proliferation and apoptosis. Ann. N. Y. Acad. Sci. 1257, 133–141.

Gopalakrishnan, S., Raman, N., Atkinson, S.J., Marrs, J.A., 1998. Rho GTPase signaling regulates tight junction assembly and protects tight junctions during ATP depletion. Am. J. Physiol. 275, C798–C809.

Gu, J.M., Lim, S.O., Park, Y.M., Jung, G., 2008. A novel splice variant of occludin deleted in exon 9 and its role in cell apoptosis and invasion. FEBS J. 275, 3145–3156.

Guillemot, L., Paschoud, S., Jond, L., Foglia, A., Citi, S., 2008a. Paracingulin regulates the activity of Rac1 and RhoA GTPases by recruiting Tiam1 and GEF-H1 to epithelial junctions. Mol. Biol. Cell 19, 4442–4453.

Guillemot, L., Paschoud, S., Pulimeno, P., Foglia, A., Citi, S., 2008b. The cytoplasmic plaque of tight junctions: a scaffolding and signalling center. Biochim. Biophys. Acta 1778, 601–613.

Gumbiner, B., Lowenkopf, T., Apatira, D., 1991. Identification of a 160-kDa polypeptide that binds to the tight junction protein ZO-1. Proc. Natl. Acad. Sci. U.S.A. 88, 3460–3464.

Gunzel, D., Yu, A.S., 2009. Function and regulation of claudins in the thick ascending limb of Henle. Pflugers Arch. 458, 77–88.
Gunzel, D., Stuiver, M., Kausalya, P.J., Haisch, L., Krug, S.M., Rosenthal, R., Meij, I.C., Hunziker, W., Fromm, M., Muller, D., 2009. Claudin-10 exists in six alternatively spliced isoforms that exhibit distinct localization and function. J. Cell Sci. 122, 1507–1517.
Gunzel, D., Zakrzewski, S.S., Schmid, T., Pangalos, M., Wiedenhoeft, J., Blasse, C., Ozboda, C., Krug, S.M., 2012. From TER to trans- and paracellular resistance: lessons from impedance spectroscopy. Ann. N. Y. Acad. Sci. 1257, 142–151.
Hall, A., 2005. Rho GTPases and the control of cell behaviour. Biochem. Soc. Trans. 33, 891–895.
Hartsock, A., Nelson, W.J., 2008. Adherens and tight junctions: structure, function and connections to the actin cytoskeleton. Biochim. Biophys. Acta 1778, 660–669.
Harvey, K.F., Hariharan, I.K., 2012. The hippo pathway. Cold Spring Harb. Perspect. Biol. 4, a011288.
Haskins, J., Gu, L., Wittchen, E.S., Hibbard, J., Stevenson, B.R., 1998. ZO-3, a novel member of the MAGUK protein family found at the tight junction, interacts with ZO-1 and occludin. J. Cell Biol. 141, 199–208.
Himmerkus, N., Shan, Q., Goerke, B., Hou, J., Goodenough, D.A., Bleich, M., 2008. Salt and acid-base metabolism in claudin-16 knockdown mice: impact for the pathophysiology of FHHNC patients. Am. J. Physiol. Renal Physiol. 295, F1641–F1647.
Hopkins, A.M., Walsh, S.V., Verkade, P., Boquet, P., Nusrat, A., 2003. Constitutive activation of Rho proteins by CNF-1 influences tight junction structure and epithelial barrier function. J. Cell Sci. 116, 725–742.
Hou, J., 2012. Regulation of paracellular transport in the distal nephron. Curr. Opin. Nephrol. Hypertens. 21, 547–551.
Hou, J., Goodenough, D.A., 2010. Claudin-16 and claudin-19 function in the thick ascending limb. Curr. Opin. Nephrol. Hypertens. 19, 483–488.
Hou, J., Paul, D.L., Goodenough, D.A., 2005. Paracellin-1 and the modulation of ion selectivity of tight junctions. J. Cell Sci. 118, 5109–5118.
Hou, J., Gomes, A.S., Paul, D.L., Goodenough, D.A., 2006. Study of claudin function by RNA interference. J. Biol. Chem. 281, 36117–36123.
Hou, J., Shan, Q., Wang, T., Gomes, A.S., Yan, Q., Paul, D.L., Bleich, M., Goodenough, D.A., 2007. Transgenic RNAi depletion of claudin-16 and the renal handling of magnesium. J. Biol. Chem. 282, 17114–17122.
Hou, J., Renigunta, A., Konrad, M., Gomes, A.S., Schneeberger, E.E., Paul, D.L., Waldegger, S., Goodenough, D.A., 2008. Claudin-16 and claudin-19 interact and form a cation-selective tight junction complex. J. Clin. Invest. 118, 619–628.
Hou, J., Renigunta, A., Gomes, A.S., Hou, M., Paul, D.L., Waldegger, S., Goodenough, D.A., 2009. Claudin-16 and claudin-19 interaction is required for their assembly into tight junctions and for renal reabsorption of magnesium. Proc. Natl. Acad. Sci. U.S.A. 106, 15350–15355.
Hou, J., Renigunta, A., Yang, J., Waldegger, S., 2010. Claudin-4 forms paracellular chloride channel in the kidney and requires claudin-8 for tight junction localization. Proc. Natl. Acad. Sci. U.S.A. 107, 18010–18015.
Hou, J., Rajagopal, M., Yu, A.S., 2012. Claudins and the kidney. Annu. Rev. Physiol. 75, 479–501.
Huber, D., Balda, M.S., Matter, K., 2000. Occludin modulates transepithelial migration of neutrophils. J. Biol. Chem. 275, 5773–5778.
Huerta, M., Munoz, R., Tapia, R., Soto-Reyes, E., Ramirez, L., Recillas-Targa, F., Gonzalez-Mariscal, L., Lopez-Bayghen, E., 2007. Cyclin D1 is transcriptionally down-regulated by ZO-2 via an E box and the transcription factor c-Myc. Mol. Biol. Cell 18, 4826–4836.

Ichimura, T., Asseldonk, E.J., Humphreys, B.D., Gunaratnam, L., Duffield, J.S., Bonventre, J.V., 2008. Kidney injury molecule-1 is a phosphatidylserine receptor that confers a phagocytic phenotype on epithelial cells. J. Clin. Invest. 118, 1657–1668.

Ikari, A., Sato, T., Takiguchi, A., Atomi, K., Yamazaki, Y., Sugatani, J., 2011a. Claudin-2 knockdown decreases matrix metalloproteinase-9 activity and cell migration via suppression of nuclear Sp1 in A549 cells. Life Sci. 88, 628–633.

Ikari, A., Takiguchi, A., Atomi, K., Sato, T., Sugatani, J., 2011b. Decrease in claudin-2 expression enhances cell migration in renal epithelial Madin-Darby canine kidney cells. J. Cell. Physiol. 226, 1471–1478.

Ikari, A., Takiguchi, A., Atomi, K., Sugatani, J., 2011c. Epidermal growth factor increases clathrin-dependent endocytosis and degradation of claudin-2 protein in MDCK II cells. J. Cell. Physiol. 226, 2448–2456.

Ikenouchi, J., Matsuda, M., Furuse, M., Tsukita, S., 2003. Regulation of tight junctions during the epithelium-mesenchyme transition: direct repression of the gene expression of claudins/occludin by Snail. J. Cell Sci. 116, 1959–1967.

Ikenouchi, J., Furuse, M., Furuse, K., Sasaki, H., Tsukita, S., 2005. Tricellulin constitutes a novel barrier at tricellular contacts of epithelial cells. J. Cell Biol. 171, 939–945.

Ikenouchi, J., Sasaki, H., Tsukita, S., Furuse, M., 2008. Loss of occludin affects tricellular localization of tricellulin. Mol. Biol. Cell 19, 4687–4693.

Itoh, M., Tsukita, S., Yamazaki, Y., Sugimoto, H., 2012. Rho GTP exchange factor ARHGEF11 regulates the integrity of epithelial junctions by connecting ZO-1 and RhoA-myosin II signaling. Proc. Natl. Acad. Sci. U.S.A. 109, 9905–9910.

Ivanov, A.I., 2008. Actin motors that drive formation and disassembly of epithelial apical junctions. Front. Biosci. 13, 6662–6681.

Ivanov, A.I., McCall, I.C., Parkos, C.A., Nusrat, A., 2004. Role for actin filament turnover and a myosin II motor in cytoskeleton-driven disassembly of the epithelial apical junctional complex. Mol. Biol. Cell 15, 2639–2651.

Ivanov, A.I., Nusrat, A., Parkos, C.A., 2005. Endocytosis of the apical junctional complex: mechanisms and possible roles in regulation of epithelial barriers. Bioessays 27, 356–365.

Jaffe, A.B., Hall, A., 2005. Rho GTPases: biochemistry and biology. Annu. Rev. Cell Dev. Biol. 21, 247–269.

Jain, S., Suzuki, T., Seth, A., Samak, G., Rao, R., 2011. Protein kinase Czeta phosphorylates occludin and promotes assembly of epithelial tight junctions. Biochem. J. 437, 289–299.

Jou, T.S., Schneeberger, E.E., Nelson, W.J., 1998. Structural and functional regulation of tight junctions by RhoA and Rac1 small GTPases. J. Cell Biol. 142, 101–115.

Kakiashvili, E., Speight, P., Waheed, F., Seth, R., Lodyga, M., Tanimura, S., Kohno, M., Rotstein, O.D., Kapus, A., Szaszi, K., 2009. GEF-H1 mediates tumor necrosis factor-{alpha}-induced Rho activation and myosin phosphorylation: role in the regulation of tubular paracellular permeability. J. Biol. Chem. 284, 11454–11466.

Kakiashvili, E., Dan, Q., Vandermeer, M., Zhang, Y., Waheed, F., Pham, M., Szaszi, K., 2011. The epidermal growth factor receptor mediates tumor necrosis factor-alpha-induced activation of the ERK/GEF-H1/RhoA pathway in tubular epithelium. J. Biol. Chem. 286, 9268–9279.

Kalluri, R., Weinberg, R.A., 2009. The basics of epithelial-mesenchymal transition. J. Clin. Invest. 119, 1420–1428.

Kapus, A., Szaszi, K., 2006. Coupling between apical and paracellular transport processes. Biochem. Cell Biol. 84, 870–880.

Katsuno, T., Umeda, K., Matsui, T., Hata, M., Tamura, A., Itoh, M., Takeuchi, K., Fujimori, T., Nabeshima, Y., Noda, T., Tsukita, S., 2008. Deficiency of zonula occludens-1 causes embryonic lethal phenotype associated with defected yolk sac angiogenesis and apoptosis of embryonic cells. Mol. Biol. Cell 19, 2465–2475.

Kavanagh, E., Buchert, M., Tsapara, A., Choquet, A., Balda, M.S., Hollande, F., Matter, K., 2006. Functional interaction between the ZO-1-interacting transcription factor ZONAB/DbpA and the RNA processing factor symplekin. J. Cell Sci. 119, 5098–5105.

Kellerman, P.S., Bogusky, R.T., 1992. Microfilament disruption occurs very early in ischemic proximal tubule cell injury. Kidney Int. 42, 896–902.

Keon, B.H., Schafer, S., Kuhn, C., Grund, C., Franke, W.W., 1996. Symplekin, a novel type of tight junction plaque protein. J. Cell Biol. 134, 1003–1018.

Kim, S.K., 2000. Cell polarity: new PARtners for Cdc42 and Rac. Nat. Cell Biol. 2, E143–E145.

Kinsey, G.R., Li, L., Okusa, M.D., 2008. Inflammation in acute kidney injury. Nephron Exp. Nephrol. 109, e102–e107.

Kirk, A., Campbell, S., Bass, P., Mason, J., Collins, J., 2010. Differential expression of claudin tight junction proteins in the human cortical nephron. Nephrol. Dial. Transplant. 25, 2107–2119.

Kiuchi-Saishin, Y., Gotoh, S., Furuse, M., Takasuga, A., Tano, Y., Tsukita, S., 2002. Differential expression patterns of claudins, tight junction membrane proteins, in mouse nephron segments. J. Am. Soc. Nephrol. 13, 875–886.

Knipp, G.T., Ho, N.F., Barsuhn, C.L., Borchardt, R.T., 1997. Paracellular diffusion in Caco-2 cell monolayers: effect of perturbation on the transport of hydrophilic compounds that vary in charge and size. J. Pharm. Sci. 86, 1105–1110.

Konrad, M., Schaller, A., Seelow, D., Pandey, A.V., Waldegger, S., Lesslauer, A., Vitzthum, H., Suzuki, Y., Luk, J.M., Becker, C., Schlingmann, K.P., Schmid, M., Rodriguez-Soriano, J., Ariceta, G., Cano, F., Enriquez, R., Juppner, H., Bakkaloglu, S.A., Hediger, M.A., Gallati, S., Neuhauss, S.C., Nurnberg, P., Weber, S., 2006. Mutations in the tight-junction gene claudin 19 (CLDN19) are associated with renal magnesium wasting, renal failure, and severe ocular involvement. Am. J. Hum. Genet. 79, 949–957.

Krause, G., Winkler, L., Mueller, S.L., Haseloff, R.F., Piontek, J., Blasig, I.E., 2008. Structure and function of claudins. Biochim. Biophys. Acta 1778, 631–645.

Krug, S.M., Amasheh, S., Richter, J.F., Milatz, S., Gunzel, D., Westphal, J.K., Huber, O., Schulzke, J.D., Fromm, M., 2009a. Tricellulin forms a barrier to macromolecules in tricellular tight junctions without affecting ion permeability. Mol. Biol. Cell 20, 3713–3724.

Krug, S.M., Fromm, M., Gunzel, D., 2009b. Two-path impedance spectroscopy for measuring paracellular and transcellular epithelial resistance. Biophys. J. 97, 2202–2211.

Krug, S.M., Gunzel, D., Conrad, M.P., Rosenthal, R., Fromm, A., Amasheh, S., Schulzke, J.D., Fromm, M., 2012. Claudin-17 forms tight junction channels with distinct anion selectivity. Cell. Mol. Life Sci. 69, 2765–2778.

Lal-Nag, M., Morin, P.J., 2009. The claudins. Genome Biol. 10, 235.

Laukoetter, M.G., Nava, P., Lee, W.Y., Severson, E.A., Capaldo, C.T., Babbin, B.A., Williams, I.R., Koval, M., Peatman, E., Campbell, J.A., Dermody, T.S., Nusrat, A., Parkos, C.A., 2007. JAM-A regulates permeability and inflammation in the intestine in vivo. J. Exp. Med. 204, 3067–3076.

Lautrette, A., Li, S., Alili, R., Sunnarborg, S.W., Burtin, M., Lee, D.C., Friedlander, G., Terzi, F., 2005. Angiotensin II and EGF receptor cross-talk in chronic kidney diseases: a new therapeutic approach. Nat. Med. 11, 867–874.

Lechner, J., Krall, M., Netzer, A., Radmayr, C., Ryan, M.P., Pfaller, W., 1999. Effects of interferon alpha-2b on barrier function and junctional complexes of renal proximal tubular LLC-PK1 cells. Kidney Int. 55, 2178–2191.

Lee, H.J., Zheng, J.J., 2010. PDZ domains and their binding partners: structure, specificity, and modification. Cell Commun. Signal 8, 8.

Lee, D.B., Huang, E., Ward, H.J., 2006a. Tight junction biology and kidney dysfunction. Am. J. Physiol. Renal Physiol. 290, F20–F34.
Lee, N.P., Tong, M.K., Leung, P.P., Chan, V.W., Leung, S., Tam, P.C., Chan, K.W., Lee, K.F., Yeung, W.S., Luk, J.M., 2006b. Kidney claudin-19: localization in distal tubules and collecting ducts and dysregulation in polycystic renal disease. FEBS Lett. 580, 923–931.
Lee, J.W., Hsiao, W.T., Chen, H.Y., Hsu, L.P., Chen, P.R., Lin, M.D., Chiu, S.J., Shih, W.L., Hsu, Y.C., 2010. Upregulated claudin-1 expression confers resistance to cell death of nasopharyngeal carcinoma cells. Int. J. Cancer 126, 1353–1366.
Lee, D.W., Faubel, S., Edelstein, C.L., 2011. Cytokines in acute kidney injury (AKI). Clin. Nephrol. 76, 165–173.
Leone, A.K., Chun, J.A., Koehler, C.L., Caranto, J., King, J.M., 2007. Effect of proinflammatory cytokines, tumor necrosis factor-alpha and interferon-gamma on epithelial barrier function and matrix metalloproteinase-9 in Madin Darby canine kidney cells. Cell. Physiol. Biochem. 19, 99–112.
Li, W.Y., Huey, C.L., Yu, A.S., 2004. Expression of claudin-7 and -8 along the mouse nephron. Am. J. Physiol. Renal Physiol. 286, F1063–F1071.
Li, J., Ananthapanyasut, W., Yu, A.S., 2011. Claudins in renal physiology and disease. Pediatr. Nephrol. 26, 2133–2142.
Lima, W.R., Parreira, K.S., Devuyst, O., Caplanusi, A., N'Kuli, F., Marien, B., Van Der Smissen, P., Alves, P.M., Verroust, P., Christensen, E.I., Terzi, F., Matter, K., Balda, M.S., Pierreux, C.E., Courtoy, P.J., 2010. ZONAB promotes proliferation and represses differentiation of proximal tubule epithelial cells. J. Am. Soc. Nephrol. 21, 478–488.
Liu, F.Y., Cogan, M.G., 1986. Axial heterogeneity of bicarbonate, chloride, and water transport in the rat proximal convoluted tubule. Effects of change in luminal flow rate and of alkalemia. J. Clin. Invest. 78, 1547–1557.
Liu, Y., Nusrat, A., Schnell, F.J., Reaves, T.A., Walsh, S., Pochet, M., Parkos, C.A., 2000. Human junction adhesion molecule regulates tight junction resealing in epithelia. J. Cell Sci. 113 (Pt. 13), 2363–2374.
Lo, C.M., Keese, C.R., Giaever, I., 1999. Cell-substrate contact: another factor may influence transepithelial electrical resistance of cell layers cultured on permeable filters. Exp. Cell Res. 250, 576–580.
Lochter, A., Galosy, S., Muschler, J., Freedman, N., Werb, Z., Bissell, M.J., 1997. Matrix metalloproteinase stromelysin-1 triggers a cascade of molecular alterations that leads to stable epithelial-to-mesenchymal conversion and a premalignant phenotype in mammary epithelial cells. J. Cell Biol. 139, 1861–1872.
Lu, C.Y., Winterberg, P.D., Chen, J., Hartono, J.R., 2012. Acute kidney injury: a conspiracy of Toll-like receptor 4 on endothelia, leukocytes, and tubules. Pediatr. Nephrol. 27, 1847–1854.
Ly, D.L., Waheed, F., Lodyga, M., Speight, P., Masszi, A., Nakano, H., Hersom, M., Pedersen, S.F., Szaszi, K., Kapus, A., 2013. Hyperosmotic stress regulates the distribution and stability of myocardin-related transcription factor, a key modulator of the cytoskeleton. Am. J. Physiol. Cell Physiol. 304, C115–C127.
Madara, J.L., Barenberg, D., Carlson, S., 1986. Effects of cytochalasin D on occluding junctions of intestinal absorptive cells: further evidence that the cytoskeleton may influence paracellular permeability and junctional charge selectivity. J. Cell Biol. 102, 2125–2136.
Makarova, O., Roh, M.H., Liu, C.J., Laurinec, S., Margolis, B., 2003. Mammalian Crumbs3 is a small transmembrane protein linked to protein associated with Lin-7 (Pals1). Gene 302, 21–29.
Mandai, K., Nakanishi, H., Satoh, A., Obaishi, H., Wada, M., Nishioka, H., Itoh, M., Mizoguchi, A., Aoki, T., Fujimoto, T., Matsuda, Y., Tsukita, S., Takai, Y., 1997.

Afadin: a novel actin filament-binding protein with one PDZ domain localized at cadherin-based cell-to-cell adherens junction. J. Cell Biol. 139, 517–528.
Mandell, K.J., Parkos, C.A., 2005. The JAM family of proteins. Adv. Drug Deliv. Rev. 57, 857–867.
Mandell, K.J., Babbin, B.A., Nusrat, A., Parkos, C.A., 2005. Junctional adhesion molecule 1 regulates epithelial cell morphology through effects on beta1 integrins and Rap1 activity. J. Biol. Chem. 280, 11665–11674.
Mankertz, J., Waller, J.S., Hillenbrand, B., Tavalali, S., Florian, P., Schoneberg, T., Fromm, M., Schulzke, J.D., 2002. Gene expression of the tight junction protein occludin includes differential splicing and alternative promoter usage. Biochem. Biophys. Res. Commun. 298, 657–666.
Marchiando, A.M., Shen, L., Graham, W.V., Weber, C.R., Schwarz, B.T., Austin 2nd, J.R., Raleigh, D.R., Guan, Y., Watson, A.J., Montrose, M.H., Turner, J.R., 2010. Caveolin-1-dependent occludin endocytosis is required for TNF-induced tight junction regulation in vivo. J. Cell Biol. 189, 111–126.
Mariano, C., Sasaki, H., Brites, D., Brito, M.A., 2011. A look at tricellulin and its role in tight junction formation and maintenance. Eur. J. Cell Biol. 90, 787–796.
Martin, T.A., Jiang, W.G., 2009. Loss of tight junction barrier function and its role in cancer metastasis. Biochim. Biophys. Acta 1788, 872–891.
Martinez-Estrada, O.M., Culleres, A., Soriano, F.X., Peinado, H., Bolos, V., Martinez, F.O., Reina, M., Cano, A., Fabre, M., Vilaro, S., 2006. The transcription factors Slug and Snail act as repressors of Claudin-1 expression in epithelial cells. Biochem. J. 394, 449–457.
Martin-Martin, N., Ryan, G., McMorrow, T., Ryan, M.P., 2010. Sirolimus and cyclosporine A alter barrier function in renal proximal tubular cells through stimulation of ERK1/2 signaling and claudin-1 expression. Am. J. Physiol. Renal Physiol. 298, F672–F682.
Martin-Martin, N., Slattery, C., McMorrow, T., Ryan, M.P., 2011. TGF-beta1 mediates sirolimus and cyclosporine A-induced alteration of barrier function in renal epithelial cells via a noncanonical ERK1/2 signaling pathway. Am. J. Physiol. Renal Physiol. 301, F1281–F1292.
Martin-Martin, N., Dan, Q., Amoozadeh, Y., Waheed, F., McMorrow, T., Ryan, M.P., Szaszi, K., 2012. RhoA and Rho kinase mediate cyclosporine A and sirolimus-induced barrier tightening in renal proximal tubular cells. Int. J. Biochem. Cell Biol. 44, 178–188.
Masszi, A., Kapus, A., 2011a. Organ fibrosis: when epithelia are muscled to change. Cell Cycle 9, 2263–2264.
Masszi, A., Kapus, A., 2011b. Smaddening complexity: the role of Smad3 in epithelial-myofibroblast transition. Cells Tissues Organs 193, 41–52.
Masszi, A., Fan, L., Rosivall, L., McCulloch, C.A., Rotstein, O.D., Mucsi, I., Kapus, A., 2004. Integrity of cell-cell contacts is a critical regulator of TGF-beta 1-induced epithelial-to-myofibroblast transition: role for beta-catenin. Am. J. Pathol. 165, 1955–1967.
Masszi, A., Speight, P., Charbonney, E., Lodyga, M., Nakano, H., Szaszi, K., Kapus, A., 2010. Fate-determining mechanisms in epithelial-myofibroblast transition: major inhibitory role for Smad3. J. Cell Biol. 188, 383–399.
Masuda, S., Oda, Y., Sasaki, H., Ikenouchi, J., Higashi, T., Akashi, M., Nishi, E., Furuse, M., 2011. LSR defines cell corners for tricellular tight junction formation in epithelial cells. J. Cell Sci. 124, 548–555.
Matsuda, M., Kubo, A., Furuse, M., Tsukita, S., 2004. A peculiar internalization of claudins, tight junction-specific adhesion molecules, during the intercellular movement of epithelial cells. J. Cell Sci. 117, 1247–1257.
Matter, K., Aijaz, S., Tsapara, A., Balda, M.S., 2005. Mammalian tight junctions in the regulation of epithelial differentiation and proliferation. Curr. Opin. Cell Biol. 17, 453–458.

McCarthy, K.M., Skare, I.B., Stankewich, M.C., Furuse, M., Tsukita, S., Rogers, R.A., Lynch, R.D., Schneeberger, E.E., 1996. Occludin is a functional component of the tight junction. J. Cell Sci. 109 (Pt. 9), 2287–2298.

McCrea, P.D., Gu, D., Balda, M.S., 2009. Junctional music that the nucleus hears: cell-cell contact signaling and the modulation of gene activity. Cold Spring Harb. Perspect. Biol. 1, a002923.

McMorrow, T., Gaffney, M.M., Slattery, C., Campbell, E., Ryan, M.P., 2005. Cyclosporine A induced epithelial-mesenchymal transition in human renal proximal tubular epithelial cells. Nephrol. Dial. Transplant. 20, 2215–2225.

Medici, D., Hay, E.D., Goodenough, D.A., 2006. Cooperation between snail and LEF-1 transcription factors is essential for TGF-beta1-induced epithelial-mesenchymal transition. Mol. Biol. Cell 17, 1871–1879.

Meza, I., Ibarra, G., Sabanero, M., Martinez-Palomo, A., Cereijido, M., 1980. Occluding junctions and cytoskeletal components in a cultured transporting epithelium. J. Cell Biol. 87, 746–754.

Milatz, S., Krug, S.M., Rosenthal, R., Gunzel, D., Muller, D., Schulzke, J.D., Amasheh, S., Fromm, M., 2010. Claudin-3 acts as a sealing component of the tight junction for ions of either charge and uncharged solutes. Biochim. Biophys. Acta 1798, 2048–2057.

Mineta, K., Yamamoto, Y., Yamazaki, Y., Tanaka, H., Tada, Y., Saito, K., Tamura, A., Igarashi, M., Endo, T., Takeuchi, K., Tsukita, S., 2011. Predicted expansion of the claudin multigene family. FEBS Lett. 585, 606–612.

Miyake, Y., Inoue, N., Nishimura, K., Kinoshita, N., Hosoya, H., Yonemura, S., 2006. Actomyosin tension is required for correct recruitment of adherens junction components and zonula occludens formation. Exp. Cell Res. 312, 1637–1650.

Molitoris, B.A., 2004. Actin cytoskeleton in ischemic acute renal failure. Kidney Int. 66, 871–883.

Moon, S.Y., Zheng, Y., 2003. Rho GTPase-activating proteins in cell regulation. Trends Cell Biol. 13, 13–22.

Mullin, J.M., Laughlin, K.V., Marano, C.W., Russo, L.M., Soler, A.P., 1992. Modulation of tumor necrosis factor-induced increase in renal (LLC-PK1) transepithelial permeability. Am. J. Physiol. 263, F915–F924.

Murakami, T., Felinski, E.A., Antonetti, D.A., 2009. Occludin phosphorylation and ubiquitination regulate tight junction trafficking and vascular endothelial growth factor-induced permeability. J. Biol. Chem. 284, 21036–21046.

Muresan, Z., Paul, D.L., Goodenough, D.A., 2000. Occludin 1B, a variant of the tight junction protein occludin. Mol. Biol. Cell 11, 627–634.

Muto, S., Hata, M., Taniguchi, J., Tsuruoka, S., Moriwaki, K., Saitou, M., Furuse, K., Sasaki, H., Fujimura, A., Imai, M., Kusano, E., Tsukita, S., Furuse, M., 2010. Claudin-2-deficient mice are defective in the leaky and cation-selective paracellular permeability properties of renal proximal tubules. Proc. Natl. Acad. Sci. U.S.A. 107, 8011–8016.

Muto, S., Furuse, M., Kusano, E., 2012. Claudins and renal salt transport. Clin. Exp. Nephrol. 16, 61–67.

Nava, P., Capaldo, C.T., Koch, S., Kolegraff, K., Rankin, C.R., Farkas, A.E., Feasel, M.E., Li, L., Addis, C., Parkos, C.A., Nusrat, A., 2011. JAM-A regulates epithelial proliferation through Akt/beta-catenin signalling. EMBO Rep. 12, 314–320.

Nelson, W.J., 2003. Epithelial cell polarity from the outside looking in. News Physiol. Sci. 18, 143–146.

Nie, M., Aijaz, S., Leefa Chong San, I.V., Balda, M.S., Matter, K., 2009. The Y-box factor ZONAB/DbpA associates with GEF-H1/Lfc and mediates Rho-stimulated transcription. EMBO Rep. 10, 1125–1131.

Nie, M., Balda, M.S., Matter, K., 2012. Stress- and Rho-activated ZO-1-associated nucleic acid binding protein binding to p21 mRNA mediates stabilization, translation, and cell survival. Proc. Natl. Acad. Sci. U.S.A. 109, 10897–10902.
Nishimura, N., Sasaki, T., 2009. Rab family small G proteins in regulation of epithelial apical junctions. Front. Biosci. 14, 2115–2129.
Nunbhakdi-Craig, V., Machleidt, T., Ogris, E., Bellotto, D., White 3rd, C.L., Sontag, E., 2002. Protein phosphatase 2A associates with and regulates atypical PKC and the epithelial tight junction complex. J. Cell Biol. 158, 967–978.
Nusrat, A., Giry, M., Turner, J.R., Colgan, S.P., Parkos, C.A., Carnes, D., Lemichez, E., Boquet, P., Madara, J.L., 1995. Rho protein regulates tight junctions and perijunctional actin organization in polarized epithelia. Proc. Natl. Acad. Sci. U.S.A. 92, 10629–10633.
Ogita, H., Rikitake, Y., Miyoshi, J., Takai, Y., 2010. Cell adhesion molecules nectins and associating proteins: implications for physiology and pathology. Proc. Jpn. Acad. Ser. B Phys. Biol. Sci. 86, 621–629.
Ohkubo, T., Ozawa, M., 2004. The transcription factor Snail downregulates the tight junction components independently of E-cadherin downregulation. J. Cell Sci. 117, 1675–1685.
Ohnishi, H., Nakahara, T., Furuse, K., Sasaki, H., Tsukita, S., Furuse, M., 2004. JACOP, a novel plaque protein localizing at the apical junctional complex with sequence similarity to cingulin. J. Biol. Chem. 279, 46014–46022.
Ohta, H., Adachi, H., Takiguchi, M., Inaba, M., 2006. Restricted localization of claudin-16 at the tight junction in the thick ascending limb of Henle's loop together with claudins 3, 4, and 10 in bovine nephrons. J. Vet. Med. Sci. 68, 453–463.
Ooshio, T., Kobayashi, R., Ikeda, W., Miyata, M., Fukumoto, Y., Matsuzawa, N., Ogita, H., Takai, Y., 2010. Involvement of the interaction of afadin with ZO-1 in the formation of tight junctions in Madin-Darby canine kidney cells. J. Biol. Chem. 285, 5003–5012.
Otani, T., Ichii, T., Aono, S., Takeichi, M., 2006. Cdc42 GEF Tuba regulates the junctional configuration of simple epithelial cells. J. Cell Biol. 175, 135–146.
Pannekoek, W.J., Kooistra, M.R., Zwartkruis, F.J., Bos, J.L., 2009. Cell-cell junction formation: the role of Rap1 and Rap1 guanine nucleotide exchange factors. Biochim. Biophys. Acta 1788, 790–796.
Patrick, D.M., Leone, A.K., Shellenberger, J.J., Dudowicz, K.A., King, J.M., 2006. Proinflammatory cytokines tumor necrosis factor-alpha and interferon-gamma modulate epithelial barrier function in Madin-Darby canine kidney cells through mitogen activated protein kinase signaling. BMC Physiol. 6, 2.
Pertz, O., 2011. Spatio-temporal Rho GTPase signaling—where are we now? J. Cell Sci. 123, 1841–1850.
Pieczynski, J., Margolis, B., 2011. Protein complexes that control renal epithelial polarity. Am. J. Physiol. Renal Physiol. 300, F589–F601.
Prozialeck, W.C., Edwards, J.R., Lamar, P.C., Smith, C.S., 2006. Epithelial barrier characteristics and expression of cell adhesion molecules in proximal tubule-derived cell lines commonly used for in vitro toxicity studies. Toxicol. In Vitro 20, 942–953.
Quaggin, S.E., Kapus, A., 2011. Scar wars: mapping the fate of epithelial-mesenchymal-myofibroblast transition. Kidney Int. 80, 41–50.
Rajasekaran, A.K., Rajasekaran, S.A., 2003. Role of Na-K-ATPase in the assembly of tight junctions. Am. J. Physiol. Renal Physiol. 285, F388–F396.
Raleigh, D.R., Marchiando, A.M., Zhang, Y., Shen, L., Sasaki, H., Wang, Y., Long, M., Turner, J.R., 2010. Tight junction-associated MARVEL proteins marveld3, tricellulin, and occludin have distinct but overlapping functions. Mol. Biol. Cell 21, 1200–1213.
Raleigh, D.R., Boe, D.M., Yu, D., Weber, C.R., Marchiando, A.M., Bradford, E.M., Wang, Y., Wu, L., Schneeberger, E.E., Shen, L., Turner, J.R., 2011. Occludin S408

phosphorylation regulates tight junction protein interactions and barrier function. J. Cell Biol. 193, 565–582.
Rathinam, R., Berrier, A., Alahari, S.K., 2011. Role of Rho GTPases and their regulators in cancer progression. Front. Biosci. 17, 2561–2571.
Rector Jr., F.C., 1983. Sodium, bicarbonate, and chloride absorption by the proximal tubule. Am. J. Physiol. 244, F461–F471.
Reyes, J.L., Lamas, M., Martin, D., del Carmen Namorado, M., Islas, S., Luna, J., Tauc, M., Gonzalez-Mariscal, L., 2002. The renal segmental distribution of claudins changes with development. Kidney Int. 62, 476–487.
Riazuddin, S., Ahmed, Z.M., Fanning, A.S., Lagziel, A., Kitajiri, S., Ramzan, K., Khan, S.N., Chattaraj, P., Friedman, P.L., Anderson, J.M., Belyantseva, I.A., Forge, A., Friedman, T.B., 2006. Tricellulin is a tight-junction protein necessary for hearing. Am. J. Hum. Genet. 79, 1040–1051.
Roberts, S., Delury, C., Marsh, E., 2012. The PDZ protein discs-large (DLG): the 'Jekyll and Hyde' of the epithelial polarity proteins. FEBS J. 279, 3549–3558.
Rodgers, L.S., Fanning, A.S., 2011. Regulation of epithelial permeability by the actin cytoskeleton. Cytoskeleton (Hoboken) 68, 653–660.
Rodriguez-Iturbe, B., Garcia Garcia, G., 2010. The role of tubulointerstitial inflammation in the progression of chronic renal failure. Nephron Clin. Pract. 116, c81–c88.
Roh, M.H., Liu, C.J., Laurinec, S., Margolis, B., 2002. The carboxyl terminus of zona occludens-3 binds and recruits a mammalian homologue of discs lost to tight junctions. J. Biol. Chem. 277, 27501–27509.
Rorth, P., 2009. Collective cell migration. Annu. Rev. Cell Dev. Biol. 25, 407–429.
Rosenthal, R., Milatz, S., Krug, S.M., Oelrich, B., Schulzke, J.D., Amasheh, S., Gunzel, D., Fromm, M., 2010. Claudin-2, a component of the tight junction, forms a paracellular water channel. J. Cell Sci. 123, 1913–1921.
Rosin, D.L., Okusa, M.D., 2011. Dangers within: DAMP responses to damage and cell death in kidney disease. J. Am. Soc. Nephrol. 22, 416–425.
Rossman, K.L., Der, C.J., Sondek, J., 2005. GEF means go: turning on RHO GTPases with guanine nucleotide-exchange factors. Nat. Rev. Mol. Cell Biol. 6, 167–180.
Rudini, N., Dejana, E., 2008. Adherens junctions. Curr. Biol. 18, R1080–R1082.
Runkle, E.A., Sundstrom, J.M., Runkle, K.B., Liu, X., Antonetti, D.A., 2011. Occludin localizes to centrosomes and modifies mitotic entry. J. Biol. Chem. 286, 30847–30858.
Russ, P.K., Pino, C.J., Williams, C.S., Bader, D.M., Haselton, F.R., Chang, M.S., 2011. Bves modulates tight junction associated signaling. PLoS One 6, e14563.
Saitou, M., Furuse, M., Sasaki, H., Schulzke, J.D., Fromm, M., Takano, H., Noda, T., Tsukita, S., 2000. Complex phenotype of mice lacking occludin, a component of tight junction strands. Mol. Biol. Cell 11, 4131–4142.
Sakakibara, A., Furuse, M., Saitou, M., Ando-Akatsuka, Y., Tsukita, S., 1997. Possible involvement of phosphorylation of occludin in tight junction formation. J. Cell Biol. 137, 1393–1401.
Sallee, J.L., Burridge, K., 2009. Density-enhanced phosphatase 1 regulates phosphorylation of tight junction proteins and enhances barrier function of epithelial cells. J. Biol. Chem. 284, 14997–15006.
Samarin, S., Nusrat, A., 2009. Regulation of epithelial apical junctional complex by Rho family GTPases. Front. Biosci. 14, 1129–1142.
Samarin, S.N., Ivanov, A.I., Flatau, G., Parkos, C.A., Nusrat, A., 2007. Rho/ROCK-II signaling mediates disassembly of epithelial apical junctions. Mol. Biol. Cell 18, 3429–3439.
Sato, T., Fujita, N., Yamada, A., Ooshio, T., Okamoto, R., Irie, K., Takai, Y., 2006. Regulation of the assembly and adhesion activity of E-cadherin by nectin and afadin for the formation of adherens junctions in Madin-Darby canine kidney cells. J. Biol. Chem. 281, 5288–5299.

Schafer, J.A., Troutman, S.L., Andreoli, T.E., 1974. Volume reabsorption, transepithelial potential differences, and ionic permeability properties in mammalian superficial proximal straight tubules. J. Gen. Physiol. 64, 582–607.
Schluter, M.A., Margolis, B., 2012. Apicobasal polarity in the kidney. Exp. Cell Res. 318, 1033–1039.
Schneeberger, E.E., Lynch, R.D., 2004. The tight junction: a multifunctional complex. Am. J. Physiol. Cell Physiol. 286, C1213–C1228.
Schnoor, M., Parkos, C.A., 2008. Disassembly of endothelial and epithelial junctions during leukocyte transmigration. Front. Biosci. 13, 6638–6652.
Schulzke, J.D., Gitter, A.H., Mankertz, J., Spiegel, S., Seidler, U., Amasheh, S., Saitou, M., Tsukita, S., Fromm, M., 2005. Epithelial transport and barrier function in occludin-deficient mice. Biochim. Biophys. Acta 1669, 34–42.
Schulzke, J.D., Ploeger, S., Amasheh, M., Fromm, A., Zeissig, S., Troeger, H., Richter, J., Bojarski, C., Schumann, M., Fromm, M., 2009. Epithelial tight junctions in intestinal inflammation. Ann. N. Y. Acad. Sci. 1165, 294–300.
Schulzke, J.D., Gunzel, D., John, L.J., Fromm, M., 2012. Perspectives on tight junction research. Ann. N. Y. Acad. Sci. 1257, 1–19.
Schwarz, B.T., Wang, F., Shen, L., Clayburgh, D.R., Su, L., Wang, Y., Fu, Y.X., Turner, J.R., 2007. LIGHT signals directly to intestinal epithelia to cause barrier dysfunction via cytoskeletal and endocytic mechanisms. Gastroenterology 132, 2383–2394.
Sebe, A., Masszi, A., Zulys, M., Yeung, T., Speight, P., Rotstein, O.D., Nakano, H., Mucsi, I., Szaszi, K., Kapus, A., 2008. Rac, PAK and p38 regulate cell contact-dependent nuclear translocation of myocardin-related transcription factor. FEBS Lett. 582, 291–298.
Seth, A., Sheth, P., Elias, B.C., Rao, R., 2007. Protein phosphatases 2A and 1 interact with occludin and negatively regulate the assembly of tight junctions in the CACO-2 cell monolayer. J. Biol. Chem. 282, 11487–11498.
Severson, E.A., Lee, W.Y., Capaldo, C.T., Nusrat, A., Parkos, C.A., 2009. Junctional adhesion molecule A interacts with Afadin and PDZ-GEF2 to activate Rap1A, regulate beta1 integrin levels, and enhance cell migration. Mol. Biol. Cell 20, 1916–1925.
Shan, Q., Himmerkus, N., Hou, J., Goodenough, D.A., Bleich, M., 2009. Insights into driving forces and paracellular permeability from claudin-16 knockdown mouse. Ann. N. Y. Acad. Sci. 1165, 148–151.
Shang, X., Lin, X., Alvarez, E., Manorek, G., Howell, S.B., 2012. Tight junction proteins claudin-3 and claudin-4 control tumor growth and metastases. Neoplasia 14, 974–985.
Shen, L., 2012. Tight junctions on the move: molecular mechanisms for epithelial barrier regulation. Ann. N. Y. Acad. Sci. 1258, 9–18.
Shen, L., Black, E.D., Witkowski, E.D., Lencer, W.I., Guerriero, V., Schneeberger, E.E., Turner, J.R., 2006. Myosin light chain phosphorylation regulates barrier function by remodeling tight junction structure. J. Cell Sci. 119, 2095–2106.
Shen, L., Weber, C.R., Raleigh, D.R., Yu, D., Turner, J.R., 2011. Tight junction pore and leak pathways: a dynamic duo. Annu. Rev. Physiol. 73, 283–309.
Singh, A.B., Harris, R.C., 2004. Epidermal growth factor receptor activation differentially regulates claudin expression and enhances transepithelial resistance in Madin-Darby canine kidney cells. J. Biol. Chem. 279, 3543–3552.
Singh, P., Okusa, M.D., 2011. The role of tubuloglomerular feedback in the pathogenesis of acute kidney injury. Contrib. Nephrol. 174, 12–21.
Singh, A.B., Sugimoto, K., Dhawan, P., Harris, R.C., 2007. Juxtacrine activation of EGFR regulates claudin expression and increases transepithelial resistance. Am. J. Physiol. Cell Physiol. 293, C1660–C1668.
Slattery, C., Campbell, E., McMorrow, T., Ryan, M.P., 2005. Cyclosporine A-induced renal fibrosis: a role for epithelial-mesenchymal transition. Am. J. Pathol. 167, 395–407.

Smutny, M., Cox, H.L., Leerberg, J.M., Kovacs, E.M., Conti, M.A., Ferguson, C., Hamilton, N.A., Parton, R.G., Adelstein, R.S., Yap, A.S., 2010. Myosin II isoforms identify distinct functional modules that support integrity of the epithelial zonula adherens. Nat. Cell Biol. 12, 696–702.
Sohl, G., Willecke, K., 2004. Gap junctions and the connexin protein family. Cardiovasc. Res. 62, 228–232.
Somlyo, A.P., Somlyo, A.V., 2003. Ca2+ sensitivity of smooth muscle and nonmuscle myosin II: modulated by G proteins, kinases, and myosin phosphatase. Physiol. Rev. 83, 1325–1358.
Sonoda, N., Furuse, M., Sasaki, H., Yonemura, S., Katahira, J., Horiguchi, Y., Tsukita, S., 1999. Clostridium perfringens enterotoxin fragment removes specific claudins from tight junction strands: evidence for direct involvement of claudins in tight junction barrier. J. Cell Biol. 147, 195–204.
Sourisseau, T., Georgiadis, A., Tsapara, A., Ali, R.R., Pestell, R., Matter, K., Balda, M.S., 2006. Regulation of PCNA and cyclin D1 expression and epithelial morphogenesis by the ZO-1-regulated transcription factor ZONAB/DbpA. Mol. Cell. Biol. 26, 2387–2398.
Staehelin, L.A., 1973. Further observations on the fine structure of freeze-cleaved tight junctions. J. Cell Sci. 13, 763–786.
Staehelin, L.A., 1974. Structure and function of intercellular junctions. Int. Rev. Cytol. 39, 191–283.
Stevenson, B.R., Siliciano, J.D., Mooseker, M.S., Goodenough, D.A., 1986. Identification of ZO-1: a high molecular weight polypeptide associated with the tight junction (zonula occludens) in a variety of epithelia. J. Cell Biol. 103, 755–766.
Suh, Y., Yoon, C.H., Kim, R.K., Lim, E.J., Oh, Y.S., Hwang, S.G., An, S., Yoon, G., Gye, M.C., Yi, J.M., Kim, M.J., Lee, S.J., 2012. Claudin-1 induces epithelial-mesenchymal transition through activation of the c-Abl-ERK signaling pathway in human liver cells. Oncogene 32, 4873–4882.
Suzuki, T., Elias, B.C., Seth, A., Shen, L., Turner, J.R., Giorgianni, F., Desiderio, D., Guntaka, R., Rao, R., 2009. PKC eta regulates occludin phosphorylation and epithelial tight junction integrity. Proc. Natl. Acad. Sci. U.S.A. 106, 61–66.
Szaszi, K., Sirokmany, G., Di Ciano-Oliveira, C., Rotstein, O.D., Kapus, A., 2005. Depolarization induces Rho-Rho kinase-mediated myosin light chain phosphorylation in kidney tubular cells. Am. J. Physiol. Cell Physiol. 289, C673–C685.
Szaszi, K., Vandermeer, M., Amoozadeh, Y., 2012. Epithelial wound healing and the effects of cytokines investigated by ECIS. In: Jiang, W.G. (Ed.), Electric cell-substrate impedance sensing and cancer metastasis. Springer, The Netherlands, pp. 131–175.
Takehara, M., Nishimura, T., Mima, S., Hoshino, T., Mizushima, T., 2009. Effect of claudin expression on paracellular permeability, migration and invasion of colonic cancer cells. Biol. Pharm. Bull. 32, 825–831.
Tamura, A., Kitano, Y., Hata, M., Katsuno, T., Moriwaki, K., Sasaki, H., Hayashi, H., Suzuki, Y., Noda, T., Furuse, M., Tsukita, S., 2008. Megaintestine in claudin-15-deficient mice. Gastroenterology 134, 523–534.
Tapia, R., Huerta, M., Islas, S., Avila-Flores, A., Lopez-Bayghen, E., Weiske, J., Huber, O., Gonzalez-Mariscal, L., 2009. Zona occludens-2 inhibits cyclin D1 expression and cell proliferation and exhibits changes in localization along the cell cycle. Mol. Biol. Cell 20, 1102–1117.
Tatum, R., Zhang, Y., Salleng, K., Lu, Z., Lin, J.J., Lu, Q., Jeansonne, B.G., Ding, L., Chen, Y.H., 2010. Renal salt wasting and chronic dehydration in claudin-7-deficient mice. Am. J. Physiol. Renal Physiol. 298, F24–F34.
Terai, T., Nishimura, N., Kanda, I., Yasui, N., Sasaki, T., 2006. JRAB/MICAL-L2 is a junctional Rab13-binding protein mediating the endocytic recycling of occludin. Mol. Biol. Cell 17, 2465–2475.

Terry, S.J., Zihni, C., Elbediwy, A., Vitiello, E., Leefa Chong San, I.V., Balda, M.S., Matter, K., 2011. Spatially restricted activation of RhoA signalling at epithelial junctions by p114RhoGEF drives junction formation and morphogenesis. Nat. Cell Biol. 13, 159–166.

Thorleifsson, G., Holm, H., Edvardsson, V., Walters, G.B., Styrkarsdottir, U., Gudbjartsson, D.F., Sulem, P., Halldorsson, B.V., de Vegt, F., d'Ancona, F.C., den Heijer, M., Franzson, L., Christiansen, C., Alexandersen, P., Rafnar, T., Kristjansson, K., Sigurdsson, G., Kiemeney, L.A., Bodvarsson, M., Indridason, O.S., Palsson, R., Kong, A., Thorsteinsdottir, U., Stefansson, K., 2009. Sequence variants in the CLDN14 gene associate with kidney stones and bone mineral density. Nat. Genet. 41, 926–930.

Thurman, J.M., 2007. Triggers of inflammation after renal ischemia/reperfusion. Clin. Immunol. 123, 7–13.

Tiruppathi, C., Malik, A.B., Del Vecchio, P.J., Keese, C.R., Giaever, I., 1992. Electrical method for detection of endothelial cell shape change in real time: assessment of endothelial barrier function. Proc. Natl. Acad. Sci. U.S.A. 89, 7919–7923.

Tsukamoto, T., Nigam, S.K., 1999. Role of tyrosine phosphorylation in the reassembly of occludin and other tight junction proteins. Am. J. Physiol. 276, F737–F750.

Tsukita, S., Furuse, M., 1998. Overcoming barriers in the study of tight junction functions: from occludin to claudin. Genes Cells 3, 569–573.

Tsukita, S., Furuse, M., 2000. The structure and function of claudins, cell adhesion molecules at tight junctions. Ann. N. Y. Acad. Sci. 915, 129–135.

Tsukita, S., Yamazaki, Y., Katsuno, T., Tamura, A., 2008. Tight junction-based epithelial microenvironment and cell proliferation. Oncogene 27, 6930–6938.

Turksen, K., Troy, T.C., 2011. Junctions gone bad: claudins and loss of the barrier in cancer. Biochim. Biophys. Acta 1816, 73–79.

Turner, J.R., 2000. Show me the pathway! Regulation of paracellular permeability by Na(+)-glucose cotransport. Adv. Drug Deliv. Rev. 41, 265–281.

Umeda, K., Matsui, T., Nakayama, M., Furuse, K., Sasaki, H., Furuse, M., Tsukita, S., 2004. Establishment and characterization of cultured epithelial cells lacking expression of ZO-1. J. Biol. Chem. 279, 44785–44794.

Umeda, K., Ikenouchi, J., Katahira-Tayama, S., Furuse, K., Sasaki, H., Nakayama, M., Matsui, T., Tsukita, S., Furuse, M., 2006. ZO-1 and ZO-2 independently determine where claudins are polymerized in tight-junction strand formation. Cell 126, 741–754.

Utech, M., Ivanov, A.I., Samarin, S.N., Bruewer, M., Turner, J.R., Mrsny, R.J., Parkos, C.A., Nusrat, A., 2005. Mechanism of IFN-gamma-induced endocytosis of tight junction proteins: myosin II-dependent vacuolarization of the apical plasma membrane. Mol. Biol. Cell 16, 5040–5052.

Vallon, V., 2011. The proximal tubule in the pathophysiology of the diabetic kidney. Am. J. Physiol. Regul. Integr. Comp. Physiol. 300, R1009–R1022.

Van Itallie, C.M., Anderson, J.M., 1997. Occludin confers adhesiveness when expressed in fibroblasts. J. Cell Sci. 110 (Pt. 9), 1113–1121.

Van Itallie, C.M., Anderson, J.M., 2004. The role of claudins in determining paracellular charge selectivity. Proc. Am. Thorac. Soc. 1, 38–41.

Van Itallie, C.M., Anderson, J.M., 2006. Claudins and epithelial paracellular transport. Annu. Rev. Physiol. 68, 403–429.

Van Itallie, C., Rahner, C., Anderson, J.M., 2001. Regulated expression of claudin-4 decreases paracellular conductance through a selective decrease in sodium permeability. J. Clin. Invest. 107, 1319–1327.

Van Itallie, C.M., Fanning, A.S., Anderson, J.M., 2003. Reversal of charge selectivity in cation or anion-selective epithelial lines by expression of different claudins. Am. J. Physiol. Renal Physiol. 285, F1078–F1084.

Van Itallie, C.M., Gambling, T.M., Carson, J.L., Anderson, J.M., 2005. Palmitoylation of claudins is required for efficient tight-junction localization. J. Cell Sci. 118, 1427–1436.
Van Itallie, C.M., Rogan, S., Yu, A., Vidal, L.S., Holmes, J., Anderson, J.M., 2006. Two splice variants of claudin-10 in the kidney create paracellular pores with different ion selectivities. Am. J. Physiol. Renal Physiol. 291, F1288–F1299.
Van Itallie, C.M., Holmes, J., Bridges, A., Gookin, J.L., Coccaro, M.R., Proctor, W., Colegio, O.R., Anderson, J.M., 2008. The density of small tight junction pores varies among cell types and is increased by expression of claudin-2. J. Cell Sci. 121, 298–305.
Van Itallie, C.M., Fanning, A.S., Holmes, J., Anderson, J.M., 2010. Occludin is required for cytokine-induced regulation of tight junction barriers. J. Cell Sci. 123, 2844–2852.
Van Itallie, C.M., Mitic, L.L., Anderson, J.M., 2012a. SUMOylation of claudin-2. Ann. N. Y. Acad. Sci. 1258, 60–64.
Van Itallie, C.M., Tietgens, A.J., Logrande, K., Aponte, A., Gucek, M., Anderson, J.M., 2012b. Phosphorylation of claudin-2 on serine 208 promotes membrane retention and reduces trafficking to lysosomes. J. Cell Sci. 125, 4902–4912.
Vezzoli, G., Terranegra, A., Arcidiacono, T., Soldati, L., 2011. Genetics and calcium nephrolithiasis. Kidney Int. 80, 587–593.
Vincent, T., Neve, E.P., Johnson, J.R., Kukalev, A., Rojo, F., Albanell, J., Pietras, K., Virtanen, I., Philipson, L., Leopold, P.L., Crystal, R.G., de Herreros, A.G., Moustakas, A., Pettersson, R.F., Fuxe, J., 2009. A SNAIL1-SMAD3/4 transcriptional repressor complex promotes TGF-beta mediated epithelial-mesenchymal transition. Nat. Cell Biol. 11, 943–950.
Waheed, F., Speight, P., Kawai, G., Dan, Q., Kapus, A., Szaszi, K., 2010. Extracellular signal-regulated kinase and GEF-H1 mediate depolarization-induced Rho activation and paracellular permeability increase. Am. J. Physiol. Cell Physiol. 298, C1376–C1387.
Waheed, F., Dan, Q., Amoozadeh, Y., Zhang, Y., Tanimura, S., Speight, P., Kapus, A., Szaszi, K., 2013. Central role of the exchange factor GEF-H1 in TNF-alpha-induced sequential activation of Rac, ADAM17/TACE, and RhoA in tubular epithelial cells. Mol. Biol. Cell 24, 1068–1082.
Walsh, S.V., Hopkins, A.M., Chen, J., Narumiya, S., Parkos, C.A., Nusrat, A., 2001. Rho kinase regulates tight junction function and is necessary for tight junction assembly in polarized intestinal epithelia. Gastroenterology 121, 566–579.
Watson, C.J., Rowland, M., Warhurst, G., 2001. Functional modeling of tight junctions in intestinal cell monolayers using polyethylene glycol oligomers. Am. J. Physiol. Cell Physiol. 281, C388–C397.
Wells, C.D., Fawcett, J.P., Traweger, A., Yamanaka, Y., Goudreault, M., Elder, K., Kulkarni, S., Gish, G., Virag, C., Lim, C., Colwill, K., Starostine, A., Metalnikov, P., Pawson, T., 2006. A Rich1/Amot complex regulates the Cdc42 GTPase and apical-polarity proteins in epithelial cells. Cell 125, 535–548.
Westphal, J.K., Dorfel, M.J., Krug, S.M., Cording, J.D., Piontek, J., Blasig, I.E., Tauber, R., Fromm, M., Huber, O., 2010. Tricellulin forms homomeric and heteromeric tight junctional complexes. Cell. Mol. Life Sci. 67, 2057–2068.
Wu, C.F., Chiang, W.C., Lai, C.F., Chang, F.C., Chen, Y.T., Chou, Y.H., Wu, T.H., Linn, G.R., Ling, H., Wu, K.D., Tsai, T.J., Chen, Y.M., Duffield, J.S., Lin, S.L., 2013. Transforming growth factor beta-1 stimulates profibrotic epithelial signaling to activate pericyte-myofibroblast transition in obstructive kidney fibrosis. Am. J. Pathol. 182, 118–131.
Xu, J., Kausalya, P.J., Phua, D.C., Ali, S.M., Hossain, Z., Hunziker, W., 2008. Early embryonic lethality of mice lacking ZO-2, but Not ZO-3, reveals critical and nonredundant roles for individual zonula occludens proteins in mammalian development. Mol. Cell. Biol. 28, 1669–1678.

Yamada, S., Nelson, W.J., 2007. Localized zones of Rho and Rac activities drive initiation and expansion of epithelial cell-cell adhesion. J. Cell Biol. 178, 517–527.
Yamamura, R., Nishimura, N., Nakatsuji, H., Arase, S., Sasaki, T., 2008. The interaction of JRAB/MICAL-L2 with Rab8 and Rab13 coordinates the assembly of tight junctions and adherens junctions. Mol. Biol. Cell 19, 971–983.
Yamanaka, T., Horikoshi, Y., Suzuki, A., Sugiyama, Y., Kitamura, K., Maniwa, R., Nagai, Y., Yamashita, A., Hirose, T., Ishikawa, H., Ohno, S., 2001. PAR-6 regulates aPKC activity in a novel way and mediates cell-cell contact-induced formation of the epithelial junctional complex. Genes Cells 6, 721–731.
Yamauchi, K., Rai, T., Kobayashi, K., Sohara, E., Suzuki, T., Itoh, T., Suda, S., Hayama, A., Sasaki, S., Uchida, S., 2004. Disease-causing mutant WNK4 increases paracellular chloride permeability and phosphorylates claudins. Proc. Natl. Acad. Sci. U.S.A. 101, 4690–4694.
Yoshizaki, H., Ohba, Y., Kurokawa, K., Itoh, R.E., Nakamura, T., Mochizuki, N., Nagashima, K., Matsuda, M., 2003. Activity of Rho-family GTPases during cell division as visualized with FRET-based probes. J. Cell Biol. 162, 223–232.
Yu, A.S., 2009. Molecular basis for cation selectivity in claudin-2-based pores. Ann. N. Y. Acad. Sci. 1165, 53–57.
Yu, A.S., McCarthy, K.M., Francis, S.A., McCormack, J.M., Lai, J., Rogers, R.A., Lynch, R.D., Schneeberger, E.E., 2005. Knockdown of occludin expression leads to diverse phenotypic alterations in epithelial cells. Am. J. Physiol. Cell Physiol. 288, C1231–C1241.
Yu, A.S., Cheng, M.H., Angelow, S., Gunzel, D., Kanzawa, S.A., Schneeberger, E.E., Fromm, M., Coalson, R.D., 2009. Molecular basis for cation selectivity in claudin-2-based paracellular pores: identification of an electrostatic interaction site. J. Gen. Physiol. 133, 111–127.
Zavala-Zendejas, V.E., Torres-Martinez, A.C., Salas-Morales, B., Fortoul, T.I., Monta, X.f.O.L.F., Rendon-Huerta, E.P., 2010. Claudin-6, 7, or 9 overexpression in the human gastric adenocarcinoma cell line AGS increases its invasiveness, migration, and proliferation rate. Cancer Investig. 29, 1–11.
Zhao, B., Li, L., Lu, Q., Wang, L.H., Liu, C.Y., Lei, Q., Guan, K.L., 2011. Angiomotin is a novel Hippo pathway component that inhibits YAP oncoprotein. Genes Dev. 25, 51–63.

CHAPTER SEVEN

Making of a Retinal Cell: Insights into Retinal Cell-Fate Determination

Jillian J. Goetz, Caitlin Farris, Rebecca Chowdhury, Jeffrey M. Trimarchi[1]

Department of Genetics, Development and Cell Biology, Iowa State University, Ames, Iowa, USA
[1]Corresponding author: e-mail address: jtrimarc@iastate.edu

Contents

International Review of Cell and Molecular Biology, Volume 308
ISSN 1937-6448
http://dx.doi.org/10.1016/B978-0-12-800097-7.00007-5

Abstract

Understanding the process by which an uncommitted dividing cell produces particular specialized cells within a tissue remains a fundamental question in developmental biology. Many tissues are well suited for cell-fate studies, but perhaps none more so than the developing retina. Traditionally, experiments using the retina have been designed to elucidate the influence that individual environmental signals or transcription factors can have on cell-fate decisions. Despite a substantial amount of information gained through these studies, there is still much that we do not yet understand about how cell fate is controlled on a systems level. In addition, new factors such as noncoding RNAs and regulators of chromatin have been shown to play roles in cell-fate determination and with the advent of "omics" technology more factors will most likely be identified. In this chapter we summarize both the traditional view of retinal cell-fate determination and introduce some new ideas that are providing a challenge to the older way of thinking about the acquisition of cell fates.

1. INTRODUCTION

1.1. Retina

The proper integration of sensory information as vital as vision requires a precisely functioning instrument. In vertebrates, this process begins in the retina. The retina is responsible for phototransduction—the conversion of light energy to neural signals—and the initial processing of visual information before the signals are passed on to the brain (Burns and Arshavsky, 2005). Specialized retinal neurons contribute to basic signal modulation even before those features are forwarded on to the visual centers of the brain. These retinal nerve cells range from the light-sensing photoreceptors with their unique outer segments to the long axon bearing retinal ganglion cells that must connect with specific partners in the brain. Interestingly, each mature retinal neuron emanates from the same retinal progenitor population and precisely integrates into the retinal circuitry to perform its own specific role in vision.

Understanding the factors directing each progenitor cell to its final fate as a specialized neuron is important for a couple of reasons. First, the factors that drive the transition from an uncommitted progenitor cell to a fully functioning neuron may be shared among additional developing central nervous system (CNS) neurons. Knowledge regarding how these factors function in concert would, therefore, inform our understanding of how different neuronal populations are generated. Second, a greater understanding of how

each retinal progenitor cell chooses a cell fate is of great interest not only for developmental biologists, but also for those interested in diseases of the visual system. Many degenerative conditions affecting the retina potentially could be treated through cellular replacement therapy. These cell-based treatments involve either regenerating lost retinal neurons in the diseased tissue or injecting new cells that have been produced in culture to replace those that have been lost (Schmeer et al., 2012). Therapies such as these require a solid knowledge of how to generate a significant number of different types of neurons to replace those that are deteriorating. Only through studies of the mechanisms behind retinal cell-fate decisions will we uncover all of these factors to be used in these cutting edge replacement strategies.

1.2. Cell types that comprise retina

Although much remains to be elucidated regarding how the precise retinal circuitry is established, there is a significant amount that is understood about the different cells that make up the retina. The retina possesses a laminar organization that is well conserved throughout vertebrate evolution. It is composed of six major types of neurons and one type of glia, all of which are located within specific layers of the retina (Altshuler et al., 1991; Masland, 2012; Rodieck, 1998). The two types of photoreceptors, rods and cones, array themselves at the outer portion of the eye in the outer nuclear layer (ONL) (Fig. 7.1A). Rod photoreceptors, containing the photopigment rhodopsin, are best suited for low-light conditions and distinguish between light and dark (Morrow et al., 1998). Cone photoreceptor cells are distinguishable from rod photoreceptors by the presence of specialized opsins that react to ranges of light at different wavelengths (Masland, 2012). In general, photoreceptors are depolarized in the absence of light, which leads to a constant sodium influx and release of the neurotransmitter glutamate to activate downstream interneurons (Yau, 1994). Conversely, when stimulated by light, photoreceptors hyperpolarize and cease to release glutamate (Yau, 1994). The main role of photoreceptors is the conversion of photons of light into chemical signals, which can then be passed on to interneurons in the inner nuclear layer (INL) for further processing.

Among the interneuron cell classes, horizontal cells function to even out signals from bright and dim areas of the visual field (Masland, 2012). In general, mammals (except rodents) possess two types of horizontal cells, distinguishable by the presence or absence of an axon that communicates signals back to photoreceptors (Masland, 2001). Bipolar interneurons are generally referred to as either cone or rod bipolar cells, since they are exclusively

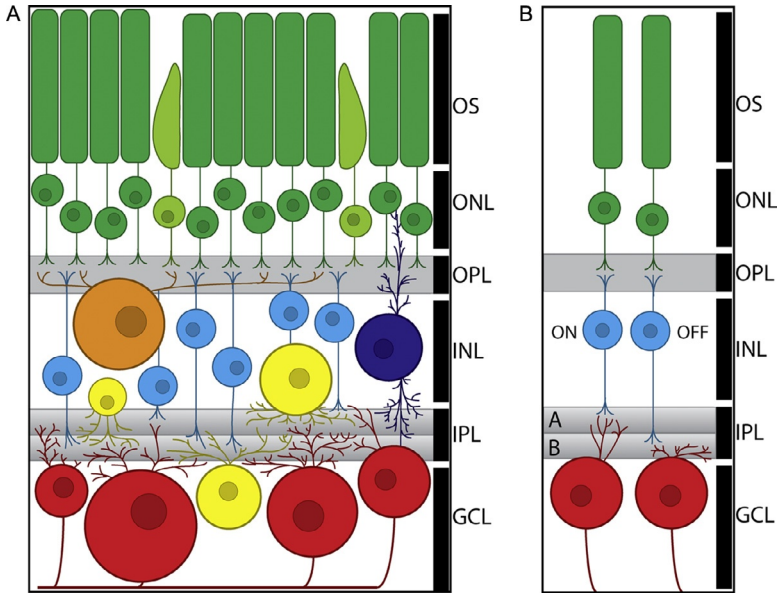

Figure 7.1 Retinal organization. (A) The organization of vertebrate retina. Retinal layers are labeled, including the photoreceptor outer segments (OSs), the ONL containing photoreceptor cell bodies, the outer plexiform layer (OPL) containing synapses between photoreceptors and interneurons, the INL containing the cell bodies of interneurons and Muller glia, the inner plexiform layer (IPL) containing synapses between interneurons and retinal ganglion cells, and the ganglion cell layer (GCL) containing ganglion cells as well as displaced amacrine interneurons. Some cell types, such as the red ganglion cells or yellow amacrine cells, show diverse morphologies. (B) Examples of the diversity within the major kinds of retinal cells. Bipolar cells are largely classified as either ON or OFF based on the location and connectivity of their dendrites within the sublaminae of the IPL, as well as their reactivity to light.

connected to one or the other type of photoreceptor. Studies of the anatomy, physiology, and gene expression place the number of different kinds of bipolar cells at 12 (Kim et al., 2008; Masland, 2001). The main function of bipolar cells varies based on their connectivity, but their two most prominent subdivisions are OFF and ON bipolar cells (Masland, 2012). When photoreceptors depolarize and release glutamate, these cells take up the glutamate and depolarize in turn. Therefore, OFF bipolar cells are active when light is off. ON bipolar cells, on the other hand, are inhibited by glutamate and hyperpolarize in its presence. Only when photoreceptors cease releasing glutamate—that is, when they are hyperpolarized due to the presence of light—do these ON bipolar cells depolarize (Masland, 2012). The ON

and OFF subtypes are distinguishable by the location of their dendrites in the inner plexiform layer where the processes meet those of the ganglion cells (Masland, 2001)—OFF cells do not extend far from the INL (Fig. 7.1B—sublamina A), while ON cells extend farther past their OFF neighbors (Fig. 7.1B—sublamina B).

The final two retinal neurons are also the most diverse. The most highly diverse class of cells in the retina is the amacrine interneurons. Morphological studies estimate that there are somewhere between 20 and 30 different subtypes of amacrines (depending on the species examined) with an array of receptive fields (MacNeil and Masland, 1998). These cells are generally inhibitory, using the neurotransmitters glycine or γ-aminobutyric acid (GABA). The most common amacrine cell type, named AII, connects rods to bipolar cells with added modulation from cones to heighten the signal intensity even in low light (Strettoi et al., 1992). Others, such as starburst amacrines, form highly branched and overlapping receptive fields that contribute to directional sensitivity in downstream signaling (Vaney et al., 1988). The retinal ganglion cells, the main output neurons of the retina, are another diverse group of retinal cells. Over 20 subtypes of ganglion cells have been isolated with functionality ranging from feature and color detection, direction and motion selectivity, and even photoreception (Rockhill et al., 2002). One ganglion cell subtype in particular has been receiving much attention recently. These intrinsically photosensitive retinal ganglion cells react to light independently of rods and cones using their own photopigment, melanopsin, and are important in establishing circadian rhythms and the normal pupillary reaction to light (Munch and Kawasaki, 2013).

Each retinal cell type is present in different proportions within the adult retina, although those proportions are conserved within a given species. For example, rods are very common at around 75% of the total retinal cell population in mice, while ganglion cells comprise only 2.5% (Drager and Olsen, 1981; Young, 1985a). It is challenging to develop a full catalog of the subtypes of the most diverse types of retinal neurons such as amacrine and ganglion cells, especially given the rarity of those cell types in general and their subtypes specifically. Nevertheless, to fully understand the control of retinal cell-fate decisions, we must have a better appreciation for the diversity of neuronal end points. It is only then that we can understand how progenitor cells sort through the myriad cues available to them and decide on a final cell fate. These decisions must be coordinated with the goal of generating the full cohort of retinal cells and functionally distinctive retinal cell subtypes in the right place and time.

2. RETINAL CELL-FATE SPECIFICATION

Since the retina is not only where the first step in the processing of visual information occurs but also a relatively simple and easily manipulated extension of the CNS, it is a widely used model system for studying nervous system development. The complex processing that is initiated by retinal cells is stunning, and their wide range of responsibilities is only more impressive given the understanding that all this diversity arises from a common progenitor population (Holt et al., 1988; Turner and Cepko, 1987; Turner et al., 1990). Each progenitor cell's multivariate fates are directed through a combination of intrinsic signals and differential reactions to extrinsic signals (Livesey and Cepko, 2001). Intrinsic signals include significant differences in gene expression, even among progenitor cells examined at the same developmental time point (Trimarchi et al., 2008). In addition to the intrinsic gene expression of individual progenitor cells, there are also cell-extrinsic factors—signals in the extracellular environment that help push progenitor cells toward a certain cell fate and assist in their path to final differentiation. Studies involving both types of signaling mechanisms are ongoing. Although many important discoveries have been made regarding the control of retinal cell-fate decisions, much about the precise combinations of genes and environmental factors and how they interact remains to be discovered. With a greater understanding of the forces driving retinal progenitor cells to a specific neuronal or glial cell fate, we can grow closer to a better understanding of how neurogenesis is accomplished in general.

Though the lessons learned from retinal development can be generalized to other parts of the nervous system, elucidation of how normal retinal development occurs is also important for its own sake. For example, retinal degeneration can specifically or preferentially affect individual subsets of retinal cell types, such as photoreceptors (retinitis pigmentosa or macular degeneration) or ganglion cells (glaucoma). Though current treatments can ameliorate symptoms and possibly delay degeneration, there are no current interventions that stimulate regeneration of the full functional cohort of lost cells (Kuehn et al., 2005). The only way regeneration could be possible is with a full understanding of the gene expression pathways that drive undifferentiated progenitors to take on those specified roles. With that knowledge, it could be possible to generate the necessary cell types *in vitro* using cultures such as induced pluripotent stem cells (Tucker et al., 2011) or, perhaps, *in vivo* by stimulating the stem cell potential of Muller glia (Karl et al., 2008).

In this review, we will discuss some of the critical players in retinal cell-fate determination, with a particular focus on some of the most recent ones. We will focus on key environmental factors as well as different families of transcription factors that have been shown to influence cell-fate decisions. Recently, new factors including epigenetic mechanisms and different types of noncoding RNAs have been shown to play crucial roles in the determination of retinal cell fates. As in many biological fields, the expansion of new technologies and techniques in transcriptomics has opened new windows into how progenitor cells arrive at a particular developmental destination. With this increased understanding in recent years, new stochastic and probabilistic models of cell fate have been proposed. As the field seeks additional evidence for one model or the other, it becomes even more critically important to understand the early differences between progenitor cells that are responsible for cell-fate decisions.

2.1. Multipotency of retinal progenitor cells

Various approaches have been utilized to uncover the mechanisms through which a progenitor cell chooses its eventual fate during retinal development. One method, called birthdating, stems from the notion that the final division of a progenitor cell is the newly developing daughter cell's "birthday." Birthdating aims to label cells during the DNA synthesis step of the cell cycle by exposing cells to a nucleotide analog such as radioactive thymidine or bromodeoxyuridine (BrdU) for a period of time (Cepko et al., 1996). After its uptake during DNA synthesis, the marker becomes diluted by successive cell divisions and strongly marks only those cells that terminally divided immediately after exposure to the marker. Early birthdating studies in the murine retina demonstrated that the different retinal cell types are generated at distinct but overlapping time points throughout development (Sidman, 1961; Young, 1985a,b). The first retinal cells to be generated are the retinal ganglion cells, followed closely by horizontal cells, amacrines, and cone photoreceptors (Farah and Easter, 2005). Later-born cell types include rod photoreceptors, bipolar cells, and Muller glia (Altshuler et al., 1991; Fig. 7.2). These birth orders are highly conserved across a multitude of different species. More recent studies examining amacrine cells more closely have discovered that even some subtypes have distinct birthdays, such that glycinergic amacrine cells are born earlier than their GABAergic relatives (Cherry et al., 2009; Voinescu et al., 2009).

In addition to birthdating, one can track the lineage of a single progenitor cell—that is, all the different cell types produced—by injecting a developing

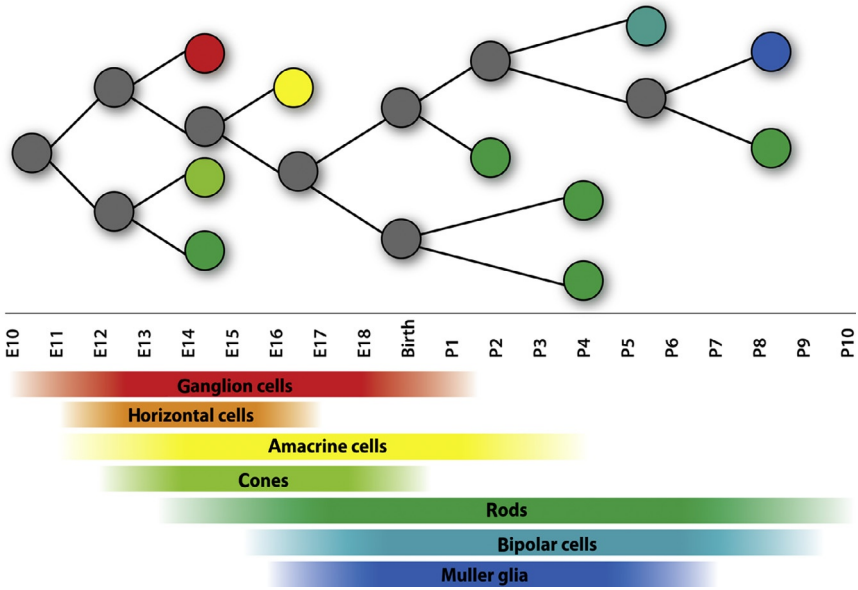

Figure 7.2 The competence model of retinal development. A timeline of retinal progenitor cell competence during mouse development is shown at the top. The lineage that is displayed is from a hypothetical retinal progenitor cell. Although the ratios of cells generated are not directly proportionate to the retina as a whole, this figure illustrates progenitor multipotency. A single progenitor cell may undergo a proliferative division yielding two progenitor cells for daughters, a neurogenic division resulting in two differentiated neurons, or an asymmetric division to produce a differentiated neuron as well as a dividing progenitor. It is important to note that while progenitor cells appear to be capable of generating any given retinal cell type, a single progenitor does not necessarily produce them all. At the bottom, a timeline of progenitor competence is shown. This diagram demonstrates the distinct but overlapping timepoints during which a progenitor cell may generate a given type of retinal neuron. These timepoints correspond to the lineage diagrammed above.

retina with a low-titer retrovirus expressing a reporter, such as GFP, or a fluorescent dye to allow visualization. Investigations of progenitor lineages demonstrated that retinal progenitor cells are multipotent throughout development, or capable of generating multiple kinds of cells including neurons and glia (Holt et al., 1988; Turner and Cepko, 1987; Turner et al., 1990; Fig. 7.2). These progenitor cells show transient biases in the proportion of cell types they generate, as seen through comparisons of the population of daughter cell types generated at either embryonic or postnatal time points. Specifically, retroviral injections of mouse progenitor cells at birth resulted

in labeling of rod photoreceptors, bipolar cells, amacrine cells, and Muller glia (Turner and Cepko, 1987). When the injections were performed during the embryonic period many progenitor cells were observed to now produce all of the cell types (Turner et al., 1990). Therefore, the current understanding is that a given progenitor cell is capable of generating several, if not all, of the cell types present in the mature retina. With this knowledge, retinal development studies have focused on elucidating the influence of intrinsic gene expression patterns and the extrinsic environment on each progenitor cells' fate decision.

2.2. Competence model of retinal cell-fate choice

Based on the data from the lineage experiments, we know that individual retinal progenitor cells are capable of generating an array of cell types. A progenitor cell which is not yet determined to give rise to a particular cell type, but rather has the capability to become any of a variety of retinal cells, is said to have the competence to generate those cell types (Cepko et al., 1996). Retinal progenitor cells are competent to generate a different set of cells at distinct and overlapping timepoints (Fig. 7.2). The probability that a progenitor cell will generate a daughter cell of one type or another changes as development progresses (Fig. 7.2). One example is that early-born retinal cells such as ganglion cells or cone photoreceptors are less likely to emerge from late-stage progenitors. The proposed progression of retinal progenitor cells through distinct states of competence is highly reminiscent of the generation of neurons from neuroblast progenitor cells in Drosophila. These neuroblasts produce intermediate cells called ganglion mother cells that in turn produce a stereotyped set of neurons in a distinct order (Pearson and Doe, 2004). Particular transcription factors (*hunchback*, *kruppel*, *PDM*, and *castor*) are sequentially activated to control the transition in neuron production (Pearson and Doe, 2004). Extension in the time that Hunchback is expressed, for example, results in an extension in the generation of the first-born neurons (Isshiki et al., 2001). Misexpression of Ikaros, the mouse ortholog of *hunchback*, can prolong the window during which early-born cells are generated, while loss of Ikaros specifically leads to a loss of early-born cells (Elliott et al., 2008). However, these effects were not as pronounced as those induced by *hunchback*. Additionally, single cell profiling analyses failed to uncover distinct genetic programs that may be regulating changes in competence (Trimarchi et al., 2008). Currently, it is unclear exactly which factor(s) control these changes in retinal neuron production over time.

The likelihood of a progenitor cell producing one cell type over another could be determined by intrinsic factors (the genes expressed by that progenitor cell), extrinsic factors (signals contributed by the progenitor's environment), or some combination of the two. The extent to which intrinsic and extrinsic signals influence a progenitor cell's fate decision is still a hotly debated topic. Several studies have attempted to address the relative importance of these signals. In the first study, embryonic retinal progenitor cells were isolated, mixed with an excess of postnatal cells and their resulting cell fates analyzed. Importantly, no embryonically derived progenitor cells were observed to prematurely adopt any postnatally generated cell fate (Belliveau and Cepko, 1999). The same basic idea held true during the converse experiment. Progenitor cells derived from postnatal retinas did not adopt early-generated cell fates when mixed with an excess of embryonic cells (Belliveau et al., 2000). While there were some slight changes in the relative proportions of some cells, these experiments point to intrinsic signaling as the driving force behind a progenitor cell's ability to become a given cell type, in spite of any environmental signals. In one final experiment, progenitor cells that were dissociated from one another and cultured *in vitro* generated the normal proportions of the different retinal cells with the correct timing (Cayouette et al., 2003). Again, these results demonstrate that retinal cell-fate decisions proceed normally even in the extreme case where there are no external signals at all.

3. EXTRINSIC SIGNALING

3.1. Importance of environment in retinal cell-fate determination

Since we know that each retinal cell fate can develop without the input from external signals, why should we even bother to examine the environment as it relates to retinal cell fate? There are hints that setting up the relative proportions of all the retinal cell types relies on extrinsic signals. In addition, the required developmental synchronization *in vivo* suggests a coordinated mechanism of intercellular communication that goes beyond cell-intrinsic factors that are needed *in vitro*. Indeed, secreted signaling proteins are an important part of coordinating development among populations of progenitor cells in many contexts. The retina is no exception, as external signaling molecules have been strongly implicated in the control of progenitor cell proliferation and cell-fate decisions (Livesey and Cepko, 2001). These signaling molecules come in many different varieties, including secreted

proteins, small molecules, and cell-surface factors. In this section, we will explore the effects that many different environmental factors have on the cell-fate choices of retinal progenitor cells.

3.2. Secreted signaling proteins

3.2.1 Hedgehog

The first *hedgehog* (*hh*) gene was discovered as part of a classic screen for mutants that disrupted the basic body plan of Drosophila. True to its name, *hedgehog* mutant flies are covered in extra spike-like processes that convey the appearance of a hedgehog (Ingham and McMahon, 2001). As it turns out, fruit fly *hh* also plays an important role in eye development. Hh activates the gene *atonal*, which is responsible for the generation of the Drosophila R8 cell, the first photoreceptor cell generated in any cluster in the fly eye (Amato et al., 2004). The Hedgehog family soon grew with the discovery of three vertebrate members, Sonic Hedgehog (Shh), Desert Hedgehog (Dhh), and Indian Hedgehog (Ihh) (Ingham and McMahon, 2001). For the purposes of murine retinal cell-fate control, Shh is the key family member. Both Ihh and Dhh have been shown to be secreted from the nearby retinal pigment epithelium, but any roles these factors have on retinal cell fate remain to be determined (Amato et al., 2004).

Classic studies in chick demonstrated that retinal ganglion cells secrete a factor that feeds back and inhibits the production of additional ganglion cells (Amato et al., 2004). This cell-fate control mechanism is important for ensuring that ganglion cells are produced at the correct time and in expected amounts during development. As it turns out, Shh is the factor that mediates this effect. Overexpression of Shh-expressing retroviruses in the developing chick led to a decrease in ganglion cell numbers while blocking Shh with an antibody led to an increase in these cells (Zhang and Yang, 2001). However, a conserved role for Shh in general cell-fate determination across different organisms has been difficult to discern. Blocking all Hh family activity with the drug cyclopamine led to a complete inhibition of retinal neurogenesis in the zebrafish, while deletion of *Shh* from the mouse retina resulted in a premature induction of photoreceptors and an overproduction of ganglion cells (Neumann and Nuesslein-Volhard, 2000; Wang et al., 2005). These observations suggest a key role for Shh in retinal cell-fate acquisition, although the various roles played by Shh, including the maintenance of progenitor cell division, the correct layering of the retina, and the prevention of programmed cell death complicate this interpretation (Stenkamp et al., 2002; Wang et al., 2002, 2005). Interference with cell proliferation, for

example, can appear as a cell-fate effect with an increase in early-generated cells and a decrease in late-generated cells. Furthermore, Shh concentration gradients may also determine which cell fate is adopted, much as it does in the developing neural tube (Amato et al., 2004).

In an attempt to further clarify the role of Shh in retinal cell fates, researchers have moved to studying the downstream signaling components of the pathway. Hedgehog signaling relies on binding of the ligand to a transmembrane receptor called Patched (Ingham and McMahon, 2001). In the absence of Shh, Patched interacts with another transmembrane protein, Smoothened (SMO), and represses the ability of SMO to alter the activity of the Gli family of transcription factors (Zhu et al., 2003). Using a conditional knockout strategy to remove SMO from cycling retinal cells resulted in a significant increase in ganglion cells and a smaller increase in cone photoreceptor cells (Sakagami et al., 2009). This was not merely the result of premature cell cycle exit, as horizontal cells, which are also generated during early development, were not affected (Sakagami et al., 2009). Deletion of *suppressor of fused* (*Sufu*), an antagonist of the Shh pathway, led to the production of only amacrine and horizontal cells in the mutant retinal cells and no other retinal cell types (Cwinn et al., 2011). This effect was mediated through Gli2, as removal of Gli2 together with Sufu appeared to restore the ability of retinal progenitor cells to produce the normal diversity of fates (Cwinn et al., 2011). In all of these cases one observation was consistently seen: the Shh signaling pathway mediates its effects on retinal development and cell fate through the modulation of numerous transcription factor families, including bHLH-transcription factors such as Math5. A detailed global analysis of how all the connections between the Shh signal and distinct transcription factors regulate cell fate specifically will be needed to reveal all the roles for this pathway.

3.2.2 FGF signaling

Additional extrinsic cell-fate factors have been identified using a combination of expression studies and *in vitro* assays. For example, many different members of the fibroblast growth factor (FGF) family and their receptors are expressed during retinal development (Blackshaw et al., 2004; Lillien and Cepko, 1992; Trimarchi et al., 2008). Since so many FGFs are expressed in the retina, a dominant negative receptor approach was used to elucidate any cell-fate role played by FGF signaling. Injection of the mutant receptor into Xenopus resulted in a 50% loss of amacrine cells and photoreceptors with a corresponding increase in Muller glia (McFarlane et al., 1998). This

effect appears to be specific to these cell fates since no alterations in either cell death or cell proliferation were observed in this system (McFarlane et al., 1998). However, this does not mean that the role of FGF signaling in retinal cell-fate determination is straightforward. Using a specific inhibitor (SU5402) to block FGF receptor signaling in either the developing chicken or zebrafish retina led to a complete blockage in ganglion cell genesis (Martinez-Morales et al., 2005; McCabe et al., 1999). This result appears to be a generalized inhibition of neurogenesis as none of the retinal cell types were generated. These observations leave open the exact role for FGF signaling in the acquisition of specific retinal cell fates.

One alternative approach is to examine the effects of specific members of the FGF family on retinal cell fate. Overexpression of FGF2 in Xenopus increased ganglion cells by 35% while decreasing Muller glia by 50% (Patel and McFarlane, 2000). Additionally, FGF2 changed the relative proportions of rods and cones, but did not alter the overall number of photoreceptors (Patel and McFarlane, 2000). Again, there are species-specific differences in the effects of FGF on retinal cell fate. In rat retinal cultures, addition of FGF2 resulted in a large increase in opsin-positive photoreceptor cells, while not significantly altering the genesis of other retinal cells (Hicks and Courtois, 1992). Further examination of additional FGFs revealed that in the developing chick retina, treatment with FGF1 could drive the production of retinal ganglion cells, but treatment with FGF8 did not (McCabe et al., 1999). Unfortunately, the overall effects of FGF signaling *in vivo* are much less clear. Mice either deficient for *FGF2* or misexpressing FGF2 showed no apparent retinal defects (Ozaki et al., 1998). Many other single FGF deletions in mice have showed no discernable retinal cell-fate defect as well. With a total of 22 FGFs and 4 FGF receptors present in the genome, it is reasonable to believe that some overlap and crosstalk occurs among the different FGFs themselves and with other signaling pathways. Teasing apart the exact roles for each FGF in retinal cell determination will require the development of tools to look at the gain and loss of combinations of these factors at the same time.

One other approach to uncovering the effects of FGF signaling in the developing retina is to focus on the downstream components of the pathway. Shp2 is a protein tyrosine phosphatase that is believed to be required to achieve maximal FGF downstream signaling (Feng, 1999). Interestingly, removal of *Shp2* conditionally from developing retinas using either a Six3-cre or αPax6-cre did not lead to an observable phenotype (Cai et al., 2010). However, using an Rx-Cre to remove the *Shp2* gene led to a loss of all the

retinal cell fates as the retinal tissue was converted into retinal pigment epithelium (Cai et al., 2010). This phenomenon had been observed previously in a variety of retinal culture experiments (Guillemot and Cepko, 1992). These results indicate that FGF signaling is precisely regulated and controls an early step in the acquisition of retinal identity, but not necessarily controlling the determination of any specific retinal cell fate. Pea3 is an Ets-family transcription factor that is also downstream of FGF signaling. This factor is expressed in the developing retina and is an example of other proteins downstream of FGF signaling that will be studied in the future to shed more light on the role of the FGF pathway in different retinal cell fates (McCabe et al., 2006).

3.2.3 Ciliary neurotrophic factor signaling

Ciliary neurotrophic factor (CNTF) stimulates a signaling cascade through its interaction with a receptor (CNTFRα) that contains significant homology to cytokine receptors (Rhee and Yang, 2010). Cytokines play various roles in the development of immune cells, including the ability to influence their cell fates (Murphy and Reiner, 2002). Given its presence in the retina, it was, therefore, reasonable to believe that CNTF could affect retinal cell fates as well. This prediction was borne out as *in vitro* treatment of retinas with CNTF led to a decrease in rod photoreceptor cells, a slight increase in amacrine cells and Muller glia and a substantial increase in bipolar cells (Ezzeddine et al., 1997). Furthermore, removal of the CNTF receptor yielded the opposite result of additional rod photoreceptors being produced (Ezzeddine et al., 1997). However, additional experiments have produced confusion regarding the true role of CNTF in cell-fate determination. Treatment of chick retinal cells with CNTF resulted in an increase in the number of cone photoreceptors generated (Fuhrmann et al., 1995). *In vivo* retinal injection of a virus engineered to produce CNTF resulted in fewer rod photoreceptors, but because of an increase in cell death and not a change in cell-fate specification (Elliott et al., 2006). Overexpression of leukemia inhibitory factor (LIF), which is highly related to CNTF, also resulted in an interference with photoreceptor development, but not a blockage of cell-fate decisions (Graham et al., 2005). One recurring theme in the CNTF experiments is that the timing of the signal is of paramount importance. This may be due to the expression dynamics of the CNTF receptor or to other downstream signaling components (Fuhrmann et al., 1995). Taken together these studies make it clear that factors such as CNTF and LIF can play critical roles in photoreceptor development and

differentiation, but leave many unanswered questions regarding any potential role for these signaling molecules in cell-fate acquisition specifically.

3.3. Notch pathway

No review of retinal cell-fate determination would be complete without an examination of the Notch signaling pathway. Much like the other extrinsic signals discussed here, the Notch pathway can regulate a multitude of processes, including cell proliferation, cell death, and cell fate. Both the Notch receptor and its ligands, Delta or Serrate, are transmembrane proteins, requiring direct cell-to-cell contact (Guruharsha et al., 2012). When activated by its ligand, the Notch intracellular domain (NICD) is cleaved and translocates to the nucleus where it directly affects transcription of target genes (Guruharsha et al., 2012). The networks formed by these target genes are complex and context-specific, as Notch has been shown to play roles in cell-fate determination in practically every tissue (Fortini, 2012). We will focus our attention on the role of Notch signaling in retinal cell fate.

The initial studies aimed at elucidating the role of Notch signaling in retinal cell-fate decisions used an antisense oligonucleotide strategy to lower the levels of Notch expressed. In the chick retina, a decrease in Notch levels led to a corresponding increase in retinal ganglion cells produced (Austin et al., 1995; Silva et al., 2003). Conversely, retroviral introduction of a constitutively active form of Notch decreased the number of ganglion cells (Austin et al., 1995). Introduction of activated Notch into newborn rat retinas led to a block in differentiation of all cell types (Bao and Cepko, 1997; Furukawa et al., 2000). Similar experiments performed in Xenopus and zebrafish showed either a similar block in differentiation or an increase in Muller glia (Dorsky et al., 1995; Scheer et al., 2001). Since Notch has a documented role in the control of cell proliferation, it was reasonable to believe that the changes in ganglion cell number might have reflected either premature or prolonged cell cycles. However, there was no observed alteration in the incorporation of radioactive thymidine (a marker for the S-phase of the cell cycle) in these experiments (Austin et al., 1995). These results identify Notch as a key regulator retinal development, but left its precise role in regulating cell fate (specifically ganglion cell fate) unclear.

In an attempt to resolve these differences, conditional Notch1-deficient mice were generated. Using a Chx10-cre, a Foxg1-cre, or an αPax6-cre to ablate Notch1 from early in retinal development resulted in a substantial increase in cone photoreceptors (Jadhav et al., 2006; Yaron et al., 2006).

Surprisingly, no additional ganglion cells were observed. In fact, the opposite result was found with ganglion cells decreasing in number (Jadhav et al., 2006; Yaron et al., 2006). Removal of Notch1 at a later developmental time led to an increase in rod photoreceptors instead of the previously observed increase in cone photoreceptors (Jadhav et al., 2006). At this time it is still unclear why removal of Notch1 leads to different cell-fate consequences in the mouse versus the chick. One possible model postulates that different levels of Notch1 are read out differently and have distinct cell-fate outcomes (Jadhav et al., 2006). Experiments where the levels of Notch1 can be carefully controlled will be required to address the validity of this hypothesis. One way to approach this problem is through the use of pharmacological inhibitors. As mentioned above, when Notch is activated, the NICD is cleaved. This cleavage is facilitated by the presenilin/γ-secretase enzyme complex, which is in turn inhibited by a compound called DAPT (Saxena et al., 2001). Treatment of early stage mouse or chick retinas with DAPT led to an increase in cone photoreceptors and ganglion cells, while treatment at later stages led to an increase in rod photoreceptors (Nelson et al., 2007). These results are consistent with both the early chick antisense experiments and the observations from the knockout mice. The most likely explanation for the lack of a ganglion cell phenotype in the Notch1-deficient mouse appears to be the presence of additional Notch proteins (such as Notch3) in the developing retina (Bao and Cepko, 1997). In fact, removal of Notch3 led to a slight increase in ganglion cells (Riesenberg et al., 2009b). When retinas are treated with DAPT, all Notch activity is inhibited, thereby revealing all of the cell-fate functions of Notch signaling in the retina.

As with other signaling pathways, one additional strategy to gain insight into the cell-fate role of Notch signaling is to examine the roles of other proteins in the pathway. Overexpression of a Notch ligand, *delta*, inhibited the ganglion cell production (Austin et al., 1995). However, overexpression of Delta-1 mRNA in the early Xenopus retina coaxed progenitor cells to prematurely differentiate into ganglion cells and cone photoreceptors (Dorsky et al., 1997). Again, experiments performed in two different organisms yielded two different results. There are a couple of potential explanations for these differences. First, the cellular environment has proven to be critically important when it comes to the Notch/Delta signaling cell-fate readout. Delta-expressing cells surrounded by wild-type cells react differently from Delta-expressing cells surrounded by additional Delta-expressing cells (Dorsky et al., 1997). Second, there are four related Delta family members

and at least three of these are expressed during retinal development (Trimarchi et al., 2008). This redundancy no doubt affects the outcome of the Notch signaling pathway in distinct progenitor cells.

Other downstream components of the Notch signaling pathway also show profound cell-fate effects during retinal development. When the NICD translocates into the nucleus, it forms a complex with additional proteins, RBPJ and Mastermind, to activate the transcription of the Hairy/enhancer of split bHLH-transcription factors. Hes5-deficient mice have a substantial decrease in Muller glia cells, but show no defects in retinal neurons (Hojo et al., 2000). Hes1 knockout mice, on the other hand, display an increase in amacrine and horizontal cells, while also showing a decrease in bipolar cells (Tomita et al., 1996a). In mice lacking Rbpj in the retina ganglion cells and cone photoreceptors are overproduced just as in the DAPT experiments (Riesenberg et al., 2009b). All of these experiments point to a critical role for Notch signaling in the inhibition of the ganglion cell and cone photoreceptor cell fate and also a second important positive role in the acquisition of the later Muller glia cell fate.

4. INTRINSIC SIGNALS AND RETINAL DEVELOPMENT

In addition to external signaling molecules, intrinsic factors expressed inside retinal progenitor cells can also play critical roles in determining final cell-fate decisions. Most often, these intrinsically expressed proteins are transcription factors that bind specific DNA sequences and control the expression of cohorts of downstream genes that execute the cellular differentiation program. However, more recent studies have revealed that other factors, such as noncoding RNAs and DNA-modifying enzymes, can also have substantial effects on retinal transcription and, therefore, retinal cell-fate acquisition. We begin by examining a few of the myriad transcription factors that have been shown to influence retinal cell fate and then discuss the roles of more recently identified cell-fate controllers.

4.1. Basic helix–loop–helix factors

Members of the basic helix–loop–helix (bHLH) transcription factor family have been shown to be involved in multiple developmental processes, including retinal neurogenesis (Lee, 1997). These proteins are composed of a helix–loop–helix domain that contributes to dimerization with other bHLH factors, and a basic region that binds to the E-box sequence (CANNTG) of DNA (Murre et al., 1989). In addition, bHLH proteins

can either repress or activate the transcription of downstream genes. Generally the bHLH activators promote neurogenesis, while the repressors work to inhibit neuronal differentiation (Hatakeyama and Kageyama, 2004). Given that different combinations of all the bHLH factors are expressed in different subsets of retinal progenitors (Brzezinski et al., 2011; Trimarchi et al., 2008), their contributions to individual retinal cell fates have proven to be a bit more complicated than was initially predicted.

4.1.1 Ath5

Ath5 belongs to a subfamily of bHLH-transcription factors that is homologous to the Drosophila atonal protein. Atonal is required for the specification of the initial photoreceptor (R8) during Drosophila eye development (Jarman et al., 1994, 1995). Given this result, it was of great interest to test whether vertebrate homologs of *atonal* could play similar roles. Overexpression of the frog homolog, Xath5, significantly increased the population of retinal ganglion cells and led to fewer amacrine cells, bipolar cells, and Muller glia (Kanekar et al., 1997). This effect appeared specific to Xath5 as overexpression of different bHLH factor, NeuroD, did not lead to a change in ganglion cell numbers, but rather to an increase in amacrine and bipolar cells (Kanekar et al., 1997). However, it is unclear whether this effect of Xath5 is generalizable or species-specific. Overexpression of the mouse homolog, Math5, in the same assay resulted in an increase in bipolar cells and not an increase in ganglion cells (Brown et al., 1998). Using viruses to misexpress either Math5 or the chicken homolog (Cath5) in developing chicken retinas did lead to an increase in the number of cells expressing ganglion markers (Liu et al., 2001). In total, misexpression of Ath5 in different organisms pointed toward a role in retinal cell-fate acquisition with a specific emphasis on retinal ganglion cells. The exact nature of that cell-fate role was not fully clear as homologs from different species displayed different potencies.

To better understand the role of Math5 in cell-fate determination, it helps to know exactly which cells in the mature retina have a history of Math5 expression. To trace the lineage of Math5-positive progenitor cells, cre recombinase was inserted into the *Math5* locus and these mice were crossed to a cre-dependent reporter mouse for cell visualization. These mice demonstrated that the lineage of Math5-expressing cells includes most of the ganglion cells and some photoreceptors, amacrine cells, and horizontal cells (Yang et al., 2003). A second cross of the Math5-cre mice to a GFP reporter confirmed the earlier lineage results and showed that Math5-expressing cells

contribute to both rod and cone photoreceptor populations and to a subset of amacrine cells (GABAergic, cholinergic, and AII subtypes) (Feng et al., 2010). Given the multitude of cell types with a history of Math5 expression, a simple model where Math5 instructively drives the formation of ganglion cells seems unlikely.

The role of Math5 in retinal cell-fate determination was further investigated through the generation of Math5-deficient mice by several laboratories. In the absence of Math5, many cell-fate-related phenotypes were observed including some that differed between the mice from distinct labs. The most consistent phenotype was a severe reduction in ganglion cell populations (80–90% of ganglion cells lost) (Brown et al., 2001; Wang et al., 2001). In fact, complete loss of ganglion cells is also observed in the Lakritz zebrafish mutant for Ath5 (Kay et al., 2001). However, additional scrutiny revealed other retinal phenotypes in the Math5 knockout mice. In at least one study, the number of cone photoreceptors increased (Brown et al., 2001). This observation suggested a possible simple cell-fate switch from ganglion cells with Math5 to cone photoreceptors without Math5. The situation has proven to be more complicated than that simple model, though, as the amacrine cell population is also affected in the absence of Math5. One study found that a syntaxin, a marker of all amacrine cells, was expressed normally in the absence of Math5 (Brown et al., 2001). Even with this normal expression, however, the numbers of two subtypes of amacrine cells, A2 and dopaminergic, were substantially decreased in Math5 mutant mice (Brown et al., 2001). Surprisingly, in a different study with a different Math5 mutant mouse, syntaxin staining was increased and cholinergic amacrine cells (as defined by ChAT staining) were also increased (Wang et al., 2001). Altogether the results from the Math5-deficient mice demonstrate the importance of this bHLH factor in cell-fate acquisition in the early developing retina.

Recent Math5-related studies have focused on the deciphering the complexity of bHLH interactions and compensation. When Math5-null mice instead express the related bHLH factors NeuroD1 or Math3 under the Math5 promoter, retinal ganglion cell development is partially rescued to 40% and 10% of wild-type populations, respectively (Mao et al., 2008). Conversely, insertion of Math5 into the NeuroD1 locus reprogrammed future amacrine cells into retinal ganglion cells (Mao et al., 2013). However, this is not a universal feature of Math5 since it could not convert rod photoreceptor precursor cells into ganglion cells when inserted into the Crx gene locus (Prasov and Glaser, 2012). All bHLH factors were not created

equal either as replacement of Math5 with a different bHLH, Ascl1, failed to rescue ganglion cell production (Hufnagel et al., 2013). These results demonstrate that bHLH factors in general and Ath5 specifically execute their functions in a context-dependent manner. Under certain conditions, Ath5 expression provides a permissive environment for the production of ganglion cells, whereas under other conditions it fails to do so. Unraveling the additional factors and precise conditions are challenges for future research.

4.1.2 NeuroD family

The NeuroD family of bHLH-transcription factors is also important in eye development, though the various family members have a range of overlapping, though not identical, expression patterns and effects. Overexpression of NeuroD1 leads to an increase in rod photoreceptors at the expense of Muller glia (Morrow et al., 1999; Ochocinska and Hitchcock, 2009). However, mice engineered to lack NeuroD1 only show a slight increase in bipolar cells (Morrow et al., 1999). Amacrine cell differentiation is delayed, but by adulthood the total number of amacrine cells is normal in NeuroD1-deficient mice (Morrow et al., 1999). Generating a compound mutant mouse where both NeuroD1 and another bHLH factor, Math3, are deleted resulted in a loss of amacrine cells and an increase in both ganglion cells and Muller glia (Inoue et al., 2002). Overexpression experiments, meanwhile, have demonstrated that while these bHLH factors are necessary for amacrine cell fates, they are not sufficient (Inoue et al., 2002). Other factors, either bHLH factors or factors belonging to additional transcription factor families, are clearly necessary to combine with these bHLHs to drive the cell-fate determination of amacrine cells. In an interesting twist on these overexpression experiments, NeuroD1 was recently knocked into the Math5 locus in mice. This meant that there was no endogenous Math5 present and NeuroD1 was now expressed under the control of Math5 regulatory sequences. When this is the case, NeuroD1 is capable of partially rescuing the production of ganglion cells in a Math5-deficient mouse (Mao et al., 2008). These results show that while NeuroD1 has evolved its own functions in amacrine and photoreceptor cell-fate specification, it still has the capacity to behave similarly as a completely distinct bHLH factor when expressed at a different time and place.

Recently, other NeuroD family members also have been implicated in retinal cell-fate determination. Loss of NeuroD2 in mice led to a specific decrease in AII amacrine cells while overexpression led to an increase in amacrine cells at the expense of bipolar cells and Muller glia (Cherry

et al., 2011). Surprisingly, overexpression of NeuroD2 at postnatal day 0 (P0) led to an increase in the production of ganglion cells beyond the time when retinal progenitor cells are normally competent to produce these cells (Cherry et al., 2011). Removal of another related family member, NeuroD6, also leads to a change in amacrine cell fate. In this case, more glycinergic amacrine cells are produced at the expense of GABAergic cells (Kay et al., 2011). These experiments show that to fully understand the generation of all retinal cells, studies of cell-fate determination must be brought to the level of small subtypes of retinal neurons.

4.1.3 Acsl1/Mash1

Acsl1, also referred to as Mash1, is the mammalian homolog of the Drosophila achaete-scute like family of bHLH-transcription factors. Mice deficient for Acsl1 die at birth, making a thorough assessment of early- and late-generated retinal fates *in vivo* impossible (Guillemot et al., 1993). Experiments in which retinas were explanted and cultured *ex vivo* revealed a possible cell-fate connection between Ascl1 and bipolar cells (Tomita et al., 1996b). Retinas that were mutant for both Ascl1 and another bHLH factor Math3 displayed a complete loss of bipolar cells and an increase in Muller glia in explant culture experiments (Tomita et al., 2000). Taken together, these mouse results point to a role for Ascl1 in bipolar cell-fate determination, but since *in vitro* culture experiments can be difficult to interpret in the absence of the *in vivo* environment, further experimentation is warranted. Recently, some interesting results have come to light regarding Ascl1 and its ability to promote neurogenesis at the expense of gliogenesis. In the zebrafish, *ascl1a* is upregulated rapidly after retina injury and is required for retinal regeneration (Fausett et al., 2008). In mouse, forced expression of Ascl1 in Muller glia led to a downregulation of glial gene expression and an acquisition of the capacity to produce retinal neurons (Pollak et al., 2013). These observations reinforce the idea that insights gleaned from retinal cell-fate experiments will be crucial for informing efforts to achieve regeneration of particular retinal cells or entire retinas.

To gain further insight into the role of Acsl1 in retinal cell-fate acquisition, lineage tracing studies were performed to determine which cells had a history of Acsl1 expression. In general, all major cell classes in the retina were represented except for the almost complete lack of retinal ganglion cells derived from Acsl1-positive progenitors (Brzezinski et al., 2011). This was somewhat surprising since Acsl1-deficient retinas produce a normal number of ganglion cells. Additionally, the other early-generated retinal

neurons (horizontal cell, cone photoreceptors, and amacrine cells) were overrepresented in the Acsl1-lineage, while rod photoreceptors were underrepresented (Brzezinski et al., 2011). These results indicate that the heterogeneity in transcription factor expression observed in retinal progenitor cells can affect the competence of particular cells to choose a certain cell fate.

4.1.4 Additional bHLH family members

In addition to the very well-studied bHLH-transcription factors, other bHLH-transcription factors are also expressed in the developing retina (Blackshaw et al., 2004; Trimarchi et al., 2008) and are, most likely, also involved in retinal cell-fate determination. For instance, deletion of Bhlhb5 in the mouse results in a decrease in GABAergic amacrine cells and a subset of bipolar cells (Feng et al., 2006). Olig2, another bHLH from the Olig subfamily, is expressed in only a small subset of retinal progenitor cells (Hafler et al., 2012). Cone photoreceptors, horizontal cells, amacrine cells, and bipolar cells all displayed a history of Olig2 expression. Overexpression of Olig2, however, did not convey any specific cell fate, but rather led to a general cell cycle exit (Hafler et al., 2012). In addition, loss of Olig2 did not lead to any observable cell-fate defect (Hafler et al., 2012). These results point to the fact that distinct bHLH factors have distinct roles in retinal cell-fate determination. Further studies will be required to fully elucidate any overlapping and combinatorial roles these transcription factors might play.

Pancreas transcription factor 1a (Ptf1a) is a bHLH factor that had been linked to cell-fate acquisition in the developing pancreas (Kawaguchi et al., 2002). Lineage tracing analyses in the retina showed that only horizontal and amacrine cells have a history of expressing Ptf1a (Fujitani et al., 2006; Nakhai et al., 2007). Loss of *Ptf1a* in the developing mouse retina led to a complete loss of horizontal cells, a significant decrease in amacrine cells and a corresponding increase in ganglion cells (Fujitani et al., 2006; Nakhai et al., 2007). Along these same lines, overexpression of Xenopus Ptf1a led to an increase of GABAergic cell types, such as horizontal and amacrine cells (Dullin et al., 2007). While it is currently unclear if Ptf1a will be sufficient to drive amacrine and horizontal cell fates in the mouse, these experiments demonstrate that this bHLH factor is a key player in the cell-fate determination of horizontal and amacrine cells.

4.2. Homeodomain-containing transcription factors

Homeotic genes are perhaps most well known for the Drosophila mutants where one body segment has transformed into another such that the mutant

flies can have a pair of legs emanating from their head (Gehring and Hiromi, 1986). However, homeodomain-containing proteins can regulate many different developmental processes including cell-fate determination. These proteins contain a widely conserved homeobox domain that is 180 bp in length and is responsible for conferring sequence-specific DNA-binding activity on this set of transcriptional regulators (Gehring et al., 1994). Homeodomain-containing transcription factors are well known for their importance in the initial formation of the eye field itself (Zuber et al., 2003), but we will not discuss these roles in detail here. Not surprisingly, many homeodomain transcription factors are involved in the determination of particular retinal fates and we will discuss several examples here to provide a framework for understanding the functions of this family.

Visual system homeobox 2 (Vsx2), formerly known as Chx10, is one member of the homeodomain transcription factor family. Mice that harbor a mutation in the Vsx2 gene display microphthalmia (small eye) (Burmeister et al., 1996), primarily due to the upregulation of a cyclin-dependent kinase inhibitor, $p27^{Kip1}$, in retinal progenitor cells (Green et al., 2003). In fact, removal of $p27^{Kip1}$ in a Vsx2 mutant mouse significantly rescues the small eye phenotype by restoring progenitor cell proliferation (Green et al., 2003). However, these mice also showed that Vsx2 is critically important for the production of bipolar cells, as they are absent in both Vsx2 mouse models (Burmeister et al., 1996; Green et al., 2003). Vsx2 is not simply instructive for bipolar cell production on its own. This is observed through Vsx2 overexpression experiments that led to an increase in Muller glia cells (Hatakeyama et al., 2001). However, when Vsx2 was expressed in combination with either of two bHLH proteins, Math3 or Mash1, an increase in bipolar interneurons was observed (Hatakeyama et al., 2001). These experiments demonstrate that homeodomain proteins play important roles in specific retinal cell fates and that combinations of transcription factors from different families will prove critical for driving cell-fate acquisition in different retinal cell types.

A second homeodomain transcription factor expressed during retinal development is Otx2 (Baas et al., 2000). Conditional removal of mouse Otx2 in the retina leads to a complete loss of photoreceptor and bipolar cells with a corresponding increase in several different types of amacrine cells (Koike et al., 2007; Nishida et al., 2003). Misexpression of Otx2 in P0 rat retinas promotes a photoreceptor cell fate at the expense of the other late-generated cells (amacrine, bipolar, and Muller glia) (Nishida et al., 2003). These results point to Otx2 as a key inducer of the photoreceptor

fate and, perhaps, as a repressor of the amacrine fate. It is noteworthy that a highly related transcription factor, Crx, is not involved in photoreceptor cell fate, but rather in the further downstream terminal differentiation of photoreceptors (Chen et al., 1997; Furukawa et al., 1997). This indicates that there is an exquisite specificity operating at the level of these cell-fate-inducing transcription factors. In fact, it has recently been demonstrated that another homeodomain transcription factor, Rax, can activate the Otx2 promoter, while the Notch pathway has been implicated in the repression of Otx2 (Muranishi et al., 2011). Deciphering the interplay of these intrinsic mechanisms and extrinsic signaling pathways is an important future direction for gaining a complete understanding of how retinal cell-fate determination is controlled.

Retinal homeobox 1 (Rax) is homeodomain-containing transcription factor that is essential for the development of the eye (Mathers et al., 1997). Retroviral misexpression of Rax resulted in an inhibition of neurogenesis and a promotion of Muller glia formation (Furukawa et al., 2000). This glial induction may be occurring through a Notch1-dependent mechanism (Furukawa et al., 2000). However, it is still not known what role endogenous Rax is playing in retinal cell-fate determination, since removal of murine Rax results in a complete loss of eyes. A fuller understanding of the role of Rax in cell-fate determination awaits the characterization of cell-type-specific knockout mice. One potential hint as to the role of Rax in individual cell types come from studies on the zebrafish homologues. Zebrafish contain three Rax-related genes (rx1, rx2, and rx3). Morpholino-mediated knockdown of either rx1 or rx2 during the period of photoreceptor production led to a decrease in many photoreceptor-expressed mRNAs (Nelson et al., 2009). Through the use of these "late-injected morphants" these studies were able to reveal a possible role for rx genes in the acquisition or maintenance of the photoreceptor fate.

The paired-type homeobox transcription factor Pax6 has powerful functions in eye development. It is essential for the development of the eye field and, when overexpressed in Drosophila, generates ectopic eyes on wings, legs, and antennae (Grindley et al., 1995; Halder et al., 1995; Nornes et al., 1998). To bypass the early requirement for Pax6 and to better understand its downstream cell-fate effects, the gene was conditionally inactivated in older retinal progenitor cells. In the absence of Pax6, progenitor cells surprisingly produced only amacrine interneurons (Marquardt et al., 2001). The mechanism by which Pax6 normally controls the multipotency of progenitor cells is still unclear, but it most likely involves the regulation of a

network of other transcription factors. For example, Pax6 has been shown to positively regulate the bHLH factor Math5 and negatively regulate the photoreceptor transcription factor Crx (Oron-Karni et al., 2008; Riesenberg et al., 2009a). It will be important, as part of future studies, to fully define the gene networks downstream of Pax6 and to link each of those networks to specific functions of this important transcription factor.

Other homeodomain-containing transcription factors also play significant roles in retinal cell-fate acquisition. When both of the Distal-less homeobox proteins Dlx1/Dlx2 are removed from the retina, a subset of the ganglion cell population is absent (de Melo et al., 2005). These double-knockout mice are embryonic lethal so it is difficult to discern the precise downstream targets of the Dlxs and whether they play any additional roles in other cell types. Postnatal misexpression of the homeodomain transcription factor Prox1 led to an increase in horizontal cells (Dyer et al., 2003). Along the same lines, deletion of mouse Prox1 led to the complete absence of horizontal cells demonstrating that this factor is both necessary and sufficient for the production of horizontal cells (Dyer et al., 2003). These experiments also showed a potential role for Prox1 in amacrine cells, rod photoreceptors, and Muller glia (Dyer et al., 2003). As with all the other factors involved in retinal cell determination, it will be of interest to delineate the exact downstream targets that are involved in the cell-fate controls of the different retinal cell types.

4.3. Other transcription factors and their effects on retinal cell fate

While the bHLH and HD families are two of the largest with identified roles in retinal cell-fate determination, there are many additional intrinsic factors that also influence retinal cell fate. Many members of the forkhead/winged helix family of transcription factors are expressed in the developing retina (Trimarchi et al., 2008). Mice deficient for one of these members, Foxn4, show a near complete loss of amacrine cells, a complete ablation of horizontal cells and an increase in photoreceptor cells (Li et al., 2004). Misexpression of Foxn4 results in the overproduction of amacrine cells, showing that Foxn4 is both necessary and sufficient for this retinal cell fate (Li et al., 2004). The downstream mechanisms through which Foxn4 exerts its effects are still being worked out, but this factor has been shown to impact numerous pathways, including upregulating bHLH and HD transcription factors and influencing Notch activity through the regulation of a Delta (Dll4) (Li et al., 2004; Luo et al., 2012). Given the plethora of Forkhead factors

expressed during retinal development, it will be of interest to determine the phenotypes of all the others, alone or in combination.

Undoubtedly, we have only scratched the surface in our understanding of the roles played by different transcription factors and their downstream networks in retinal cell-fate determination. We have highlighted some of the larger transcription factor families in this review, but there are certainly additional factors that we have omitted. Each year, phenotypes related to additional factors are identified and added to our growing knowledge of the cell-fate process. In the future, the biggest challenge will be to integrate all of these distinct factors and their regulatory networks into a comprehensive snapshot of how the cell-fate programs are initiated and executed to produce not only each retinal cell type, but their subtypes as well. With this information in hand, we will be better able to produce or regenerate any retinal cell types that may be dying or dysfunctional in different retinal disorders.

5. RECENT DISCOVERIES CONTRIBUTING TO RETINAL FATE DECISIONS

5.1. Noncoding RNAs

Throughout this review thus far, we have focused on classic experiments and well-studied effectors of cell-fate decisions. However, since the large-scale Encyclopedia of DNA elements (ENCODE) project revealed that ~75% of the human genome is transcribed (Djebali et al., 2012), we must reevaluate the repertoire of potential cell-fate factors and consider some that have been largely ignored. Included among these factors are long noncoding RNAs (lncRNAs), opposite strand transcripts (OSTs), and micro-RNAs (miRNAs). These different RNA species are expressed in a number of CNS locations (Maiorano and Hindges, 2012), including the retina, and although their exact mechanisms of action are still being actively investigated, it is clear that these types of RNAs can play important roles in the cell-fate acquisition process in the developing retina.

5.1.1 LncRNAs and OSTs

Different types of lncRNAs have been found in many distinct regions of the nervous system (including the retina) throughout development (Mercer et al., 2008). One of the more abundant lncRNAs present in the developing retina, retinal noncoding RNA #2 (RNCR2), is a long (9 kb) nuclear RNA originally found in a SAGE screen of retinal expressed transcripts (Blackshaw

et al., 2004). Decreasing the levels of RNCR2 in the retina led to an increase in both amacrine cells and Muller glia, revealing that this lncRNA normally acts to block the generation of these cell types (Rapicavoli et al., 2010). However, RNCR2 was only necessary and not sufficient for the cell-fate specification of amacrine cells and Muller glia as overexpression of this lncRNA failed to produce an increase in these cells (Rapicavoli et al., 2010). Intriguingly, mislocalization outside of the nucleus led to the same phenotype as RNCR2 knockdown, demonstrating that whatever function RNCR2 plays in retinal cell-fate determination occurs in the nucleus (Rapicavoli et al., 2010).

OSTs have been observed for numerous retina-expressed genes, most prominently the homeodomain transcription factors (Alfano et al., 2005). These noncoding RNAs derive their names from the fact that their transcription begins nearby in the promoter of a well characterized gene and proceeds in the opposite direction (Rapicavoli and Blackshaw, 2009). While it has been tempting to speculate that the function of these OSTs would involve the regulation of their counterpart "sense" transcript, there has been little evidence to back up this hypothesis. Gain and loss of function experiments targeting one particular OST, Six3OS, have shown its important role in retinal cell-fate acquisition (Rapicavoli et al., 2011). Removal of Six3OS expression resulted in retinas with fewer bipolar cells and a concomitant increase in Muller glia cells (Rapicavoli et al., 2011). Further experimentation revealed that Six3OS could act to regulate the transcription factor Six3, but that SixOS might also influence retinal cell fate through a Six3 independent mechanism (Rapicavoli et al., 2011). The precise mechanism by which Six3OS regulates cell fate appears to be through the recruitment of transcriptional repressive complexes to DNA sites, including those of Six3 target genes (Rapicavoli et al., 2011). These complexes contain members of the polycomb family of repressor proteins along with histone-modifying enzymes, but their exact biochemical composition still remains to be identified. These results, as well as those concerning RNCR2 above, suggest that lncRNAs play critical and varied roles in the cell-fate determination of many different retinal cell types, but it will take time and further experiments are needed to fully elucidate the precise mechanisms these novel RNA species play in retinal development.

5.1.2 Dicer and miRNAs

miRNAs are small (21 nucleotide), enzymatically processed RNAs that can regulate gene expression by binding to a complementary mRNA sequence

and targeting that mRNA for either destruction or translational inhibition through association with the RNA-inducing silencing complex (Maiorano and Hindges, 2012). Numerous profiling studies have been performed to identify all of the miRNAs expressed during retinal development (Hackler et al., 2010; Karali et al., 2010). While informative, these studies did not address questions of functionality for these miRNAs.

Dicer is an RNA endonuclease required for the processing of miRNAs. Mice deficient for this enzyme have been constructed, but these mice die during early embryonic development (E7.5) (Bernstein et al., 2003), making it impossible to assess the global role of miRNAs in these mice. Therefore, to study the effects of Dicer loss on the fates of developing retinal cells, a conditional knockout strategy had to be employed. Accordingly, the Dicer gene was flanked by LoxP sites (floxed) and has now been deleted in the retina by crossing it to multiple different cre-expressing mouse lines. Surprisingly, these distinct Dicer retinal conditional knockout mice have yielded different phenotypes. We will review each of them here and attempt to reconcile these disparate results.

The first retinal-specific knockout inactivated Dicer using a transgenic Chx10-cre mouse (Damiani et al., 2008). No defects were observed in the Dicer-deficient retinas during early development of the $Dicer^{flox}/Dicer^{flox}$; Chx10-cre mice (Damiani et al., 2008). In fact, all of the different retinal cells were present, indicating that retinal progenitor cells acquired their cell fates normally in the absence of Dicer. However, as the mice matured, photoreceptor rosettes developed and it became apparent that the vision of these mice was compromised (Damiani et al., 2008). These results suggest that Dicer is not required for early retinal development, but rather functions in the maintenance of a wild-type retina. One caveat to these experiments is the fact that the Chx10-cre is mosaic in its expression in the developing retina (Rowan and Cepko, 2004). Along these lines, a spot-check of miRNA expression in the $Dicer^{flox}/Dicer^{flox}$;Chx10-cre mice showed several miRNAs were present at wild-type levels as late as one month of age (Damiani et al., 2008). These observations provide a potential explanation for the lack of a developmental phenotype in these mice and led to the generation of additional Dicer-deficient mouse models.

Further insight into Dicer's role in retinal development was gained by crossing the floxed Dicer mice to the αPax6cre mice ($Dicer^{flox}/Dicer^{flox}$;αPax6cre). In this conditional mouse there were clearly observable defects in retinal cell fate. There was an increase in early-born retinal cell types, such as ganglion and horizontal cells and a corresponding failure of later-born cell

types, such as rod photoreceptors and Muller glia to be generated (Georgi and Reh, 2010). Additionally, the developmental time window during which ganglion cells are produced was extended beyond the normal range (Georgi and Reh, 2010), indicating that miRNAs are strong candidates to control the changes in competence of retinal progenitor cells. To attempt to explain these phenotypes, Notch signaling was examined and found to be decreased in the Dicer conditional knockout animals (Georgi and Reh, 2011). However, overexpression of a constitutively active Notch protein (NICD) failed to rescue all the phenotypes of the Dicer knockout mice, except for a restoration of the number of horizontal cells generated (Georgi and Reh, 2011). To further elucidate the role of Dicer in retinal development, two additional cre-expressing mice (Dkk3-cre and Rx-cre) have also been crossed to the floxed Dicer mice. In each of these mice, a small eye phenotype was observed due to massive increases in cell death in the developing retina, but no changes in cell fate were reported (Iida et al., 2011; Pinter and Hindges, 2010). Taken together, the results from these Dicer-deficient mice reveal that miRNAs are critical and potent controllers of both retinal cell-fate determination and retinal competence and that different miRNAs most likely operate at distinct time points during development.

The challenge that remains involves deciphering which miRNAs are operating to control each of the different Dicer phenotypes. Recently, there has been progress in this area. Three miRNAs (let-7, miR-9, and miR-125) were identified as upregulated during the early embryonic developmental time window (La Torre et al., 2013). Expression of these miRNAs led to a significant decrease in the number of horizontal and ganglion cells produced, while antagonizing these miRNAs led to an increase in the numbers of these cells (La Torre et al., 2013). Perhaps most informative, introduction of these three miRNAs into the Dicer-deficient retinas significantly rescued the production of later-born rod photoreceptors, but not later-born bipolar cells (La Torre et al., 2013). Two potential target genes, Lin28b and Protogenin, were also identified and shown to be capable of extending the early competence window in a similar fashion as the miRNAs (La Torre et al., 2013). These experiments demonstrate that different RNA species, besides just the traditional mRNAs, can have profound effects on retinal development and cell-fate acquisition. Integrating the functions of these noncoding RNAs with those of the more "traditional" intrinsic and extrinsic factors will lead to a more comprehensive picture of how retinal cells decide on a specific cell fate.

5.2. Epigenetics

5.2.1 Methyltransferases

Epigenetic modifications are also a potential source of regulation of cell-fate decisions in the developing retina. In general, DNA methylation and modifications to histone proteins are the two most prominent epigenetic changes that have been linked to stable alterations in gene expression (Jaenisch and Bird, 2003). At the moment, it is not clear what exact role DNA methylation plays in the acquisition or maintenance of retinal cell fates, but DNA methyltransferase enzymes, which are responsible for transferring the methyl group to DNA, are expressed in the developing retina (Nasonkin et al., 2011). Their expression places them in the right place and the right time to exert significant effects on the expression of key genes involved in cell-fate decisions.

In addition to direct DNA methylation, methylation of lysine residues in histone proteins has been shown to affect gene transcription and to correlate with cellular differentiation (Mohn and Schubeler, 2009). G9a histone methyltransferase, which is expressed at high levels in the developing retina, is an enzyme that can di-methylate the lysine residue at position 9 in histone H3. In a G9a conditional knockout mouse, there is a significant increase in cell death throughout development and an extension of the window in which cycling progenitor cells can be detected (Katoh et al., 2012). Somewhat surprisingly, however, cell-fate determination appears not to have been affected in these mice, even though differentiation of all retinal cell types has been compromised (Katoh et al., 2012). How DNA methylation and histone methylation may be coordinated to regulate gene expression during retinal cell-fate acquisition is an open question. Future experiments will examine the roles of these methylation marks in specific cell types and at specific time points of retinal development.

Epigenetic factors do not act in isolation and, in fact, are most likely coordinated with many or all of the intrinsic transcription factors discussed earlier. Along those lines, repressive complexes containing chromatin remodeling proteins and histone methyltransferases have profound impacts on the activity of transcription factors that control retinal cell fate. Blocking the function of these complexes inhibits most retinal neuron fates and leads to an expansion in Muller glia cells (Aldiri et al., 2013). Furthermore, it has been shown in chicken that as the expression of the bHLH-transcription factor Cath5 increases, so does the methylation of lysine 4 on histone H3 (Skowronska-Krawczyk et al., 2004). The Cath5 promoter sequences affect the methylation of lysine 4 only in the retina and only around the time of

ganglion cell production (Skowronska-Krawczyk et al., 2004). The fact that this activity is highly regulated suggests that the retina has its particular set of histone marks (histone "code") operating during development and that this code could be different for different transcription factor networks active as different cells acquire their final cell fates.

5.2.2 Histone acetylation

Covalent modifications of the tails of histone proteins play important regulatory roles in activation and repression of transcription (Jenuwein and Allis, 2001). Perhaps the most well-studied histone modification is histone lysine acetylation. Enzymes called histone acetyltransferases catalyze the addition of an acetyl group onto conserved lysine residues in histone tails while histone deacetylases (Hdacs) remove these acetyl groups. In general the presence of acetylated lysine residues correlates with an "open" chromatin conformation and, therefore, an increase in gene transcription, while the removal of the acetyl group is most often associated with gene repression (Roth et al., 2001). The exact role of these enzymes in retinal cell-fate determination is currently under investigation. In zebrafish, mutations in Hdac1 lead to a compromised ability of retinal progenitor cells to exit the cell cycle (Yamaguchi et al., 2005). Hdac1 was further shown to downregulate both the Wnt and Notch signaling pathways leading to cell cycle exit and neuron production (Yamaguchi et al., 2005). Any role for this enzyme in the cell-fate decisions of specific retinal cell types is currently unknown though. These roles most likely exist since pharmacological removal of histone deacetylase activity in retinal cultures led to a loss of rod photoreceptor cells and Muller glia with a concomitant increase in bipolar cells (Chen and Cepko, 2007). Additional retina-specific removal of the enzymes that control these chromatin alterations should increase our understanding of the precise role that the histone modifications play in determining and maintaining different retinal cell fates.

6. "OMICS" APPROACHES TO UNDERSTANDING RETINAL CELL-FATE DECISIONS

6.1. Whole retina studies

Classic studies designed to identify and characterize retinal cell-fate determinants traditionally focused on the role of a single factor or, in rare instances, several factors simultaneously. However, it is undoubtedly combinations of genes (networks) that work together in concert to produce the distinct types

and subtypes of retinal neurons. Therefore, in the search for intrinsic and extrinsic factors that work together to drive the fate of retinal progenitor cells, it is important to leave no stone unturned. Forward genetics, the technique by which an interesting phenotype (such as microphthalmia or lack of optic nerve development) is discovered and studied to determine its genetic root, is an extremely powerful approach to determine genes that drastically affect large-scale developmental cascades. However, many genes may be missed by forward genetics. A converse approach, called reverse genetics, starts with a gene in mind and works backward to determine the role that gene plays in a system. The process of reverse genetics may seem less exciting at first, but it allows for a much more thorough understanding of developmental factors. The key to a reverse genetics approach is knowing the transcriptome—the full collection of mRNA transcripts that are expressed, whether in the whole retina, a subset of retinal cells, or just within a single developing cell. Many recent studies have tackled the problem of identifying all the mRNA transcripts associated with different stages of retinal development and distinct retinal cell populations.

Several groups have examined retinal gene expression using microarrays or expressed sequence tag-based approaches to catalog all the transcripts expressed at distinct times during normal retinal development (Chowers et al., 2003; Livesey et al., 2004; Swaroop and Zack, 2002). Additionally, comparisons of transcriptomes between wild-type and mutant organisms can help to reveal previously uncharacterized factors involved in the development of particular retinal cells. For instance, a screen for genes differentially expressed between embryonic day (E)14.5 wild-type and Brn3b knockout mice revealed a host of candidate genes to be tested for their functional roles in ganglion cell development (Mu et al., 2001). Additionally, comparisons have been made between the transcriptomes of wild-type mice and Math5-deficient mice at multiple developmental time points. These microarray experiments revealed a wealth of potential downstream targets of Math5 that may be important in the cell-fate determination of several early-generated retinal cell types (Mu et al., 2005). As with all of these large-scale profiling studies, the future challenge is to understand which of these genes are the critical cell-fate regulators and how all of these different genes work together to produce the different retinal cells.

To further expand our knowledge of gene expression, serial analysis of gene expression, or SAGE, was employed at 2-day intervals throughout retinal development (Blackshaw et al., 2004). This technique has the added advantage of not relying solely on those genes that are spotted down on a

microarray. Additionally, this study further characterized the expression of >1000 genes by *in situ* hybridization (Blackshaw et al., 2004). Mining this dataset has already identified transcription factors and signaling molecules that could play key roles in setting up distinct cell-fate choices. As sequencing techniques have improved, RNA-seq has now become a widely used profiling technique. Thus far it has only been used to identify mRNAs expressed in the adult retina (Gamsiz et al., 2012), but it will soon be utilized for multiple different time points. RNA-seq allows for the identification of novel splice isoforms and long noncoding RNAs to add to the repertoire of potential cell-fate determinants (Wang et al., 2009). These studies will continue to produce candidate factors for study for many years to come.

6.2. Single cell studies

Since the developing retina contains a complex mixture of uncommitted retinal progenitor cells and different cell types in various stages of maturation (Young, 1985a), identifying programs that drive distinct cell fates is challenging with classic whole tissue approaches. Given these issues, single cell-based profiling techniques were adapted to retinal cells to achieve the resolution necessary to examine gene networks in even rare cell types. After retinal dissection and dissociation, individual cells were isolated using a small glass needle and cDNA libraries were generated through amplification-based strategies (Goetz and Trimarchi, 2012). The resulting microarray data from these single cell libraries revealed a treasure trove of marker genes for mouse retinal progenitor cells at different stages of development (Trimarchi et al., 2008) and, specifically, for developing retinal ganglion and amacrine cells (Trimarchi et al., 2007). In addition to the new markers, the single cell retinal profiling studies revealed a surprising level of gene expression heterogeneity, even among retinal progenitor cells isolated from the same embryonic time point (Trimarchi et al., 2008). Much of this observed heterogeneity was observed to derive from the differential expression of transcription factors from diverse sets of transcription factor families, including those described in this review and many others. Despite this wealth of expression-based information, precisely how these genes work together to produce each specific type and subtype of retinal neuron is not fully understood. A combination of more sophisticated computational tools and functional studies will be necessary to generate a more complete picture of the role(s) for each of these genes in retinal cell-fate determination.

Since it was known that retinal progenitor cells change their competence as they progress through developmental time (Cepko et al., 1996) and that this progression appeared to be largely controlled by intrinsic mechanisms (Cayouette et al., 2003), one would predict that clusters of genes would track specifically with either early or late single retinal progenitor cells. While this was indeed found to be the case, the number of genes and their expression patterns proved to be a surprise. Only a single gene, Secreted frizzled-related protein 2 (Sfrp2), was found to be broadly expressed primarily in early embryonic progenitor cells. A handful of additional genes showed expression that was restricted to early progenitor cells, but each of these genes was only observed in a small subset of cells. What these results mean in terms of the competence model of retinal development remains unclear. Perhaps competence is not driven by changes in mRNAs expressed in progenitor cells, but rather by changes in protein expression (see Ikaros), changes in miRNA expression, or some combination of both. Alternatively, the gene expression heterogeneity revealed by the single cell profiling could be pointing to a more stochastic model of retinal development. No matter which model proves to be ultimately correct, collecting more single cell profiles will help to sort through the meaning of all the gene expression heterogeneity. For these future studies either genetically encoded or electroporated fluorescent reporters (Cherry et al., 2009) will enable the isolation of more specific sets of cells. This refinement, combined with the change from microarray technology to RNA-seq technology, will expand the amount of information collected and the number of single cells analyzed.

7. ADDITIONAL FACTORS CONTRIBUTING TO RETINAL FATE DETERMINATION

7.1. Asymmetric versus symmetric cell divisions

We have discussed many intrinsic and extrinsic factors and the roles they play in retinal cell-fate decisions, but there are other aspects to the story. For example, the position and activity of a progenitor cell during its progression through the cell cycle may confer information about its final cell fate beyond its internal composition and the nearby environmental factors. It is well documented that the nuclei of cycling progenitor cells follow a predictable progression (Dyer and Cepko, 2001b). They migrate to the apical, or outer, surface of the retina to undergo mitosis. As they move forward through the first gap (G1) phase, these progenitor cells shift basally, toward the vitreal surface of the retina. At their basal nadir, progenitor cells pass through G1

and start the S-phase of the cell cycle. They then move apically in G2 phase before entering mitosis again at their apical peak. By studying the kinetic trends of progenitor cells, it was found that cells that travel much farther basally than their neighbors tend to generate two neurons instead of another proliferating progenitor cell (Baye and Link, 2007). However, whether this phenomenon is linked to specific retinal fates or just neurogenesis in general remains to be determined.

In *Drosophila* and *Caenorhabditis elegans*, asymmetric distribution of cell-fate determinants prior to cell division is widely known to bias the cell-fate decision-making process (Roegiers and Jan, 2004). Uneven distribution of mRNAs or proteins within a dividing parent cell can produce different fates between its two daughter cells. One identified factor that is asymmetrically localized at mitosis is Numb, a negative regulator of Notch. When Numb is misexpressed in a progenitor cell, it has a higher chance of producing rod photoreceptors at the expense of amacrine cells, bipolar cells and Muller glia (Cayouette and Raff, 2003). Since Numb inhibits Notch signaling, these results are consistent with those where Notch itself was perturbed. Loss of Notch1 late in retinal development led to an increase in rod photoreceptors much like overexpression of Numb. Removal of Numb from the retina leads to a corresponding decrease in asymmetric cell divisions that produce a photoreceptor cell. However, symmetric divisions producing rod photoreceptors are increased, indicating that Numb is not generally required for this particular cell fate (Kechad et al., 2012). What are the determinants that drive rod photoreceptor fate in symmetric divisions versus asymmetric ones? Why does there need to be a difference in how these cells acquire their fates? The answers to these questions await further experimentation.

7.2. Cell cycle's influence on cell fate

Underlying all of the stimuli (extrinsic and intrinsic) that influence retinal cell fate is the fact that this process must be coordinated with cell proliferation so that the retina produces the correct amount of total cells. Many extrinsic and intrinsic factors that we have discussed influence the cell cycle in addition to cell fate. Cell cycle regulators also aid in the cell-fate decision-making process and perhaps, in some cases, help drive the specification of particular fates. One well-studied factor that is critically involved in the regulation of cell cycle exit is the retinoblastoma tumor suppressor protein (Rb) (Weinberg, 1995). Conditional knockout mice where Rb is deleted from the retina do in fact show a defect in the ability of progenitor cells to exit

the cell cycle (Zhang et al., 2004). Interestingly, loss of Rb also leads to the production of fewer rod photoreceptors specifically (Zhang et al., 2004). This cell-fate phenotype occurs only in rod photoreceptors and is separate from the effect of Rb loss on the cell cycle. Instead, transcription factors that are important for rod development, such as Nrl, are absent in Rb-deficient retinas (Zhang et al., 2004). These results demonstrate that factors can play different roles in determining different cell fates and that, for some factors, their cell cycle roles are separate from other roles in cell-fate determination.

Another family of cell cycle regulators, the cyclin kinase inhibitors (CKIs), can block the cell cycle at a number of places and, in some contexts, promote differentiation. Overexpression of a CKI from Xenopus, $p27^{Xic1}$, inhibits retinal progenitor cell proliferation, but also shows a specific cell-fate effect. Muller glia cells are increased, while bipolar cells are decreased (Ohnuma et al., 1999). Interestingly, the domain that is responsible for kinase inhibition was not required to facilitate the cell-fate switch, suggesting a potential novel mechanism (Ohnuma et al., 1999). Both gain and loss of the mouse homolog of this CKI, $p27^{Kip1}$, show cell cycle phenotypes in a similar fashion as $p27^{Xic1}$. However, in the case of the mouse, neither gain nor loss of function showed significant alterations in any retinal cell fates (Dyer and Cepko, 2001a). Perturbation of another related mouse CKI, $p57^{Kip2}$, displays aspects of both a cell cycle and cell-fate phenotype, much as in the case of Xenopus. When $p57^{Kip2}$ was removed from embryonic retinal progenitor cells, these cells could not properly exit the cell cycle and subsequently died (Dyer and Cepko, 2000). On the other hand, when $p57^{Kip2}$ was removed from postnatal retinal progenitor cells, there was an increase in amacrine cells (Dyer and Cepko, 2000). All of these experiments point to the precise regulation of intrinsic factors (transcription factors and otherwise) in response to extrinsic cues leading to a coordinated exit from the cell cycle and the acquisition of specific retinal cell fates. It is important to consider how all of these processes are coregulated when examining any experimental results dealing with cell-fate determination.

8. RECENT PERSPECTIVES

8.1. New models of retinal cell-fate acquisition: Stochastic models

A discussion of the influences that different intrinsic and extrinsic factors can have on the acquisition of different retinal cell fates suggests that retinal progenitor cells are enacting discrete programs that lead to the reproducible

production of particular types of cells. These programs are represented in the deterministic model of cell-fate determination (Fig. 7.3A). Perhaps, the most infamous example of such a deterministic organization of cell fate occurs in *C. elegans*. Researchers have discovered the identity and number of all the cells in this nematode and even have mapped out the lineages for all cells, as they do not change from one animal to another (Hobert, 2010). While the case of *C. elegans* is an extreme one, it has been presumed for some time that cell-fate determination generally follows the same basic rules. In the retina this would be that cells enact a specific intrinsic program, at a specific time and specific position. The results of that intrinsic cell-fate program would be the production of a specific cell type. This program would be the same each time this particular retinal neuron type was produced. As development proceeds, the competence of the progenitor cells would change, but the intrinsic programs they enact would be the same for any particular cell type. However, more recent data suggest that not all the cell-fate decisions of retinal progenitor cells are deterministic, but instead there may be more randomness to these decisions than was previously appreciated (Fig. 7.3B).

Stochastic cell-fate determination has been demonstrated in Drosophila eye development, where progenitors are randomly recruited to clusters of eight photoreceptors, or ommatidia, and adopt a photoreceptor fate based on their position and timing of recruitment. Extracellular Notch/Delta signaling plays a critical role in the differentiation of cells in the ommatidia. Progenitor cells are initially indistinguishable until small changes in the cells' reaction to Notch signals initiate feedback loops to differentiate those cells further (Johnston and Desplan, 2008). Removal of the *sevenup* gene, which is repressed by Notch and is necessary to generate R1 and R6 photoreceptors, prevents progenitor cells from developing properly, and leaves them to decide randomly between an R7 or an R8 photoreceptor fate (Miller et al., 2008). The cells forced into these fates decide to become either R7 or R8 regardless of spatial considerations, and express genes specific to one photoreceptor type completely exclusively of the other (Miller et al., 2008).

The gene networks involved in the cell-fate decision-making process in vertebrates are complex and dynamic, which impedes experiments designed to differentiate between a stochastic and deterministic model. To begin to gain insight into which process is operating, researchers first set out to understand the types of divisions that progenitor cells undergo. These divisions can be classified as proliferative (generating two new progenitors), self-renewing (generating one progenitor cell and one differentiated retinal cell), and terminal (generating two nonproliferative retinal cells). In zebrafish, marked

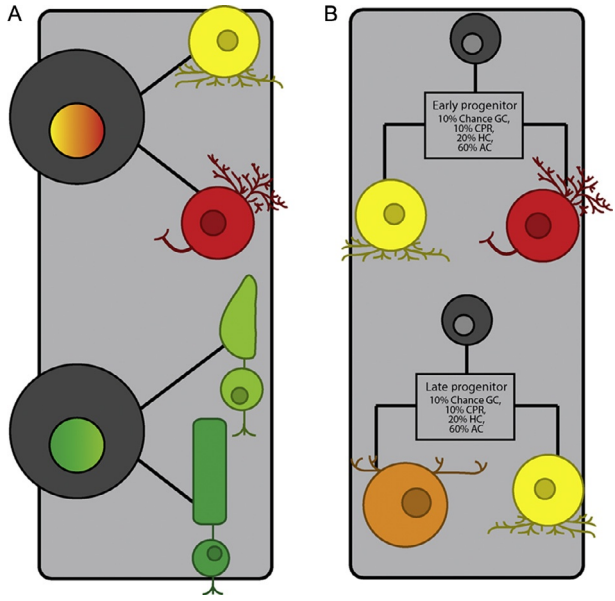

Figure 7.3 Models of retinal cell-fate determination. (A) The deterministic model states that progenitor cells are fated to produce a certain subset of retinal cells, and this determination cannot be changed. For instance, the top progenitor cell will divide to yield an amacrine cell and a ganglion cell, whereas the bottom cell will produce a cone photoreceptor and a rod photoreceptor. (B) The stochastic model of cell-fate determination posits that the fate of progenitor cells is not determined, but is instead subject to changing probabilities. As shown, the probability of producing an early retinal cell versus a late retinal cell changes throughout the development of the retina.

lineages of progenitor cells were monitored through multiple cell divisions and the resulting data used to generate a mathematical model of retinal development. The best model to explain the data was one where the progenitor cells produced progeny without adherence to a strictly deterministic pattern (He et al., 2012). The model is not consistent with a fully stochastic model either, but rather one in which progenitor cells make "random" cell-fate choices based on a weighted probability that changes throughout development (Fig. 7.3). Interestingly, this study also showed that the bHLH factor *ath5* can "tip the scales" in favor of ganglion cell production, linking a factor with a wealth of previous literature to this new model of retinal development (He et al., 2012). This probabilistic mode of cell-fate determination is not unique to zebrafish. When videomicroscopy was used to monitor rat progenitor cells and the cell fates they produce over time, it was found that again

the most consistent model of cell-fate acquisition was a more stochastic one (Gomes et al., 2011). Specifically, a progenitor cell was able to generate a late-born neuron and then an early-born retinal neuron in succession (Gomes et al., 2011). These observations suggest a stochastic probability that each progenitor cell could differentiate into any of a few given cell types, as opposed to a more deterministic timed cell lineage.

8.2. Concluding remarks

As we move to the future, how are we to make sense of the strategies retinal progenitor cells use to acquire all the distinct cell fates (both cell types and subtypes). It is apparent that a simple model wherein cells proceed along an intrinsically determined linear pathway and arrive at a specific fate is insufficient. It is here that single cell gene expression profiling studies will be invaluable for revealing the gene networks operating to push cells down one cell-fate pathway or another. Experiments performed on individual developing retinal cells have already demonstrated an incredible amount of gene expression heterogeneity in the cycling cell population (Trimarchi et al., 2008). Nowhere is this more apparent than when examining different subsets of transcription factors. The challenge for the future will be to determine just which combinations of factors are the critical ones for biasing a progenitor cell toward one fate or another. One way that this may be possible is by combining single cell profiling with videomicroscopy and mathematical modeling. Recently, an algorithm was developed that could predict, with incredible accuracy, whether a progenitor cell would produce a neuron or not (Cohen et al., 2010). In addition, this algorithm could, in some cases, predict which type of neuron would be generated (Cohen et al., 2010). Using this strategy, single cells could be profiled for their gene expression with the knowledge of precisely which cell fate they were about to generate. Correlating this information across a multitude of individual cells would allow for specific networks to be identified and tested for their ability to bias the production of distinct fates. With all of this information in hand, we will be better able to control the production of particular cell types from stem cell populations for more efficient use in cellular replacement strategies for retinal diseases.

REFERENCES

Aldiri, I., Moore, K.B., Hutcheson, D.A., Zhang, J., Vetter, M.L., 2013. Polycomb repressive complex PRC2 regulates Xenopus retina development downstream of Wnt/beta-catenin signaling. Development 140, 2867–2878.

Alfano, G., Vitiello, C., Caccioppoli, C., Caramico, T., Carola, A., Szego, M.J., McInnes, R.R., Auricchio, A., Banfi, S., 2005. Natural antisense transcripts associated with genes involved in eye development. Hum. Mol. Genet. 14, 913–923.

Altshuler, D.M., Turner, D.L., Cepko, C.L., 1991. Specification of cell type in the vertebrate retina. In: Lam, D.M.-K., Shatz, C.J. (Eds.), Develoment of the Visual System. MIT Press, Cambridge, pp. 37–58.

Amato, M.A., Boy, S., Perron, M., 2004. Hedgehog signaling in vertebrate eye development: a growing puzzle. Cell. Mol. Life Sci. 61, 899–910.

Austin, C.P., Feldman, D.E., Ida, J.A., Cepko, C.L., 1995. Vertebrate retinal ganglion cells are selected from competent progenitors by the action of Notch. Development 121, 3637–3650.

Baas, D., Bumsted, K.M., Martinez, J.A., Vaccarino, F.M., Wikler, K.C., Barnstable, C.J., 2000. The subcellular localization of Otx2 is cell-type specific and developmentally regulated in the mouse retina. Brain Res. Mol. Brain Res. 78, 26–37.

Bao, Z.Z., Cepko, C.L., 1997. The expression and function of Notch pathway genes in the developing rat eye. J. Neurosci. 17, 1425–1434.

Baye, L.M., Link, B.A., 2007. Interkinetic nuclear migration and the selection of neurogenic cell divisions during vertebrate retinogenesis. J. Neurosci. 27, 10143–10152.

Belliveau, M.J., Cepko, C.L., 1999. Extrinsic and intrinsic factors control the genesis of amacrine and cone cells in the rat retina. Development 126, 555–566.

Belliveau, M.J., Young, T.L., Cepko, C.L., 2000. Late retinal progenitor cells show intrinsic limitations in the production of cell types and the kinetics of opsin synthesis. J. Neurosci. 20, 2247–2254.

Bernstein, E., Kim, S.Y., Carmell, M.A., Murchison, E.P., Alcorn, H., Li, M.Z., Mills, A.A., Elledge, S.J., Anderson, K.V., Hannon, G.J., 2003. Dicer is essential for mouse development. Nat. Genet. 35, 215–217.

Blackshaw, S., Harpavat, S., Trimarchi, J., Cai, L., Huang, H., Kuo, W.P., Weber, G., Lee, K., Fraioli, R.E., Cho, S.H., Yung, R., Asch, E., Ohno-Machado, L., Wong, W.H., Cepko, C.L., 2004. Genomic analysis of mouse retinal development. PLoS Biol. 2, E247.

Brown, N.L., Kanekar, S., Vetter, M.L., Tucker, P.K., Gemza, D.L., Glaser, T., 1998. Math5 encodes a murine basic helix-loop-helix transcription factor expressed during early stages of retinal neurogenesis. Development 125, 4821–4833.

Brown, N.L., Patel, S., Brzezinski, J., Glaser, T., 2001. Math5 is required for retinal ganglion cell and optic nerve formation. Development 128, 2497–2508.

Brzezinski, J.A.t., Kim, E.J., Johnson, J.E., Reh, T.A., 2011. Ascl1 expression defines a subpopulation of lineage-restricted progenitors in the mammalian retina. Development 138, 3519–3531.

Burmeister, M., Novak, J., Liang, M.-Y., Basu, S., Ploder, L., Hawes, N.L., Vidgen, D., Hoover, F., Goldman, D., Kalnins, V.I., Roderick, T.H., Taylor, B.A., Hankin, M.H., McInnes, R.R., 1996. Ocular retardation mouse caused by Chx10 homeobox null allele: impaired retinal progenitor proliferation and bipolar cell defferentiation. Nature 12, 376–383.

Burns, M.E., Arshavsky, V.Y., 2005. Beyond counting photons: trials and trends in vertebrate visual transduction. Neuron 48, 387–401.

Cai, Z., Feng, G.S., Zhang, X., 2010. Temporal requirement of the protein tyrosine phosphatase Shp2 in establishing the neuronal fate in early retinal development. J. Neurosci. 30, 4110–4119.

Cayouette, M., Raff, M., 2003. The orientation of cell division influences cell-fate choice in the developing mammalian retina. Development 130, 2329–2339.

Cayouette, M., Barres, B.A., Raff, M., 2003. Importance of intrinsic mechanisms in cell fate decisions in the developing rat retina. Neuron 40, 897–904.

Cepko, C.L., Austin, C.P., Yang, X., Alexiades, M., Ezzeddine, D., 1996. Cell fate determination in the vertebrate retina. Proc. Natl. Acad. Sci. U. S. A. 93, 589–595.

Chen, B., Cepko, C.L., 2007. Requirement of histone deacetylase activity for the expression of critical photoreceptor genes. BMC Dev. Biol. 7, 78.

Chen, S., Wang, Q.L., Nie, Z., Sun, H., Lennon, G., Copeland, N.G., Gilbert, D.J., Jenkins, N.A., Zack, D.J., 1997. Crx, a novel Otx-like paired-homeodomain protein, binds to and transactivates photoreceptor cell-specific genes. Neuron 19, 1017–1030.

Cherry, T.J., Trimarchi, J.M., Stadler, M.B., Cepko, C.L., 2009. Development and diversification of retinal amacrine interneurons at single cell resolution. Proc. Natl. Acad. Sci. U. S. A. 106, 9495–9500.

Cherry, T.J., Wang, S., Bormuth, I., Schwab, M., Olson, J., Cepko, C.L., 2011. NeuroD factors regulate cell fate and neurite stratification in the developing retina. J. Neurosci. 31, 7365–7379.

Chowers, I., Gunatilaka, T.L., Farkas, R.H., Qian, J., Hackam, A.S., Duh, E., Kageyama, M., Wang, C., Vora, A., Campochiaro, P.A., Zack, D.J., 2003. Identification of novel genes preferentially expressed in the retina using a custom human retina cDNA microarray. Invest. Ophthalmol. Vis. Sci. 44, 3732–3741.

Cohen, A.R., Gomes, F.L., Roysam, B., Cayouette, M., 2010. Computational prediction of neural progenitor cell fates. Nat. Methods 7, 213–218.

Cwinn, M.A., Mazerolle, C., McNeill, B., Ringuette, R., Thurig, S., Hui, C.C., Wallace, V.A., 2011. Suppressor of fused is required to maintain the multipotency of neural progenitor cells in the retina. J. Neurosci. 31, 5169–5180.

Damiani, D., Alexander, J.J., O'Rourke, J.R., McManus, M., Jadhav, A.P., Cepko, C.L., Hauswirth, W.W., Harfe, B.D., Strettoi, E., 2008. Dicer inactivation leads to progressive functional and structural degeneration of the mouse retina. J. Neurosci. 28, 4878–4887.

de Melo, J., Du, G., Fonseca, M., Gillespie, L.A., Turk, W.J., Rubenstein, J.L., Eisenstat, D.D., 2005. Dlx1 and Dlx2 function is necessary for terminal differentiation and survival of late-born retinal ganglion cells in the developing mouse retina. Development 132, 311–322.

Djebali, S., Davis, C.A., Merkel, A., Dobin, A., Lassmann, T., Mortazavi, A., Tanzer, A., Lagarde, J., Lin, W., Schlesinger, F., Xue, C., Marinov, G.K., Khatun, J., Williams, B.A., Zaleski, C., Rozowsky, J., Roder, M., Kokocinski, F., Abdelhamid, R.F., Alioto, T., Antoshechkin, I., Baer, M.T., Bar, N.S., Batut, P., Bell, K., Bell, I., Chakrabortty, S., Chen, X., Chrast, J., Curado, J., Derrien, T., Drenkow, J., Dumais, E., Dumais, J., Duttagupta, R., Falconnet, E., Fastuca, M., Fejes-Toth, K., Ferreira, P., Foissac, S., Fullwood, M.J., Gao, H., Gonzalez, D., Gordon, A., Gunawardena, H., Howald, C., Jha, S., Johnson, R., Kapranov, P., King, B., Kingswood, C., Luo, O.J., Park, E., Persaud, K., Preall, J.B., Ribeca, P., Risk, B., Robyr, D., Sammeth, M., Schaffer, L., See, L.H., Shahab, A., Skancke, J., Suzuki, A.M., Takahashi, H., Tilgner, H., Trout, D., Walters, N., Wang, H., Wrobel, J., Yu, Y., Ruan, X., Hayashizaki, Y., Harrow, J., Gerstein, M., Hubbard, T., Reymond, A., Antonarakis, S.E., Hannon, G., Giddings, M.C., Ruan, Y., Wold, B., Carninci, P., Guigo, R., Gingeras, T.R., 2012. Landscape of transcription in human cells. Nature 489, 101–108.

Dorsky, R.I., Rapaport, D.H., Harris, W.H., 1995. Xotch inhibits cell differentiation in the Xenopus retina. Neuron 14, 487–496.

Dorsky, R.I., Chang, W.S., Rapaport, D.H., Harris, W.A., 1997. Regulation of neuronal diversity in the Xenopus retina by Delta signalling. Nature 385, 67–70.

Drager, U.C., Olsen, J.F., 1981. Ganglion cell distribution in the retina of the mouse. Invest. Ophthalmol. Vis. Sci. 20, 285–293.

Dullin, J.P., Locker, M., Robach, M., Henningfeld, K.A., Parain, K., Afelik, S., Pieler, T., Perron, M., 2007. Ptf1a triggers GABAergic neuronal cell fates in the retina. BMC Dev. Biol. 7, 110.
Dyer, M.A., Cepko, C.L., 2000. p57(Kip2) regulates progenitor cell proliferation and amacrine interneuron development in the mouse retina. Development 127, 3593–3605.
Dyer, M.A., Cepko, C.L., 2001a. p27Kip1 and p57Kip2 regulate proliferation in distinct retinal progenitor cell populations. J. Neurosci. 21, 4259–4271.
Dyer, M.A., Cepko, C.L., 2001b. Regulating proliferation during retinal development. Nat. Rev. Neurosci. 2, 333–342.
Dyer, M.A., Livesey, F.J., Cepko, C.L., Oliver, G., 2003. Prox1 function controls progenitor cell proliferation and horizontal cell genesis in the mammalian retina. Nat. Genet. 34, 53–58.
Elliott, J., Cayouette, M., Gravel, C., 2006. The CNTF/LIF signaling pathway regulates developmental programmed cell death and differentiation of rod precursor cells in the mouse retina in vivo. Dev. Biol. 300, 583–598.
Elliott, J., Jolicoeur, C., Ramamurthy, V., Cayouette, M., 2008. Ikaros confers early temporal competence to mouse retinal progenitor cells. Neuron 60, 26–39.
Ezzeddine, Z.D., Yang, X., DeChiara, T., Yancopoulos, G., Cepko, C.L., 1997. Postmitotic cells fated to become rod photoreceptors can be respecified by CNTF treatment of the retina. Development 124, 1055–1067.
Farah, M.H., Easter Jr., S.S., 2005. Cell birth and death in the mouse retinal ganglion cell layer. J. Comp. Neurol. 489, 120–134.
Fausett, B.V., Gumerson, J.D., Goldman, D., 2008. The proneural basic helix-loop-helix gene ascl1a is required for retina regeneration. J. Neurosci. 28, 1109–1117.
Feng, G.S., 1999. Shp-2 tyrosine phosphatase: signaling one cell or many. Exp. Cell Res. 253, 47–54.
Feng, L., Xie, X., Joshi, P.S., Yang, Z., Shibasaki, K., Chow, R.L., Gan, L., 2006. Requirement for Bhlhb5 in the specification of amacrine and cone bipolar subtypes in mouse retina. Development 133, 4815–4825.
Feng, L., Xie, Z.H., Ding, Q., Xie, X., Libby, R.T., Gan, L., 2010. MATH5 controls the acquisition of multiple retinal cell fates. Mol. Brain 3, 36.
Fortini, M.E., 2012. Introduction—Notch in development and disease. Semin. Cell Dev. Biol. 23, 419–420.
Fuhrmann, S., Kirsch, M., Hofmann, H.-D., 1995. Ciliary neurotrophic factor promotes chick photoreceptor development in vitro. Development 121, 2695–2706.
Fujitani, Y., Fujitani, S., Luo, H., Qiu, F., Burlison, J., Long, Q., Kawaguchi, Y., Edlund, H., MacDonald, R.J., Furukawa, T., Fujikado, T., Magnuson, M.A., Xiang, M., Wright, C.V., 2006. Ptf1a determines horizontal and amacrine cell fates during mouse retinal development. Development 133, 4439–4450.
Furukawa, T., Morrow, E.M., Cepko, C.L., 1997. *Crx*, a novel *otx*-like homeobox gene, shows photoreceptor-specific expression and regulates photoreceptor differentiation. Cell 91, 531–541.
Furukawa, T., Mukherjee, S., Bao, Z.Z., Morrow, E.M., Cepko, C.L., 2000. rax, Hes1, and notch1 promote the formation of Muller glia by postnatal retinal progenitor cells. Neuron 26, 383–394.
Gamsiz, E.D., Ouyang, Q., Schmidt, M., Nagpal, S., Morrow, E.M., 2012. Genome-wide transcriptome analysis in murine neural retina using high-throughput RNA sequencing. Genomics 99, 44–51.
Gehring, W.J., Hiromi, Y., 1986. Homeotic genes and the homeobox. Annu. Rev. Genet. 20, 147–173.
Gehring, W.J., Affolter, M., Burglin, T., 1994. Homeodomain proteins. Annu. Rev. Biochem. 63, 487–526.

Georgi, S.A., Reh, T.A., 2010. Dicer is required for the transition from early to late progenitor state in the developing mouse retina. J. Neurosci. 30, 4048–4061.
Georgi, S.A., Reh, T.A., 2011. Dicer is required for the maintenance of notch signaling and gliogenic competence during mouse retinal development. Dev. Neurobiol. 71, 1153–1169.
Goetz, J.J., Trimarchi, J.M., 2012. Single-cell profiling of developing and mature retinal neurons. J. Vis. Exp. 62, e3824. http://dx.doi.org/10.3791/3824.
Gomes, F.L., Zhang, G., Carbonell, F., Correa, J.A., Harris, W.A., Simons, B.D., Cayouette, M., 2011. Reconstruction of rat retinal progenitor cell lineages in vitro reveals a surprising degree of stochasticity in cell fate decisions. Development 138, 227–235.
Graham, D.R., Overbeek, P.A., Ash, J.D., 2005. Leukemia inhibitory factor blocks expression of Crx and Nrl transcription factors to inhibit photoreceptor differentiation. Invest. Ophthalmol. Vis. Sci. 46, 2601–2610.
Green, E.S., Stubbs, J.L., Levine, E.M., 2003. Genetic rescue of cell number in a mouse model of microphthalmia: interactions between Chx10 and G1-phase cell cycle regulators. Development 130, 539–552.
Grindley, J.C., Davidson, D.R., Hill, R.E., 1995. The role of Pax-6 in eye and nasal development. Development 121, 1433–1442.
Guillemot, F., Cepko, C., 1992. Retinal fate and ganglion cell differentiation are potentiated by acidic FGF in an in vitro assay of early retinal development. Development 114, 743–754.
Guillemot, F., Lo, L.C., Johnson, J.E., Auerbach, A., Anderson, D.J., Joyner, A.L., 1993. Mammalian achaete-scute homolog 1 is required for the early development of olfactory and autonomic neurons. Cell 75, 463–476.
Guruharsha, K.G., Kankel, M.W., Artavanis-Tsakonas, S., 2012. The Notch signalling system: recent insights into the complexity of a conserved pathway. Nat. Rev. Genet. 13, 654–666.
Hackler Jr., L., Wan, J., Swaroop, A., Qian, J., Zack, D.J., 2010. MicroRNA profile of the developing mouse retina. Invest. Ophthalmol. Vis. Sci. 51, 1823–1831.
Hafler, B.P., Surzenko, N., Beier, K.T., Punzo, C., Trimarchi, J.M., Kong, J.H., Cepko, C.L., 2012. Transcription factor Olig2 defines subpopulations of retinal progenitor cells biased toward specific cell fates. Proc. Natl. Acad. Sci. U. S. A. 109, 7882–7887.
Halder, G., Callaerts, P., Gehring, W.J., 1995. Induction of ectopic eyes by targeted expression of the eyeless gene in Drosophila. Science 267, 1788–1792.
Hatakeyama, J., Kageyama, R., 2004. Retinal cell fate determination and bHLH factors. Semin. Cell Dev. Biol. 15, 83–89.
Hatakeyama, J., Tomita, K., Inoue, T., Kageyama, R., 2001. Roles of homeobox and bHLH genes in specification of a retinal cell type. Development 128, 1313–1322.
He, J., Zhang, G., Almeida, A.D., Cayouette, M., Simons, B.D., Harris, W.A., 2012. How variable clones build an invariant retina. Neuron 75, 786–798.
Hicks, D., Courtois, Y., 1992. Fibroblast growth factor stimulates photoreceptor differentiation in vitro. J. Neurosci. 12, 2022–2033.
Hobert, O., 2010. Neurogenesis in the nematode Caenorhabditis elegans. WormBook 1–24.
Hojo, M., Ohtsuka, T., Hashimoto, N., Gradwohl, G., Guillemot, F., Kageyama, R., 2000. Glial cell fate specification modulated by the bHLH gene Hes5 in mouse retina. Development 127, 2515–2522.
Holt, C.E., Bertsch, T.W., Ellis, H.M., Harris, W.A., 1988. Cellular determination in the *Xenopus* retina is independent of lineage and birth date. Neuron 1, 15–26.
Hufnagel, R.B., Riesenberg, A.N., Quinn, M., Brzezinski, J.A.t., Glaser, T., Brown, N.L., 2013. Heterochronic misexpression of Ascl1 in the Atoh7 retinal cell lineage blocks cell cycle exit. Mol. Cell. Neurosci. 54, 108–120.

Iida, A., Shinoe, T., Baba, Y., Mano, H., Watanabe, S., 2011. Dicer plays essential roles for retinal development by regulation of survival and differentiation. Invest. Ophthalmol. Vis. Sci. 52, 3008–3017.
Ingham, P.W., McMahon, A.P., 2001. Hedgehog signaling in animal development: paradigms and principles. Genes Dev. 15, 3059–3087.
Inoue, T., Hojo, M., Bessho, Y., Tano, Y., Lee, J.E., Kageyama, R., 2002. Math3 and NeuroD regulate amacrine cell fate specification in the retina. Development 129, 831–842.
Isshiki, T., Pearson, B., Holbrook, S., Doe, C.Q., 2001. Drosophila neuroblasts sequentially express transcription factors which specify the temporal identity of their neuronal progeny. Cell 106, 511–521.
Jadhav, A.P., Mason, H.A., Cepko, C.L., 2006. Notch 1 inhibits photoreceptor production in the developing mammalian retina. Development 133, 913–923.
Jaenisch, R., Bird, A., 2003. Epigenetic regulation of gene expression: how the genome integrates intrinsic and environmental signals. Nat. Genet. 33 (Suppl), 245–254.
Jarman, A.P., Grell, E.H., Ackerman, L., Jan, L.Y., Jan, Y.N., 1994. Atonal is the proneural gene for Drosophila photoreceptors. Nature 369, 398–400.
Jarman, A.P., Sun, Y., Jan, L.Y., Jan, Y.N., 1995. Role of the proneural gene, atonal, in formation of Drosophila chordotonal organs and photoreceptors. Development 121, 2019–2030.
Jenuwein, T., Allis, C.D., 2001. Translating the histone code. Science 293, 1074–1080.
Johnston Jr., R.J., Desplan, C., 2008. Stochastic neuronal cell fate choices. Curr. Opin. Neurobiol. 18, 20–27.
Kanekar, S., Perron, M., Dorsky, R., Harris, W.A., Jan, L.Y., Jan, Y.N., Vetter, M.L., 1997. Xath5 participates in a network of bHLH genes in the developing Xenopus retina. Neuron 19, 981–994.
Karali, M., Peluso, I., Gennarino, V.A., Bilio, M., Verde, R., Lago, G., Dolle, P., Banfi, S., 2010. miRNeye: a microRNA expression atlas of the mouse eye. BMC Genomics 11, 715.
Karl, M.O., Hayes, S., Nelson, B.R., Tan, K., Buckingham, B., Reh, T.A., 2008. Stimulation of neural regeneration in the mouse retina. Proc. Natl. Acad. Sci. U. S. A. 105, 19508–19513.
Katoh, K., Yamazaki, R., Onishi, A., Sanuki, R., Furukawa, T., 2012. G9a histone methyltransferase activity in retinal progenitors is essential for proper differentiation and survival of mouse retinal cells. J. Neurosci. 32, 17658–17670.
Kawaguchi, Y., Cooper, B., Gannon, M., Ray, M., MacDonald, R.J., Wright, C.V., 2002. The role of the transcriptional regulator Ptf1a in converting intestinal to pancreatic progenitors. Nat. Genet. 32, 128–134.
Kay, J.N., Finger-Baier, K.C., Roeser, T., Staub, W., Baier, H., 2001. Retinal ganglion cell genesis requires lakritz, a Zebrafish atonal Homolog. Neuron 30, 725–736.
Kay, J.N., Voinescu, P.E., Chu, M.W., Sanes, J.R., 2011. Neurod6 expression defines new retinal amacrine cell subtypes and regulates their fate. Nat. Neurosci. 14, 965–972.
Kechad, A., Jolicoeur, C., Tufford, A., Mattar, P., Chow, R.W., Harris, W.A., Cayouette, M., 2012. Numb is required for the production of terminal asymmetric cell divisions in the developing mouse retina. J. Neurosci. 32, 17197–17210.
Kim, D.S., Ross, S.E., Trimarchi, J.M., Aach, J., Greenberg, M.E., Cepko, C.L., 2008. Identification of molecular markers of bipolar cells in the murine retina. J. Comp. Neurol. 507, 1795–1810.
Koike, C., Nishida, A., Ueno, S., Saito, H., Sanuki, R., Sato, S., Furukawa, A., Aizawa, S., Matsuo, I., Suzuki, N., Kondo, M., Furukawa, T., 2007. Functional roles of Otx2 transcription factor in postnatal mouse retinal development. Mol. Cell. Biol. 27, 8318–8329.

Kuehn, M.H., Fingert, J.H., Kwon, Y.H., 2005. Retinal ganglion cell death in glaucoma: mechanisms and neuroprotective strategies. Ophthal. Clin. North Am. 18, 383–395.
La Torre, A., Georgi, S., Reh, T.A., 2013. Conserved microRNA pathway regulates developmental timing of retinal neurogenesis. Proc. Natl. Acad. Sci. U. S. A. 110, E2362–E2370.
Lee, J.E., 1997. Basic helix-loop-helix genes in neural development. Curr. Opin. Neurobiol. 7, 13–20.
Li, S., Mo, Z., Yang, X., Price, S.M., Shen, M.M., Xiang, M., 2004. Foxn4 controls the genesis of amacrine and horizontal cells by retinal progenitors. Neuron 43, 795–807.
Lillien, L., Cepko, C., 1992. Control of proliferation in the retina: temporal changes in responsiveness to FGF and TGF alpha. Development 115, 253–266.
Liu, W., Mo, Z., Xiang, M., 2001. The Ath5 proneural genes function upstream of Brn3 POU domain transcription factor genes to promote retinal ganglion cell development. Proc. Natl. Acad. Sci. U. S. A. 98, 1649–1654.
Livesey, F.J., Cepko, C.L., 2001. Vertebrate neural cell-fate determination: lessons from the retina. Nat. Rev. Neurosci. 2, 109–118.
Livesey, F.J., Young, T.L., Cepko, C.L., 2004. An analysis of the gene expression program of mammalian neural progenitor cells. Proc. Natl. Acad. Sci. U. S. A. 101, 1374–1379.
Luo, H., Jin, K., Xie, Z., Qiu, F., Li, S., Zou, M., Cai, L., Hozumi, K., Shima, D.T., Xiang, M., 2012. Forkhead box N4 (Foxn4) activates Dll4-Notch signaling to suppress photoreceptor cell fates of early retinal progenitors. Proc. Natl. Acad. Sci. U. S. A. 109, E553–E562.
MacNeil, M.A., Masland, R.H., 1998. Extreme diversity among amacrine cells: implications for function. Neuron 20, 971–982.
Maiorano, N.A., Hindges, R., 2012. Non-coding RNAs in retinal development. Int. J. Mol. Sci. 13, 558–578.
Mao, C.A., Wang, S.W., Pan, P., Klein, W.H., 2008. Rewiring the retinal ganglion cell gene regulatory network: Neurod1 promotes retinal ganglion cell fate in the absence of Math5. Development 135, 3379–3388.
Mao, C.A., Cho, J.H., Wang, J., Gao, Z., Pan, P., Tsai, W.W., Frishman, L.J., Klein, W.H., 2013. Reprogramming amacrine and photoreceptor progenitors into retinal ganglion cells by replacing Neurod1 with Atoh7. Development 140, 541–551.
Marquardt, T., Ashery-Padan, R., Andrejewski, N., Scardigli, R., Guillemot, F., Gruss, P., 2001. Pax6 is required for the multipotent state of retinal progenitor cells. Cell 105, 43–55.
Martinez-Morales, J.R., Del Bene, F., Nica, G., Hammerschmidt, M., Bovolenta, P., Wittbrodt, J., 2005. Differentiation of the vertebrate retina is coordinated by an FGF signaling center. Dev. Cell 8, 565–574.
Masland, R.H., 2001. The fundamental plan of the retina. Nat. Neurosci. 4, 877–886.
Masland, R.H., 2012. The neuronal organization of the retina. Neuron 76, 266–280.
Mathers, P.H., Grinberg, A., Mahon, K.A., Jamrich, M., 1997. The Rx homeobox gene is essential for vertebrate eye development. Nature 387, 603–607.
McCabe, K.L., Gunther, E.C., Reh, T.A., 1999. The development of the pattern of retinal ganglion cells in the chick retina: mechanisms that control differentiation. Development 126, 5713–5724.
McCabe, K.L., McGuire, C., Reh, T.A., 2006. Pea3 expression is regulated by FGF signaling in developing retina. Dev. Dyn. 235, 327–335.
McFarlane, S., Zuber, M.E., Holt, C.E., 1998. A role for the fibroblast growth factor receptor in cell fate decisions in the developing vertebrate retina. Development 125, 3967–3975.
Mercer, T.R., Dinger, M.E., Sunkin, S.M., Mehler, M.F., Mattick, J.S., 2008. Specific expression of long noncoding RNAs in the mouse brain. Proc. Natl. Acad. Sci. U. S. A. 105, 716–721.

Miller, A.C., Seymour, H., King, C., Herman, T.G., 2008. Loss of seven-up from Drosophila R1/R6 photoreceptors reveals a stochastic fate choice that is normally biased by Notch. Development 135, 707–715.
Mohn, F., Schubeler, D., 2009. Genetics and epigenetics: stability and plasticity during cellular differentiation. Trends Genet. 25, 129–136.
Morrow, E.M., Furukawa, T., Cepko, C.L., 1998. Vertebrate photoreceptor cell development and disease. Trends Cell Biol. 8, 353–358.
Morrow, E.M., Furukawa, T., Lee, J.E., Cepko, C.L., 1999. NeuroD regulates multiple functions in the developing neural retina in rodent. Development 126, 23–36.
Mu, X., Zhao, S., Pershad, R., Hsieh, T.F., Scarpa, A., Wang, S.W., White, R.A., Beremand, P.D., Thomas, T.L., Gan, L., Klein, W.H., 2001. Gene expression in the developing mouse retina by EST sequencing and microarray analysis. Nucleic Acids Res. 29, 4983–4993.
Mu, X., Fu, X., Sun, H., Beremand, P.D., Thomas, T.L., Klein, W.H., 2005. A gene network downstream of transcription factor Math5 regulates retinal progenitor cell competence and ganglion cell fate. Dev. Biol. 280, 467–481.
Munch, M., Kawasaki, A., 2013. Intrinsically photosensitive retinal ganglion cells: classification, function and clinical implications. Curr. Opin. Neurol. 26, 45–51.
Muranishi, Y., Terada, K., Inoue, T., Katoh, K., Tsujii, T., Sanuki, R., Kurokawa, D., Aizawa, S., Tamaki, Y., Furukawa, T., 2011. An essential role for RAX homeoprotein and NOTCH-HES signaling in Otx2 expression in embryonic retinal photoreceptor cell fate determination. J. Neurosci. 31, 16792–16807.
Murphy, K.M., Reiner, S.L., 2002. The lineage decisions of helper T cells. Nat. Rev. Immunol. 2, 933–944.
Murre, C., McCaw, P.S., Vaessin, H., Caudy, M., Jan, L.Y., Jan, Y.N., Cabrera, C.V., Buskin, J.N., Hauschka, S.D., Lassar, A.B., et al., 1989. Interactions between heterologous helix-loop-helix proteins generate complexes that bind specifically to a common DNA sequence. Cell 58, 537–544.
Nakhai, H., Sel, S., Favor, J., Mendoza-Torres, L., Paulsen, F., Duncker, G.I., Schmid, R.M., 2007. Ptf1a is essential for the differentiation of GABAergic and glycinergic amacrine cells and horizontal cells in the mouse retina. Development 134, 1151–1160.
Nasonkin, I.O., Lazo, K., Hambright, D., Brooks, M., Fariss, R., Swaroop, A., 2011. Distinct nuclear localization patterns of DNA methyltransferases in developing and mature mammalian retina. J. Comp. Neurol. 519, 1914–1930.
Nelson, B.R., Hartman, B.H., Georgi, S.A., Lan, M.S., Reh, T.A., 2007. Transient inactivation of Notch signaling synchronizes differentiation of neural progenitor cells. Dev. Biol. 304, 479–498.
Nelson, S.M., Park, L., Stenkamp, D.L., 2009. Retinal homeobox 1 is required for retinal neurogenesis and photoreceptor differentiation in embryonic zebrafish. Dev. Biol. 328, 24–39.
Neumann, C.J., Nuesslein-Volhard, C., 2000. Patterning of the zebrafish retina by a wave of sonic hedgehog activity. Science 289, 2137–2139.
Nishida, A., Furukawa, A., Koike, C., Tano, Y., Aizawa, S., Matsuo, I., Furukawa, T., 2003. Otx2 homeobox gene controls retinal photoreceptor cell fate and pineal gland development. Nat. Neurosci. 6, 1255–1263.
Nornes, S., Clarkson, M., Mikkola, I., Pedersen, M., Bardsley, A., Martinez, J.P., Krauss, S., Johansen, T., 1998. Zebrafish contains two pax6 genes involved in eye development. Mech. Dev. 77, 185–196.
Ochocinska, M.J., Hitchcock, P.F., 2009. NeuroD regulates proliferation of photoreceptor progenitors in the retina of the zebrafish. Mech. Dev. 126, 128–141.
Ohnuma, S., Philpott, A., Wang, K., Holt, C.E., Harris, W.A., 1999. p27Xic1, a Cdk inhibitor, promotes the determination of glial cells in Xenopus retina. Cell 99, 499–510.

Oron-Karni, V., Farhy, C., Elgart, M., Marquardt, T., Remizova, L., Yaron, O., Xie, Q., Cvekl, A., Ashery-Padan, R., 2008. Dual requirement for Pax6 in retinal progenitor cells. Development 135, 4037–4047.
Ozaki, H., Okamoto, N., Ortega, S., Chang, M., Ozaki, K., Sadda, S., Vinores, M.A., Derevjanik, N., Zack, D.J., Basilico, C., Campochiaro, P.A., 1998. Basic fibroblast growth factor is neither necessary nor sufficient for the development of retinal neovascularization. Am. J. Pathol. 153, 757–765.
Patel, A., McFarlane, S., 2000. Overexpression of FGF-2 alters cell fate specification in the developing retina of Xenopus laevis. Dev. Biol. 222, 170–180.
Pearson, B.J., Doe, C.Q., 2004. Specification of temporal identity in the developing nervous system. Annu. Rev. Cell Dev. Biol. 20, 619–647.
Pinter, R., Hindges, R., 2010. Perturbations of microRNA function in mouse dicer mutants produce retinal defects and lead to aberrant axon pathfinding at the optic chiasm. PLoS One 5, e10021.
Pollak, J., Wilken, M.S., Ueki, Y., Cox, K.E., Sullivan, J.M., Taylor, R.J., Levine, E.M., Reh, T.A., 2013. ASCL1 reprograms mouse Muller glia into neurogenic retinal progenitors. Development 140, 2619–2631.
Prasov, L., Glaser, T., 2012. Pushing the envelope of retinal ganglion cell genesis: context dependent function of Math5 (Atoh7). Dev. Biol. 368, 214–230.
Rapicavoli, N.A., Blackshaw, S., 2009. New meaning in the message: noncoding RNAs and their role in retinal development. Dev. Dyn. 238, 2103–2114.
Rapicavoli, N.A., Poth, E.M., Blackshaw, S., 2010. The long noncoding RNA RNCR2 directs mouse retinal cell specification. BMC Dev. Biol. 10, 49.
Rapicavoli, N.A., Poth, E.M., Zhu, H., Blackshaw, S., 2011. The long noncoding RNA Six3OS acts in trans to regulate retinal development by modulating Six3 activity. Neural Dev. 6, 32.
Rhee, K.D., Yang, X.J., 2010. Function and mechanism of CNTF/LIF signaling in retinogenesis. Adv. Exp. Med. Biol. 664, 647–654.
Riesenberg, A.N., Le, T.T., Willardsen, M.I., Blackburn, D.C., Vetter, M.L., Brown, N.L., 2009a. Pax6 regulation of Math5 during mouse retinal neurogenesis. Genesis 47, 175–187.
Riesenberg, A.N., Liu, Z., Kopan, R., Brown, N.L., 2009b. Rbpj cell autonomous regulation of retinal ganglion cell and cone photoreceptor fates in the mouse retina. J. Neurosci. 29, 12865–12877.
Rockhill, R.L., Daly, F.J., MacNeil, M.A., Brown, S.P., Masland, R.H., 2002. The diversity of ganglion cells in a mammalian retina. J. Neurosci. 22, 3831–3843.
Rodieck, R.W., 1998. The First Steps in Seeing. Sinauer, Sunderland, MA.
Roegiers, F., Jan, Y.N., 2004. Asymmetric cell division. Curr. Opin. Cell Biol. 16, 195–205.
Roth, S.Y., Denu, J.M., Allis, C.D., 2001. Histone acetyltransferases. Ann. Rev. Biochem. 70, 81–120.
Rowan, S., Cepko, C.L., 2004. Genetic analysis of the homeodomain transcription factor Chx10 in the retina using a novel multifunctional BAC transgenic mouse reporter. Dev. Biol. 271, 388–402.
Sakagami, K., Gan, L., Yang, X.J., 2009. Distinct effects of Hedgehog signaling on neuronal fate specification and cell cycle progression in the embryonic mouse retina. J. Neurosci. 29, 6932–6944.
Saxena, M.T., Schroeter, E.H., Mumm, J.S., Kopan, R., 2001. Murine notch homologs (N1-4) undergo presenilin-dependent proteolysis. J. Biol. Chem. 276, 40268–40273.
Scheer, N., Groth, A., Hans, S., Campos-Ortega, J.A., 2001. An instructive function for Notch in promoting gliogenesis in the zebrafish retina. Development 128, 1099–1107.
Schmeer, C.W., Wohl, S.G., Isenmann, S., 2012. Cell-replacement therapy and neural repair in the retina. Cell Tissue Res. 349, 363–374.

Sidman, R.L., 1961. Histogenesis of mouse retina studied with thymidine-H^3. In: Smelser, G.K. (Ed.), The Structure of the Eye. Academic, New York, NY, pp. 487–506.
Silva, A.O., Ercole, C.E., McLoon, S.C., 2003. Regulation of ganglion cell production by Notch signaling during retinal development. J. Neurobiol. 54, 511–524.
Skowronska-Krawczyk, D., Ballivet, M., Dynlacht, B.D., Matter, J.M., 2004. Highly specific interactions between bHLH transcription factors and chromatin during retina development. Development 131, 4447–4454.
Stenkamp, D.L., Frey, R.A., Mallory, D.E., Shupe, E.E., 2002. Embryonic retinal gene expression in sonic-you mutant zebrafish. Dev. Dyn. 225, 344–350.
Strettoi, E., Raviola, E., Dacheux, R.F., 1992. Synaptic connections of the narrow-field, bistratified rod amacrine cell (AII) in the rabbit retina. J. Comp. Neurol. 325, 152–168.
Swaroop, A., Zack, D.J., 2002. Transcriptome analysis of the retina. Genome Biol. 3, REVIEWS1022.
Tomita, K., Ishibashi, M., Nakahara, K., Ang, S.L., Nakanishi, S., Guillemot, F., Kageyama, R., 1996a. Mammalian hairy and Enhancer of split homolog 1 regulates differentiation of retinal neurons and is essential for eye morphogenesis. Neuron 16, 723–734.
Tomita, K., Nakanishi, S., Guillemot, F., Kageyama, R., 1996b. Mash1 promotes neuronal differentiation in the retina. Genes Cells 1, 765–774.
Tomita, K., Moriyoshi, K., Nakanishi, S., Guillemot, F., Kageyama, R., 2000. Mammalian achaete-scute and atonal homologs regulate neuronal versus glial fate determination in the central nervous system. EMBO J. 19, 5460–5472.
Trimarchi, J.M., Stadler, M.B., Roska, B., Billings, N., Sun, B., Bartch, B., Cepko, C.L., 2007. Molecular heterogeneity of developing retinal ganglion and amacrine cells revealed through single cell gene expression profiling. J. Comp. Neurol. 502, 1047–1065.
Trimarchi, J.M., Stadler, M.B., Cepko, C.L., 2008. Individual retinal progenitor cells display extensive heterogeneity of gene expression. PLoS One 3, e1588.
Tucker, B.A., Park, I.H., Qi, S.D., Klassen, H.J., Jiang, C., Yao, J., Redenti, S., Daley, G.Q., Young, M.J., 2011. Transplantation of adult mouse iPS cell-derived photoreceptor precursors restores retinal structure and function in degenerative mice. PLoS One 6, e18992.
Turner, D.L., Cepko, C.L., 1987. A common progenitor for neurons and glia persists in rat retina late in development. Nature 328, 131–136.
Turner, D.L., Snyder, E.Y., Cepko, C.L., 1990. Lineage-independent determination of cell type in the embryonic mouse retina. Neuron 4, 833–845.
Vaney, D.I., Peichl, L., Boycott, B.B., 1988. Neurofibrillar long-range amacrine cells in mammalian retinae. Proc. R. Soc. Lond. B Biol. Sci. 235, 203–219.
Voinescu, P.E., Kay, J.N., Sanes, J.R., 2009. Birthdays of retinal amacrine cell subtypes are systematically related to their molecular identity and soma position. J. Comp. Neurol. 517, 737–750.
Wang, S.W., Kim, B.S., Ding, K., Wang, H., Sun, D., Johnson, R.L., Klein, W.H., Gan, L., 2001. Requirement for math5 in the development of retinal ganglion cells. Genes Dev. 15, 24–29.
Wang, Y.P., Dakubo, G., Howley, P., Campsall, K.D., Mazarolle, C.J., Shiga, S.A., Lewis, P.M., McMahon, A.P., Wallace, V.A., 2002. Development of normal retinal organization depends on Sonic hedgehog signaling from ganglion cells. Nat. Neurosci. 5, 831–832.
Wang, Y., Dakubo, G.D., Thurig, S., Mazerolle, C.J., Wallace, V.A., 2005. Retinal ganglion cell-derived sonic hedgehog locally controls proliferation and the timing of RGC development in the embryonic mouse retina. Development 132, 5103–5113.
Wang, Z., Gerstein, M., Snyder, M., 2009. RNA-Seq: a revolutionary tool for transcriptomics. Nat. Rev. Genet. 10, 57–63.
Weinberg, R.A., 1995. The retinoblastoma protein and cell cycle control. Cell 81, 323–330.

Yamaguchi, M., Tonou-Fujimori, N., Komori, A., Maeda, R., Nojima, Y., Li, H., Okamoto, H., Masai, I., 2005. Histone deacetylase 1 regulates retinal neurogenesis in zebrafish by suppressing Wnt and Notch signaling pathways. Development 132, 3027–3043.

Yang, Z., Ding, K., Pan, L., Deng, M., Gan, L., 2003. Math5 determines the competence state of retinal ganglion cell progenitors. Dev. Biol. 264, 240–254.

Yaron, O., Farhy, C., Marquardt, T., Applebury, M., Ashery-Padan, R., 2006. Notch1 functions to suppress cone-photoreceptor fate specification in the developing mouse retina. Development 133, 1367–1378.

Yau, K.W., 1994. Phototransduction mechanism in retinal rods and cones. The Friedenwald Lecture. Invest. Ophthalmol. Vis. Sci. 35, 9–32.

Young, R.W., 1985a. Cell differentiation in the retina of the mouse. Anat. Rec. 212, 199–205.

Young, R.W., 1985b. Cell proliferation during postnatal development of the retina in the mouse. Dev. Brain Res. 21, 229–239.

Zhang, X.M., Yang, X.J., 2001. Regulation of retinal ganglion cell production by Sonic hedgehog. Development 128, 943–957.

Zhang, J., Gray, J., Wu, L., Leone, G., Rowan, S., Cepko, C.L., Zhu, X., Craft, C.M., Dyer, M.A., 2004. Rb regulates proliferation and rod photoreceptor development in the mouse retina. Nat. Genet. 36, 351–360.

Zhu, A.J., Zheng, L., Suyama, K., Scott, M.P., 2003. Altered localization of Drosophila Smoothened protein activates Hedgehog signal transduction. Genes Dev. 17, 1240–1252.

Zuber, M.E., Gestri, G., Viczian, A.S., Barsacchi, G., Harris, W.A., 2003. Specification of the vertebrate eye by a network of eye field transcription factors. Development 130, 5155–5167.

CHAPTER EIGHT

Adhesion Networks of Cnidarians: A Postgenomic View

Richard P. Tucker[*,1], **Josephine C. Adams**[†,1]
[*]Department of Cell Biology and Human Anatomy, University of California, Davis, California, USA
[†]School of Biochemistry, University of Bristol, Bristol, United Kingdom
[1]Corresponding authors: e-mail address: rptucker@ucdavis.edu; jo.adams@bristol.ac.uk

Contents

Abstract

Cell–extracellular matrix (ECM) and cell–cell adhesion systems are fundamental to the multicellularity of metazoans. Members of phylum Cnidaria were classified historically by their radial symmetry as an outgroup to bilaterian animals. Experimental study of *Hydra* and jellyfish has fascinated zoologists for many years. Laboratory studies, based on dissection, biochemical isolations, or perturbations of the living organism, have identified the ECM layer of cnidarians (mesoglea) and its components as important determinants of stem cell properties, cell migration and differentiation, tissue morphogenesis, repair,

International Review of Cell and Molecular Biology, Volume 308
ISSN 1937-6448
http://dx.doi.org/10.1016/B978-0-12-800097-7.00008-7

and regeneration. Studies of the ultrastructure and functions of intercellular gap and septate junctions identified parallel roles for these structures in intercellular communication and morphogenesis. More recently, the sequenced genomes of sea anemone *Nematostella vectensis*, *Hydra magnipapillata*, and coral *Acropora digitifera* have opened up a new frame of reference for analyzing the cell–ECM and cell–cell adhesion molecules of cnidarians and examining their conservation with bilaterians. This chapter integrates a review of literature on the structure and functions of cell–ECM and cell–cell adhesion systems in cnidarians with current analyses of genome-encoded repertoires of adhesion molecules. The postgenomic perspective provides a fresh view on fundamental similarities between cnidarian and bilaterian animals and is impelling wider adoption of species from phylum Cnidaria as model organisms.

1. INTRODUCTION

Cnidarians are early diverging metazoans descended from a common ancestor of both protostomes and deuterostomes (Fig. 8.1). The phylum contains approximately 10,000 species, most of which live in the oceans and other marine environments. The following common features define membership in the phylum: (1) digestion takes place within a central space called the gastrovascular cavity, with the opening to the gastrovascular cavity performing double duty as mouth and anus, (2) surrounding the opening to the gastrovascular cavity is an array of tentacles that help capture food, (3) they have specialized cells called cnidocytes ("cnido" is from the Greek word meaning "nettle") that contain organelles known as nematocysts that are discharged explosively and can envenomate or adhere to potential prey, and (4) they have a trilaminate body wall composed of an outer epidermis and inner gastrodermis (sometimes referred to as "ectoderm" and "endoderm") that sandwich an extracellular matrix (ECM) layer termed the mesoglea. Radial symmetry is often listed as another feature of the phylum, hence their inclusion in the group Radiata. However, the radial symmetry is often only superficial and closer examination of at least some members of the phylum reveals dorsal–ventral features as well as the appropriate expression of genes that regulate the development of the dorsal–ventral axis in bilaterian animals (Darling et al., 2005).

Much of the morphological diversity found in phylum Cnidaria results from the presence of two different body forms, the polyp and the medusa (Fig. 8.2A–C). Polyps are generally sessile, with the aboral end of a cylindrical body attached to the substratum and the tentacles circling the mouth at the opposite end. This is in contrast to the swimming medusa, which often

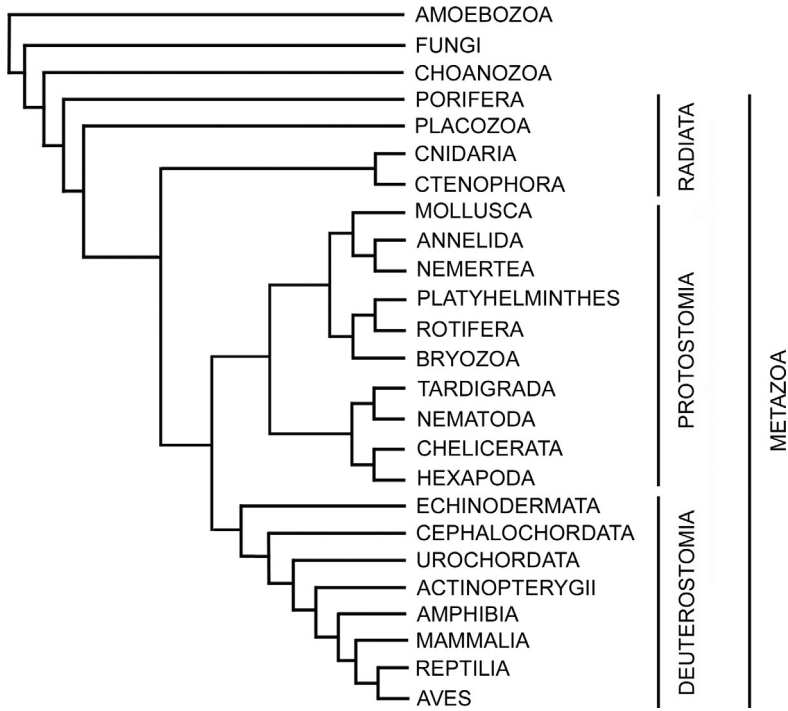

Figure 8.1 A diagrammatic representation of one widely accepted version of the tree of life for the unikonts showing the evolutionary relationships between representative metazoan phyla as well as the groups considered to be most closely related to the metazoa.

takes the shape of an open umbrella with the tentacles hanging from or near the edge of the umbrella surrounding a centrally located mouth. Cnidarians of class Anthozoa, which includes the corals and sea anemones, exist only in the polyp form (Fig. 8.3A). Adult polyps are dioecious or hermaphroditic, releasing sperm or oocytes into the water where fertilization takes place. A free swimming larval stage, the planula, will metamorphose into a miniature polyp. Asexual reproduction can take place through transverse or longitudinal fission, pedal laceration, or fragmentation (Fig. 8.2D). Members of other classes of cnidarians belong to the clade Medusozoa (Fig. 8.3A). Medusozoans belonging to the class Scyphozoa (true jellyfish) and class Cubozoa (the cube jellies) typically have more complex life cycles (Fig. 8.2C and D). Scyphozoan medusae are usually dioecious, with a free swimming planula larva developing after external fertilization. The planula becomes a sessile polyp, and medusae are usually formed by asexual transverse budding of the polyp. Most members of the class Hydrozoa also have polypoid and

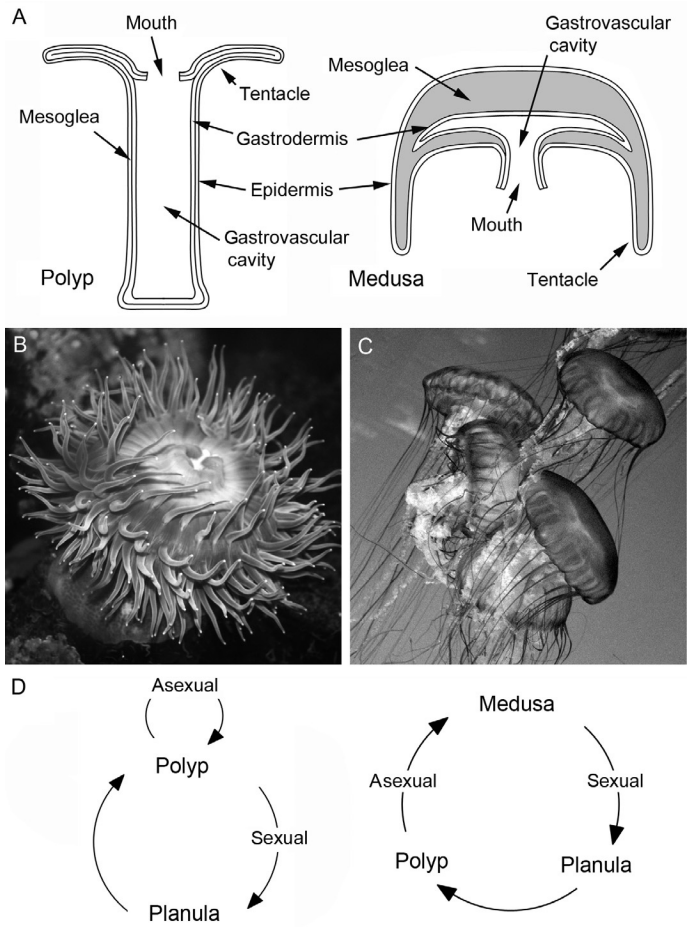

Figure 8.2 Cnidarian morphologies and life cycles. (A) Cnidarians exist as either a polyp or a medusa; some exist as either a polyp or a medusa at different stages of the life cycle. Both the polyp and the medusa are composed of an outer epidermis and an inner gastrodermis separated by an extracellular matrix termed mesoglea. (B) A typical polyp is illustrated by the sea anemone *Anthopleura xanthogrammica*. (C) A typical medusa is illustrated by the scyphozoan *Chrysaora fuscescens*. (D) The life cycle of a typical anthozoan (sea anemone) is illustrated on the left and can involve both sexual and asexual reproduction. The life cycle of a typical scyphozoan (jellyfish) is illustrated on the right.

medusoid stages in their life cycle, but some are exclusively medusae and others exist only as polyps (Fig. 8.3A). Finally, the members of class Staurozoa have only a medusoid stage, but the medusa has a stalk that attaches it to the substratum.

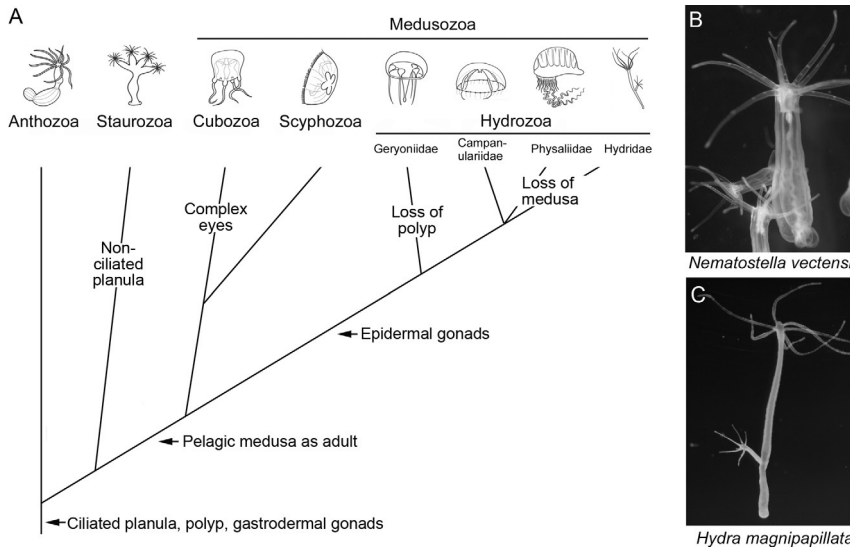

Figure 8.3 The classes of cnidarians and experimental models. (A) The relationships between the cnidarian classes as proposed by Collins et al. (2006), with key features discussed in the text indicated. Four of the many families of hydrozoans are shown to illustrate some of the diversity found in this particular class. (B) The anthozoan *Nematostella vectensis*, the starlet sea anemone. These juvenile polyps are about 5 mm in length. (C) The freshwater hydrozoan *Hydra magnipapillata*. Though outwardly similar, *N. vectensis* and *H. magnipapillata* are representative of opposite ends of the cnidarian phylogenetic spectrum. Note the mesenteries inside the body column of *N. vectensis* (B) and the asexual bud on *H. magnipapillata* (C). *The photograph* of H. magnipapillata *is courtesy of Hiroshi Shimizu, National Institute of Genetics, Mishima, Japan (from the NIH Image Gallery).*

The traditional, textbook taxonomy of the cnidarians has been upgraded in part due to closer examination of the life cycles of some members (Werner et al., 1971), but also due to analysis of nucleic acid sequences. For example, Collins et al. (2006) compared the sequences of 28S and 18S ribosomal DNA sequences from dozens of cnidarians and concluded that the staurozoans were a sister group to all other medusozoans, that the cubozoans and scyphozoans belong to the same clade, and that hydrozoans are a sister group to the cubozoan/scyphozoan clade (Fig. 8.3A). These authors and others (Bridge et al., 1992) also conclude that the anthozoans were the earliest class of cnidarians to diverge from an ancient common ancestor. Cnidarians are estimated to have diverged from the Bilateria around 750 million years ago (Ryan et al., 2007). The fossil record of cnidarians extends back to the Cambrian period (Cartwright et al., 2007).

In this review, we bring together the growing literature on the molecular components and functions of cell–cell and cell–ECM adhesion systems in cnidarians. This topic is of special interest at this time because the availability of complete genome sequences for several species of cnidarians has stimulated many questions about the relationships between cnidarian and bilaterian organisms. The broad evidence for many conserved cell adhesion networks between cnidarians and mammals is reactivating interest in cnidarians as experimental models or potential sources for tissue engineering materials. We will briefly describe the organisms selected for genomic analysis and then concentrate on the anthozoan *Nematostella vectensis* and the hydrozoan *Hydra magnipapillata*, for both of which genome sequences are available. In addition to discussing data on adhesion molecules and their functions from biochemical, molecular cloning, and functional studies, and identifications from postgenomic analyses to date, we will present some novel postgenomic analyses to compare predicted proteins from these cnidarians with those from widely studied eumetazoan experimental organisms. We will not discuss the fascinating-related fields of ECM production in corals (Helman et al., 2008) or the specialized ECM of nematocysts. Excellent articles on these topics are provided by David et al. (2008), Özbek (2011), and Balasubramanian et al. (2012).

2. CNIDARIAN GENOMES

To date the genomes of three cnidarians have been sequenced: the sea anemone *N. vectensis* (Putnam et al., 2007), the hydrozoan *H. magnipapillata* (Chapman et al., 2010; Steele, 2012; Steele et al., 2011), and the stony coral *Acropora digitifera* (Shinzato et al., 2011). Other members of phylum Cnidaria have been the subjects of large-scale transcriptome analysis and expressed sequence tag (EST)-sequencing projects (Iguchi et al., 2011; Siebert et al., 2011; Soza-Ried et al., 2010; Sun et al., 2013). Such projects are becoming a focus of interest for examining the effects of climate change on the reef-building capacities of corals (Meyer et al., 2009; Moya et al., 2012; Polato et al., 2011).

2.1. *Nematostella vectensis*

N. vectensis is the starlet sea anemone, an anthozoan that burrows in muddy estuaries along the Atlantic and Pacific coasts of the United States, as well as along the southern coast of England (Fig. 8.3B). It was selected to be the first member of its phylum to have its genome sequenced because of its relatively

small genome. Also, it is relatively easy to culture in the laboratory: the small (1–5 cm long) sexually mature polyps can be kept in diluted sea water at room temperature in Petri dishes on the bench top; if kept well fed with *Artemia* nauplii, they spawn at regular intervals, and their offspring reach sexual maturity in half a year or less (Hand and Uhlinger, 1992). Several laboratories have refined these methods and have learned how to synchronize the spawning to simplify studies of early development (Darling et al., 2005; Fritzenwanker and Technau, 2002). Although established only recently as an animal model, several 100 publications have appeared featuring this hardy anthozoan in studies of evolution, development, differentiation, responses to stress, and regeneration.

The genome sequence of *N. vectensis* was described by Putnam et al. (2007). The genome contains approximately 18,000 genes encoded on 30 chromosomes. Approximately 12,000 of the 27,000-predicted protein-coding transcripts have clear orthologs in either protostomes or deuterostomes. The numbers of exons found in *N. vectensis* genes were comparable to those found in humans and pufferfish, and splice sites were nearly identical. Analyses also provided insights into the origins of metazoan genes: about 80% of the genes or gene families shared between *N. vectensis* and bilaterians are also found in non-metazoan eukaryotes. Of the remaining shared genes, the largest group (about 15%) contains genes that are novel to metazoans. These include the Wnt family of signal transduction proteins and the fibroblast growth factor family. Smaller numbers of genes encode proteins with novel combinations of previously evolved domains or proteins with both novel and previously evolved domains (e.g., Notch). When the authors analyzed integrin signaling and cell–cell adhesion pathways, they found that most of the intracellular signaling molecules were ancient, but other components contained novel domains.

2.2. *Hydra magnipapillata*

In contrast to *N. vectensis*, which is a relative newcomer to experimental biology, members of the genus *Hydra* have been studied experimentally since pioneering studies by Abraham Trembley in the eighteenth century (Galliot, 2012). Unlike the vast majority of cnidarians, *Hydra* live in fresh water. *Hydra* are small (up to about 1 cm, but usually only a few millimeter long) hydrozoans that exist only as polyps (Fig. 8.3C). There is abundant literature on the anatomy of *Hydra* and detailed knowledge of their cell types. These comprise the epithelial cells of the two cell layers, cnidocytes, nerve, muscle, and gland cells and, in the interstices of the epithelial layers, cells of the interstitial (I) stem cell lineage (Bode, 1996; Galliot and Chera,

2010). The species and standard wild-type strain that was selected for genomic analysis, strain 105 of *H. magnipapillata*, is used widely for research on development, pattern formation, and regeneration. It is interesting to note that even though *N. vectensis* and *H. magnipapillata* share a similar outward appearance (Fig. 8.3B and C), they diverged about 500 MYA and represent different ends of the phylogenetic spectrum within phylum Cnidaria.

The *H. magnipapillata* genome (Chapman et al., 2010) contains approximately 20,000 predicted protein-coding transcripts. A recent description of the transcriptome of the closely related species *Hydra vulgaris* (Wenger and Galliot, 2013) finds the number to be somewhat higher (between 24,500 and 28,000), probably because their method also identifies pseudogenes and transposons. There has been a relatively high rate of intron loss, with 22% of the introns shared between *N. vectensis* and humans lost from *H. magnipapillata*. The *H. magnipapillata* genome also lacks many of the homeobox genes found in *N. vectensis*, suggesting again that hydrozoans in general, and *Hydra* in particular, are a relatively specialized and modern group that has diverged in significant ways from the common eumetazoan ancestor. Key signaling pathways featuring Wnt, Hedgehog, and Notch, however, are conserved, as are many gene products required for cell–cell and cell–ECM interactions.

2.3. *Acropora digitifera*

Reef-building corals are at tremendous risk from warming seawater; understanding their molecular foundations was a major motivating factor for sequencing the genome of *A. digitifera*, a staghorn coral that is abundant in Indo-Pacific reefs. Like *N. vectensis*, the staghorn corals are anthozoans, though their polyps are partially housed in a tough calcium carbonate exoskeleton. Analysis of the *A. digitifera* genome revealed approximately 24,000 predicted genes as well as evidence that *N. vectensis* and *A. digitifera* diverged from a common ancestor about 500 million years ago (Shinzato et al., 2011). To date, this genome has been studied primarily to understand the effects of stress on corals and the molecular basis for the symbiotic relationship between corals and photosynthetic dinoflagellates. In our review of adhesion networks, we will therefore concentrate on *N. vectensis* and *Hydra*.

3. THE ANATOMY OF *N. VECTENSIS* AND *HYDRA* POLYPS

Though outwardly similar (Fig. 8.3B and C), the adult polyps of *N. vectensis* and *Hydra* have significantly different internal anatomies. The

mesoglea of *Hydra* is acellular (Hess et al., 1957) whereas the mesoglea of *N. vectensis* contains multiple cell types (Tucker et al., 2011, 2013). In addition, both the epidermis (a.k.a. ectoderm) and gastrodermis (a.k.a. endoderm) of *Hydra* contain myoepithelial cells, whereas these cells are only found in the gastrodermis of *N. vectensis* (Fig. 8.4A). The epidermis of the mouth of anthozoans is connected to a tubular pharynx, and the gastrodermis of *N. vectensis*, like that of all sea anemones and unlike that of *Hydra*, is thrown into a series of infoldings known as mesenteries (Fig. 8.4B). The mesenteries contain cell types that give it region-specific functions. For example, projecting toward the lumen of the gastrovascular cavity is the mesenteric filament, which contains numerous cnidoblasts for neutralizing ingested prey and ciliated cells that circulate the cavity's contents. Also embedded within the mesentery is the testicular or ovarian cyst, which bursts to release its contents into the gastrovascular cavity. Within the stalk that connects the reproductive cyst to the body wall are two sets of retractor muscles composed of longitudinal arrays of myonemes that arise from myoepithelial cells.

Epithelial and I cells in the gastric region of the body column of *Hydra* proliferate continuously. This leads to axial displacement of the cells, either apically into the tentacles where the epithelial cells undergo terminal differentiation as hypostome or tentacle cells, or basally into developing buds or the basal disk; in the latter, cells undergo terminal differentiation to the basal disk phenotype. With time, nonproliferating cells are lost from the extremities of the organism, thus allowing for continuous renewal of the tentacles or foot (Fig. 8.5A). During these displacements, the epithelial cells undergo major changes in cell shape and differentiation status. For example, epidermal cells are cuboidal within the body column but become spindle-shaped upon displacement into the tentacles, due to weakening of cell–cell contacts. Basal displacement results in differentiation to columnar, mucus-producing cells of the basal disk (Anton-Erxleben et al., 2009). Sexual reproduction in *Hydra* depends on the differentiation of gamete cells from migratory I stem cells that aggregate and proliferate in response to environmental cues such as temperature or nutrient availability. The surrounding epithelium forms a temporary gonad from which gametes are released to the exterior (Künzel et al., 2010). *Hydra* polyps have separate sexes and sperm- or egg-restricted stem cells are derived from multipotent stem cells during embryogenesis and maintained in offspring during asexual reproduction. Grafting experiments demonstrate that the sex of polyps can be determined by interactions between multipotent, egg-restricted, and sperm-restricted stem cells (Nishimiya-Fujisawa and Kobayashi, 2012).

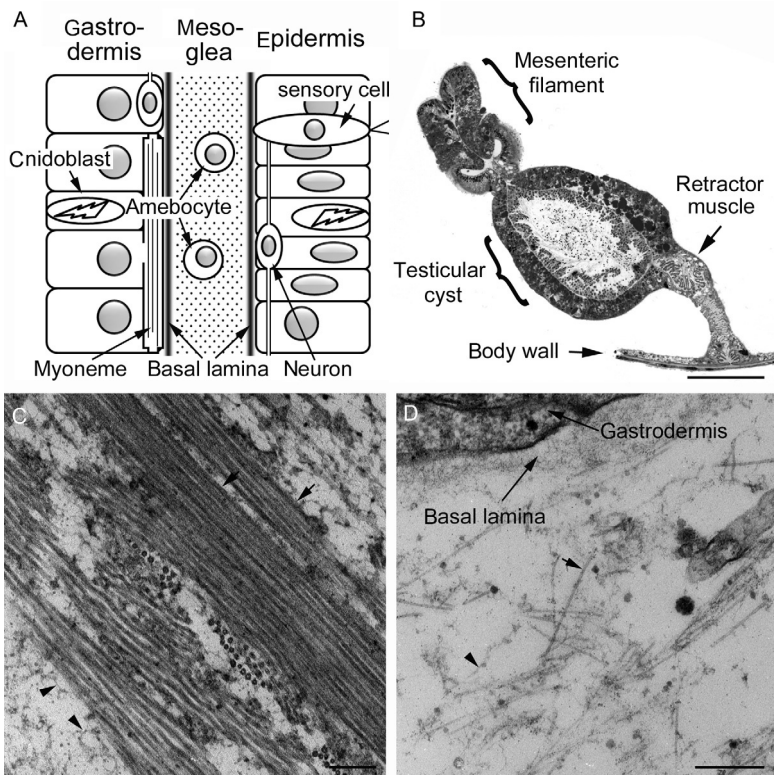

Figure 8.4 Anthozoan anatomy. (A) A schematic of the bilaminar organization of the body wall of an anthozoan. An outer epidermis and an inner gastrodermis sandwich an extracellular matrix called the mesoglea. In contrast to the mesoglea of hydrozoans, the mesoglea of *Nematostella vectensis* is cellular. Note the diversity of cells making up the two epithelial layers. Some cells form long muscle-like processes called myonemes. Others are the specialized cnidoblasts (indicated by lightning bolts). (B) The gastrodermis of *N. vectensis* forms double-layered mesenteries that project into the gastrovascular cavity from the body wall. Longitudinally arrayed myonemes are found in the retractor muscle. Gonadal cysts will burst and release either sperm or eggs into the gastrovascular cavity. The central free edge of the mesentery is the mesenteric filament, which contains ciliated cells, secretory cells, and batteries of cnidoblasts. (C) Electron microscopy reveals the organization of the mesoglea found in the body wall of an adult *N. vectensis*. Note the bundles of faintly striated fibrils that in this section are running parallel to the myonemes of the body wall. (D) Mesoglea ultrastructure is different in different parts of *N. vectensis*. In the mesenteric filament the extracellular matrix is sparse (arrowheads). Note the fuzzy basal lamina underlying the gastrodermis. Scale bars: 100 μm (B), 250 nm (C) and 500 nm (D).

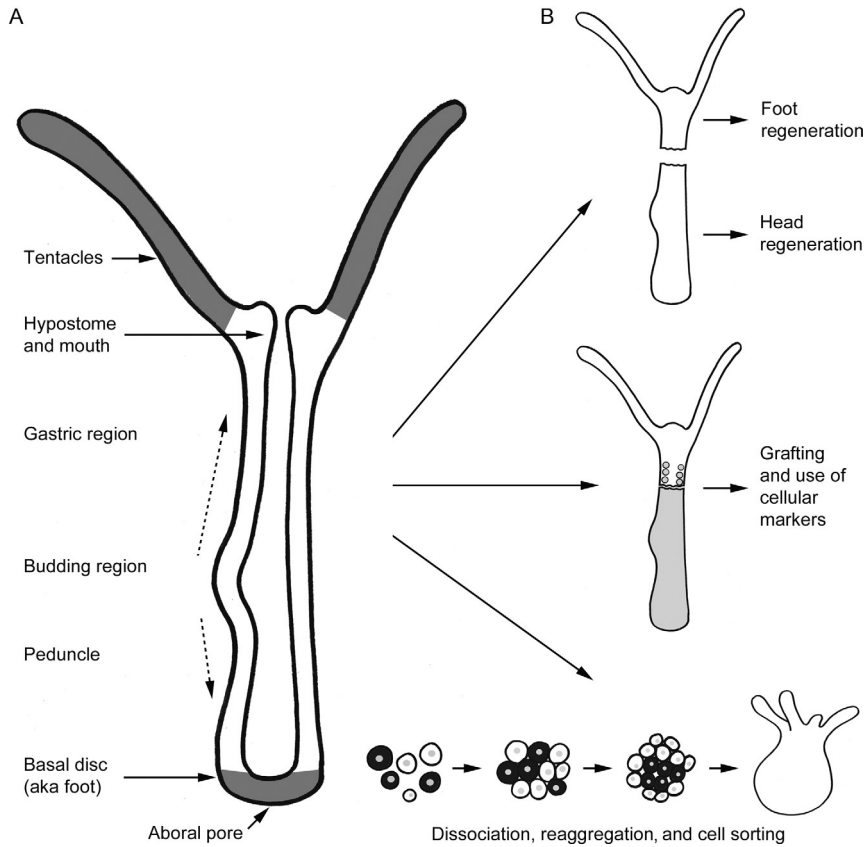

Figure 8.5 Organization of the *Hydra* polyp and methods used to study regeneration in *Hydra*. (A) Schematic view of a *Hydra* polyp with the main regions of the body column labeled. Gray shading indicates the regions of nonproliferative epithelial cells in the tentacles and basal disk. Dotted arrows indicate the apical or basal movement of proliferating epithelial cells along the axis of the body column. (B) Some of the prominent methods used to study regeneration in *Hydra*, as mentioned in this article, that include transection of the body column, grafting of body regions with labeled cells to enable study of cell movements or transdifferentiation, and reaggregation, cell sorting and tissue assembly after mechanical or enzymatic dissociation of cells from intact *Hydra*.

4. ECM IN CNIDARIANS

4.1. The ultrastructure and mechanical properties of mesoglea

The mesoglea of *Hydra* includes meshwork-like basal laminae (Davis, 1975) as well as ground substance, fibrils of between 5 and 50 nm diameter, 10-nm thick fibrils that are typically beaded in appearance, and thicker and clearly

striated fibrils (Davis and Haynes, 1968). Cellular processes from both cell layers of the body wall extend across the mesoglea to mediate direct cell–cell interactions (Haynes et al., 1968; Hess et al., 1957; Wood, 1961). In accord with the large scale changes in body length that occur when *Hydra* extend to full length or contract sporadically (Passano and McCullough, 1965; Shimizu and Fujisawa, 2003), the mesoglea is very elastic. Fluorescent antibody tagging of *Hydra* collagen-1 or laminin in the intact animal by microinjection revealed that the mesoglea is a dynamic structure: in the body column and tentacles the mesoglea undergoes continual displacement toward the foot or tentacle tips, respectively. This is likely driven in association with the continual proliferation and displacement of cells of the body column toward the apical or aboral ends (see Section 3). The mesoglea is also reorganized during the formation of asexual buds, as the bud expands outward (Aufschnaiter et al., 2011).

The ultrastructure of the mesoglea of sexually mature *N. vectensis* is quite different in different parts of the polyp (Tucker et al., 2011). In the body wall, the mesoglea is composed primarily of bundles of faintly striated fibrils approximately 20–25 nm in diameter found near the gastrodermis that generally course circumferentially (Fig. 8.4C). The same fibrils are abundant in the mesoglea of the retractor muscles, where they run longitudinally (i.e., these fibrils run parallel to the fibers of the myoepithelial cells, or myonemes, found in different parts of the gastrodermis). The mesoglea of both the body wall and retractor muscles also contains a finer set of fibrils of approximately 5 nm diameter that appear to lack any particular orientation, as well as a particulate ground substance. Elsewhere in the mesenteries the fibrous mesoglea is sparse (Fig. 8.4D), but a fuzzy basal lamina underlies both epithelial layers throughout the organism.

In medusozoans, the mesoglea of the bell of the medusa is thicker and less rigid than the mesoglea of polyps. It has a distinct ultrastructure, including a jelly-like, water-retaining ground substance, collagen fibrils, and other fibrils of various morphologies including radial fibrils that contain fibrillin (Beigel-Heuwinkel, 1982; Bouillon and Coppois, 1977; Chapman, 1953; Reber-Müller et al., 1995; Weber and Schmid, 1985). The notable pulsatile contractions of swimming medusae have made jellyfish a favored model for studies on the biophysical properties of mesoglea. The swimming movements depend on cycles (with periodicity of about 1 s) of muscle-driven contraction of the bell of the medusa to displace aquatic fluid rearward, followed by reopening (relaxation) of the bell and reinflux of fluid. The relaxation and refilling stage is powered by energy stored by the shape

change of the bell during contraction. In comparison to anthozoan mesoglea, jellyfish mesoglea has much higher elastic compliance (Alexander, 1964). The biophysical properties of jellyfish mesoglea implicated that energy sufficient for extension could be stored by contraction of the mesoglea (DeMont and Gosline, 1988). The question of which structures might store energy was addressed by Megill et al. (2005), with reference to the hydrozoan jellyfish *Polyorchis penicillatus*. In this organism, the bell contains inner and outer layers of mesoglea separated by a layer of gastrodermal cells (Gladfelter, 1972). The outer layer contains radial bundles of fibrillin-containing microfibrils, between 1.5 and 2.3 μm in diameter, at a density of over 200 bundles/mm (Megill et al., 2005; Reber-Müller et al., 1995; Weber and Schmid, 1985). The inner mesoglea is less stiff and contains a network of fibers. Megill et al. (2005) demonstrated that isolated, intact mesoglea was indeed jelly-like with a compressive stiffness of 131 Pa. The radial microfibril bundles were calculated to have an elastic modulus of 0.9 MPa; sufficiently stiff to store the energy needed for reexpansion of the bell.

These measurements of mesoglea properties were expanded recently by Gambini et al. (2012) to microrheology, the measurement of stress and deformation at the microscopic scale. Using fluorescent microbeads as tracers in the mesoglea of *Aurelia aurita*, the viscoelastic properties were found to be very heterogeneous at the local scale, perhaps reflecting the heterogeneous networks of small fibrils and microfibril bundles. The mesoglea of adult *A. aurita* was found to be more rigid than that of juveniles. This change correlated with the aggregation of fibrils, leading to the suggestion that progressive stiffening of mesoglea occurs as part of aging.

4.2. ECM components of cnidarians

4.2.1 ECM components identified by biochemistry or molecular cloning

Dissection has been a popular approach to isolate the thick mesoglea of jellyfish medusae, yet an experimental advantage, used widely in studies of *Hydra*, is that mesoglea can be isolated from its surrounding cell layers by a detergent extraction and freezing procedure (Barzansky et al., 1975; Day and Lenhoff, 1981). Initial biochemical or immunohistochemical studies identified that *Hydra* mesoglea has characteristics similar to those of the basement membranes of vertebrates with amino acid profiles indicative of the presence of collagens (Barzansky et al., 1975; Sarras et al., 1991a). Abundant fibrillar collagens isolated from several anthozoans are homotrimeric

(Katzman and Kang, 1972; Nordwig et al., 1973; Nowack and Nordwig, 1974); however, heterotrimeric collagens have been isolated from the hydrozoan sea-pen *Veretillum cynomorium* (Tillet-Barret et al., 1992) and jellyfish *Stomolophus nomurai* (Miura and Kimura, 1985) and *Catostylus tagi* (Calejo et al., 2009).

Through the combined approaches of protein isolation, peptide sequencing, immunohistochemistry, and molecular cloning, a fibrillar collagen, collagen IV, and laminin subunits have been identified as prominent components of *Hydra* mesoglea (Deutzmann et al., 2000; Fowler et al., 2000; Sarras et al., 1994; Shimizu et al., 2008; Zhang et al., 2002). Purified *Hydra* laminin appears in rotary-shadowed electron microscopy images as a heterotrimer of the same molecular form as laminins from bilaterians (Zhang et al., 2002). The laminin alpha and beta subunit proteins have the same domain organization and are highly conserved with those of bilaterians (Sarras et al., 1994; Zhang et al., 2002). Further molecular cloning studies revealed that the repertoire of collagens in *Hydra* is quite complex and includes in *H. vulgaris* four fibrillar collagens (Hcol1, Hcol2, Hcol3, and Hcol5; the Arabic numerals are used to signify that these collagens should not be assumed to be orthologs of the bilaterian collagens I, II, etc.), a collagen IV (Hcol4), and a unique form of collagen in which von Willebrand factor A domains are interspersed with interrupted triple helical domains (Hcol6). Whereas Hcol1 and Hcol2 are expressed throughout the adult organism, Hcol3 and -5 are expressed most strongly in tentacles and buds. Hcol1, -2, -4, -5, and -6 were reported to be conserved in *H. magnipapillata*, which was also found to express an additional collagen, Hcol7 (Zhang et al., 2007; Table 8.1). Eight fibrillar collagen alpha chains have been identified in *N. vectensis*; these include three with a whey acidic protein domain in their N-propeptide and two that have an N-propeptide corresponding to a TSPN domain (Exposito et al., 2008).

In terms of understanding how *Hydra* mesoglea is assembled, it is noteworthy that, even though it appears to be a symmetrically organized structure, all the fibrillar collagens are principally expressed in the epidermis, whereas laminin subunits are expressed by the gastrodermis (Sarras et al., 1994; Shimizu et al., 2002; Zhang et al., 2002, 2007). It is not understood how the "sided" secretion of ECM components is converted to the final symmetrical structure. Antibody staining studies show that Hcol1 forms a fibrillar network in the central region of the mesoglea, whereas laminin and Hcol4 form the dense sheet of the basement membranes and also line the 0.5–1 μ diameter channels or pores that traverse the mesoglea. These

Table 8.1 Extracellular matrix components of *Hydra magnipapillata* and *Nematostella vectensis* that are conserved with bilaterians

Species	Extracellular matrix component	GenBank accession number
H. magnipapillata	Fibrillar collagen Hcol1	XP_002158319 (AAM77398[a])
	Fibrillar collagen Hcol2	XP_002164888 (ABG80449[a])
	Fibrillar collagen Hcol3	XR_181671 (ABG80450[a])
	Fibrillar collagen Hcol5	XP_002161962 (ABG80451[a])
	Novel interrupted collagen Hcol6	XR_053617 (ABG80452[a])
	Collagen IV, Hcol4	XP_004212647 (AAG40729[a])
	Fibrillin	XP_001630852
	Fibulin/Hemicentin	XP_002154934
	Laminin (LNα)	XP_002170373
	Laminin (LNβ1)	XP_002168125
	Laminin (LNβ2)	XP_002165286
	Nidogen	Not detected
	Perlecan	XP_002168817
	SPARC	XP_002167014
	Thrombospondin	XP_002164610
N. vectensis	Fibrillar collagen	XP_001635016
	Collagen IV	XP_001626265
	Fibrillin	XP_001630852
	Fibulin/hemicentin	XP_001636480
	Fibulin/hemicentin	XP_001625395
	Laminin (LNα, partial)	XP_001623203
	Laminin (LNβ1)	XP_001631565
	Laminin (LNβ2)	XP_001628586
	Nidogen	XP_001625225
	Perlecan	XP_001627394
	SPARC	XP_001629356

Continued

Table 8.1 Extracellular matrix components of *Hydra magnipapillata* and *Nematostella vectensis* that are conserved with bilaterians—cont'd

Species	Extracellular matrix component	GenBank accession number
	SPARC	XP_001626442
	SPARC	XP_001641541
	Thrombospondin (Nv22035)	22035[b]
	Thrombospondin (Nv168100)	JX680803
	Thrombospondin (Nv85341)	XP_1639928
	Thrombospondin (Nv30790)	30790[b]

[a]Cloned from *Hydra vulgaris* (see Zhang et al., 2007).
[b]JGI transcript ID.

pores appear to provide the extracellular spaces by which cell processes extending from the epidermal and gastrodermal cell layers make transverse cell–cell contacts (Shimizu et al., 2008).

As mentioned in Section 4.1, examination of mesoglea ultrastructure in the jellyfish *Podocoryne carnea* identified 10 nm, beaded fibrils that strikingly resemble the beaded fibrillin microfibrils that are prominent in interstitial ECM of vertebrates. Fibrillins are large, dimeric proteins that contains around 46 epidermal growth factor (EGF)-like domains and seven TB (for transforming growth factor β-binding protein) domains, and which assemble into beaded microfibrils by intermolecular interactions of their N-terminal regions. With benefit of an antibody that stained ECM fibrils, a *P. carnea* fibrillin was cloned; remarkably, this has over 40% sequence identity to human fibrillins (Reber-Müller et al., 1995).

Secreted protein rich in aspartic residues and cysteine (SPARC), also known as osteonectin or BM40, is an ECM glycoprotein expressed widely in mammals that plays important roles in osteogenesis, basement membrane organization, and the regulation of cell adhesion (Bradshaw, 2012). SPARC is characterized by an N-terminal acidic domain, a central follistatin domain, and a calcium-binding and collagen-binding C-terminal domain. Major functions are collagen binding and modulation of collagen fibril organization, with basement membrane-associated functions predominating in *Drosophila* and *Caenorhabditis elegans*, and binding to fibrillar collagens being an additional function in vertebrates (Mosher and Adams, 2012). It appears likely that collagen-binding activity is conserved in cnidarian SPARCs and represents an ancestral function. Four SPARC homologs are encoded in

N. vectensis, all of which are expressed only by gastrodermal cells and in all of which the collagen-binding domain is well conserved (Koehler et al., 2009).

Proteolytic cleavage is essential for the processing of collagen propeptides and collagen fibril assembly, and more generally for dynamic extracellular turnover of ECM. Several matrix proteases have been cloned in *Hydra*. *H. vulgaris* metalloproteinase 1 and 2 (Hmp1 and Hmp2) were identified through analysis of gelatinolytic activities in whole animal extracts. A major peak of activity was identified around 26 kDa, and subsequent protein purification, peptide sequencing, and molecular cloning led to the identification of Hmp1 as a member of the astacin family of zinc-binding metalloproteinases (Yan et al., 1995, 2000a), with homology to a cloned jellyfish astacin (Pan et al., 1998). Hmp2 was identified subsequently by homology cloning (Yan et al., 2000b). *In vitro*, Hmp1 degrades fibronectin (Yan et al., 1995), although this cannot be a physiologically relevant substrate as fibronectin is only found in chordates (Tucker and Chiquet-Ehrismann, 2009). Hmp1 mRNA is expressed by gastrodermal cells in the upper part of the body column, with highest levels at the base of the tentacles, and is not expressed in the foot process. It appears that Hmp1 is released extracellularly once the endodermal cells migrate to the base of the tentacles. Hmp1 protein localizes specifically in the mesoglea of the tentacles and in gastrodermal cells of the upper body (Yan et al., 1995). Interestingly, the meprin-like Hmp2 has a reciprocal pattern of expression within the gastrodermis, both transcript and protein being highest in the lower region of the body column and absent from the tentacles (Sarras et al., 2002; Yan et al., 2000b). A third astacin-like protease, foot activator responsive metalloproteinase (Farm1), was cloned from *H. vulgaris* as a transcript regulated downstream of *Hydra* foot activator peptide, a peptide which promotes foot-specific differentiation of epithelial cells. *Farm1* transcript is expressed in epidermal and gastrodermal cells within the gastric region of the body column and in early bud regions and is down-regulated by foot activator peptide or lithium chloride (Kumpfmuller et al., 1999).

A matrix metalloproteinase (MMP), with around 33% sequence identity to mammalian MMPs, was identified by homology cloning from *H. vulgaris* (Leontovich et al., 2000). This MMP has a similar domain organization to vertebrate MMPs but also includes a furin cleavage site (Sarras et al., 2002). The MPP exhibits gelatinase activity *in vitro*, and has proteolytic activity against components of isolated mesoglea including laminin. *Hydra* MMP is expressed by gastrodermal cells throughout the body, with highest levels in the foot process and tentacles, similar to the expression pattern of laminin

beta1 subunit. During foot regeneration in transected *Hydra*, the transcript is upregulated at the regenerating pole (Leontovich et al., 2000).

4.2.2 ECM components identified by postgenomic analyses

Following the publication of their genomes, the *N. vectensis* and *H. magnipapillata* genome sequences have been examined for additional ECM components conserved with those of bilaterians. Together, the experimental and *in silico* studies have identified a repertoire that includes many of the central structural components of basement membranes and interstitial ECM, as defined from studies of bilaterian ECM (Table 8.1). As discussed in Sections 4.1 and 4.2.1, fibrillin was already identified in a jellyfish and beaded microfibrils have been reported in *Hydra* mesoglea. With reference to the *N. vectensis* and *H. magnipapillata* genome sequences, it is clear that fibrillin orthologs are encoded in both genomes (Özbek et al., 2010; Table 8.1). The TB domain of fibrillins originated in cnidarians and thus fibrillins are a component of ECM specific to cnidarians and bilaterians (Robertson et al., 2011). Fibulins, proteins that associate with fibrillin microfibrils, are also encoded in cnidarians (Segade, 2010; Table 8.1). Of additional interest is the general conservation of bone morphogenetic protein (BMP) and a disintegrin and metalloproteinase with thrombospondin repeats (ADAMTS) proteases and nonfibril forming components of ECM: SPARC and thrombospondin. We discuss here in more detail some of the components identified through phylogenomics.

Thrombospondins are large, multidomain glycoproteins that interact with cell surfaces, cytokines and proteases, and other ECM components. In mammals and chicken, some thrombospondins are abundant in the nervous system, and others are expressed at high levels in dense connective tissues. Mammalian thrombospondins have many roles, including in synaptogenesis (Risher and Eroglu, 2012), wound repair (Sweetwyne and Murphy-Ullrich, 2012), the cardiovascular system and ECM organization and function in cartilage and other connective tissues (Adams and Lawler, 2011). All mammalian thrombospondins are oligomeric and conform to two domain architectures termed subgroup A (trimeric) and subgroup B (pentameric); however, other domain architectures have been identified in protostomes and basal deuterostomes that include monomeric forms (Bentley and Adams, 2010). The postgenomic analyses show that four thrombospondins are encoded in the *N. vectensis* genome and a single thrombospondin in the *H. magnipapillata* genome (Bentley and Adams, 2010; Özbek et al., 2010; Tucker et al., 2013; Fig. 8.6A; Table 8.1). The

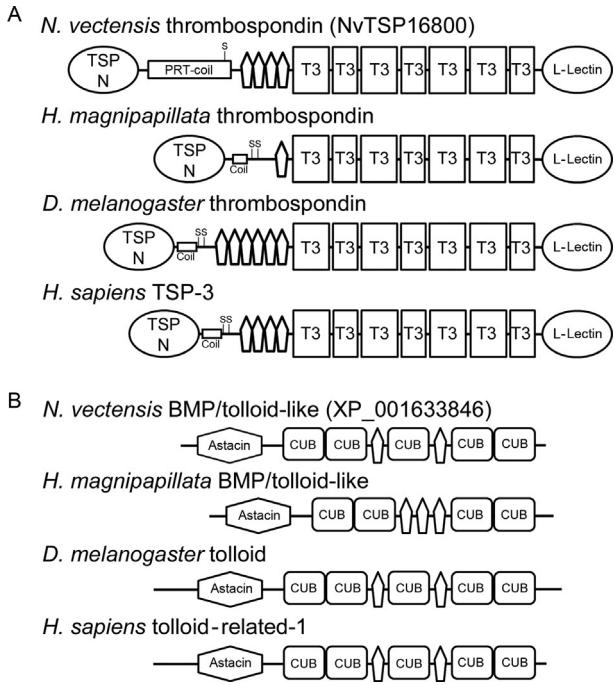

Figure 8.6 Diagrams illustrating the domain architecture of representative extracellular matrix molecules and proteases described in the text. (A) The extracellular matrix glycoprotein thrombospondin is highly conserved in *N. vectensis*, *H. magnipapillata*, *D. melanogaster*, and *Homo sapiens*. There are four thrombospondins in *N. vectensis* and five in *H. sapiens*; only one is shown here from each species. Note the presence of one or two cysteine residues (S) that may stabilize oligomerization by the coiled-coil domain (coil). (B) Homologs of the *D. melanogaster* fibrillar collagen protease tolloid are found in cnidarian genomes and in man. Key: Epidermal growth factor domains are indicated by narrow pentagons; astacin and CUB domains are indicated on the models. LamN, N- terminal domain; FN3, fibronectin type III domain; LamG, laminin G domain; TSPN, thrombospondin N-terminal domain; PRT-coil, domain rich in proline, arginine, and threonine; T3, thrombospondin type 3 domain; L-lectin, L-lectin-like domain.

predicted *H. magnipapillata* thrombospondin has a single EGF-like domain, but is otherwise closely related in domain organization to the subgroup B thrombospondins of deuterostomes (Bentley and Adams, 2010; Fig. 8.6A).

All the *N. vectensis* thrombospondin genes are expressed in adult polyps. Two genes are found on the same genomic scaffold and appear to be the result of gene duplication. The gene product of one of these related thrombospondin genes has been cloned in its entirety and is referred to by its JGI identification number: NvTSP16800. NvTSP16800 has features of the

expected domain organization of a subgroup B thrombospondin, but is unusual in containing a novel proline-rich domain near its N-terminus and only a short coiled-coil (Fig. 8.6A). An antibody raised against a fragment of NvTSP16800 labels neuron-like cells in the mesoglea of retractor muscles and pharynx (Tucker et al., 2013). This not only suggests a highly conserved role for thrombospondins in the nervous system, but also shows that the cellular elements of the anthozoan mesoglea are more diverse than previously thought. *In situ* hybridization and quantitative polymerase chain reaction (PCR) show that NvTSP16800 is upregulated during regeneration, and immunohistochemistry of regenerating polyps identified anti-thrombospondin labeling in the exterior glycocalyx of the epidermis. This similarity with localizations of mammalian thrombospondins suggests a conserved role for TSPs in responses to stress and wounding.

Secreted proteoglycans (e.g., decorin, versican, aggrecan) are prominent in the ECM of vertebrates, yet surprisingly, only the basement membrane proteoglycan perlecan is identifiable in the cnidarian genomes sequenced to date (Özbek et al., 2010; Table 8.1). Chemical analysis of *Hydra* extracts has identified that chondroitin and heparan sulfate glycosaminoglycans are present (Yamada et al., 2007): it would be expected that these are substituted onto protein cores. It is possible that these glycosaminoglycans are associated only with membrane-associated proteins because several membrane-associated proteoglycans are conserved between cnidarians and vertebrates (see Table 8.3). Alternatively, there may be lineage-specific mechanisms for extracellular interactions. A recent study of the glycocalyx of *Hydra* identified chondroitin and chondroitin 6-sulfate disaccharides; however, these did not appear to be associated with large core proteins (Böttger et al., 2012). The salt-extractable fraction of *Hydra* glycocalyx also included seven proteins belonging to two protein families: the PPOD (for putative peroxidase domain) and SWT (for sweet-tooth domain) families. The PPOD proteins were identified to have lectin activity inhibitable by heparin or chondroitin (Böttger et al., 2012). Thus, one possibility is that these glycosaminoglycans are substituted onto small peptides and bind into ECM by extracellular interactions. A further possibility is that cnidarian mesoglea includes lineage-specific secreted proteoglycan core proteins. Since these cannot be identified by sequence homology, approaches such as proteoglycan isolation and proteomic identification will need to be applied to address this question.

As discussed in Section 4.2.1, MMP and astacin-type matrix proteases are known mediators of matrix proteolysis in *Hydra*. Astacins are conserved in

N. vectensis (Table 8.2). In bilaterians, the C-propeptides of fibrillar collagens are cleaved by BMP1/tolloid proteases (Hopkins et al., 2007) and representatives of this family are conserved in both *N. vectensis* and *H. magnipapillata* (Fig. 8.6B; Table 8.2). From the *N. vectensis* and *H. magnipapillata* genome sequences, additional MMP family members have been identified and another major category of ECM proteases, the ADAMTS proteases, has been revealed to be conserved in cnidarians (Table 8.2; Özbek et al., 2010). In mammals, ADAMTS-2, -3 and -14 act as N-propeptidases for fibrillar collagens, thus representation of this family would be expected for efficient collagen fibril assembly to proceed. Large numbers of MMPs and ADAMTSs are encoded, with the former predominating in *H. magnipapillata* and the latter in *N. vectensis* (Table 8.2). These findings open up new prospects for experimental investigations of the roles of all these family members throughout the life cycle. The nature of the repertoire of ADAMTS substrates in both species is of particular interest, because many mammalian ADAMTS family members have specific roles in degrading proteoglycans such as aggrecan, or thrombospondin family members such as TSP5 (Stanton et al., 2011). Tissue inhibitors of metalloproteinases (TIMPs) are important physiological inhibitors of ECM metalloproteinase activity that are also conserved in *H. magnipapillata* and *N. vectensis* (Brew and Nagase, 2010).

4.2.3 Novel ECM components of cnidarians

In addition to the conserved ECM proteins described in Section 4.2, novel components of the mesoglea have been identified by biochemical analyses. One interesting example comes from studies of the scyphozoan *A. aurita* (Matveev et al., 2007). This jellyfish has a thick mesoglea filled with motile amoeboid cells that engage in phagocytosis. A major protein component of the mesoglea with an apparent molecular mass of 47 kDa was extracted at low pH and peptide sequences were used to design PCR primers to obtain nucleotide sequences. The resulting PCR products revealed a partial sequence for a novel protein with a zona pellucida (ZP) domain that the authors named mesoglein. *In situ* hybridization revealed that the amoeboid cells found within the mesoglea itself were the source of mesoglein. Potential insight into the complete sequence of mesoglein can be gained by using the ZP domain of *A. aurita* mesoglein to identify the homologous sequence in *N. vectensis*. The most similar predicted gene (JGI protein ID 245497) encodes two CUB domains and a ZP domain. This suggests that cnidarian mesoglein is related to human CUZD1 (from "cub and zona pellucida

Table 8.2 Matrix proteases of *Hydra magnipapillata* and *Nematostella vectensis* as predicted from their genomes

Species	Matrix proteases[a]	GenBank accession number
H. magnipapillata	ADAMTS6-like	XP_002168102
	ADAMTS20-like	XP_002166940
	ADAMTS-like	XP_002169841 (partial[b])
	ADAM-like	XP_002161708
	Astacin-type metalloprotease-1[c]	XP_004209002 (AAA92361[d])
	Astacin-type metalloprotease-2[e]	XP_002165576 (AAD33860[d])
	Farm1 astacin-type metalloproteinase	XP_002159980 (AF125506[d])
	Matrix metalloproteinase[f]	XP_002163794; XP_0000215860; XP_00168433; XP_002164979; XP_002160477; XP_002168462; XP_002161129; XP_002170324; XP_002166835; XP_002155089; XP_002168334
	BMP/tolloid-like	XP_002154412
N. vectensis	ADAMTS6-like	XP_001626083; XP_001639247; XP_001626094; XP_001627322
	ADAMTS10-like	XP_001626087
	ADAMTS20-like	XP_001636439
	ADAMTS-like	XP_001627302; XP_001637268; XP_001637265; XP_001628428 (partial[b]); XP_001620798 (partial[b]); XP_001628429 (partial[b])
	ADAM-like	XP_001629192 (partial); XP_001629194 (partial)
	Astacin-type metalloprotease-1[c]	XP_001626821
	Astacin-type metalloprotease-2[e]	XP_001628402
	Farm1-like astacin-type metalloprotease	XP_001633483

Table 8.2 Matrix proteases of *Hydra magnipapillata* and *Nematostella vectensis* as predicted from their genomes—cont'd

Species	Matrix proteases	GenBank accession number
	Matrix metalloproteinase[f]	XP_001640669; XP_001633230; XP_001640565; XP_001629775; XP_001635184
	BMP/tolloid-like	XP_001633846; XP_001635534

[a]Metalloproteinase and BMP/tolloid domain hits were also identified in additional short partial sequences from the *H. magnipapillata* and *N. vectensis* genome predicted proteins; these are not included in the table.
[b]Partial = ADAMTS-like sequences that were identified by the presence of a Zinc metalloproteinase-ADAMTS subfamily domain and thrombospondin type 1 domains in sequences of <1000 amino acids.
[c]Identified by presence of zinc metalloproteinase-astacin-like domain and ShK domain.
[d]Cloned from *H. vulgaris*.
[e]Identified by the presence of zinc metalloproteinase-astacin-like domain, MAM domain, and ShK domain.
[f]Identified by the presence of zinc metalloproteinase domain and hemopexin-like domain.

domain containing protein 1"), a protein of unknown function that nevertheless shows promise as a serum marker for ovarian cancer (Leung et al., 2012).

Thrombospondins belonging to subgroup A contain thrombospondin type 1 repeats (TSRs) in addition to the EGF domains and thrombospondin type 3 repeats that are found throughout the thrombospondin family. Many specific functions of subgroup A thrombospondins can be traced to the TSRs, and TSRs are also found in a variety of other ECM and transmembrane proteins, many of which are found in the nervous system (Tucker, 2004). Both *H. magnipapillata* and *N. vectensis* have a number of genes encoding repeated TSR domains, many of which are combined with other domains in unique and mostly uncharacterized proteins. The expression of one such TSR-containing protein in *H. vulgaris* was described by Miljkovic-Licina et al. (2004). The TSR-containing protein was expressed in a subset of neurons found in the head of the polyp, and was upregulated during regeneration. Further characterization of this family of proteins may prove interesting to those studying the evolution of the nervous system. Other interesting TSR proteins include the rhamnospondins, which contain repeated TSR domains and a C-terminal galactose-binding domain. First identified in *Hydractinia symbiolongicarpus* and found to be expressed specifically in the hypostome of the mouth (Schwarz et al., 2007), these proteins are well conserved in *N. vectensis* and *H. magnipapillata* (e.g., XP_001639688 and XP_004212403).

4.3. ECM receptors: Identification and functional investigations

Surprisingly, few cnidarian ECM adhesion receptors have been identified by biochemical methods. An analysis of binding of radiolabeled laminin to isolated *H. vulgaris* cells identified around 10,000 binding sites per cell of nanomolar affinity. Screening of the cells with antibodies against adhesion proteins of vertebrates identified that monoclonal antibody JG22 to the avian beta 1 integrin subunit could bind to *Hydra* cells and blocked their interaction with laminin. Proteins immunoprecipitated by this antibody had apparent molecular masses suggestive of integrin heterodimers. Treatment of living *Hydra* cells with the antibody blocked morphogenesis of *Hydra* cell aggregates and I cell migration *in vivo* (Ağbaş and Sarras, 1994).

The presence of integrin receptors in members of the phylum Cnidaria was established definitely over a decade ago by homology cloning of an integrin beta subunit from the coral *Acropora millepora* (Brower et al., 1997) and the cloning of single alpha and beta subunits from the jellyfish *P. carnea* (Reber-Müller et al., 2001). In this jellyfish, integrin transcripts are present at all life cycle stages including unfertilized eggs and during asexual budding; RNA analysis of dissected medusae and *in situ* hybridization indicated expression of both subunits in all adult tissues of polyps and medusae. Strong expression was noted in early developing buds and in both cell layers of planular larvae. Isolated muscle cells treated with collagenase, to induce transdifferentiation, maintained expression of both subunits, further indicating that most cell types of the medusa are integrin-positive.

An EST sequencing project in *A. millipora* identified a second coral integrin beta subunit, designated beta 2, and an alpha subunit with highest similarity to the vertebrate alpha4/alpha9 clade. All three *A. millipora* integrin genes are present in unfertilized eggs and throughout early development, with highest expression in the gastrodermal cell layer (Knack et al., 2008). An initial search of the *N. vectensis* genome for integrin-encoding sequences by these authors identified four integrin beta subunits and also an alpha subunit (as listed in Table 8.3).

ECM–integrin signaling in bilaterians involves interactions of the integrin beta subunit cytoplasmic domain with intracellular proteins of the focal adhesion complex, talin, and kindlin. Integrin signaling activity has not yet been demonstrated directly for any cnidarian integrin, but both talin and kindlin are conserved in cnidarians (Khan et al., 2011; Reber-Müller et al., 2001). In mammals, sharpin is an alpha subunit-binding protein that inhibits integrin signaling (Rantala et al., 2011) and related

Table 8.3 Extracellular matrix adhesion receptors of *Hydra magnipapillata* and *Nematostella vectensis* that are conserved with bilaterians

Species	Adhesion receptor	GenBank accession number
H. magnipapillata	Discoidin domain receptor	XP_002168413
	Dystroglycan receptor	XP_002164217
	Glypican	XP_002157574
	Integrin α	XP_002161020.1 (partial)
	Integrin β	XP_002164638.1 (partial)
	Syndecan	Hma2.224712[a]
N. vectensis	Discoidin domain receptor	XP_001636332 (partial)
	Dystroglycan receptor	XP_001629936
	Glypican	XP_001624312
	Integrin α (NvItgα1)	XP_001641435
	Integrin β (NvItgβ1)	XP_001641468
	Integrin β (NvItgβ2)	XP_001627336
	Integrin β (NvItgβ3)	XP_001637894
	Integrin β (NvItgβ4)	XP_001621822
	Syndecan	FC288353

[a]Hydra genome project.

C3HC4 zinc finger domain proteins are encoded in both *N. vectensis* and *H. magnipapillata* (XP_001631290 and XP_002166020).

Syndecan transmembrane proteoglycans have independent adhesion and signaling activities and frequently act as integrin coreceptors by interaction of negatively charged regions of their glycosaminoglycan side chains with clusters of positively charged residues in ECM integrin ligands (Couchman, 2010). Recognizable by their very highly conserved cytoplasmic domains, syndecans are conserved in cnidarians and postgenomic analyses have clarified that *N. vectensis* and *H. magnipapillata* encode single syndecans (Chakravarti and Adams, 2006; Özbek et al., 2010; Table 8.3). Other membrane-bound proteoglycans encoded in *N. vectensis* and *H. magnipapillata* as single genes include dystroglycan and glypican. A discoidin domain receptor-like protein is encoded in *H. magnipapillata* but not *N. vectensis*. NG2 or betaglycan-like proteoglycans were not identified (Özbek et al., 2010; Table 8.3).

5. FUNCTIONAL IMPORTANCE OF CELL–ECM INTERACTIONS FOR TISSUE ORGANIZATION AND REGENERATION IN CNIDARIANS

To date, *Hydra* species and jellyfish have been the predominant experimental models for analyses of cell–ECM adhesion processes and functions in cnidarians. Isolated *Hydra* cells will reattach and spread on isolated mesoglea, irrespective of the species of *Hydra* used to prepare the cells or the mesoglea. However, *Hydra* cells do not attach to purified mammalian ECM proteins such as collagen, fibronectin, or serum/vitronectin (Day and Lenhoff, 1981). Fibronectin and vitronectin are now known to be chordate-specific ECM components, and so a physiological interaction with these proteins would not be expected. Whether the lack of attachment to mammalian fibrillar collagen reflects a requirement for the native 3D organization or mechanical properties of intact mesoglea, or species specificity of collagen adhesion receptors, is unclear. Interestingly, mammalian and insect cell lines attached to plastic in preference to *Hydra* mesoglea, whereas *Xenopus* A6 cells attached equivalently to both substrata (Day and Lenhoff, 1981). Conservation of adhesion mechanisms in cnidarians is also indicated by the finding that isolated, decellularized mesoglea from the jellyfish *Rhopilema nomadica* can support the attachment, spreading, and migration of cells isolated from five species of anthozoans. This activity was not retained by acid-extracted mesoglea (Frank and Rinkevich, 1999).

Because of the enormous regeneration capacity of cnidarians, complete organisms can be regenerated over several days from dissected portions. In the case of *Hydra*, a minimum of one-fiftieth of an adult polyp is needed to achieve regeneration (Shimizu et al., 1993). Experimental designs that have been used widely to investigate morphogenesis, tissue assembly and cell differentiation in *Hydra* include transecting the body column into separate head and "foot" regions, each of which will regenerate the missing structures. Cell movements can also be traced by grafting together head and foot regions, in which one region contains a lineage tracer such as a fluorescent tag (Fig. 8.5B; Lenhoff, 1983). Integration of these classic methods with the application of pharmacological inhibitors, antibodies or antisense reagents has led to the identification of functional roles for ECM components including Hcol-1, laminin beta subunit, Hmp1, Hmp2, and MMP in regenerative processes (Deutzmann et al., 2000; Shimizu et al., 2002; Yan et al., 1995, 2000a,b; Zhang et al., 2002). Blockade of glycosaminoglycan substitutions

by β-xyloside has implicated roles for glycosaminoglycans in head regeneration (Sarras et al., 1991b, 1993; Zhang et al., 2002).

In agreement with its localization in the body, Hmp1 has particular roles in head regeneration and affects the differentiation status of tentacle epidermal cells. Loading of purified Hmp1 stimulated cell proliferation along the body column, perhaps indicating an effect on signaling pathways (Yan et al., 1995). In transected *H. vulgaris*, Hmp1 transcript levels are upregulated in the lower body region during head regeneration (initially at the cut site and then more generally), but are not upregulated in the head portion. Introduction of a Hmp1-neutralizing antibody or Hmp1 antisense oligonucleotides in the apical pole blocked head regeneration (Sarras et al., 2002; Yan et al., 2000a). Hmp2 also participates functionally in foot regeneration: transcript levels are elevated at the transection site during regeneration of the foot, and introduction of antisense oligonucleotides into the basal regenerating pole blocks foot regeneration and basal disk cell differentiation (Yan et al., 2000b). Studies on the role of MMP in foot regeneration provide further evidence for the importance of ECM proteolysis in polyp homeostasis and regeneration. Treatment of intact polyps with GM6001, a competitive inhibitor of mammalian MMPs, led to dedifferentiation of cells of the basal disk, resulting in reduced attachment of polyps to glass surfaces. MMP inhibition by GM6001 or recombinant human TIMP-1 also blocked foot regeneration in a process again involving dedifferentiation of basal cells (Leontovich et al., 2000; Sarras et al., 2002).

Using decapitated adult *Hydra* as the regeneration model, Shimizu et al. (2002) identified that after transection the mesoglea retracted from the area of the cut, such that the epidermal and gastrodermal cell layers made direct contact. Lateral resealing of the two cell layers across the cut site then took place within 1 h. Between 3 and 96 h posttransection, first mRNA and then protein levels of the studied ECM components increased around the cut site: as in the intact organism, Hcol-1 mRNA was expressed mainly in the epidermis and laminin beta1 subunit and MMP were expressed in the gastrodermis. Laminin was detectable in reforming basement membranes from 7 h onward, whereas Hcol-1 was not detected in the central fibrillar layer until around 15 h after transection. Introduction of antisense oligonucleotides to either laminin beta1 or MMP inhibited head regeneration; in the case of laminin, this effect could be reversed by addition of purified *Hydra* laminin. Thus, assembly of the mesoglea, especially the basement membrane layers, along with an associated capacity for proteolytic remodeling, are required to drive regenerative tissue organization (Shimizu et al., 2002).

Remarkably, cnidarians also regenerate from mechanically or enzymatically dissociated cell suspensions. *Hydra* has again been the main experimental model for these experiments that have allowed investigation of initial cell–cell and cell–ECM reassembly processes and how these can lead to tissue assembly (Fig. 8.5B). In *H. vulgaris*, clusters of dissociated cells reform into an epithelial bilayer within the first 24 h. Mesoglea reassembly is detectable by immunofluorescence microscopy after 17 h, with full assembly of the layered structure by 48 h. Tentacles begin to reform around this time, and regeneration of the complete organism with a head and crown of tentacles is completed over 96 h to 7 days (Sarras et al., 1993). In line with the microscopy observations, pulse-labeling experiments show that synthesis of ECM components is maximal between 24 to 48 h after cell dissociation. Reassembly of a complete ECM is an essential step for full morphogenesis in this system, as evidenced by experiments in which collagen cross-linking or proteoglycan biosynthesis were perturbed by pharmacological agents: these treatments led to reversible blockade of head and tentacle regeneration (Sarras et al., 1993). Application of fragments of mammalian collagen IV, or collagen IV antibodies, also altered cell differentiation and reduced cell proliferation, resulting in a blockade of morphogenesis from cell aggregates (Zhang et al., 1994).

I cells of *Hydra* are a heterogenous population of fast-proliferating cells with multipotent stem cell properties that are located between the epithelial cells throughout the body column (Bode, 1996). Migration of I cells is important for differentiation of the head and foot regions of the *Hydra* polyp. The role of ECM in I cell migration was analyzed through grafting experiments, in which the head regions of polyps depleted of I cells (by hydroxyurea treatment) were grafted onto a normal distal region containing lineage-labeled I cells. Under control conditions, I cells migrated and repopulated the head region over a 24 h period. The number of migrating I cells was strongly reduced by treatment of grafts with β-amino propionitrile, an inhibitor of lysyl oxidase-mediated collagen cross-linking. Migration was partially reduced in the presence of RGD peptide, but was not affected by β-xyloside treatment (Zhang and Sarras, 1994). Thus, specific attributes of mesoglea, collagen cross-linking and RGD-dependent interactions, are important to enable I cell migration. Studies with a *Hydra* laminin-derived peptide indicate that laminin is also needed for I cell migration (Zhang et al., 2002).

The above studies all focused on the functions of cell–ECM interactions in the asexual polyp. The role of integrins in fertilization has also been

studied with the coral *A. millipora*. Transcripts for integrin beta 1 and alpha 1 are present in unfertilized eggs. Antibodies against an N-terminal fragment of the extracellular domain of the beta 1 subunit blocked the binding of sperm to eggs, resulting in decreased fertilization rates. In contrast, antibodies against an N-terminal fragment of the alpha 1 subunit did not reduce sperm binding or fertilization rates. Whether this reflects that the epitope targeted in the alpha subunit is not part of the ligand-binding site, or whether a different alpha subunit partners with beta 1 in the egg remains to be established (Iguchi et al., 2007). As a role for mammalian integrins in fertilization is well established, these studies implicate wide conservation of a functional role of integrins in fertilization.

6. CELL–CELL ADHESION MOLECULES IN CNIDARIANS

In the following sections, we will discuss the cellular structures and molecular components that have been identified to participate in cell–cell interactions in cnidarians. We will then address additional molecules homologous to bilaterian cell–cell adhesion molecules that have been identified through phylogenomics. Most of the work that has been done to date is descriptive in nature. The emerging postgenomic data once again point to many conserved proteins between chordates and cnidarians. However, little is known about the specific roles or cell–cell adhesion activities of many of the proteins discussed here. Some insights have been gained into the possible evolution of the foundations of development and morphogenesis.

6.1. Ultrastructural and functional studies of cell–cell adhesion systems in cnidarians

6.1.1 Septate junctions

Septate junctions were identified first in *Drosophila* salivary glands as closely apposed regions of plasma membrane, below adherens junctions, that have a ladder-like appearance of electron-dense extracellular material (Wiener et al., 1964; Fig. 8.7). In *Hydra*, the first electron microscopy studies of intercellular junctions (Wood, 1959) identified septate junctions as ladder-like intercellular structures located between the outer lateral edges of adjacent epidermal cells and between the inner, luminal edges of cells in the gastrodermal layer. In these areas, the intercellular space between plasma membranes is around 15–20 nm across. Analysis of conventional fixed or freeze/fracture preparations in planes across the cell layers showed the septa to be like rungs in a ladder: parallel, electron-dense structures that extend

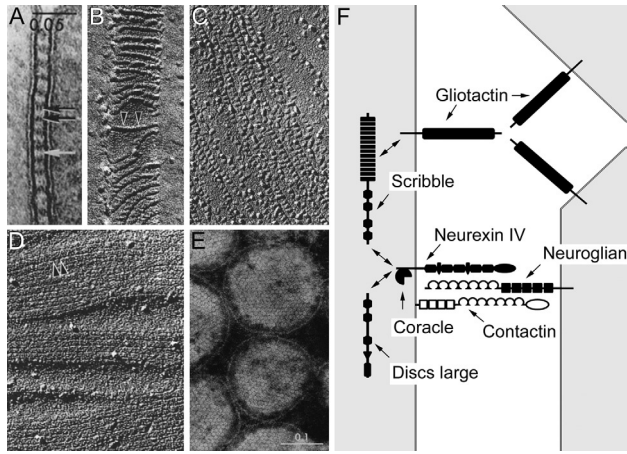

Figure 8.7 Septate junctions and gap junction in cnidarians. (A) Uranyl-acetate stained, transmission electron microscope image of a septate junction from the gastrodermis of *Hydra oligactis* in longitudinal view, showing two apposed plasma membranes and the septa of the junction that span the inter-membrane space (white arrow). Black arrows indicate the projections from a septum, 243,000 ×. (B) Longitudinal view of a septate junction in the epidermis of *Hydra littoralis* from a fast-frozen, freeze-fractured sample, 170,000 ×. (C) and (D). En-face freeze-fracture views of septate junctions from the epidermis of *H. littoralis*. Intramembranous particles are visible on the E-face (C), and grooves with periodic puncta on the P face (D). Both 200,000 ×. (E) En-face transmission electron microscope view of lanthanum-stained gap junctions in the gastrodermis of *H. oligactis*. Each plaque contains many hexagonally packed gap junction units and is surrounded by an electron-lucent band that separates it from the intercellular space, 185,000 ×. (F) A model of a septate junction from *D. melanogaster* showing interactions between different molecules. The molecules that have been filled in with black are encoded in both *D. melanogaster* and cnidarians. *This schematic is adapted from a figure found in Hortsch and Margolis (2003). Panels (A) and (E) are reproduced, with permission, from Hand and Gobel (1972). © 1972 Rockefeller University Press. J. Cell Biol. 52, 397–408. Panels (B)–(D) are reproduced, with permission, from Kachar et al. (1986).*

across the intercellular space and are around 2–3 nm thick and spaced at 13–17 nm intervals. Additional projections from each septum extend toward adjacent septa (Filshie and Flower, 1977; Hand and Gobel, 1972; Kachar et al., 1986; Fig. 8.7A–D). Studies with electron-dense, extracellular tracer dyes led to the model that the junctions are built from chains of hexagonal units, of around 6 nm, with projections that extend above and below the units and link the chain to cell membranes. Low penetration of the junctions by molecules such as horseradish peroxidase implicated a barrier function for these junctions (Hand and Gobel, 1972). These results were in line with prior measurements of transcellular resistance in *Hydra*, that

had demonstrated a transepithelial resting potential of around 40 mV and a transepithelial resistance of around 166 kOhm (Josephson and Macklin, 1967). Freeze–fracture studies of several species of New Zealand sea anemones later identified septate junctions with distinctive and unusual morphologies. In septate junctions of the gastrodermis, each septum appeared, not as a continuous rung, but as two twin septa separated by a 6- to 7-nm gap (Green and Flower, 1980). In the epidermis, the septate junctions contained single, wavy septa, each with many lateral projections of around 7 nm in length. Unlike the junctions described in *Hydra*, these projections extended on one side of the septum only. A clearer understanding of the molecular composition of cnidarian septate junctions is needed to understand more fully the significance of these morphological differences, which may reflect specializations for the organisms' life style or ecological niche.

A study of tissue reformation in grafts of transected *Hydra* showed that the process begins with extension of finger-like protrusions from the bases of epithelial cells. These bridges reach across to neighboring cells to reseal the epidermis. Septate junctions start to form early in this process, initially locally and then with larger-scale organization (Bibb and Campbell, 1973). The rapid reformation of these large structural junctions during dynamic tissue remodeling presumably reflects the importance of restoring the epidermal barrier against pathogens and the external environment. Given the large changes in body shape that many cnidarians are capable of, it is interesting to consider how septate junctions are maintained during tissue deformation. This question has been examined with regard to the septate junctions of myoepithelial cells of mesenteries of the sea anemone *Metridium senile*. Stretching of the mesenteries resulted in a decrease in cell thickness from 32 to 8 μm. The integrity of the septate junctions and the spacing of septa were maintained throughout stretching, yet the depth of the junctions decreased and their perimeter length increased (Holley, 1985). These studies implied mobility of the junctional structures within the plane of the plasma membrane and potential for "sliding" interactions of extracellular elements of the junctions. Since these early microscopy studies, the molecular components of invertebrate septate junctions have been elucidated principally in *Drosophila* (Banerjee et al., 2006). Below, in Section 6.3.4, we discuss the encoding of known proteins of protostome septate junctions in *H. magnipapillata* and *N. vectensis*.

6.1.2 Gap junctions

Gap junctions in *Hydra* are located at the apical regions of the lateral membranes of the epithelial cell layers and also along the muscle processes at the

base of the cells (Hand and Gobel, 1972). The junctions have a width of 17–20 nm. In *en face* electron microscope images, they appear as arrays of hexagonally packed structures of about 8 nm diameter (Fig. 8.7E). Dye transfer and electrical coupling activities take place between *Hydra* epithelial cells as in other animal epithelia (Fraser and Bode, 1981; Fraser et al., 1987). These functional activities were identified to be mediated by gap junctions through inhibition experiments using antibodies raised against rat liver connexins (the major proteins of gap junctions in chordates). Introduction of these antibodies into cells in intact *Hydra* led to loss of cell coupling. Furthermore, antibody-treated organisms used as graft recipients had a greater tendency to form secondary body axes. These results demonstrated the importance of gap junctions for morphogenetic cues necessary for patterning of the body plan, as well as for local signaling between epithelial cells (Fraser et al., 1987).

The formation of gap junctions is influenced by ECM. If cultured in suspension, cells from the subumbrella plate gastrodermis of the anthomedusa *P. carnea* form spheres in which cells do not form gap junctions. However, adhesion of the spheres to sheets of isolated mesoglea results in assembly of functional gap junctions (Weber and Schmid, 1984).

Gap junctions have other important functions in the lineage-specific cells of cnidarians. For example, as demonstrated in the sea anemone *Haliplanella luciae*, mechanical vibration is a stimulus for the discharge of nematocysts from the tentacles, as a result of deflection of hair bundles on the cell surfaces. The epidermal cells of tentacles contain connexin-positive gap junctions and mechanical stimulation results in increased gap junctional communication. This is needed for nematocyte discharge, as demonstrated by reversible inhibition of discharge upon uncoupling of gap junctions (Mire et al., 2000). Communication between cells can also result from the electrical potential generated by epithelial cells, as demonstrated in *Hydra* (Josephson and Macklin, 1967), with transmission of depolarization between cells via gap junctions. Many cnidarians exhibit bioluminescence due to light emission from photocytes that are scattered within the gastrodermis. Photocytes exhibit gap junction structures and cell–cell coupling with surrounding epithelial cells (Germain and Anctil, 1996). In the hydrozoan *Obelia geniculata*, luminescence in the photocytes is activated by gap junction-mediated, intracellular calcium signaling from adjacent supporting epithelial cells. The calcium signaling is initiated by mechanical, chemical, or electrical stimuli that activate depolarization of the plasma membrane in the epithelial cells (Dunlap et al., 1987).

6.1.3 Cell–cell interactions

Although few cell–cell adhesion molecules of cnidarians were identified definitively prior to the availability of genome sequences (see Section 6.2), functional investigations of cell–cell interactions and processes of cell sorting leading to tissue organization have been vibrant areas of research, especially with *Hydra*. Many of the major recent questions of developmental biology relating to cell sorting, the set up of morphogen gradients and the molecular identity of morphogens have been applied to *Hydra* and resulted in the identification of a crucial importance of Wnt signaling in axial patterning of the body column (Hobmayer et al., 2000; Holstein, 2008). Here, we discuss some of the publications that provide insight into the functional importance of cell–cell interactions as effectors of patterning and morphogenesis.

The *Hydra* cell dissociation and regeneration system has been used widely to trace cell–cell interactions and the sorting out of epidermal and gastrodermal cells during tissue reassembly. In initial aggregates, epidermal and gastrodermal cells are randomly located, but after 1 h cells begin to show homotypic preference, that is, epidermal cells cluster preferentially with other epidermal cells, and gastrodermal cells with other gastrodermal cells. In short-term assays, homotypic cell aggregates predominate over heterotypic clusters (Sato et al., 1992; Sato-Maeda et al., 1994; Technau and Holstein, 1992). These early stage interactions are calcium-dependent (Hobmayer et al., 2001). Quantified analysis of attachment between pairs of single cells, through use of collagenase to remove mesoglea fragments and a laser trap to manipulate two cells into contact, demonstrated preferential attachment of cells from the same tissue layer and that gastrodermal-derived cell pairs formed more stable attachments than epidermal cell pairs. By using the laser beam to detach cells from each other, the adhesive force was estimated as >50 pN between gastrodermal cells and around 27 pN between epidermal cells (Sato-Maeda et al., 1994).

Once clusters reached a size of 10–20 cells/cluster, heterotypic interactions between epidermal and gastrodermal cells contributed to establishment of heterotypic aggregates. In addition, epidermal cells preferentially spread over the surface of the gastrodermal cells (epiboly), a process that can also be demonstrated after recombination of cell layer tissue pieces (Kishimoto et al., 1996). By around 12 h after dissociation, reformation of the epidermal layer was complete (Technau and Holstein, 1992). These experiments demonstrated that organization of the cell layers of the *Hydra* body wall depend on a defined sequence of homotypic and heterotypic cell interactions, differential adhesion, and migration of epidermal cells.

During regeneration of *Hydra*, the correct reorganization of the body column depends firstly on organization of the head region. Initial experiments demonstrated that head induction in aggregates is *de novo* and not driven by cells derived originally from the head region (Technau and Holstein, 1992). The preassembly of clusters of 5–15 cells is an important prerequisite for induction of a head. This "community effect" relates to the production of Wnt morphogen within the head region. The clusters also provide cues to inhibit the induction of another head within an approximately 800 μ range (Technau et al., 2000). During formation of buds, epidermal cells widen at their bases and gastrodermal cells curve toward the epidermal cell layer, enabling evagination of the bud and temporary disruption of muscle fibers. These cell shape changes are accompanied by lateral intercalation of adjacent epithelial cells that move into the bud zone. Thus, initial evagination of the bud depends on altered cell–cell interactions in the absence of increased cell proliferation. The cell shape changes and local motility of cells from the mother polyp are driven by canonical and noncanonical Wnt signaling (Philipp et al., 2009).

6.2. Cell–cell adhesion molecules identified by biochemistry and molecular cloning

Investigations of cnidarian cell–cell adhesion molecules by biochemical or molecular cloning approaches have been less extensive than those of ECM components, likely due to the greater experimental accessibility of isolating the mesoglea. Cadherins are a prominent family of cell–cell adhesion molecules in bilaterians, which are linked intracellularly to the actin cytoskeleton by interactions of the cadherin cytoplasmic domain with catenin family proteins including β-catenin. The existence of cadherin-mediated adhesion systems in members of the phylum Cnidaria was first implicated by the homology cloning of a *H. magnipapillata* ortholog of β-catenin. In this molecule, the central armadillo repeats are highly conserved with the β-catenins of bilaterians, whereas the N- and C-terminal regions are more divergent (Hobmayer et al., 1996).

Zona occludens-1 (ZO-1) is one of the major proteins of craniate tight junctions and is important for their barrier function. A ZO-1-like protein cloned from *H. vulgaris* contains all the major domains of ZO-1 from craniates, but is distinct in having an extended region between the N-terminal PDZ domains and a longer C-terminal region. The *HZO-1* transcript is expressed throughout the epidermal cell layer, and in these cells HZO-1 protein localizes specifically to the apical region of the plasma membrane

(Fei et al., 2000). Further investigations of the function of this protein would be of great interest.

6.3. New views on cell–cell adhesion molecules in *N. vectensis* and *H. magnipapillata* from postgenomic analyses

6.3.1 Usherin

Usherin is large glycoprotein with transmembrane and basement membrane-associated ECM variants that are derived through alternative splicing. The name comes from the transmembrane variant, which is found in the ankle link complex of the stereocilia of the chordate cochlea: in humans, mutations can lead to a form of Usher syndrome, or congenital deaf/blindness. Analysis of the *N. vectensis* genome revealed a predicted protein with an identical domain organization to the transmembrane variants of human usherin (AY481573) and 49% amino acid sequence similarity (Tucker, 2010; Fig. 8.8A). The domain architecture and also the number of domains are phylogenetically conserved. The only significant differences between human and anthozoan usherin are: (1) one fewer fibronectin type III domain in *N. vectensis* usherin, and (2) a short intracellular domain in the anthozoan usherin homolog (Fig. 8.5A). Interestingly, despite this extraordinary high conservation of domain architecture between primates and cnidarians, usherin genes are not found in *C. elegans* or *Drosophila melanogaster*. Thus, usherin is an example of a gene found in the common ancestor of cnidarians and deuterostomes that was lost in ecdysozoans. Usherin transcripts and evidence of alternative splicing are found in developing and adult *N. vectensis* (Tucker, 2010) leading to the exciting possibility that usherin also links stereocilia in cnidarians, perhaps in the trigger-like mechanosensory cone of the cnidoblast. This could not, however, be confirmed by *in situ* hybridization, which revealed widespread expression in the epidermis. It is unknown if the ECM variants of usherin are associated with basement membranes in cnidarians.

6.3.2 Cadherin and protocadherin superfamily

The cadherins are a major superfamily of calcium-dependent, homotypic cell–cell adhesion molecules. Many nomenclatures are used to describe this superfamily; for clarity, the nomenclature used by Hulpiau et al. (2013) is adopted here. Classical type I cadherins (e.g., E-cadherin or cadherin-1) are transmembrane proteins with short strings of extracellular cadherin domains and an intracellular domain that can interact with β-catenin and p120 catenin. The classical type I cadherins appear to be unique to chordates.

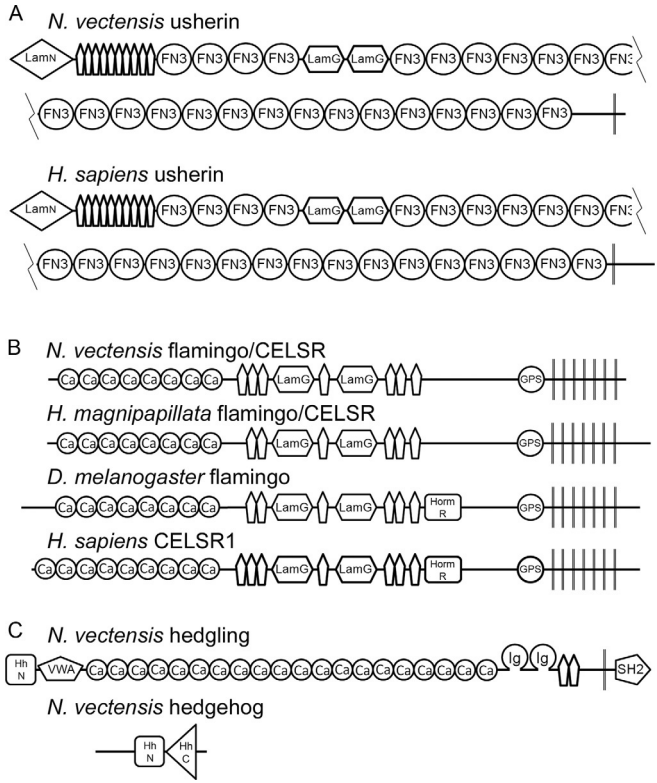

Figure 8.8 Domain architectures of some of the cell–cell adhesion molecules discussed in this chapter. (A) Schematic representations of the transmembrane protein usherin from *N. vectensis* and *Homo sapiens*. Note the remarkable similarity in the arrangement and numbers of domains. Usherin homologs are not found in *D. melanogaster* or *C. elegans*. (B) Schematic representations of flamingo/CELSR1 homologs from *N. vectensis*, *H. magnipapillata*, *D. melanogaster*, and *Homo sapiens*. In bilaterians, flamingo/CELSR1 plays an important role in dendrite development; it is highly conserved in *N. vectensis* and *Hydra*. (C) *N. vectensis* hedgling and hedgehog. Hedgling is a form of cadherin found in sponges and cnidarians that is not found in deuterostomes or protostomes. Evidence suggests that the N-terminal hedgehog domain (Hh N) of hedgling became joined with a C-terminal hedgehog domain (Hh C) to make the signaling molecule hedgehog in an early ancestral metazoan. Key: Epidermal growth factor domains are indicated by narrow pentagons, and transmembrane domains are indicated with vertical lines. Ca, cadherin domain; FN3, fibronectin type III domain; LamN, N-terminal domain; LamG, laminin G domain; GPS, GPCR proteolytic site; Horm R, diuretic hormone receptor domain; VWA, von Willebrand factor domain type A; Ig, immunoglobulin domain; SH2, src homology domain 2.

Type II cadherins are also known as atypical cadherins, and include desmocollins and desmogleins, that mediate cell–cell adhesion in desmosomes. These also appear to be specific to deuterostomes (Hulpiau and van Roy, 2009). Type I and type II cadherins are considered to belong to cadherin major branch-1. Cadherin major branch-2 includes the type III cadherins, the nonchordate metazoans' version of classical cadherins. Type III cadherins have additional features of one or more LamG domains and one or more EGF domains between the cadherin domains and the transmembrane domain (Hulpiau et al., 2013; Magie and Martindale, 2008; Nichols et al., 2012). At least three type III cadherins were identified in the genome of *N. vectensis* (Hulpiau and van Roy, 2011; Table 8.4). Termed NvCDH1-3, these huge predicted proteins have between 25 and 32 extracellular cadherin domains and two LamG domains flanked by two or three single EGF-like domains. The intracellular domains of NvCDH1 and NvCDH3 are also predicted by the domain architecture program pfam (http://pfam.sanger.ac.uk/) to have β-catenin and p120 catenin-binding

Table 8.4 Cadherin and cadherin-related proteins of *Hydra magnipapillata* and *Nematostella vectensis*, as predicted from their genomes

Species/type	Cell–cell adhesion molecule	GenBank accession number
H. magnipapillata		
Cadherin major branch-2	Flamingo/CELSR	XP_002163205
Cadherin-related branch-3	Fat-like	XP_002162352
Unique cadherin-related	Hedgling	XP_002161856
N. vectensis		
Cadherin major branch-2	NvCadherin1	XP_001631293
	NvCadherin2	XP_001641031
	NvCadherin3	XP_001638547
	Flamingo/CELSR	XP_001640300
Cadherin-related branch-1a	NvProtocadherin	XP_001637727
Cadherin-related branch-1b	NvDachsous	XP_001632533
Cadherin-related branch-3	Fat/fat-like	XP_001617773
	Fat/fat-like	XP_001633830
Unique cadherin-related	Hedgling	ABX84114

domains, demonstrating the likely conserved function of these proteins in catenin-mediated signaling. Homologs were not identified in the present version of the *H. magnipapillata* genome sequence; future analysis of the recently described transcriptome of *H. vulgaris* (Wenger and Galliot, 2013) may lead to the identification of a *Hydra* type III cadherin. Another protein family that belongs to cadherin major group-2 includes the flamingo/CELSR proteins. First identified in *D. melanogaster*, flamingo/CELSR proteins play crucial roles in regulating the branching of dendrites in both the insect and mammalian nervous systems. *N. vectensis* and *H. magnipapillata* both have flamingo/CELSR homologs, which share remarkably similar domain architecture to the proteins of flies and man (Fig. 8.7B; Table 8.4).

The superfamily also includes three branches of cadherin-related proteins. Branch 1a includes the protocadherins. These proteins feature extracellular cadherin domains, a transmembrane domain and a conserved intracellular "protocadherin" domain. Mammals have over 50 protocadherin genes that are involved in many roles, including dendritic self/nonself recognition (Lefebvre et al., 2012). Because protocadherins are missing from *D. melanogaster* and *C. elegans*, it was long assumed that they evolved together with the deuterostome lineage. However, Hulpiau and van Roy (2009) found a typical protocadherin gene in *N. vectensis* that encodes seven extracellular cadherin domains and the highly conserved protocadherin intracellular domain (Table 8.4). Thus, protocadherins, like usherins (Section 6.3.1), appear to have evolved in basal metazoans and were lost subsequently in ecdysozoans. A comparable protocadherin has yet to be identified in the current version of *H. magnipapillata*'s genome sequence.

Representatives of two other branches of cadherin-related proteins are also encoded in cnidarian genomes. *N. vectensis* has a representative of branch 1b, dachsous. Dachsous is a transmembrane protein composed of a long series of extracellular cadherin domains and an intracellular domain that contains the catenin-binding region. *N. vectensis* dachsous (Table 8.4) has 27 extracellular cadherin domains and the conserved intracellular catenin-binding region. Both *N. vectensis* and *H. magnipapillata* have homologs of the cadherin-related branch 3 protein Fat (or the related Fat-like protein; Table 8.4). Fat and Fat-like proteins are composed of long strings of extracellular cadherin domains as well as one or two LamG domains and a string of EGF-like domains. Fat and fat-like bind to dachsous, and Fat/dachsous interactions mediate cell and tissue growth through the Hippo pathway (Sharma and McNeill, 2013). The presence of a Fat-like protein in

H. magnipapillata (Table 8.4) suggests that a dachsous protein, which has not been identified in the current genome sequence, is likely to be present.

While the cadherins and cadherin-related proteins of cnidarians described above have clear homologs in other metazoa, others appear to be unique to basal metazoans. One example is hedgling (Table 8.4). This huge transmembrane protein has an N-terminal Hedge domain, a von Willebrand factor A domain, 21 cadherin domains, two Ig domains, two EGF domains, and a type 2 Src-homology (SH2) domain in its intracellular tail. A similar cadherin with fewer cadherin domains and no SH2 domain is found in the sponge *Amphimedon queenslandica* (Adamska et al., 2007). The expression of hedgling was studied in *N. vectensis* and *A. queenslandica* by *in situ* hybridization. In the former, it is found just after gastrulation in cells associated with the pigment ring, in the latter it is expressed in the developing mesenteries. Interestingly, Adamska et al. (2007) have proposed that hedgehog originated by domain shuffling of the N-terminal Hedge domain from a hedgling in an ancestor to bilaterians to become joined with the C-terminal Hog domain of a gene not unlike the Hog domain-containing genes of modern choanoflagellates. A hedgehog-encoding gene is present in *N. vectensis* (Fig. 8.8C) and in *H. magnipapillata* (XP_004207437), but hedgling, which likely regulates some aspect of cell–cell interactions in sponges and cnidarians, has been lost in eumetazoans.

Cadherin-23 is a cadherin-related protein of deuterostomes composed of 27 repeated cadherin domains, a transmembrane domain, and a short intracellular tail. As with usherin (Section 6.3.1) mutations of human cadherin-23 can result in Usher syndrome, and cadherin-23 is another component of the so-called tip complex that links stereocilia in the inner ear (Müller, 2008). Watson et al. (2008) used the cadherin-23 sequence from zebrafish to identify the most similar sequence in the *N. vectensis* genome. They identified a novel cadherin with a single Ig domain, 44 cadherin domains, and three transmembrane domains that they propose folds like a paperclip with the cadherin domains available for adhesion (Table 8.4). Antibodies to this cadherin-23-like protein stain the hair bundles that act as nematocyst triggers on the tentacles of the sea anemone *H. luciae*. Immunoelectron microscopy shows clusters of gold particles along links between the stereocilia and the inner stereocilium of the sea anemone hair bundles. This striking localization suggests that the mechanosensory organs of the chordate inner ear and cnidarian nematocysts share some of the same conserved building blocks.

The description of cadherins and cadherin-related proteins in cnidarians above is very likely to be incomplete. Hulpiau and van Roy (2009) found

13 predicted proteins in *N. vectensis* with more than one extracellular cadherin domain and a transmembrane domain, and three other incomplete sequences with long strings of extracellular cadherin domains. However, Pfam searches reveal 41 complete or incomplete predicted proteins with more than one extracellular cadherin domain in *N. vectensis*, suggesting that this superfamily may be even larger than previously reported.

6.3.3 The immunoglobulin family of cell adhesion molecules

Calcium-independent homotypic interactions between mammalian cells are frequently mediated by members of the immunoglobulin family of cell adhesion molecules, sometimes referred to simply as CAMs. These molecules have been studied mostly in chordates and include L1CAM and N-CAM, both of which are transmembrane proteins with extracellular Ig domains and fibronectin type III domains. The former also has a distinctive intracellular Bravo domain that includes the highly conserved amino acid motif FIGEY, the function of which is unknown. L1CAM, which is also known as neuroglian (in *D. melanogaster*) or simply as L1, is able to bind homophilically or heterophilically to contactin (see Section 6.3.4). These interactions are critical for normal human brain development; mutations in L1CAM can lead to mental retardation (Wei and Ryu, 2012). Mouse knock-out models indicate that homotypic cell–cell interactions mediated by N-CAMs are important for proper motor function and long-term potentiation (Becker et al., 1996).

Pfam was used to identify the representatives of these molecules in cnidarians by searching for predicted proteins encoded in the *N. vectensis* genome that include Ig domains, fibronectin type III domains, and a transmembrane domain. Predicted proteins with this domain architecture include a homolog of L1CAM/neuroglian and at least three homologs of N-CAM (Table 8.5). The N-CAM homologs include one that is most similar to N-CAM2 from *Danio rerio* (listed in Table 8.5 as N-CAM2-like) and two that are most similar to N-CAMs from *Gallus gallus*. A fourth N-CAM homolog is described by Marlow et al. (2009) with only a single Ig domain (not unlike the single N-CAM found in *H. magnipapillata*). An apparent homolog of deleted in colorectal cancer (DCC) in *N. vectensis*, with two Igs and a fibronectin type III domain, was also identified with this search. The DCC homolog in *H. magnipapillata* is yet to be identified in the current version of the genome sequence; possibly, future analysis of the transcriptome dataset of *H. vulgaris* (Wenger and Galliot, 2013) may prove

Table 8.5 Immunoglobulin family cell adhesion molecules of *Hydra magnipapillata* and *Nematostella vectensis*, as predicted from their genomes

Species	Cell–cell adhesion molecule	GenBank accession number
H. magnipapillata	L1CAM/neuroglian	XP_002165052
	Protogenin	XP_004208692
	N-CAM	XP_002160592
N. vectensis	L1CAM/neuroglian	XP_001637406
	Protogenin	XP_001633563
	N-CAM2-like	A7RYG0[a]
	N-CAM	XP_001635578
	N-CAM	XP_001635579
	DCC-like	XP_001625780

[a]UniProt ID.

fruitful. Cnidarian homologs of protogenin, a CAM present during gastrulation in the chicken embryo, were also identified (Table 8.5).

The *N. vectensis* L1CAM homolog is illustrated in Fig. 8.9A with the similar proteins from *H. magnipapillata*, *D. melanogaster*, and *Homo sapiens*. Of note is the intracellular Bravo domain, which is conserved in each of the proteins. However, the FIGEY sequence found in the Bravo domain of chordate L1CAMs is not. Expression of this CAM in cnidarians has not been studied. In contrast, the expression patterns of the *N. vectensis* N-CAMs (one is illustrated in Fig. 8.9B) were studied by whole mount in situ hybridization by Marlow et al. (2009). One of the three N-CAMs (it is unclear which one corresponds to which sequence in Table 8.5) is expressed in the epidermal cells of planulae and early polyps, though it is missing from the cells of the apical ciliary tuft. The expression of a second N-CAM, in contrast, appears to be limited to the sensory apical tuft of the planula, and to the gastrodermis of the early polyp. The third N-CAM is expressed widely, though the signal is strongest in the polyp in the vicinity of the pharynx.

6.3.4 Proteins of cell–cell junctions

Tight junctions are not found in sponges or placozoans, but are found in cnidarians. Analyses by Chapman et al. (2010) led to the identification of claudin, one of the principal homophilic interacting transmembrane

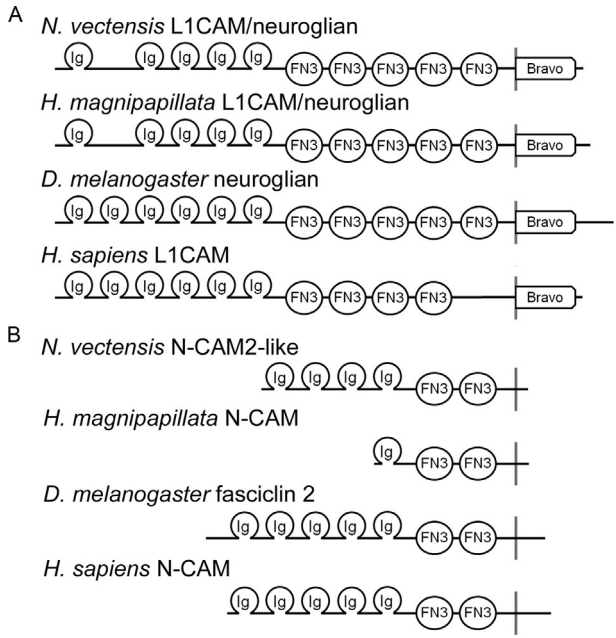

Figure 8.9 Key cell–cell adhesion molecules that are conserved between cnidarians, protostomes, and deuterostomes. Domain architectures of L1CAM (A) and N-CAM (B) homologs from *N. vectensis*, *Hydra magnipapillata*, *D. melanogaster*, and *Homo sapiens* are illustrated. Transmembrane domains are indicated with vertical lines. Bravo, Bravo FIGEY domain; FN3, fibronectin type III domain; Ig, immunoglobulin domain.

proteins found in the tight junctions of chordates, in the genomes of both *H. magnipapillata* and *N. vectensis* (Table 8.6). A second four-pass transmembrane protein found in vertebrate tight junctions, occludin, is not encoded. Chapman et al. (2010) also reported other proteins that are associated with tight junctions in these cnidarian genomes. Notably, a homolog of ZO-1 is found in both *H. magnipapillata* and *N. vectensis* genomes (see Section 6.2; Table 8.6). ZO-1 is a cytoplasmic protein related to disk large, which is found in septate junctions (see below); the N-terminal half contains PDZ domains, an SH3 domain and a guanylate kinase domain, while the C-terminal half is rich in prolines. The predicted ZO-1-like proteins from cnidarians have this same architecture, though the predicted *N. vectensis* ZO-1 protein may be missing some N-terminal sequence. The presence of ZO-1 is surprising, since ZO-1 is associated with the cytoplasmic domains of occludin in chordate tight junctions, and occludin has not been found in cnidarians. Future studies of ZO-1 binding partners in *Hydra* or *N. vectensis* may shed light on the evolution of these junctional complexes,

Table 8.6 Cell–cell junction proteins of *Hydra magnipapillata* and *Nematostella vectensis* as predicted from their genomes

Species/type	Junction protein	GenBank accession number
H. magnipapillata		
Tight junctions	Claudin	XP_002154363
	ZO-1	UPI00019264D6[a]
	Stardust/PALS1	XP_002165318
	PATJ	XP_002167180
	PAR3	XP_002165602
	PAR6	XP_004209525
Septate junctions	Neurexin	XP_002157821
	Disks large	XP_002168436
	Scribble	XP_002165472
	Coracle	XP_002160141
Gap junctions	Innexin	XP_002154796; XP_002160488; XP_002166931; XP_002170247; XP_002164746; XP_002170241; XP_002165350; XP_002155033; XP_002160898; XP_004208200
N. vectensis		
Tight junctions	Claudin	XP_001642058
	ZO-1	XP_001633912
	Stardust/PALS	XP_001625677
	PATJ	XP_001625806
	PAR3	XP_001637950
	PAR6	XP_001627416
Septate junctions	Neurexin	XP_001637897
	Gliotactin	XP_001629673
	Disks large	XP_001638123
	Scribble	XP_001625532
	Coracle	XP_001622324
Gap junctions	Innexin	XP_001623899

Adapted in part from Chapman et al. (2010).
[a]Uniprot sequence ID.

and also on potential novel interactions. Other intracellular tight junction-related proteins associated with junction assembly and cell polarity (stardust/PALS1, PATJ, PAR3, and PAR6) are also found in cnidarians (Table 8.6).

Septate junctions have been particularly well characterized in *D. melanogaster*, and interactions between the various players have been demonstrated experimentally or can be assumed because of interactions known between homologs in other species (Fig. 8.7F; Hortsch and Margolis, 2003). Heterophilic interactions between neurexin, contactin, and neuroglian (also known as L1CAM, see Section 6.3.2) are key to septate junction formation, and homologs of each of these transmembrane proteins were found to be encoded in the genomes of *H. magnipapillata* and *N. vectensis* (Chapman et al., 2010). The *H. magnipapillata* and *N. vectenis* neurexin homologs (Table 8.6) have the same overall domain organization as neurexin IV in *D. melanogaster*, though the latter also has a discoidin domain at its extracellular N-terminus that is missing from the predicted cnidarian homologs. The contactin homologs listed in the paper by Chapman et al. (2010), however, are problematic. The *H. magnipapillata* homolog (XP_002154651) does not have the characteristic contactin domain architecture, and the *N. vectensis* homolog (XP_001639008) is a partial predicted protein composed of two fibronectin type III domains. A tblastn search of cnidarian sequences with the *D. melanogaster* contactin sequence reveals the L1CAM/neuroglian homologs described earlier, but no other significant hits. A Pfam architecture search also failed to reveal a contactin in *N. vectensis*. Thus, septate junctions in cnidarians may form through interaction between neuroglian and neurexin, but might not include contactin. Interestingly, Fahey and Degnan (2010) failed to find neuroglian or neurexin homologs in the *Amphimedon* genome, suggesting that septate junctions, like tight junctions, may have evolved with the cnidarians. Another large transmembrane protein found in *Drosophila* septate junctions is gliotactin; this protein is concentrated at sites where three cells meet. The accession number for the *H. magnipapillata* homolog found in Chapman et al. (2010) has been removed from the database, but there is a clear gliotactin homolog encoded in the *N. vectensis* genome (Table 8.6). In addition to these transmembrane components of septate junctions, a number of intracellular-interacting proteins have been identified. These include coracle, which binds to the intracellular domain of neurexin IV, and scribble and disks large, which are proposed to interact with the PDZ-binding domains found in the intracellular regions of both neurexin IV and gliotactin. Partial predicted proteins with homologous domain architecture to *Drosophila* coracle are encoded

in both the *H. magnipapillata* and *N. vectensis* genomes (Table 8.6). A disks large homolog is encoded in both *H. magnipapillata* and *N. vectensis*, and a partial predicted scribble sequence and a potentially complete scribble sequence are also encoded in the *H. magnipapillata* and *N. vectensis* genomes, respectively (Table 8.6).

The gap junctions of chordates are assembled from either connexins or pannexins (Abascal and Zardoya, 2013). Connexins are specific for the chordate lineage, but pannexins (referred to as "innexins" outside the phylum Chordata) are found in most metazoans. Pfam recognizes the four-pass transmembrane domain of innexins as a distinctive domain, simplifying their identification. *Caenorhadbitis elegans* has 25 innexin genes, and *D. melanogaster* has 8. However, only one predicted protein in *N. vectensis* has an innexin domain (Chapman et al., 2010; Table 8.6). In contrast, Chapman et al. (2010) reported up to 17 innexin genes in *H. magnipapillata*. Unfortunately, only 10 of these could be confirmed at the present time (Table 8.6). The diversity of innexin genes in *H. magnipapillata* may be related to the direct contacts observed between cells of the gastrodermis and epidermis, an interaction that is not seen in *N. vectensis*. As innexins have not been found in sponges or placozoans, studies of the innexins of cnidarians may give particularly important insights into the evolution of gap junctions.

7. CONCLUSIONS AND FUTURE DIRECTIONS

Postgenomic analyses of the mesoglea, cell–matrix adhesion molecules, and cell–cell adhesion molecules of the hydrozoan *H. magnipapillata* and anthozoan *N. vectensis* reveal that there are often multiple copies of related genes in the anthozoan, whereas *Hydra* has only one. In cases where this occurs (e.g., SPARC, thrombospondins, integrins, cadherins, and N-CAM), *Hydra* may prove a more tractable model for knockout or knockdown studies of gene function. However, this is not always the case: notable exceptions are the innexins and MMPs, which are much more diverse in *H. magnipapillata* than in *N. vectensis*. It is important to note that relatively few of the predicted genes listed in the tables of this review have actually been cloned and their expression studied by *in situ* hybridization or, even more rarely, by immunohistochemistry. Given the ease with which these model cnidarians can be kept in a laboratory, and their small size and transparency, such expression studies should be completed quickly to provide the foundations for future experimental work.

Another exciting feature of the cnidarian genomes described here is the similarity between cnidarian adhesion network proteins and their homologs

in chordates: domain architecture is well-conserved, even in huge proteins such as usherin, L1CAM, and flamingo. These conserved proteins are often more similar between cnidarians and chordates than they are between chordates and protostomes, which leads us to suggest that novel insights into the functions of, and interaction between, chordate proteins will be gleaned from experimental studies of their homologs in *Hydra* and *N. vectensis*. In fact, several of the proteins described here that are found in cnidarians and chordates are not found in ecdysozoans, which also argues the case for more experimental studies with cnidarian models. Some gene families have undergone lineage-specific expansion in cnidarians: for example, both *Hydra* and *N. vectensis* encode more collagens than *D. melanogaster*. For evolutionary studies, cnidarian genomes provide a unique glimpse into the origins of many key genes: many of the genes described here appear to have evolved in an ancestral cnidarian or ctenophore (e.g., protocadherins), together with their complex musculature and nervous systems.

Ultrastructural studies of the cell junctions of *N. vectensis* should be initiated as a first step in understanding the organization of tight and septate junctions in this organism, which apparently has many of the key proteins found in these junctions in bilaterians. Localization studies on individual molecules now identified from the genome sequence, combined with *in vitro* studies of protein-protein interactions, are likely to yield significant information about the development and maintenance of junctional complexes in metazoans.

A number of elegant studies have been published on the matrix proteases of *Hydra*, but postgenomic analyses reveal numerous novel proteases. Identifying the targets of these proteases should prove interesting and might provide insight into matrix remodeling more widely. The available methods to generate *Hydra* transgenics will be important for reaching these goals.

Historically, as discussed in this article, jellyfish have been widely used as experimental models; however, at present, a genome sequence from a cubozoan, scyphozoan, or even a hydrozoan with a medusoid form, is lacking. This information will be important for further understanding the evolution of phylum Cnidaria and is also needed to provide insight in the molecules that underpin the medusa body form and the more complex life cycles of these classes of cnidarians. A first step is the ongoing EST and genome project for *Clytia hemisphaerica*, a hydrozoan that has medusa and polyp stages in its life cycle (Houliston et al., 2010).

The great conservation of adhesion proteins between cnidarians and mammals, and the advantages of cnidarians for laboratory experiments, also

makes them attractive as models for studying cellular and molecular mechanisms of epithelial tissue organization, stem cell niches, regeneration, or the role of ECM in human disease. For example, effects of high glucose on basement membrane thickening, a frequent pathological complication in diabetic patients, have been examined in the *Hydra* aggregation system (Zhang et al., 1990). In tissue engineering there is a major need for xeno-free preparations of fibrillar collagen that has prompted evaluation of jellyfish collagen for prospective biomedical use (Addad et al., 2011). With these expanding frontiers, and all the benefits arising from knowledge of cnidarian genome sequences, we anticipate further growth of research interest in cnidarians.

ACKNOWLEDGMENT

We thank Suat Özbek for helpful comments.

REFERENCES

Abascal, F., Zardoya, R., 2013. Evolutionary analyses of gap junction protein families. Biochim. Biophys. Acta 1828, 4–14.

Adams, J.C., Lawler, J., 2011. The thrombospondins. In: Hynes, R.O., Yamada, K.M. (Eds.), Extracellular Matrix Biology. Cold Spring Harbor Laboratory Press, Cold Spring Harbor, NY, pp. 99–127.

Adamska, M., Matus, D.Q., Adamski, M., Green, K., Rokhsar, D.S., Martindale, M.Q., Degnan, B.M., 2007. The evolutionary origin of hedgehog proteins. Curr. Biol. 17, R836–R837.

Addad, S., Exposito, J.Y., Faye, C., Ricard-Blum, S., Lethias, C., 2011. Isolation, characterization and biological evaluation of jellyfish collagen for use in biomedical applications. Mar. Drugs 9, 967–983.

Ağbaş, A., Sarras Jr., M.P., 1994. Evidence for cell surface extracellular matrix binding proteins in *Hydra vulgaris*. Cell Adhes. Commun. 2, 59–73.

Alexander, R. McN, 1964. Visco-elastic properties of the mesogloea of jellyfish. J. Exp. Biol. 41, 363–369.

Anton-Erxleben, F., Thomas, A., Wittlieb, J., Fraune, S., Bosch, T.C., 2009. Plasticity of epithelial cell shape in response to upstream signals: a whole-organism study using transgenic Hydra. Zoology (Jena) 112, 185–194.

Aufschnaiter, R., Zamir, E.A., Little, C.D., Özbek, S., Münder, S., David, C.N., Li, L., Sarras Jr., M.P., Zhang, X., 2011. In vivo imaging of basement membrane movement: ECM patterning shapes *Hydra* polyps. J. Cell Sci. 124, 4027–4038.

Balasubramanian, P.G., Beckmann, A., Warnken, U., Schnölzer, M., Schüler, A., Bornberg-Bauer, E., Holstein, T.W., Ozbek, S., 2012. Proteome of *Hydra* nematocyst. J. Biol. Chem. 287, 9672–9681.

Banerjee, S., Sousa, A.D., Bhat, M.A., 2006. Organization and function of septate junctions: an evolutionary perspective. Cell Biochem. Biophys. 46, 65–77.

Barzansky, B., Lenhoff, H.M., Bode, H., 1975. *Hydra* mesoglea: similarity of its amino acid and neutral sugar composition to that of vertebrate basal lamina. Comp. Biochem. Physiol. B 50, 419–424.

Becker, C.G., Artola, A., Gerardy-Schahn, R., Becker, T., Welzl, H., Schachner, M., 1996. The polysialic acid modification of the neural cell adhesion molecule is involved in spatial learning and hippocampal long-term potentiation. J. Neurosci. Res. 45, 143–152.
Beigel-Heuwinkel, U., 1982. Helical fibrils in the mesoglea of a hydropolyp. Tissue Cell 14, 225–230.
Bentley, A.A., Adams, J.C., 2010. The evolution of thrombospondins and their ligand-binding activities. Mol. Biol. Evol. 27, 2187–2197.
Bibb, C., Campbell, R.D., 1973. Tissue healing and septate desmosome formation in hydra. Tissue Cell 5, 23–35.
Bode, H.R., 1996. The interstitial cell lineage of hydra: a stem cell system that arose early in evolution. J. Cell Sci. 109, 1155–1164.
Böttger, A., Doxey, A.C., Hess, M.W., Pfaller, K., Salvenmoser, W., Deutzmann, R., Geissner, A., Pauly, B., Altstätter, J., Münder, S., Heim, A., Gabius, H.J., McConkey, B.J., David, C.N., 2012. Horizontal gene transfer contributed to the evolution of extracellular surface structures: the freshwater polyp hydra is covered by a complex fibrous cuticle containing glycosaminoglycans and proteins of the ppod and swt (sweet tooth) families. PLoS One 7, e52278.
Bouillon, J., Coppois, G., 1977. Comparative-study of mesoglea of cnidarians. Cah. Biol. Mar. 18, 339–368.
Bradshaw, A.D., 2012. Diverse biological functions of the SPARC family of proteins. Int. J. Biochem. Cell Biol. 44, 480–488.
Brew, K., Nagase, H., 2010. The tissue inhibitors of metalloproteinases (TIMPs): an ancient family with structural and functional diversity. Biochim. Biophys. Acta 1803, 55–71.
Bridge, D., Cunningham, C.W., Schierwater, B., DeSalle, R., Buss, L.W., 1992. Class-level relationships in the phylum Cnidaria: evidence from mitochondrial genome structure. Proc. Natl. Acad. Sci. U. S. A. 89, 8750–8753.
Brower, D.L., Brower, S.M., Hayward, D.C., Ball, E.E., 1997. Molecular evolution of integrins: genes encoding integrin beta subunits from a coral and a sponge. Proc. Natl. Acad. Sci. U. S. A. 94, 9182–9187.
Calejo, M.T., Morais, Z.B., Fernandes, A.I., 2009. Isolation and biochemical characterisation of a novel collagen from *Catostylus tagi*. J. Biomater. Sci. Polym. Ed. 20, 2073–2087.
Cartwright, P., Halgedahl, S.L., Hendricks, J.R., Jarrard, R.D., Marques, A.C., Collins, A.G., Lieberman, B.S., 2007. Exceptionally preserved jellyfishes from the middle Cambrian. PLoS One 2, e1121.
Chakravarti, R., Adams, J.C., 2006. Comparative genomics of the syndecans defines an ancestral genomic context associated with matrilins in vertebrates. BMC Genomics 7, 83.
Chapman, G., 1953. Studies of the mesoglea of coelenterates. 1. Histology and chemical properties. Q. J. Microsc. Sci. 94, 155–176.
Chapman, J.A., Kirkness, E.F., Simakov, O., Hampson, S.E., Mitros, T., Weinmaier, T., Rattei, T., Balasubramanian, P.G., Borman, J., Busam, D., Disbennet, K., Pfannkoch, C., Sumin, N., Sutton, G.G., Viswanathan, L.D., Walenz, B., Goodstein, D.M., Hellsten, U., Kawashima, T., Prochnik, S.E., Putnam, N.H., Shu, S., Blumberg, B., Dana, C.E., Gee, L., Kibler, D.F., Law, L., Lindgens, D., Martinez, D.E., Peng, J., Wigge, P.A., Bertulat, B., Guder, C., Nakamura, Y., Ozbek, S., Watanabe, H., Khalturin, K., Hemmrich, G., Franke, A., Augustin, R., Fraune, S., Hayakawa, E., Hayakawa, S., Hirose, M., Hwang, J.S., Ikeo, K., Nishimiya-Fujisawa, C., Ogura, A., Takahashi, T., Steinmetz, P.R., Zhang, X., Aufschnaiter, R., Eder, M.K., Gorny, A.K., Salvenmoser, W., Heimberg, A.M., Wheeler, B.M., Peterson, K.J., Böttger, A., Tischler, P., Wolf, A., Gojobori, T., Remington, K.A., Strausberg, R.L., Venter, J.C., Technau, U., Hobmayer, B., Bosch, T.C., Holstein, T.W., Fujisawa, T., Bode, H.R., David, C.N., Rokhsar, D.S., Steele, R.E., 2010. The dynamic genome of Hydra. Nature 464, 592–596.

Collins, A.G., Schuchert, P., Marques, A.C., Jankowski, T., Medina, M., Schierwater, B., 2006. Medusozoan phylogeny and character evolution clarified by new large and small subunit rDNA data and an assessment of the utility of phylogenetic mixture models. Syst. Biol. 55, 97–115.

Couchman, J.R., 2010. Transmembrane signaling proteoglycans. Annu. Rev. Cell Dev. Biol. 26, 89–114.

Darling, J.A., Reitzel, A.R., Burton, P.M., Mazza, M.E., Ryan, J.F., Sullivan, J.C., Finnerty, J.R., 2005. Rising starlet: the starlet sea anemone, *Nematostella vectensis*. Bioessays 27, 211–221.

David, C.N., Ozbek, S., Adamczyk, P., Meier, S., Pauly, B., Chapman, J., Hwang, J.S., Gojobori, T., Holstein, T.W., 2008. Evolution of complex structures: minicollagens shape the cnidarian nematocyst. Trends Genet. 24, 431–438.

Davis, L.E., 1975. Histological and ultrastructural studies of the basal disk of Hydra. III. The gastrodermis and the mesoglea. Cell Tissue Res. 162, 107–118.

Davis, L.E., Haynes, J.F., 1968. An ultrastructural examination of the mesoglea of Hydra. Z. Zellforsch. Mikrosk. Anat. 92, 149–158.

Day, R.M., Lenhoff, H.M., 1981. *Hydra* mesoglea: a model for investigating epithelial cell-basement membrane interactions. Science 211, 291–294.

DeMont, M.E., Gosline, J.M., 1988. Mechanics of jet propulsion in the hydromedusan jellyfish, *Polyorchis penicillatus*. II. Energetics of the jet cycle. J. Exp. Biol. 134, 333–345.

Deutzmann, R., Fowler, S., Zhang, X., Boone, K., Dexter, S., Boot-Handford, R.P., Rachel, R., Sarras Jr., M.P., 2000. Molecular, biochemical and functional analysis of a novel and developmentally important fibrillar collagen (Hcol-I) in hydra. Development 127, 4669–4680.

Dunlap, K., Takeda, K., Brehm, P., 1987. Activation of a calcium-dependent photoprotein by chemical signalling through gap junctions. Nature 325, 60–62.

Exposito, J.Y., Larroux, C., Cluzel, C., Valcourt, U., Lethias, C., Degnan, B.M., 2008. Demosponge and sea anemone fibrillar collagen diversity reveals the early emergence of A/C clades and the maintenance of the modular structure of type V/XI collagens from sponge to human. J. Biol. Chem. 283, 28226–28235.

Fahey, B., Degnan, B.M., 2010. Origin of animal epithelia: insights from the sponge genome. Evol. Dev. 12, 601–617.

Fei, K., Yan, L., Zhang, J., Sarras Jr., M.P., 2000. Molecular and biological characterization of a zonula occludens-1 homologue in *Hydra vulgaris*, named HZO-1. Dev. Genes Evol. 210, 611–616.

Filshie, B.K., Flower, N.E., 1977. Junctional structures in hydra. J. Cell Sci. 23, 151–172.

Fowler, S.J., Jose, S., Zhang, X., Deutzmann, R., Sarras Jr., M.P., Boot-Handford, R.P., 2000. Characterization of hydra type IV collagen. Type IV collagen is essential for head regeneration and its expression is up-regulated upon exposure to glucose. J. Biol. Chem. 275, 39589–39599.

Frank, U., Rinkevich, B., 1999. Scyphozoan jellyfish's mesoglea supports attachment, spreading and migration of anthozoans' cells in vitro. Cell Biol. Int. 23, 307–311.

Fraser, S.E., Bode, H.R., 1981. Epithelial cells of *Hydra* are dye-coupled. Nature 294, 356–358.

Fraser, S.E., Green, C.R., Bode, H.R., Gilula, N.B., 1987. Selective disruption of gap junctional communication interferes with a patterning process in hydra. Science 237, 49–55.

Fritzenwanker, J.H., Technau, U., 2002. Induction of gametogenesis in the basal cnidarian *Nematostella vectensis* (Anthozoa). Dev. Genes Evol. 212, 99–103.

Galliot, B., 2012. Hydra, a fruitful model system for 270 years. Int. J. Dev. Biol. 56, 411–423.

Galliot, B., Chera, S., 2010. The *Hydra* model: disclosing an apoptosis-driven generator of Wnt-based regeneration. Trends Cell Biol. 20, 514–523.

Gambini, C., Abou, B., Ponton, A., Cornelissen, A.J., 2012. Micro- and macrorheology of jellyfish extracellular matrix. Biophys. J. 102, 1–9.
Germain, G., Anctil, M., 1996. Evidence for intercellular coupling and connexin-like protein in the luminescent endoderm of *Renilla koellikeri* (Cnidaria, Anthozoa). Biol. Bull. 191, 353–366.
Gladfelter, W.G., 1972. Structure and function of the locomotory system of the Scyphomedusa *Cyanea capillata*. Mar. Biol. 14, 150–160.
Green, C.R., Flower, N.E., 1980. Two new septate junctions in the phylum Coelenterata. J. Cell Sci. 142, 43–59.
Hand, A.R., Gobel, S., 1972. The structural organization of the septate and gap junctions of Hydra. J. Cell Biol. 152, 397–408.
Hand, C., Uhlinger, K.R., 1992. The culture, sexual and asexual reproduction, and growth of the sea anemone *Nematostella vectensis*. Biol. Bull. 182, 169–176.
Haynes, J.F., Burnett, A.L., Davis, L.E., 1968. Histological and ultrastructural study of the muscular and nervous systems in *Hydra*. I. The muscular system and the mesoglea. J. Exp. Zool. 167, 283–293.
Helman, Y., Natale, F., Sherrell, R.M., Lavigne, M., Starovoytov, V., Gorbunov, M.Y., Falkowski, P.G., 2008. Extracellular matrix production and calcium carbonate precipitation by coral cells in vitro. Proc. Natl. Acad. Sci. U. S. A. 105, 54–58.
Hess, A., Cohen, A.I., Robson, E.A., 1957. Observations on the structure of hydra as seen with the electron and light microscopes. Q. J. Microsc. Sci. 98, 315–326.
Hobmayer, E., Hatta, M., Fischer, R., Fujisawa, T., Holstein, T.W., Sugiyama, T., 1996. Identification of a *Hydra* homologue of the beta-catenin/plakoglobin/armadillo gene family. Gene 172, 155–159.
Hobmayer, B., Rentzsch, F., Kuhn, K., Happel, C.M., von Laue, C.C., Snyder, P., Rothbächer, U., Holstein, T.W., 2000. WNT signalling molecules act in axis formation in the diploblastic metazoan Hydra. Nature 407, 186–189.
Hobmayer, B., Snyder, P., Alt, D., Happel, C.M., Holstein, T.W., 2001. Quantitative analysis of epithelial cell aggregation in the simple metazoan Hydra reveals a switch from homotypic to heterotypic cell interactions. Cell Tissue Res. 304, 147–157.
Holley, M.C., 1985. Changes in the distribution of filament-containing septate junctions as coelenterate myoepithelial cells change shape. Tissue Cell 17, 1–11.
Holstein, T.W., 2008. Wnt signaling in cnidarians. Methods Mol. Biol. 469, 47–54.
Hopkins, D.R., Keles, S., Greenspan, D.S., 2007. The bone morphogenetic protein 1/Tolloid-like metalloproteinases. Matrix Biol. 26, 508–523.
Hortsch, M., Margolis, B., 2003. Septate and paranodal junctions: kissing cousins. Trends Cell Biol. 13, 557–561.
Houliston, E., Momose, T., Manuel, M., 2010. *Clytia hemisphaerica*: a jellyfish cousin joins the laboratory. Trends Genet. 26, 159–167.
Hulpiau, P., van Roy, F., 2009. Molecular evolution of the cadherin superfamily. Int. J. Biochem. Cell Biol. 41, 349–369.
Hulpiau, P., van Roy, F., 2011. New insights into the evolution of metazoan cadherins. Mol. Biol. Evol. 28, 647–657.
Hulpiau, P., Gul, I.S., van Roy, F., 2013. New insights into the evolution of metazoan cadherins and catenins. Prog. Mol. Biol. Transl. Sci. 116, 71–94.
Iguchi, A., Márquez, L.M., Knack, B., Shinzato, C., van Oppen, M.J., Willis, B.L., Hardie, K., Catmull, J., Miller, D.J., 2007. Apparent involvement of a beta1 type integrin in coral fertilization. Mar. Biotechnol. (NY) 9, 760–765.
Iguchi, A., Shinzato, C., Forêt, S., Miller, D.J., 2011. Identification of fast-evolving genes in the scleractinian coral Acropora using comparative EST analysis. PLoS One 6, e20140.
Josephson, R.K., Macklin, M., 1967. Transepithelial potentials in Hydra. Science 156, 1629–1631.

Kachar, B., Christakis, N.A., Reese, T.S., Lane, N.J., 1986. The intramembrane structure of septate junctions based on direct freezing. J. Cell Sci. 80, 13–28.
Katzman, R.L., Kang, A.H., 1972. The presence of fucose, mannose, and glucosamine-containing heteropolysaccharide in collagen from the sea anemone *Metridium dianthus*. J. Biol. Chem. 247, 5486–5489.
Khan, A.A., Janke, A., Shimokawa, T., Zhang, H., 2011. Phylogenetic analysis of kindlins suggests subfunctionalization of an ancestral unduplicated kindlin into three paralogs in vertebrates. Evol. Bioinform. Online 7, 7–19.
Kishimoto, Y., Murate, M., Sugiyama, T., 1996. Hydra regeneration from recombined ectodermal and endodermal tissue. I. Epibolic ectodermal spreading is driven by cell intercalation. J. Cell Sci. 109, 763–772.
Knack, B.A., Iguchi, A., Shinzato, C., Hayward, D.C., Ball, E.E., Miller, D.J., 2008. Unexpected diversity of cnidarian integrins: expression during coral gastrulation. BMC Evol. Biol. 8, 136.
Koehler, A., Desser, S., Chang, B., MacDonald, J., Tepass, U., Ringuette, M., 2009. Molecular evolution of SPARC: absence of the acidic module and expression in the endoderm of the starlet sea anemone, *Nematostella vectensis*. Dev. Genes Evol. 219, 509–521.
Kumpfmuller, G., Rybakine, V., Takahashi, T., Fujisawa, T., Bosch, T.C., 1999. Identification of an astacin matrix metalloprotease as target gene for Hydra foot activator peptides. Dev. Genes Evol. 209, 601–607.
Künzel, T., Heiermann, R., Frank, U., Müller, W., Tilmann, W., Bause, M., Nonn, A., Helling, M., Schwarz, R.S., Plickert, G., 2010. Migration and differentiation potential of stem cells in the cnidarian *Hydractinia* analysed in eGFP-transgenic animals and chimeras. Dev. Biol. 348, 120–129.
Lefebvre, J.L., Kostadinov, D., Chen, W.V., Maniatis, T., Sanes, J.R., 2012. Protocadherins mediate dendritic self-avoidance in the mammalian nervous system. Nature 488, 517–521.
Lenhoff, H.M., 1983. Hydra: Research Methods. Plenum Press, New York, NY, 463 p.
Leontovich, A.A., Zhang, J., Shimokawa, K., Nagase, H., Sarras Jr., M.P., 2000. A novel hydra matrix metalloproteinase (HMMP) functions in extracellular matrix degradation, morphogenesis and the maintenance of differentiated cells in the foot process. Development 127, 907–920.
Leung, F., Soosaipillai, A., Kulasingam, V., Diamandis, E.P., 2012. CUB and zona pellucida-like domain-containing protein 1 (CUZD1): a novel serological biomarker for ovarian cancer. Clin. Biochem. 45, 1543–1546.
Magie, C.R., Martindale, M.Q., 2008. Cell-cell adhesion in the cnidaria: insights into the evolution of tissue morphogenesis. Biol. Bull. 214, 218–232.
Marlow, H.Q., Srivastava, M., Matus, D.Q., Rokhsar, D., Martindale, M.Q., 2009. Anatomy and development of the nervous system of *Nematostella vectensis*, an anthozoan cnidarian. Dev. Neurobiol. 69, 235–254.
Matveev, I.V., Shaposhnikova, T.G., Podgornaya, O.I., 2007. A novel *Aurelia aurita* protein mesoglein contains DSL and ZP domains. Gene 399, 20–25.
Megill, W.M., Gosline, J.M., Blake, R.W., 2005. The modulus of elasticity of fibrillin-containing elastic fibres in the mesoglea of the hydromedusa *Polyorchis penicillatus*. J. Exp. Biol. 208, 3819–3834.
Meyer, E., Aglyamova, G.V., Wang, S., Buchanan-Carter, J., Abrego, D., Colbourne, J.K., Willis, B.L., Matz, M.V., 2009. Sequencing and de novo analysis of a coral larval transcriptome using 454 GSFlx. BMC Genomics 10, 219.
Miljkovic-Licina, M., Gauchat, D., Galliot, B., 2004. Neuronal evolution: analysis of regulatory genes in a first-evolved nervous system, the hydra nervous system. Biosystems 76, 75–87.
Mire, P., Nasse, J., Venable-Thibodeaux, S., 2000. Gap junctional communication in the vibration-sensitive response of sea anemones. Hear. Res. 144, 109–123.

Miura, S., Kimura, S., 1985. Jellyfish mesogloea collagen. Characterization of molecules as alpha 1 alpha 2 alpha 3 heterotrimers. J. Biol. Chem. 260, 15352–15356.
Mosher, D.F., Adams, J.C., 2012. Adhesion-modulating/matricellular ECM protein families: a structural, functional and evolutionary appraisal. Matrix Biol. 31, 155–161.
Moya, A., Huisman, L., Ball, E.E., Hayward, D.C., Grasso, L.C., Chua, C.M., Woo, H.N., Gattuso, J.P., Forêt, S., Miller, D.J., 2012. Whole transcriptome analysis of the coral *Acropora millepora* reveals complex responses to CO_2-driven acidification during the initiation of calcification. Mol. Ecol. 21, 2440–2454.
Müller, U., 2008. Cadherins and mechanotransduction by hair cells. Curr. Opin. Cell Biol. 20, 557–566.
Nichols, S.A., Roberts, B.W., Richter, D.J., Fairclough, S.R., King, N., 2012. Origin of metazoan cadherin diversity and the antiquity of the classical cadherin/β-catenin complex. Proc. Natl. Acad. Sci. U. S. A. 109, 13046–13051.
Nishimiya-Fujisawa, C., Kobayashi, S., 2012. Germline stem cells and sex determination in Hydra. Int. J. Dev. Biol. 56, 499–508.
Nordwig, A., Nowack, H., Hieber-Rogall, E., 1973. Sea anemone collagen: further evidence for the existence of only one α-chain type. J. Mol. Evol. 2, 175–180.
Nowack, H., Nordwig, A., 1974. Sea-anemone collagen: isolation and characterization of the cyanogen-bromide peptides. Eur. J. Biochem. 45, 333–342.
Özbek, S., 2011. The cnidarian nematocyst: a miniature extracellular matrix within a secretory vesicle. Protoplasma 248, 635–640.
Özbek, S., Balasubramanian, P.G., Chiquet-Ehrismann, R., Tucker, R.P., Adams, J.C., 2010. The evolution of extracellular matrix. Mol. Biol. Cell 21, 4300–4305.
Pan, T., Gröger, H., Schmid, V., Spring, J., 1998. A toxin homology domain in an astacin-like metalloproteinase of the jellyfish Podocoryne carnea with a dual role in digestion and development. Dev. Genes Evol. 208, 259–266.
Passano, L.M., McCullough, C.B., 1965. Co-ordinating systems and behaviour in Hydra. II. The rhythmic potential system. J. Exp. Biol. 42, 205–231.
Philipp, I., Aufschnaiter, R., Ozbek, S., Pontasch, S., Jenewein, M., Watanabe, H., Rentzsch, F., Holstein, T.W., Hobmayer, B., 2009. Wnt/beta-catenin and non-canonical Wnt signaling interact in tissue evagination in the simple eumetazoan Hydra. Proc. Natl. Acad. Sci. U. S. A. 106, 4290–4295.
Polato, N.R., Vera, J.C., Baums, I.B., 2011. Gene discovery in the threatened elkhorn coral: 454 sequencing of the *Acropora palmata* transcriptome. PLoS One 6, e28634.
Putnam, N.H., Srivastava, M., Hellsten, U., Dirks, B., Chapman, J., Salamov, A., Terry, A., Shapiro, H., Lindquist, E., Kapitonov, V.V., Jurka, J., Genikhovich, G., Grigoriev, I.V., Lucas, S.M., Steele, R.E., Finnerty, J.R., Technau, U., Martindale, M.Q., Rokhsar, D.S., 2007. Sea anemone genome reveals ancestral eumetazoan gene repertoire and genomic organization. Science 317, 86–94.
Rantala, J.K., Pouwels, J., Pellinen, T., Veltel, S., Laasola, P., Mattila, E., Potter, C.S., Duffy, T., Sundberg, J.P., Kallioniemi, O., Askari, J.A., Humphries, M.J., Parsons, M., Salmi, M., Ivaska, J., 2011. SHARPIN is an endogenous inhibitor of β1-integrin activation. Nat. Cell Biol. 13, 1315–1324.
Reber-Müller, S., Spissinger, T., Schuchert, P., Spring, J., Schmid, V., 1995. An extracellular matrix protein of jellyfish homologous to mammalian fibrillins forms different fibrils depending on the life stage of the animal. Dev. Biol. 169, 662–672.
Reber-Müller, S., Studer, R., Muller, P., Yanze, N., Schmid, V., 2001. Integrin and talin in the jellyfish *Podocoryne carnea*. Cell Biol. Int. 25, 753–769.
Risher, W.C., Eroglu, C., 2012. Thrombospondins as key regulators of synaptogenesis in the central nervous system. Matrix Biol. 31, 170–177.
Robertson, I., Jensen, S., Handford, P., 2011. TB domain proteins: evolutionary insights into the multifaceted roles of fibrillins and LTBPs. Biochem. J. 433, 263–276.

Ryan, J.F., Mazza, M.E., Pang, K., Matus, D.Q., Baxevanis, A.D., Martindale, M.Q., Finnerty, J.R., 2007. Pre-bilaterian origins of the Hox cluster and the Hox code: evidence from the sea anemone, *Nematostella vectensis*. PLoS One 2, e153.

Sarras Jr., M.P., Madden, M.E., Zhang, X.M., Gunwar, S., Huff, J.K., Hudson, B.G., 1991a. Extracellular matrix (mesoglea) of *Hydra vulgaris*. I. Isolation and characterization. Dev. Biol. 148, 481–494.

Sarras Jr., M.P., Meador, D., Zhang, X.M., 1991b. Extracellular matrix (mesoglea) of *Hydra vulgaris*. II. Influence of collagen and proteoglycan components on head regeneration. Dev. Biol. 148, 495–500.

Sarras Jr., M.P., Zhang, X., Huff, J.K., Accavitti, M.A., St. John, P.L., Abrahamson, D.R., 1993. Extracellular matrix (mesoglea) of *Hydra vulgaris* III. Formation and function during morphogenesis of hydra cell aggregates. Dev. Biol. 157, 383–398.

Sarras Jr., M.P., Yan, L., Grens, A., Zhang, X., Agbas, A., Huff, J.K., St. John, P.L., Abrahamson, D.R., 1994. Cloning and biological function of laminin in *Hydra vulgaris*. Dev. Biol. 164, 312–324.

Sarras Jr., M.P., Yan, L., Leontovich, A., Zhang, J.S., 2002. Structure, expression, and developmental function of early divergent forms of metalloproteinases in hydra. Cell Res. 12, 163–176.

Sato, M., Tashiro, H., Oikawa, A., Sawada, Y., 1992. Patterning in hydra cell aggregates without the sorting of cells from different axial origins. Dev. Biol. 151, 111–116.

Sato-Maeda, M., Uchida, M., Graner, F., Tashiro, H., 1994. Quantitative evaluation of tissue-specific cell adhesion at the level of a single cell pair. Dev. Biol. 162, 77–84.

Schwarz, R.S., Hodes-Villamar, L., Fitzpatrick, K.A., Fain, M.G., Hughes, A.L., Cadavid, L.F., 2007. A gene family of putative immune recognition molecules in the hydroid Hydractinia. Immunogenetics 59, 233–246.

Segade, F., 2010. Molecular evolution of the fibulins: implications on the functionality of the elastic fibulins. Gene 464, 17–31.

Sharma, P., McNeill, H., 2013. Fat and dachsous cadherins. Prog. Mol. Biol. Transl. Sci. 116, 215–235.

Shimizu, H., Fujisawa, T., 2003. Peduncle of Hydra and the heart of higher organisms share a common ancestral origin. Genesis 36, 182–186.

Shimizu, H., Sawada, Y., Sugiyama, T., 1993. Minimum tissue size required for hydra regeneration. Dev. Biol. 155, 287–296.

Shimizu, H., Zhang, X., Zhang, J., Leontovich, A., Fei, K., Yan, L., Sarras Jr., M.P., 2002. Epithelial morphogenesis in hydra requires de novo expression of extracellular matrix components and matrix metalloproteinases. Development 129, 1521–1532.

Shimizu, H., Aufschnaiter, R., Li, L., Sarras Jr., M.P., Borza, D.B., Abrahamson, D.R., Sado, Y., Zhang, X., 2008. The extracellular matrix of hydra is a porous sheet and contains type IV collagen. Zoology (Jena) 111, 410–418, Erratum in: Zoology (Jena) 2009, 112, 76.

Shinzato, C., Shoguchi, E., Kawashima, T., Hamada, M., Hisata, K., Tanaka, M., Fujie, M., Fujiwara, M., Koyanagi, R., Ikuta, T., Fujiyama, A., Miller, D.J., Satoh, N., 2011. Using the *Acropora digitifera* genome to understand coral responses to environmental change. Nature 476, 320–323.

Siebert, S., Robinson, M.D., Tintori, S.C., Goetz, F., Helm, R.R., Smith, S.A., Shaner, N., Haddock, S.H., Dunn, C.W., 2011. Differential gene expression in the siphonophore *Nanomia bijuga* (Cnidaria) assessed with multiple next-generation sequencing workflows. PLoS One 6, e22953.

Soza-Ried, J., Hotz-Wagenblatt, A., Glatting, K.H., del Val, C., Fellenberg, K., Bode, H.R., Frank, U., Hoheisel, J.D., Frohme, M., 2010. The transcriptome of the colonial marine hydroid *Hydractinia echinata*. FEBS J. 277, 197–209.

Stanton, H., Melrose, J., Little, C.B., Fosang, A.J., 2011. Proteoglycan degradation by the ADAMTS family of proteinases. Biochim. Biophys. Acta 1812, 1616–1629.

Steele, R.E., 2012. The Hydra genome: insights, puzzles and opportunities for developmental biologists. Int. J. Dev. Biol. 56, 535–542.
Steele, R.E., David, C.N., Technau, U., 2011. A genomic view of 500 million years of cnidarian evolution. Trends Genet. 27, 7–13.
Sun, J., Chen, Q., Lun, J.C., Xu, J., Qiu, J.W., 2013. PcarnBase: development of a transcriptomic database for the brain coral *Platygyra carnosus*. Mar. Biotechnol. (NY) 15, 244–251.
Sweetwyne, M.T., Murphy-Ullrich, J.E., 2012. Thrombospondin1 in tissue repair and fibrosis: TGF-β-dependent and independent mechanisms. Matrix Biol. 31, 178–186.
Technau, U., Holstein, T.W., 1992. Cell sorting during the regeneration of Hydra from reaggregated cells. Dev. Biol. 15, 117–127.
Technau, U., Cramer von Laue, C., Rentzsch, F., Luft, S., Hobmayer, B., Bode, H.R., Holstein, T.W., 2000. Parameters of self-organization in Hydra aggregates. Proc. Natl. Acad. Sci. U. S. A. 97, 12127–12131.
Tillet-Barret, E., Franc, J.M., Franc, S., Garrone, R., 1992. Characterization of heterotrimeric collagen molecules in a sea-pen (Cnidaria, Octocorallia). Eur. J. Biochem. 203, 179–184.
Tucker, R.P., 2004. The thrombospondin type 1 repeat superfamily. Int. J. Biochem. Cell Biol. 36, 969–974.
Tucker, R.P., 2010. Expression of usherin in the anthozoan *Nematostella vectensis*. Biol. Bull. 218, 105–112.
Tucker, R.P., Chiquet-Ehrismann, R., 2009. Evidence for the evolution of tenascin and fibronectin early in the chordate lineage. Int. J. Biochem. Cell Biol. 41, 424–434.
Tucker, R.P., Shibata, B., Blankenship, T.N., 2011. Ultrastructural analysis of the mesoglea of the sea anemone *Nematostella vectensis* (Edwardsiidae). Invertebr. Biol. 130, 11–24.
Tucker, R.P., Hess, J.F., Gong, Q., Garvey, K., Shibata, B., Adams, J.C., 2013. A thrombospondin in the anthozoan *Nematostella vectensis* is associated with the nervous system and upregulated during regeneration. Biol. Open 2, 217–226.
Watson, G.M., Pham, L., Graugnard, E.M., Mire, P., 2008. Cadherin 23-like polypeptide in hair bundle mechanoreceptors of sea anemones. J. Comp. Physiol. A Neuroethol. Sens. Neural. Behav. Physiol. 194, 811–820.
Weber, C., Schmid, V., 1984. The influence of extracellular matrix on reversible gap junction formation in vitro. Exp. Cell Res. 155, 153–162.
Weber, C., Schmid, V., 1985. The fibrous system in the extracellular matrix of hydromedusae. Tissue Cell 17, 811–822.
Wei, C.H., Ryu, S.E., 2012. Homophilic interaction of the L1 family of cell adhesion molecules. Exp. Mol. Med. 44, 413–423.
Wenger, Y., Galliot, B., 2013. RNAseq versus genome-predicted transcriptomes: a large population of novel transcripts identified in an Illumina-454 *Hydra* transcriptome. BMC Genomics 14, 204.
Werner, B., Cutress, C.E., Studebaker, J.P., 1971. Life cycle of *Tripedalla cystophora* Conant (Cubomedusae). Nature 232, 582–583.
Wiener, J., Spiro, D., Loewenstein, W.B., 1964. Studies on an epithelial (gland) cell junction. II. Surface structure. J. Cell Biol. 22, 587–598.
Wood, R.L., 1959. Intercellular attachment in the epithelium of Hydra as revealed by electron microscopy. J. Biophys. Biochem. Cytol. 6, 343–352.
Wood, R.L., 1961. The fine structure of intercellular and mesogleal attachments of the epithelial cells in *Hydra*. In: Lenhoff, H.M., Loomis, W.F. (Eds.), The Biology of Hydra. University of Miami Press, Coral Gables, FL, pp. 51–67.
Yamada, S., Morimoto, H., Fujisawa, T., Sugahara, K., 2007. Glycosaminoglycans in *Hydra magnipapillata* (Hydrozoa, Cnidaria): demonstration of chondroitin in the developing

nematocyst, the sting organelle, and structural characterization of glycosaminoglycans. Glycobiology 17, 886–894.
Yan, L., Pollock, G.H., Nagase, H., Sarras Jr., M.P., 1995. A 25.7 × 10(3) M(r) hydra metalloproteinase (HMP1), a member of the astacin family, localizes to the extracellular matrix of *Hydra vulgaris* in a head-specific manner and has a developmental function. Development 121, 1591–1602.
Yan, L., Leontovich, A., Fei, K., Sarras Jr., M.P., 2000a. Hydra metalloproteinase 1: a secreted astacin metalloproteinase whose apical axis expression is differentially regulated during head regeneration. Dev. Biol. 219, 115–128.
Yan, L., Fei, K., Zhang, J., Dexter, S., Sarras Jr., M.P., 2000b. Identification and characterization of hydra metalloproteinase 2 (HMP2): a meprin-like astacin metalloproteinase that functions in foot morphogenesis. Development 127, 129–141.
Zhang, X., Sarras Jr., M.P., 1994. Cell-extracellular matrix interactions under in vivo conditions during interstitial cell migration in *Hydra vulgaris*. Development 120, 425–432.
Zhang, X., Huff, J.K., Hudson, B.G., Sarras Jr., M.P., 1990. A non-mammalian in vivo model for cellular and molecular analysis of glucose-mediated thickening of basement membranes. Diabetologia 33, 704–707.
Zhang, X., Hudson, B.G., Sarras Jr., M.P., 1994. Hydra cell aggregate development is blocked by selective fragments of fibronectin and type IV collagen. Dev. Biol. 164, 10–23.
Zhang, X., Fei, K., Agbas, A., Yan, L., Zhang, J., O'Reilly, B., Deutzmann, R., Sarras Jr., M.P., 2002. Structure and function of an early divergent form of laminin in hydra: a structurally conserved ECM component that is essential for epithelial morphogenesis. Dev. Genes Evol. 212, 159–172.
Zhang, X., Boot-Handford, R.P., Huxley-Jones, J., Forse, L.N., Mould, A.P., Robertson, D.L., Lili, Athiyal, M., Sarras Jr., M.P., 2007. The collagens of hydra provide insight into the evolution of metazoan extracellular matrices. J. Biol. Chem. 282, 6792–6802.

INDEX

Note: Page numbers followed by "*f*" indicate figures and "*t*" indicate tables.

D

E

F

G

P

R

S